

**JONIX**  
pure living

**SCIENTIFIC  
DOSSIER**



## Jonix NTP technology application for indoor and environmental sanitizing



**Jonix** devices use **"Non Thermal Plasma"** generators covered by an industrial patent "IONIZING DEVICE PROVIDED WITH A IONIZING TUBE TO REMOVE POLLUTANTS / CONTAMINANTS IN A FLUID AND RELATED OPERATING METHOD"  
- license number 0001429908 - application number 102015902351864

# 1. INDEX

<b>2. JONIX DEVICES</b> .....	7
<b>3. PRINCIPLE OF OPERATION</b> .....	7
<b>4. CERTIFICATIONS</b> .....	7
<b>5. COLD PLASMA (NTP – NONTHERMAL PLASMA)</b> .....	9
5.1. PLASMA PRODUCTION BY MEANS OF DBD (DIELECTRIC BARRIER DISCHARGE) .....	9
5.2. JONIX AND THE COLD PLASMA.....	10
5.3. THE CHEMISTRY OF NON-THERMAL PLASMA IN THE GAS FLOW .....	11
<b>6. EFFECTS ON CHEMICAL POLLUTANTS</b> .....	12
6.1. EFFECT ON INORGANIC MOLECULES .....	12
6.2. REACTION MECHANISMS WITH VOCs .....	13
6.3. FOCUS ON INDOOR APPLICATIONS .....	13
<b>7. SANITISING EFFECTS: MECHANISMS OF ACTION AGAINST VIRUSES, MOULDS AND BACTERIA</b> .....	14
<b>8. STUDIES BY THE JONIX RESEARCH AND DEVELOPMENT CENTRE</b> .....	15
8.1 LABORATORY STUDY ON THE BIOCIDAL ACTIVITY OF OXIDIZING SPECIES GENERATED VIA NTP .....	15
8.2 LABORATORY STUDY ON THE SANITIZING EFFECTS PRODUCED BY A MATE – JONIX.....	15
8.3 USE OF NTP TECHNOLOGY AGAINST ODORS ASSOCIATED WITH THE USE OF FOOTWEAR.....	15
8.4. SANITATION OF NON-CRITICAL ULTRASOUND PROBES .....	15
8.5. LABORATORY STUDIES ON THE USE OF NTP FOR VOC ABATEMENT: REVIEW .....	15
8.6. TEST EVALUATING THE EFFECTIVENESS OF MICRO-ORGANISM REDUCTION THAT HAVE BEEN INTENTIONALLY INOCULATED INTO PLATES BY USING THE JONIX MATE AIR IONIZATION SYSTEM .....	16
8.7. STUDY OF THE SANITIZING POWER OF A JONIX DEVICE INSTALLED INTO A COMMERCIAL FAN COIL .....	16
8.8. EVALUATION OF THE SANITIZING CAPACITY OF PHOTOCATALYTIC DEVICES IN COMPARISON WITH JONIX NTP SYSTEMS .	16
8.9. REPORT ON THE ANTIMICROBIAL EFFECTS OF THE JONIX NTP TECHNOLOGY .....	17
<b>9. CASE STUDY: STUDIES ON PRACTICAL APPLICATIONS OF INDOOR SANITIZING SYSTEMS JONIX</b> .....	67
9.1. CASE STUDY 1: REDUCTION OF ODOR IMPACTS ON WASTE MANAGEMENT PLANT .....	67
9.2. CASE STUDY 2: STUDY OF AIR SANITATION IN A VETERINARY CLINIC .....	67
9.3. CASE STUDY 3: SANITIZING EFFECTS OF THE MATE DEVICE IN THE LARGE-SCALE FOOD DISTRIBUTION SECTOR.....	68
9.4. CASE STUDY 4: SANITIZING EFFECTS OF THE MATE DEVICE IN HOSPITAL OPERATING ROOMS .....	68
9.5. CASE STUDY 5: SANITIZING EFFECTS OF THE MATE DEVICE IN HOSPITAL WARDS .....	68
<b>10. CONCLUSIONS</b> .....	69
<b>11. BIBLIOGRAPHY</b> .....	70
<b>12. ATTACHMENTS</b> .....	73
ATTACHMENT 12.0 .....	75
<b>BACTERICIDAL EFFICACY TEST REPORT: QUANTITATIVE SUSPENSION TEST FOR THE EVALUATION OF BACTERICIDAL ACTIVITY AGAINST MDR BACTERIA</b> .....	77
ATTACHMENT 12.1 .....	89
<b>VIRUCIDAL EFFECTIVENESS REPORT: QUANTITATIVE TEST IN SUSPENSION FOR THE EVALUATION OF VIRUCIDAL ACTIVITY AGAINST THE SARS-CoV-2 VIRUS</b> .....	91
ATTACHMENT 12.2 .....	101
LABORATORY STUDY ON THE BIOCIDAL ACTIVITY OF OXIDIZING SPECIES GENERATED VIA NTP .....	103
ATTACHMENT 12.3 .....	105
LABORATORY STUDY ON THE SANITIZING EFFECTS PRODUCED BY A MATE – JONIX .....	107
ATTACHMENT 12.4 .....	109
USE OF NTP TECHNOLOGY AGAINST ODORS ASSOCIATED WITH THE USE OF FOOTWEAR .....	111
ATTACHMENT 12.5 .....	113
SANITATION OF NON-CRITICAL ULTRASOUND PROBES .....	115

ATTACHMENT 12.6 .....	117
LABORATORY STUDIES ON THE USE OF NTP FOR VOC ABATEMENT: REVIEW .....	118
ATTACHMENT 12.7 .....	121
ATTACHMENT 12.8 .....	131
STUDY OF THE SANITISING POWER OF A JONIX DEVICE APPLIED TO A COMMERCIAL FAN COIL .....	133
ATTACHMENT 12.9 .....	149
EVALUATION OF THE SANITIZING CAPACITY OF PHOTOCATALYTIC DEVICES IN COMPARISON WITH JONIX NTP SYSTEMS .....	151
ATTACHMENT 12.10 .....	169
CASE STUDY 1: REDUCTION OF ODOR IMPACTS ON WASTE MANAGEMENT PLANT.....	171
ATTACHMENT 12.11 .....	179
CASE STUDY 2: STUDY OF AIR SANITATION IN A VETERINARY CLINIC .....	181
ATTACHMENT 12.12 .....	193
CASE STUDY 3: SANITIZING EFFECTS OF THE MATE DEVICE IN THE LARGE-SCALE FOOD DISTRIBUTION SECTOR.....	195
ATTACHMENT 12.13 .....	201
CASE STUDY 4: SANITIZING EFFECTS OF THE MATE DEVICE IN HOSPITAL OPERATING ROOMS.....	203
ATTACHMENT 12.14 .....	219
CASE STUDY 5: SANITIZING EFFECTS OF THE MATE DEVICE IN HOSPITAL WARDS .....	221
ATTACHMENT 13.1 .....	239
SCIENTIFIC ARTICLES ON VIRAL AND BACTERIAL SANITIZATION BY MEANS OF NON THERMAL PLASMA .....	241
ATTACHMENT 13.2 .....	317
SCIENTIFIC ARTICLES ON INORGANIC POLLUTANT REMOVAL.....	319
ATTACHMENT 13.3 .....	327

## 2. JONIX DEVICES

All JONIX devices use NTP (Non Thermal Plasma or Cold Plasma) technology which produces oxidizing, and therefore sanitizing, species through the "JONIX generators" (or "actuators"), consisting of cylindrical tubes with metal foils.



## 3. PRINCIPLE OF OPERATION

The *non-thermal plasma (NTP - Non Thermal Plasma)* produces various reactive species collectively known as ROS (*Reactive Oxygen Species*) and these provide the **sanitizing power** of the JONIX systems. Based on what is known about cold plasma, it is possible to posit that sanitization processes can take place by direct interaction between the plasma (actuator surface) and the contaminant, and by the interaction with the species produced by the passage of air into the plasma, which are removed in the gas stream.

Jonix devices, subject to correct use according to the technical specifications, facilitate the **reduction of bacteria, moulds and viruses** both in the ambient air and on the surfaces.

The air filters in the devices of the MATE family (MiniMate, Mate, MaxiMate) increase the sanitizing efficacy of the machines.

## 4. CERTIFICATIONS

All Jonix devices have the following certifications and acknowledgments:



### CE Marking

Products in compliance with EU regulations

Through a declaration of conformity or declaration of performance, the manufacturer declares that the supplied product meets all the safety requirements of the applicable EC directives.



## TÜV PROFICERT

### Constantly-monitored and validated Products

The TÜV logo certifies the truthfulness of the data and performances declared in the scientific dossiers and in the product catalogs.

#### The TÜV logo on products guarantees that:

- The technical dossier complies with current regulations
- The reliability of the devices has been checked and verified over time.
- The history of maintenance operations conducted within guarantee period has been monitored
- Spare parts requests were monitored,
- After-sales assistance has been assessed
- The truthfulness of data and performances indicated in the catalogs and scientific dossiers was checked on a sample basis through tests conducted in laboratories.
- The laboratories used for scientific research have applied reliable protocols that comply with current regulations.

#### Furthermore:

The TÜV Authority has the right to carry out tests at other facilities and / or attend at tests conducted on Jonix products .



### Ongreening® & ProductMAP®

The Green Building Platform

Ongreening® is an independent digital platform dedicated to sustainability-focused practices and material data. Ongreening's mission is to make green building easier and more accessible to all.

Ongreening combines invaluable resources on green building with an innovative material database, called ProductMAP®, which enables informed product selection and decisions based on material performance and sustainability criteria. ProductMAP® assesses products eligibility and contribution to major green building rating schemes such as LEED, WELL, BREEAM, Estidama, HK Beam and the Italian Green Public Procurement Criteria (CAM).

Jonix devices for air sanitizing contribute to fulfill assessment requirements of ecologic buildings: LEED, BREEAM, ESTIDAMA, HB Beam, WELL.



### Bio-Safe

Bio-Safe® certification: certifies excellent indoor living comfort.

#### Validated products

Jonix products have been tested, according to the patented Bio-Safe® protocol which has verified and certified their effectiveness in reducing pollutants. The products have been tested, according to the Bio-Safe® protocol, through laboratory tests conducted inside test chambers (UNI EN

16000) to verify their emission potential and through environmental sampling (UNI EN 14412) to assess the level of indoor air purification achieved within the premises of use.

Passing all the stringent assessment thresholds has led these products to obtain the Bio-Safe® Validation Seal: a guarantee mark which certifies excellent indoor living comfort

#### Environmental health certification

Bio-Safe® certifies environments equipped with Jonix air purification systems, through a patented analysis protocol

## 5. COLD PLASMA (NTP – NONTHERMAL PLASMA)

There are various types of plasma; in general, it is defined as a fully or partially ionized gas, consisting of various particles such as electrons, ions, atoms and molecules, which together as a whole is electrically neutral. Among these, a nonthermal plasma (NTP) is characterized by the fact that it is not in thermodynamic equilibrium: due to their small mass, its electrons can be easily accelerated under the influence of an electric field and can therefore reach high temperatures, while other, non-accelerated particles, remain at room temperature.

Overall, the temperature reached is a few tens of degrees centigrade, and it is for this reason this plasma is called "cold". As almost all the energy imparted is converted into high energy electrons rather than heat, it has a high energy efficiency compared to a conventional plasma, and this makes the technology interesting for various environmental applications (Hao Zhang, 2017). The accelerated electrons induce ionization, excitation and dissociation of the gas molecules, leading to the formation of excited molecules, atoms, ions and radicals which, if in the presence of oxygen, collectively take the name of ROS (*Reactive Oxygen Species*). The ROS are responsible for the oxidative power acquired by the gas flow. The mix is highly responsive and capable of attacking a large variety of polluting compounds with different mechanisms that are discussed further.

Special actuators are used to ionize the gas flow and generate an NTP.

### 5.1. Plasma production by means of DBD (Dielectric Barrier Discharge)

Cold plasma is produced using actuators in a wide variety of geometric configurations and with different principles of operation. These can differ in their configurations and power consumption, and usually involve alternating current (with frequency from 50 up to several kHz) and a potential difference of several kilovolts. This creates discharges within which the process of electron ionization takes place (Figure 1) (U. Kogelschatz, 1997). One of the most widespread and established methods, adopted by Jonix in that it combines a discrete plasma production efficiency with not excessively complex constructional aspects, is based on the principle of dielectric barrier discharge (DBD). It is called that, because there is a dielectric material between the electrodes that prevents the development of high currents.

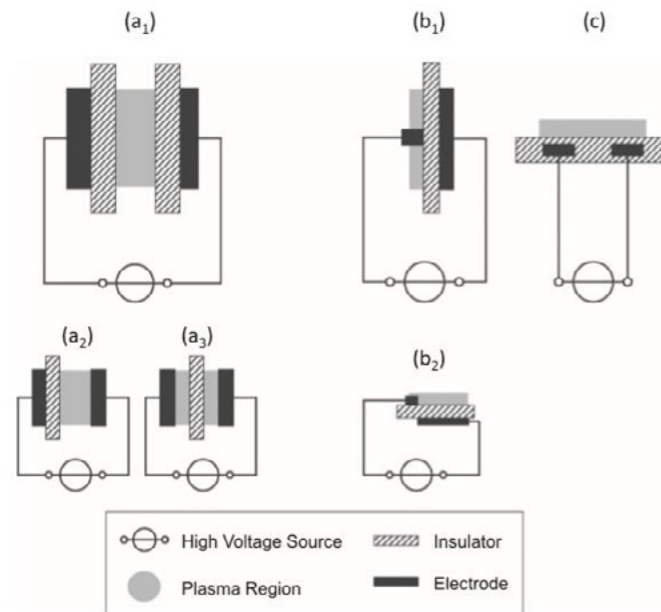


Figure 1 – Examples of DBD reactor configurations: (a) DBD volume (1-symmetric, 2-asymmetric, 3-floated dielectric); (b) surface DBD (1-symmetric, 2-asymmetric 'actuator' design); (c) coplanar discharge (Brandenburg R., 2017)

In most applications, the dielectric material limits the average current density in the gas space, acting as a resistor that, in the ideal case, does not consume energy, preventing the discharge to the arc. When a "streamer", or a transient electrical discharge, propagates towards the barrier, it creates a surface charge that opposes the applied electric field, shielding it. As a consequence, the streamer is interrupted (if the dielectric force of the barrier is sufficient). To remove the surface charge, the voltage is reversed. This type of discharge functions only in the alternating current, since the dielectric material between the electrodes, being an insulator, cannot be crossed by a direct current. The preferred materials for the dielectric barrier are glass or silica glass, in special cases also ceramic materials, and thin veneers and polymeric layers. Some applications use additional protective or functional coatings. The limitation of the current by the dielectric material becomes less effective at very high frequencies. For this reason, the DBD discharges normally operate at frequencies between the frequency of the electricity supply grid and about 1 MHz.

## 5.2. JONIX and the cold plasma

The Jonix plasma actuators (ionizing tubes) consist of a quartz cylinder covered with a metal mesh (exposed electrode) in which there are numerous holes, in number ranging from 30 to 45 per square centimeter, and a coaxial electrode placed inside internal (encapsulated electrode) (Figure 2).



Figure 2 – Jonix plasma DBD actuator

The system is powered by an alternating electric current with mains frequency (50Hz) and voltage of 2850V (nominal voltage). The discharge is generated thanks to the sinusoidal current with such a high potential difference, leading to the generation of micro-arcs on the exposed electrode that take place thanks to the accumulation of electrons on the dielectric layer, that is on the metal mesh (Figure 3), where the cold plasma is generated (surface discharge): the gaseous flow that touches this surface is then ionized (CL Enloe, 2008).

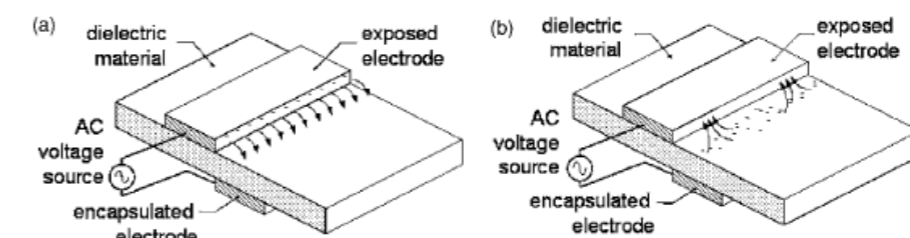
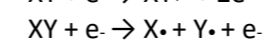
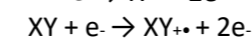
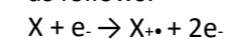


Figure 3 – DBD functioning: (a) negative semi-cycle and (b) positive semi-cycle

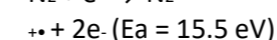
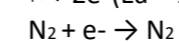
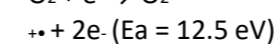
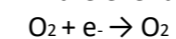
As the internal electrode is placed inside the quartz tube, and it is therefore encapsulated, there is no generation of plasma on it.

## 5.3. The chemistry of non-thermal plasma in the gas flow

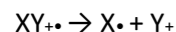
The chemistry of the reactions that take place in a nonthermal plasma is extremely complex and varies according to the gas being ionized, the contact times, the power supply characteristics and the geometry of the reactor. In general, since the main ionization mechanism in the electric discharges is the electron impact ionization, the reactions that initiate the processes can be generically described as follows:



In the event that the ionized gas is air, the main reactions that can occur are:



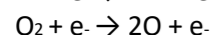
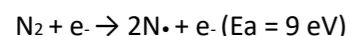
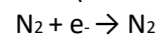
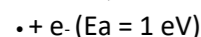
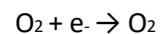
Ionization in air is accompanied by fragmentation processes with the formation of free radicals:



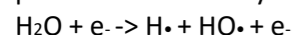
10

Other processes that occur in a plasma involve the excitation of atomic or molecular species; again, in the case

of air:



The products of these primary reactions are highly reactive species that can subsequently recombine to yield nitrogen oxides, NO and NO<sub>2</sub>, and ozone. Another species generated in nonthermal plasmas is the hydroxyl radical, •OH, extremely important for its great oxidizing power. It is formed only in the presence of humidity as follows:



In conclusion, therefore, **the main species generated in a non-thermal plasma in air** are:

- ions O<sub>2+•</sub>, N<sub>2+•</sub>, NO<sub>+•</sub>, O<sub>+•</sub>, O<sub>2+•</sub>, O<sub>3+•</sub>;
- the atomic oxygen species O and the radical •OH;
- excited species of molecular and atomic oxygen (O<sub>2+•</sub>) and molecular nitrogen (N<sub>2+•</sub>);
- the neutral oxygen species O<sub>3</sub> and NO<sub>x</sub>.

The reactions that these species can give rise to are numerous and are still subject of study in the literature due to the considerable complexity of such a heterogeneous set of species. Radical decomposition reactions are accompanied by oxidation reactions, such as the addition of ozone (i.e. Criegee Mechanism Ozonolysis), which reacts even with small carbon particles (2.5 microns) thus removing the fine particulate. The same polluting molecules, in contact with the electron excitation of the plasma, can in turn be ionized, hence generate reaction initiators. The oxidation mechanisms are generalized and can also involve inorganic molecules transported within the plasma.

## 6. EFFECTS ON CHEMICAL POLLUTANTS

This section is divided according to the molecule type: inorganic and organic (VOCs).

### 6.1. Effect on inorganic molecules

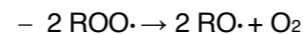
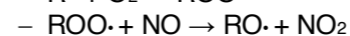
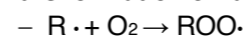
NTP technologies offer a promising scenario for the treatment of typical air-polluting inorganic molecules, such as sulphur and nitrogen oxides, as well as hydrogen sulphide in industrial emission applications (Bratislav M. Obradovic, 2011), this is because NTP is also able to act on inorganic pollutants (Zulfam Adnana, 2017): oxygen radicals react with carbon monoxide (CO) to form carbon dioxide (CO<sub>2</sub>), with sulphur dioxide (SO<sub>2</sub>) to form sulphur trioxide (SO<sub>3</sub>), and with nitrogen oxides (NO<sub>x</sub>), which in the presence of moisture can form nitric acid. Nitrogen oxides and ozone, being persistent, may be considered unwanted by-products.

The new applications appear interesting and are the subject of studies, as plasma treatment allows the simultaneous removal of pollutants, and by managing the applied power according to the requirements, to attain low consumption, as evidenced by the authors of various studies (Wen-Jun Liang, 2011).

### 6.2. Reaction mechanisms with VOCs

Various industrial applications of cold plasma are already established (packaging, polymer functionalization, etc.). Others are still being studied. These include the abatement of VOCs in emissions as an alternative to activated carbon systems, scrubbers, biofilters or combustion systems, because in these plasmas, the polluted organic volatiles can be oxidized to CO<sub>2</sub> already at room temperature with an efficacy dependent on the molecule, contact times and other factors (Arne M. Vandembroucke, 2011) (Kim, 2004).

This is possible because, if air (formed almost exclusively by nitrogen and oxygen) is subjected to the bombardment by these high-energy electrons, the molecules with a stable state (N<sub>2</sub>, O<sub>2</sub>) become metastable, (N<sub>2m</sub>, O<sub>2m</sub>) or excited (N<sub>2\*</sub>, O<sub>2\*</sub>). These forms collide with each other or with others left at the base level, or are bombarded again by excited electrons. The result is a summation of ionization processes (including Penning ionization), even if the most accredited reaction pathways still involve the formation of radicals (Seinfeld & Pandis, 1998):



The result of these step reactions is the formation of ions and free radicals with very high oxidizing power which, in contact with contaminants, theoretically lead to products such as carbon dioxide and water vapour, similarly to what happens in high-temperature combustion systems. However, a partial efficacy, occurring when some pollutants are oxidized only partially (Oda, 2003), as well as the formation of decomposition intermediates as by-products (K. Urashima, 2000) should be tested experimentally. These limitations must be assessed on a case-by-case basis to determine the suitability of the process and any possible issues.

Ultimately, the NTP technology represents a promising solution for the treatment of any VOC, even in exceptional conditions, or for inert and persistent molecules, such as haloalkanes, both in the conditions of low (<100 ppmv) and of high (>1000 ppmv) concentration of pollutants (Penetrante, 2011) (S. Schmid, 2010), demonstrating thus a remarkable flexibility of use. One of its possible applications, for example, could be for odorous compounds, which often cause adverse effects already at extremely low levels (ppb). In comparison with the various technologies for the removal of VOCs from the air available today, the NTP systems show their strength in the conditions of medium to low concentrations (<1000 ppmv) (J. Karuppiah, 2012) of poorly water-soluble contaminants (Schiavon M. T., 2017). In industrial applications, the expectations linked to the increased solubility of the by-products of the treatments are interesting, especially if combined with catalysts, as they improve the functioning of biofilters and absorption columns. As for the indoor applications, they are of special interest due to the expected low concentration of by-products.

### 6.3. Focus on indoor applications

In this context, nonthermal plasma (NTP) systems offer interesting possibilities in the area of indoor air purification systems because, as has been said, they are particularly useful in conditions that are typical of environments intended for human presence, namely:

- Low concentrations;
- Numerous types of pollutants
- Ambient temperature and pressure

Compared to the alternatives, the NTP proves flexible and a more environmentally friendly and promising technique for removing numerous air pollutants (Stasiulaitiene et al., 2015; Thevenet et al., 2014). Among the many types of plasma and of ways to generate it, those generated by the corona and the dielectric barrier discharges (DBD) are the most studied within the scope of the air-cleaning objectives (Moscosa-Santillan et al., 2008).

The abatement values are dependent on the pollutant type and generally, in the specified low concentration conditions, range from 50 to 90 %<sup>1</sup> (for an NTP generated with DBD) (Osman Karatum, A comparative study of dilute VOCs treatment in a non-thermal, 2016). The highest percentages apply to the hydrogen richer molecular structures. In these cases there are no partial oxidation products and it can be postulated that once a chain of reactions has been initiated, the enthalpy generates heat allowing the oxidation to carbon dioxide to be completed. (Carlos M. Nunez, 2012)!!

## 7. SANITISING EFFECTS: MECHANISMS OF ACTION AGAINST VIRUSES, MOULDS AND BACTERIA

There are numerous studies in the literature that demonstrate the nonthermal plasma's ability to inactivate many different types of microorganisms, such as moulds, viruses and bacteria (Michael J. Gallagher, 2004), both on surfaces and in the air. In the latter case, this technology generates particular interest, because high-efficiency particulate filters (HEPAs), commonly used to remove most microorganisms, are effective for particles up to 0.5 microns in size, but lose their effectiveness against viruses present in the air (via droplets), as these are among the smallest microorganisms (20-300 nm) (Harstad, 1969).

As regards surface treatments, biomedical applications are cited among the most interesting applications studied, thanks to the effects of microbial inactivation, sterilisation and disinfection confirmed by the authors. In this case the benefits comprise a broad spectrum of action, the use of non-toxic gases and the absence of toxic residues (Kong M.G., 2009).

Given the advantages over other sanitization technologies, many studies have focused on identifying the mechanisms of action against different types of viruses, considering also the increase in resistance to treatments. (Chulkyoon, Non-thermal plasmas (NTPs) for inactivation of viruses in abiotic environment, 2016). Several researchers have stated that chemically reactive neutral species such as O, O<sub>2</sub><sup>\*</sup>, O<sub>3</sub>, OH<sup>•</sup>, NO and NO<sub>2</sub> can contribute significantly to the plasma sterilization process, in particular at atmospheric pressures (Laroussi, 2005), whilst the ionization of oxygen-containing gases provided the most consistent germicidal effects (Herrmann H.W., 1999), in that the presence of ozone (known bactericide) and hydroxyl radicals (OH) makes it possible to chemically attack the external structures of the bacterial cells, meaning the oxidizing power acts on the integrity of the virus both structurally and genomically, affecting the proteins as well as the nucleic acids. Other authors attribute some virucidal effects to other nitrogen mechanisms (Wu Y., 2015). However, almost all the authors agree that neither the UV radiation, nor the thermal component, although present in cold plasma, have any impact on the sanitization effect (Arijana Filipi, 2020) (M. Laroussi, 2004) (Leipold, 2004).

It should be remembered that there are many types of NTP that differ in energy density, production method and other parameters. Although all the studies clearly agree on the virucidal effects, the degree of inactivation depends on the category of viruses and the type of plasma, as well as on the experimental parameters, such as the exposure time.

<sup>1</sup> Es. specific input energy (SIE) of 350 J L: 1, methyl ethyl ketone (50%), benzene (58%), toluene (74%), 3-pentanone (76%), methyl tert-butyl ether (80%), ethylbenzene (81%), and n-hexane (90%)

## 8. STUDIES BY THE JONIX RESEARCH AND DEVELOPMENT CENTRE

Over the years, numerous laboratory-scale studies have been conducted by Jonix Research & Development Center in order to increase the knowledge of the Jonix NTP systems produced effects in different applications. The main results are here below reported with a summary of the carried-out activities.

### 8.1 Laboratory study on the biocidal activity of oxidizing species generated via NTP

**PURPOSE:** checking the bactericidal capacity of ionized air on culture plates.

**RESULT:** NTP is effective from the very first minutes of use. After just 5 minutes, all tested species are completely eradicated from the surface of the plates. A further element that positively characterizes the success of the test consists in the fact that, contrary to the provisions of some methods that require carrying out the experiments on stainless steel surfaces, the above described tests were performed in optimal conditions for the microorganisms both from an ecological point of view and for the quantity of organic substance involved.

The details of the trial are reported in ANNEX 1.

### 8.2 Laboratory study on the sanitizing effects produced by a MATE – Jonix

**PURPOSE:** checking the spontaneous reduction of microbial contamination in a workplace in the presence and in absence of the NTP treatment generated by a MATE device.

**RESULT:** after about 30 minutes of treatment the percentage of microbial reduction is very close to 100%. This confirms the effectiveness of MATE in sanitizing living or working environments.

The details of the trial are reported in ANNEX 2.

### 8.3 Use of NTP technology against odors associated with the use of footwear

**PURPOSE:** testing the effectiveness of the Jonix NTP system to reduce the concentration of chemical molecules (VOCs) responsible for the odor associated with the use of footwear.

**RESULT:** the test result led to the conclusion that using a NTP air treatments for sufficiently long time (from 6 hours onwards) is EFFECTIVE and the treatment breaks down and completely destroys the molecules in subject

The details of the trial are reported in ANNEX 3

### 8.4. Sanitation of non-critical ultrasound probes

**PURPOSE:** comparing the sanitizing effect on “non-critical” ultrasound probes by NTP enriched flow of air, compared to the sanitization carried out by traditional commercial devices.

**RESULT:** The tests have shown that the effectiveness of an NTP treatment is absolutely comparable to that of the devices that are traditionally designed and used for the purpose

The details of the trial are reported in ANNEX 4.

### 8.5. Laboratory studies on the use of NTP for VOC abatement: review

**PURPOSE:** summary of some laboratory internal tests to rationalize the obtained results and evaluate possible applications.



**RESULT:** The abatement percentages, generally higher than 95%, indicate the NTP capability of acting on certain compounds, mostly odorous. Interesting scenarios emerge as for odor impact reduction applications on purification or waste treatment plants.  
 The details of the trial are reported in ANNEX 5.

**8.6. Test evaluating the effectiveness of micro-organism reduction that have been intentionally inoculated into plates by using the Jonix Mate air ionization system**

**PURPOSE:** checking the reduction of microorganisms that have been intentionally inoculated in cultural soils and exposed for a pre-established time to the effect of ionized air. For each test a control test was performed using the same inoculated soils but not subject to NTP treatment.

**RESULT:** the microbial abatement in presence of the Jonix Mate air ionization system, on organic material simulants surfaces that have been inoculated with different microbial species, is high. Jonix ionizing system completely inhibits most of the inoculated species within 12-24 hours. In many cases, the obtained reduction is higher than 95%. The microbial reduction effect of ionized air is similar on both Gram positive, Gram negative, yeasts and molds, although the effectiveness is often depending on the involved species.

The details of the trial are reported in ANNEX 6.

**8.7. Study of the sanitizing power of a Jonix device installed into a commercial fan coil**

**PURPOSE:** checking the biological sanitizing effectiveness of a Jonix NTP device installed inside a fan coil for wall installation. The purpose of the test is to check whether the production of oxidizing species can solve the problem of pollution by molds of some parts of the equipment, as well as sanitizing the air in the room where it is installed.

**RESULT:** the obtained results show how the use of a Jonix sanitization device allows getting over time a marked reduction of an environmental microbial contamination both in terms of bacteria, molds and yeasts.

The details of the trial are reported in ANNEX 7.

**8.8. Evaluation of the sanitizing capacity of Photocatalytic devices in comparison with Jonix NTP systems**

**PURPOSE:** the target was to quantify and then compare the possible sanitizing effect performed by two types of commercial devices, Jonix NTP and SHU900X, a photocatalytic device. They have been installed inside a 30 cm diameter steel pipe 12 m long. By means of a fan, an air flow blew at different speeds and flow rates, thus simulating what happens inside a ventilation duct in the event of microbiological contamination and in presence or absence of "sanitizing" devices such as those tested. For this purpose, ARCHA have designed and carried out a series of experiments in which, in a controlled manner, different types and quantity of microorganisms have been exposed inside the tube to air flow while different types of air sanitizing devices were activated.

**RESULT:** Both Jonix NTP and Photocatalytic systems are effective as for the total abatement of yeasts. The Photocatalytic system is more efficient than the Jonix system as for the sanitization effect on molds on plate but is inefficient on bio-aerosol, unlike Jonix. In conclusion, Jonix systems have a broad spectrum of action that allows sanitizing both surfaces and air.

The details of the trial are reported in ANNEX 8.

8.9. Report on the antimicrobial effects of the Jonix NTP technology



JOnix S.p.a.

Benefit Croporation

REGISTERED OFFICE

Viale Spagna 31-33

35020 Tribano (PD) - Italy

HEADQUARTERS

Via dell'Artigianato 1,

35020 San Pietro

Vinimario (PD) - Italy

REPORT ON THE ANTIMICROBIAL EFFECTS OF THE JONIX NTP TECHNOLOGY

May-June 2021

**Laboratori ARCHA S.r.l. unipersonale**

Via di Tegulaia 10/a - 56121 - PISA - ph. +39 050 985165 - fax +39 050 985233 - www.archa.it - archainf@archa.it  
 C.F., P.IVA, Iscr. Reg. Impr. di Pisa n. 01115340505 - Rep. Econ. Amm. di Pisa n°101169 - Capitale Sociale 101.400,00 i.v.

## INDEX

INDEX .....	18
INTRODUCTION AND GLOSSARY.....	20
TECHNICIANS IN CHARGE OF THE TRIAL.....	22
JONIX EQUIPMENT AND DEVICES .....	23
MEASUREMENT INSTRUMENTS .....	23
JONIX DEVICES USED FOR THE TESTS .....	24
PERFORMED TESTS.....	25
TEST A.....	26
<i>Summary of the test</i> .....	26
<i>Description of the test</i> .....	26
<i>Ozone concentration in the test environment</i> .....	26
<i>Photo evidence</i> .....	27
<i>Results</i> .....	28
<i>Summary conclusions on the results of the test</i> .....	31
TEST B .....	32
<i>Summary of the test</i> .....	32
<i>Description of the test</i> .....	32
<i>Ozone concentration in the test environment</i> .....	33
<i>Photo evidence</i> .....	34
<i>Results</i> .....	35
<i>Summary conclusions on the results of the test</i> .....	37
PROVA C .....	39
<i>Summary of the test</i> .....	39
<i>Description of the test</i> .....	39
<i>Ozone concentration in the test environment</i> .....	40
<i>Photo evidence (fotografiche)</i> .....	41
<i>Results</i> .....	42
<i>Summary conclusions on the results of the test</i> .....	43
TEST D.....	46
<i>Summary of the test</i> .....	46
<i>Description of the test</i> .....	46

**Laboratori ARCHA S.r.l. unipersonale**

Via di Tegulaia 10/a - 56121 - PISA - ph. +39 050 985165 - fax +39 050 985233 - www.archa.it - archainf@archa.it  
C.F., P.IVA, Iscr. Reg. Impr. di Pisa n. 01115340505 - Rep. Econ. Amm. di Pisa n°101169 - Capitale Sociale 101.400,00 i.v.

<i>Ozone concentration in the test environment</i> .....	46
<i>Photo evidence</i> .....	48
<i>Results</i> .....	49
<i>Summary conclusions on the results of the test</i> .....	51
TEST E .....	53
5.5.1 <i>Summary of the test</i> .....	53
1.1.2 <i>Ozone in the outside air</i> .....	53
<i>Description of the test</i> .....	56
<i>Ozone concentration in the test environment</i> .....	56
5.5.5 <i>Photo evidence (fotografiche)</i> .....	60
5.5.6 <i>Results</i> .....	61
1.1.7 <i>Summary conclusions on the results of the test</i> .....	63
SUMMARY AND CONCLUSIONS.....	64

**Laboratori ARCHA S.r.l. unipersonale**

Via di Tegulaia 10/a - 56121 - PISA - ph. +39 050 985165 - fax +39 050 985233 - www.archa.it - archainf@archa.it  
C.F., P.IVA, Iscr. Reg. Impr. di Pisa n. 01115340505 - Rep. Econ. Amm. di Pisa n°101169 - Capitale Sociale 101.400,00 i.v.

## INTRODUCTION AND GLOSSARY

The following report describes the results of the main experiments conducted on behalf of JONIX S.p.A. in order to evaluate/assess the antimicrobial effect (bacteriostatic or bactericidal) of the devices, also in relation to similar effects that occur in nature.

For this, experimental tests were conducted by exposing bacterial colonies both in the air emitted by Jonix devices and in the natural air on a day with good weather.

Below is the definition of the terms used in the report:

Antimicrobial	Substance or product capable of killing microorganisms (biocide) or slowing their growth (biostatic)
Bactericidal	Substance or product capable of killing bacteria (biocide)
Bacteriostatic	Substance or product capable of inhibiting or slowing bacterial replication without killing the microorganism (biostatic)
Enterococcus	Gram-positive, catalase-negative, rounded or oval-shaped bacteria, often arranged in chains
Escherichia Coli	Gram-negative bacteria that normally reside in the intestines of healthy people; however, some strains can cause infections in the digestive tract, urinary tract or many other parts of the body.
Gram-negative	Bacteria that remain pink stained after the Gram staining. Gram-negatives have a wall consisting of a simpler structure, always based on peptidoglycan and also have an external lipid membrane.
Gram-positive	Bacteria that remain blue or purple stained after the Gram staining. Gram-positive bacteria have a wall with a complex, rigid and thick structure based on peptidoglycan.
Ozone	Allotropic form of oxygen with formula O <sub>3</sub> , with a characteristic garlic odour. It is present in nature due to the effect of solar radiation. Strong oxidizer used for disinfection operations.
Pseudomonas	Gram-negative bacteria, obligate aerobes, positive oxidase, catalase positive and have polar flagella that allow them to move. They are found in the soil and in water but also on plants.
ROS	The reactive oxygen species, ROS, are the most widespread free radicals. The most important ROS are the superoxide anion O <sub>2</sub> <sup>-</sup> , the hydrogen peroxide H <sub>2</sub> O <sub>2</sub> and the hydroxyl radical •OH.
Staphylococcus	Aerobic Gram-positive spherical bacteria (i.e., able to live only in the presence of oxygen) or facultative anaerobic (i.e., normally requiring oxygen, but which can survive even without if necessary). These microbes are normally found on

the skin and in the nose of healthy individuals, where in most cases they do not cause any problems or result in minor skin infections. In some circumstances, they can trigger very dangerous infections.

## TECHNICIANS IN CHARGE OF THE TRIAL

The trials were conducted by the following qualified technicians:

**Dott.ssa Francesca Gambineri** Graduated in Industrial Chemistry, 20 years of experience in the field of chemical research, materials science and innovative technologies  
10 years of experience in the study of NTP and its effects on chemicals and materials  
Co-inventor of 3 patents  
Co-author in numerous scientific publications, 6 of which concerning the potential use of NTP  
Coordinator of the experiments

**Dott. Fabrizio Cervelli** Graduated in Biology, PhD in Cellular and Molecular Pathology  
Expert in Hygiene of living and working environments and water resources  
10 years of experience in Basic Biological Research  
20 years of experience in microbiology and applied research  
Coordinator and performer of microbiological experiments in the study of NTP and its effects on microorganisms  
Co-author of numerous publications in national and international scientific journals

**Dott. Lamberto Corsi** Graduated in Chemistry  
20 years of experience in conducting research projects  
Coordinator and executor of the chemical-physical measurements

## JONIX EQUIPMENT AND DEVICES

### Measurement instruments

JONIX NTP technology is based on Non-Thermal Plasma and produces oxidizing species around the generators that are also conveyed into the environment through the ventilation of the devices themselves and the help of air humidity.

Among the oxidizing species that are generated, there is also Ozone which appears to be the only measurable species. The concentration of environmental Ozone is therefore not only an important and necessary reference to be measured to ensure compliance with all the regulations that provide for exposure limits in living environments, but also a reference on the "potential" of the devices in generating oxidizing species.


A Horiba analyser was used to measure environmental Ozone concentrations.

HORIBA is a leader in the field of instrumentation for environmental analysis, and the instrument used is the APOA 370 model.

It is based on the NDUV method (Principle of non-dispersive ultra-violet-absorption) and allows to detect concentrations between 0 and 100 ppb using the low range and up to 1,000 ppb using the higher range, with a detectability of 0.1 ppb.

It has a repeatability of  $\pm 1.0\%$  of the full scale and a linearity of  $\pm 1.0\%$  of the full scale.

The instrument is periodically subjected to calibration and the latest report is shown alongside:

 Laboratorio di Taratura Via A. Volta, 25/6 35020 Vegliano (PD) Italy Tel: +39 049 9006911 Fax: +39 049 9006929 Web: www.orion-srl.it Email: info@orion-srl.it		Laboratorio di Taratura Calibration Laboratory	
RAPPORTO DI TARATURA 014 - 2020 Calibration Report 014 - 2020			
Pagina 1 di 4 Page 1 of 4			
- data di emissione date of issue	2020-11-27	- cliente customer	Jonix SRL
- destinatario receiver	Dott.ssa Francesca Gambineri Jonix SRL Viale Spagna, 31/33 35020 Tribano PD	- Si riferisce a Referring to	
- oggetto item	Analizzatore di Ozono	- costruttore manufacturer	HORIBA
- modello model	APOA - 370	- matricola serial number	89R3WGTY
- data ricevimento oggetto date of receipt of item	2020-10-30	- data delle misure date of measurements	2020-11-27
- registro di laboratorio laboratory reference	MOD_LS02 01 012/2020		

Le incertezze di misura dichiarate in questo documento sono state determinate conformemente alla Guida ISO/IEC 98 e al documento EA-4/02. Solitamente sono espresse come incertezza estesa ottenuta moltiplicando l'incertezza tipo per il fattore di copertura k corrispondente ad un livello di fiducia di circa il 95%. Normalmente tale fattore k vale 2.  
The measurement uncertainties stated in this document have been determined according to the ISO/IEC Guide 98 and to EA-4/02. Usually, they have been estimated as expanded uncertainty obtained multiplying the standard uncertainty by the coverage factor k corresponding to a confidence level of about 95%. Normally, this factor k is 2.

**Jonix devices used for the tests**

For the tests described below, commercial Jonix MiniMate and Jonix Cube devices were used, in some cases electrically modified to simulate the correct sizing within the testing rooms.

The use, sizing and management of the devices was therefore such as to keep the environmental Ozone levels below 50 ppb which is the target for the correct sizing of the devices in the premises.



**PERFORMED TESTS**

The following experimental tests were carried out, in addition to other undocumented ones that were preparatory for the development of the methods:

TEST	CODE	DESCRIPTION	OBJECTIVE
A	S20/005800001	Exposure of plates with Escherichia coli and Staphylococcus aureus microorganisms, at different distances from the JONIX device	Evaluating the antimicrobial effect of NTP at different distances from the device
B	S20/005800003	Exposure of plates with fecal Enterococcus and Pseudomonas aeruginosa, at different distances from the JONIX device	Evaluating the antimicrobial effect of NTP at different distances from the device
C	S20/005800004	Exposure of plates with Staphylococcus aureus, fecal Enterococcus, Escherichia coli and Pseudomonas aeruginosa in small cases (theca), keeping the internal humidity at about 50%	Evaluating the antimicrobial effect of NTP under controlled humidity conditions
D	S20/005800009	Exposure of plates with Staphylococcus aureus, fecal Enterococcus, Escherichia coli and Pseudomonas aeruginosa in small cases (theca), keeping the internal humidity at about 80%	Evaluating the antimicrobial effect of NTP at high humidity conditions
E	S20/005800008	Exposure of plates with Staphylococcus aureus, fecal Enterococcus, Escherichia coli and Pseudomonas aeruginosa in a natural environment	Evaluating the effect of external air, containing naturally occurring oxidizing species

TEST A

Summary of the test

Test code	S20/005800001
Date	21 April 2021
Description of the test	Exposure of plates with Escherichia coli and Staphylococcus aureus microorganisms, at different distances from the JONIX device
Objective of the test	Evaluating the antimicrobial effect of NTP at different distances from the device
Jonix device used	JONIX MiniMate
Test environment	Room with plan dimensions of 9.2 m x 6.8 m x 2.8 m (h) for a floor area of 62.6 square meters and a volume of 175 m <sup>3</sup>
Summary of the results	Reduction of the microbial load up to 100% for Staphylococcus aureus and up to 9% for Escherichia coli

Description of the test

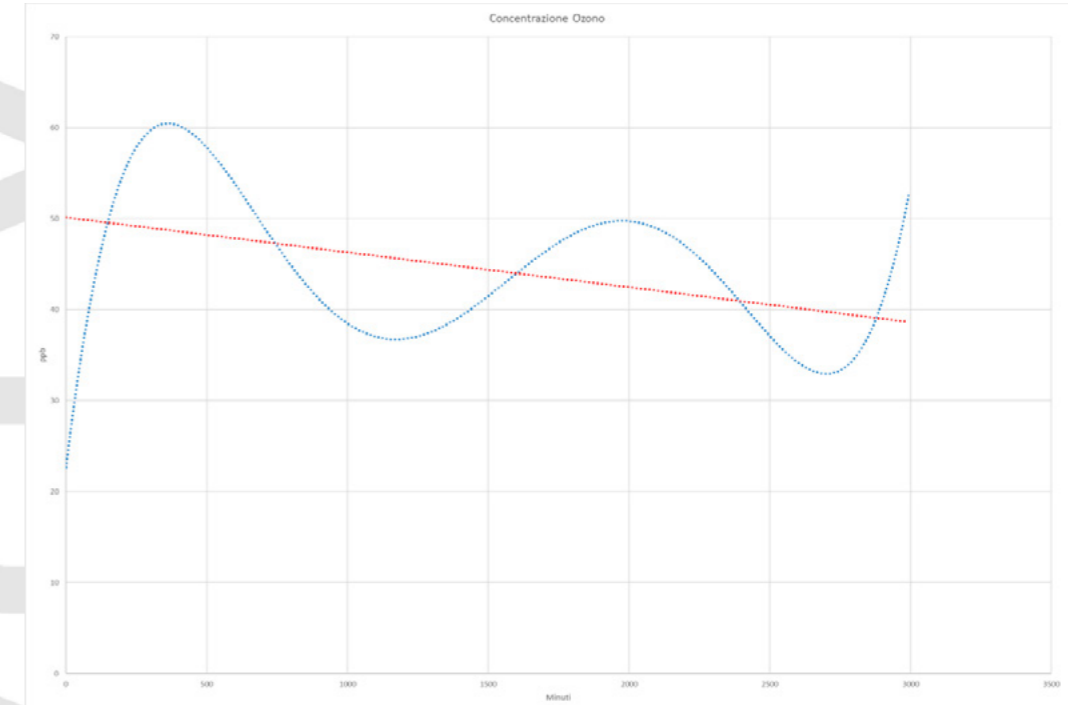
For this test, cultures of gram-negative (Escherichia coli) and Gram-positive (Staphylococcus aureus) bacteria were used, since a different sensitivity to biocidal agents is known between the two types of bacteria.

The microorganisms were seeded, in duplicate, on double sector petri dishes filled with PCA agar (non-selective medium) at a density of about 200 CFU/sector. Subsequently, the plates were exposed, uncovered, to the NTP, keeping them at a distance of 1, 2 and 4 meters from the device for a total time of 24 hours. The control plates were kept inside the laboratory, closed with their lid, thus avoiding any possible exposure to NTP.

After exposure, the plates were photographed and then kept in an incubator at 37° C for 24 + 24 hours.

Ozone concentration in the test environment

The Ozone measurements to which the plates were exposed during the 24 hours of treatment revealed an average value of 45 ppb during the test period as shown in the following graph:



Test environment Ozone concentration during Test A (red line = average)

Photo evidence

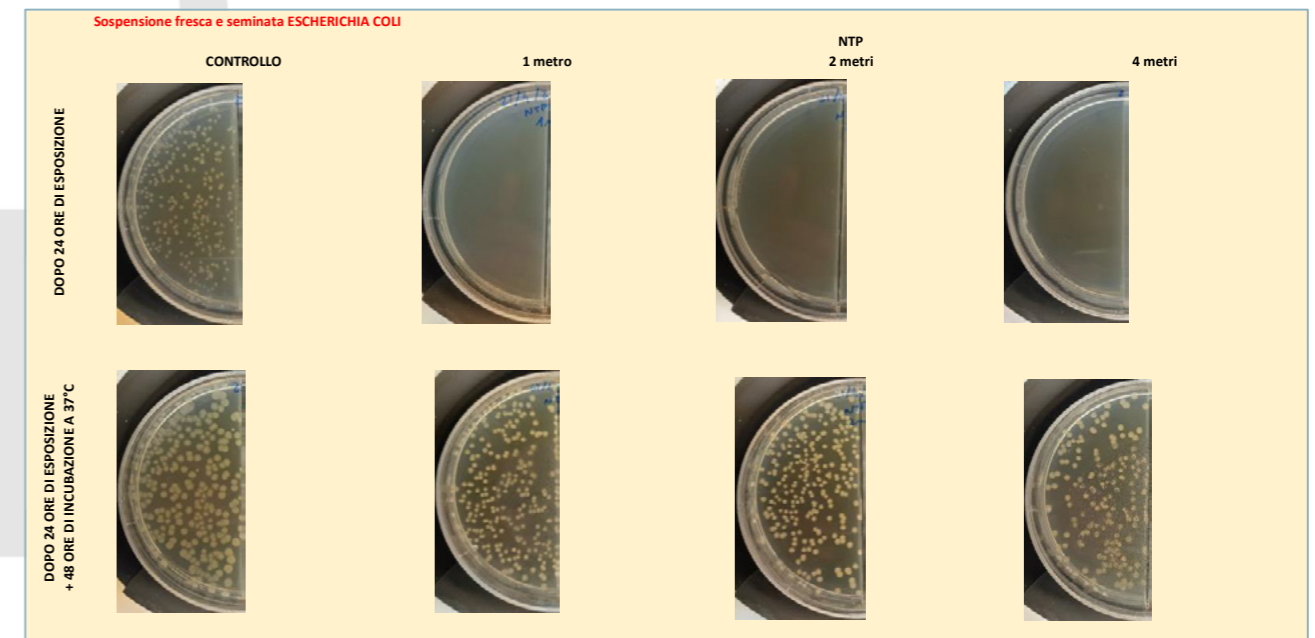


Immagine: Suspension seeded with ESCHERICHIA COLI  
Control – 0 meter – NTP 2 meters – 4 meters  
After 24-hours exposition  
After 24-hours exposition + 48 hours of incubation at 37° C

*Antimicrobial effects: detail of the sectors containing Escherichia coli*

*Top row: the appearance of the culture plates after 24-hour exposure to NTP (comparison with the control plate, not exposed) as the distance from the device varies*

*Bottom row: same plates but after 48 hours of incubation at 37° C*

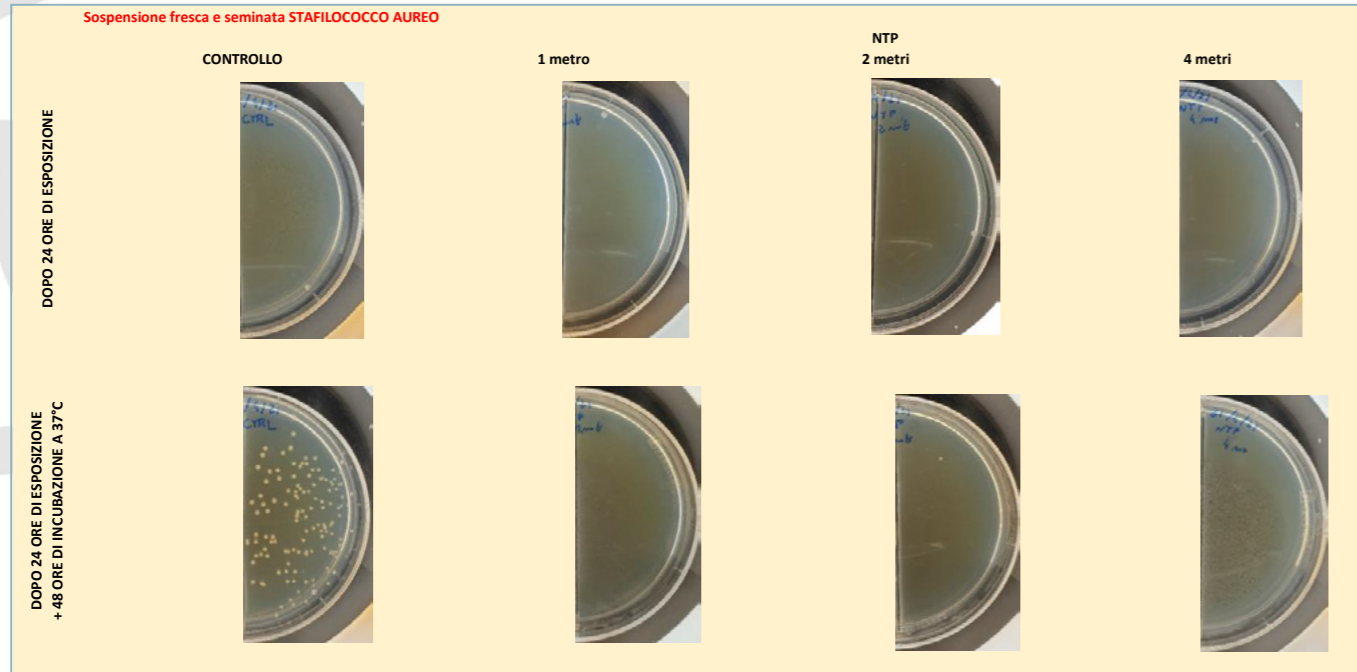


Immagine: Suspension seeded with STAPHYLOCOCCUS AUREUS

Control – 0 meter – NTP 2 meters – 4 meters

After 24-hours exposition

After 24-hours exposition + 48 hours of incubation at 37° C

*Antimicrobial effects: detail of the sectors containing Staphylococcus aureus*

*Top row: the appearance of the culture plates after 24-hour exposure to NTP (comparison with the control plate, not exposed) as the distance from the device varies*

*Bottom row: same plates but after 48 hours of incubation at 37° C*

## Results

From the previous image, it is easy to see how there is a substantial difference in the effects exerted by NTP on the two different types of bacteria. In particular, we observe, for all three exposure distances, an effect of almost total inhibition of growth against Staphylococcus aureus (right sectors) and a limited action against Escherichia coli.

It is also interesting to observe how at the end of the 24 hours of exposure to NTP, it was not possible to recognise any microbial growth in all sectors, including those containing Escherichia coli, which instead does not occur after the subsequent incubation, in which colonies of Escherichia coli also

appear in plates exposed to NTP. This data, together with the smaller size of the bacterial colonies, demonstrate the bacteriostatic effect produced by NTP.

On the other hand, the situation relating to Staphylococcus aureus is different, which instead showed an almost absolute effect of microbial reduction after exposure to NTP.

Following are the values of the microbial count of the colonies grown in the plate:

Microbial concentration in each sector of the plates used.

Ecoli	UFC/sector		plate 1	plate 2	Average	St Dev
		Ctrl	291	272	<b>281,5</b>	13
	NTP 1 mt	263	260	<b>262</b>	2	
	NTP 2 mt	259	257	<b>258</b>	1	
	NTP 4 mt	178	170	<b>174</b>	6	
Log UFC/sector		Ctrl	2,45	2,43	<b>2,45</b>	0,02
		NTP 1 mt	2,42	2,41	<b>2,42</b>	0,00
		NTP 2 mt	2,41	2,41	<b>2,41</b>	0,00
		NTP 4 mt	2,25	2,23	<b>2,24</b>	0,01

Saureo	UFC/sector		plate 1	plate 2	Average	St Dev
		Ctrl	108	134	<b>121</b>	18
	NTP 1 mt	0	0	<b>0</b>	0	
	NTP 2 mt	0	2	<b>1</b>	1	
	NTP 4 mt	0	0	<b>0</b>	0	
Log UFC/sector		Ctrl	2,03	2,13	<b>2,08</b>	0,07
		NTP 1 mt	0,00	0,00	<b>0,00</b>	0,00
		NTP 2 mt	0,00	0,30	<b>0,15</b>	0,21
		NTP 4 mt	0,00	0,00	<b>0,00</b>	0,00

## Summary conclusions on the results of the test

The graphic transposition of the data highlights better the results obtained:

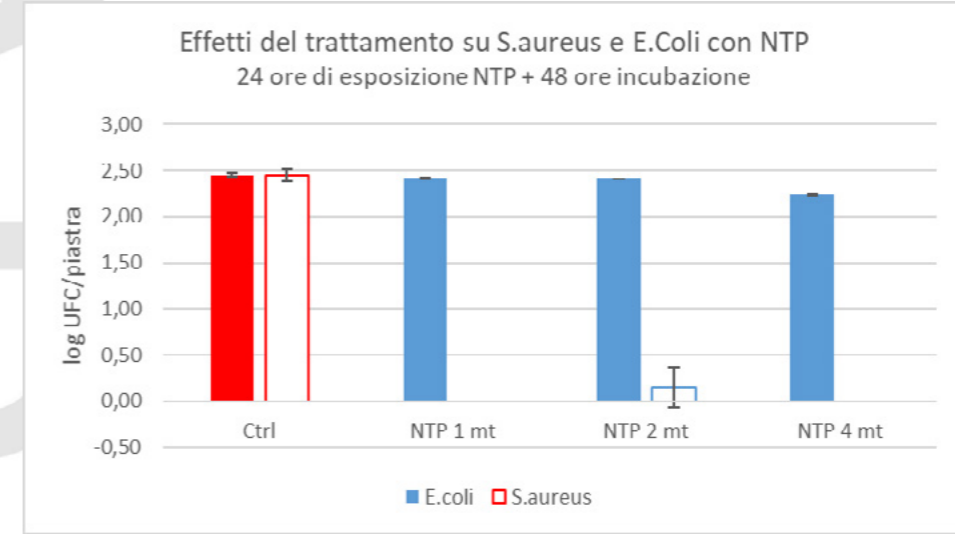


Immagine: log CFU/plate

Effects of the treatment on S.aureus and E.Coli with NTP  
24 hours of NTP exposure + 48 hours of incubation

Comparison of the effects of NTP treatment, values expressed as the average of two plates

On the other hand, by expressing the data obtained in terms of percentage reduction of growth compared to the control plates, it can be clearly highlighted how this was very high exclusively for Staphylococcus aureus and present only at a distance of 4 meters from the device for Escherichia coli.

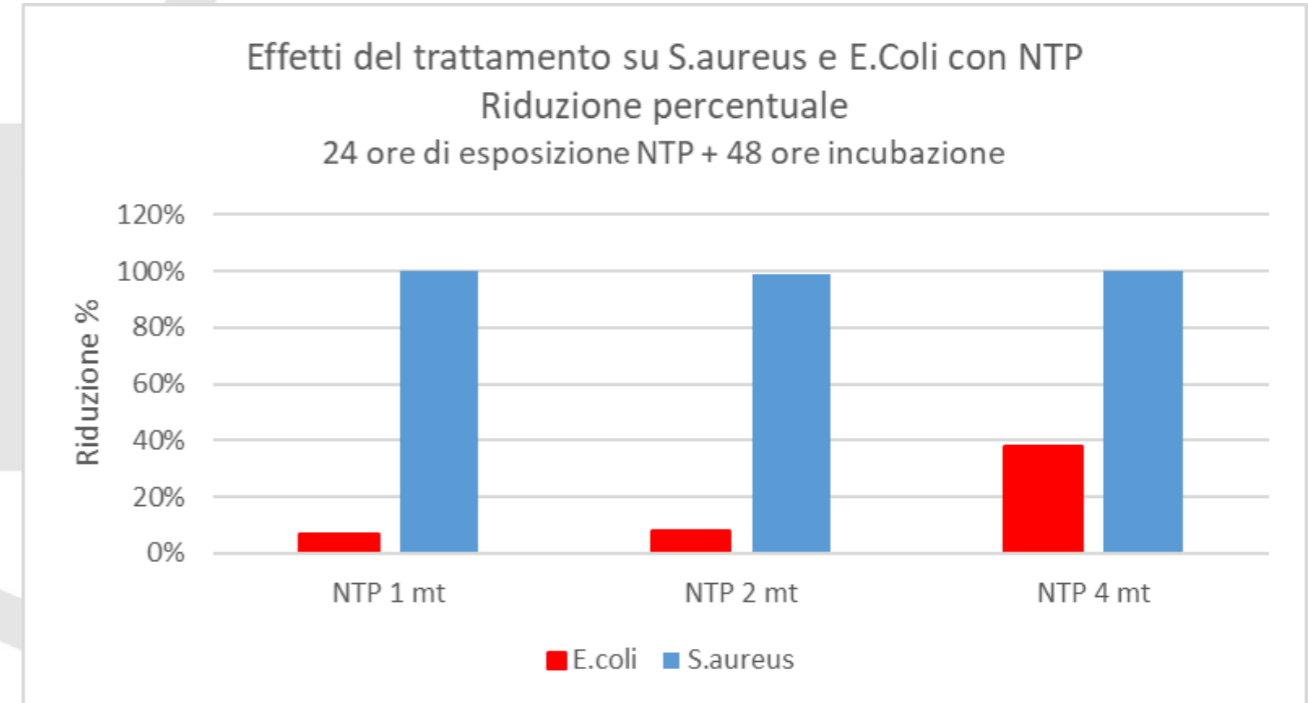




Immagine: Reduction%  
 Effects of the treatment on S.aureus and E.Coli with NTP  
 Percentage reduction  
 24 hours of NTP exposure + 48 hours of incubation

*Comparison of the percentage reductions in microbial growth between the two tested microorganisms*

The distance from the NTP device did not show any significant differences.

**TEST B**

*Summary of the test*

Test code	S20/005800003
Date	29/04/2021
Description of the test	Exposure of plates with fecal Enterococcus and Pseudomonas aeruginosa, at different distances from the JONIX device
Objective of the test	Evaluating the antimicrobial effect of NTP at different distances from the device
Jonix device used	JONIX MiniMate
Test environment	Room with plan dimensions of 9.2 m x 6.8 m x 2.8 m (h) for a floor area of 62.6 square meters and a volume of 175 m <sup>3</sup>
Summary of the results	Reduction of the microbial load up to 56% for Enterococcus and up to 9% for Escherichia coli

*Description of the test*

Having ascertained the different effect on the two microorganisms Escherichia coli and Staphylococcus aureus (Test A), we wanted to verify whether this was a distinctive trait of the microbial groups to which they belong.

Two other Gram-positive (Enterococcus fecal) and Gram-negative (Pseudomonas aeruginosa) microorganisms were thus exposed to NTP.

Just like for the previous test, the microorganisms were seeded, in duplicate, on double sector petri dishes filled with PCA agar (non-selective medium) at a density of about 200 CFU/sector. Subsequently, the plates were exposed, uncovered, to the NTP, keeping them at a distance of 1, 2 and 4 meters from the device for a total time of 24 hours. The control plates were kept inside the laboratory, closed with their lid, thus avoiding any possible exposure to NTP.

After exposure, the plates were photographed and then kept in an incubator at 37° C for 24 + 24 hours.

*Ozone concentration in the test environment*

The Ozone measurements to which the plates were exposed during the 24 hours of treatment revealed an average value of 24 ppb during the test period as shown in the following graph:

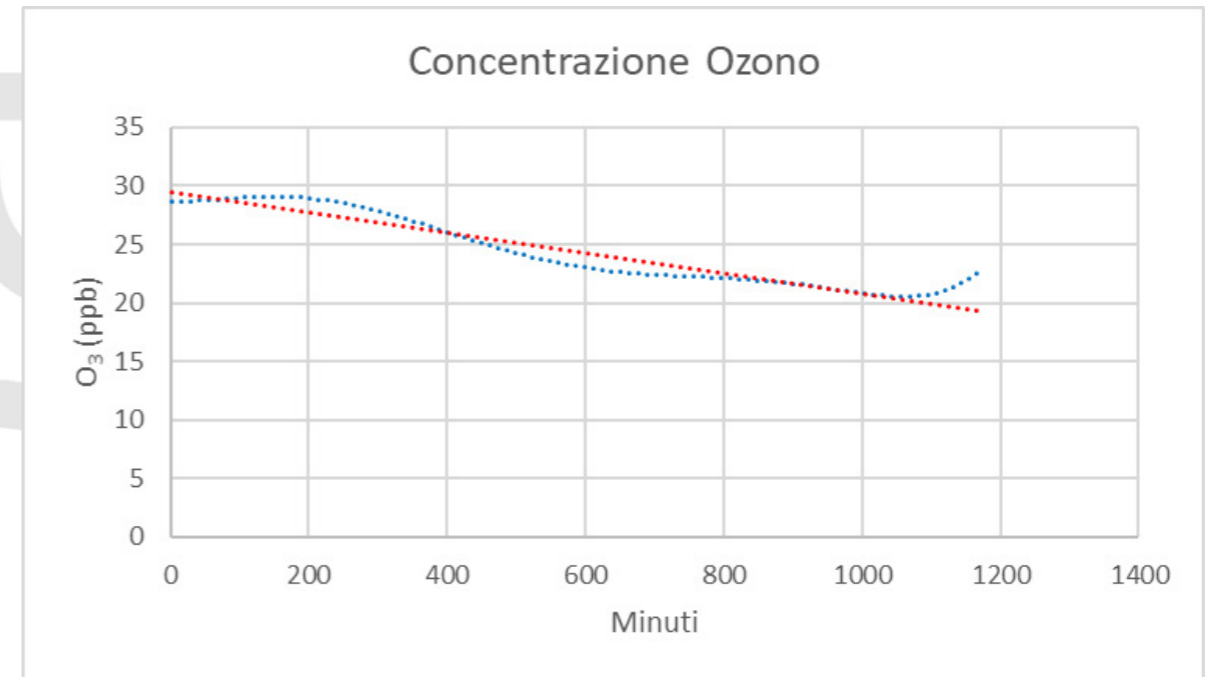


Immagine: Ozone Concentration

O<sub>3</sub> (ppb)

Minutes

*Test environment Ozone concentration during Test B (red line = average)*

Photo evidence

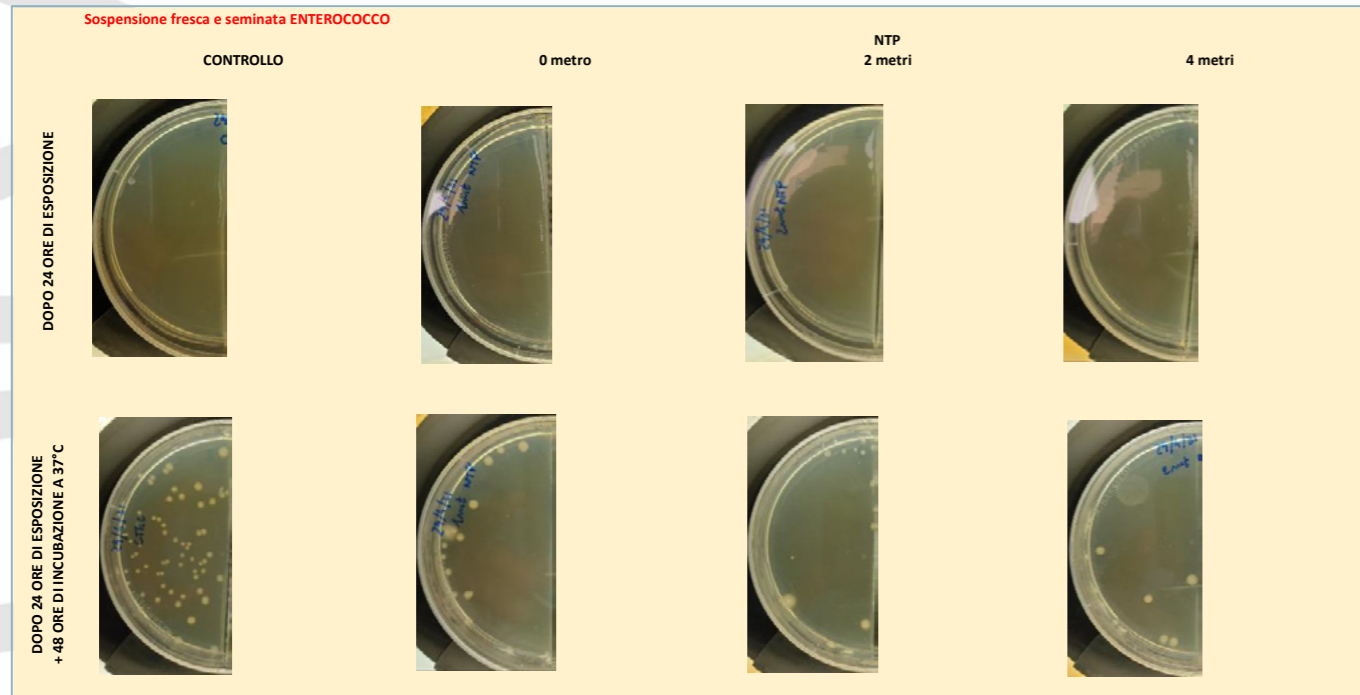


Immagine: Suspension seeded with E. Coli  
 Control – 0 meter – NTP 2 meters – 4 meters  
 After 24-hours exposition  
 After 24-hours exposition + 48 hours of incubation at 37° C

Antimicrobial effects: detail of the sectors containing fecal Enterococcus

Top row: the appearance of the culture plates after 24-hour exposure to NTP (comparison with the control plate, not exposed) as the distance from the device varies

Bottom row: same plates but after 48 hours of incubation at 37° C

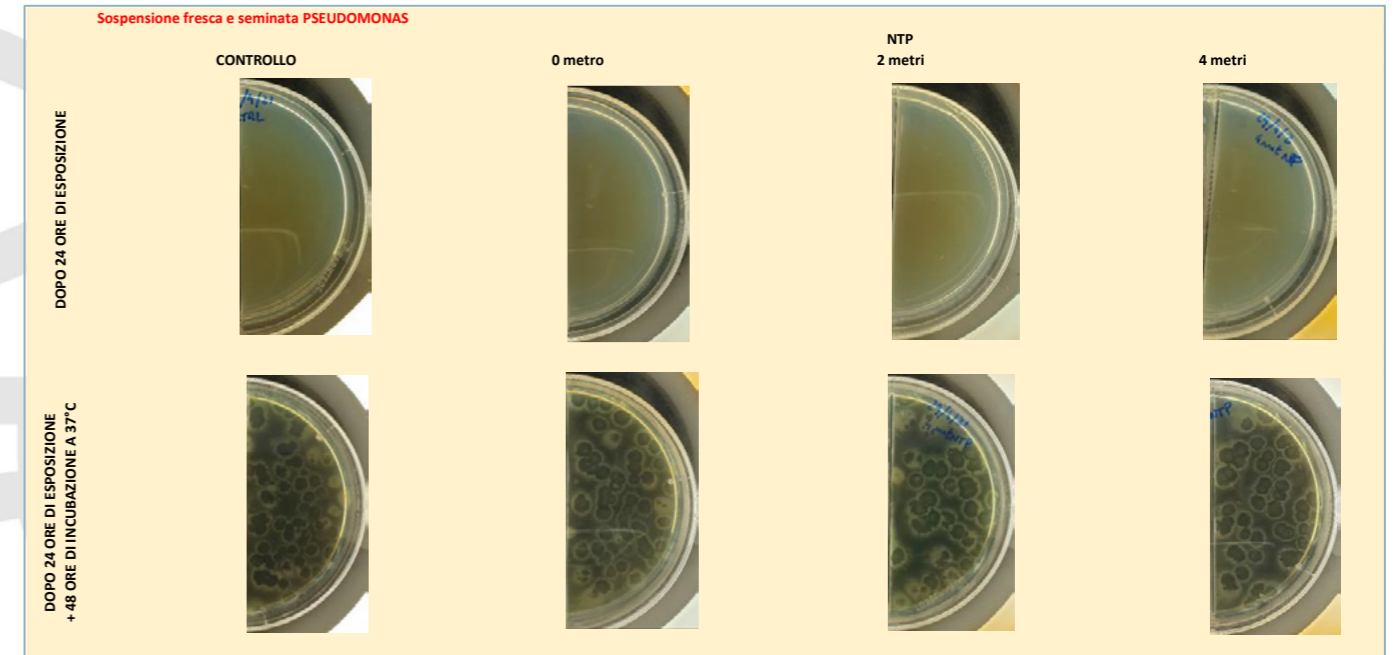


Immagine: Suspension seeded with PSEUDOMONAS  
 Control – 0 meter – NTP 2 meters – 4 meters  
 After 24-hours exposition  
 After 24-hours exposition + 48 hours of incubation at 37° C

Antimicrobial effects: detail of the sectors containing Pseudomonas aeruginosa  
 Upper row: the appearance of the culture plates after 24-hour exposure to NTP (comparison with the control plate, not exposed) as the distance from the device varies  
 Bottom row: same plates but after 48 hours of incubation at 37° C

Results

Also, in this case it is possible to observe an important inhibitory effect against gram-positive (fecal Enterococcus) unlike what happens for gram-negative (Pseudomonas aeruginosa).

Again, there is also a total absence of growth in the plates after 24 hours of exposure, both in the gram-positive and in the gram-negative sectors, which instead disappears after incubation at 37° C, confirming the bacteriostatic effect of the NTP.

Following are the values of the microbial count of the colonies grown in the plate:

Microbial concentration in each sector of the plates used.

			plate 1	plate 2	average	St. Dev.
Fecal Enterococcus	CFU/sector	Ctrl	66	61	<b>63,5</b>	4
		NTP 1 mt	11	14	<b>13</b>	2
		NTP 2 mt	5	8	<b>7</b>	2
		NTP 4 mt	4	10	<b>7</b>	4
	Log CFU/sector	Ctrl	1,82	1,79	<b>1,80</b>	0,02
		NTP 1 mt	1,04	1,15	<b>1,09</b>	0,07
		NTP 2 mt	0,70	0,90	<b>0,80</b>	0,14
		NTP 4 mt	0,60	1,00	<b>0,80</b>	0,28

			plate 1	plate 2	average	St. Dev.
Pseudomonas aureog.	CFU/sector	Ctrl	65	54	<b>59,5</b>	8
		NTP 1 mt	56	44	<b>50</b>	8
		NTP 2 mt	38	53	<b>46</b>	11
		NTP 4 mt	45	43	<b>44</b>	1
	Log CFU/sector	Ctrl	1,81	1,73	<b>1,77</b>	0,06
		NTP 1 mt	1,75	1,64	<b>1,70</b>	0,07
		NTP 2 mt	1,58	1,72	<b>1,65</b>	0,10
		NTP 4 mt	1,65	1,63	<b>1,64</b>	0,01

Summary conclusions on the results of the test

The graphic transposition of the data highlights better the results obtained:

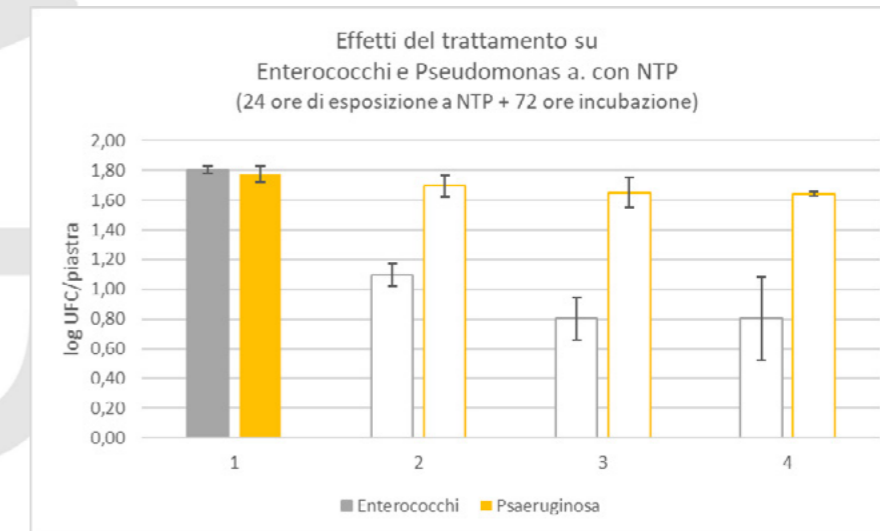


Immagine: log CFU/plate

Effects of the treatment on Enterococcus and Pseudomonas a. with NTP (24 hours of NTP exposure + 72 hours of incubation)

Comparison of the effects of NTP treatment, values expressed as the average of two plates

On the other hand, by expressing the data obtained in terms of percentage reduction in growth compared to control plates, it can be seen that this was once again highlighted for gram-positive bacteria (Enterococcus), extremely limited for gram-negative bacteria, represented in this case by Pseudomonas.

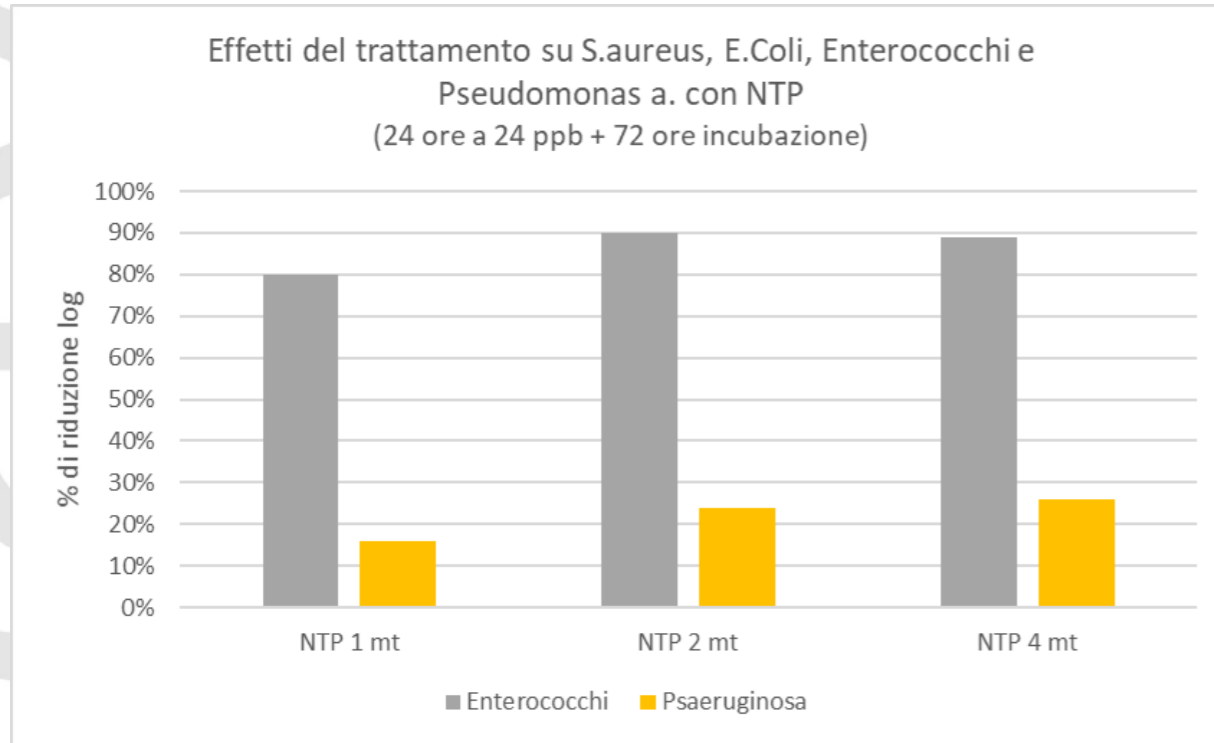


Immagine: % of log reduction  
 Effects of the treatment on S.aureus, E.Coli, Enterococcus and Pseudomonas a. with NTP  
 (24 hours to 24 ppb + 72 hours of incubation)  
 Enterococcus - Psaeruginosa

*Comparison of the percentage reductions in microbial growth between the two tested microorganisms*

PROVA C

Summary of the test

Test code	S20/005800004
Date	11 May 2021
Description of the test	Exposure of plates with Staphylococcus aureus, fecal Enterococcus, Escherichia coli and Pseudomonas aeruginosa in small cases (theca), keeping the internal humidity at about 50%
Objective of the test	Evaluating the antimicrobial effect of NTP under controlled humidity conditions
Jonix device used	Modified JONIX Cube
Test environment	Plastic cases with dimensions of 100 cm x 50 cm x 50 cm for a volume of 0.250 m <sup>3</sup>
Summary of the results	Reduction of the microbial load up to 3% for Ecoli, 20% Staphilococcus aureus, 30% Enterococcus.  Not detected for Pseudomonas

Description of the test

In this test, and in the subsequent one, an attempt was made to replicate what was observed in a larger environment, within a small confined environment in which it is easier to control the environmental conditions.

For this purpose, a special case (50 cm x 50 cm x 100 cm) was used in which to insert an NTP generator (CUBE) powered with a voltage regulated specifically to keep the exposure as low as possible under 50 ppb, precisely to simulate the functioning of a Jonix device in real conditions. Preliminary tests made it possible to establish that the best power supply conditions for this purpose were 850 volts at 50 Hz.

The exposure test was conducted using both Gram-positive (Staphylococcus aureus and fecal Enterococcus) and Gram-negative (Escherichia coli and Pseudomonas aeruginosa) bacteria.

As for the other tests, the bacteria were seeded, in duplicate, on double sector petri dishes filled with PCA agar (non-selective medium) at a density of about 200 CFU/sector. Subsequently, the plates were exposed, uncovered, to the NTP inside the case in which an NTP generator (CUBE) was placed, kept constantly on for the entire time of the test. The control plates were kept inside the laboratory, closed with their lid, thus avoiding any possible exposure to NTP.

After exposure, the plates were photographed and then kept in an incubator at 37° C for 24 + 24 hours.

**Ozone concentration in the test environment**

The Ozone produced was measured with the HORIBA with data acquisition every three minutes.

The Ozone values that were kept inside the case were quite variable with a continuous increasing trend and, on average, slightly higher than expected. The average concentration in the entire test was 64 ppb.

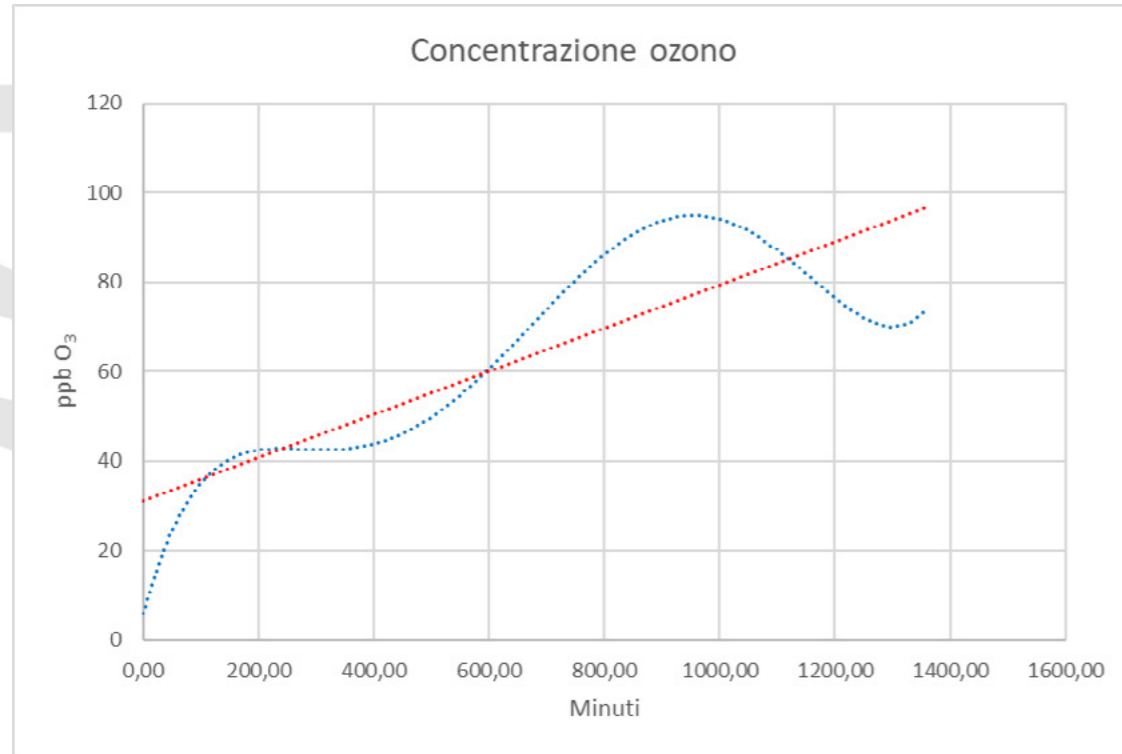
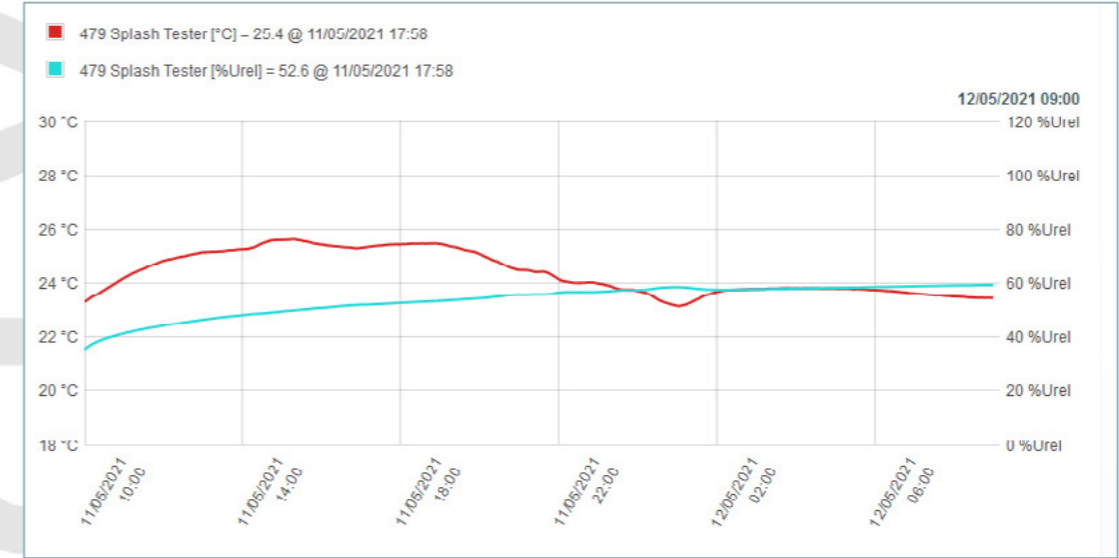


Immagine: Ozone concentration  
Ppb O<sub>3</sub>  
Minutes

Ozone concentration trend (red line = average)

An average humidity of about 54% was measured inside the case.



Temperature trend (red line) and humidity trend (blue line) inside the case

**Photo evidence (fotografiche)**

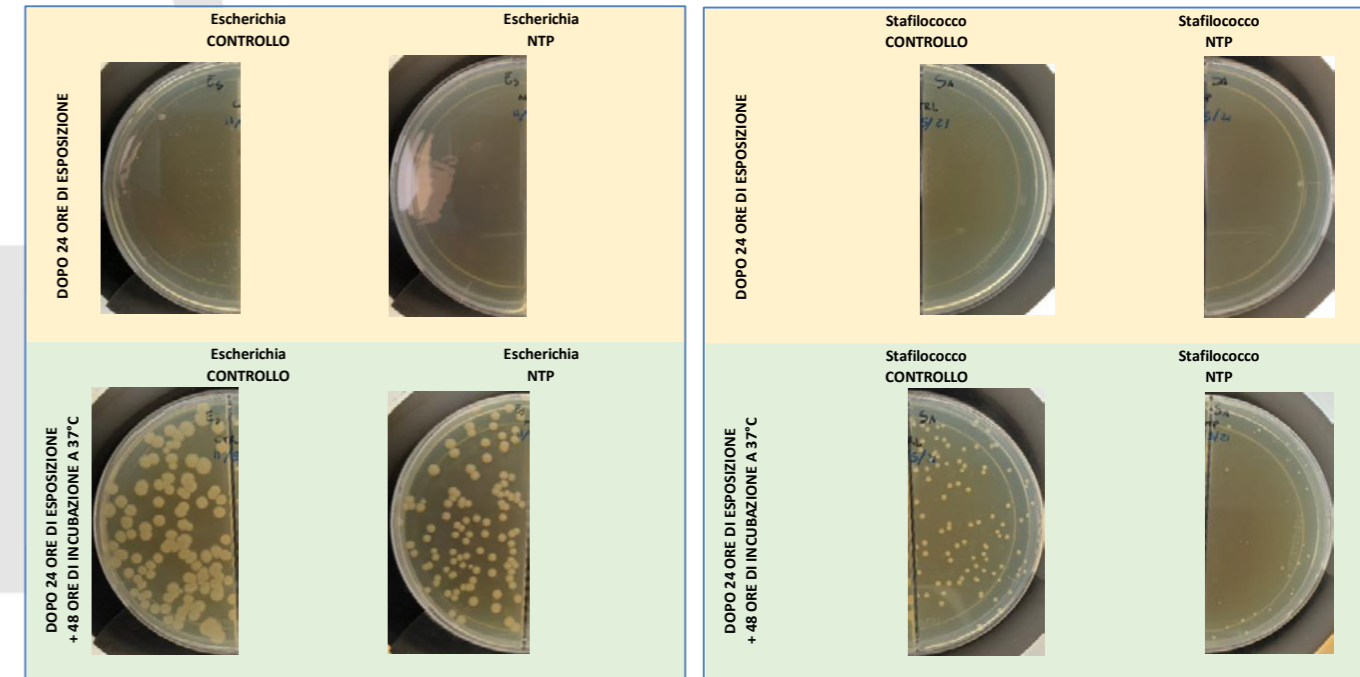


Immagine sx: Escherichia CONTROL – Escherichia NTP  
After 24-hour exposure

Escherichia CONTROL – Escherichia NTP

After 24-hour exposure + 48 hours of incubation at 37°C

Immagine dx: Staphylococcus CONTROL – Staphylococcus NTP  
After 24-hour exposure

Staphylococcus CONTROL – Staphylococcus NTP  
After 24-hour exposure + 48 hours of incubation at 37°C

Top row: the appearance of the culture plates after 24-hour exposure to NTP (comparison with the control plates, not exposed)

Bottom row: same plates but after 48 hours of incubation at 37°C

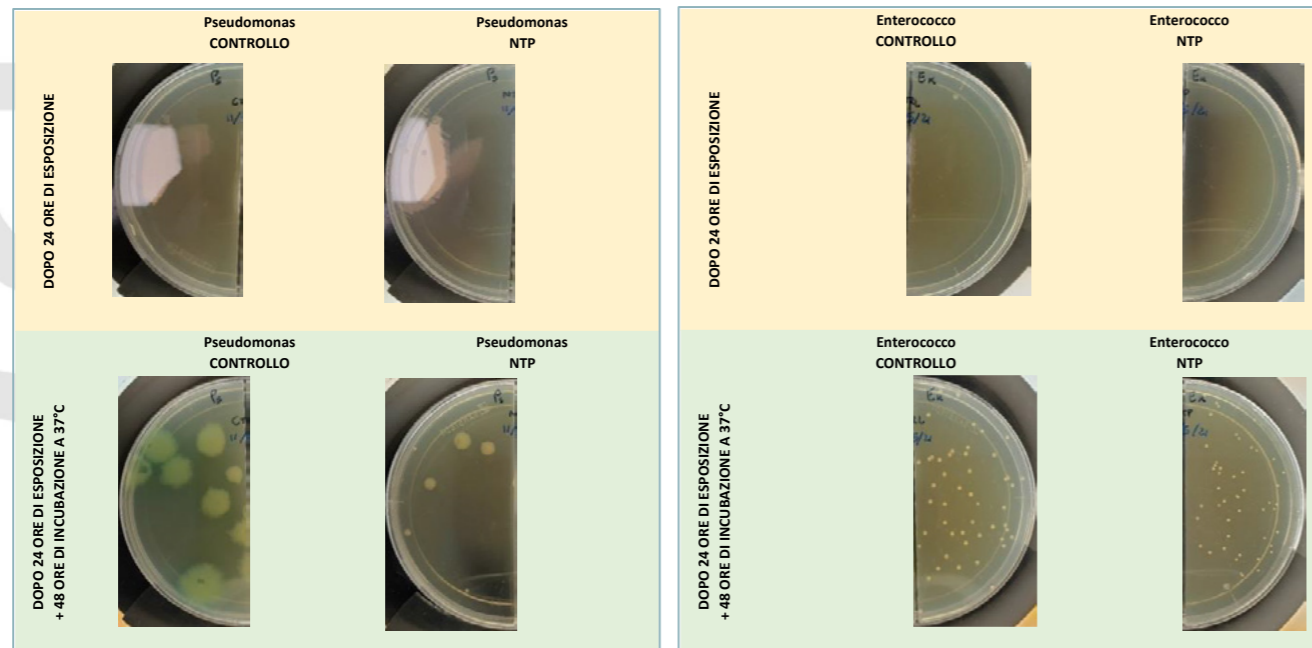


Immagine sx: Pseudomonas CONTROL – Pseudomonas NTP  
After 24-hour exposure

Pseudomonas CONTROL – Pseudomonas NTP  
After 24-hour exposure + 48 hours of incubation at 37°C

Immagine dx: Enterococcus CONTROL – Enterococcus NTP  
After 24-hour exposure

Enterococcus CONTROL – Enterococcus NTP  
After 24-hour exposure + 48 hours of incubation at 37°C

Top row: the appearance of the culture plates after 24-hour exposure to NTP (comparison with the control plates, not exposed)

Bottom row: same plates but after 48 hours of incubation at 37°C

## Results

Once again, the “differential” effect towards Gram-positive versus a modest efficacy towards Gram-negative is confirmed.

Laboratori ARCHA S.r.l. unipersonale

Via di Tegulaia 10/a - 56121 - PISA - ph. +39 050 985165 - fax +39 050 985233 - www.archa.it - archainf@archa.it  
C.F., P.IVA, Iscr. Reg. Impr. di Pisa n. 01115340505 - Rep. Econ. Amm. di Pisa n°101169 - Capitale Sociale 101.400,00 i.v.

Again, the bacteriostatic “phenomenon” is very well appreciated, that is, the delay in microbial growth of crops exposed to NTP compared to the control ones.

Following are the values of the microbial count of the colonies grown in the plate:

Microbial concentration in each sector of the plates used.

Ecoli	CFU/sector	Ctrl	plate 1	plate 2	average	St. Dev.
		NTP	113	n.e.	n.a	n.a.
	Log CFU / sector	Ctrl	2,05	n.e.	n.a	n.a.
		NTP	2,03	n.e.	n.a	n.a.

Saureo	CFU / sector	Ctrl	plate 1	plate 2	average	St. Dev.
		NTP	97	n.e.	n.a	n.a.
	Log CFU / sector	Ctrl	1,99	n.e.	n.a	n.a.
		NTP	1,58	n.e.	n.a	n.a.

Fecal E	CFU / sector	Ctrl	plate 1	plate 2	average	St. Dev.
		NTP	10	n.e.	n.a	n.a.
	Log CFU / sector	Ctrl	1	n.e.	n.a	n.a.
		NTP	0,7	n.e.	n.a	n.a.

Paureog	CFU / sector	Ctrl	plate 1	plate 2	average	St. Dev.
		NTP	48	n.e.	n.a	n.a.
	Log CFU /sector	Ctrl	1,68	n.e.	n.a	n.a.
		NTP	1,71	n.e.	n.a	n.a.

## Summary conclusions on the results of the test

The graphic transposition of the data highlights better the results obtained:

Laboratori ARCHA S.r.l. unipersonale

Via di Tegulaia 10/a - 56121 - PISA - ph. +39 050 985165 - fax +39 050 985233 - www.archa.it - archainf@archa.it  
C.F., P.IVA, Iscr. Reg. Impr. di Pisa n. 01115340505 - Rep. Econ. Amm. di Pisa n°101169 - Capitale Sociale 101.400,00 i.v.

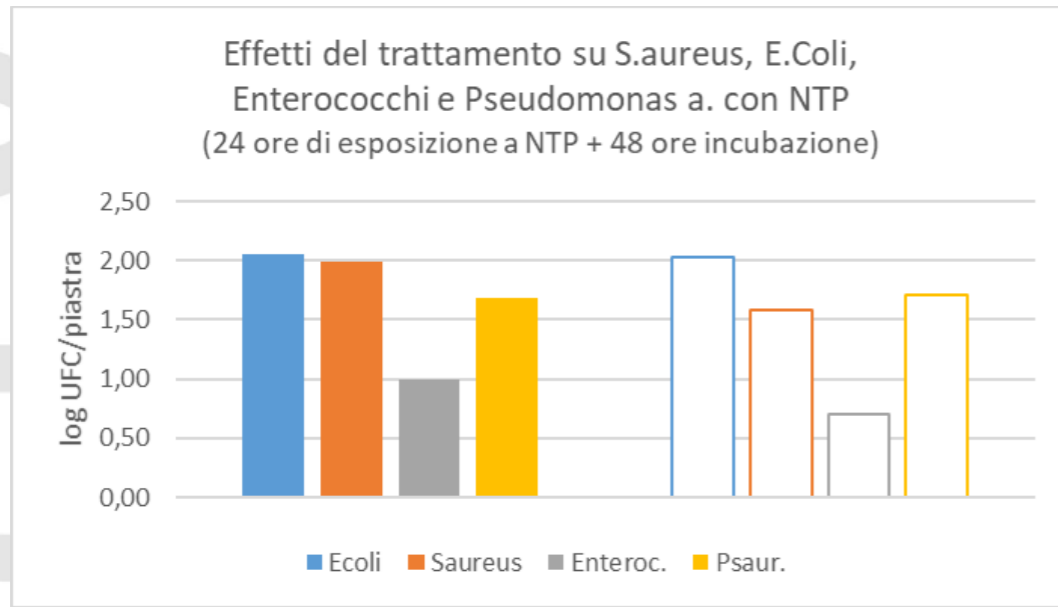


Immagine: log CFU/plate  
 Effects of the treatment on S.aureus, E.Coli, Enterococcus and Pseudomonas a. with NTP (24 hours of NTP exposition + 48 hours of incubation)

Comparison of the effects of NTP treatment

If expressed in terms of percentage reduction of growth compared to the controls, it can be noted again that this was practically evident only for Gram-positive bacteria (Staphylococcus and Enterococcus).

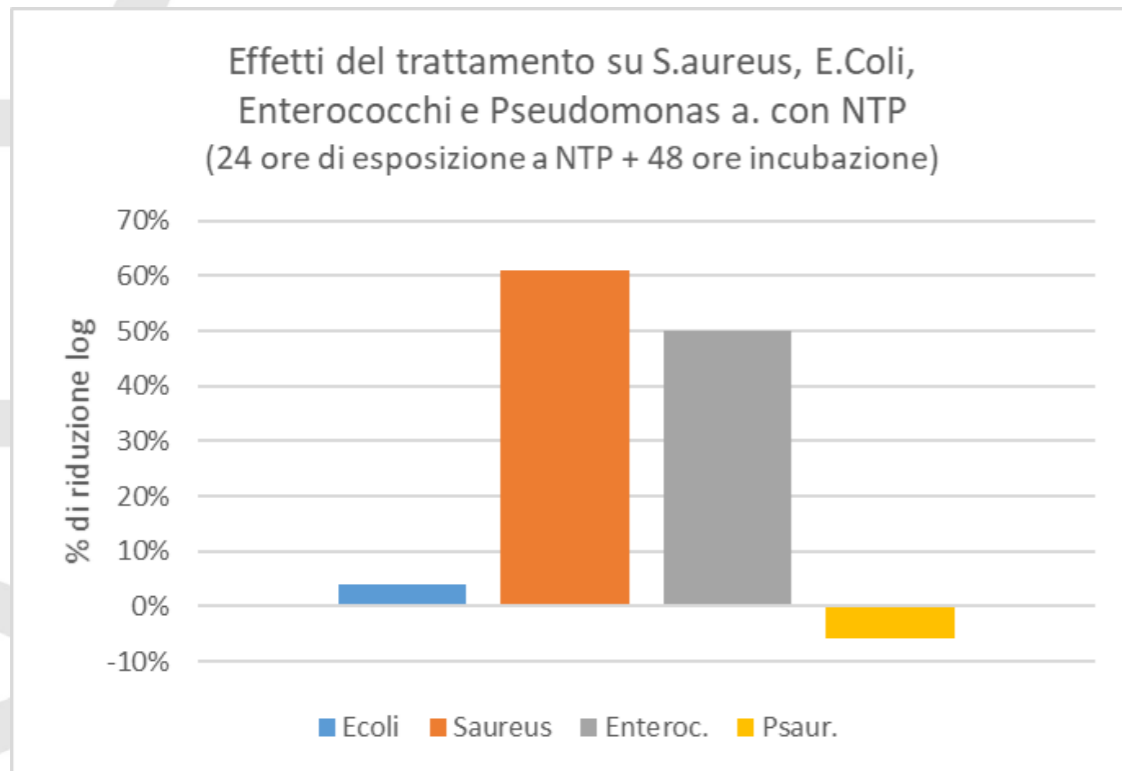


Immagine: % of log reduction  
 Effects of the treatment on S.aureus, E.Coli, Enterococcus and Pseudomonas a. with NTP (24 hours of NTP exposition + 48 hours of incubation)

Comparison of the percentage reductions in microbial growth between the two tested microorganisms

TEST D

Summary of the test

Test code	S20/005800009
Date	27 May 2021
Description of the test	Exposure of plates with Staphylococcus aureus, fecal Enterococcus, Escherichia coli and Pseudomonas aeruginosa in small cases (theca), keeping the internal humidity at about 80%
Objective of the test	Evaluating the antimicrobial effect of NTP under controlled humidity conditions
Jonix device used	Modified JONIX Cube
Test environment	Plastic box with dimensions of 100 cm x 50 cm x 50 cm for a volume of 0.250 m <sup>3</sup>
Summary of the results	Reduction of the microbial load up to 51% for the Enterococcus, and 59% for the Staphylococcus aureus

Description of the test

As for the previous test, both Gram-positive (Staphylococcus aureus and fecal Enterococcus) and Gram-negative (Escherichia coli and Pseudomonas aeruginosa) bacteria were used, seeded, in duplicate, on double-sector petri dishes filled with PCA agar (non-selective medium) at a density of about 200 CFU/sector. Subsequently, the plates were exposed, uncovered, to the NTP inside the case in which an NTP generator (CUBE) was placed, kept constantly on for the entire time of the test. The control plates were kept inside the laboratory, closed with their lid, thus avoiding any possible exposure to NTP.

Thanks to the use of a supersaturated NaCl solution, an environment with relative humidity values higher than 80% was created inside the case.

Ozone concentration in the test environment

In order to avoid instrumental damage, the Ozone measurements in the case did not take place continuously as in the other tests, but in a discontinuous and timely manner, interrupting it only during the night. In any case, the measured values made it possible to establish a “trend” substantially overlapping the previous ones. The average value found was 47 ppb, lower than that of the previous test.

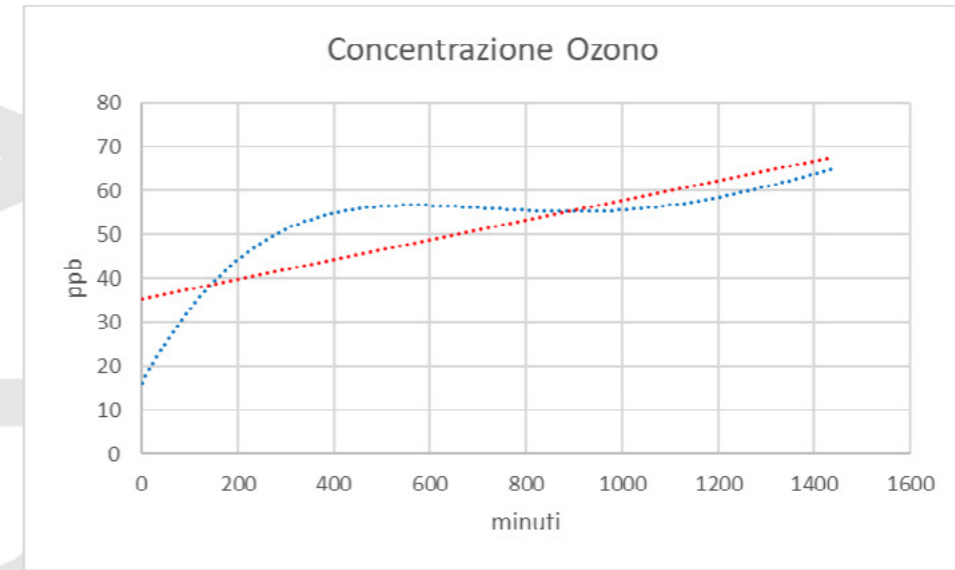


Immagine: Ozone Concentration

Ppb  
 minutes

Ozone concentration trend. Red line = average

Since the power supply conditions of the generator were identical (850 volts at 50 Hz), the lower quantity of Ozone detected could be due precisely to the presence of greater humidity in the air which, carrying water, would have worked as a “sequestering” agent of the Ozone diffused in a gaseous form giving rise to different chemical species (e.g., H<sub>2</sub>O<sub>2</sub>) which would also explain the greater effectiveness of the treatment.

The temperature in the case and that of the control environment was found to be of little influence with only one degree of difference (average T° NTP: 24.7; average T° CTRL: 23.7).

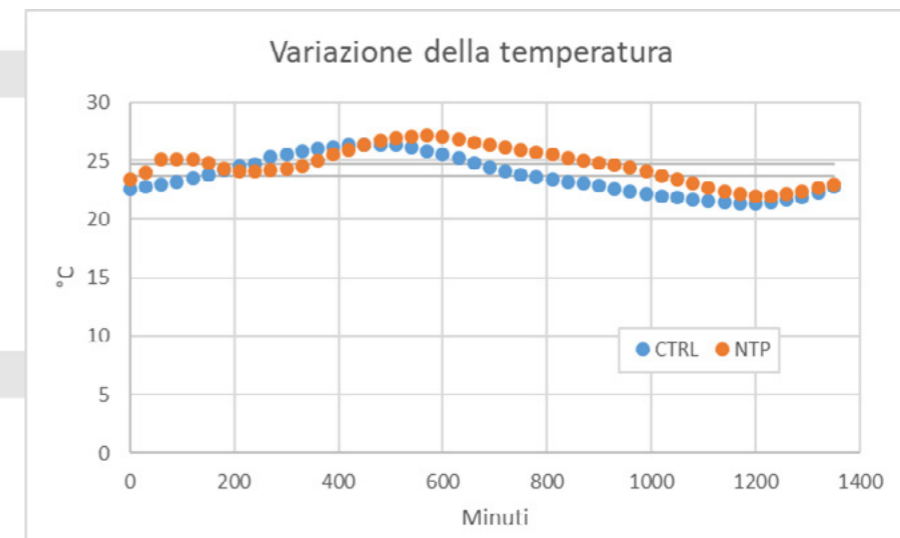


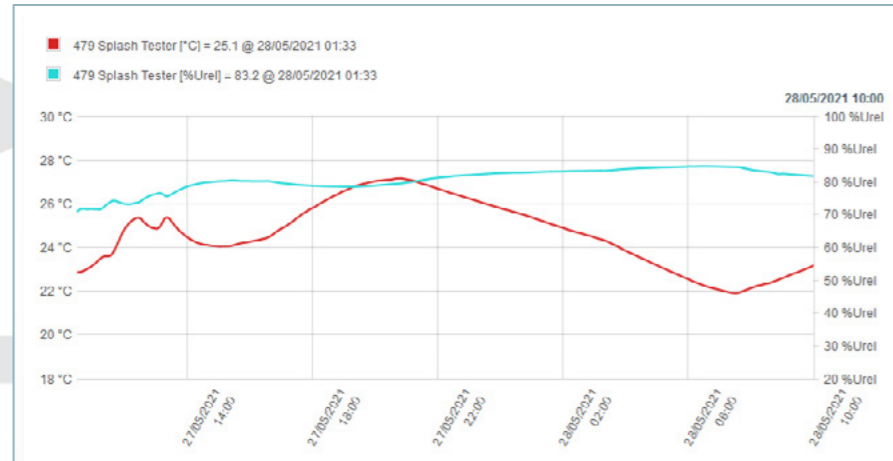
Immagine: temperature variation

Minutes

Comparison between the two exposure temperatures over 24 hours. CTRL: plates stored in the laminar flow hood; NTP: plates stored in a case.



Furthermore, an average humidity of about 80% was measured inside the case.



Temperature trend (red line) and humidity trend (blue line) inside the case

### Photo evidence

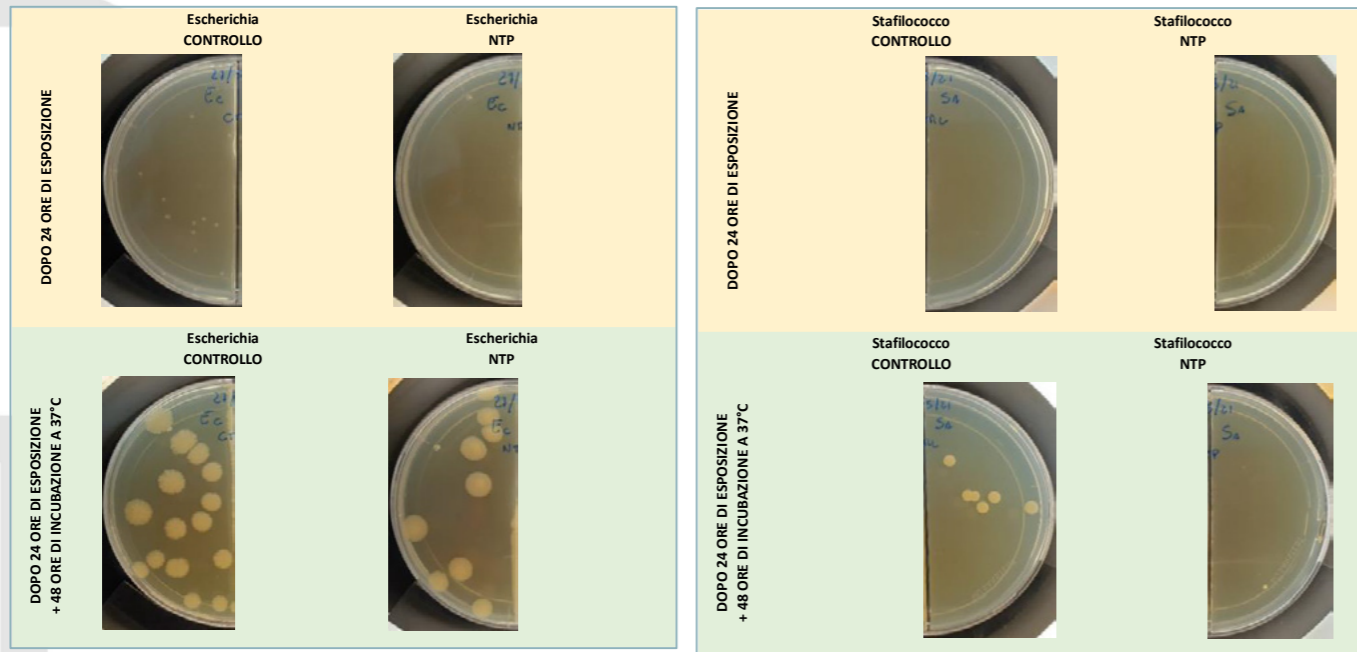


Immagine sx: Escherichia CONTROL – Escherichia NTP

After 24-hour exposure

Escherichia CONTROL – Escherichia NTP

After 24-hour exposure + 48 hours of incubation at 37°C

Immagine dx: Staphylococcus CONTROL – Staphylococcus NTP

After 24-hour exposure

Staphylococcus CONTROL – Staphylococcus NTP

After 24-hour exposure + 48 hours of incubation at 37°C

**Laboratori ARCHA S.r.l. unipersonale**

Via di Tegulaia 10/a - 56121 - PISA - ph. +39 050 985165 - fax +39 050 985233 - www.archa.it - archainf@archa.it  
C.F., P.IVA, Iscr. Reg. Impr. di Pisa n. 01115340505 - Rep. Econ. Amm. di Pisa n°101169 - Capitale Sociale 101.400,00 i.v.

Top row: the appearance of the culture plates after 24-hour exposure to NTP (comparison with the control plates, not exposed)

Bottom row: same plates but after 48 hours of incubation at 37°C

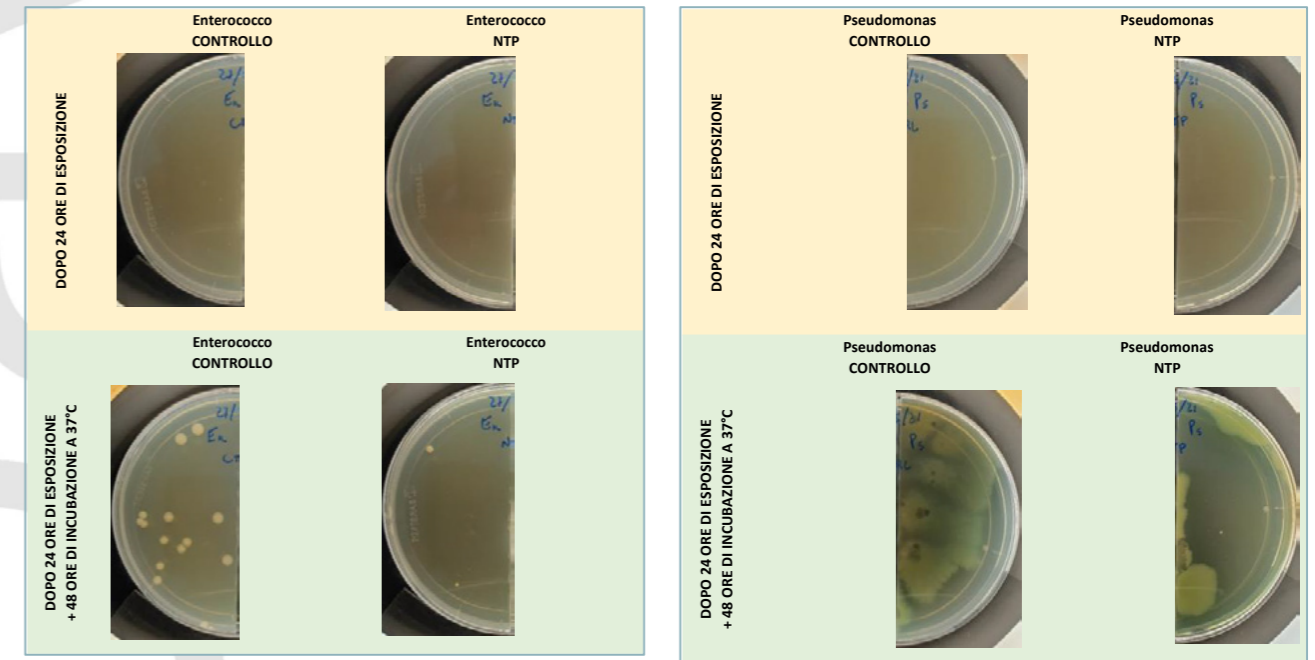


Immagine sx: Enterococcus CONTROL – Enterococcus NTP

After 24-hour exposure

Enterococcus CONTROL – Enterococcus NTP

After 24-hour exposure + 48 hours of incubation at 37°C

Immagine dx: Pseudomonas CONTROL – Pseudomonas NTP

After 24-hour exposure

Pseudomonas CONTROL – Pseudomonas NTP

After 24-hour exposure + 48 hours of incubation at 37°C

Top row: the appearance of the culture plates after 24-hour exposure to NTP (comparison with the control plates, not exposed)

Bottom row: same plates but after 48 hours of incubation at 37°C

### Results

In this case, the test highlighted an inhibitory effect (biocide) also against Gram-negative bacteria (Escherichia coli and Pseudomonas aeruginosa), a phenomenon not observed in the lower humidity test.

Following are the values of the microbial count of the colonies grown in the plate:

**Laboratori ARCHA S.r.l. unipersonale**

Via di Tegulaia 10/a - 56121 - PISA - ph. +39 050 985165 - fax +39 050 985233 - www.archa.it - archainf@archa.it  
C.F., P.IVA, Iscr. Reg. Impr. di Pisa n. 01115340505 - Rep. Econ. Amm. di Pisa n°101169 - Capitale Sociale 101.400,00 i.v.

Microbial concentration in each sector of the plates used.

Ecoli	CFU/ sector		plate 1	plate 2	average	St. Dev.
		Ctrl	15	16	15,5	1
	NTP	13	9	11	3	
	Log CFU/ sector					
Ctrl	-	-	1,19	0,02		
NTP	-	-	1,04	0,11		

Saureo	CFU/ sector		plate 1	plate 2	average	St. Dev.
		Ctrl	7	6	6,5	1
	NTP	3	1	2	1	
	Log CFU/ sector					
Ctrl	-	-	0,81	0,05		
NTP	-	-	0,30	0,34		

Fecale	CFU/ sector		plate 1	plate 2	average	St. Dev.
		Ctrl	18	15	16,5	2
	NTP	2	0	1	1	
	Log CFU/ sector					
Ctrl	-	-	1,22	0,06		
NTP	-	-	0,02	0,92		

Paureog	CFU/ sector		plate 1	plate 2	average	St. Dev.
		Ctrl	4	15	9,5	8
	NTP	4	2	3	1	
	Log CFU/ sector					
Ctrl	-	-	0,98	0,41		
NTP	-	-	0,48	0,21		

## Summary conclusions on the results of the test

The graphic transposition of the data highlights better the results obtained:

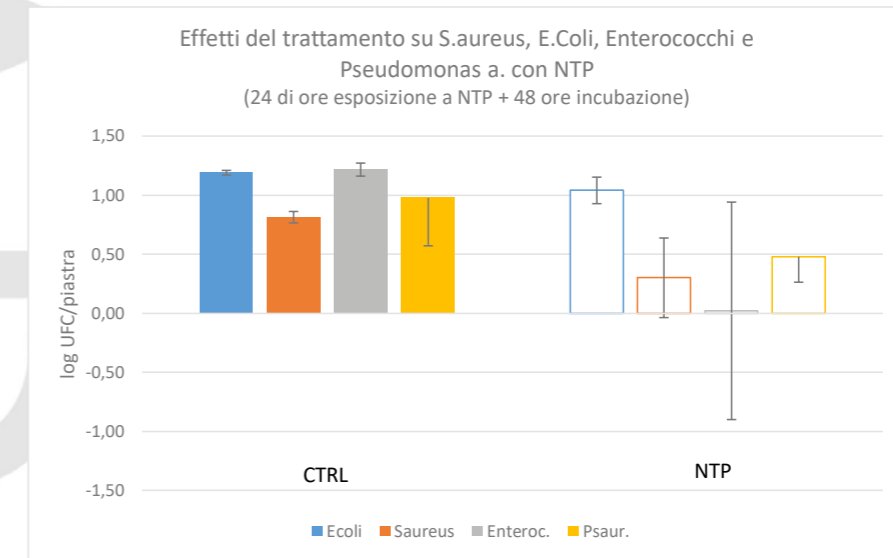
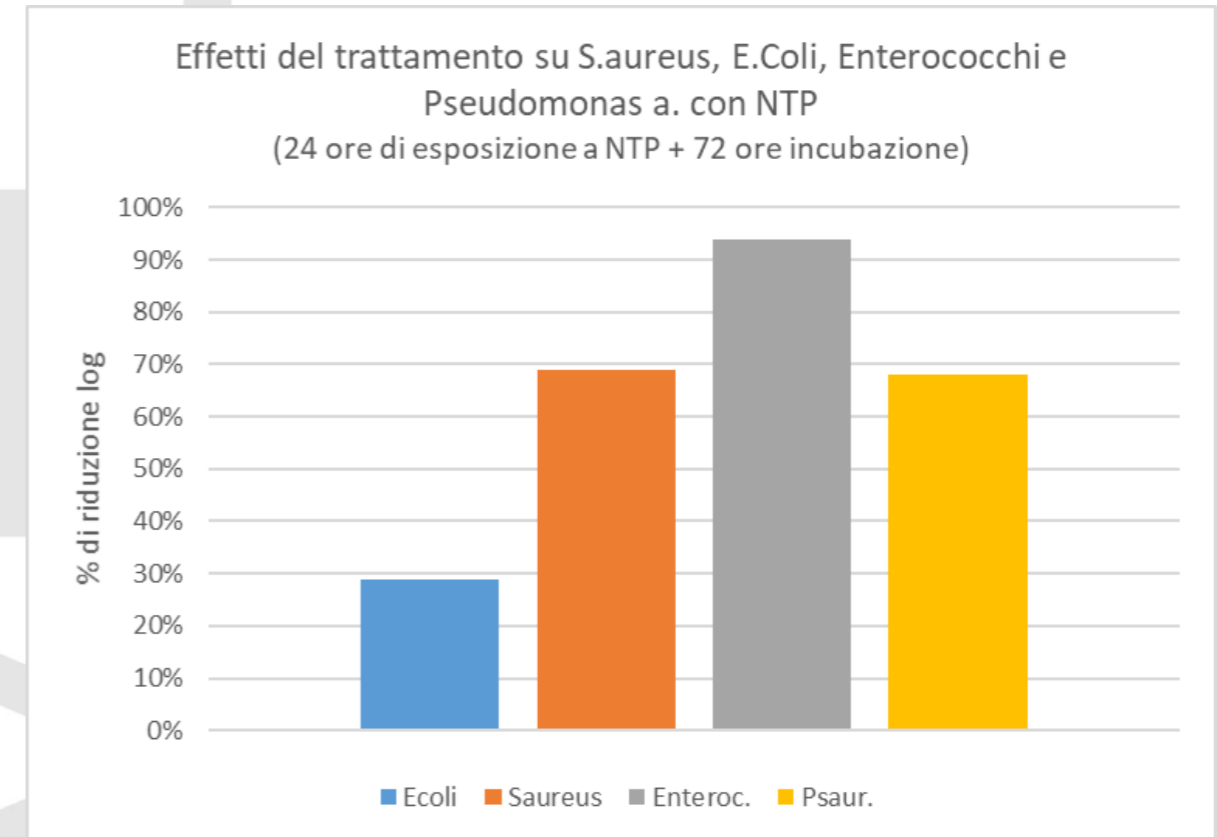


Immagine: log CFU/plate

Effects of the treatment on S.aureus, E.Coli, Enterococcus and Pseudomonas a. with NTP (24 hours of NTP exposition + 48 hours of incubation)

## Comparison of the effects of NTP treatment



Laboratori ARCHA S.r.l. unipersonale

Via di Tegulaia 10/a - 56121 - PISA - ph. +39 050 985165 - fax +39 050 985233 - www.archa.it - archainf@archa.it  
C.F., P.IVA, Iscr. Reg. Impr. di Pisa n. 01115340505 - Rep. Econ. Amm. di Pisa n°101169 - Capitale Sociale 101.400,00 i.v.

Laboratori ARCHA S.r.l. unipersonale

Via di Tegulaia 10/a - 56121 - PISA - ph. +39 050 985165 - fax +39 050 985233 - www.archa.it - archainf@archa.it  
C.F., P.IVA, Iscr. Reg. Impr. di Pisa n. 01115340505 - Rep. Econ. Amm. di Pisa n°101169 - Capitale Sociale 101.400,00 i.v.

Immagine: % of log reduction  
Effects of the treatment on S.aureus, E.Coli, Enterococcus and Pseudomonas a. with NTP  
(24 hours of NTP exposition + 72 hours of incubation)

Comparison of the percentage reductions in microbial growth between the two tested microorganisms

The comparison of the percentage reductions clearly highlights a new phenomenon.

Having exposed the microorganisms to NTP in an environment of high relative humidity considerably increased the biocidal capacity exerted by the treatment.

In fact, by comparing the results of test C conducted at a Relative Humidity of approximately 54% and those of test D conducted at a Relative Humidity of approximately 80%, it can be seen how the humidity influences the effectiveness of the NTP, as it was conceivable as the natural droplet acts as a vehicle for oxidizing species.

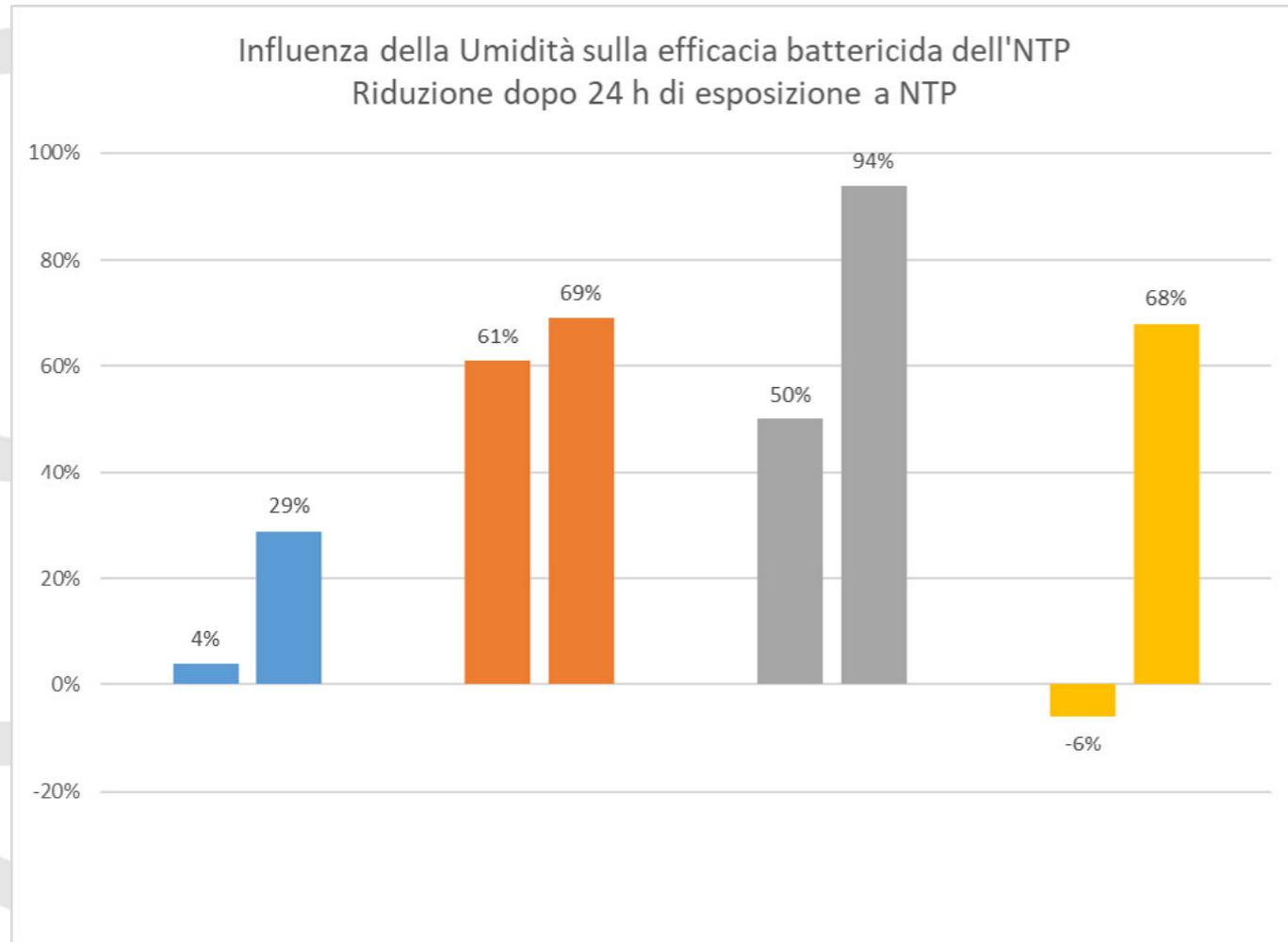


Immagine: influence of Humidity on the effectiveness of the NTP  
Reduction after 24 hours of NTP exposure

Laboratori ARCHA S.r.l. unipersonale

Via di Tegulaia 10/a - 56121 - PISA - ph. +39 050 985165 - fax +39 050 985233 - www.archa.it - archainf@archa.it  
C.F., P.IVA, Iscr. Reg. Impr. di Pisa n. 01115340505 - Rep. Econ. Amm. di Pisa n°101169 - Capitale Sociale 101.400,00 i.v.

Comparison between the percentages of bacterial reduction in different humidity conditions

TEST E

5.5.1 Summary of the test

Test code	S20/005800008
Date	24 May 2021
Description of the test	Exposure of plates with Staphylococcus aureus, fecal Enterococcus, Escherichia coli and Pseudomonas aeruginosa in a natural environment
Objective of the test	Evaluating the effect of external air, containing naturally occurring oxidizing species
Jonix device used	NONE
Test environment	Room facing outwards
Summary of the results	Reduction of the microbial load up to 51% for the Enterococcus, and 59% for Staphylococcus aureus

1.1.2 Ozone in the outside air

It is known that Ozone is also found in the atmosphere as a result of the interaction of solar radiation which, interacting with atmospheric oxygen, leads to the production of this gas.

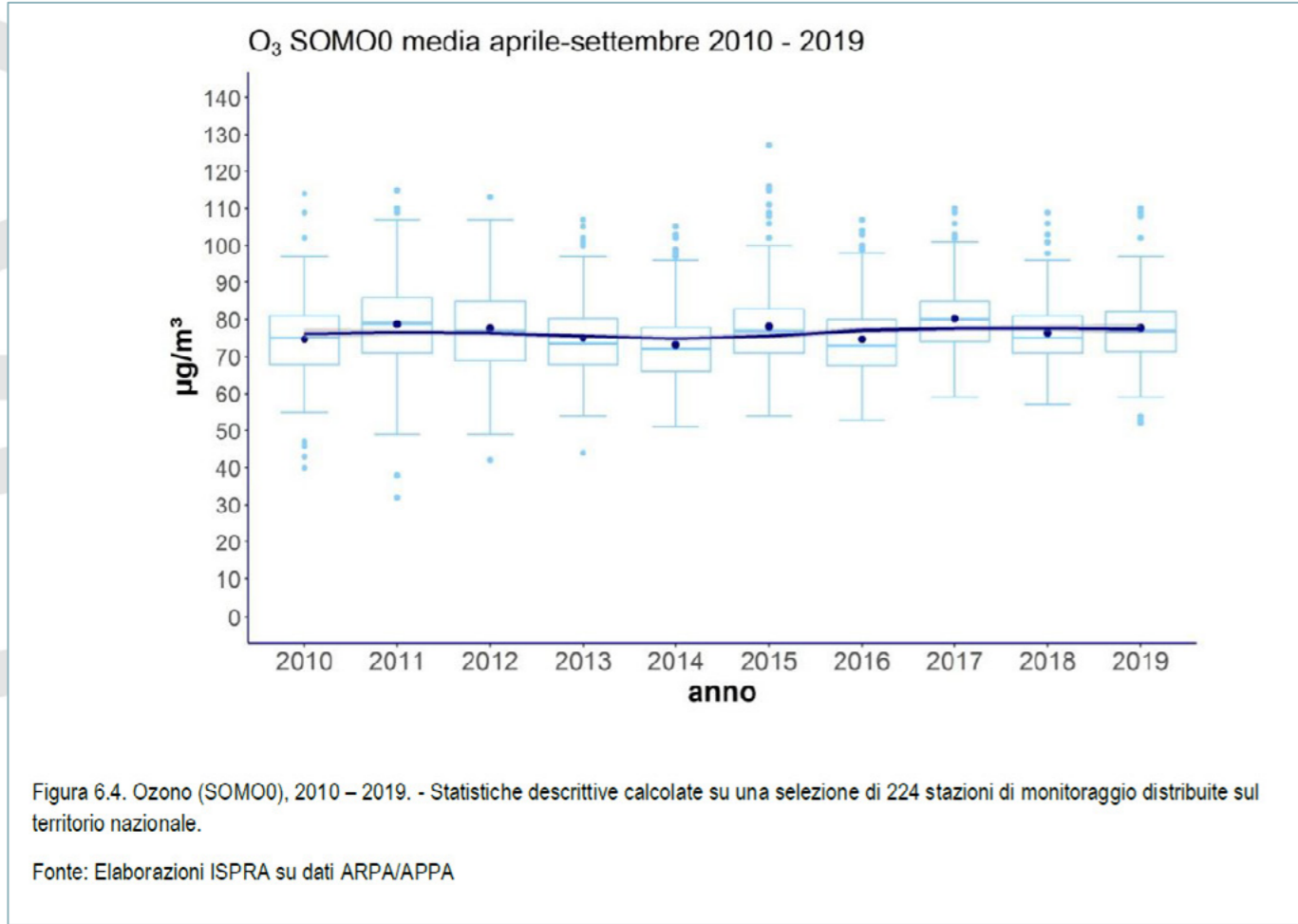
Typically, as it is easy to see from the environmental monitoring data detected by the control units of the various ARPAs scattered throughout the country, the concentration of Ozone increases significantly on days of good weather, when solar radiation is stronger.

As also indicated in the report of the National System for Environmental Protection "Air quality in Italy 2020 edition", in lowland areas or at sea level, O<sub>3</sub> concentrations follow the intensity profile of solar radiation quite well (thus tending to increase during maximum insolation and to decrease at night).

The same report also shows the average statistics of Ozone concentrations detected by 224 monitoring stations indicating an average of about 35 ppb (remember that µg/m<sup>3</sup> are double the ppb) with peaks that even exceed 50-60 ppb.

Laboratori ARCHA S.r.l. unipersonale

Via di Tegulaia 10/a - 56121 - PISA - ph. +39 050 985165 - fax +39 050 985233 - www.archa.it - archainf@archa.it  
C.F., P.IVA, Iscr. Reg. Impr. di Pisa n. 01115340505 - Rep. Econ. Amm. di Pisa n°101169 - Capitale Sociale 101.400,00 i.v.



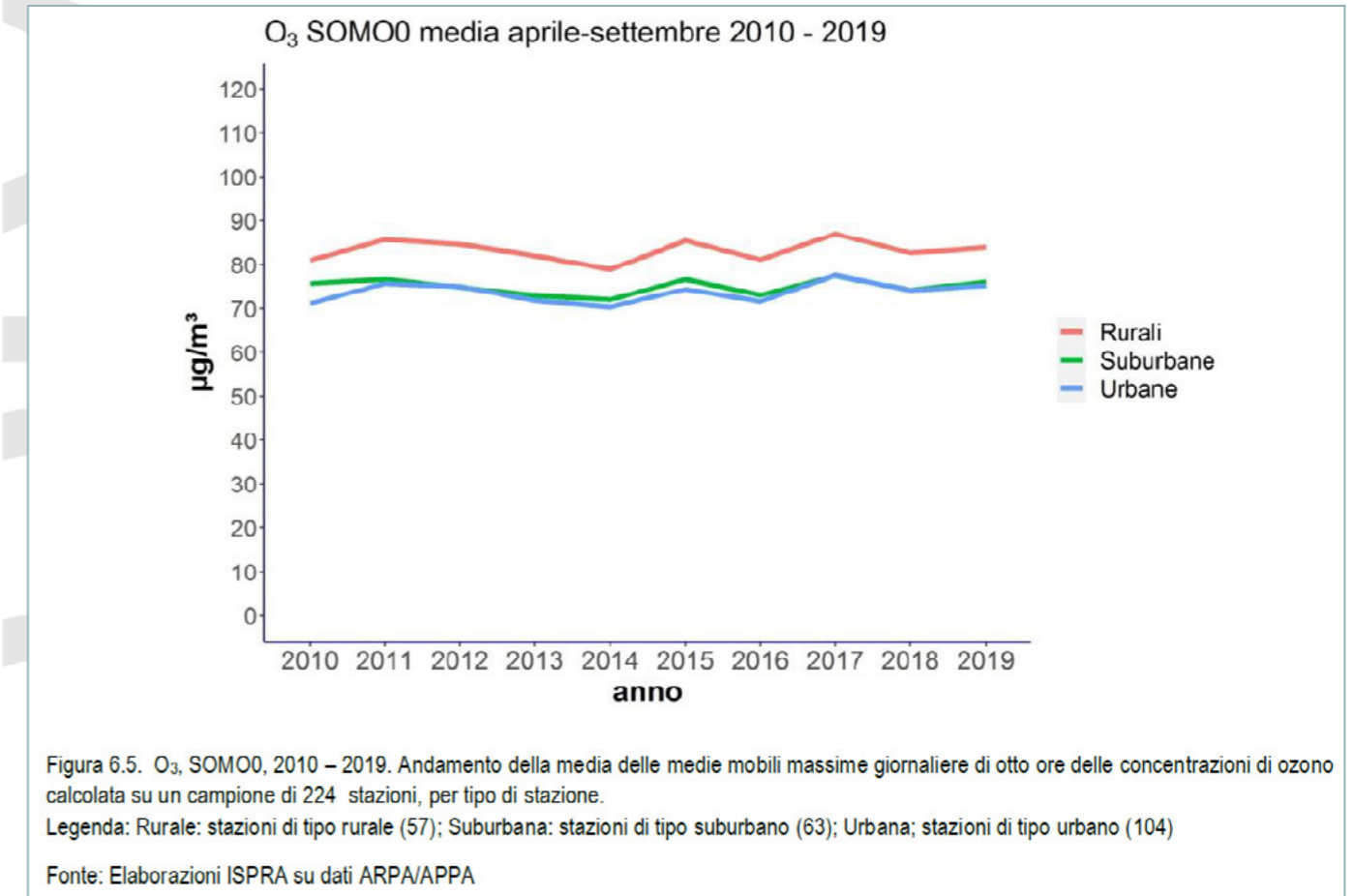
O<sub>3</sub> SOMO0 April-September average 2010-2019

Year

Figure 6.4. Ozone (SOMO0), 2010-2019. – Descriptive statistics calculated by 224 monitoring stations all over the national territory.

Source: ISPRA based on ARPA/APPA data

Also interesting is the graph that shows the average statistics in relation to the position of the stations from which it is noted that the highest concentrations, 40-45 ppb, occur in rural areas, therefore, places that we all consider to have “clean air”. In fact, the pollution of urban areas that “steals” the Ozone by making it react with the pollutants produced by vehicular traffic, heating, etc.



O<sub>3</sub> SOMO0 April-September average 2010-2019

Year

Rural

Suburban

Urban

Figure 6.5. Ozone (SOMO0), 2010-2019. –

Year

The trend of the average of the eight-hour daily maximum moving averages of ozone concentrations calculated on a sample of 224 stations, divided by type of station.

Legend: Rural: Rural stations (57); Suburban: suburban stations (63); Urban: urban stations (104).

Source: ISPRA, based on ARPA/APPA data

It should also be considered that where Ozone is present, other oxidizing species, free radicals, hydroxyls, etc. are presumably also present. They play a role in producing the O<sub>3</sub> molecule.

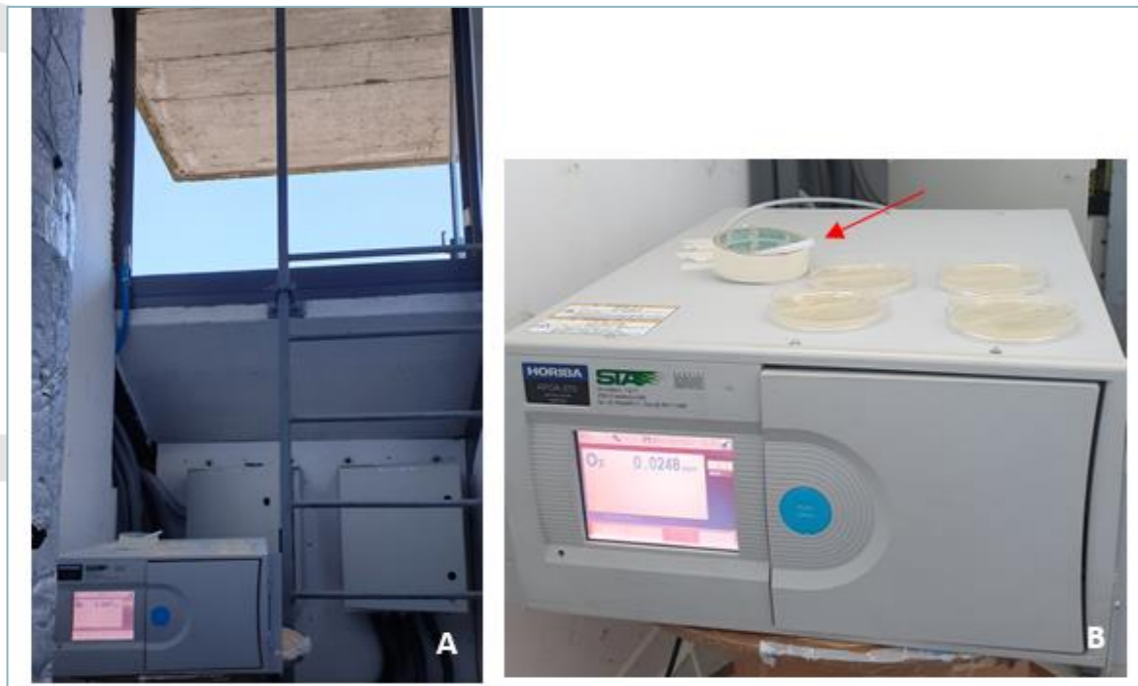
## Description of the test

This experimental test aimed to verify whether the effects of exposure of bacterial colonies on plates to concentrations of Ozone (and presumably of other natural oxidizing species) naturally present in the outside air were similar and comparable to those detected inside the case.

For this purpose, as for the previous tests, both Gram-positive (*Staphylococcus aureus* and fecal *Enterococcus*) and Gram-negative (*Escherichia coli* and *Pseudomonas aeruginosa*) bacteria were used, seeded, in duplicate, on double-sector petri dishes filled with PCA agar (non-selective medium) at a density of about 200 CFU/sector.

Exposure to atmospheric Ozone occurred by placing the plates in a room leaving the window completely open to allow atmospheric air to saturate the room. Exposure to outside air was thus possible, but without solar radiation or turbulence due to winds and breezes.

## Ozone concentration in the test environment

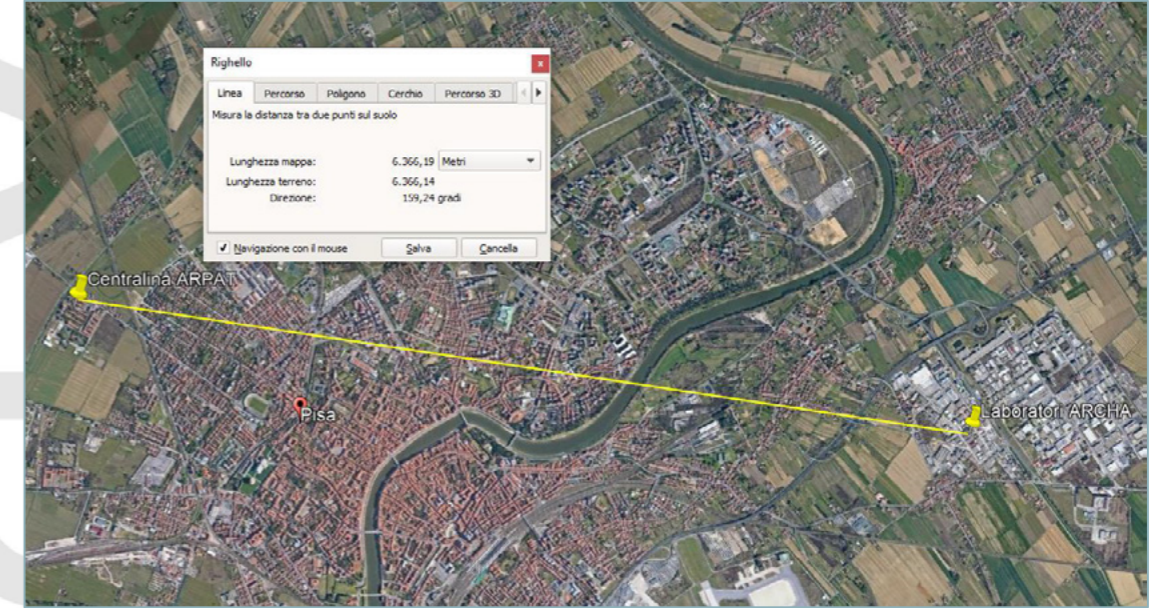


Test layout.

A) location of the Horiba and the plates with respect to the open window;

B) detail of the exposed plates with the Horiba air sampling tube (red arrow)

The Ozone value measured by HORIBA was compared with that recorded by the nearest ARPAT control unit located in the "I Passi" district of Pisa, about 6 km away from the test site.



Location of the ARPAT control unit with respect to the test site

Previous tests have in fact made it possible to establish that there is an excellent correspondence between the values recorded by the ARPAT control unit and those measured in the environment outside the test site with the HORIBA, despite the distance that separates the two measurement points.

Together with the atmospheric Ozone value, the ambient temperature and humidity were also measured.

In this case too, as in all other experiments, Ozone is to be considered the indicator of the "oxidizing species" because it is certainly the longest-lived species and above all the only measurable substance.

The control plates were kept inside the laboratory, closed with their lid, thus avoiding any possible exposure to environmental Ozone. As usual, after 24 hours of exposure all the plates were placed inside the incubator at 37° C to facilitate the growth of microorganisms.

To compare the environmental Ozone values measured by the ARPAT control unit and the Horiba, it was necessary to partially process the data collected by the latter, since only the values in  $\mu\text{g}/\text{m}^3$  expressed as an hourly average are shown from the ARPAT site. Consequently, it was necessary to perform an hourly average of all the measurements made by Horiba and convert the ARPAT data into ppb (dividing by 2).

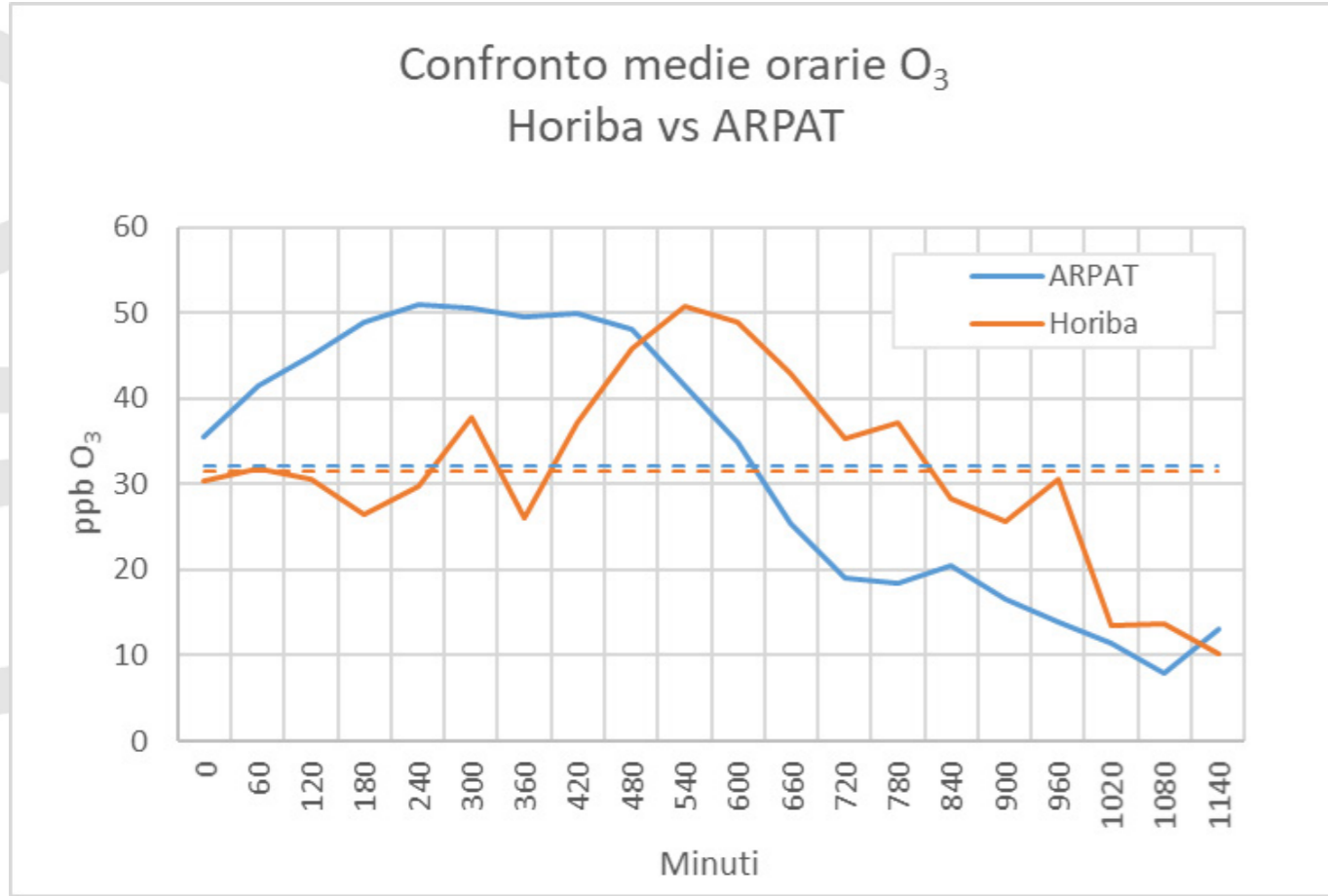


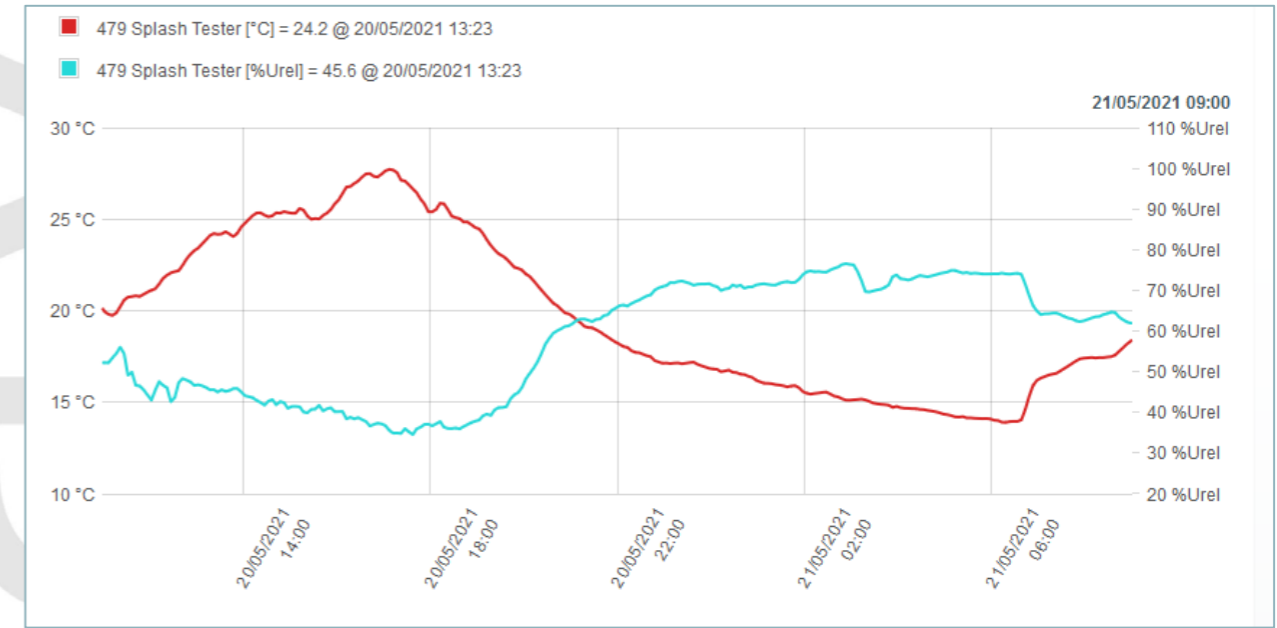
Immagine: average hourly comparison  
 Horiba vs ARPAT

*Environmental Ozone values to which the plates were exposed. Comparison between ARPAT and HORIBA measures*

As can be seen from the previous graph, the curves are quite similar but above all the average value detected (dashed lines) is practically identical: 32.2 ppb (ARPAT value) against 31.6 ppb (HORIBA value).

Consequently, it is possible to conclude that the plates have been exposed to values of Ozone (and presumably of other oxidizing species) which, on average, are absolutely similar to others previously tested with NTP treatments.

Finally, as regards the environmental temperature and humidity values, the following graph shows the data recorded by the monitoring data logger.



*Trend of temperature (red curve) and humidity (light blue curve) in the test environment*

In this case, (average) humidity values of 57.9% and a temperature of 19.9° C were recorded.

5.5.5 Photo evidence (fotografiche)

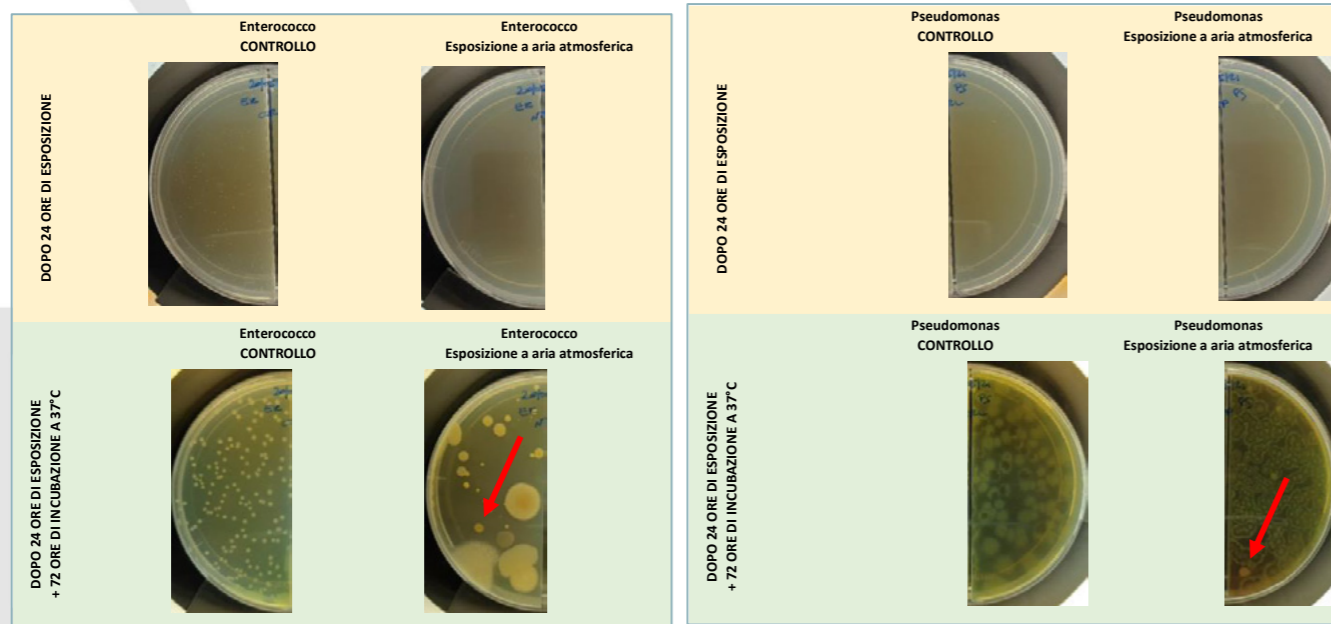
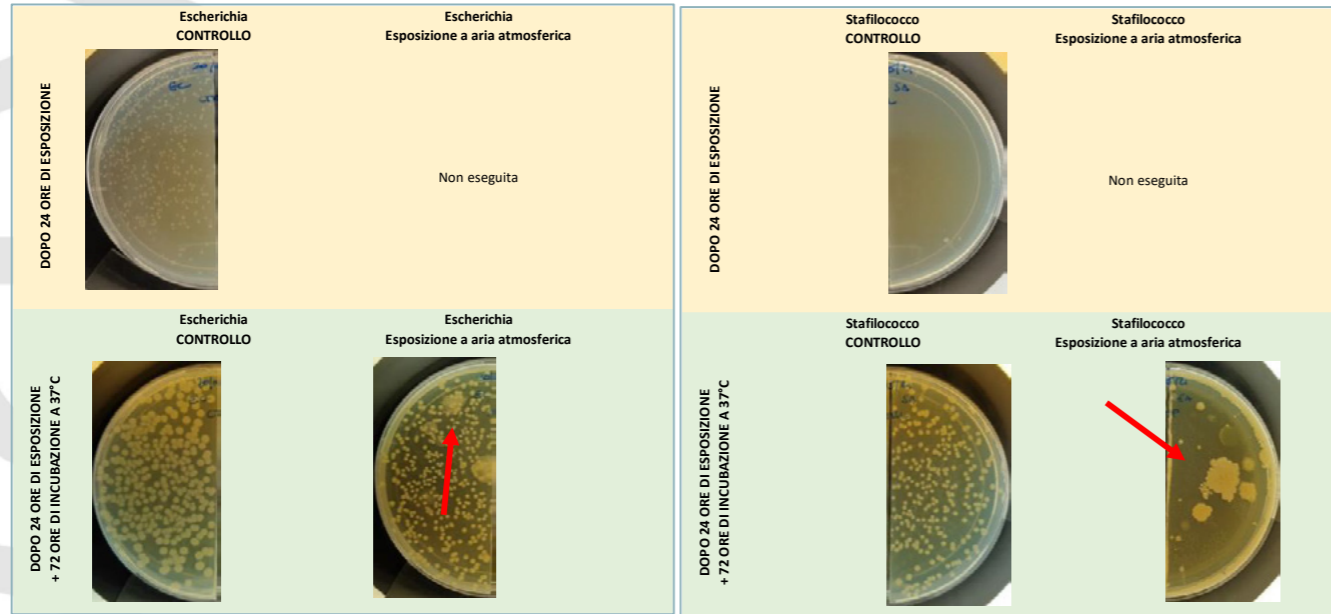


Immagine 2 sx: Enterococcus CONTROL – Enterococcus exposed to outside air  
After 24-hour exposure  
Enterococcus CONTROL – Enterococcus exposed to outside air  
After 24-hour exposure + 48 hours of incubation at 37°C  
Immagine dx: Pseudomonas CONTROL – Pseudomonas exposed to outside air  
After 24-hour exposure  
Staphylococcus CONTROL – Staphylococcus exposed to outside air  
After 24-hour exposure + 48 hours of incubation at 37°C

Top row: the appearance of the culture plates after 24-hour exposure to environmental Ozone (comparison with the control plates, not exposed).  
Bottom row: same plates but after 72 hours of incubation at 37° C.  
Arrows indicate the presence of colonies of contaminating environmental microorganisms.

5.5.6 Results

As can be appreciated from the previous figures, the effects of “simple” exposure to outside air (containing natural Ozone) replicated what was observed regarding the action of NTP in a confined environment (room or case) with a significant effect of growth inhibition against Gram-positive bacteria and no effect against Gram-negative bacteria.

From the observation of the plates, it is possible to notice a presence of contaminating microorganisms of environmental origin that have developed on the surface of the culture agar. The greater the presence of the microorganisms, the lower the presence of test microorganisms. This fact finds an obvious explanation in the common phenomena of ecological competition that arise when a common environment (with its nutrients) is shared by several species; in this case the strongest and/or most numerous takes over, preventing or limiting the development of the others.

Furthermore, it is clear once again that there was an inhibitory (biocidal) effect on differential growth depending on the type of microorganism.

Following are the values of the microbial count of the colonies grown in the plate:

Immagine 1 sx: Escherichia CONTROL – Escherichia exposed to outside air – not performed  
After 24-hour exposure  
Escherichia CONTROL – Escherichia exposed to outside air  
After 24-hour exposure + 48 hours of incubation at 37°C  
Immagine dx: Staphylococcus CONTROL – Staphylococcus exposed to outside air – not performed  
After 24-hour exposure  
Staphylococcus CONTROL – Staphylococcus exposed to outside air  
After 24-hour exposure + 48 hours of incubation at 37°C

Microbial concentration in each sector of the plates used.

Ecoli	CFU/sector	plate 1	plate 2	average	St. Dev.
		Ctrl	369	355	362
	O <sub>3</sub>	438	318	378	85
	Log CFU/sector				
Ctrl	-	-	2,56	0,01	
O <sub>3</sub>	-	-	25,58	0,1	

Saureo	CFU / sector	plate 1	plate 2	average	St. Dev.
		Ctrl	220	301	260,5
	O <sub>3</sub>	14	6	10	6
	Log CFU / sector				
Ctrl	-	-	2,42	0,1	
O <sub>3</sub>	-	-	1	0,26	

FecalE	CFU / sector	plate 1	plate 2	average	St. Dev.
		Ctrl	164	110	137
	O <sub>3</sub>	9	13	11	3
	Log CFU / sector				
Ctrl	-	-	2,14	0,12	
O <sub>3</sub>	-	-	1,04	0,11	

Paureog	CFU / sector	plate 1	plate 2	average	St. Dev.
		Ctrl	82	145	113,5
	O <sub>3</sub>	164	174	169	7
	Log CFU / sector				
Ctrl	-	-	2,05	0,18	
O <sub>3</sub>	-	-	2,23	0,02	

## 1.1.7 Summary conclusions on the results of the test

The graphic transposition of the data highlights better the results obtained:

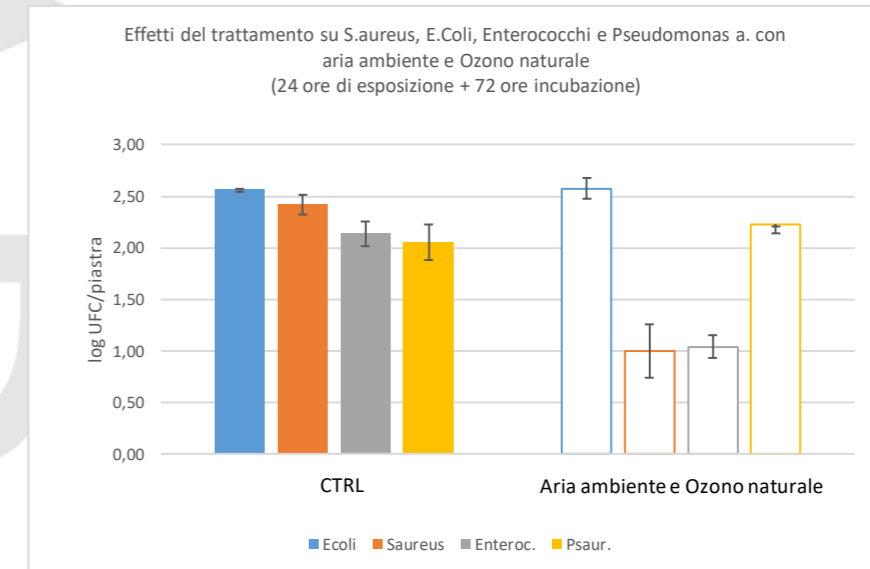


Immagine: log CFU/plate

Effects of the treatment on S.aureus, E.Coli, Enterococcus and Pseudomonas a. with outside air and natural Ozone (CTRL – Outside air and natural Ozone)

Comparison of the effects of the exposure to outside air and natural ozone



The usual conversion of the data into percentage reduction values highlights the effects obtained on the two main bacterial strains.

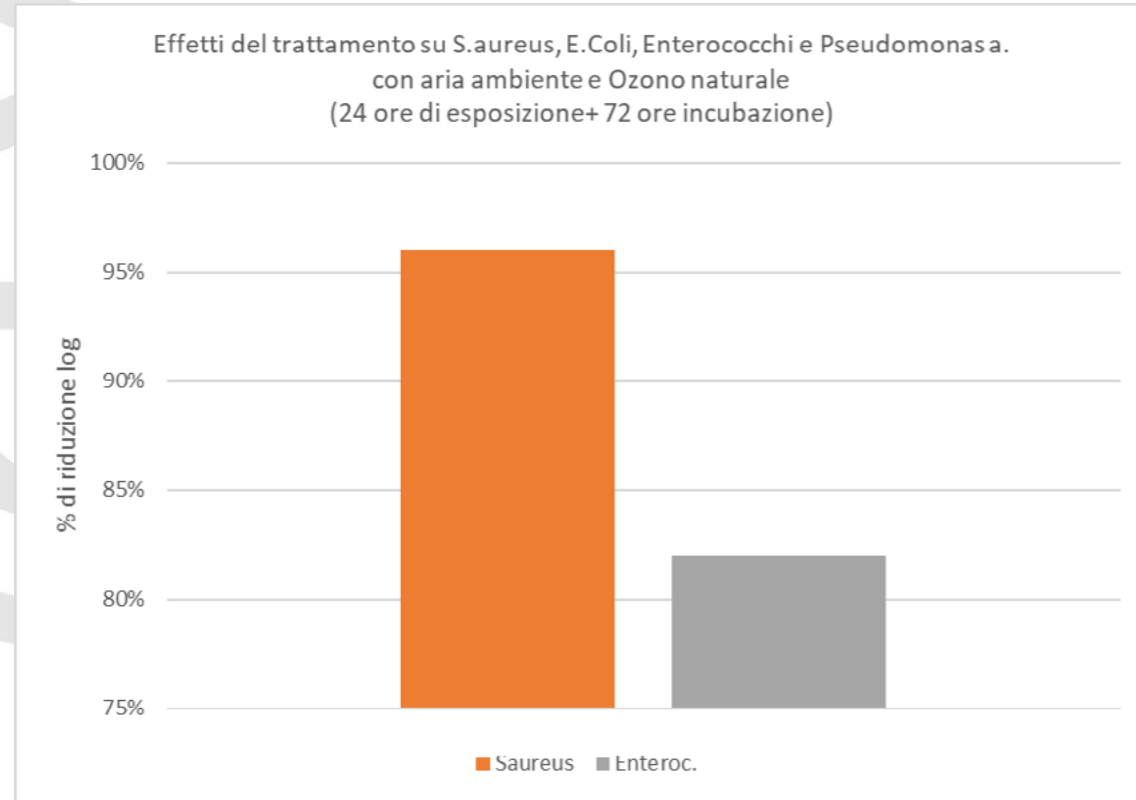


Immagine: % of log reduction  
 Effects of the treatment on S.aureus, E.Coli, Enterococcus and Pseudomonas a. with outside air and natural Ozone  
 (24 hours of exposition + 72 hours of incubation)

Comparison of the percentage reductions in microbial growth between the two tested microorganisms

## SUMMARY AND CONCLUSIONS

The following table compares the results obtained with the various tests. When available, the environmental data of temperature and relative humidity (both of the environment in which the treatment took place and that of the control plate) are reported, in addition to the concentration of Ozone (both natural or generated by the NTP) and the percentage reduction value of microbial growth (R). This latter value in the case of the first two tests A and B is indicated as the average value of that measured at the three distances evaluated.

Summary table of results. N.r. not detected

Test i.d.	T°		UR (%)	O <sub>3</sub> (ppb)	R (%)			
	NTP	CTRL			GRAM-NEGATIVE		GRAM-POSITIVE	
					Ecoli	P. Aeruginosa	S. Aureus	Fecal E.
TEST A	19,7	25,2	42	45	7		100	
TEST B	n.r.	n.r.	58	24		26		90
TEST C	24,4	22,4	54	64			61	50
TEST D	24,7	23,7	80	47	29	68	69	94
TEST E	19,9	23,9	58	32			96	92

As can be seen from the colored cells, the percentages (%) of reduction of the microbial load are almost similar in the case of exposure to "artificial=Jonix" NTP and exposure to "natural" NTP.

## 9. CASE STUDY: STUDIES ON PRACTICAL APPLICATIONS OF INDOOR SANITIZING SYSTEMS JONIX

### 9.1. Case study 1: reduction of odor impacts on waste management plant

**PURPOSE:** study and analysis of the environmental aspects related to the odor impact measurements in connection to waste management; implementation of a pilot-scale experiment related to the treatment of gaseous effluents in order to reduce effectively the present odor load.

**RESULTS:** the test results show how NTP technology positively abates the species that are present in the gaseous flow generated by a waste, with a percentages varying between 25% and 40%. This result has been obtained by carrying out a complex experimentation on a pilot plant that was equipped with NTP technology. The treatment was tested on different type of waste and by mixing them too. Both the Electronic Nose and the Gas chromatography with Mass detector (GC-MS) have been used as analytical techniques for the "quantification" of the efficiency. The obtained results suggest a wide possibility of applications of this technology as a system for the abatement of both the organic pollutants present in an emission and, as regards more specifically the topic of the project, the abatement of odorous molecules. Organic molecules, as it has been verified on aliphatic and aromatic chains by means of GC-MS, are reduced up to about 40%. The odorous substances, as it was possible to verify thanks to the Electronic Nose, decreased in their concentration down to a 30%. A possible further development of the study and of the proposed technology could concern different waste matrices characterized by olfactory impacts due to inorganic compounds, such as for example ammonia and hydrogen sulphide. In these cases, the analytical methods to be applied could be the Electronic Nose and specific techniques for the determination of these compounds.

The details of the trial are reported in ANNEX 9.

### 9.2. Case study 2: Study of air sanitation in a veterinary clinic

**PURPOSE:** testing the effectiveness of Non Thermal Plasma technology in veterinary health system. The trial was conducted at a Veterinary Clinic with the aim of achieving a reduction in perceived odors and a reduction in airborne microbial contamination in premises where concentrations could be significant and have a negative impact on animals and people. The test required a series of samplings that have been taken before the installation of the devices, during the normal activity of the clinic, to evaluate the initial conditions, to be compared with the measurements made after switching on the Jonix devices.

**RESULTS:** In the veterinary hospital room, the observed trend indicates a reduction of the total microbial content and staphylococci, while the fungi have a slight tendency to increase. This can be explained by the frequent opening of the doors that overlook the outside of the building, surrounded by hedges and plants. The sampling points were about 50 cm from the doors consequently the sucked air was mixed with that coming from outside. In the waiting room there was a general trend line of slight increase in the initially detected parameters due to the promiscuity with the air coming from the opening and closing of the doors. The effect of bacterial reduction over time is evident, the prolonged supply of ionizing molecules to the air makes the air becoming inhospitable for contaminants. **The deodorization effect of the air was sensibly appreciable in both controlled rooms:** the odor present was significantly reduced. Users perceived almost odorless air in the waiting room after switching on the Jonix devices. To conduct a more detailed evaluation of the antimicrobial effect of ionization, that has already been documented in the bibliography and with the same devices in other application, it would be necessary to set up a research protocol in premises with a greater

control of the variables or with environmental indicators that are less affected by the variables in place.

The details of the trial are reported in ANNEX 10.

### 9.3. Case study 3: Sanitizing effects of the MATE device in the large-scale food distribution sector

**PURPOSE:** evaluation of the sanitizing effects in a hypermarket, where an ionization and air filtration device model JONIX MINIMATE has been installed. The device was placed in the packaging area of the meat processing department.

**RESULTS:** the test results show that Jonix Minimate device significantly reduced the contamination present in the air, despite the influence of the air coming from adjacent rooms.

The details of the trial are reported in ANNEX 11.

### 9.4. Case study 4: Sanitizing effects of the MATE device in hospital operating rooms

**PURPOSE:** to study the action of the Jonix MATE device on the contamination levels of two operating rooms in private hospital.

**RESULTS:** as for the work surfaces, the collected data highlighted a substantial low microbial contamination; the continuous use of MATE has exercised an important and significant adjuvant action to the cleaning operations, without any use of additional chemical compounds to be nebulized in the environment

As regards the ambient air, it was possible to detect a low airborne microbial contamination, with the same type of isolated microorganisms (exclusively CBT37 and sporadically SC +). In this case also, the test on the air showed the same contamination decreasing trend, as if over time it was increasingly protected during the operations (even if the mate is off) and its remediation during the night became more and more effective.

The details of the trial are reported in ANNEX 12.

### 9.5. Case study 5: Sanitizing effects of the MATE device in hospital wards

**PURPOSE:** to establish the action of NTP technology against microorganisms that can be potentially found within the wards. For this purpose, ionizing systems of reduced dimensions have been used. They are specially designed for their less "invasive" location and more easily placement in a context of everyday life. The equipment was placed in different points of a ward and left in almost constant operation throughout the study period. The comparison of the effects was performed by evaluating the contamination levels in a "control" lane without NTP systems. In this way, the study was able to respond effectively and extremely pertinently to the need to evaluate innovative systems for the prevention of infections in the operating room in particular, and hospital infections in general, allowing the identification of a technology that is capable of supporting the usual environmental remediation activities, maximizing their effectiveness and helping to create safer environments with a lower infectious risk.

**RESULTS:** An AVERAGE ABATEMENT \* of 86% was verified in the ward (\* values referring to the total airborne bacterial load). The use of NTP technology, with its proven ability in the wards to reduce airborne microbial contamination over time and facilitate the sanitizing of surfaces, can contribute to the achievement and maintenance of better hygienic-sanitary conditions, helping the hospital personnel in handling the clinical risk.

The details of the trial are reported in ANNEX 13.

## 10. CONCLUSIONS

In conclusion, a nonthermal plasma can be used to inactivate a wide range of microorganisms such as bacteria, spores, fungi, viruses and prions.

The mechanism of a plasma's interaction with living systems is undoubtedly very complex and not well-understood, both because of the complexity of the biology and of plasma. Generally speaking, charged species, in particular ions, are believed to play a key role in the interaction between living cells (Dobrynin D., 2009), interacting chemically, and not through physical phenomena, such as shear stress, ion bombardment damage, thermal effects or UV radiation. Charged particles could play a significant role in the rupture of external cell membranes, *especially in gram-negative bacteria* that have thinner outer membranes.

The specific mechanisms leading to the inactivation of a virus by an NTP are as yet unclear. Studies have shown that the exposure to NTP causes a modification and/or degradation of viral proteins and nucleic acids, as well as of lipids in enveloped viruses (Yasuda H., 2010). In addition, reactive species can damage the viral RNA, leading to a reduction in gene expression and the elimination of viral RNA.

The use of NTP in sanitization processes appears interesting, regardless of the interpretation of the phenomena, due to its broad spectrum of activity. The technology is therefore flexible and easily applicable in many contexts, in particular in the sanitization of indoor environments from airborne particles, where other technologies may be unsuitable or ineffective.

## 11. BIBLIOGRAPHY

- Alex Lindsay, B. B. (2014). Fertilization of Radishes, Tomatoes, and Marigolds Using a Large-Volume Atmospheric Glow Discharge. *Plasma Chem Plasma Process*, 34 1271 - 1290.
- Arijana Filipić, I. G.-A. (2020). Cold plasma, a new hope in the field of virus inactivation . *Trends in Biotechnology*.
- Arne M. Vandenbroucke, R. M. (2011). Non-thermal plasmas for non-catalytic and catalytic VOC abatement. *Journal of Hazardous Materials*, 195, 30 - 54.
- Brandenburg, R. (2017). Dielectric barrier discharges: progress on plasma sources and on the understanding of regimes and single filaments. *Plasma Sources Sci. Technol.* 26, 053001 (29pp).
- Brandenburg, R. K.-D. (2014). Plasma based pollutant degradation in gas streams: status, examples and outlook. *Contrib. Plasma Phys.* 54,, 202 - 214.
- Bratislav M. Obradović, G. B. (2011). A dual-use of DBD plasma for simultaneous NOx and SO2 removal from coalcombustion flue gas. *Journal of Hazardous Materials volume 185, Issues 2–3*, 1280-1286.
- Carlos M. Nunez, G. H. (2012). Corona Destruction: An Innovative Control Technology for VOCs and Air Toxics. *Waste*, 242-247.
- Chulkyoon, P. P. (2016). Non-thermal plasmas (NTPs) for inactivation of viruses in abiotic environment. *Research Journal of Biotechnology* , Vol. 11 (6) .
- Chulkyoon, P. P. (2016). Non-thermal plasmas (NTPs) for inactivation of viruses in abiotic environments. *Research Journal of Biotechnology*, Vol. 11 (6) .
- CL Enloe, M. M. (2008). Time-correlated force production measurements of the dielectric barrier discharge plasma aerodynamic actuator. *Journal of applied physics*, 103(7), 073302-073302.
- Dayonna P. Park, K. D.-A. (2013). Reactive nitrogen species produced in water by non-equilibrium plasma increase plant growth rate and nutritional yield. *Current Applied Physics*, 13 S19 - S29.
- Dobrynin D., F. G. (2009). Physical and biological mechanisms of direct plasma interaction with living tissue. *New J. Phys.*, 11.
- Hao Zhang, D. M. (2017). Non-thermal plasma technology for organic contaminated soil remediation: A review. *Chemical Engineering Journal* (313), 157-170.
- Harstad, J. (1969). Evaluation of air filters with submicron viral aerosols and bacterial aerosols. *American Industrial Hygiene Association Journal*.
- Herrmann H.W., H. I. (1999). Decontamination of chemical and biological warfare, (CBW) agents using an atmospheric pressure plasma jet (APPJ). *Phys. Plasmas*, 6, 2284-2289 .
- J. Han, B. P. (July 5-10, 2015). Non-equilibrium plasmas in agriculture. *22nd International Symposium on Plasma Chemistry*.
- J. Karuppiaha, E. L. (2012). Abatement of mixture of volatile organic compounds (VOCs) in a catalytic non-thermal plasma reactor. *Journal of Hazardous Materials* (2012) , 283– 289.
- K. Urashima, J. C. (2000). Removal of volatile organic compounds from air streams and industrial flue gases by nonthermal plasma technology. *IEEE Transactions on Dielectrics and Electrical Insulation* ( Volume: 7, Issue: 5), 602 - 614.
- Kim, H. (2004). Nonthermal plasma processing for air-pollution control: a historical review, current issues, and future prospects. *Plasma Processes and Polymers*, 91-110.
- Kong M.G., K. G. (2009). Plasma medicine: an introductory review. *New J. Phys.*, 11.
- Laroussi, M. (2005). Low temperature plasma-based sterilization: Overview and state-of-the-art. *Plasma Process Polym.*, 391-400.
- Leipold, M . L . (2004). E valuation o f the roles o f reactive species, heat, and UV radiation in the inactivation of bacterial cells by air plasmas at atmospheric pressure. *nternational Journal of Mass Spectrometry*, 233 (1– 3), 81-86.
- M. Laroussi, F. ( 2004). E valuation of the roles of reactive species, heat, and UV radiation in theinactivation of bacterial cells by air plasmas at atmospheric pressure. *International Journal of Mass Spectrometry* 233, 81–86.
- Marco Schiavon, M. S. (2015). Potential of non-thermal plasmas for helping the biodegradation of volatile organic compounds (VOCs) released by waste management plants. *Journal of Cleaner Production* 104, 211 - 219.
- Marco Schiavon, M. S. (2017). Non-thermal plasma assisting the biofiltration of volatile organic compounds. *Journal of Cleaner Production* 148, 498-508.
- Michael J. Gallagher, A. G. (2004). Non-thermal plasma application in air sterilization. *Conference Paper in IEEE International Conference on Plasma Science*.
- Mráz, P. B. (2014). EFFECT OF LOW-TEMPERATURE PLASMA TREATMENT ON THE GROWTH AND REPRODUCTION RATE OF SOME PLANT PATHOGENIC BACTERIA. *Journal of Plant Pathology*, 96 (1), 63-67.
- Oda, T. (2003). Non-thermal plasma processing for environmental protection: decomposition of dilute VOCs in air. *J. Electrostat* 57, 293-311.
- Osman K aratum, M. A . ( 2016). A c omparative s tudy o f dilute VOCs treatment in a non-thermal. *Chemical Engineering Journal* 294, 308-315.
- Osman Karatum, M. A. (2016). A comparative study of dilute VOCs treatment in a non-thermal plasma reactor. *Chemical Engineering Journal* 294, 308–315.
- Penetrante, B. S. (2011). Non-thermal plasma techniques for pollution control: Part A-overview, fundamentals and supporting technologies and part B-electron beam and electrical discharge processing. *NATO ASI Ser Ser G 84*, 1296–1300.
- S. Schmid, M. J. (2010). Degradation of volatile organic compounds in a non-thermal plasma air purifier. *Chemosphere*, 124 - 130.

- Sang-Hye Ji, K.-H. C.-H. (2016). Effects of high voltage nanosecond pulsed plasma and micro DBD plasma on seed germination, growth development and physiological activities in spinach. *Archives of Biochemistry and Biophysics* 605, 117 - 128.
- Schiavon, M. R. (2016). Comparison between conventional biofilters and biotrickling filters applied to waste biodegradation in terms. *Environ. Technol.* 37, 975-982.
- Schiavon, M. T. (2017). Non-thermal Plasma as an Innovative Option for the Abatement of Volatile Organic Compounds: a Review. *Water Air Soil Pollut* , 228,388.
- Seinfeld, J., & Pandis, S. (1998). Atmospheric Chemistry and Physics. From Air Pollution to. In *John Wiley & sons, inc.*
- U. Kogelschatz, B. E. (1997). Dielectric-Barrier Discharges. Principle and Applications . *Journal de Physique IV Colloque, 07, C4-47-C4-66.*
- Wen-Jun Liang, H.-P. F.-X.-Q. (2011). Performance of non-thermal DBD plasma reactor during the removal of hydrogen sulfide. *Journal of Electrostatics Volume 69, Issue 3, 206-213.*
- Wu Y., L. Y. ( 2015). MS2 virus inactivation by atmospheric-pressure cold plasma using different gas carriers and power levels. *Appl. Environ. Microbiol.*, 81, 996-1002.
- Yasuda H., M. T. (2010). A., Biological evaluation of DNA damage in bacteriophages inactivated by atmospheric pressure cold plasma. *Plasma Process Polym.*, 7, 301–308 .
- Zulfam Adnana, S. M. (2017). Exhaust gases depletion using non-thermal plasma (NTP). *Atmospheric Pollution Research (volume 8 issue 2)*, 338-343.

## 12. ATTACHMENTS

- ATTACHMENT 12.0 - **VIRUCIDAL EFFECTIVENESS REPORT:** Quantitative test in suspension for the evaluation of virucidal activity against the SARS-CoV-2 virus
- ATTACHMENT 12.1 - **VIRUCIDAL EFFECTIVENESS REPORT:** Quantitative test in suspension for the evaluation of virucidal activity against the SARS-CoV-2 virus
- ATTACHMENT 12.2 - Laboratory study on the biocidal activity of oxidizing species generated via NTP
- ATTACHMENT 12.3 – Laboratory study on the sanitizing effects produced by a MATE – Jonix
- ATTACHMENT 12.4 – Use of NTP technology against odors associated with the use of footwear
- ATTACHMENT 12.5 – Sanitation of non-critical ultrasound probes
- ATTACHMENT 12.6 – Laboratory studies on the use of NTP for VOC abatement: review
- ATTACHMENT 12.7 – Test evaluating the effectiveness of micro-organism reduction that have been intentionally inoculated into plates by using the Jonix Mate air ionization system
- ATTACHMENT 12.8 – Study of the sanitizing power of a Jonix device installed into a commercial fan coil
- ATTACHMENT 12.9 – Evaluation of the sanitizing capacity of Photocatalytic devices in comparison with Jonix NTP systems
- ATTACHMENT 12.10 – Case study 1: reduction of odor impacts on waste management plant
- ATTACHMENT 12.11 – Case study 2: Study of air sanitation in a veterinary clinic
- ATTACHMENT 12.12 – Case study 3: Sanitizing effects of the MATE device in the large-scale food distribution sector
- ATTACHMENT 12.13 – Case study 4: Sanitizing effects of the MATE device in hospital operating rooms
- ATTACHMENT 12.14 – Case study 5: Sanitizing effects of the MATE device in hospital wards

## ATTACHMENT 12.0

---

*BACTERICIDAL EFFICACY TEST REPORT: Quantitative suspension test for the evaluation of bactericidal activity against MDR bacteria*

## INDEX

1. PURPOSE	79
2. TERMS AND DEFINITIONS	79
3. INTRODUCTION	79
4. SAMPLE CHARACTERIZATION	80
5. EXPERIMENTAL CONDITIONS	80
6. MATERIALS AND REAGENTS	80
7. EQUIPMENT	81
8. EFFECTIVENESS TEST	81
9. RESULTS	84
10. BACTERICIDAL EFFECTIVENESS	86
11. CONCLUSIONS	87
12. REFERENCES	87

## 1. PURPOSE

The following report has the purpose of defining in a clear and detailed way the methods of execution of the analysis in order to guarantee maximum precision and accuracy in compliance with the European standard UNI EN 17272:2020. This standard, employed for the validation of chemical disinfectants and antiseptics, was used for the verification of the bactericidal activity of equipment that uses the Non-Thermal-Plasma technology, or cold plasma. The bactericidal activity was performed using a control strain of *Escherichia coli* and in succession strains of MDR microorganisms (MultiDrug Resistant).

## 2. TERMS AND DEFINITIONS

**Bactericidal activity:** the ability of a product to produce a reduction in the number of bacterial colonies through experimental procedures that include precise and defined test conditions.

**Colony Forming Units (CFU):** number of colonies per mL.

**Airborne disinfection contact (ADC) time:** time from the first release of the product to the point where the carriers are recovered.

**Sensitive microorganism:** microorganism in which desiccation causes a log reduction greater than 1.5.

## 3. INTRODUCTION

The test method to verify the bactericidal activity of the Jonix Cube device (test product) against MDR bacteria was conducted in compliance with the European standard UNI EN 17272:2020 chemical disinfectants and antiseptics- Method for airborne room disinfection using automatic processes. Cold plasma emits light with wavelengths both in the visible and in the ultraviolet part of the spectrum. In addition to the emission of UV radiation, an important property of low-temperature plasma is the presence of highly reactive and high-energy electrons, which cause numerous chemical and physical processes such as oxidation, excitation of atoms and molecules, production of free radicals and other reactive particles.

#### 4. SAMPLE CHARACTERIZATION

**Product:** Jonix Cube Non-Thermal-Plasma Device (hereinafter referred to as Jonix Cube)

**Product Description:** Jonix CUBE is an air purification device; with a design that uses an advanced technology called cold plasma to eliminate bacteria, moulds, viruses, pollutants and odours

**Storage conditions:** room temperature

**Equipment instructions:** see attachment

#### 5. EXPERIMENTAL CONDITIONS

**Test temperature:**  $20 \pm 2$  °C

**Relative humidity (RH):** 50-75%

**Contact time:** 12 h - 14 h - 16 h

**Analysis period:** test start date: 25-05-2020 to Test end date 28-05-2021

#### 6. MATERIALS AND REAGENTS

**Microorganisms used in the experimental phase:**

- **Strain of *Escherichia coli* ATCC 10536:** *Escherichia coli* is a Gram-negative bacillus. It is an integral part of the normal intestinal flora of humans and other animals. While most *E. coli* strains are harmless, some endanger human health.
- ***Acinetobacter baumannii* MDR strain:** OXA-23 type carbapenemase-producing strain. *Acinetobacter baumannii* is a ubiquitous Gram-negative bacillus. It is able to survive about one month on dry surfaces.
- ***Klebsiella pneumoniae* MDR:** KPC type carbapenemase-producing strain. *Klebsiella pneumoniae* is a Gram-negative bacillus capable of causing bacterial pneumonia, although it is more commonly associated with urinary tract infections acquired from hospitals. *Klebsiella pneumoniae* has become a growing nosocomial infection as antibiotic-resistant strains continue to appear.

- ***Pseudomonas aeruginosa* MDR:** OXA-48 type carbapenemase-producing strain. *Pseudomonas aeruginosa* is a ubiquitous Gram-negative bacillus. It causes numerous types of infections.

\* ATCC (American Type Culture Collections)

#### ***MEDIUMS OF CULTURE AND REAGENTS***

The reagents used are pure for analysis and/or suitable for microbiological applications.

#### **Culture medium for bacterial count**

The culture medium used for cell counting is TSA (Tryptone Soya Agar).

#### **Diluent for microbial suspensions**

The diluent for microbial suspensions, prepared according to the UNI EN 17272:2020 standard, was used to prepare the microbial suspension and to carry out the dilutions required by the standard indicated above.

#### 7. EQUIPMENT

- Steel carriers
- DensiCheck Plus Biomerieux
- Stopwatch
- Vortex stirrer
- Incubator with a controlled temperature of  $36^{\circ}\text{C} \pm 1^{\circ}\text{C}$ .
- “BioHazard” class II vertical laminar flow hood
- pH meter
- Refrigerator with a controlled temperature of  $4^{\circ}\text{C}$
- Graduated pipettes
- Petri dishes
- Scale
- Beaker
- Scrapers

#### 8. EFFECTIVENESS TEST



## PREPARATION OF THE BACTERIAL SUSPENSION

### Bacterial suspension

A TSA subculture was prepared from the mother culture and incubated at  $37 \pm 1^\circ \text{C}$  for 18-24 hours. The step was repeated and incubated for another 24 hours. Finally, a third subculture was generated from the second (subculture II and III are considered working cultures). A loop was taken from the working cultures and transferred into a tube containing the diluent for the microbial suspensions until 0.5 McF was obtained with DensiCheck Plus Biomerieux corresponding to  $1 \times 10^8$  cfu/mL.

### Interfering substance

The interfering substance (BSA 3g/l) was added to the suspension in order to obtain a 1/10 dilution, and then an adaptation was performed for sensitive microorganisms, adding skimmed milk (100g/l) in concentration 1:20.

## DETERMINATION OF THE TITLE

To determine the title of the stock solution, serial dilutions up to  $10^{-8}$  were made. 1 ml of dilution  $10^{-6}$ ,  $10^{-7}$  and  $10^{-8}$  was included in TSA agar. In addition, 1 ml of the dilution  $10^{-6}$ ,  $10^{-7}$  and  $10^{-8}$  was filtered through the use of filter membranes.

All tests were conducted twice.

## EVALUATION OF THE DISINFECTION PROCESS

### Survival of the test organism in control carriers

The control carriers were placed inside uncovered Petri dishes and contaminated with 50  $\mu\text{l}$  of microbial suspension, which was then well distributed and dried. At the end of the drying period, the lid of the corresponding plate was applied. Each plate, containing the control carrier, was left in the laboratory for the duration of the exposure period. At the end of the exposure period, the control carriers were transferred into a beaker containing 100 ml of diluent for microbial suspensions. A first phase of scraping, lasting 1 minute, was followed by a second phase of mechanical stirring to allow the detachment of any microorganisms remaining adhered to the carrier. Serial dilutions up to  $10^{-3}$  were carried out from the solution obtained. 1 ml of the  $10^{-2}$

$10^{-2}$  dilution and 1 ml of the  $10^{-3}$  dilution were added in TSA medium with the inclusion technique; the tests carried out were duplicate. The plates were placed in an incubator at  $37 \pm 1^\circ \text{C}$  for 24 hours, for the first count and reincubated for another 24 hours for the second count.

### Preparatory tests to evaluate the absence of residual effects

To evaluate the absence of residual effects, 50  $\mu\text{l}$  of interfering substance were deposited in other carriers. When completely dry, the carriers were placed in the display case to be exposed to the action of the NTP. At the end of the exposure period, the carriers were transferred into a beaker containing 100 ml of diluent for microbial suspensions. A first phase of scraping, lasting 1 minute, was followed by a second phase of mechanical stirring to allow the detachment of any microorganisms adhering to the carrier, thus obtaining a solution, defined as S.

A screening was then performed to evaluate any inhibitory effects in the agar; therefore, 1 ml of solution S was included in the TSA agar together with 1 ml of the known bacterial suspension. The plate was incubated at  $37 \pm 1^\circ \text{C}$  for 24 hours for the first count and reincubated for another 24 hours for the second count. Further screening was performed to assess any inhibitory effects with the filter membranes. To do this, 98 ml of solution S were filtered with 0.45  $\mu\text{m}$  filter membranes, followed by 3 washes with 50 ml of diluent for microbial suspensions. Subsequently, 1 ml of dilution of the known microbial suspension was filtered. The membrane was transferred to a plate containing TSA agar and incubated at  $37 \pm 1^\circ \text{C}$  for 24 hours for the first count, and reincubated for another 24 hours for the second count. Finally, to evaluate a possible carrier-related inhibitory effect, 1 ml of the known microbial suspension was transferred together with the exposed carrier in a Petri dish. Agar was added and the plate was incubated at  $37 \pm 1^\circ \text{C}$  for 24 hours for the first count, and reincubated for another 24 hours for the second count.

Preliminary tests were conducted for each microorganism tested.

### Effectiveness test

#### **Exposure of carriers to the test product**

The carriers were placed inside empty Petri dishes. 50  $\mu\text{l}$  of microbial suspension (contaminated carriers) were deposited, then well distributed on the carrier through the use of a loop, and kept under a hood until the microbial suspension was completely dry.

When the microbial suspension was completely dry, the carriers to be exposed to the NTP were placed in the case provided with the lid open, in the opposite position to the location of the test device, to allow the carriers to be exposed to the test product. The duration of the exposure was weighted according to the results obtained.

### Recovery of carriers

The exposed carriers were deposited inside a beaker containing 100 ml of diluent for microbial suspensions. A first phase of scraping, lasting 1 minute, was followed by a second phase of mechanical stirring to allow the detachment of any microorganisms remaining adhered to the carrier, thus obtaining a solution. 1 ml of solution was used to perform a direct seeding by inclusion in TSA; subsequently, the plate was incubated at  $37 \pm 1^\circ \text{C}$  for 24 hours, for the first count and reincubated for another 24 hours for the second count. 10 ml of solution were filtered with 0.45  $\mu\text{m}$  filter membranes, followed by 3 rinses with recovery liquid. The membrane was then transferred to a TSA plate which was incubated at  $37 \pm 1^\circ \text{C}$  for 24 hours for the first count, and reincubated for another 24 hours for the second count. Finally, the carrier was transferred to a TSA plate to which more TSA agar was then added to completely cover the carrier. The plate was incubated at  $37 \pm 1^\circ \text{C}$  for 24 hours for the first count and reincubated for another 24 hours for the second count.

## 9. RESULTS

### Escherichia coli ATCC 10536

In the first experimental phase, the efficacy test was carried out on *E. coli* ATCC 10536 as required by the UNI EN 17272:2020 standard to evaluate the efficacy of the test product on a known microorganism.

Microorganism test	Title of the initial suspension (cfu/mL)	Validation test	Title of the suspension of the carrier of control (cfu/mL)	Log Reduction (R)
<i>E. coli</i> ATCC 10536	$4.55 \cdot 10^8$	Valid	$1.46 \cdot 10^6$	6.2

12 h				
<i>E. coli</i> ATCC 10536 14 h		Valid	$1.45 \cdot 10^6$	5.9
<i>E. coli</i> ATCC 10536 16 h		Valid	$1.44 \cdot 10^6$	6.2

Table 1 - *E. coli* - NTP exposure for 12, 14 and 16 hours.

Having demonstrated that the requirements of the standard with *E. coli* ATCC 10536 are met, the experimental phase continued by testing strains of multidrug-resistant Gram-Negative microorganisms (MDR): *K. pneumoniae* KPC, *A. baumannii* OXA-23 and *P. aeruginosa* OXA-48.

### Klebsiella pneumoniae MDR

Microorganism test	Title of the initial suspension (cfu/mL)	Validation test	Title of the suspension of the carrier of control (cfu/mL)	Log Reduction (R)
<i>K. pneumoniae</i> KPC 12 h	$4.45 \cdot 10^8$	Valid	$1.61 \cdot 10^6$	6.3
<i>K. pneumoniae</i> KPC 14 h		Valid	$1.38 \cdot 10^6$	6.3
<i>K. pneumoniae</i> KPC 16 h		Valid	$1.83 \cdot 10^6$	6.3

Table 2 - *K. pneumoniae* - NTP exposure for 12, 14 and 16 hours.

### Acinetobacter baumannii MDR

Microorganism test	Title of the initial suspension (cfu/mL)	Validation test	Title of the suspension of the carrier of control (cfu/mL)	Log Reduction (R)
<i>A. baumannii</i> OXA-23 12 h	$4.93 \cdot 10^8$	Valid	$3.93 \cdot 10^6$	3.1

<i>A. baumannii</i> OXA-23 14 h		Valid	2.45 10 <sup>6</sup>	4.1
<i>A. baumannii</i> OXA-23 16 h		Valid	2.56 10 <sup>6</sup>	6.4

Table 3. *A. baumannii* - NTP exposure for 12, 14 and 16 hours.

***Pseudomonas aeruginosa* MDR**

Microorganism test	Title of the initial suspension (cfu/mL)	Validation test	Title of the suspension of the carrier of control (cfu/mL)	Log Reduction (R)
<i>P. aeruginosa</i> OXA-48 12 h	2.59 - 10 <sup>8</sup>	Valid	1.17 10 <sup>6</sup>	4.1
<i>P. aeruginosa</i> OXA-48 14 h		Valid	1.13 10 <sup>6</sup>	4.8
<i>P. aeruginosa</i> OXA-48 16 h		Valid	1.15 10 <sup>6</sup>	6.1

Table 4. *P. aeruginosa* - NTP exposure for 12, 14 and 16 hours.

**10. BACTERICIDAL EFFECTIVENESS**

The product in question is considered **bactericidal** when, after the contact time, there is a **reduction in the vitality of at least 10<sup>5</sup>**, corresponding to a reduction equal to 5 logarithms concerning the bacterial strain test based on the method and the acceptability criteria of UNI EN 17272:2020.

To obtain the reduction of the bacterial load (R), the logarithm of the ratio between the microorganisms presents on the control carrier and the microorganisms surviving in the carrier after exposure to NTP was carried out.

**11. CONCLUSIONS**

The results obtained showed that the device is effective from as quick as 12 hours, determining a reduction of the total bacterial load both for the *E. coli* strain ATCC 10536 (R>5) and for the *K. pneumoniae* KPC strain (R>5).

For the strains of *A. baumannii* OXA-23 and *P. aeruginosa* OXA-48, the reduction of the bacterial load is not sufficient to demonstrate the efficacy of the device after 12 hours (respectively R=3.1 and R=4.1) and 14 hours (respectively R=4.1 and R=4.8) of exposure. However, after 16 hours of exposure for both microorganisms, the reduction of the bacterial load is total, demonstrating the effectiveness of the device, with R>5.

The results obtained show that the Jonix Cube device has an effective bacterial activity against various multidrug-resistant microorganisms after a microorganism-related exposure phase.

**12. REFERENCES**

- EUROPEAN STANDARD UNI EN 17272:2020 Chemical disinfectants and antiseptics - Method for airborne room disinfection using automatic processes
- EUROPEAN STANDARD EN 14476:2019 Chemical disinfectants and antiseptics - Quantitative suspension test for the evaluation of virucidal activity in the medical area
- ISO 15189: 2012 Medical laboratories - Requirements for quality and competence

Il Responsabile Scientifico  
  
(dott.ssa Claudia Del Vecchio)

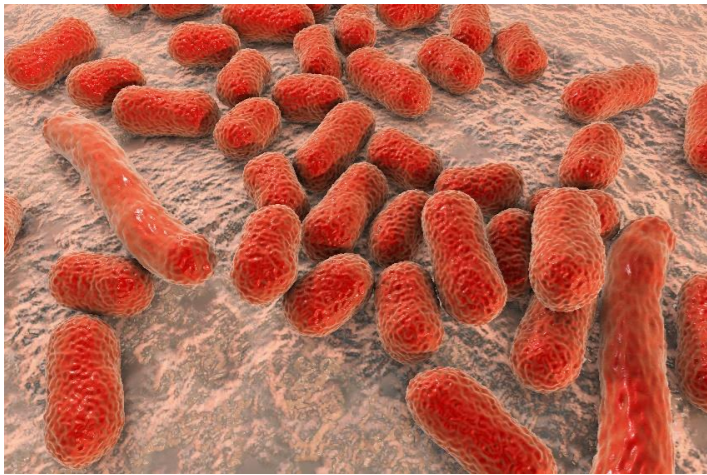
Il Direttore del Dipartimento  
  
(Prof. Andrea Crisanti)



*Escherichia coli*



*Klebsiella pneumoniae*



*Acinetobacter baumannii*



*Pseudomonas aeruginosa*

## ATTACHMENT 12.1

*VIRUCIDAL EFFECTIVENESS REPORT: Quantitative test in suspension for the evaluation of virucidal activity against the SARS-CoV-2 virus*



Via A. Gabelli 63 - 35121 Padova  
C.F. 80006480281 - P.IVA 00742430283

## VIRUCIDAL EFFECTIVENESS REPORT

Quantitative test in suspension for the evaluation of virucidal activity  
against the SARS-CoV-2 virus

PRODUCT:

**JONIX CUBE**  
air purification device

### CLIENT

Jonix S.r.l. Address: Viale Spagna, 31/33 - 35020 Tribano (PD)  
VAT and Tax Code 04754080283

### SCIENTIFIC RESPONSIBLE:

Prof. Andrea Crisanti

Research assistants: Dott.ssa Claudia Del Vecchio, Dott.ssa Manuela Sciro, Dott. Di Pietra  
Giuseppe

Report Date: 22/09/2020

## INDEX

1. PURPOSE .....	93
2. TERMS AND DEFINITIONS .....	93
3. INTRODUCTION .....	93
4. CHARACTERIZATION OF THE SAMPLE .....	93
5. EXPERIMENTAL CONDITIONS.....	94
6. MATERIALS AND REAGENTS .....	94
7. EQUIPMENT.....	95
8. PRELIMINARY TESTS .....	95
9. INACTIVATION VERIFICATION – TEST WITH FORMALDEHYDE .....	96
10. VERIFICATION OF THE VIRUCIDAL ACTIVITY OF THE DEVICES.....	96
11. CALCULATION OF THE EXPRESSION OF THE RESULTS.....	97
12. VIRUCIDAL EFFECTIVENESS .....	97
13. RESULTS AND VIRUCIDAL ACTIVITIES.....	98
14. CONCLUSIONS .....	98
15. REFERENCES.....	98

## 1. PURPOSE

The purpose of the following report is the clearly and in detail definition of the performing methods and of the results of a research evaluating the virucidal activity on surfaces of a device using Cold Plasma (Non-Thermal Plasma) technology by emitting oxidizing species.

## 2. TERMS AND DEFINITIONS

**Virucidal or antiviral activity:** the ability of a product to produce a reduction in the number of infecting viral particles through testing procedures that require precise and defined test conditions.

**Plate Forming Units (PFUs):** number of infecting viral particles per mL.

**ID<sub>50</sub>:** dose infecting 50% of the viral suspension or of the dilution of the viral suspension which induces 50% viral cytotoxic effect (CPE) in cell cultures.

**Viral cytotoxic effect (CPE – cytopathologic effect):** morphological alteration and/or destruction of cells following the multiplication of the virus.

**Inactivation of viruses:** reduction of the infectivity of a virus towards the product concerned.

## 3. INTRODUCTION

In order to guarantee maximum precision and accuracy, the test was performed in compliance with the EN 14476:2019 standard "Chemical disinfectants and antiseptics - quantitative suspension test for the evaluation of virucidal activity in the medical area - Test method and requirements (Phase 2/Stage 1)" and to the EN 17272:2020 standard "Chemical and antiseptic disinfectants: methods of indoor air disinfection through automated processes - Determination of bactericidal, mycobactericidal, sporicidal, fungicidal, yeasticidal, virucidal and phagocytic activities" (limited to the use of the described metal supports).

The virucidal activity was tested using the SARS-CoV-2 strain. All experiments were conducted in the Biosafety Level 3 Laboratory (BSL3)

## 4. CHARACTERIZATION OF THE SAMPLE

Product: Jonix Cube Non-Thermal Plasma Device (hereinafter referred to as Jonix Cube)

Product description: Jonix CUBE is an air purification device; a design piece that uses an advanced technology called cold plasma to eliminate bacteria, molds, viruses, pollutants and odors

Storage conditions: room temperature

Device instructions: see attachment

## 5. TEST CONDITIONS

**Test temperature:** it was performed at + 20 ° C ± 1 ° C.

**Contact time:** 30'-60'-120'-240'

**Analysis period:** test start date: 01-08-2020 ÷ Test end date 01-09-2020

## 6. MATERIALS AND REAGENTS

**Test microorganisms:**

SARS-CoV-2

**Cell line:**

VERO E 6 (ATCC CCL-81) \*

\* ATCC (American Type Culture Collections)

### Viral stock suspension

Each viral suspension was prepared and amplified on a large scale in monolayer cell cultures. After the infection and multiplication of the virus, the cellular debris was removed by double centrifugation at low speed (2500 rpm for 10 min), and the supernatant, containing the virus, is taken to determine the viral titer. It was divided into aliquots with known titer of 2 ml volume in Eppendorf and stored at -80 ° C in the freezer.

### Cell cultures

VERO E6 cells, cells of epithelial origin taken from monkey kidney (solid line).

### Supports (carriers)

35 mm diameter AISI 316 stainless steel discs were used, previously sterilized in an autoclave.

## MEDIUMS OF CULTURE AND REAGENTS

Reagents must be pure for analysis and/or suitable for microbiological applications.

### **Cell culture medium**

Each cell line is kept in a thermostat at 37°C with 5% (v/v) CO<sub>2</sub> in DMEM (Dulbecco's Modified Eagle Medium) medium supplemented with 10% (v/v) of fetal bovine serum (FBS) and 1% (w/v) of penicillin - streptomycin (pen-strep).

### **Phosphate Buffered Saline (PBS)**

Solution containing: 8 g of NaCl, 0.2 g of KCl, 2.89 g Na<sub>2</sub>HPO<sub>4</sub> 12 H<sub>2</sub>O, 0.20 g KH<sub>2</sub>PO<sub>4</sub> in 1000 ml of distilled H<sub>2</sub>O.

## 7. EQUIPMENT

- Inverted microscope for the observation of cell cultures
- Stopwatch
- Vortex stirrer
- Centrifuge
- CO<sub>2</sub> incubator (5% v/v) capable of maintaining the temperature at 37 ° C ± 1 ° C.
- "BioHazard" class II vertical laminar flow hood
- Freezers

## 8. PRELIMINARY TESTS

### **PREPARATION OF VIRAL SUSPENSION - VIRAL TITER**

0.2 ml of viral suspension (stock solution) + 1.8 ml of serum-free DMEM were mixed and serial dilutions from 10<sup>-2</sup> to 10<sup>-9</sup> (dilutions 1:10) were prepared.

250 µl of each dilution was transferred to 24 well plates containing the cell monolayer at confluence (> 90%) after aspiration of the growth medium. Each dilution of the viral suspension was plated in sextuple. 12 wells were left uninoculated, (cell line control). After 1 hour of incubation at 37 ° C (viral adsorption time), the inoculum was removed, washed with PBS and added 500 µl of DMEM with 2% (v/v) FBS and 0.75% (v/v) of carboxymethylcellulose.

### Thermostat incubation conditions

Infections were incubated with 5% (v/v) CO<sub>2</sub> at 37 ° C ± 1 ° C and observed under an inverted microscope to detect lysis plaque formation caused by the cytopathic effect (CPE) of the viral suspension.

The plaques present in the wells at counted dilution after fixation with formaldehyde and staining with a crystal violet solution were counted under an inverted microscope.

The CPE (quantitative test) results of each dilution are expressed with the percentage of positive results ranging from 100% to 0% and recorded as "0" for no CPE and "1" (25% CPE) to "4" (100% CPE) depending on the degree of cell damage.

Viral titer was calculated using the Spaerman-Karber method (ID<sub>50</sub> assessment).

### 9. INACTIVATION CHECK – TEST WITH FORMALDEHYDE

2 mL of viral suspension was mixed with 8 mL of PBS and 10 mL of 1.4% (w/v) formaldehyde solution to check the validity of the system. Immediately after a contact of 30 minutes and 60 minutes, 0.2 mL of this solution was mixed with 1.8 mL of DMEM + 2% FBS in ice. Serial dilutions from 10<sup>-2</sup> to 10<sup>-6</sup> (1:10 dilutions) with PBS + 2% FBS were performed. For each dilution 250 µl were distributed in 6 wells of the 24-well microplate and placed in the incubator at 37 ° C for 1 hour. After 1 hour in the incubator at 37 ° C (viral adsorption time), the inoculum was removed, washed with PBS and added 500 µl of DMEM with 2% (v/v) FBS and 0.75% (v/v) of carboxymethylcellulose were added.

The cell culture was placed in the incubator at 5% (v/v) of CO<sub>2</sub> at 37 ° C ± 1 ° C and observed under an inverted microscope for the detection of the cytopathic effect (CPE) of the viral suspension.

Plaques in the wells at counting dilution after fixation and staining with crystal violet-methanol solution were counted. The CPE (quantitative test) results of each dilution are expressed with the percentage of positive results ranging from 100% to 0% and recorded as "0" for no CPE and "1" (25% CPE) to "4" (100% CPE) depending on the degree of cell damage.

Viral titer was calculated using the Spaerman-Karber method (ID<sub>50</sub> assessment).

### Cytotoxicity of the formaldehyde test solution

1 ml of 1.4% (w/v) formaldehyde was added to 1 ml of PBS. From this dilution the serial dilutions from 10<sup>-2</sup> to 10<sup>-4</sup> (dilutions 1:10) were prepared by taking 0.2 ml of the obtained mixture + 1.8 ml DMEM serum-free.

0.1 ml of each dilution was plated in sextuple into monolayer cell cultures at confluence (>90%). The mixture was not added to 6 wells (cell line control). After 1 hour at 37 ° C ± 1 ° C, 100 µl of DMEM + 10% FBS were added and the cell culture was placed in an incubator at 37 ° C ± 1 ° C, at 5% of CO<sub>2</sub> and constantly observed under an inverted microscope for the next 9 days for the detection of the cytopathic effect (CPE), caused by the cytotoxic action of the formaldehyde solution.

### 10. VERIFICATION OF THE VIRUCIDAL ACTIVITY OF THE DEVICES

The virucidal test was performed at 20°C.

50 µl of viral suspension was inoculated on each carrier and left to dry under a laminar flow hood. The discs inoculated were used to verify virucidal activity by exposing them to the action of the Jonix Cube device or left inside petri dishes using them as control discs. The treated discs were placed inside a special box containing the Jonix device and exposed to its action for a time equal to 30'-60'-120'-240'. Subsequently, the discs (both treated and control ones) were eluted with 1 ml of culture medium and serial dilutions of 10<sup>-2</sup> to 10<sup>-9</sup> (dilutions 1:10) were prepared. 250 µl of each dilution was transferred to 24-well plates containing the cell monolayer at confluence (>90%) after aspiration of the culture medium. Each dilution of the viral suspension was plated in sextuple. 12 wells were left uninoculated (cell line control). After 1 hour of incubation at 37 ° C (viral adsorption time), the inoculum was removed, washed with PBS and 500 µl of DMEM with 2% (v/v) FBS and 0.75% (v/v) of carboxymethylcellulose were added.

### 11. CALCULATION OF THE EXPRESSION OF THE RESULTS

#### Determination of the infectivity titer (ID<sub>50</sub>).

The infecting activity was determined with the Spaerman-Kärber method, which uses the following formula to calculate the ID<sub>50</sub> value:

$$-\text{Log}_{10} \text{ID}_{50} = - (x_0) - \left\{ \left[ \frac{R}{100} \right] - 0,5 \right\} \times \log_{10} \text{dilution factor}$$

Where:

$x_0$  = log<sub>10</sub> of the lowest dilution with 100% positive reaction  
(CPE) R = summation (%) of the positive cultures

The virucidal activity test is valid when this condition occurs in the preliminary tests: the viral test suspension must have a viral concentration to determine the reduction of at least 4 lg of the initial viral titer: **ID<sub>50</sub> = 10<sup>7</sup>/mL**.

### 12. VIRUCIDAL EFFECTIVENESS

The product under examination is considered **VIRUCID** when at 20 ° C, after the contact time under consideration, it demonstrates a **reduction in vitality of at least 10<sup>4</sup>**, corresponding to a reduction of 4 logarithms (99.99%) compared to the test viral strain (EN 14476: 2019 and EN 17272: 2020).



### 13. RESULTS AND VIRUCIDAL ACTIVITIES

The results obtained are shown in the following table

Table 1 - Effects of treatment with Jonix CUBE. The viral load reduction values are expressed both in terms of logarithmic units and in percentage.

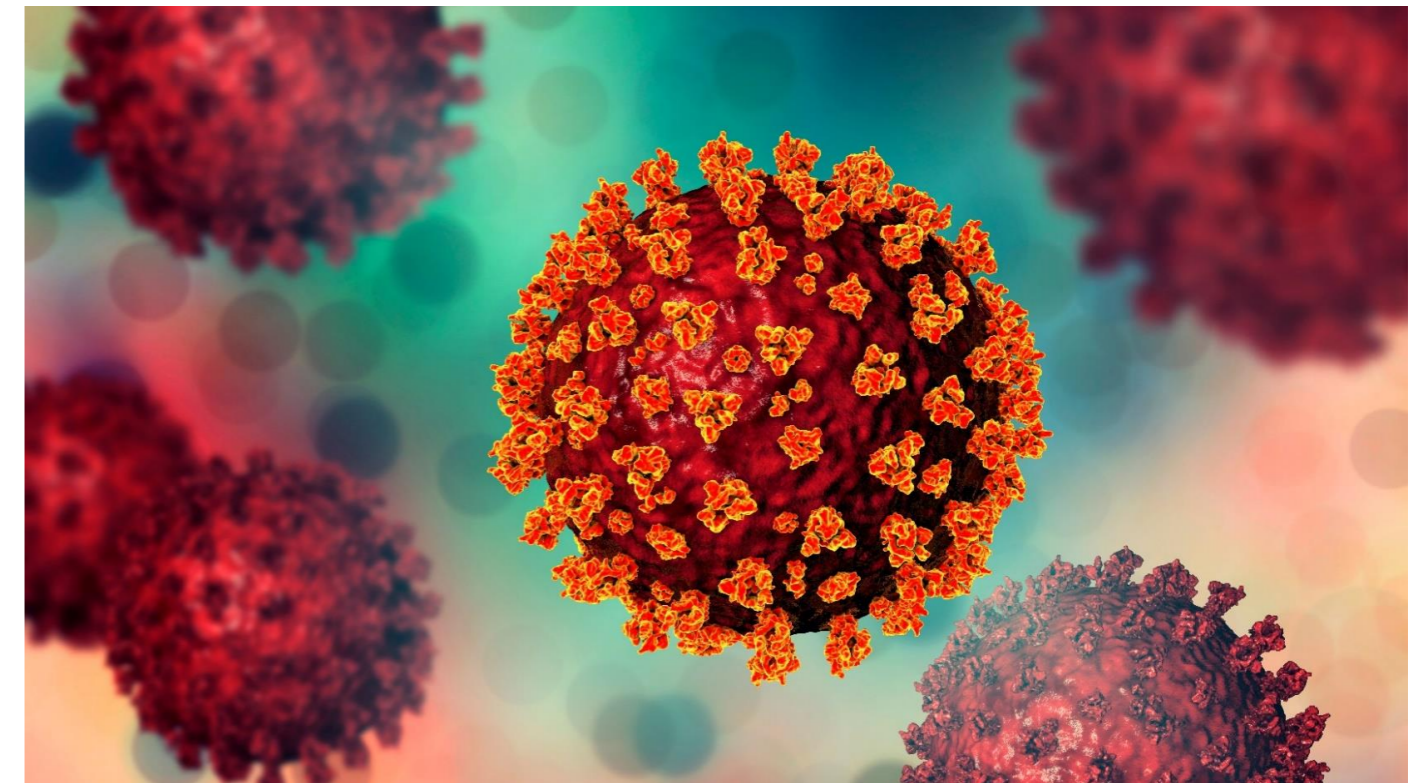
Exposition time (minutes)	Control		Treated		Reduction	
	PFU/ml	log(PFU/ml)	PFU/ml	log(PFU/ml)	U <sub>logaritmiche</sub>	%
0	10.000.000	7	10.000.000	7	0	0
30	10.000.000	7	1,07	0,03	6,97	99,99999
60	10.000.000	7	1,02	0,01	6,99	99,99999
120	10.000.000	7	1,02	0,01	6,99	99,99999
240	10.000.000	7	1,02	0,01	6,99	99,99999

### 14. CONCLUSION

The results obtained show that the Jonix Cube device (Non-Thermal Plasma Technology (NTP)) has an **effective antiviral activity against SARS-CoV-2 with a reduction of the viral load equal to 99.99999% (about 7 logarithmic units) after only 30 minutes of exposure; this suggests that the achievement of the reduction level required by the technical standards (4 logarithmic units) may also occur for considerably shorter times.**

### 15. REFERENCES

- EUROPEAN STANDARD EN 17272: 2020 Chemical disinfectants and antiseptics - Method for environmental disinfection using automatic processes
- EUROPEAN STANDARD EN 14476: 2019 Chemical disinfectants and antiseptics - Quantitative suspension test for the evaluation of virucidal activity in the medical area
- ISO / IEC 17025: 2017 General requirements for the competence of testing and calibration laboratories
- ISO 15189: 2012 Medical laboratories - Requirements for quality and competence



*SARS-CoV-2 virus*

## ATTACHMENT 12.2

---

*Laboratory study on the biocidal activity of oxidizing species generated via NTP*

## PURPOSE OF THE TEST

Attesting biocidal activity of NTP air (ionized air via Non Thermal Plasma) of different microbial strains

## PROCEDURE

Petri dishes have been contaminated with *Salmonella* spp., *Escherichia coli*, *Listeria monocytogenes*, *Staphylococcus aureus* and *Pseudomonas aeruginosa* and then exposed for different timeframes (2.5 and 10 minutes) to ambient air flow or ionized air via NTP. In this way it is possible to get a direct comparison between the Petri dishes and evaluate the proliferation of the microorganisms.

## RESULTS

The images below show the comparison of the different cases:



Foto 1 - Attività su *Salmonella* spp.

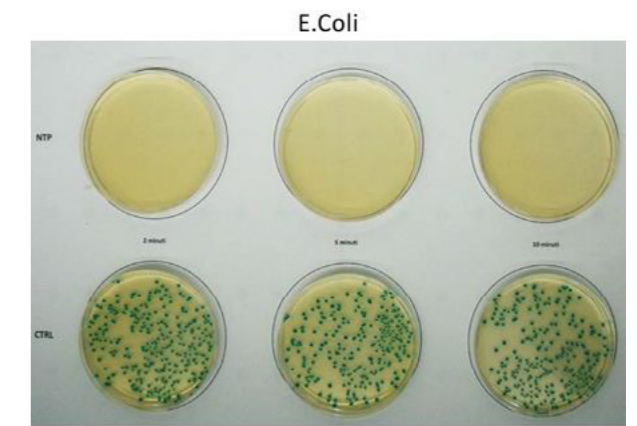


Foto 2 - Attività su *Escherichia coli*

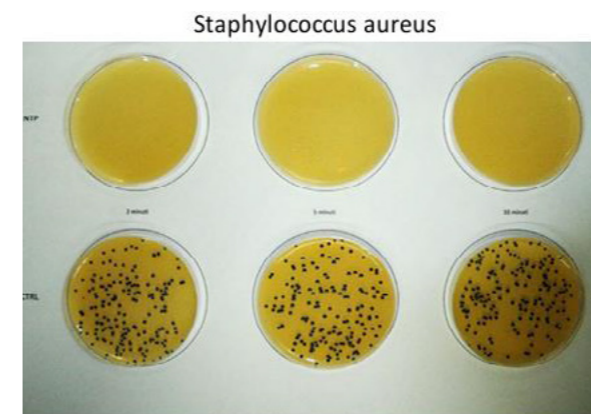


Foto 4 - Attività su *Staphylococcus aureus*

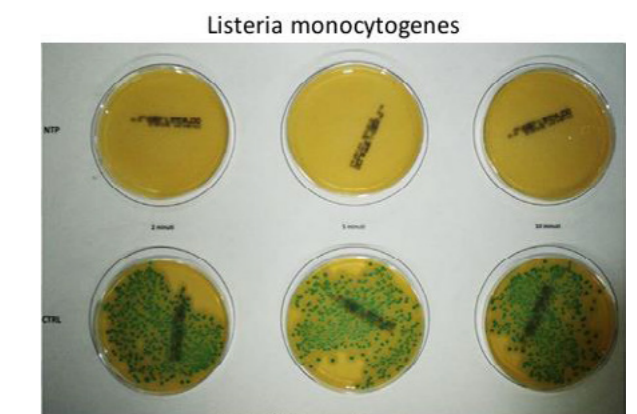


Foto 1 - Attività su *Listeria monocytogenes*



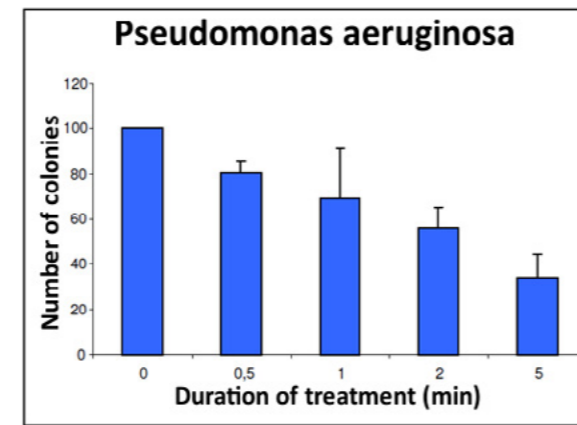
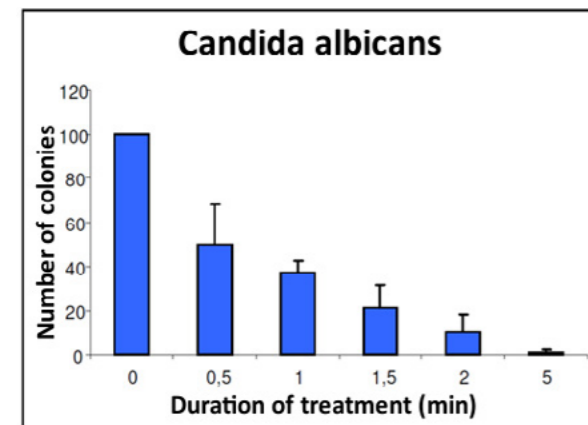
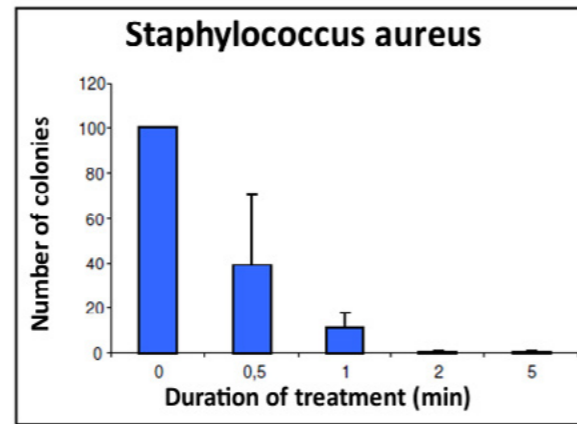
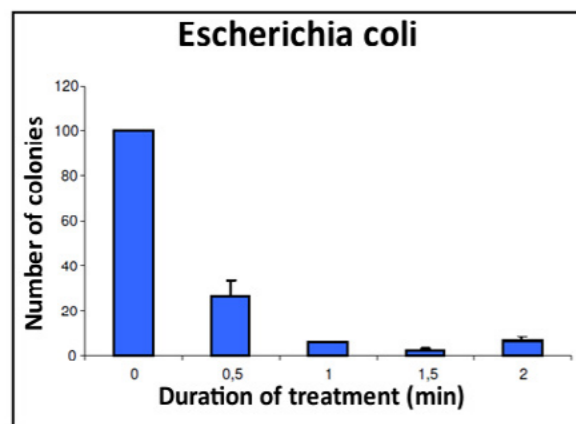
Foto 5 - Attività su *Pseudomonas aeruginosa*

The following table summarises the average results.

**Table 1.** Results of treatment tests

Strain \ treatment	Treatment time (minutes)						
	0	1	3	5	10	15	30
Escherichia coli \ air	~ 500	~ 500	~ 500	~ 500	~ 500	~ 500	~ 500
Escherichia coli \ NTP	~ 500	0	0	0	0	0	0
Candida Albicans \ air	~ 600	~ 600	~ 600	~ 600	~ 600	~ 600	~ 600
Candida Albicans \ NTP	~ 600	38	20	0	0	0	0
Staphylococcus aureus \ air	~ 300	~ 300	~ 300	~ 300	~ 300	~ 300	~ 300
Staphylococcus aureus \ NTP	~ 300	78	1	0	0	0	0

The above results in graphic format:



From the photos, it is evident that even with short contact times (2 minutes), the biocidal activity of NTP air is total: the plates exposed to NTP air show no development of microbial strains tested, which, instead, are normally developed on plates just exposed to air

As shown in the photo, the NTP treatment is effective from the first few minutes of use. In fact, after just 5 minutes, all species tested were completely eradicated from the surface of the plates. An additional element that positively characterises the success of the experiment consists in the fact that, contrary to what is foreseen by certain methods that require the execution of experiments on stainless steel surfaces, the described above tests were carried out in perfect conditions for microorganisms, both with regard to the ecological point of view (humidity, perfect pH, presence of nutrients, etc.) and for the presence of great quantity of organic substance, which is known to interfere with the classical biocides.

## ATTACHMENT 12.3

*Laboratory study on the sanitizing effects produced by a MATE – Jonix*

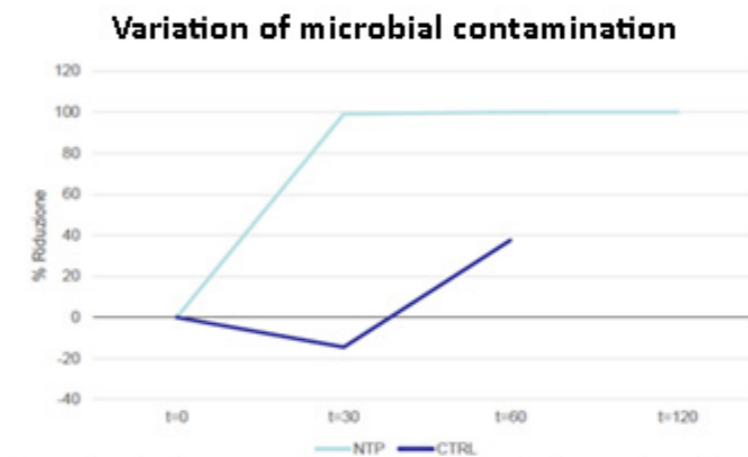
### Environmental Sanitisation with JONIX™ MATE

MATE device by JONIX™ is a sanitizing cabinet system that uses NTP cold plasma technology to ionize the air. Its use is focused on sanitizing industrial, medical and ambulatory environments and it is suitable for many other applications, amongst which the agri-food industry (cultivation and food preservation).



ARCHA srl laboratories have compared the spontaneous reduction of microbial contamination in a workplace with and without NTP treatment (respectively with MATE in operation and with non-operating unit).

The results are shown in the graph below.



Comparison between spontaneous reduction of airborne microbial contamination (CTRL) and what is determined by the treatment (NTP). Negative values indicate an increase in contamination with regard to zero time (end of atomization)

From the graph, it is possible to observe how, just after 30 minutes of treatment with the device, the microbial reduction percentage is really close to 100%. This confirms the efficiency of the JONIX™ MATE to sanitize living and working environments

## ATTACHMENT 12.4

---

*Use of NTP technology against odors associated with the use of footwear*

## Introduction

The effectiveness of NTP air was tested as for the abatement of chemical molecules and as for the microbiological sanitization to eliminate bad odours that are associated with use of footwear.

In particular, NTP air resulted effective in eliminating the following species:

- Chemical molecules responsible for odours.
- Microorganisms responsible for producing odours.

With regard to the elimination of chemical molecules, the experiment led to the conclusion that the air treatment using NTP for sufficiently long timeframes (from 6 hours onwards), is EFFECTIVE and able to eliminate and destroy completely the molecules in object, as shown in the following table

chemical molecules	Elimination % of molecules compared to the initial concentration, via NTP air		
	60 min	6 h	17 h
Acetic acid	69%	100%	100%
Propionic acid	45%	100%	100%
Isobutyric acid	31%	100%	100%
Butyric acid	21%	100%	100%
Isovaleric acid	0%	100%	100%
Valeric Acid	10%	100%	100%
Caproic Acid	6%	100%	100%
Caprylic Acid	6%	99%	99%
Caprylic Acid	6%	88%	95%

## ATTACHMENT 12.5

---

*Sanitation of non-critical ultrasound probes*



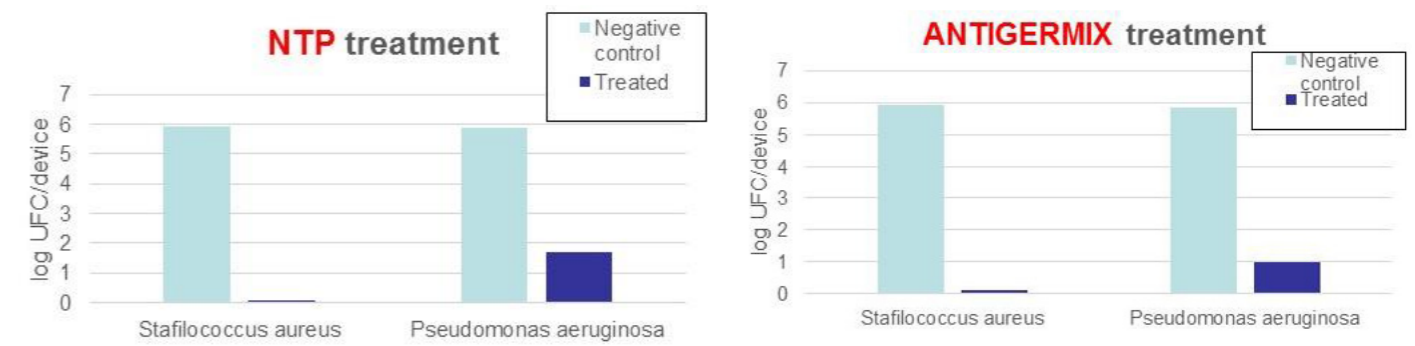
## Purpose of the test

Tests of sanitation were carried out on “Non-critical” ultrasound probes by using NTP AIR, and the results were compared to the sanitisation carried out by usual commercial devices.

The tests have shown an efficiency of NTP that is absolutely comparable to that of the devices commonly found in the market for the purpose.

## Results

The figures below show the abatement of microbial species provided by NTP air and by commercial devices after the same disinfection procedure.



## ATTACHMENT 12.6

---

*Laboratory studies on the use of NTP for VOC abatement: review*

## Laboratory studies on the use of NTP for VOC abatement: review

One of the most investigated fields is the abatement of VOCs (Volatile Organic Compounds – a wide range of gas-phase pollutants) as in these plasmas they can be oxidized to CO<sub>2</sub> already at room temperatures. The efficacy of this process depends on the VOC type and the duration of the contact. It is worth noting that these plasmas are able to treat even the extremely unreactive Halon (a haloalkane).

In addition to organic molecules, NTP is also able to act on inorganic pollutants, such as nitrogen oxides (NO<sub>x</sub>), sulphur dioxide (SO<sub>2</sub>), hydrogen sulphide (H<sub>2</sub>S) etc..., for example, such as those in the exhaust gases of motor vehicles.

The NTP technology's broad effectiveness spectrum means it can be applied in many fields, being easily scalable for both small and large applications.

In reality, there are many factors that impact the efficacy of pollutant abatement with NTP systems. From the geometry of plasma production systems to the power supply systems, from the concentration of pollutants to air humidity, and so on.

The case studies performed by ARCHA<sup>2</sup> laboratories represent the application areas in which the Jonix cold plasma production system has been tested. Their scope was to work out the best treatment conditions as well as to identify and, using the appropriate analytical methods, to measure the effectiveness of the abatement of the contaminant molecules. These cases are therefore just an example and an introduction to the application possibilities of the NTP technology, providing a robust and reliable set of data indicating the potential of this technology.

The table below shows the organic and inorganic compounds that have been treated during the various case studies and the abatement effectiveness of the NTP Jonix treatment.

The abatement rate refers to the individual case studies, yet it is indicative of the system's ability to act on the particular compound.

VOC – Volatile Organic Compounds	Abatement % following Jonix NTP treatment
Toluene	> 95
TBA (Tribromoanisole)	> 95
Ethyl acetate	> 95
Butyl acetate	> 95
Acetaldehyde	> 95
Butanal	> 95
Dichloroethylene	> 95
TCE	> 95
1, 2-DCP	> 95
Methylcyclohexane	> 95

Volatile/Gassy Inorganic Compounds	Abatement % following Jonix NTP Treatment
NO <sub>x</sub>	> 95
Sox	> 95
H <sub>2</sub> S	> 95
CO	> 95
	> 95
NH <sub>3</sub>	> 95

<sup>2</sup> ARCHA, acronym of **Analisi e Ricerche di CHimica Applicata** (Applied Chemistry Analysis and Research), founded in 1989 in Pisa, on the initiative of a group of professionals in the field of chemistry. It is a state-of-the-art chemical laboratory, fully equipped and with qualified staff.

Over the years, the company has grown in every respect: scientific expertise, service efficiency and market results.

Today, the different areas of expertise and/or the different companies within the ARCHA group are organised into **three sectors** (Technical – ICT- Industrialization).

Octane	> 95
PCE	> 95
Xylenes	> 95
C9 Aromatics	> 95
Aceti acid	> 95
Propionic acid	> 95
Isobutyric acid	> 95
Butyric acid	> 95
Isovaleric acid	> 95
Valeric acid	> 95
Hexanoic acid	> 95
Caprylic acid	> 95
Aliphatic compounds (C5-12)	> 95
Aromatic compounds (C7-C10)	> 95
Volatile organic compounds	> 95

The definition of VOCs is broad and includes odorous compounds and, improperly, often also inorganic compounds.

The application contexts in which The Jonix NTP technology has been tested and where the VOC abatement effectiveness in the previous tables was assessed are as follows:

NTP pilot plants for the abatement of odorous emissions of hazardous solid waste (VOCs and inorganic compounds - H<sub>2</sub>S, NO<sub>x</sub>, NH<sub>3</sub>...)

NTP pilot plants for the abatement of odorous emissions in civil and industrial wastewater treatment plants (various VOCs and inorganic compounds - H<sub>2</sub>S, NO<sub>x</sub>, NH<sub>3</sub>...)

NTP treatment systems for highly odorous/irritating organic substances (carboxylic acids: acetic acid, propionic acid, butyric acid...)

NTP pilot plants for VOC abatement in industrial painting and varnishing systems (toluene, ethyl acetate, butyl acetate...)

NTP treatment systems of post-combustion exhaust gases (diesel combustion engine exhaust gas): SO<sub>x</sub>, NO<sub>x</sub>, CO...

## ATTACHMENT 12.7

*Test evaluating the effectiveness of micro-organism reduction that have been intentionally inoculated into plates by using the Jonix Mate air ionization system*

## Technical report

Test protocol for assessing the effectiveness of the reduction of micro-organisms intentionally inoculated in plates using the Jonix Mate air ionisation system.

**Prof. Giuseppe Comi**  
**Department of Agri-Food, Environmental and**  
**Animal Husbandry Sciences, University of Udine, via**  
**Sondrio 2/a, 33100 Udine.**

**28 February 2016**

### **Introduction**

This protocol has been implemented to verify reduction of micro-organisms intentionally inoculated in culture media and exposed for predetermined periods of time to the effect of ionized air. A control test has been effected for each trial using the same inoculated media not subject to treatment.

### **Inoculated strains**

The following micro-organisms were tested:

- *Staphylococcus aureus* (Gram + , asporogenous, aerobe - facultative anaerobe)
- *Listeria monocytogenes* (Gram + , asporogenous, aerobe - facultative anaerobe)
- *Aspergillus niger* (fungus - Mould)
- *Kluyveromyces marxianus* (perfect form of *Candida pseudotropicalis*)
- Various micro-organisms in association (Enterobacteriaceae – Total bacterial count)

### **Materials and methods**

Various micro-organisms were directly inoculated in Plate Count agar (Oxoid, Italy) and Malt Agar (yeasts and moulds) (Oxoid, Italy), treated for various times 0 (control), 30, 60, 90, 120 min and 12 and 24 h with the ioniser. After treatment the plates were incubated at 25 °C for 2-5 days. After that the colonies that survived treatment were counted. The results were expressed in % of inactivation/decay.  $100 - (\text{Initial number} / \text{Final number} \%)$

### **Preparation of the microbial suspension and inoculation**

#### ***Staphylococcus aureus***

Inoculation consisted of 2 strains of *Staphylococcus aureus* from international collections (DSMZ 4910) and Collection of the Department of Agri-Food, Environmental and Animal Husbandry Sciences of the University of Udine (DIAL). Individual suspensions were prepared with one loop of *St. aureus* added to sterile peptone water (0.8% NaCl). The spectrophotometer evaluated optical density equal to 0.1 at 600 nm. In order to evaluate the load of each suspension, the same were diluted in sterile peptone water. After that 0.1 ml of each dilution was inoculated in Plate Count Agar (Oxoid, Italy). The plates were incubated at 37 °C for 48 hours and the grown colonies were counted. Each suspension contained on average approximately 10<sup>7</sup> CFU/ml. Decimal dilutions were carried out and 0.1 ml of dilution 10<sup>-3</sup> CFU/ml was spread in Plate Count Agar. The open plates were placed in the chamber with ioniser turned on 24 hours before. At the above time frames the plates were recovered and placed to incubate at 37 °C for 48 hours. 5 replicas (samples) were analysed at each interval.

#### ***Listeria monocytogenes***

Inoculation consisted of 2 strains of *Listeria monocytogenes*: *L. monocytogenes* , *L. monocytogenes* from International Collections and plants and stored in the Collection of the Department of Foodstuff Sciences of the Faculty of Agriculture of the University of Udine (DIAL). Individual suspensions were prepared with one loop of *L. monocytogenes* added to sterile peptone water (0.8% NaCl). The spectrophotometer evaluated optical density equal to 0.1 at 600 nm. In order to evaluate the load of each suspension, the same were diluted in sterile peptone water. After that 0.1 ml of each dilution was inoculated in Plate Count Agar (Oxoid, Italy). The plates were incubated at 37 °C for 48 hours and the grown colonies were counted. Each suspension contained on average approximately 10<sup>7</sup> CFU/ml. Five ml of each suspension were mixed and diluted in sterile peptone water and 0.1 ml of dilution 10<sup>-3</sup> CFU/ml was spread in Plate Count Agar. The open plates were placed in the chamber with ioniser turned on 24 hours before. At the above time frames the plates were recovered and placed to incubate at 37 °C for 48 hours. 5 replicas (samples) were analysed at each interval.

### ***Kluyveromyces marxianus***

*Kluyveromyces marxianus* was seeded in malt agar {Oxoid, Italy}, incubated at 25 °C for 3 days, then one colony was diluted in sterile peptone water {NaCl 0.1%, Peptone 0.8%, ater 1000 ml). The spectrophotometer evaluated optical density equal to 0.1 at 600 nm. In order to evaluate the load of the suspension, the same were diluted in sterile peptone water. After that 0.1 ml of each dilution was inoculated in plates containing Malt Agar {Oxoid, Italy). The plates were incubated at 25 °C for 3-5 days and the grown colonies were counted. The suspension contained on average approximately 107 CFU/ml. Decimal dilutions were carried out and 0.1 ml of dilution 10<sup>-4</sup> CFU/ml was spread in Malt Agar. The open plates were placed in the chamber with ioniser turned on 24 hours before. At the above time frames the plates were recovered and placed to incubate at 25 °C for 3-5 days. 5 replicas {samples) were analysed at each interval.

### ***Coliforms and Escherichia coli (environmental/faecal contamination)***

The inoculation consisted of 2 strains of *E. coli* isolated from flours and stored in the Collection of the Department of Foodstuff Sciences of the Faculty of Agriculture of the University of Udine {DIAL), one strain of *Pantoea (Enterobacter) agglomerans* of environmental origin. Individual suspensions were prepared with one loop of each micro-organism added to sterile peptone water {0.8% NaCl).

The spectrophotometer evaluated optical density equal to 0.1 at 600 nm. In order to evaluate the load of each suspension, the same were diluted in sterile peptone water. After that 0.1 ml of each dilution was inoculated in Plate Count Agar {Oxoid, Italy). The plates were incubated at 37 °C for 48 hours and the grown colonies were counted. Each suspension contained on average approximately 107 CFU/ml. Five ml of each suspension were mixed and diluted in sterile peptone water and 0.1 ml of dilution 10<sup>-3</sup> CFU/ml was spread in Plate Count Agar. The open plates were placed in the chamber with ioniser turned on 24 hours before. At the above time frames the plates were recovered and placed to incubate. 5 replicas {samples) were analysed at each interval.

### ***Aspergillus niger***

Spores, produced from colonies of *Aspergillus niger*, seeded in Malt agar {Oxoid, Italy) incubated at 25 °C for 5 days, were diluted in peptone water {NaCl 0.1%, Peptone 0.8%, ater 1000 ml). After homogenisation the spores, following dilution, were counted in Malt agar plates {Oxoid, Italy) and 0.1 ml of dilution 10<sup>-3</sup> were spread in Malt Agar plates. The open plates were placed in the chamber with ioniser turned on 24 hours before. At the above time frames the plates were recovered and placed to incubate at 25 °C for 3-5 days. 5 replicas {samples) were analysed at each interval.

Ozone concentration was also measured during treatment in order to evaluate the healthiness of the method.

### ***Ioniser model used***

A Jonix Mate ioniser model by the company Jonix srl was used. Viale Spagna 31-33, 31020 Tribano {PD). The ioniser, placed in a food grade cold store room of approximately 60 m<sup>3</sup> {6x3.6x 2.70 m) kept at average temperature of 15 °C., had been switched on 2 days prior to the start of the experimentation in order to eliminate interference due to air contamination in the cold store room. The open plates were positioned on metal shelves and subject to treatment leaving the ioniser on throughout the tests.



### **Results**

The outcome of the tests are outlined below. The figures are the approximate average result of five plates. The data are expressed in UFC/ml in 90 mm plate.

Table 1: Change in concentration of *Staphylococcus aureus*

Time min/h	Average UFC/ml	st. dev.	% decrease
0	58400000	10822199.41	
30	31320000	7121235.84	37.1
60	34100000	3090307.42	31.5
90	21640000	3710525.56	56.5
120	4600000	854400.37	90.8
12 h	40000	89442.71	99.9
24 h	0	0	100.0

Key: st. dev.: standard deviation

Table 2: Change in the concentration of *Listeria monocytogenes*

Time min/h	Average UFC/ml	st. dev.	% decrease
0	65280000	1752712.18	
30	65080000	7150314.67	0.3
60	51360000	25677772.49	21.3
90	3520000	1605303.71	94.6
120	2006000	1080823.76	96.9
12 h	980000	752994.02	98.5
24 h	960000	409878.03	98.5

Key: st. dev.: standard deviation

Table 3: Change in the concentration of *Kluyveromyces marxianus*

Time min/h	Average UFC/ml	st. dev.	% decrease
0	2184480	505268.19	
30	2292400	622791.13	4.9
60	2336000	782642.95	6.9
90	2266000	979938.77	3.7
120	2158000	864823.68	1.2
12 h	0	0	100.0
24 h	0	0	100.0

Key: st. dev.: standard deviation

Table 4: Change in the total bacterial count

Time min/h	Average UFC/ml	st. dev.	% decrease
0	70240000	7029082.44	
30	63420000	3692153.84	9.7
60	82480000	16818799.01	17.4
90	54800000	10471867.07	21.9
120	57960000	16288277.99	17.5
12 h	0	0	100.0
24 h	0	0	100.0

Key: st. dev.: standard deviation

Table 5: Change in the concentration of *Aspergillus niger*

Time min/h	Average UFC/ml	st. dev.	% decrease
0	1300000	200000	
30	740000	54772.25	43.1
60	1000000	519615.24	23.1
90	1000000	353553.39	23.1
120	1260000	421900.46	30.8
12 h	360000	207364.41	72.3
24 h	180000	130384.04	82.7

Key: st. dev.: standard deviation

#### Comment on results

As may be inferred from the results of the above mentioned tests, the microbial reduction obtained with the Jonix Mate air ionisation system on surfaces simulating organic material inoculated with various microbial strains is high and allows most inoculated strains to be completely inhibited within 12 - 24 hours. In fact in many cases the reduction obtained is higher than 95%. The microbial reduction effect of ionised air is similar both on Gram positives and Gram negatives as well as on yeasts and moulds, although the effectiveness often appears to depend on the species considered, specifically:

- 1) *Staphylococcus aureus* (Table 1). This micro-organism is typical of human and animal mucosa. It is a potential pathogen, since the species includes enterotoxin-producing strains (A, B, C, D, E, F). Enterotoxin A seems the most widespread one at food level. In fact it has been the culprit in a number of poisoning cases since it is produced -- like the other enterotoxins -- in food stored in thermal abuse. Foodstuff may be naturally contaminated by *Staphylococcus aureus* or come into contact with it due to human manipulation and contaminated environments and equipment. In the event of development the toxin persists since it is thermostable hence it is not eliminated by pasteurisation and/or cooking. Using the ionising treatment assures complete inhibition of said micro-organism. In fact, continuous inactivation over time is observed (Table 1). In fact after 2 hours reduction is 90% and 99.9-100% at 12 and 24 hours.
- 2) *Listeria monocytogenes* (Table 2). This is an environmental origin psychrotrophic micro-organism. It contaminates any environment and consequently any food either as ingredient or finished product (Cocolin et al., 2005). Its presence in foodstuff (ready to eat) is regulated by microbiology criteria set out in Reg. EC 2073/05 and 1414/08, since it is a pathogen and highly virulent. Every year, in fact, a number of listeriosis cases are reported (0.4/100,000 inhabitants) following consumption of food products. Consequently, the food industry uses a number of technologies to eradicate or prevent its presence in food, as well as to prevent its



growth. The Jonix system assures reduction already after 90 min of 94% of *L. monocytogenes* present, and at 12-24 hours reduction is greater than 98%. To achieve total eradication (100%) prolonged treatment is required (36 hours).

- 3) *Kluyveromyces marxianus* (Table 3). *K. marxianus* is an innocuous yeast, considered as the perfect form of *Candida pseudotropicalis*; which, however, is a recognised pathogen, although less virulent than *Candida albicans*, a typical pathogen of human and animal mucosa. It is widespread in nature, particularly in milk and fermented milk (i.e. Kefir). It is used in the production of bio-ethanol. This yeast is particularly resistant to short ionising treatment (< 120 min). However, its presence may be eradicated from organic substrates after 12/24 hours of treatment, as effectively reported in table 3.
- 4) Total bacterial count (Table 4). For an assessment of the effect of the ionising treatment on the total bacterial count various micro-organisms typical of faecal (*Escherichia coli*) and environmental (*Pantoea agglomerans*) contamination were used. Also in this case treatment shorter than 120 minutes do not lead to significant reductions, while treatment of 12 and 24 hours lead to complete eradication of the 2 species considered.
- 5) *Aspergillus niger* (Table 5). Mould (fungus) of environmental origin and typical of vegetables, even if it has often been isolated on the surface of cured meats. It features mycotoxigenic strains. In fact black aspergilli may produce Ochratoxin A and B; Ochratoxin A is undesirable in foodstuff as it has been classified by IARC (International Agency for Research of Cancer) in group "2B" as a possible carcinogen. A number of studies, in fact, have proved its teratogenic, neurotoxic, genotoxic, immunotoxic and nephrotic properties (IARC, 1993; JEFCA, 2001). As a matter of fact in Italy the limit of 1 µg/Kg has been suggested for its presence in meat and meat-based products (Circular of the Ministry of Health no. 10-09/06/1999). Ionisation is conducive to variable reduction of said micro-organism, linked to the treatment time. In fact 12 or 24 hours are required to reduce 72 and 82 % of the *A. niger* load inoculated in organic media. To achieve complete inactivation of inoculated spores a 36-48 hour treatment is required.

#### **Conclusion**

The Jonix Mate system based on air ionisation makes it possible to inactivate microbial strains intentionally inoculated in organic culture media. The reduction percentage is strictly linked to the microbial species considered and the treatment time.

#### **Bibliography**

- Abarca, M.L., Bragulat, M.R., Castellà, G., Cabanes, F.J. (1994) Ochratoxin A production by strain of *Aspergillus niger* var. *niger*. Appl. Environ. Microbiol., 60 (7), 2650-2652.
- Cocolin, L., Stella, S., Nappi, R., Bozzetta, E., Cantoni, C., Comi, G. (2005) Analysis of PCR-based methods for characterization of *Listeria monocytogenes* strains isolated from different sources. Int. J. Food Microbiol., 103, 167-178.
- Comi, G., Iacumin, L. (2013) Ecology of moulds during the pre-ripening and ripening of San Daniele dry cured ham. Food Research Int. 54, 1113-1119.
- Comi, G., Lovo, A., Bortolussi, N., Paiani, M., Berton, A., Bustreo, G. (2005) Ionisers to decontaminate air in the production premises of San Daniele ham. Ind. Alim., XLIV, October, 1-9.
- Comi, G., Osualdini, M., Manzano, M., Lovo, A., Bortolussi, N., Berton, A., Bustreo, G. (2006) Decontamination of the surfaces of facilities and equipment used in foodstuff companies by using ionisers. Ind. Alim., XLV, June, 661-669.
- JEFCA, 2001. Ochratoxin A. First Draft 47 series.
- Iacumin, L., Manzano, M., Comi, G. (2012) Prevention of *Aspergillus ochraceus* growth on and Ochratoxin A contamination of Sausages using ozonated air. Food Microbiol., 29 (2), 229-232.
- I.A.R.C., 1993. Ochratoxin A. In Some naturally occurring substances: Food items and constituents, heterocyclic aromatic amines and mycotoxins. IARC Monograph on the evolution of carcinogenic risks to humans, vol. 56, pp. 489-521. Geneva: International Agency for Research on Cancer.

## ATTACHMENT 12.8

*Study of the sanitising power of a Jonix device applied to a commercial fan coil*

## Study of the sanitising power of a Jonix device applied to a commercial fan coil



**Pisa, February 2017**

## 1. Introduction

The experiment described below involved the performance of a series of tests aiming to verify the sanitising effectiveness at biological level of an NTP Jonix device installed inside a wall-mounted fan coil unit.

The purpose of the experiment is to test whether or not the production of oxidising species is able to solve the issue of pollution of certain parts of the equipment from moulds, and to sanitise the air of the premises in which it is installed.

### 1.1 Setup of the first test

The test was performed with the use of two twin devices placed in two rooms of the same size. A fan coil equipped with the NTP system was placed in the first room; an identical fan coil without any sanitising device was placed in the second room. Both devices were switched on at the minimum possible flow and were artificially polluted with moulds, after which they were activated and left to work for a time period of 7 days.

The pollution was applied to the impeller, before the NTP actuator. In fact, the impeller is one of the components where, in similar systems, it has been observed that moulds form and dirt in general is deposited.

Samples were taken at the end of the test period and the decrease was measured at two points:

- 1) **Directly on the fins of the impeller**, both because it is the most critical point and to check the effect of the release in the environment of sanitising molecules which are then conveyed again into the device, also sanitising the parts before the NTP generator;
- 2) **At the outlet**, to check, taking into account differences with the concentration of incoming pollutants, whether there was a direct decrease:

Parameters of the experiment:

- Room size: 25 m<sup>3</sup> (2.7x3.8x2.5)
- Fan coil model: ESTRO\_GT FL 7 – Galletti brand
- Sanitising device: Jonix Model “C/2”
- Recirculating air flow: 320 m<sup>3</sup>/h

### 1.2 Setup of the second test

The test was performed with the use of two twin devices placed at 2 points of a single large room. Both fan coils were equipped with the NTP system, with ventilation set at the highest possible flow.

The two fan coils were artificially polluted with moulds, after which they were activated and allowed to work for a time period of 15 days.

The pollutants were applied to the area downstream of the cooling block, downstream of the NTP actuator, to make it possible to evaluate the self-sanitising ability in another component at risk of microbial pollution.

Samples were taken at the end of the test period and the decrease was measured at two points:

- 3) **Directly on the area contaminated with moulds**, to evaluate the sanitisation of the part downstream of the NTP generator;
- 4) **At the centre of the room**, to evaluate the degree of environmental contamination.

Parameters of the experiment:

- Room size: approximately 250 m<sup>3</sup> (2.7x3.8x2.5)
- Fan coil model: ESTRO\_GT FL 7 – Galletti brand
- Sanitising device: Jonix Model “C/2”
- Recirculating air flow: 640 m<sup>3</sup>/h for each device

## 2. Materials and methods

### 2.1 Microorganisms used

To ensure the presence of contaminating microorganisms inside the devices, since the two machines used for the experiment were brand new, they were contaminated with a solution containing 10<sup>6</sup> CFU/ml of *Aspergillus brasiliensis* spores, applied with a cotton swab.

The microorganism selected, *Aspergillus brasiliensis* (*ex niger*), is a mould that is typical of domestic environments, especially in more humid locations, and is one of the main culprits behind the formation of black stains on the walls of certain rooms. During previous experiments this mould was found in large amounts inside the ventilation rotors of fan coils used for many hours every day.

Fungal spores are resistant structures that persist in the environment for long periods of time, even under adverse circumstances, such as the lack of water. **The use of spores guaranteed the near-constant presence of contamination levels throughout the experiment; it also made it possible to evaluate the sanitising effects on hard-to-eradicate microbial forms.**

### 2.2 Sampling and microbiological analyses

#### 2.2.1. Sampling methods

The following sampling methods were applied in order to determine the microbial loads:

- 1) **SAS (Surface Air System) Super 100** (International PBI): the method makes it possible to determine the quantity of airborne microorganisms and to evaluate any decrease kinetics over time. Figure 1 shows a sampling stage performed during the experiment. The SAS instrument was placed in front of the fan coil, at a distance of 50 cm from the vents.

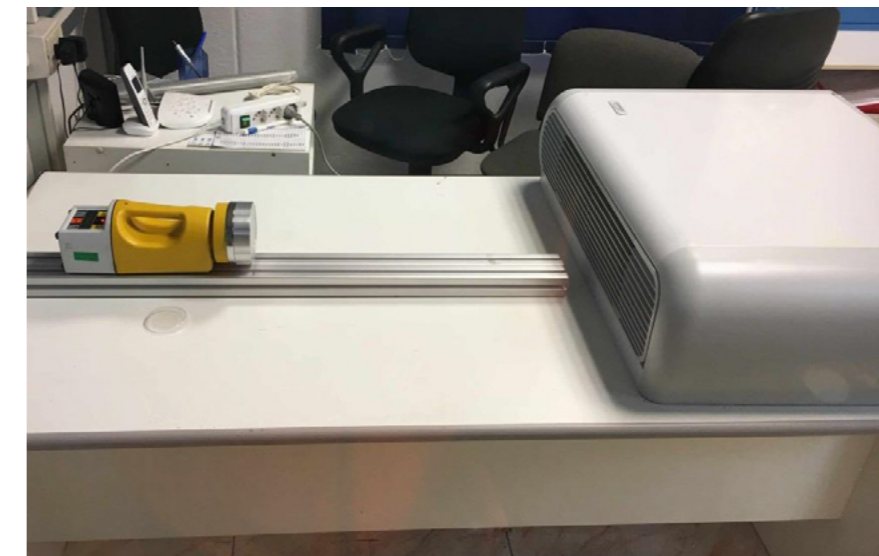


Figure 1 - harvesting of aerosol with the use of SAS Super 100

- 2) **Surface swab**: it makes it possible to evaluate the degree of surface contamination (in the first experiment, the fins of the fan coils' ventilation system): samples were harvested (figure 2) from both sides of a single fin, subsequently marked so as not to harvest from the same fin in subsequent sessions.

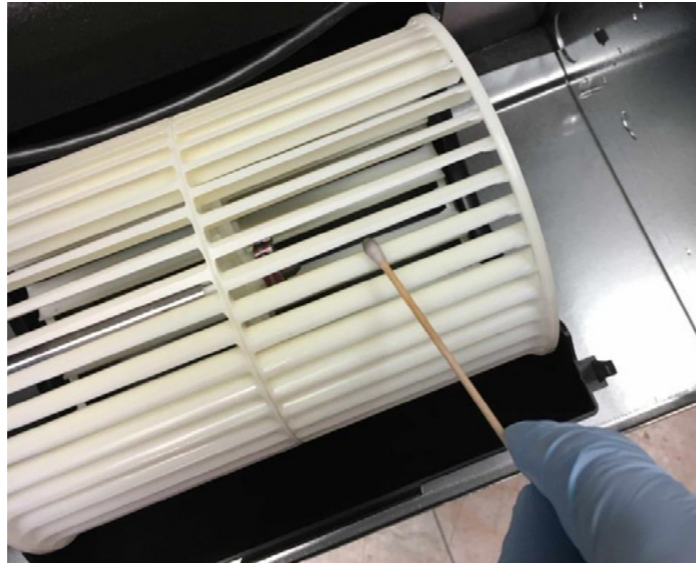


Figure 2 - harvesting microorganisms with the use of a surface swab

### 2.2.2. Analytical methods

The following official analytical methods were used to determine the microbial species:

#### Aerosol:

- Total bacterial load: Method Unichim 1962-2:2006
- Moulds and Yeasts: Method Unichim 1962-2:2006

#### Surfaces:

- Moulds and Yeasts: ISO 18593:2004 + ISO 21527-1:2008

### 2.3 Measurement of ozone levels

The levels of ozone produced inside the room where the Jonix device was installed were measured at the same time as the test.

The concentration values were measured with a Horiba - model APOA 370 measuring device. The instrument's reading range varies from 10 ppb to 3 ppm.

The measurement was launched at time zero and continued for 24 hours thereafter, in order to evaluate the accumulation kinetics and the ozone saturation levels.

## 3. Results and discussion

### 3.1 First experiment

#### 3.1.1. Experiment rooms

The twin rooms in which the experiment took place were two offices inside a shed where pilot tests of various types are performed, including tests on naturally contaminated matrices, such as compost and waste water, which is why significant environmental microbial contamination was anticipated, confirmed by the samples harvested at the start of the experiment.

In order to prevent interference due to the contamination of the external environment, the rooms were kept closed for the entire duration of the tests. To take the periodic samples, the operator entered the room quickly, and immediately closed the door. During the harvesting operations, the operator wore a coat, gloves and a respiratory mask, so as to minimise the microbial contribution linked to their presence in the room.

#### 3.1.2. Contamination of the devices

The first experiment entailed contamination with moulds of the ventilation rotors' blades (figure 3).

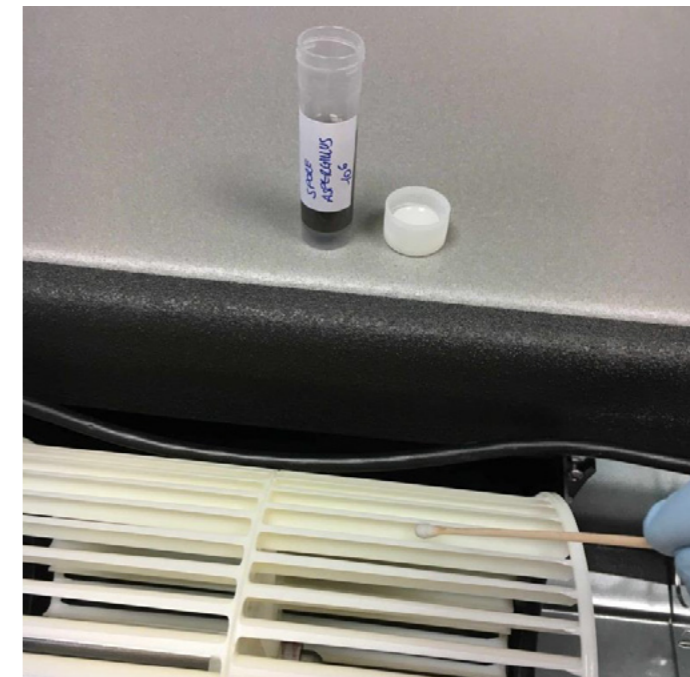


Figure 3 - contamination of the ventilation fins with fungal spores

All ventilation blades were contaminated on both sides, which entailed the consumption of approximately 3 ml of spore solution for each device, for a total of approximately 3 million fungal spores per fan coil.

#### 3.1.3. Analysis of the aerosols

Table 1 below shows the measurements of the bacterial loads (TBL) found in the aerosols harvested at various time intervals from the two experiment rooms. The "control" room contained the fan coil without a sanitising device; the "device" room contained the device equipped with the Jonix sanitising system.

Table 1 - Total airborne bacterial load at various times

Time (hours)	Total microbial load at 30 °C (CFU/m <sup>3</sup> )	
	Control	NTP device
0	520	620
3	540	600
6	470	540
24	450	190
48	400	30
72	380	20
120	260	50
144	260	20
168	240	50

The graph below (figure 4) shows the results obtained.

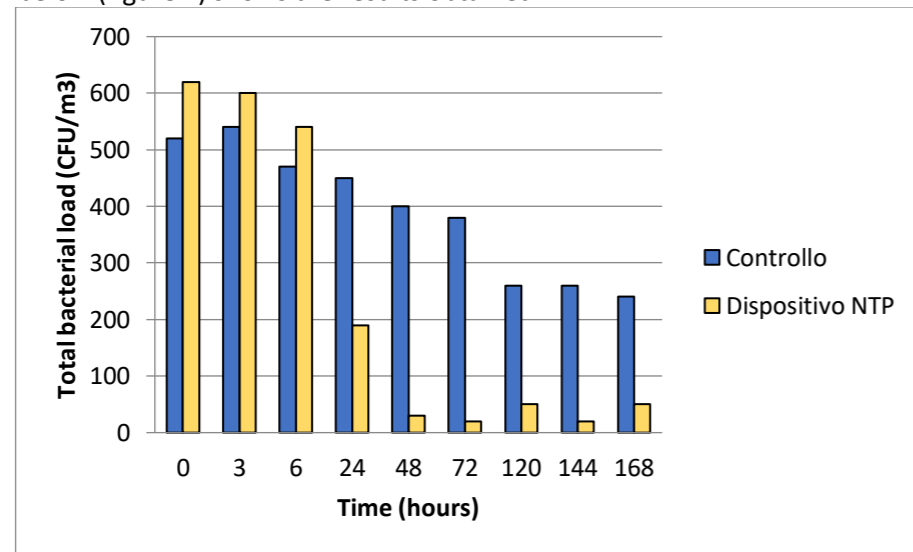


Figure 4 - Measurements of the airborne TBL in the two test rooms

It is possible to observe from the graph that the total airborne bacterial load tends to decrease inside the room that contains the fan coil equipped with the Jonix device. The slight decrease detected in the control room is attributable to the fact that the room was kept closed, hence isolated from the external environment, source of environmental contamination. Airborne microorganisms, especially bacteria, tend to lose viability due to phenomena such as dehydration or to form sediments together with the particulate matter by which they are often vehiculated; that is why, in the absence of new contamination sources, their concentration tends to decrease.

Table 2 below summarises the data pertaining to fungal contamination (moulds and yeasts) detected at various harvest times.

Table 2 - Moulds found in the air at various points in time

Time (hours)	Moulds (CFU/m <sup>3</sup> )	
	Control	NTP device
0	250	280
3	260	250
6	230	260
24	190	180
48	200	40
72	170	20
120	160	50
144	140	30
168	160	50

The graph below (figure 5) shows the results obtained.

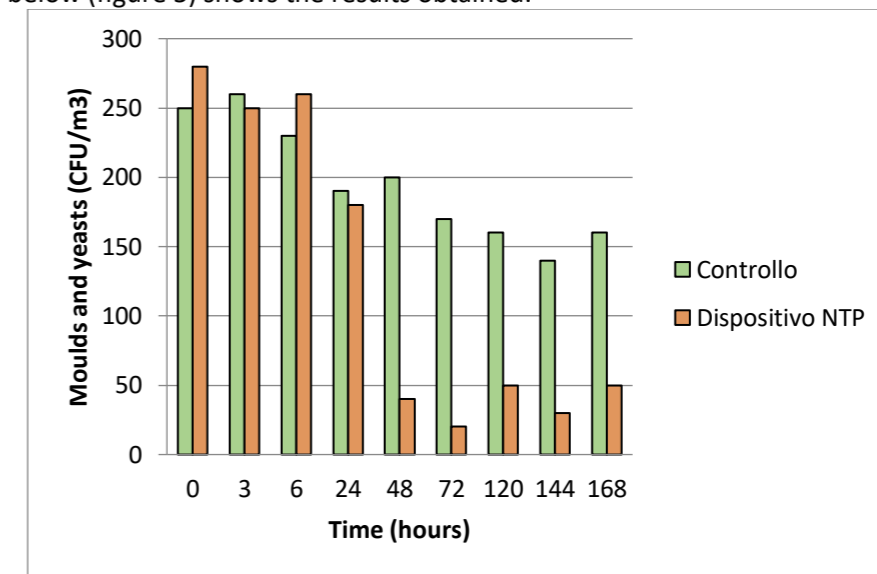


Figure 5 - Airborne moulds and yeasts in the two test rooms

From the graph it is possible to observe that moulds tend to decrease in the air of the room containing the fan coil equipped with the Jonix device, with different kinetics from those found for bacteria.

In fact, in the case of moulds, the time required to detect a significant decrease is longer, probably due to the greater resistance of the fungal spores compared to bacterial cells.

The slight decrease observed in the control room is attributable to the fact that the room was kept closed, hence isolated from the external environment, source of environmental contamination. That is why over time one sees a "sedimentation" of airborne contaminants or a loss of their viability, a phenomenon which, in the case of moulds, is decidedly less obvious than in the case of bacteria.

It should be noted that the moulds used to contaminate the fins, although detectable on the rotor's surface even days from the start of the tests (see paragraph 3.1.4), represent a very small percentage of those found in the ambient air.

The photos below show the levels of mould contamination detected after 48 hours in the control room and in that containing the Jonix device. The photos show, even more than the figures, the marked difference in contamination between the two rooms; on the surface of the slides we can see

the number of fungi found in 100 litres of air, practically the quantity of air inhaled by an adult at rest in approximately 15 minutes.



Figure 6 - Airborne moulds and yeasts in the two test rooms (control room on the left)

### 3.1.4. Measurement of the contamination levels of the impeller fins

The table below shows the fungal contamination levels of a single fin in the control fan coil and in the one equipped with an NTP generator. The theoretical contamination introduced at the time of contamination was approximately 38,000 spores per fin; however, as it was done by hand, the value may vary due to the manual nature of the operation and the quantity of liquid deposited on the individual fin. The microbial contamination levels introduced on the fins were purposely very high, so as to evaluate the effects of the sanitising system in extreme conditions.

Table 3 - Moulds found on one fin at individual harvesting times

Time (days)	Moulds (CFU/fin)	
	Control	NTP device
0	35000	40000
3	34000	32000
5	30000	21000
7	27000	11000

The graph below (figure 7) shows the results obtained.

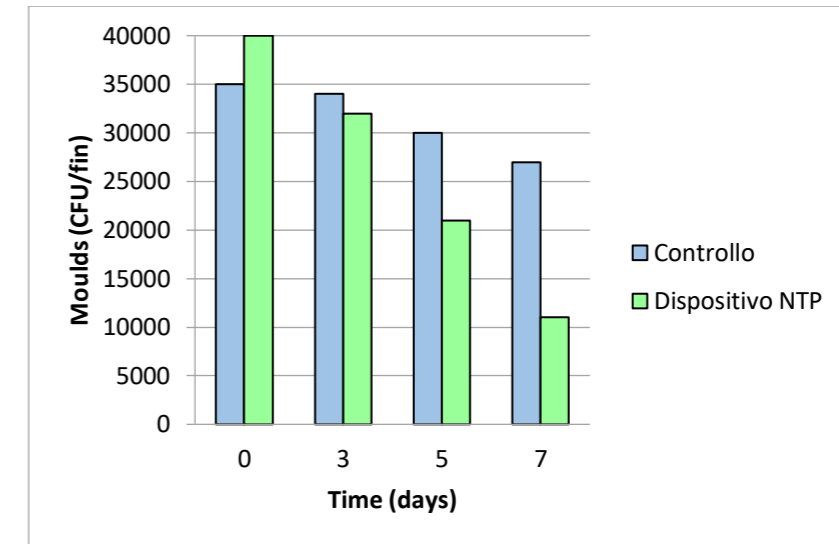


Figure 7 - Moulds found on a single fin at the various harvesting times

The levels of mould found on the fins of the control device tend to decrease due to the mechanical action of the whirling motion of the ventilation rotor, but, after 7 days, the number of spores decreases by just 20% approximately, while in the device equipped with an NTP generator, the observed decrease was over 70%. From these data, it is possible to deduce that approximately 50% of the fungal spores was killed by the oxidising species produced by the NTP generator.

The interpretation of the results should take into account the fact that the rotor is placed upstream from the NTP generator, which is why, due to the air flow generated by said rotor, the sanitising effect is due mainly to the oxidising species that return to the device after being released into the environment; hence the result obtained in a single week is certainly encouraging.

## 3.2 Second experiment

### 3.2.1. Experiment room

The large room in which the experiment took place is a service area next to offices, which is why the presence of rather low levels of environmental microbial contamination was expected, an assumption that was confirmed by the samples harvested at the start of the experiment.

As this was a large area, in order to guarantee a sufficient number of changes/hours (at least 5), 2 fan coils were used, equipped with an NTP device set to a flow of 640 m<sup>3</sup>/hour. The two devices were placed at 2 different areas of the room, so as to guarantee optimal treatment of the ambient air.

In order to prevent interference due to contamination of the external environment, the room was kept closed for the entire duration of the tests. To take the periodic samples, the operator entered the room quickly, and immediately closed the door. During the harvesting operations, the operator wore a coat, gloves and a respiratory mask, so as to minimise the microbial contribution linked to their presence in the room.

### 3.2.2. Contamination of the devices

In this case, a flat surface downstream from the NTP generator was contaminated (figure 8).

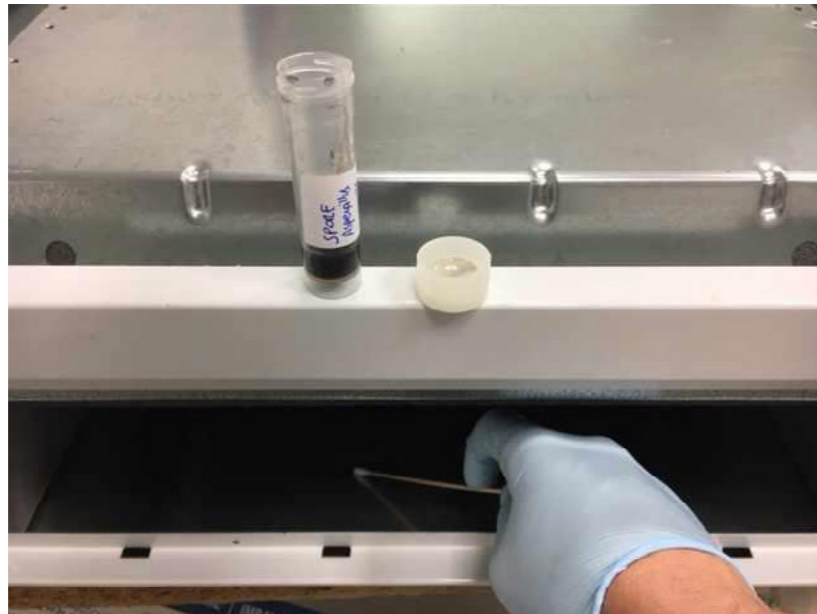


Figure 8 - contamination of the device with fungal spores

The area was contaminated with approximately 30,000 *Aspergillus brasiliensis* spores per surface square centimetre.

### 3.2.3. Analysis of the aerosols

Table 4 below shows the measurements of the bacterial loads (TBL) and Moulds found in the aerosols harvested at various intervals from the experiment room.

Table 4 - Airborne microbial contamination found at various times

Time (days)	TBL 30°C (CFU/m <sup>3</sup> )	Moulds (CFU/m <sup>3</sup> )
0	100	50
1	40	30
4	10	20
5	40	10
6	20	20
7	40	30
8	20	20
10	20	30
11	20	30
12	20	30

The graphs below (figures 9 and 10) illustrate the results.

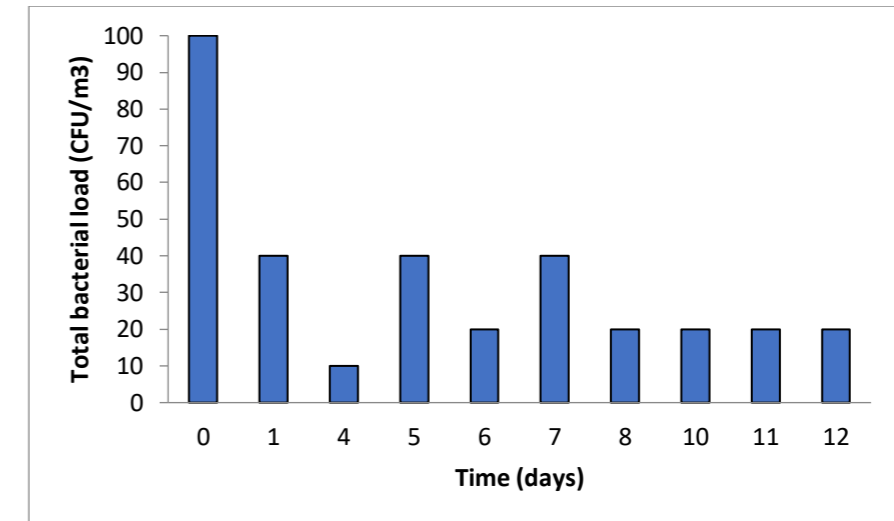


Figure 9 - Airborne TBL in the test room

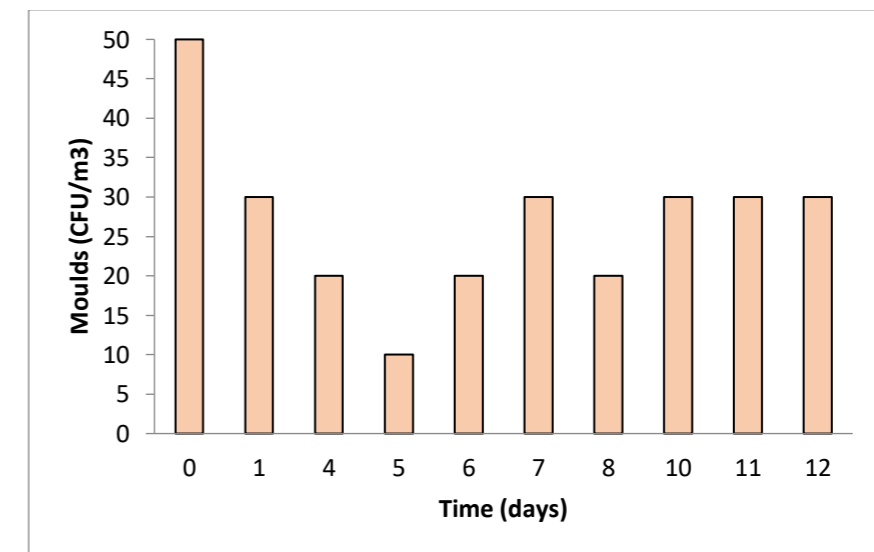


Figure 10 - Airborne moulds in the test room

Contrary to what was found during the first test, the environmental contamination values were very low already at the start of the experiment. Both TBL and Moulds decrease over time to stabilise at a “background noise” level, below which it is virtually impossible to go, since a totally sterile conditions cannot be reached.

### 3.2.4. Measurement of the contamination levels of the device’s interior

The Table below contains the average values of the samples harvested from 2 different areas of the interior surface of the device that was artificially contaminated with fungal spores.

Table 5 - Moulds found in the device at individual harvesting times

Time (days)	Moulds inside the device (CFU/cm <sup>2</sup> )
0	28800
1	26000
4	15000
5	9900
6	6900
7	5900
8	5200
10	4600
11	4000
12	3500

Figure 11 below shows the data in graphic form.

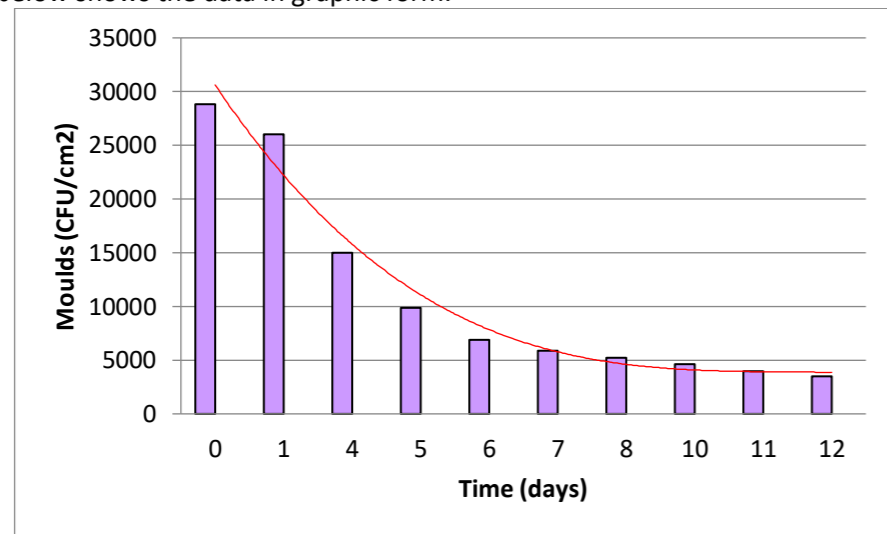


Figure 11 -- Moulds found inside the device

The fungal contamination decreases consistently, but the decrease curve (red line) shows a tendency to decrease its gradient over time. The contamination values at 12 days from the start of the test are, in any case, one-tenth of the initial values.

### 3.3 Brief experiment aiming to optimise the self-sanitisation process

The second experiment was extended by an additional 2 days (from day 12 to day 14), in order to identify a potential technical/system-engineering improvement that would make it possible to optimise the self-sanitisation process of the device containing the Jonix probe.

In practice, the still contaminated fan coils were left running for another 2 days with the same methods envisaged by the experiment described under point 3.2, with just one variation in the experiment:

- the ventilation device of one of the fan coils was switched off 3 times a day for 2 minutes, leaving the NTP generator switched on;
- during the 2 minutes that the fan was switched off, the ventilation rotor was switched on and off every 20 seconds (a total of 6 times).

In this way, during the 20 minutes of ventilation downtime, the oxidising substances accumulated in the immediate vicinity of the generator to then be conveyed in the adjacent areas, thanks to the rotor switch-on impulse; immediately switching off said rotor prevented the majority of the oxidising species from exiting the fan coil and allowed them to act on the moulds that were still present in the artificially contaminated area.

This strategy made it possible to accelerate the decrease process of the residual moulds, which, as you may remember, on day 12 still amounted to 3500 CFU/cm<sup>2</sup>.

The diagram below shows the levels of fungal loads inside the device in the 3 days of the experiment.

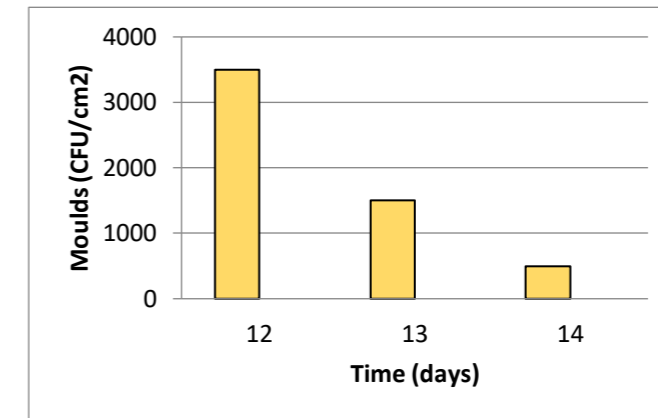


Figure 12 -- Moulds found inside the device

The diagram makes it clear that, in just 2 days, the contaminating moulds decreased from 3500 to 500 CFU/cm<sup>2</sup>.

The figure below shows the results obtained as a “coda” to the graph relating to the contaminating moulds detected during the experiment described under point 3.2.

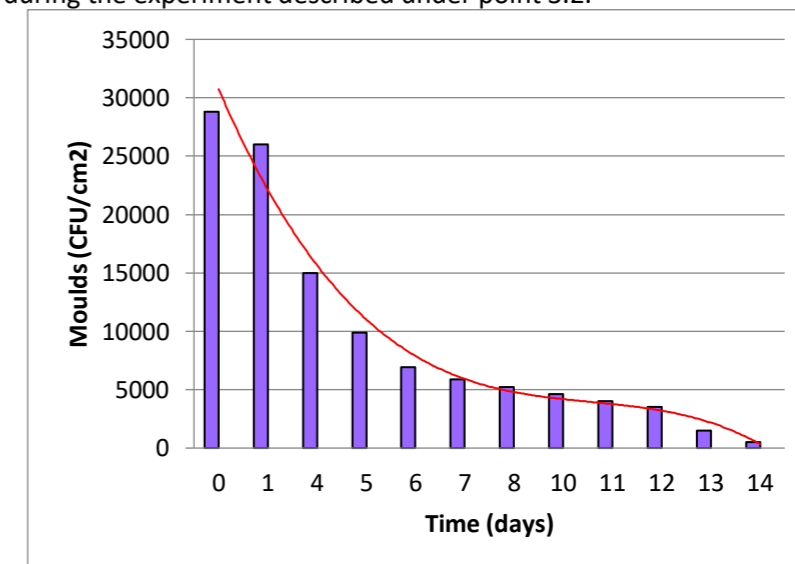


Figure 13 -- Moulds found inside the device

The data up to day 12 relate to the test described in paragraph 3.2, while the last 2 data (days 13 and 14) relate to the results obtained from the test described in this paragraph. It is interesting to observe that the trend line clearly changes its gradient, showing a significant acceleration of the microorganism reduction process.

This simple strategy was proven able to accelerate and optimise the instrument’s self-sanitisation process: measurements made with a Horiba measuring instrument showed that, in the 2 minutes



while the rotor was switched off, ozone concentrations inside the instrument (and just in that micro-environment) reached approximately 200 ppb, i.e. 10 times higher than those detected in normal operating conditions.

### 3.4. Measurement of ozone levels in the environment and at the air conditioning unit's outlet

#### 3.4.1. Measurement of the concentration of ambient ozone

The levels of ozone produced inside the room where the Jonix device was installed were measured at the same time as the test.

The Horiba analyser was placed at the centre of the test area to acquire the value of ozone levels during the test. Figure 14 shows the graph of the values acquired; each point represents the average of 30 minutes of acquisition.

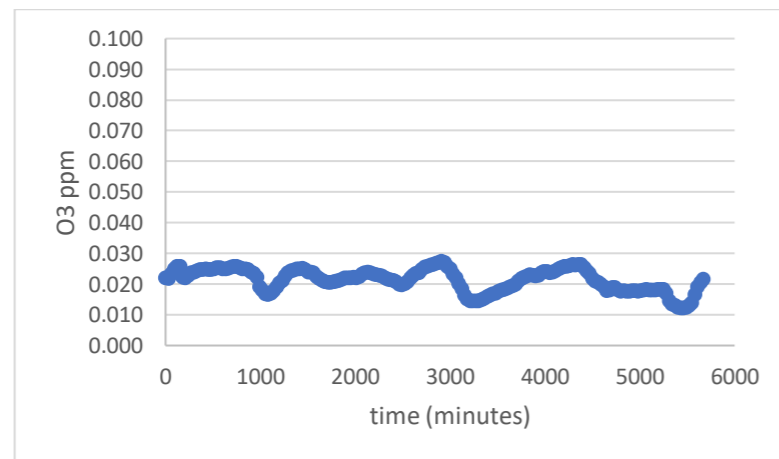


Figure 14 - ozone concentration curve

From the graph it is possible to observe that there are no significant changes in ozone levels, which remain constantly under 30 ppb and, in any case, close to the minimum detectable levels.

The slight oscillations that can be seen may be attributed to environmental factors (temperature, etc.).

#### 3.4.2. Measurement of ozone levels at the fan coil's outlet

The test was carried out to assess the uniformity in ozone distribution within the fan coil; as the pipe was placed laterally to the air flow that reaches it, one might reasonably anticipate a lack of evenness as illustrated.

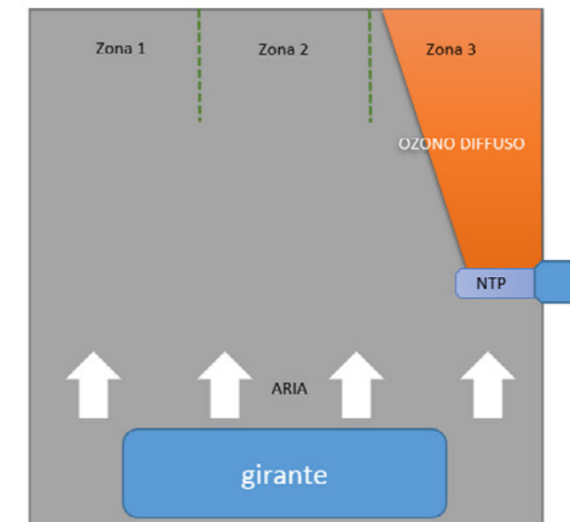


Figure 15 - hypothesis regarding ozone diffusion inside the fan coil

The outlet was, therefore, divided into three areas, as shown in the figure; the levels of ozone were measured in each area for approximately 40 minutes. The results are shown in Figure 16; each point refers to an average at three minutes of acquisition.

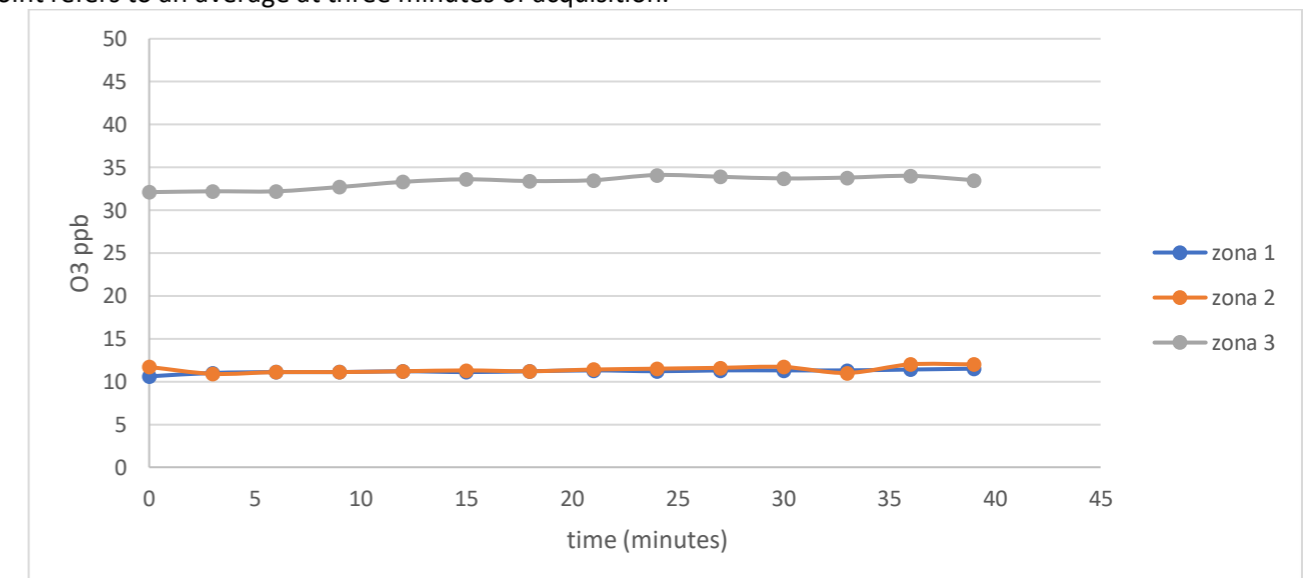


Figure 16 - ozone levels at the fan coil's outlet

The graphs show clearly that there is a marked concentration of ozone in Area 3.

## 4. Conclusions

The space used for the first experiment was selected because it featured a microbial contamination that may be defined as medium, certainly higher than the one to be found in a regularly cleaned and ventilated domestic environment or office. In fact, in planning the experiments' tests, one first aimed at assessing the effectiveness of the device in "unfavourable" conditions and, for this reason, the situation was further "aggravated" by artificially contaminating the ventilation impellers in the devices with moulds that are typically found in humid and unhygienic environments.

The results obtained show that the adoption of a Jonix sanitisation device makes it possible to obtain, over time, a marked reduction of the environmental microbial contamination from bacteria, as well as moulds and yeasts.

The kinetics of the decrease in microbial contaminants, be they bacteria, moulds, or yeasts, require at least 48 hours of continuous use of the device, keeping the room in which it is active closed; it is, therefore, to be expected that, if the device is used for a few hours per day, more time will be required to reach low levels of environmental contamination. On the other hand and as partial mitigation of this last statement, one should also take into account that the environmental conditions in which the experiment was carried out were purposely worse than those normally found in a “domestic” environment.

If the device is introduced in a space with low levels of environmental contamination, such as an office, the contamination levels are quickly reduced to very low values which we have called “background noise”, below which they may be reduced solely through the adoption of system-related strategies only required for specific spaces, such as the drug packaging white rooms (HEPA filters, positive pressure space equipped with an ante-chamber, etc.).

With regard to the device’s self-sanitising ability, the artificial contamination with moulds adopted in both experiments was purposely high, so as to evaluate the potential of the device also in very unfavourable conditions.

These conditions might occur after a fan coil without an NTP generator has been operating for a long time, while they are extremely unlikely to occur if a brand new device is equipped with an NTP generator which makes it possible to prevent the establishment and proliferation of such high levels of microbial contamination.

The adoption of a simple system-related strategy, such as the one described under point 3.3, might decidedly improve the instrument’s self-sanitisation process, without the need for costly technical modifications.

The data shown in paragraph 3.4, relating to the distribution of ozone levels inside the fan coil, imply that it would be worth considering placing the NTP generator at a different location inside the air conditioning system, so as to encourage a more homogeneous diffusion of the oxidising species it contains and releases.

In conclusion and based on the observations made during the experiment, it is possible to state that the adoption of an NTP generator inside a fan coil device may provide the double advantage of maintaining the quantity of airborne microorganisms at low levels – even in areas characterised by substantial environmental contamination – and of preventing the instrument from being contaminated by undesirable microorganisms, especially moulds.

## ATTACHMENT 12.9

---

*Evaluation of the sanitizing capacity of Photocatalytic devices in comparison with Jonix NTP systems*

**Experiment to assess the  
SANITISING ABILITY  
of  
Photocatalytic devices vs Jonix NTP Condensers**

## Table of contents

Foreword	146
Ozone measurements and number of ions	147
Test to ascertain the sanitising effect of the devices	149
Tests on exposed plate	151
Test with microbial bio-aerosol	157
Test to ascertain the sanitising effect of the devices on grown moulds	161

## Foreword

ARCHA Laboratories has set up an experimental study with the aim of assessing and quantifying the possible sanitising effect performed by two types of commercial devices (NTP-Jonix and a Photocatalytic device SHU900X), within a 12m-long steel duct of 30 cm in diameter, through which air flows, via a fan, at various speeds/flow rates.

The aim was to simulate what happens inside a ventilation duct in the event of microbiological contamination and depending on whether “sanitising” devices like the tested ones were installed or not.

To this end, ARCHA has designed and conducted a series of experiments in which various types and quantities of microorganisms were exposed in a controlled manner to air flows inside the pipe with different types of activated sanitising devices.

With regard to this type of test, since there are no technical standards of reference, ARCHA had to set up appropriate test procedures, and experimentally evaluate the most appropriate/functional operative conditions to study the phenomena and identify the setups to be implemented in terms of:

- Fan air flow rates
- Types and concentrations of the microorganisms to be tested
- Time frames and methods of contact with the sanitising systems

In terms of the air flow rate inside the test pipe, preliminary tests were conducted and it was ascertained that it was not possible to act in a controlled and reproducible manner with microorganisms and culture plates under high air flows like the ones typically reported by Dr.Marangon (2,000 m<sup>3</sup>/h).

For this reason the tests were set up and conducted with lower air flows (130 m<sup>3</sup>/h and 800 m<sup>3</sup>/h) and all the tests were conducted in a COMPARATIVE manner “NTP-Jonix vs. Photocatalytic” in order to obtain a relative reading of the phenomena (i.e. which of the 2 devices works best, the operative conditions being equal?) and thus being able to free oneself from the “realistic” nature of the operating conditions adopted.

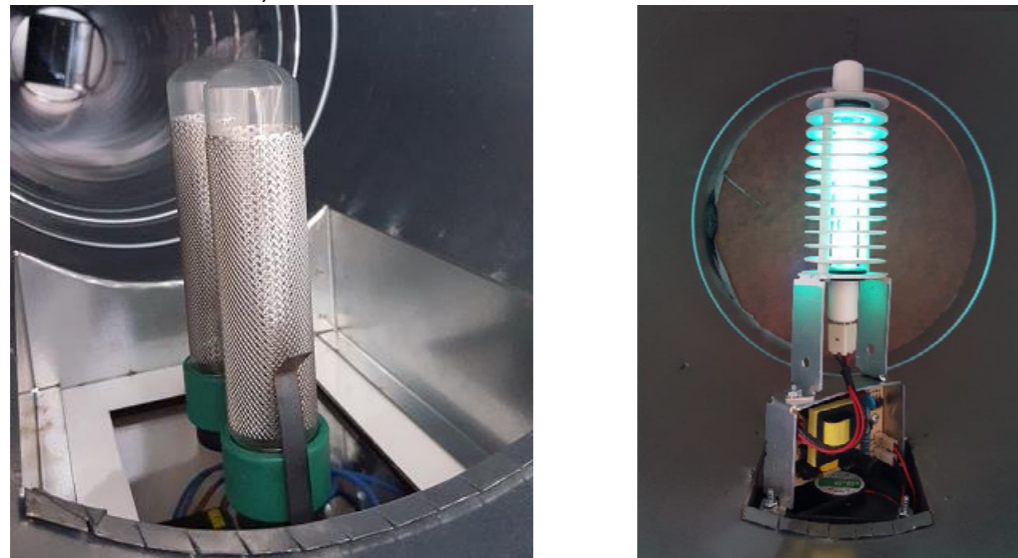
The test installation on which the tests were conducted consists of a square plenum within which an adjustable flow fan is installed, the range of which can be adjusted from 100 to 2000 m<sup>3</sup>/h. The air is conveyed from the fan into a round duct the diameter of which is 30 cm. In order to ensure the devices work in linear flow, the sanitisation systems were installed immediately downstream of a two-metre linear section, which was deemed sufficient to assure flow stabilisation, eliminating any turbulence due to air draft. The section of the system where the tests were conducted, behind the devices, consists of a 10m duct. The general diagram of the installation is shown in



Picture 1 - pilot installation layout

The following sanitising devices were tested in the experiments conducted by ARCHA:

- JONIX – NTP, set up with 2 pipes Model C;
- SHU - Model 900X;



Picture 1 - JONIX-NTP (left), SHU 900X (right)

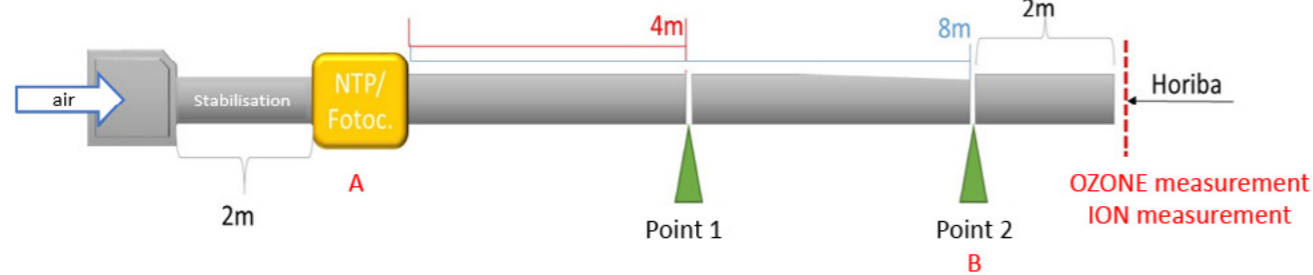
The **JONIX NTP** system is based on use of a barrier discharge system for generation of nonthermal plasma (NTP) which in its turn is able to produce the active species (Picture 1 – left).

The **SHU** system is based on a catalytic oxidation system promoted on a surface doped with a nano-Nickel catalyst and activated by a light source consisting of a UVC lamp (Picture 1 – right).

### Ozone measurements and number of ions

Measurements were conducted to quantify the ozone and ion concentration in the air when the sanitising devices covered by this study are activated.

The measurements were performed at the end of the 12m pipe, as pictured below:



The **ozone concentration** was measured by means of a continuous **HORIBA – APOA – 370** analyser, fitted with a suction probe placed at the air outlet point and in the middle of the pipe. The instrument’s reading range varies from 0,0001 ppm to 3 ppm.

The measurements were performed by setting up a 130m<sup>3</sup>/h flow rate (higher flow rates entail excessive dilution). In view of the unstable nature of ozone, as well as the low concentrations close to the instrument’s reading limit, the measurements were repeated five times and then averaged.

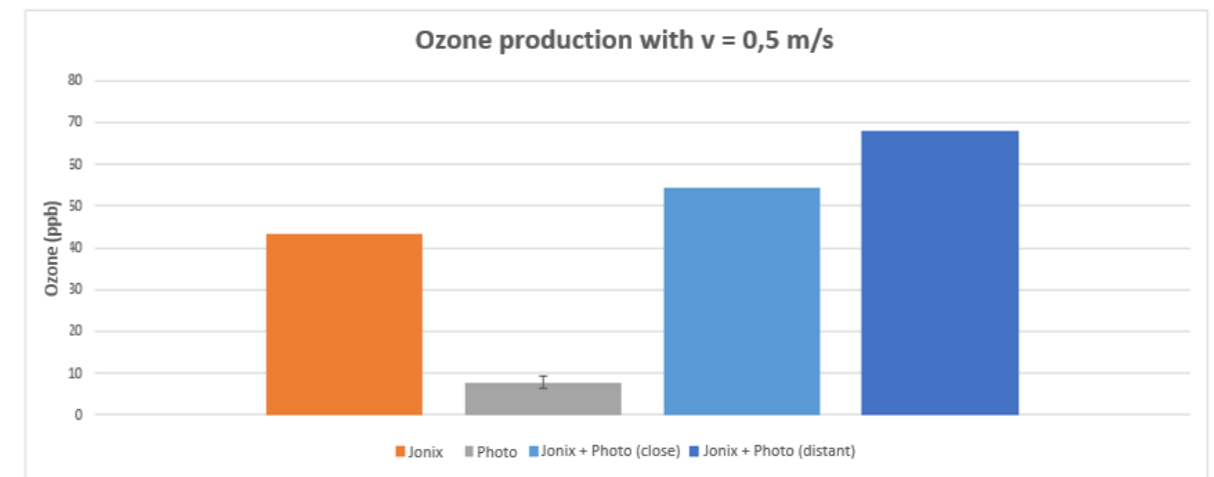
The tested sanitising devices were set up as follows (refer to the picture above):

- Jonix NTP device, positioned at point A;
- Photocatalytic device, positioned at point A;
- Photocatalytic + NTP JONIX device “close”, both at point A;
- Photocatalytic + NTP JONIX device “distant”, the NTP device is at point A, while the Photocatalytic system is at point B.

Table 1 shows the numeric results while the graph in Picture 2 illustrates the results obtained.

Table 1 - arithmetic average of ozone measurements

	Average (ppb)	Stand. dev.
Jonix	43	± 12
Photocatalytic	8	± 2
Jonix - photo (close)	54	± 7
Jonix - photo (distant)	68	± 3



Picture 2 – ozone measurements

The measurement of the **number of ions** in the air flow was conducted with an AlphaLab Inc. ion counter Mod. AIC, which is able to measure the density of ions in the air with a reading range from 10 ions/cm<sup>3</sup> (natural background concentration) up to 2x10<sup>6</sup> ions/cm<sup>3</sup>. The measurement was performed in the same sampling point used for the ozone measurements. It should be specified that the natural instability of ions means the measurements are affected by considerable uncertainty. The manufacturer indicates a 25% accuracy on the reading.

	Jonix	Δ	Photo	Δ	Jonix+ Photo	Δ
<b>Positive ions</b>	15,000	± 3750	400	± 100	15,000	± 3750
<b>Negative ions</b>	10,000	± 2500	10,000	± 2500	23,000	± 5750
<b>Total ions</b>	500	± 125	600	± 150	300	± 75

Picture 3 - ionic concentration (Ions/cm3) on outlet

The ion measurements are consistent with the reasonably expected values for the electrical devices used.

The following remarks can be made regarding the measurements:

- ✚ The photocatalytic system produces low quantities of ozone (< 10 ppb)
- ✚ The photocatalytic system produces slightly more ozone without photocatalyst (UV lamp only)

- The Jonix device with 2 C pipes produces 4 times more ozone than the Photocatalytic system (> 40 ppb)
- If the two systems are placed in series (Jonix + Photo or Photo + Jonix), either close or distant, the zone that forms is the sum of the ozone produced by the two devices: the Photo is unable to reduce the ozone produced by Jonix, on the contrary it produces ozone too.
- At the air flow rate normally used on real installations (500-2.000 m<sup>3</sup>/h) the ozone concentration is widely below the limits (50 ppb) even with the Jonix system
- The Photocatalytic system produces much fewer ions (+) than the Jonix system.
- The Photocatalytic system produces the same number of ions, even if «naked» (without photocatalyst)
- The combination of the 2 systems (Jonix + Photo) produces a number of ions that is the sum of the ions produced by the individual systems (ADDITIVE effect, as for the OZONE)
- Both the Jonix and the photocatalytic system produce «few» ions if compared with a “typical” ion generator (see the picture below):

Performance:	
• Ion density:	<b><math>3.1 \times 10^{12}</math> ions/cm<sup>3</sup> at 2.9 cm from emitter</b>
• High voltage output	9.5 Kv.
• Power use:	less than 1 watt
• Power requirements:	12VDC

Typical ion generator based on the “point” effect and its characteristic performance

Measurements have also been taken to quantify electrical consumption of the two sanitising devices: the table below sets out the measurements.

	Jonix	Photo
Power consumption (Watt)	13	11

The electrical consumption of the 2 devices are wholly comparable.

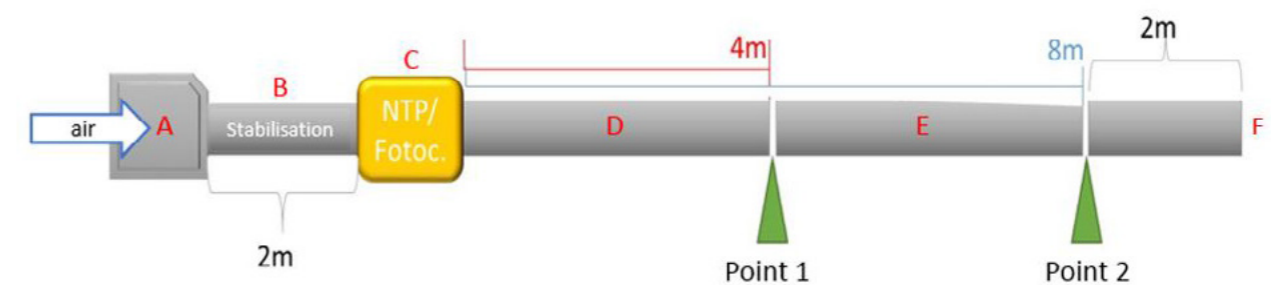
### Test to ascertain the sanitising effect of the devices

ARCHA Laboratories has set up an experimental study with the aim of assessing and quantifying the possible sanitising effect performed by two types of commercial devices (NTP-Jonix and a Photocatalytic device SHU900X), within a 12m-long steel duct of 30 cm in diameter, through which air flows, via a fan, at various speeds/flow rates.

The aim was to simulate what happens inside a ventilation duct in the event of microbiological contamination and depending on whether “sanitising” devices like the tested ones were installed or not.

To this end, ARCHA has designed and conducted a series of experiments in which various types and quantities of microorganisms were exposed in a controlled manner to air flows inside the pipe with different types of activated sanitising devices.

Specifically, the pipe simulating the aeration duct where the tests have been conducted is pictured below:



A fan (A) is able to generate air flows of different flow rate, hence different speed, inside the pipe. After a 2m section (B) required to stabilise the air flow, the tested sanitising devices have been housed (C).

The checks on microbiological contamination of the air were conducted at different points along the pipe: at Point 1 (4m after the sanitisation devices – section D), at Point 2 (8m after the sanitisation devices – section E), and at the pipe outlet (F).

In the tests conducted, two types of microbiological experiments were performed:

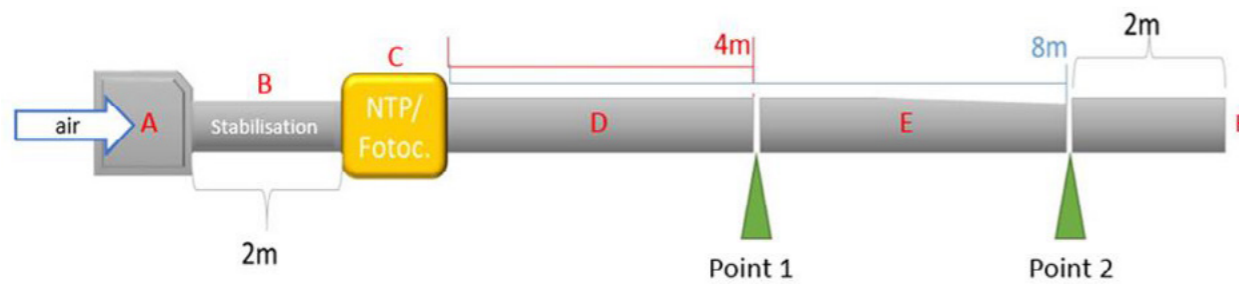
- Test on contaminated Petri plates, exposed to air flows inside the pipe;
- Test with bio-aerosol, continuously sprayed inside the pipe.

These types of test differ structurally and make it possible to provide different information on the phenomena at play:

- **Test on contaminated Petri plates, exposed to air flows inside the pipe (TESTS ON EXPOSED PLATE):** in this case, microbiological culture plates, contaminated by different types of microorganisms with known concentration, were exposed to a definite air flow inside the pipe, either activating the various sanitising devices or not. In this type of experiment, the following variables were investigated:
  - o The distance of the plates from the sanitising device (microbiological sampling was conducted at the following points: Point 1 and Point 2)
  - o The time of exposure to air and to the sanitising device (i.e. protracted measurements for different exposure times): the longer the Petri dishes remain exposed to the action of air, the better/greater the effect I should expect from any sanitisation

With this type of test, the microorganisms are in an extremely “favourable” environment, with large amounts of available nutrients (i.e. culture media), in the optimal pH conditions, in a sort of “cradle” that promotes their survival and growth, consisting of huge amounts of organic matter that might be an “interference”/“competitor” for the microorganisms in reactions with the “active” species generated by the tested sanitising devices. This test must therefore be considered a worst case scenario when it comes to assessing the effects of the devices being studied.

- **Test via bio-aerosol, sprayed continuously inside the pipe:** in this case, an aerosol of different microorganisms, at known concentration, is sprayed continuously inside the pipe, at the point shown in the picture below, at the same time as the air flow is activated.



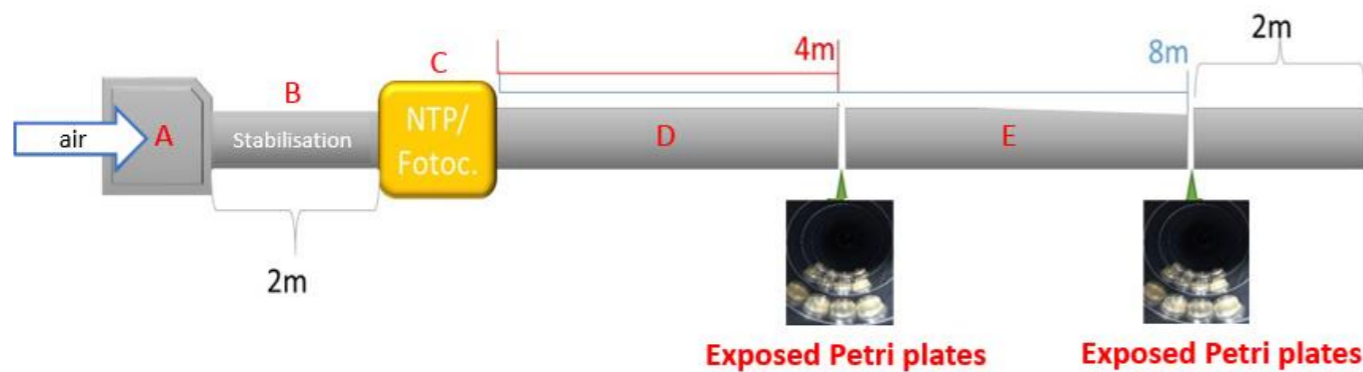
In this case, the dwell time of the microorganisms inside the pipe is a function of the air flow speed and pipe length. The microbiological sampling to evaluate the microbiological contamination of the air, in this type of setup, was conducted at the end of the pipe, at point F.

In this case, from the temporal start of the experiment, the sampling time is not a variable of the system: the time taken by the bio-aerosol to reach the end of the pipe is only a function of the air speed, as the air speed changes so does the contact time of the bio-aerosol with the species generated by the sanitising system.

The following paragraphs illustrate the results obtained in the various types of experiment conducted.

### Tests on exposed plate

The tests on contaminated Petri dishes, exposed to air flows within the pipe, were conducted according to the diagram pictured:



The experiments were conducted in the following experimental conditions:

- air flow rate = 130 m<sup>3</sup>/h ( speed = 0.5 m/sec)
- microbial concentration on the Petri dishes: 500 UFC/plate
- exposure time of the Petri dishes: 30', 1h, 90', 4h

The following microorganisms were tested:

- bacteria of 2 different types: Escherichia coli [gram (-)] and Staphylococcus aureus [gram (+)]

- moulds: Aspergillus brasiliensis
- yeasts: Saccharomyces cerevisiae

The following setups were tested in the experiments for the sanitising devices in question:

- no sanitising device on (control test, "Ctrl");
- photocatalytic device on;
- "naked" photocatalytic device: UV lamp on without nano-catalyst support;
- NTP device on
- both systems (Photocatalytic and NTP) on

The following tables show the results obtained with the tests conducted using 4h exposure time: the tests conducted with shorter contact times (30', 1h, 90') did not produce significant measurable results with neither tested device.

Each test was conducted in triplicate. The analytical results shown are therefore the average of the 3 different microbiological measurements.

### tests on BACTERIA:

Effect after 4 hours exposition with an air flow of 130 m <sup>3</sup> /h	Used microbic concentration: 500 UFC / plate	Reduction % of the microbic growth	
		gram (-) bacterium <i>E. coli</i>	gram (+) bacterium <i>S. aureus</i>
sanitizing treatment device	Distance from sanitizing device (m)		
None (Ctrl)	4	0	0
	8	0	0
Photocatalytic	4	56	15
	8	0	0
Photocatalytic "naked"	4	62	74
	8	8	52
NTP	4	0	71
	8	0	75
Photocatalytic + NTP	4	0	78
	8	0	79

The **Photocatalytic** device:

- Has medium activity on bacteria only «close» to the device: the effects are lost when moving away from it.
- It is more active on gram (-) microorganisms compared to the Jonix device
- If the photocatalyst is removed (UV lamp only), the biocidal activity increases, especially in the case of gram (+)

The **JONIX** device:

- Is not active on gram (-) microorganisms
- It is active on gram (+) microorganisms regardless of the distance from the device

There seems to be no **synergy** between the two systems (NTP + Photocatalytic)

**tests on MOULDS and YEASTS:**

Effect after 4 hours exposition with an air flow of 130 m <sup>3</sup> /h	Used microbic concentration: 500 UFC / plate	Reduction % of the microbic growth	
sanitizing treatment device	Distance from sanitizing device (m)	yeast	mould
		<i>S. cerevisiae</i>	<i>A. brasiliensis</i>
None (Ctrl)	4	0	0
	8	0	0
Photocatalytic	4	0	59
	8	0	57
Photocatalytic "naked"	4	-	56
	8	-	48
NTP	4	18	35
	8	17	47
Photocatalytic + NTP	4	0	42
	8	0	51

The **Photocatalytic** device:

- Is not active on yeasts
- is active on moulds
- If the photocatalyst is removed and only the UV lamp is used, the effect is essentially the same as with the intact photocatalyst

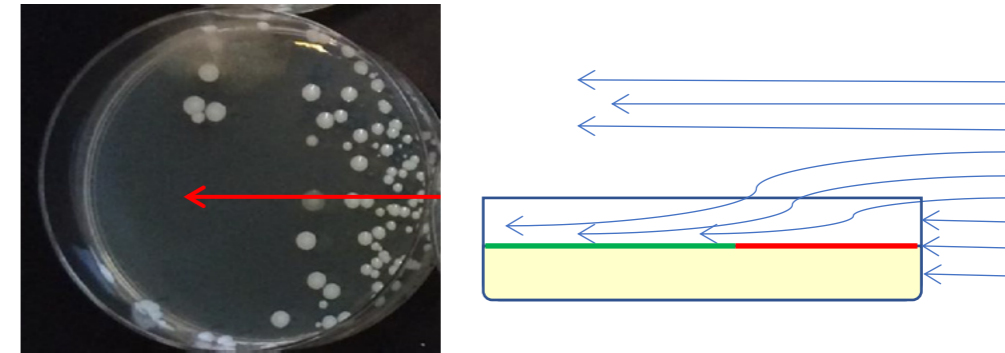
The **JONIX** device:

- Has weak activity on yeasts, regardless of the distance from the device
- Has medium activity on moulds, regardless of the distance from the device

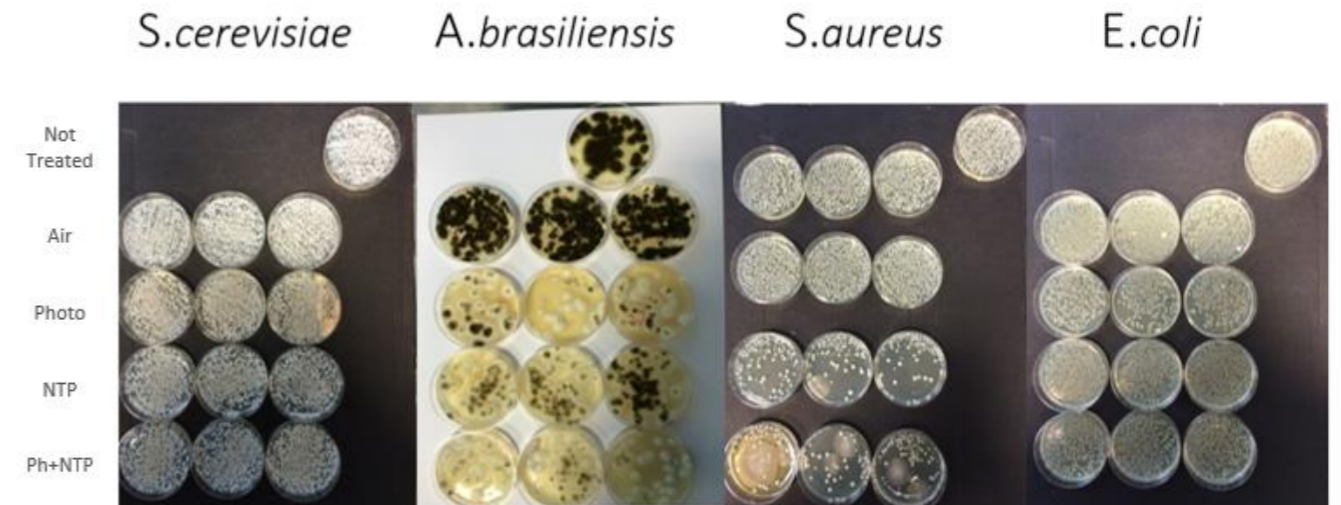
There seems to be no **synergy** between the two systems (NTP + Photocatalytic)

**REMARKS on PLATE TESTS:**

While conducting the experiments on PLATE, it was observed that the edge of the plate has a protective effect on the bacterial colonies from the flow of sanitising air, according to the diagram illustrated in the following picture:



The photographs below illustrate this effect in the tests, the results of which are set out above.





### IN DEPTH ANALYSIS of PLATE TESTS: tests on plates tilted by 30°

Following observation of the so-called “edge effect” caused by the plates on the bacterial colonies exposed to the flows of sanitising air, the PLATE exposure tests were replicated with the exposed plates tilted by 30°.

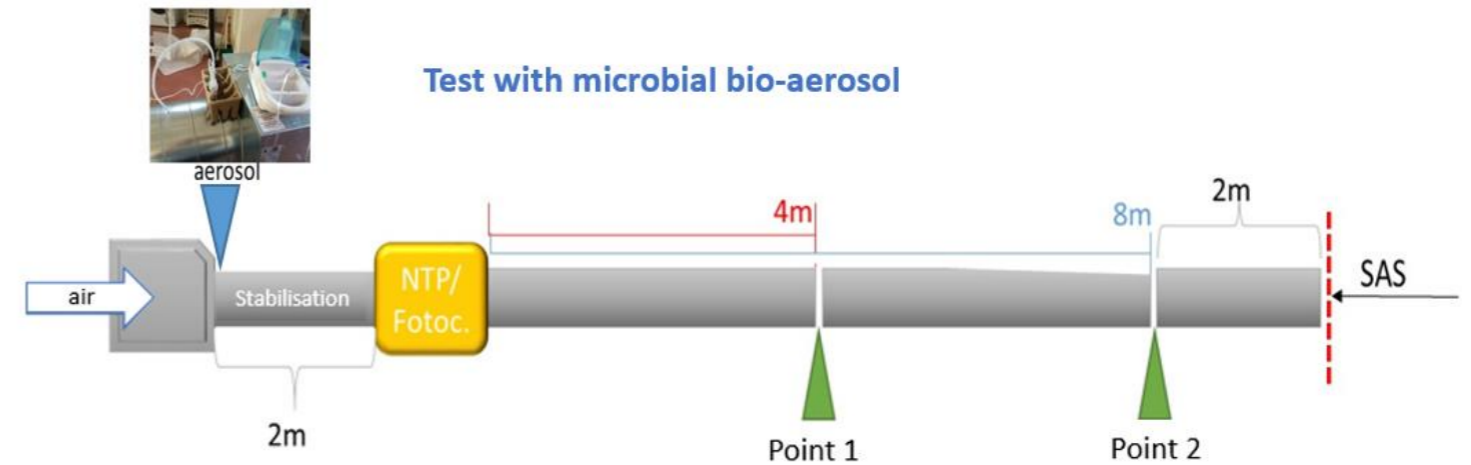
The results obtained are illustrated in the following table. Each test was conducted in triplicate. The analytical results shown are therefore the average of 3 different microbiological measurements.

Effect after 4 hours exposition with an air flow of 130 m <sup>3</sup> /h	Used microbic concentration: 500 UFC / plate	Reduction % of the microbic growth					
		gram (-) bacterium		gram (+) bacterium		mould	
		<i>E. coli</i>		<i>S. aureus</i>		<i>A. brasiliensis</i>	
		horizontal plates with "edge" effect	plates tilted by 30°	horizontal plates with "edge" effect	plates tilted by 30°	horizontal plates with "edge" effect	plates tilted by 30°
sanitizing treatment device	Distance from sanitizing device (m)						
NTP	4	0	0	71	79	35	35
	8	0	0	75	74	47	48
Photocatalytic + NTP	4	0	0	78	93	42	48
	8	0	0	79	82	51	64

The results obtained show that a slight tilt of the plates (30°) entails, in some cases, a weak increase in the sanitising ability of the air flow, but the differences are not large.

### Test with microbial bio-aerosol

The tests with microbial bio-aerosol, generated continuously through biomedical equipment and introduced into the pipe immediately downstream from the fan, were conducted according to the diagram pictured:



The following experiments were conducted:

#### TEST 1:

- air flow rate = 130 m<sup>3</sup>/h ( speed = 0.5 m/sec)
- bio-aerosol:
  - o bacteria = 70,000 UFC/min = 30 UFC/L air
  - o moulds and yeasts: 7,000 UFC/min = 3 UFC/L air
- sampling time: 30', 60', 90'

#### TEST 2:

- air flow rate = 130 m<sup>3</sup>/h ( speed = 0.5 m/sec)
- bio-aerosol:
  - o bacteria = 700,000 UFC/min = 300 UFC/L air
  - o moulds and yeasts: 70,000 UFC/min = 30 UFC/L air
- sampling time: 30', 60', 90'

#### TEST 3:

- air flow rate = 800 m<sup>3</sup>/h ( speed = 3 m/sec)
- bio-aerosol:
  - o bacteria = 700,000 UFC/min = 300 UFC/L air
  - o moulds and yeasts: 70,000 UFC/min = 30 UFC/L air
- sampling time: 30', 60', 90'

The following setups were tested in the experiments for the sanitising devices in question:

- no sanitising device on (control test, “Ctrl”);
- photocatalytic device on;
- NTP device on
- both systems (Photocatalytic and NTP) on

**REMARK:** in conducting the experiments described above, a recovery of microorganisms was observed (through SAS sampler) at the bottom of the 12m pipe, very low indeed: microbial recoveries are less than 10% of the sprayed microorganisms.

Hence the analytical results of tests 2 and 3, conducted with higher microbial concentrations than test 1, should be considered more “reliable” than those obtained with Test 1 itself.

The tables below set out the results of the tests conducted with the following microbial concentrations (Tests 2 and 3):

- bacteria = 700,000 UFC/min = 300 UFC/L air
- moulds and yeasts: 70,000 UFC/min = 30 UFC/L air

Each test was conducted in triplicate. The analytical results shown are therefore the average of the 3 different microbiological measurements.

⇒ It should be observed that with the SAS sampler, it is not possible to distinguish gram (+) from gram (-) bacteria: growth takes place in an undistinguishable manner on the same Petri dish. The test result is therefore expressed as total result “gram (+) + gram (-)”.

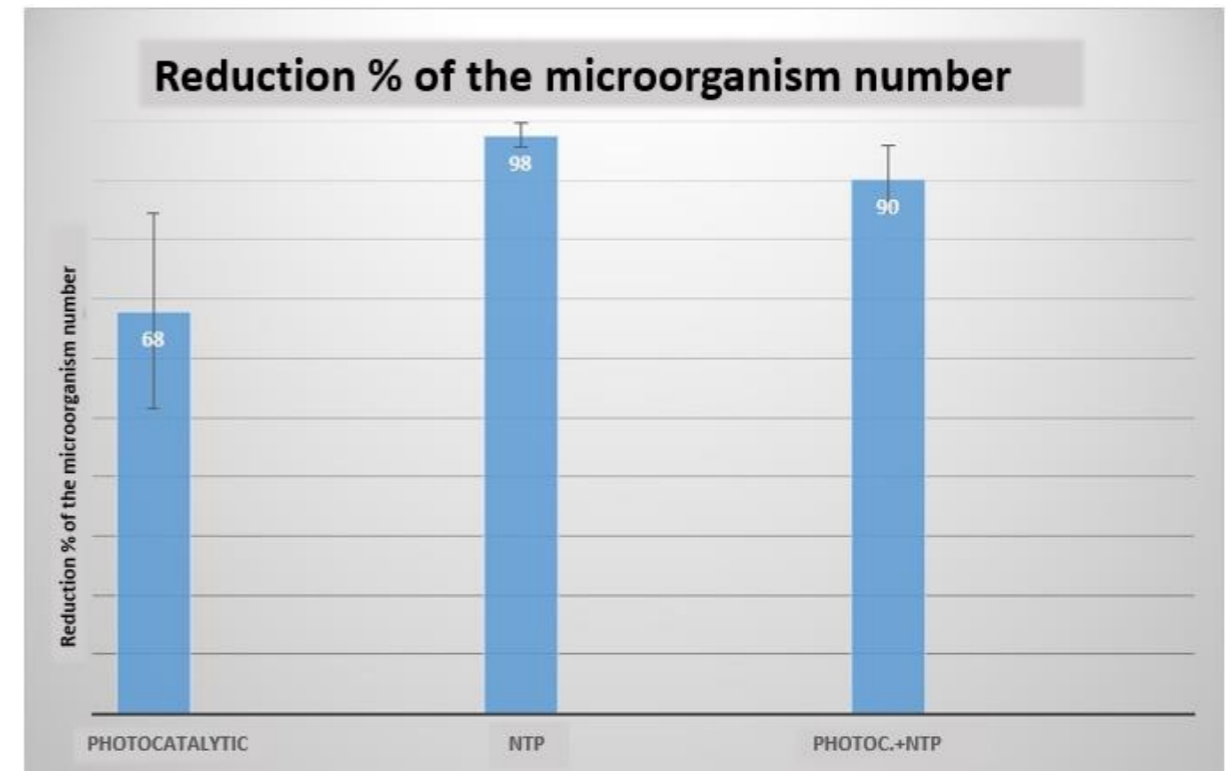
⇒ It should be observed that owing to the structure of the experiment, in this case, the time at which microbiological monitoring is conducted is not a variable of the system: the dwell time of the microorganisms inside the pipe is only a function of the air flow speed and pipe length. Hence sampling at different times by SAS should only be considered as repetitions of measurements conducted under the same experimental test conditions.

**TEST 2 - test on BACTERIA:**

Test 2	Reduction % of the micro-organism number			
130 m3/h	TOTAL BACTERIA (gram+ and gram-)			
Sanitizing device	Sampling time (min.)	Single measurement	AVERAGE	Standard deviation
Photocatalytic	30	50	68	16
	60	82		
	90	72		
NTP	30	100	98	2
	60	97		
	90	96		
Photoc.+NTP	30	84	90	6
	60	95		
	90	92		

The **Jonix NTP** system is **more efficient (+30-40%)** than the Photocatalytic system in the sanitising effect on TOT BACTERIA [gram (+) + gram (-)]

The following diagram shows the results obtained with the different sanitising devices tested.



**There is no synergy** between the Jonix system and the Photocatalytic system in the sanitising effect on TOT BACTERIA.

**TEST 2 - test on YEASTS:**

Test 2	Reduction % of the micro-organism number	
130 m3/h	<i>S. cerevisiae</i>	
Sanitizing device	Sampling time (min.)	Single measurement
Photocatalytic	30	100
	60	100
	90	100
NTP	30	100
	60	100
	90	100
Photoc.+NTP	30	100
	60	100
	90	100

Both the **Jonix NTP** and the **Photocatalytic** system prove to be **effective** in total reduction of yeasts.

Yeasts are not discriminating microorganisms to understand which of the 2 sanitising systems is more effective.

**TEST 2 - test on MOULDS:**

Test 2	Reduction % of the micro-organism number
130 m <sup>3</sup> /h	<i>A. brasiliensis</i>
Sanitizing device	Single measurement
Photocatalytic	50
	50
NTP	25
	25
Photoc.+NTP	25
	25

The **Photocatalytic** system is **more efficient** than the Jonix system in the sanitising effect on moulds.

**There is no synergy** between the Jonix system and the Photocatalytic system in the sanitising effect on MOULDS.

**TEST 3 - test on Bioaerosol:**

Test 3	Reduction % of the micro-organism number	
800 m <sup>3</sup> /h	<i>Bacteria (gram+ and gram-)</i>	<i>A. brasiliensis</i>
Photocatalytic	0	0
NTP	100	100
Photoc.+NTP	86	100

For high air flow rates (800m<sup>3</sup>/h) the **JONIX system is efficient (+100%)** both against bacteria and moulds.

**The Photocatalytic system** is wholly **inefficient** also against moulds, on which (test 2) it seemed to have a better action than NTP.

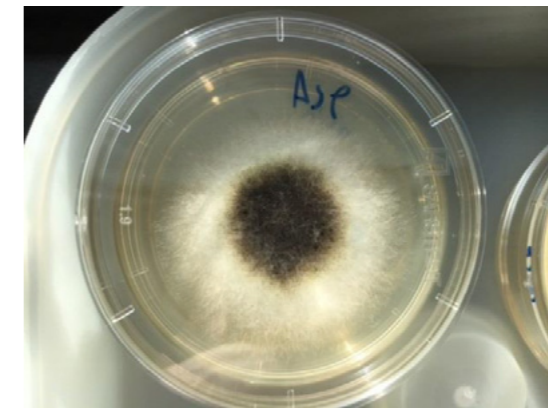
**There is no synergy** between the Jonix system and the Photocatalytic system in the sanitising effect.

**Test to ascertain the sanitising effect of the devices on grown moulds**

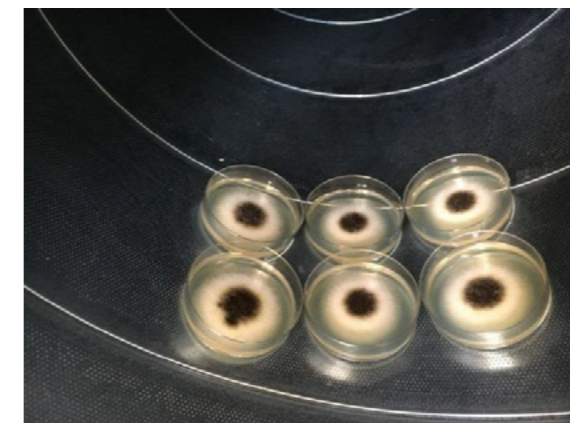
The aim of the test is to ascertain whether, and how long after installation of the sanitising device, inside an existing duct (and which has been contaminated for a long time), it is possible to observe an active sanitising action also on grown and developed microorganisms. The tests were performed on moulds (*Aspergillus brasiliensis*), as representatives of the microbial category ecologically most suitable to colonising this type of installation.

Fully grown moulds were placed inside the pipe and the air flow was activated (130 m<sup>3</sup>/h): the effect of the sanitising air produced by both technologies, is then verified on the grown moulds, at different exposure times (1, 2 and 4 days of exposure).

The microorganisms were inoculated about 4 days before the start of the tests, so as to allow the colonies to develop and the microorganisms to ripen the fruiting bodies containing the spores. In order to prevent the protection effects due to the edge of the plates, the moulds were inoculated in the centre of the plates in order to develop one single large central structure. The picture below shows one of the plates used for the test: the colony has developed away from the edges, the darker central part is the portion of mycelium that has developed the fruiting bodies, while the peripheral white crown is made up of a portion of mycelium consisting of hyphae but without any fruiting bodies.



The plates were placed in an intermediate point of the pipe, about 4 metres from the sanitising devices, and extracted at the 3 times envisaged by the test.



The viability of the microorganisms was assessed both for fruiting bodies and for hyphae, by taking portions of mycelium from the pigmented area containing the spores and from the clear one that did not have any with a sterile loop. This expedient was aimed at evaluating whether the antimicrobial

activity occurred on the vegetative portions – theoretically easier to attack – on resistance structures (spores), on both forms or on neither.

The portions of mycelium were inoculated on Sabouraud Agar and incubated at 25°C for 5 days. Since this was a qualitative test, aimed at assessing whether or not there were viable microorganisms, the exact number of microorganisms grown was not determined at the end of the incubation, but it was ascertained whether or not there were any fungal colonies.

The following table sums up the effects obtained by treatment with the photocatalytic device.

Exposure time	Portion of the mycelium	
	Spores	Hyphae
1 day	Viable	Viable
2 days	Viable	Viable
4 days	Viable	Viable

Whereas the following table shows the effects measured after treatment with the NTP device.

Exposure time	Portion of the mycelium	
	Spores	Hyphae
1 day	Viable	Non viable
2 days	Viable	Non viable
4 days	Viable	Non viable

Neither of the two devices was found to be able to completely inactivate the spores found in the pigmented portion of the mycelium, probably due to the resistance ability of these fungal structures but, most certainly, also due to the high number of spores present: in fact, the tests carried out previously with shorter exposure times (maximum 4 hours), although performed on a low number of spores, showed a survival rate that was around 30% at least. Despite assuming an exponential increase in the effects over the 4 days of the test, one ought to consider that hundreds of millions of spores are found within the pigmented area, hence the survival of a certain number of them was predictable.

The result obtained on the vegetative portion of the mycelium is much more interesting. As a matter of fact, in the case of the hyphae, the treatment with the NTP device was found to be able to inactivate the microorganisms, although a definitely high number of filaments were taken, almost certainly “contaminated” by a certain number of spores raised by the air flow and dropped back on this portion of the mycelium. The latter result means that, if the installations have already been colonised, NTP treatment might perform a three-fold positive effect, by:

- killing the vegetative part of moulds that have already grown in the ducts, and prevent their further growth;
- in the longer term, decreasing and gradually reducing to zero the number of viable spores;
- preventing the colonisation of new portions of the installation, since the hyphae germinated by any surviving spores would however be rapidly inactivated.

## ATTACHMENT 12.10

*Case study 1: reduction of odor impacts on waste management plant*

# REDUCTION OF ODOROUS IMPACTS

## INTRODUCTION

This document describes the study and analysis of the environmental aspects related to the odor impact measurements associated to waste management and the implementation of a pilot-scale test on the treatment of gaseous effluents in order to effectively reduce the odor load present.

## CLASSIFICATION OF THE ODOUR PROBLEM

This work involved a screening survey aimed at identifying the best ways to deal with the delicate issue of odor emissions generated by a waste treatment plant.

The topic addressed is very timely and urgent. It is known, in fact, how the dispersion of unpleasant odors starts from industrial activities or, in any case, from production plants that involve the presence of odorous sources. Among the wide range of activities that can be considered - in addition to specific industrial plants - we include broader categories such as wastewater treatment plants, waste treatment and sorting plants, landfills, etc.

Despite the importance of these challenges, there is currently no integrated methodology for the "control" of these phenomena; and by phenomena we mean not only its "measurement" - which is quite complex - but a real strategy to address the problem according to a precise hierarchy: interventions at source - confinement - mitigation.

In industrial-commercial contexts, which see the presence of a high number of possible odorous "sources", it becomes particularly complicated to determine, demonstrate and control the exact source of the problem, which is often highlighted by complaints - sometimes not fully reliable - by the population present in the area affected by the so-called "relapses".

In fact, the complexity of this problem arises from three fundamental reasons:

- } the difficulty of analyzing odorant substances whose concentrations in the environment are below a threshold of analytical detection (while causing, at the aforementioned concentrations, "nuisance" phenomena);
- } the variability of the intensity and characteristics of odor pollution as a function of time and meteorological conditions;
- } the great subjectivity that characterizes the perception of odorous substances.

In literature, there are very few studies carried out on the identification of odorant substances originating from odorous matrices and the evaluation of the effects of specific treatment systems on odorous substances.

Added to this is the lack of specific reference legislation, both internationally and Italian. In fact, at the national level, just a few regions have defined guidelines on the subject, mostly in recent times and applicable only to specific sectors. This "lack of legislation" is even more critical considering that, on the contrary, there is a growing awareness of society towards issues related to the environment, of which odorous impacts are, at present, one of the most subtle and elusive.

## ABATEMENT OF ODOROUS COMPONENTS ON NTP pilot-laboratory plant (BA-TEST pilot-industrial SCALE)

The activity carried out concerns the use of a pilot-industrial plant (therefore also applicable on an industrial scale) used on a laboratory scale, applied to the treatment of specific waste streams (the most critical) as well as mixed waste streams.

To carry out this experimental activity, a way was therefore designed to "manage" a flow of odorous substances of a much greater extent.

The following figure shows schematically the container that was used for the trial to be carried out with the industrial BA-TEST, which has a flow rate that can be modulated between 150 and 600 m<sup>3</sup>/h.

The system consists of a 100-liter PP drum on the bottom of which a series of holes are made, while a fitting is made on the lid for connection with the BA-TEST fan.

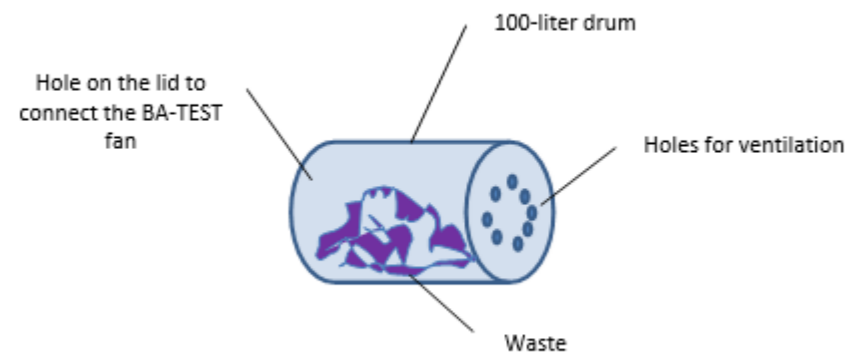


**Image showing a container for trials with BA-TEST**

The waste (30-50 kg) is placed inside the drum that is connected to the BA-TEST fan. The drum is positioned horizontally, and can be moved periodically to change the exposed surface of the waste mass.

The treatment system of the molecules (odorous and not) released by the waste contained in the drum is presented in the following photo.



**Picture of the BA-TEST pilot plant used in the trial**

LEGEND:

- A. Emission aspiration
- B. By-pass selector
- C. NTP® Generator
- D. Emission output
- E. Sampling points: (1 on top, upstream of the abatement system; 2: at the bottom, downstream of the treatment; 3 downstream of the treatment system, before the final emission)

Through the use of this system, trials and tests were carried out to verify the best plant structure, that is the one that guarantees the best results in terms of abatement of odorous substances developed from specific waste selected following the experimental activity carried out in the field of the previous operational objectives.

#### Development of the experimental conditions

This part of the experimental activity was rather complex, given that the individual responses and their variability were carefully evaluated, depending on the type of waste involved and the test condition used.

The conditions of the various tests (schematically reported in Table 5) were set using Design of Experiment (DoE) techniques. The results of the experiments obtained through the EN and the GC-MS were processed in order to identify the best operating conditions.

**Table 5. Trial conditions tested.**

	Levels		
	1	2	3
Waste quantity (kg)	30	50	
Waste type	LO	LA	MIX
Waste temperature (°C)	50		
Suction flow (m <sup>3</sup> /h)	150	300	600
By-pass	0	0,5	1
Voltage probe 1 (V)	3000		
Voltage probe 2 (V)	3000		
Voltage probe 3 (V)	3200		
Sampling points	1	2	3

The trial concerned 3 different types of waste (already known for their critical characteristics in terms of odorous impacts produced): LO (CER 19 01 05 \*), LA (CER 19 02 05 \*) and MIX (consisting of a mix of different wastes, including LO and LA, in order to simulate the average condition of the plant with the presence of odorous and non-odorous waste). This waste was placed inside the punctured drum, placed on a heating plate at about 50° C and, after 5 minutes of conditioning the tests began, taking the samples from the 3 sampling points with the probes off and, subsequently, turned on.

In order to evaluate the best test conditions, different trials were performed, varying one or more of the settings shown in Table 5.

The comparison between the sum of the areas obtained by GC-MS and the sum of the signals recorded by the 10 sensors of the EN, provided the answers sought for the identification of the best operating conditions, relative to the treatment trial of the odorous flows produced by the waste being tested, using the BA-Test on a pilot-laboratory scale.

The best test conditions, obtained using the LO waste (and then confirmed with the other tested wastes), were:

1. Waste quantity = 30 kg
2. Waste temperature = 50°C
3. Suction flow = 150 m<sup>3</sup>/h
4. By-pass = close (0)
5. Capacitor voltage = 3000, 3000, 3200 V
6. Sampling points = 1 e 3

### Results obtained with the LO CER 19 01 05 \* waste

The tests carried out for the abatement of the odorous molecules contained in the LO waste made it possible to obtain the results briefly presented in the graph in Figure 25. The sampling points considered are point 1 (upstream of the NTP treatment system) which represents the untreated gas emission and point 3 (downstream of the NTP probe) which represents, with the probe on, the emission after treatment with the probe. In this way, it is also necessary to consider the contributions of the controls and in particular the negative contribution that the probe has on the EN reading, as can be seen from the SA\_SR test in the graph on the left of Figure 26: the sum of the sensor signals of the EN decreases by about 11% following switching on of the probe itself. Similarly, it is possible to record a decrease (about 7% with the EN and 6% with the GC) due, almost certainly, to molecule adsorption phenomena along the pilot plant duct. These percentages of decrease were considered for the purposes of evaluating the reduction efficiency of the NTP system with respect to the odorous molecules, subtracting them from the overall reduction percentage determined as differences in signals recorded in points 1 and 3, during the test that used the waste and the probe turned on.

In conclusion, for the LO waste, percentages ranging between 34% (with the Electronic Nose) and 28% (with the Gas-chromatography) of abatement of the odorous molecules present were found.

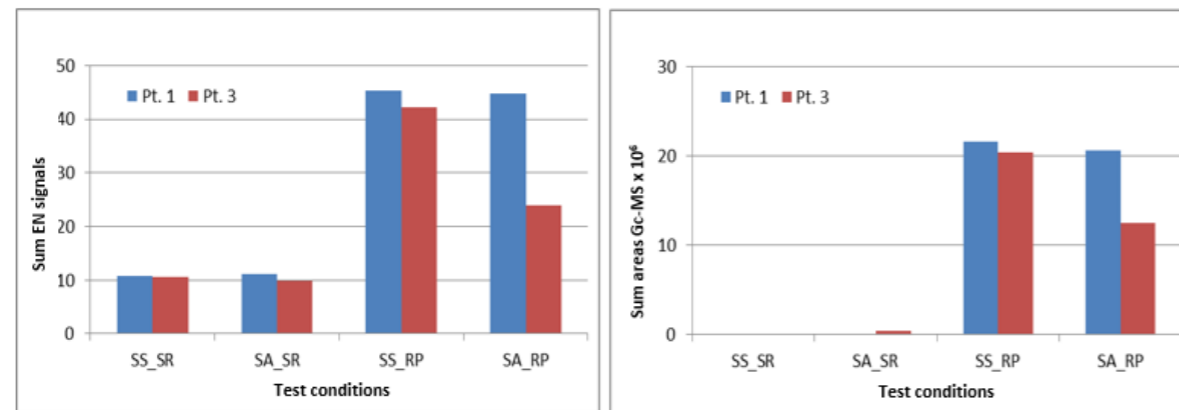


Figure 25. Results of tests conducted on LO waste (EN left; GC-MS right).

Legend: SS\_SR = probe off – no waste (no probe baseline); SA\_SR = probe on – no waste (probe baseline); SS\_RP = probe off – waste on the heating plate (emissions with the waste heated at 50°C); SA\_RP = probe on – waste on the heating plate (emissions with the waste heated at 50°C + NTP treatment)

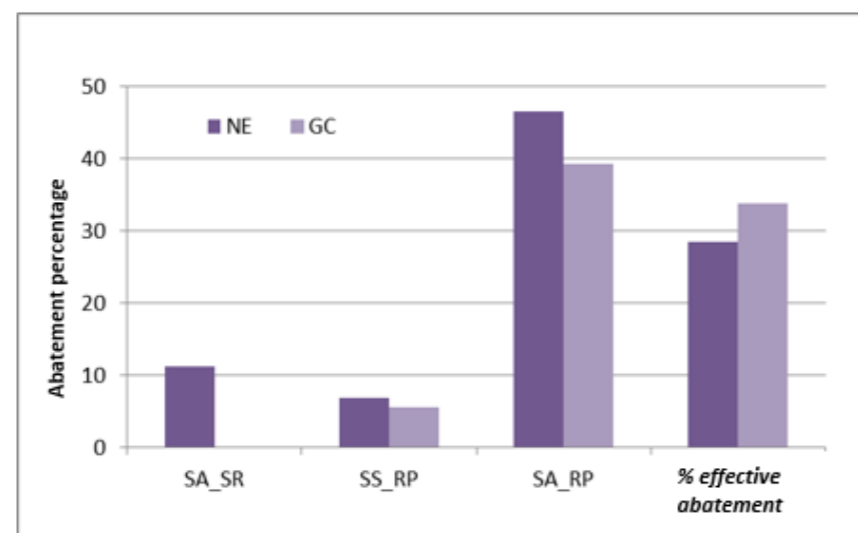


Figure 26. Results of tests conducted on LO waste expressed as abatement percentages, taken at the sampling points 1 and 3.

Legend: SA\_SR = % probe contribution; SS\_RP = % decrease due to waste emission losses along the way; SA\_RP = % abatement incorrect probe; % effective abatement = SA\_RP – SS\_RP – SA\_SR

### Results obtained with the LA CER 19 02 05 \* waste

Similarly to what was done with the LO waste, the treatment tests of the odorous molecules produced by the LA waste were carried out.

The graphs of the experimental results obtained are shown in Figure 27, on the left the values of the sum of the signals recorded by the Electronic Nose, on the right the results obtained by the SPME-GC-MS analysis.

The abatement percentages defined as described in Paragraph 5.4.3. are represented in Figure 28: the effective abatement on the odorous molecules carried out through the NTP probe is calculated as 40% by GC analysis and 26% by EN.

This difference can be easily explained through the different composition of the LA waste compared to LO, obtained by GC-FID analysis, on the solid sample (Figure 29): the first is in fact exclusively made of short-chain aliphatic Volatile Organic Compounds (C5-C12), while in the LO waste there are also more complex aromatic compounds, with a number of C8-C10 carbons (toluene, xylenes ...) which are less degradable by the species emitted by the NTP probe.

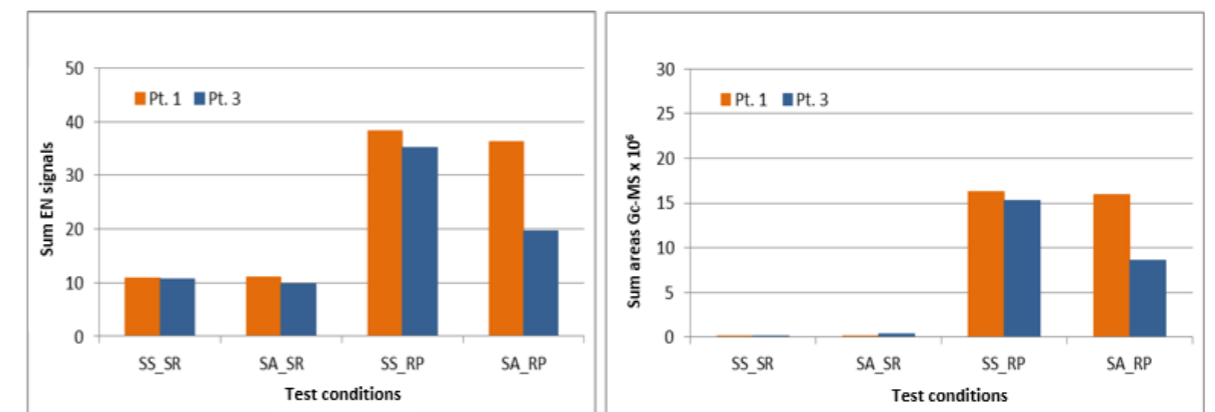


Figure 27. Results of tests conducted on LA waste (EN left; GC-MS right).

Legend: SS\_SR = probe off – no waste (no probe baseline); SA\_SR = probe on – no waste (probe baseline); SS\_RP = probe off – waste on the heating plate (emissions with the waste heated at 50°C); SA\_RP = probe on – waste on the heating plate (emissions with the waste heated at 50°C + NTP treatment)



Figure 28. Results of tests conducted on LA waste expressed as abatement percentages, taken at the sampling points 1 and 3.

Legenda: SA\_SR = % probe contribution; SS\_RP = % decrease due to waste emission losses along the way; SA\_RP = % abatement incorrect probe; % effective abatement = SA\_RP – SS\_RP – SA\_SR

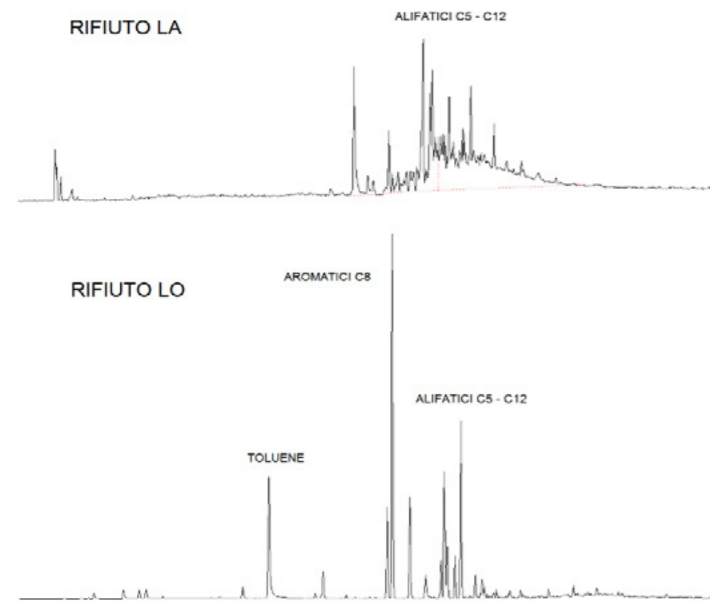


Figure 29. Chromatograms related to the analysis of LA (top) and LO (bottom) waste samples.

#### Results obtained with the mixed waste (MIX)

For the final validation of the treatment tests using NTP technology, further experiments were carried out, using mixed waste (called MIX), consisting of the two previous LO and LA, together with 4 other kinds of waste, not particularly critical, but of a dangerous nature and equally rich in volatile organic compounds.

The analyses carried out on the air samples taken in points 1 and 3, under the experimental conditions already described in the previous paragraphs, provided the trends shown in the graph of Figure 30 (EN, left; GC-MS, right).

In general, the values measured both at the EN and at the GC are lower than those found with the single waste present in the previous paragraphs. The abatement percentages that can be found during the tests carried out reach about 30% of the load of substances present in the gaseous flow leaving the BA-TEST (Figure 31).

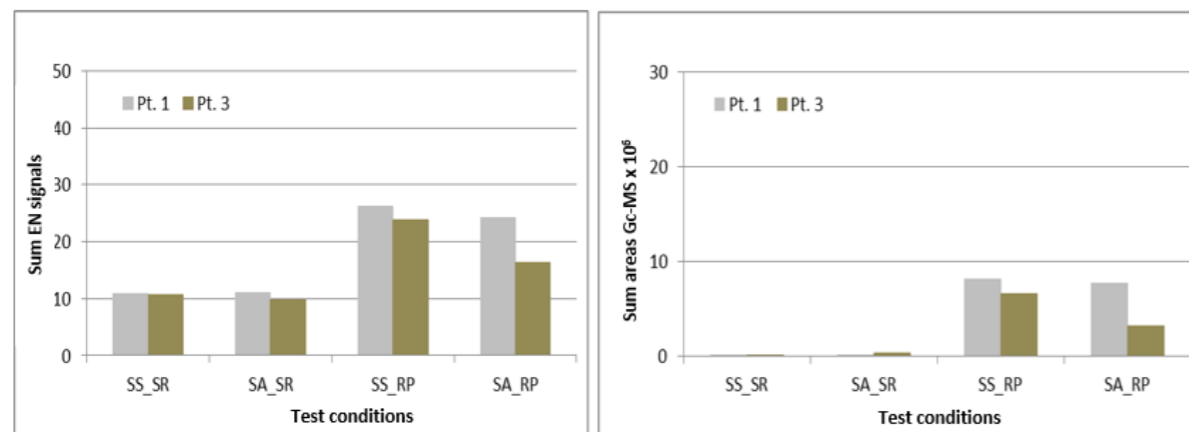


Figura 27. Results of tests conducted on MIX mixed waste (EN left; GC-MS right).

Legend: SS\_SR = probe off – no waste (no probe baseline); SA\_SR = probe on – no waste (probe baseline); SS\_RP = probe off – waste on the heating plate (emissions with the waste heated at 50°C); SA\_RP = probe on – waste on the heating plate (emissions with the waste heated at 50°C + NTP treatment)



Figure 28. Results of tests conducted on MIX waste expressed as abatement percentages, taken at the sampling points 1 and 3. Legenda: SA\_SR = % probe contribution; SS\_RP = % decrease due to waste emission losses along the way; SA\_RP = % abatement incorrect probe; % effective abatement = SA\_RP – SS\_RP – SA\_SR

#### Final considerations

From the results presented, it is clear that NTP technology has a positive effect in the abatement of the species present in the gaseous flow generated by waste, with percentages ranging between 25 and 40%.

This result was obtained by carrying out a complex trial on a pilot plant equipped with NTP technology, testing the treatment on different waste and their mixtures, and using both the Electric Nose and Gas-Chromatography with Mass Detector as analytical techniques for the "quantification" of efficiency.

The results obtained offer a wide range of use of this technology as an abatement system, both of the organic pollutants present in the emissions and, more specifically, with regards to the objective of the project, that is the abatement of odorous molecules.

The organic molecules, as has been verified in particular on the aliphatic and aromatic chains through the analyses carried out with the GC-MS, are reduced by up to about 40%. The odorous substances, as it was verified through the use of the Electronic Nose, undergo a decrease in their concentration up to 30%.

A possible further development of the study and the proposed technology could concern different kinds of waste characterized by olfactory impacts due to inorganic compounds, such as ammonia and hydrogen sulphide (H<sub>2</sub>S). In these cases, the analytical methods to be applied could be the Electronic Nose and specific techniques for the determination of such compounds.



## ATTACHMENT 12.11

---

*Case study 2: Study of air sanitation in a veterinary clinic*

## Index

<b>INTRODUCTION</b> .....	181
<b>PURPOSE</b> .....	181
<b>IONIZATION THEORY</b> .....	184
<b>DESCRIPTION OF JONIX EQUIPMENT</b> .....	184
<b>MATERIALS AND METHODS</b> .....	185
<b>RESULTS OF THE TRIALS</b> .....	186
<b>RESULTS OF THE MICROBIOLOGICAL ANALYSIS OF THE AIR</b> .....	190
RESULTS OF THE EVALUATION OF THE PERCEIVED ODOR.....	190
CONSIDERATIONS .....	190
<b>CONCLUSIONS</b> .....	191
BIBLIOGRAPHY.....	192

## Introduction

The "indoor" pollution of homes and workplaces is a chemical and microbiological problem that can be significant for the health of people and animals living in these environments. The problem is so important that it has a dedicated branch of study: Aerobiology.

It is a new multidisciplinary science that studies the particles present in the atmosphere, the sources that produce them, the ways in which they are transported by the air, their effects both indoors and outdoors.

The techniques used to improve the "healthiness" of the environments, in particular working environments, are many and different, they can be implemented in the air treatment systems or be independent mobile devices. Among the different techniques, filtration, UV lamps or ozone are used, the latter are not compatible with the presence of people.

In the last decade, research has been oriented towards air ionization, a natural phenomenon that can be artificially reproduced which has proved capable of acting on many (microbiological and chemical) particles present in the air.

There are many national and international publications on the effects of air ionization, which demonstrate, in addition to the therapeutic effects on the pathology of the respiratory system, also an effective reduction of the microbial content in the air and on surfaces.

Numerous researches and experiments have been carried out in the food and hospital healthcare sector.

Applications in veterinary clinics and surgeries are very recent. The need for constant sanitation emerged at the same time as that of general and orthopedic surgery in particular.

In fact, similar to what happens in "human" surgery, post-surgical infections can also be airborne. Although there are no real clinical trials in the veterinary field, the factors on the indoor air quality of the sector lead us to estimate that they cause a significant percentage of infections.

There is also the trend towards a holistic view of the veterinary medicine service, with a health-genetic and eco-sustainable approach; focused on the patient and his family unit; with the minimum possible use of synthetic medicines and instead the adoption, where possible, of homeopathic protocols.

These new scenarios, for consistency, must necessarily live within environments with an adequate air quality factor, microbiologically controlled, free of volatile organic substances and odors; this aspect is directly related to the perceived quality of the clinical service offered.

## Purpose

Jonix wanted to verify the effectiveness of Non Thermal Plasma technology in veterinary healthcare. This first trial was conducted at the prestigious San Marco Veterinary Clinic.

The goal was to achieve a reduction in perceived odors and a reduction in airborne microbial contamination in premises where concentrations could be significant and have a negative impact on animals and people.

The experimentation, carried out in March and April 2018, required a series of samples taken before the installation of the devices, during the normal activity of the clinic, to evaluate the initial conditions, to be compared with the measurements made after switching on Jonix devices.

Sampling and analysis were conducted by qualified technicians and an independent institute, indicated below, using a SAS-Super 180 device by PBI.

Initial evaluations. Regarding the veterinary clinics, a bibliography has not been identified to support the initial evaluation.

The veterinary clinic where the experimentation took place has a high turnout of animals both for outpatient services and in the ward that offers 30 cages, with a consequent high turnover of animals.

Animals can vary by species, size, pathology and total number of simultaneous presence. This involves a very high variability of the particles released into the air by the animals themselves and by the movement of operators inside the room.

The clinic is not equipped with air treatment systems except for the introduction of primary air. This involves a further source of variability in the microbial content of the ambient air. The conditions described created interesting conditions for the experimentation, it was therefore decided to carry out the measurements in the environments with greater variability of turnout and consequent variations in the aero dispersed bacterial concentrations:

the waiting room at the entrance (fig. 1) and the animal hospital room (see fig. 2).

In these rooms we find the greatest number of variables related to air movement: the opening and closing of the entrance and access doors to the clinics and the extreme changeability of human presence offered the possibility of "photographing" the microbial contamination of the air in a situation of ordinary activity.

The clinic operates 24 hours a day.

For a better understanding of the air variability factors, the contribution of external air coming from the opening of the doors, both those facing the inside of the building and those facing outwards, has been calculated.

In the hospitalization room the air coming from the door facing the external garden is about 1300 m<sup>3</sup>/h; while from the door facing the central corridor, about 1700 m<sup>3</sup>/h.

In the waiting room, with the three doors, entrance, entrance to the ambulatory area and exit, the volume of air that mixes with the ambient air is approximately 4500 m<sup>3</sup>/h.

The calculations are based on the average number of hourly openings observed during the sampling.

Measurements were made to understand the level of contamination present and whether, under current conditions, the proposed air ionization system could achieve the desired odor and microbial content reduction goals.

To define the contribution of air coming from the doors, a specific calculation system was used, the same that is usually used in the specific technical calculations of the sector. The factors used are shown in the table below.

Row	Text	Value
1	LEGENDA COLORI:	
2	RISULTATI DI CALCOLO	
3	RICHESTE DA COMPILARE	
4	VALORI PRE-IMPOSTATI NON MODIFICABILI	
5	DIMENSIONI PORTA	
6	larghezza (DA COMPILARE)	2,4 m
7	altezza (DA COMPILARE)	3,2 m
8		
9	CEFF (VALORI PRE-IMPOSTATI)	0,692
10		
11	DENSITA' ARIA INTERNA (VAL. PRE-IMPOSTATI)	1,24 kg/m <sup>3</sup>
12	DENSITA' ARIA ESTERNA (VAL. PRE-IMPOSTATI)	1,16 kg/m <sup>3</sup>
13		
14		
15	PORTATA ARIA IN INGRESSO (CALCOLO RISULTANTE)	0,527 m <sup>3</sup> /s
16	PORTATA ARIA IN INGRESSO (CALCOLO RISULTANTE)	1,897 m <sup>3</sup> /h
17		
18		
19	NUMERO DI APERURE IN 24 ORE (O NELLE ORE LAVORATIVE)	400 n°/gg
20	TEMPO DI APERURA IN MINUTI	0,3 min
21		
22	QUANTITA' ARIA IN INGRESSO DALLE PORTE	3,795 m <sup>3</sup> /gg



Fig. 1 – Waiting room



Fig. 2 - San Marco veterinary clinic, animal hospitalization room

### Theory of ionization with non-thermal plasma

The term “non-thermal plasma”, also known as cold plasma, indicates an evolved form of ionized gas mixture composed of a large number of charged particles, such as ions or electrons, free radicals, ROS, molecules and even neutral atoms.

The ionization of an atom occurs when an electron acquires enough energy to overcome the attractive forces of the atom's nucleus. When this is obtained with processes that generate a plasma where the temperature of the ions and neutral atoms is significantly lower than that of the electrons, we speak of cold plasma or Non-Thermal Plasma (NTP).

The cold plasma emits light with wavelengths both in the visible and in the ultraviolet part of the spectrum. In addition to the emission of UV radiation, an important property of low-temperature plasma is the presence of highly reactive high-energy electrons, which generate numerous chemical and physical processes such as oxidation, excitation of atoms and molecules, production of free radicals and other reactive particles. A plasma can be artificially generated by supplying a gas with a sufficiently high energy, that is, by applying energy to a gas in such a way as to reorganize the electronic structure of the species (atoms, molecules) and produce excited species and ions. One of the most common ways to artificially create and maintain a plasma is through an electrical discharge in a gas. The JONIX NTP technology uses the so-called non-thermal discharges with the dielectric barrier method. The ionization potential and density of charged species generated by dielectric barrier discharge (DBD) plasma are greater than those present in non-thermal plasma generated by other systems.

### Description of the Jonix equipment

JONIX steel is a sanitization unit, with cold plasma technology for air purification and decontamination.

Ideal for veterinary wards, clinics, surgical rooms, waiting rooms and where it is necessary to prevent and reduce airborne bacterial contamination. It can be easily installed on the wall or placed on a horizontal surface. The device is designed to allow the propagation of purified air in a uniform way thanks to the front ventilation system at the entrance and the openings on the sides that ensure optimal air output. Compact and silent, the JONIX steel device rapidly breaks down bacterial loads and chemical contaminants.

JONIX steel is simple and essential. For a higher quality integrated plant management, the control and functions can be managed remotely.

#### ECOLOGICAL AND COMPATIBLE WITH THE PRESENCE OF PEOPLE/SAFE AROUND PEOPLE

There is no chemical or environmental impact. It sanitizes the air continuously and eliminates odors, improving environmental comfort. It guarantees operators the healthiness of the air as required by the regulations for the safety of workers.



Fig. 2 – Ionized air flow



Fig. 3 – The device

### Materials and methods

Samplings were made in two points of two pre-established rooms: the Veterinary ward and the Waiting Room. In the veterinary ward there are animals in cages awaiting surgery/controls or recovering right after undergoing one.

In the waiting room there are secretaries on one side and customers with their pets on the other (photos 1 and 2).

The time spent in the veterinary ward and the variability of the animals is very high since the number, type and general state of each individual animal vary during the test period. There is also a flow of people who access the room directly from outside, resulting in a significant change in the air.

Also, in the waiting room the variability is very high: the number of people as well as the number, type and size of the animals change continuously, just like the frequency of the doors opening.

The samplings were taken with a PBI SAS-Super 180 device, which allows the operator to pre-establish a certain quantity of air to be taken. The air comes in direct contact with a plate containing a specific culture medium for the microorganisms to be monitored. In the test, 100 liters of air were sampled each time.

These plates are then transferred inside a refrigerated container in the laboratory which will provide for the incubation of the plates at the temperature required for the specific method.

The measured parameters are:

Parameter	Culture medium	Temperature and incubation time
Mesophilic bacterial load	Plate count agar	30°C for 48 hours
Yeasts/Mycetes	Sabouroud Dextrose Agar	30°C for 5 days
Pseudomonas ss	Pseudomonas cetrimide agar	35°C for 18-72 hours
Staphylococci spp	Baird Parker Medium E.Y.T.E.	37°C for 24-48 hours

The tests were carried out in collaboration with the Experimental Zooprophyllactic Institute delle Venezie, section of Treviso - Diagnostic Laboratory. The samplings were conducted with the collaboration of Alimentaria S.r.l. .

The trial also included the smell perceived both in the waiting room and in the veterinary ward. The test was conducted by evaluating the technicians involved in the sampling and the personnel present in the above-mentioned areas.

## Test results

### Results of microbiological analyzes in the air

Microbiological analyzes were conducted in the air by sampling a known quantity of air with an instrument called SAS. The sampling was carried out in two points per room, about 1.5 meters above the floor.

Tab. 1 – Trend of analytical results in the veterinary ward - point 1

Veterinary ward 1	Date	TBL CFU/m <sup>3</sup>	Yeasts CFU/m <sup>3</sup>	<i>Pseudomonas spp</i> CFU/m <sup>3</sup>	<i>Staphylococcus Spp</i> CFU/m <sup>3</sup>
No ionization	26/03/18	120	110	10	210
	27/03/18	270	80	10	10
	28/03/18	340	110	10	220
	29/03/18	80	190	10	50
With ionization	04/04/18	100	100	10	150
	09/04/18	160	210	30	140
	17/04/18	190	160	10	180
	18/04/18	150	200	10	40
	20/04/18	50	40	10	80

(\*) Mesophilic bacterial load

Tab. 2 – Trend of analytical results in the veterinary ward - point 2

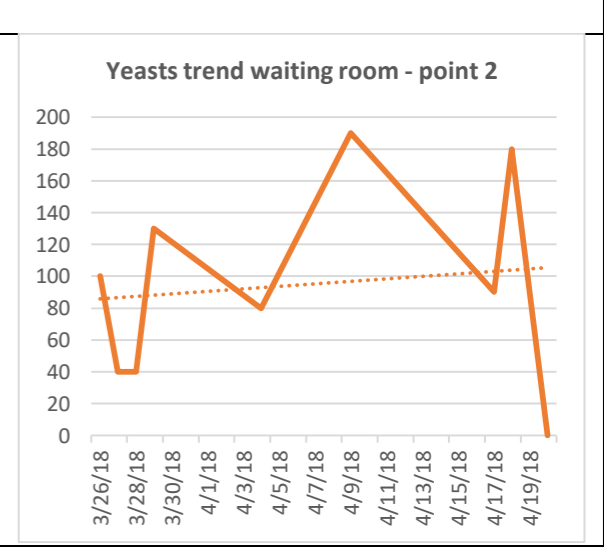
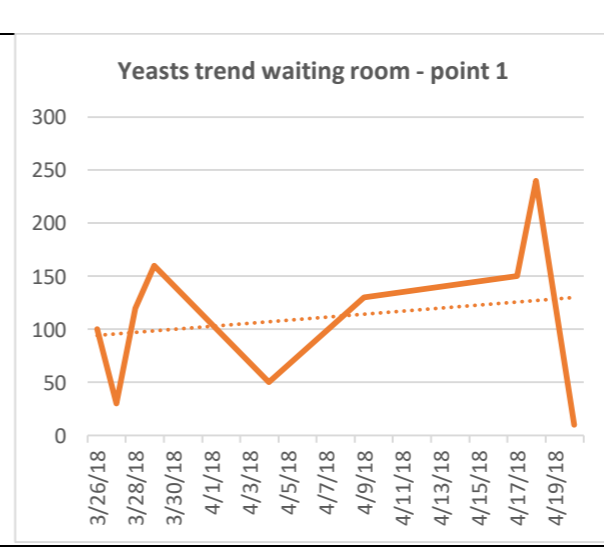
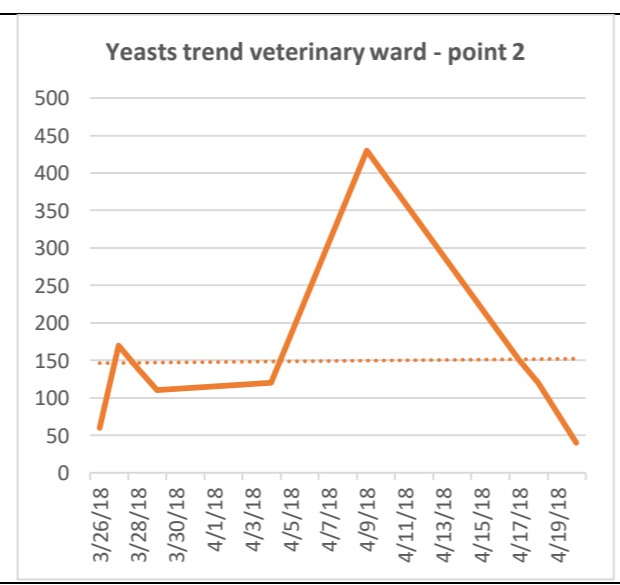
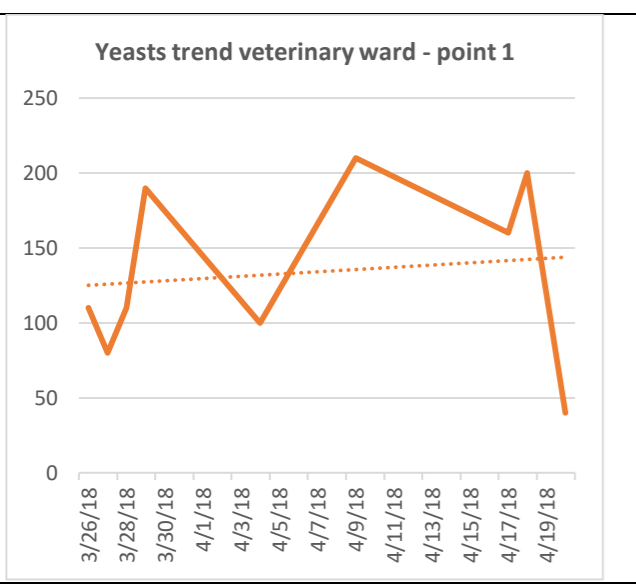
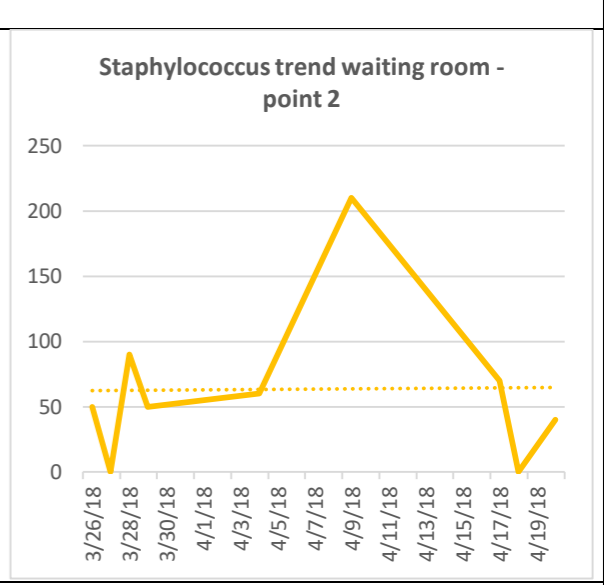
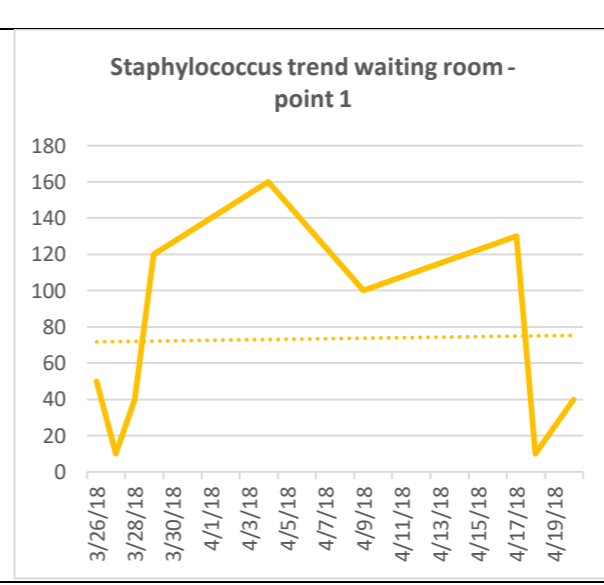
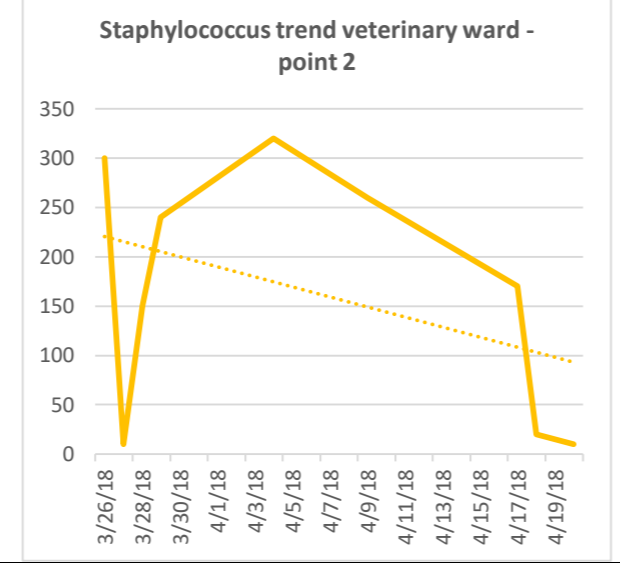
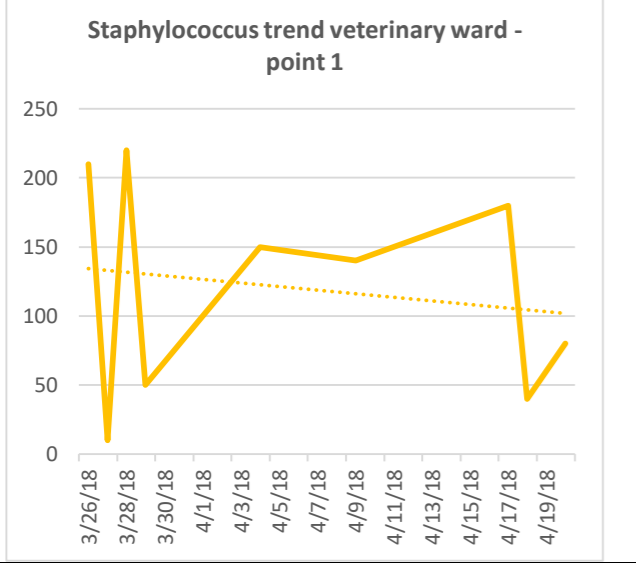
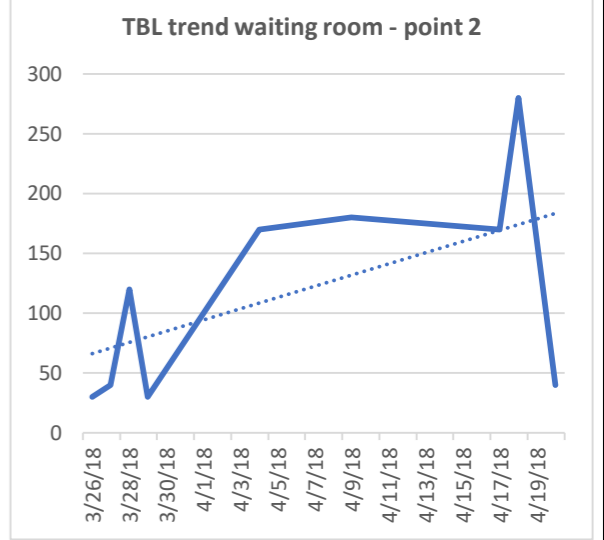
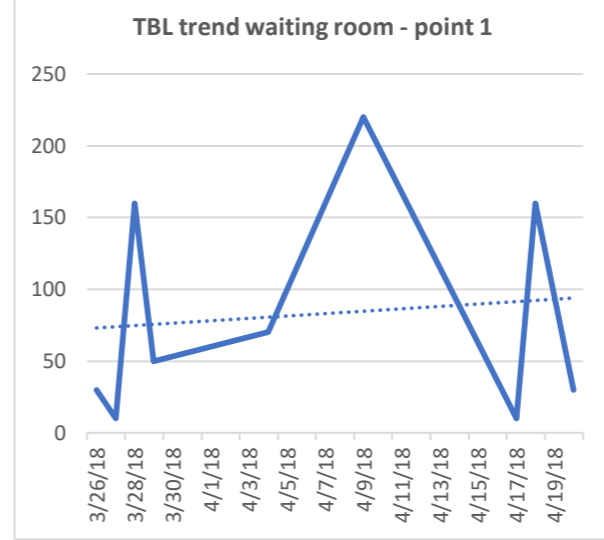
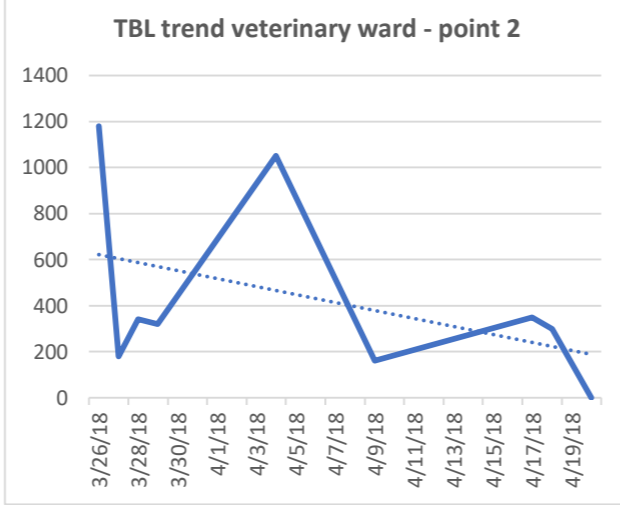
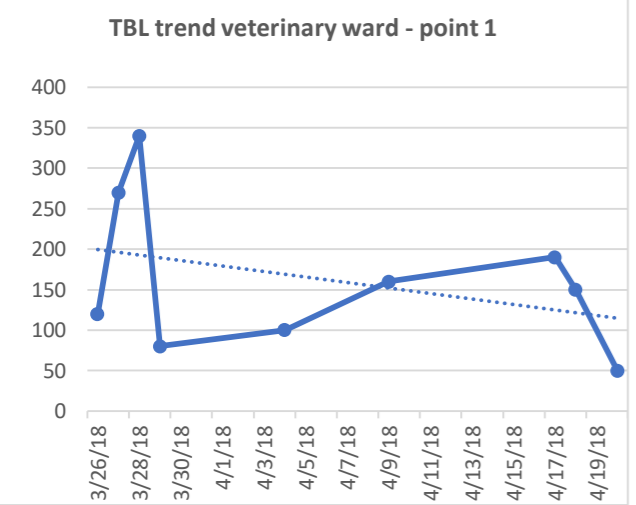
Veterinary ward 2	Date	TBL CFU/m <sup>3</sup>	Yeasts CFU/m <sup>3</sup>	<i>Pseudomonas spp</i> CFU/m <sup>3</sup>	<i>Staphylococcus Spp</i> CFU/m <sup>3</sup>
No ionization	26/03/18	1180	60	10	300
	27/03/18	180	170	10	10
	28/03/18	340	140	10	150
	29/03/18	320	110	40	240
With ionization	04/04/18	1050	120	10	320
	09/04/18	160	430	40	260
	17/04/18	350	150	20	170
	18/04/18	300	120	10	20
	20/04/18	<10	40	10	10

Tab. 3 – Trend of analytical results waiting room – point 1

Waiting room 1	Date	TBL CFU/m <sup>3</sup>	Yeasts CFU/m <sup>3</sup>	<i>Pseudomonas spp</i> CFU/m <sup>3</sup>	<i>Staphylococcus Spp</i> CFU/m <sup>3</sup>
No ionization	26/03/18	30	100	<10	50
	27/03/18	10	30	<10	10
	28/03/18	160	120	50	40
	29/03/18	50	160	20	120
With ionization	04/04/18	70	50	<10	160
	09/04/18	220	130	<10	100
	17/04/18	10	150	<10	130
	18/04/18	160	240	<10	10
	20/04/18	30	10	<10	40

Tab. 2 – Trend of analytical results - waiting room 2

Waiting room 2	Date	TBL CFU/m <sup>3</sup>	Yeasts CFU/m <sup>3</sup>	<i>Pseudomonas spp</i> CFU/m <sup>3</sup>	<i>Staphylococcus Spp</i> CFU/m <sup>3</sup>
No ionization	26/03/18	30	100	<10	50
	27/03/18	40	40	<10	<10
	28/03/18	120	40	<10	90
	29/03/18	30	130	10	50
With ionization	04/04/18	170	80	<10	60
	09/04/18	180	190	10	210
	17/04/18	170	90	<10	70
	18/04/18	280	180	<10	<10
	20/04/18	40	<10	<10	40



## Results of the assessment on perceived odor

The areas indicated above have a typical smell deriving from the animals that are housed in the premises. This smell is "normal" for those who work daily in the facility for a large number of hours. This is not the case for operators and people (clients) who occasionally enter the clinic. The effect on the odor had an appreciable and perceptible effect from the first detection.

Date	Ionization	Waiting room	Veterinary ward
26/03/18	No ionization	5	5
27/03/18		5	5
28/03/18		5	5
29/03/18		5	5
04/04/18	With ionization	1	3
09/04/18		1	3
17/04/18		1	3
18/04/18		1	3
20/04/18		1	3

The scale used during the interview ranged from 5 high odor to 1 low odor.

The test was conducted on people (5 people for each interview) in the waiting room in the period before and after the Jonix devices were switched on.

The operating staff was not suitable for the panel test because they are used to the smell.

Not being able to introduce external people to carry out the survey, the evaluation was carried out by interviewing the technicians in charge of the samplings.

### Considerations

The use of air ionization for the reduction of odors and the microbial content of the air and the surfaces in contact with it has been repeatedly demonstrated and documented (see bibliography).

All the tests reported in the bibliography were conducted having a limited number of environmental variables that could affect the results.

In the specific case, during the trial, it emerged that the variables are many and these have a significant impact on the performance of the results.

The veterinary ward has the following variables:

- Number of operators from 2 to over 10 simultaneously present
- Variable staff working hours
- Variable number of animals
- Different size, species and pathologies, as well as hygiene degrees of the animals
- Door to the outside with variable random opening throughout the day

The waiting room has the following variables:

- Number of customers ranging from none to more than 10 in a short time
- Variable number of animals depending on the number of customers
- Frequent opening of the door to the outside for the people entering and leaving

The structure where the tests were conducted has an air management system based on AHUs that introduce primary air, of which, however, the volumes of the air flow rates are not known, neither overall, nor any recirculation.

The type of sampling used foresees the collection of a known quantity of air. This sampling lasts a few minutes (3-5 minutes). During this period, normal activities take place at the sampling points, which obviously vary with each sampling.

In the veterinary ward, the number of animals, their size, the number of people who entered and the duration of their stay changed with each sample, in addition to the fact that there is a door to the outside that opens as needed.

In the waiting room, the situation has foreseen similar variables even if higher since the air is also influenced by the secretaries as well as by the number of customers and animals; in some cases, there were 1 or 2 people while in others the room also featured 10 or 15 people present with their respective animals.

The trend of the microbial content of the air is exposed to a high and unpredictable number of variables (door opening, number of customers and animals, external air influence, number of passages, etc). To obtain results on the real contribution of the ionization, it will be necessary to reduce the number of variables and/or modify the indicators used to check the effectiveness of the ionization system in highly variable environments.

From the bibliography it appears that the ionization system is effective, the research must be conducted with a protocol that must be revised in order to carry out reliable measurements.

### Conclusions

In the veterinary ward, the trend observed indicates a reduction in the total microbial content and staphylococci while the trend of the yeasts see a slight increase, attributable to the frequent opening of the doors that overlook the outside of the building, surrounded by hedges and plants. The sampling points were about 50 cm from the doors, consequently the air collected in the sample was mixed with that coming from the outside.

In the waiting room there was a general trend line of slight increase in the parameters initially detected for the promiscuity with the air coming from the opening and closing of the doors.

The sampling method used is therefore a "pinpoint photograph" of the moment being analyzed. The bacterial reduction effect over time is evident, the prolonged supply of ionizing molecules to the air makes it inhospitable for contaminants.

The deodorization effect of the air was sensorially appreciable in both rooms: the odor present was significantly reduced.

In fact, users perceived almost odorless air in the waiting room after switching on the Jonix devices.

In order to be able to conduct a more in-depth evaluation of the antimicrobial effect of ionization, already documented in the bibliography and with the same devices in other areas, it is necessary to set up a research protocol in premises with greater control of variables or with environmental indicators that are less affected by the variables in place.

Given the environmental conditions detected, where the microbial content is also linked to air-dispersed particles, a test can also be conducted using devices equipped with filtration systems combined with air ionization, a system similar to that used in human hospitals.

Test conducted in collaboration with:



Alimentaria S.r.l. Safety and environment department  
Sede legale: Parco Scientifico & Tecnologico di Venezia – Via delle Industrie 19/B/11-30175  
Venezia Marghera Tel. 041.5382629 – e-mail: [info@alimentariavenezia.it](mailto:info@alimentariavenezia.it)  
C.F. e P.IVA 03089520278 – Capitale sociale € 58.000,00 i.v.– R.E.A. VE 281802 – Reg. Imp. VE  
03089520278



Experimental Zooprophyllactic Institute delle Venezie.

SCT2 Section of Treviso, Belluno e Venezia  
Vicolo Mazzini, 4 31020 Villorba (TV) Tel. 0422 302302

#### Bibliography

Comi, G., Lovo, A., Bortolussi, N., Paiani, M., Berton, A., Bustreo, G. (2005) Ionizzatori per decontaminare l'aria nei locali di produzione del prosciutto crudo di San Daniele. Ind. Alim., XLIV, ottobre, 1-9.

Comi, G., Osualdini, M., Manzano, M., Lovo, A., Bortolussi, N., Berton, A., Bustreo, G. (2006) Decontaminazione di superfici di strutture e attrezzature utilizzate in aziende alimentari attraverso l'impiego di ionizzatori. Ind. Alim., XLV, giugno, 661-669.

JEFCA, 2001. Ochratoxin A. First Draft 47 series.

## ATTACHMENT 12.12

---

*Case study 3: Sanitizing effects of the MATE device in the large-scale food distribution sector*



## Evaluation of the effect of Jonix Minimate air sanitation devices in a hypermarket

An air sanitizing filtration device (the air ionization and filtration system model JONIX MINIMATE) is installed in a hypermarket. The device was positioned in the packaging area of the meat processing department.

The space is closed on three sides and open on the side overlooking the store.

The open side allows air mixing with the air of the store.

The air in the store was sampled near the refrigerated sections, to evaluate the bacterial concentration.

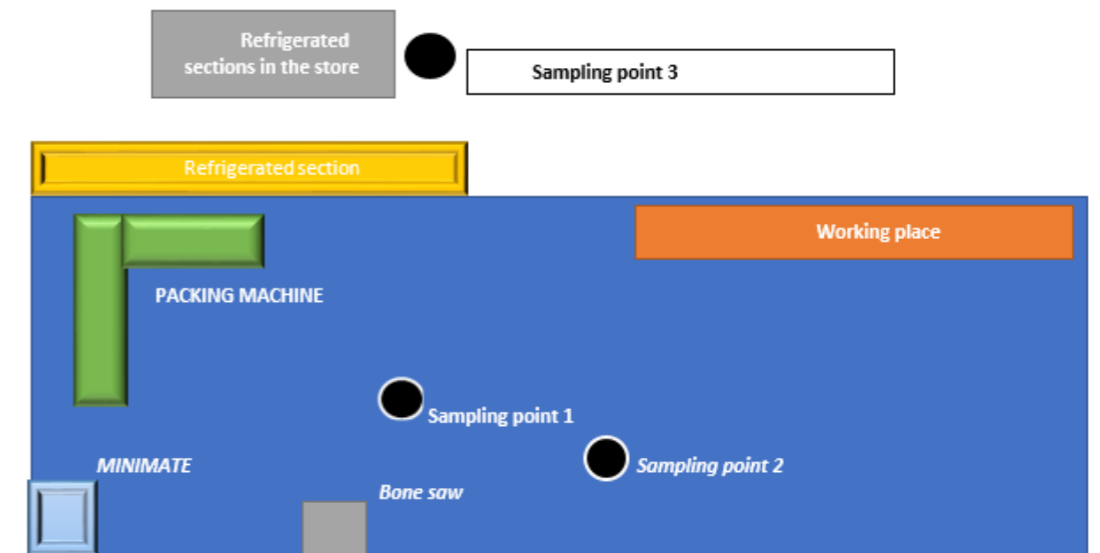


**Figure 1. Plan view of the room** Dimensions: 15x5x4h m = 75 m<sup>2</sup> - 300 mc. Open side towards the store, dimensions mt. 13 x 2.5 approx. 32.5 m<sup>2</sup> open area. The result is an air volume mix of approx. 30,904 m<sup>3</sup>/h.

The ceiling in the indicated area is gridded, allowing air in from above the room. As shown in the figure. The room therefore suffers contamination from the store and the ceiling.



**Figure 2 Front view of the room.** Upper grid, dimensions: 0.5 x 13 m = 6.5 m<sup>2</sup>. surface of the opening. Open continuously, the result is a volume of incoming air equal to 2.764 m<sup>3</sup>/h.

**Materials and methods**

The JONIX MINIMATE device was started up in the weeks preceding the test period and operated with air flows ranging from 1000 to 2000 m<sup>3</sup>/h.

To evaluate the air sanitization effects of the device, two samplings were performed, at different times and with different air flow rates, 10 days away from each other.

The first sampling was carried out on September 19<sup>th</sup> 2018 at 9.30, there were 4 employees, our expert to collect the sample and the manager of the store. For about 10 days the air flow had been set at 1000 m<sup>3</sup>/h and the 4 plasma generators of the device were active.

The second air sampling was carried out on September 28<sup>th</sup> 2018 at 20.00. From the previous 2 days the air flow of the device was set at 2000 m<sup>3</sup>/h. This time there were 4 employees, our expert to collect the sample and the store manager.

A PBI SAS-Super 180 device was used for the sampling, 100 liters of air were sampled at each sampling point. Petri dishes with PCA culture medium for CBT and Ros Bengal Agar for molds and yeasts were used.

The tables below show the results of the two samplings.

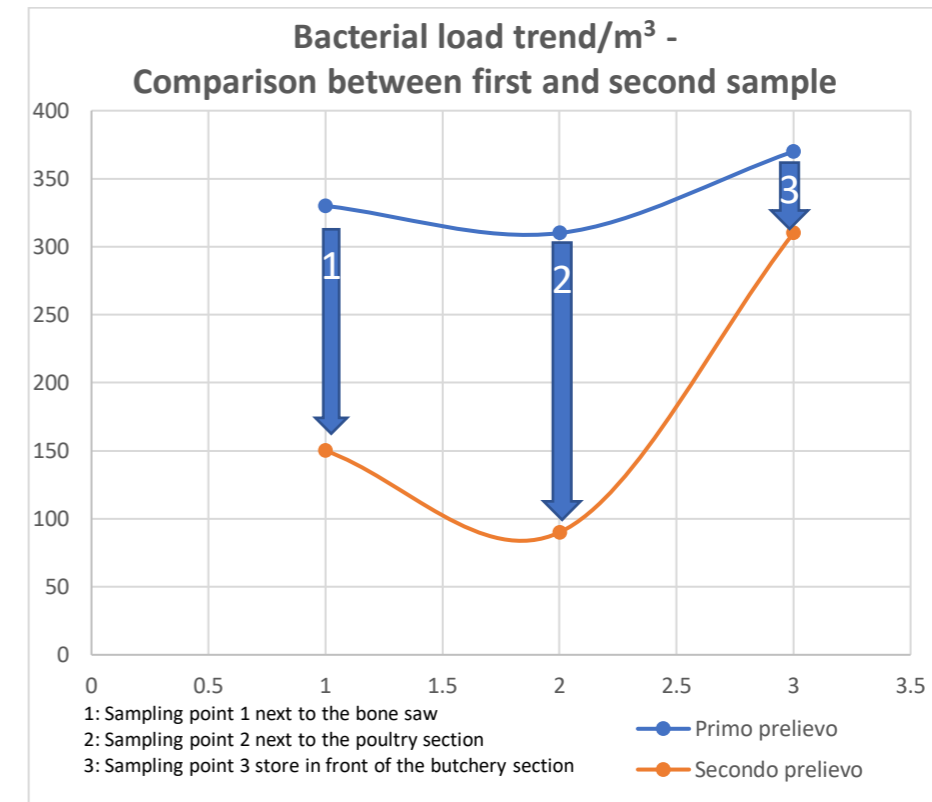
**Sampling of on September 19<sup>th</sup> 2018**

Butchery section	Total bacterial load UFC/m3	Molds and yeasts UFC/m3
Sampling point 1 next to the bone saw	330	210
Sampling point 2 next to the poultry section	310	297
Sampling point 3 in front of the butchery section	>370	//

**Sampling of on September 28<sup>th</sup> 2018**

Area	Total bacterial load UFC/m3	Molds and yeasts UFC/m3
Sampling point 1 next to the bone saw	150	57
Sampling point 2 next to the poultry section	90	63
Sampling point 3 in front of the butchery section	310	//

**Graph 1 - Comparison of first and second sampling trends - total bacterial load/m<sup>3</sup>**



Blue: First sample  
Orange: Second sample

The volume of the room is about 300 m<sup>3</sup>, which are mixed with the air coming from the store for about 30,900 m<sup>3</sup>/h and with that coming from the upper grid for about 2,700 m<sup>3</sup>/h.

We do not know the filtration characteristics provided by the centralized air treatment system, or the renewal percentages. In any case, the environment is inevitably affected.

The Jonix Minimate device in use in the analyzed area is an air sanitation system combining filtration and sanitization. It is equipped with three filters (G4+F7+F9) under which are placed the 4 cold plasma generators, as shown in figure 3.



Figure 3. Front view of the Jonix Minimate

Non-Thermal Plasma technology <https://jonixair.com/tecnology> (cold plasma) is an advanced form of ionization generating oxidizing species capable of reducing the microbial content present in the air. This system allows the continuous control of contaminants, a sort of continuous "washing" of the air minimizing airborne contamination.

Jonix Minimate has an adjustable air flow from 300 to 2,000 m<sup>3</sup>/h. The device must be sized according to the volume of air to be treated. In the space of the trial, at the maximum flow rate of 2,000 m<sup>3</sup>/h, the device "washes" the air 6,6 times every hour. At the flow rate of 1,000 m<sup>3</sup>/h 3.3 times per hour.

The total bacterial concentration values in supermarket environments can vary from 500 to 1000 colony-forming units per m<sup>3</sup>, depending on the crowd, the season and the maintenance status of the air treatment system.

### Conclusions

From graph 1 we can see that the bacterial concentration per cubic meter is lower than the average reference values already at the first sampling, and is significantly improved with increasing air flow. The values achieved are compatible with a room equipped with a filtration system for protected environments, complying with the microbiological class D. as indicated in the image below.

Clean Room classification				
Microbiologic contamination (a) – Annex 1				
Grade	air sample cfu/m <sup>3</sup>	settle plates (diameter 90mm) cfu/4 hours (b)	contact plates (diameter 55 mm) cfu/plate	glove print 5 fingers cfu/glove
A	<1	<1	<1	<1
B	10	5	5	5
C	100	50	25	-
D	200	100	50	-

Notes:  
 (a) average values  
 (b) plates exposed for less than 4 hours

It is therefore evident that the Jonix Minimate device has significantly reduced the contamination in the air, despite the influence of the air coming from adjacent rooms.

In order to further improve the results, we suggest two infrastructural interventions:

- Closing the ceiling grid with transparent material, thus allowing the passage of light but preventing the uncontrolled passage of air and dust from an unfiltered area;
- Closing the side facing the store, preventing dust and other contaminants from entering, significantly improving the air microbial content of the space that would no longer have uncontrollable influences from the outside.

Available for further clarification.

Alimentaria  
 Dr. Andrea Lovo

## ATTACHMENT 12.13

---

*Case study 4: Sanitizing effects of the MATE device in hospital operating rooms*

## Impact of MATE (air treatment system using NTP technology) on hospital operating rooms

Study conducted between February and March 2017

### Foreword

This document illustrates the results obtained during the first study on the impact of MATE cabinets on the levels of contamination in two operating rooms in a private clinic.

The study refers to the first trial period conducted between 27th February - 23rd March 2017.

### Preparation

#### MATE cabinets

One MATE cabinet was set up in each of the operating rooms in the clinic, namely in Operating Room A and Operating Room B.

The exact location was chosen together with the operators to meet the following requirements:

- Presence of a power supply point;
- Minimal disruption to routine activities carried out in the operating room;
- Adequate distance from items that could obstruct the regular flow of air through MATE.

The cabinets were positioned as shown in the following photos.



**Photo 1 - Position of MATE cabinets inside the operating rooms**

MATE was turned on only during the night and was set to manual mode, even though the internal software allows programming switching on operations: the purpose was to guarantee a certain degree of flexibility of use.

The study program was set up so as to better evaluate the effects of MATE, which had to be integrated with the routine activities carried out inside the operating room, which, at the end of surgeries, call for in-depth environmental sanitation. Furthermore, as required by industry regulations, the air of each operating room was constantly filtered by the treatment system already in place.

The purpose was therefore to use MATE as a support during the standard and ordinary environmental decontamination activities, with the aim of replacing/complementing the existing system, which requires spraying a hydrogen peroxide and silver ions disinfectant solution (400 GLOSAIR).

### Control Schedule

The action of MATE was to be monitored by running targeted analyses with the purpose of obtaining the characterisation of the following items in each operating room:

- 3 surface swabs;
- 1 sample of ambient air.

Each sample was analysed for:

### Total bacterial count at 37°C (TBC37)

*This is the sum of the all the microorganisms that can grow at 37 °C, which are therefore indicators of contamination also by potentially pathogenic germs. Their presence does not provide evidence of the presence of pathogens: it only indicates that they may be present.*

### Moulds and yeasts (M&Y)

*Microorganism that indicate environmental contamination. Together with TBC37, they allow establishing the degree of cleanliness of a certain sample.*

### Coagulase-positive Staphylococci (SC+)

*Opportunistic pathogenic microorganisms that can cause infections in humans. They are normally used as anthropic contamination indicators, often associated with dangerous hospital-acquired infections.*

Sampling was prepared based on the ordinary work activities carried out in both rooms, attempting an assessment of both intensive and low activities (figure 1), in compliance with the workflow illustrated in figure 2.

1st ACTION		2st ACTION		3rd ACTION		4th ACTION		5th ACTION		6th ACTION		7th ACTION		8th ACTION	
WORKING TIME LONG		WORKING TIME SHORT		WORKING TIME LONG		WORKING TIME SHORT		WORKING TIME LONG		WORKING TIME SHORT		WORKING TIME LONG		WORKING TIME SHORT	
27th Feb	28th Feb	1st Mar	2nd Mar	6th Mar	7th Mar	8th Mar	9th Mar	13th Mar	14th Mar	15th Mar	16th Mar	20th Mar	21st Mar	22nd Mar	23rd Mar
Mon	Tue	Wed	Thu	Mon	Tue	Wed	Thu	Mon	Tue	Wed	Thu	Mon	Tue	Wed	Thu

Figure 4 – Sampling program



Figure 5- Flow-chart of activities during the study program

Based on the above, it was possible to assess the level of contamination in the room in case of maximum contamination conditions (worst-case) at the end of the working day and compare it with the levels detected when the room is at its cleanest, by way of samples taken the following day, after manual de-contamination operations and following the uninterrupted use of MATE during the night.

The samples were taken from the same surfaces in both operating rooms, trying to focus on the areas that are more exposed to contamination due to a more intensive operator presence, or to the

fact that they are more difficult to clean by hand due to their shape. Ambient air, instead, was consistently sampled in the middle of each room, near the operating table.

All sampling and analyses were carried out by a qualified and accredited laboratory. Together with the sampling, the switching on and off times of each MATE cabinet were also recorded.

### Results

#### Work surfaces

The data collected, and illustrated in annex 1, evidenced a microbial contamination level that was substantially low.

No moulds or yeasts were isolated from the analysed samples in both sampling conditions (clean/dirty room). Staphylococci were occasionally found in some samples taken after work activities, but only during the first few days of monitoring.

Separate considerations must be made for TBC37.

First, in every case, the microbial load at 37 °C was isolated exclusively in samples taken in the dirty room and never after treatment with MATE; therefore, **after treatment, the samples were totally clean and free from any detectable levels of microorganisms**, evidencing the presence of ideal hygienic conditions.

Obviously, surfaces on which activities are carried out tend to be contaminated, regardless of the type of surface.

The interesting fact that emerged is that, as MATE was used, the average level of fouling (that is the average quantity of what was found in the six sampled surfaces in both operating rooms) tended to decrease over time, as if the treatment made them resistant to contamination during ordinary operating activities.

The chart below shows what has just been described.

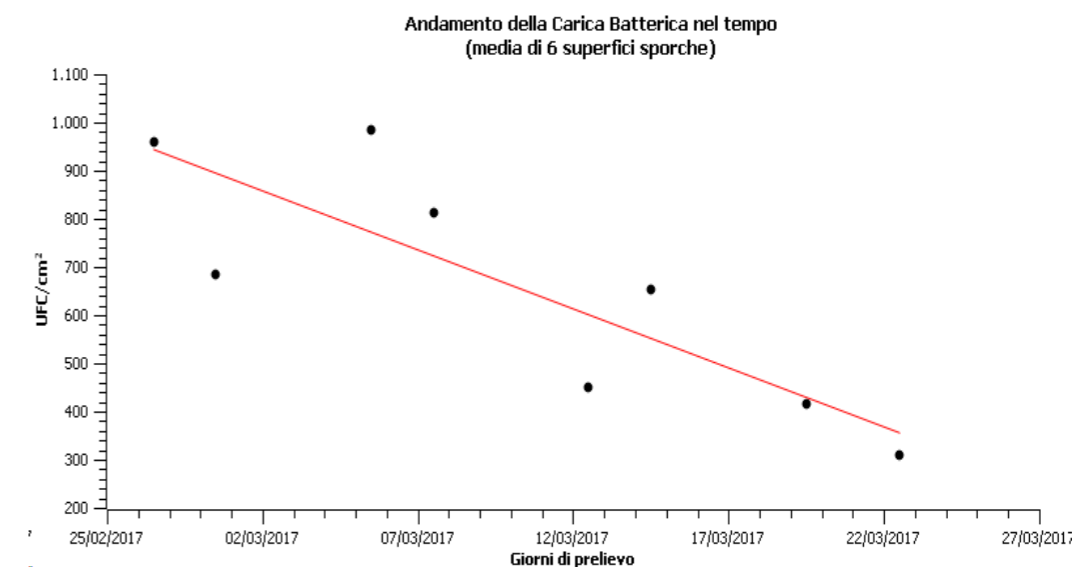


Figure 6 - Average microbial contamination; trend during the testing period. The data represent the average contamination levels detected on the six sampled surfaces in both rooms (3 per room).

The figure illustrates that the TBC37 undeniably tends to decrease, going from an average value of over 900 colony-forming units per square centimetre (CFU/cm<sup>2</sup>) to just over 300 CFU/cm<sup>2</sup> with a reduction trend of good linear approximation.

Through the analysis of the results obtained in individual rooms, it was possible to verify whether this behaviour was detected in both rooms.

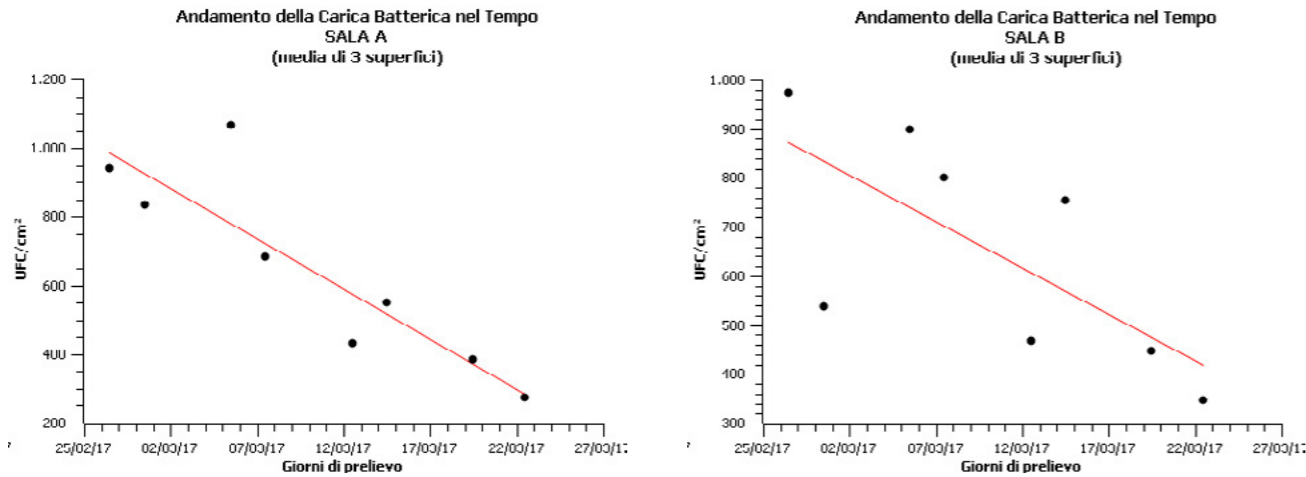


Figure7- Average microbial contamination in the two operating rooms: room A on the left and room B on the right

In this case, it is clear that the observed phenomenon is repeatable in both operating rooms.

As contamination occurs during the normal use of the operating room when MATE is off, the phenomenon seems to be produced by "something" that tends to protect surfaces from contamination, as if the action of MATE made them less hospitable for microorganisms over time.

In general, a surface is less contaminated because:

- a) It is soiled less
- or
- b) With the same level of fouling, the survival rate of microorganisms is lower.

This may be due to:

- b') the presence of biocidal elements (which, in this case, would accumulate over time);
- b'') the lack of elements favouring microbial settlement / survival (free water, nutrients, such as organic matter)

Most probably, it is possible to rule out that the surfaces are soiled less (there is no reason why this should be the case) and therefore the second hypothesis of lower microbial survival rate must be true. In this case, this is unlikely to be due to the permanence/accumulation of biocidal elements (the reactive species generated by MATE have a very short half-life) or to a reduction of free water (this doesn't appear to be correlated with the action of MATE). The most likely hypothesis is that, thanks to the use of MATE, cleaning operations are more effective not only when it comes to eliminating microorganisms (a goal that was achieved right from the beginning of the trial), but also and foremost when it comes to effectively removing the organic matter that settles on the surfaces and constitutes microbial nourishment (dirt).

Regardless of the scientific explanation of the reasons for the observed phenomenon, it seems clear that **the continuous and repeated use of MATE may have a significant adjuvant action to cleaning operations**, without any need for chemical products to be sprayed.

### Ambient air

In the same way, also airborne microbial contamination evidenced low levels of microbial contamination, with the same type of isolated microorganisms (TBC37 and only sporadically SC+).

Also in this case, the air showed the same downward trend, as if it were more and more protected over time during surgery (even if MATE is off) and its de-contamination at night became increasingly more effective.

Nell'immagine: Microbial load trend (average of 2 samples) – Air after operations – Sampling days

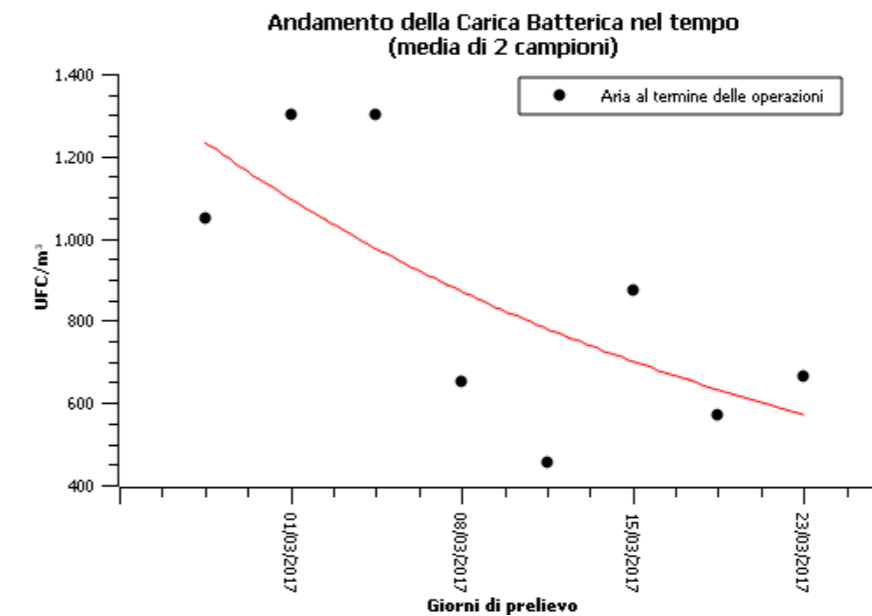


Figure 8 – Airborne contamination trend at the end of the surgery activities (dirty room). Average values detected in both operating rooms

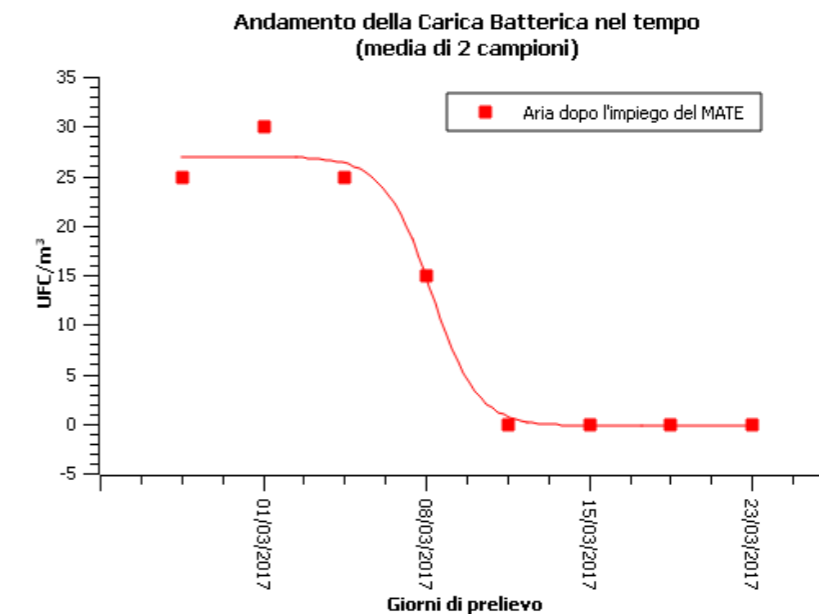
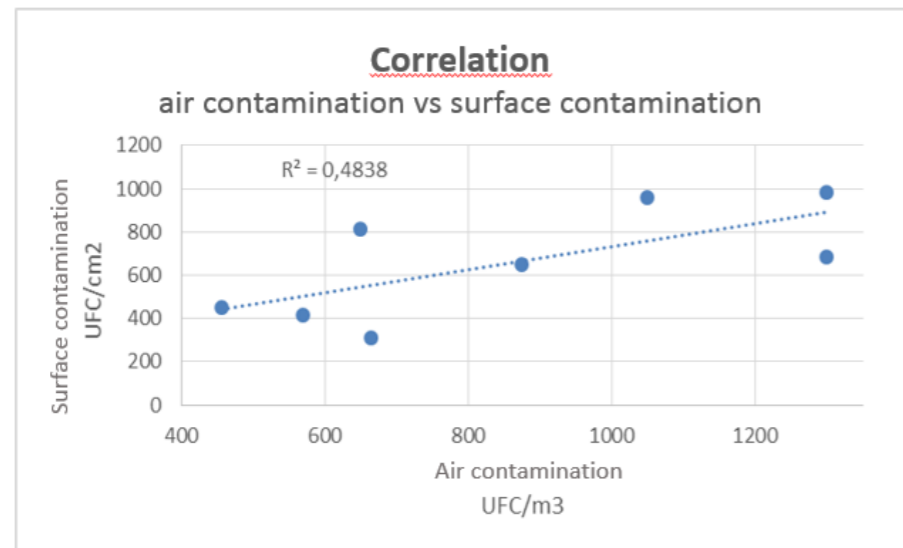


Figure 9 - Airborne contamination trend when MATE is switched off after working overnight (clean room). Average values detected in both operating rooms

The microbial load reduction is evident both in the dirty and in the clean room. In the latter case, a particular phenomenon was observed: whereas at the beginning of the experimental period a minimum amount of contamination was recorded despite the use of MATE (approximately 30 CFU/m<sup>3</sup>), such contamination suddenly disappeared during the second experimental period (sigmoid trend).

In this case the explanation of the phenomenon may be more complicated: it is in fact difficult to understand why, as MATE is used regularly, the air is less contaminated even during surgery operations, that is when the ionizing system is off.

In the case of airborne contamination, biocidal activity cannot be a reason (as it is very short), nor can be the other factors that were hypothesized for surfaces. An assumption was made regarding the existence of a correlation between the level of fouling of surfaces and airborne contamination, i.e. cleaner surfaces mean fewer microorganisms in the air.



**Figure 10 – Correlation between surface contamination and airborne contamination**

Data analysis, unfortunately, evidences a poor correlation between these factors ( $r^2 = 0.49$ ) making this assumption inaccurate.

Another option, currently impossible to verify with the data available, is that the combination of reactive species produced during the night by MATE with water vapour in the air generates hydrogen peroxide molecules characterized by a clear higher persistence in air. The prolonged use of MATE would therefore allow, over time, the accumulation of compounds with biocidal action able to contrast the presence of airborne microorganisms.

Even in this case, however, irrespective of strict scientific explanation of the observed phenomenon, it can be concluded that **the use of MATE improves air quality**, leading to a gradual decrease of microbial contamination of air, which greatly improves health and hygienic conditions.

## Annex 1

### -Analytical results -



## Surfaces

Sala A											
Ora del prelievo	Sporca	17:30	Orario MATE	Mate ON	17:51	Sportello mobile porta fili sutura		Soffietto lettino operatorio		Lampada scialitica lato dx	
	Pulita	07:35		Mate OFF	7:30	27/02/17	28/02/17	27/02/17	28/02/17	27/02/17	28/02/17
Tempo funzionamento MATE (ore:minuti)					13:39	Sporca	Pulita	Sporca	Pulita	Sporca	Pulita
CBT a 37°						1300	<1	1500	<1	30	<1
Muffe						<10	<10	<10	<10	<10	<10
Lieviti						<10	<10	<10	<10	<10	<10
Stafilococco						15	<10	<10	<10	<10	<10

Sala B											
Ora del prelievo	Sporca	17:55	Orario MATE	Mate ON	18:13	Sportello mobile porta fili sutura		Soffietto lettino operatorio		Lampada scialitica lato dx	
	Pulita	08:00		Mate OFF	07:32	27/02/17	28/02/17	27/02/17	28/02/17	27/02/17	28/02/17
Tempo funzionamento MATE (ore:minuti)					13:19	Sporca	Pulita	Sporca	Pulita	Sporca	Pulita
CBT a 37°						1400	<1	1500	<1	20	<1
Muffe						<10	<10	<10	<10	<10	<10
Lieviti						<10	<10	<10	<10	<10	<10
Stafilococco						<10	<10	<10	<10	<10	<10

Sala A											
Ora del prelievo	Sporca	20:00	Orario MATE	Mate ON	20:15	Tubo corrugato		Macchina anestesia zona pulsanti		Piano inox carrello ferri	
	Pulita	08:10		Mate OFF	07:40	01/03/17	02/03/17	01/03/17	02/03/17	01/03/17	02/03/17
Tempo funzionamento MATE (ore:minuti)					11:25	Sporca	Pulita	Sporca	Pulita	Sporca	Pulita
CBT a 37°						900	<1	1000	<1	600	<1
Muffe						<10	<10	<10	<10	<10	<10
Lieviti						<10	<10	<10	<10	<10	<10
Stafilococco						15	<10	<10	<10	<10	<10

Sala B											
Ora del prelievo	Sporca	19:30	Orario MATE	Mate ON	19:49	Tubo corrugato		Macchina anestesia zona pulsanti		Piano inox carrello ferri	
	Pulita	07:45		Mate OFF	07:42	01/03/17	02/03/17	01/03/17	02/03/17	01/03/17	02/03/17
Tempo funzionamento MATE (ore:minuti)					11:53	Sporca	Pulita	Sporca	Pulita	Sporca	Pulita
CBT a 37°						700	<1	110	<1	800	<1
Muffe						<10	<10	<10	<10	<10	<10
Lieviti						<10	<10	<10	<10	<10	<10
Stafilococco						<10	<10	<10	<10	<10	<10

Sala A											
Ora del prelievo	Sporca	18:15	Orario MATE	Mate ON	18:34	Carrello portafarmaci cassetto lato dx		Maniglia carrello assistente paziente		Sportello mobile porta fili di sutura	
	Pulita	11:20		Mate OFF	11:15	06/03/17	07/03/17	06/03/17	07/03/17	06/03/17	07/03/17
Tempo funzionamento MATE (ore:minuti)					16:41	Sporca	Pulita	Sporca	Pulita	Sporca	Pulita
CBT a 37°						1300	<1	1000	<1	900	<1
Muffe						<10	<10	<10	<10	<10	<10
Lieviti						<10	<10	<10	<10	<10	<10
Stafilococco						<10	<10	<10	<10	<10	<10

Sala B											
Ora del prelievo	Sporca	17:10	Orario MATE	Mate ON	17:31	Carrello portafarmaci cassetto lato dx		Maniglia carrello assistente paziente		Sportello mobile porta fili di sutura	
	Pulita	10:55		Mate OFF	10:52	06/03/17	07/03/17	06/03/17	07/03/17	06/03/17	07/03/17
Tempo funzionamento MATE (ore:minuti)					17:21	Sporca	Pulita	Sporca	Pulita	Sporca	Pulita
CBT a 37°						900	<1	700	<1	1100	<1
Muffe						<10	<10	<10	<10	<10	<10
Lieviti						<10	<10	<10	<10	<10	<10
Stafilococco						<10	<10	<10	<10	<10	<10

Sala A											
Ora del prelievo	Sporca	20:30	Orario MATE	Mate ON	20:46	Soffietto lettino operatorio		Lampada scialitica lato sx		Tubo corrugato	
	Pulita	11:20		Mate OFF	07:47	08/03/17	09/03/17	08/03/17	09/03/17	08/03/17	09/03/17
Tempo funzionamento MATE (ore:minuti)					11:01	Sporca	Pulita	Sporca	Pulita	Sporca	Pulita
CBT a 37°						1100	<1	840	<1	530	<1
Muffe						<10	<10	<10	<10	<10	<10
Lieviti						<10	<10	<10	<10	<10	<10
Stafilococco						<10	<10	<10	<10	<10	<10

Sala B											
Ora del prelievo	Sporca	20:10	Orario MATE	Mate ON	20:28	Soffietto lettino operatorio		Lampada scialitica lato sx		Tubo corrugato	
	Pulita	07:40		Mate OFF	07:41	08/03/17	09/03/17	08/03/17	09/03/17	08/03/17	09/03/17
Tempo funzionamento MATE (ore:minuti)					11:13	Sporca	Pulita	Sporca	Pulita	Sporca	Pulita
CBT a 37°						1300	<1	650	<1	450	<1
Muffe						<10	<10	<10	<10	<10	<10
Lieviti						<10	<10	<10	<10	<10	<10
Stafilococco						<10	<10	<10	<10	<10	<10

Sala A											
Ora del prelievo	Sporca	14:50	Orario MATE	Mate ON	15:13	Macchina anestesia zona pulsanti		Carrello portafarmaci cassetto lato sx		Piano inox carrello ferri	
	Pulita	12:45		Mate OFF	12:46	13/03/17	14/03/17	13/03/17	14/03/17	13/03/17	14/03/17
Tempo funzionamento MATE (ore:minuti)					21:33	Sporca	Pulita	Sporca	Pulita	Sporca	Pulita
<b>CBT a 37°</b>						400	<1	400	<1	500	<1
<b>Muffe</b>						<10	<10	<10	<10	<10	<10
<b>Lieviti</b>						<10	<10	<10	<10	<10	<10
<b>Stafilococco</b>						<10	<10	<10	<10	<10	<10

Sala B											
Ora del prelievo	Sporca	15:40	Orario MATE	Mate ON	16:07	Macchina anestesia zona pulsanti		Carrello portafarmaci cassetto lato sx		Piano inox carrello ferri	
	Pulita	13:10		Mate OFF	13:06	13/03/17	14/03/17	13/03/17	14/03/17	13/03/17	14/03/17
Tempo funzionamento MATE (ore:minuti)					20:59	Sporca	Pulita	Sporca	Pulita	Sporca	Pulita
<b>CBT a 37°</b>						640	<1	410	<1	350	<1
<b>Muffe</b>						<10	<10	<10	<10	<10	<10
<b>Lieviti</b>						<10	<10	<10	<10	<10	<10
<b>Stafilococco</b>						<10	<10	<10	<10	<10	<10

Sala A											
Ora del prelievo	Sporca	19:10	Orario MATE	Mate ON	19:33	Maniglia carrello assistente paziente		Sportello mobile porta fili di sutura		Soffietto lettino operatorio	
	Pulita	07:40		Mate OFF	07:37	15/03/17	16/03/17	15/03/17	16/03/17	15/03/17	16/03/17
Tempo funzionamento MATE (ore:minuti)					12:04	Sporca	Pulita	Sporca	Pulita	Sporca	Pulita
<b>CBT a 37°</b>						540	<1	710	<1	400	<1
<b>Muffe</b>						<10	<10	<10	<10	<10	<10
<b>Lieviti</b>						<10	<10	<10	<10	<10	<10
<b>Stafilococco</b>						<10	<10	<10	<10	<10	<10

Sala B											
Ora del prelievo	Sporca	19:40	Orario MATE	Mate ON	19:53	Maniglia carrello assistente paziente		Sportello mobile porta fili di sutura		Soffietto lettino operatorio	
	Pulita	08:10		Mate OFF	07:54	15/03/17	16/03/17	15/03/17	16/03/17	15/03/17	16/03/17
Tempo funzionamento MATE (ore:minuti)					12:01	Sporca	Pulita	Sporca	Pulita	Sporca	Pulita
<b>CBT a 37°</b>						730	<1	1100	<1	430	<1
<b>Muffe</b>						<10	<10	<10	<10	<10	<10
<b>Lieviti</b>						<10	<10	<10	<10	<10	<10
<b>Stafilococco</b>						<10	<10	<10	<10	<10	<10

Sala A											
Ora del prelievo	Sporca	17:30	Orario MATE	Mate ON	17:55	Lampada scialitica zona centrale		Tubo corrugato		Macchina anestesia zona pulsanti	
	Pulita	12:40		Mate OFF	12:37	20/03/17	21/03/17	20/03/17	21/03/17	20/03/17	21/03/17
Tempo funzionamento MATE (ore:minuti)					18:42	Sporca	Pulita	Sporca	Pulita	Sporca	Pulita
<b>CBT a 37°</b>						430	<1	310	<1	410	<1
<b>Muffe</b>						<10	<10	<10	<10	<10	<10
<b>Lieviti</b>						<10	<10	<10	<10	<10	<10
<b>Stafilococco</b>						<10	<10	<10	<10	<10	<10

Sala B											
Ora del prelievo	Sporca	18:15	Orario MATE	Mate ON	18:37	Lampada scialitica zona centrale		Tubo corrugato		Macchina anestesia zona pulsanti	
	Pulita	13:05		Mate OFF	13:00	20/03/17	21/03/17	20/03/17	21/03/17	20/03/17	21/03/17
Tempo funzionamento MATE (ore:minuti)					18:23	Sporca	Pulita	Sporca	Pulita	Sporca	Pulita
<b>CBT a 37°</b>						510	<1	310	<1	520	<1
<b>Muffe</b>						<10	<10	<10	<10	<10	<10
<b>Lieviti</b>						<10	<10	<10	<10	<10	<10
<b>Stafilococco</b>						<10	<10	<10	<10	<10	<10

Sala A											
Ora del prelievo	Sporca	19:05	Orario MATE	Mate ON	19:45	Piano inox carrello porta ferri		Cassetto basso carrello portafarmaci		Maniglia carrello assistente pazienti	
	Pulita	09:48		Mate OFF	09:40	23/03/17	24/03/17	23/03/17	24/03/17	23/03/17	24/03/17
Tempo funzionamento MATE (ore:minuti)					13:55	Sporca	Pulita	Sporca	Pulita	Sporca	Pulita
<b>CBT a 37°</b>						210	<1	70	<1	540	<1
<b>Muffe</b>						<10	<10	<10	<10	<10	<10
<b>Lieviti</b>						<10	<10	<10	<10	<10	<10
<b>Stafilococco</b>						<10	<10	<10	<10	<10	<10

Sala B											
Ora del prelievo	Sporca	19:30	Orario MATE	Mate ON	19:33	Piano inox carrello porta ferri		Cassetto basso carrello portafarmaci		Maniglia carrello assistente pazienti	
	Pulita	09:20		Mate OFF	09:15	23/03/17	24/03/17	23/03/17	24/03/17	23/03/17	24/03/17
Tempo funzionamento MATE (ore:minuti)					13:42	Sporca	Pulita	Sporca	Pulita	Sporca	Pulita
<b>CBT a 37°</b>						530	<1	100	<1	410	<1
<b>Muffe</b>						<10	<10	<10	<10	<10	<10
<b>Lieviti</b>						<10	<10	<10	<10	<10	<10
<b>Stafilococco</b>						<10	<10	<10	<10	<10	<10

**Ambient air**

Sala A							
Ora del prelievo	Sporca	17:30	Orario MATE	Mate ON	17:51	Aria lettino operatorio	
	Pulita	07:35		Mate OFF	7:30		
Tempo funzionamento MATE (ore:minuti)					13:39	27/02/17	28/02/17
CBT a 37°						Sporca	Pulita
						1200	50
Muffe						assente	assente
Lieviti						assente	assente
Stafilococco						70	assente
Sala B							
Ora del prelievo	Sporca	17:55	Orario MATE	Mate ON	18:13	Aria lettino operatorio	
	Pulita	08:00		Mate OFF	07:32		
Tempo funzionamento MATE (ore:minuti)					13:19	27/02/17	28/02/17
CBT a 37°						Sporca	Pulita
						900	<1
Muffe						assente	assente
Lieviti						assente	assente
Stafilococco						assente	assente

Sala A							
Ora del prelievo	Sporca	20:00	Orario MATE	Mate ON	20:15	Aria lettino operatorio	
	Pulita	08:10		Mate OFF	07:40		
Tempo funzionamento MATE (ore:minuti)					11:25	01/03/17	02/03/17
CBT a 37°						Sporca	Pulita
						1400	30
Muffe						assente	assente
Lieviti						assente	assente
Stafilococco						35	assente
Sala B							
Ora del prelievo	Sporca	19:30	Orario MATE	Mate ON	19:49	Aria lettino operatorio	
	Pulita	07:45		Mate OFF	07:42		
Tempo funzionamento MATE (ore:minuti)					11:53	01/03/17	02/03/17
CBT a 37°						Sporca	Pulita
						1200	30
Muffe						assente	assente
Lieviti						assente	assente
Stafilococco						assente	assente

Sala A							
Ora del prelievo	Sporca	18:15	Orario MATE	Mate ON	18:34	Aria lettino operatorio	
	Pulita	11:20		Mate OFF	11:15		
Tempo funzionamento MATE (ore:minuti)					16:41	06/03/17	07/03/17
CBT a 37°						Sporca	Pulita
						1400	30
Muffe						assente	assente
Lieviti						assente	assente
Stafilococco						assente	assente
Sala B							
Ora del prelievo	Sporca	17:10	Orario MATE	Mate ON	17:31	Aria lettino operatorio	
	Pulita	10:55		Mate OFF	10:52		
Tempo funzionamento MATE (ore:minuti)					17:21	06/03/17	07/03/17
CBT a 37°						Sporca	Pulita
						1200	20
Muffe						assente	assente
Lieviti						assente	assente
Stafilococco						40	assente

Sala A							
Ora del prelievo	Sporca	20:30	Orario MATE	Mate ON	20:46	Aria lettino operatorio	
	Pulita	11:20		Mate OFF	07:47		
Tempo funzionamento MATE (ore:minuti)					11:01	08/03/17	09/03/17
CBT a 37°						Sporca	Pulita
						500	30
Muffe						assente	assente
Lieviti						assente	assente
Stafilococco						assente	assente
Sala B							
Ora del prelievo	Sporca	20:10	Orario MATE	Mate ON	20:28	Aria lettino operatorio	
	Pulita	07:40		Mate OFF	07:41		
Tempo funzionamento MATE (ore:minuti)					11:13	08/03/17	09/03/17
CBT a 37°						Sporca	Pulita
						800	<1
Muffe						assente	assente
Lieviti						assente	assente
Stafilococco						assente	assente

Sala A							
Ora del prelievo	<b>Sporca</b>	14:50	Orario MATE	<b>Mate ON</b>	15:13	Aria lettino operatorio	
	<b>Pulita</b>	12:45		<b>Mate OFF</b>	12:46	13/03/17	14/03/17
Tempo funzionamento MATE (ore:minuti)					21:33	<b>Sporca</b>	<b>Pulita</b>
CBT a 37°					340	<1	
Muffe					assente	assente	
Lieviti					assente	assente	
Stafilococco					assente	assente	
Sala B							
Ora del prelievo	<b>Sporca</b>	15:40	Orario MATE	<b>Mate ON</b>		Aria lettino operatorio	
	<b>Pulita</b>	13:10		<b>Mate OFF</b>		13/03/17	14/03/17
Tempo funzionamento MATE (ore:minuti)					00:00	<b>Sporca</b>	<b>Pulita</b>
CBT a 37°					570	<1	
Muffe					assente	assente	
Lieviti					assente	assente	
Stafilococco					assente	assente	

Sala A							
Ora del prelievo	<b>Sporca</b>	17:30	Orario MATE	<b>Mate ON</b>	17:55	Aria lettino operatorio	
	<b>Pulita</b>	12:40		<b>Mate OFF</b>	12:37	20/03/17	21/03/17
Tempo funzionamento MATE (ore:minuti)					18:42	<b>Sporca</b>	<b>Pulita</b>
CBT a 37°					340	<1	
Muffe					assente	assente	
Lieviti					assente	assente	
Stafilococco					assente	assente	
Sala B							
Ora del prelievo	<b>Sporca</b>	18:15	Orario MATE	<b>Mate ON</b>	18:37	Aria lettino operatorio	
	<b>Pulita</b>	13:05		<b>Mate OFF</b>	13:00	20/03/17	21/03/17
Tempo funzionamento MATE (ore:minuti)					18:23	<b>Sporca</b>	<b>Pulita</b>
CBT a 37°					800	<1	
Muffe					assente	assente	
Lieviti					assente	assente	
Stafilococco					assente	assente	

Sala A							
Ora del prelievo	<b>Sporca</b>	19:10	Orario MATE	<b>Mate ON</b>	19:33	Aria lettino operatorio	
	<b>Pulita</b>	07:40		<b>Mate OFF</b>	07:37	15/03/17	16/03/17
Tempo funzionamento MATE (ore:minuti)					12:04	<b>Sporca</b>	<b>Pulita</b>
CBT a 37°					810	<1	
Muffe					assente	assente	
Lieviti					assente	assente	
Stafilococco					30	assente	
Sala B							
Ora del prelievo	<b>Sporca</b>	19:40	Orario MATE	<b>Mate ON</b>	19:53	Aria lettino operatorio	
	<b>Pulita</b>	08:10		<b>Mate OFF</b>	07:54	15/03/17	16/03/17
Tempo funzionamento MATE (ore:minuti)					12:01	<b>Sporca</b>	<b>Pulita</b>
CBT a 37°					940	<1	
Muffe					assente	assente	
Lieviti					assente	assente	
Stafilococco					assente	assente	

Sala A							
Ora del prelievo	<b>Sporca</b>	19:05	Orario MATE	<b>Mate ON</b>	19:45	Aria lettino operatorio	
	<b>Pulita</b>	09:48		<b>Mate OFF</b>	09:40	23/03/17	24/03/17
Tempo funzionamento MATE (ore:minuti)					13:55	<b>Sporca</b>	<b>Pulita</b>
CBT a 37°					1100	<1	
Muffe					assente	assente	
Lieviti					assente	assente	
Stafilococco					assente	assente	
Sala B							
Ora del prelievo	<b>Sporca</b>	19:30	Orario MATE	<b>Mate ON</b>	19:33	Aria lettino operatorio	
	<b>Pulita</b>	09:20		<b>Mate OFF</b>	09:15	23/03/17	24/03/17
Tempo funzionamento MATE (ore:minuti)					13:42	<b>Sporca</b>	<b>Pulita</b>
CBT a 37°					230	<1	
Muffe					assente	assente	
Lieviti					assente	assente	
Stafilococco					assente	assente	

## ATTACHMENT 12.14

---

*Case study 5: Sanitizing effects of the MATE device in hospital wards*

AXIS I - PROMOTION OF RESEARCH AND INNOVATION

**“INNOVATION OF THE PROCESS FOR THE  
PREVENTION OF HEALTHCARE-ASSOCIATED  
INFECTIONS (INPRASS)”**

*Innovation Services*

**Final report**

Service 1.1.

**Start:** 1 February 2018  
**End:** 30 April 2018

## Table of contents

<b>SUMMARY</b> .....	223
<b>INTRODUCTION</b> .....	224
CLINICAL RISK: HOSPITAL ACQUIRED INFECTIONS .....	224
STUDY IN THE WARDS .....	226
<b>RESULTS OBTAINED</b> .....	229
AMBIENT AIR .....	229
WORK SURFACES .....	230
ADVANTAGES OF THE POSSIBLE USE OF THE NTP TREATMENT FOR CLINICAL RISK – REDUCTION OF THE RISK OF INFECTION	233
<b>INDICATORS FOR THE FINAL CHECK OF THE SERVICE</b> .....	235
PERFORMANCE INDICATORS.....	235
BIBLIOGRAPHY.....	236

## Summary

The previous study activity, carried out in relation to Service 2.1 in the context of the research project called “Innovation of the process for the prevention of healthcare-associated infections (INPRASS)” and financed by ROP CALABRIA ERDF-ESF 2014-2020 in support of the adoption of innovations and new technologies, brought to light interesting possibilities for the use of NTP technology due to its ability to very significantly reduce the levels of microbial pollution inside ORs.

With a view to taking action to reduce the Clinical Risk linked to hospital infections, we strove to establish how NTP technology could potentially act also against microorganisms that may be found in hospital wards.

For this purpose, we used small ionising systems purposely designed for less “invasive” placement and easier inclusion in a daily life context. The equipment was placed at various points of a ward and left in operation almost constantly during the entire study period. The effects were compared by evaluating the contamination levels in a “control” ward that had not been equipped with NTP systems.

The study was thus able to efficiently and very pertinently meet the need to evaluate innovative systems for the prevention of infections in the OR, in particular, and of hospital infections, in general, making it possible to identify a technology that is able to be used as a complement to the usual environmental sanitisation activities, maximising their efficacy and contributing towards the creation of safer premises with a lower risk of infection.

## Introduction

### Clinical Risk: hospital acquired infections

In its “Manual for training healthcare providers – Patient safety and management of clinical risk” (1), the Ministry of Health defines Clinical Risk as “the possibility that a patient is unwillingly harmed or made uncomfortable, due to healthcare, with a consequent prolongation of hospitalisation, a worsening of the patient’s health, or death”

This possibility is closely related to errors in medical treatment, which may result in various types of harm to the patient. In healthcare, such errors are generally categorised as active errors (a nurse mistaking a medication dose), that are easily identifiable in space and time, and latent errors (a manual treatment prescription and transcription system) which, on the contrary, are harder to identify but which may result in a series of active errors as a chain reaction.

It has been recognised that such errors, which are at the source of health-related incidents, are the result of the interaction among the various components of the healthcare system (technological, human and organisational), each one of which is able to function as a protective barrier against the onset of errors but which, at times, is “faulty” and may, under specific circumstances, lead to an adverse event.

Every healthcare system is thus characterised by its own “risk level” to which contribute various factors:

- structural and technological factors;
- organisational/management-related factors and work conditions;
- human (individual and team) factors;
- the characteristics of the user.

Depending on the adverse event under consideration, one or more of these factors may contribute to its genesis.

Among the most feared adverse events in healthcare, the possibility that a patient may contract a secondary infection (in addition, that is, to the primary infections for which aid was sought from healthcare) is certainly one of the main issues which clinical risk management must deal with.

Such infections may result from patient/patient, operator/patient, or environment/patient cross-contamination and may arise either from active errors (mixed use of medical equipment, failure to use protection systems by healthcare providers, lack of compliance with hygiene rules, etc.) or latent

errors (incorrect formalisation of safety procedures, inadequate training of staff, failure to execute environmental hygiene procedures or insufficient execution thereof, etc.).

Although, at the end of the last century, hospital infections were considered “infections contracted during hospitalisation, which manifest clinically at least 48 hours following admission, during recovery or following discharge”, today the focus has shifted on the concept of infections associated to healthcare processes and to the work performed in healthcare – which may not only refer to hospitals – to the point that the National Healthcare Plan, since 2002-2004, has identified them as errors in the provision of healthcare. It is, however, important to point out that such errors are inherent to the provision of healthcare itself and, consequently, although predictable, they can never be completely eliminated, with an (ever increasing) national rate that ranges from 5 to 10%.

In this light, succeeding in keeping the environmental contamination level in the OR under control is an indispensable element of all clinical risk management; in fact, in the OR, patients are exposed more than ever before to the possibility of contracting dangerous infections to a degree that is directly proportional to the invasiveness of the operation, and, obviously, to the level of airborne and surface contamination.

Other than this “critical” environment, however, there are many others that require thorough control of the levels of environmental contamination, from outpatient clinics to waiting rooms, all the way to hospital wards. The latter are very often a source of cross infection due to the possible presence of patients who are known, but, more often, unknown carriers of infectious agents able to increase the clinical risk. On the other hand, the presence of visitors can, in certain cases, deteriorate the general environmental hygiene level, with a consequent increase of the risk of infection to patients.



### Study in the wards

With this study, we sought to understand whether the excellent results obtained in the OR could, in some way, be replicated in hospital wards as well.

For this reason, a type of equipment other than MATE was used, always based on ionising modules able to generate NTP air, but of a significantly smaller size and not equipped with a HEPA filtration module.



Figure 11 - Air handling unit used in the ward

The system used, known as CUBE, exploits the same principles that the MATE cabinet is based on and, being equipped with an automatic timer system, is able to perform treatment cycles that can be customised to meet needs.

Two hospital wards were identified for the purpose of the study, exactly similar in terms of type of hospitalised patients (orthopaedic patients), number of patients, and the frequency of visits from members of the patients' families.

Both wards are of exactly the same size and are subjected to the same sanitisation activities by auxiliary personnel.

One of the two wards was equipped with three CUBE units placed in such a manner as to cover the entire length of the corridor, with particular focus on the most frequented areas (coffee area).



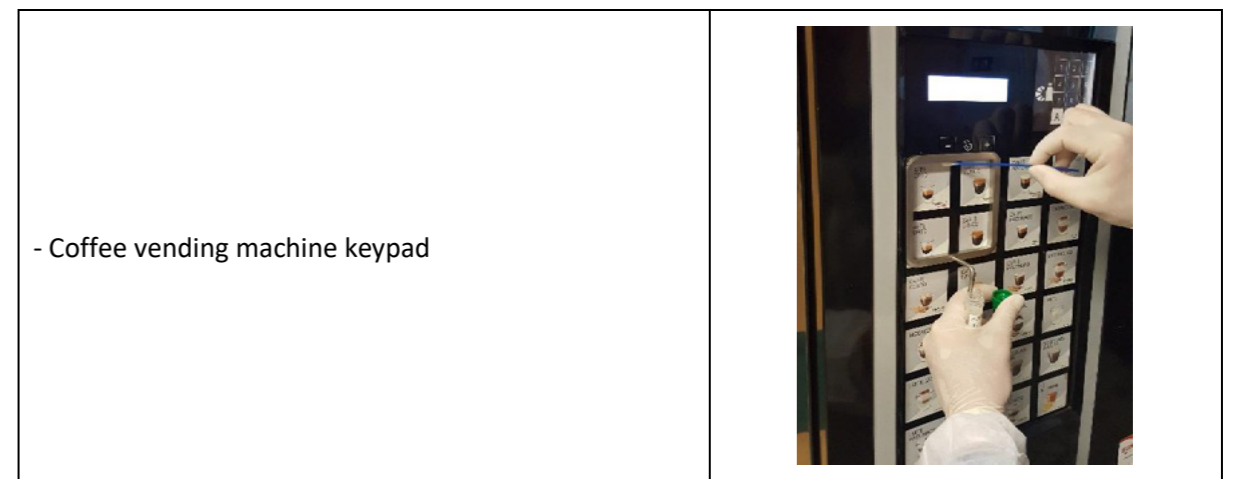
Figure 12 - Placement of the three CUBE units in the "treated" ward. A) coffee area - waiting room; B) ward centre; C) ward end

The CUBE units were programmed to guarantee continuous operation in accordance with a cycle that envisaged 2 minutes switched on followed by an 8-minute pause, 24 hours a day.

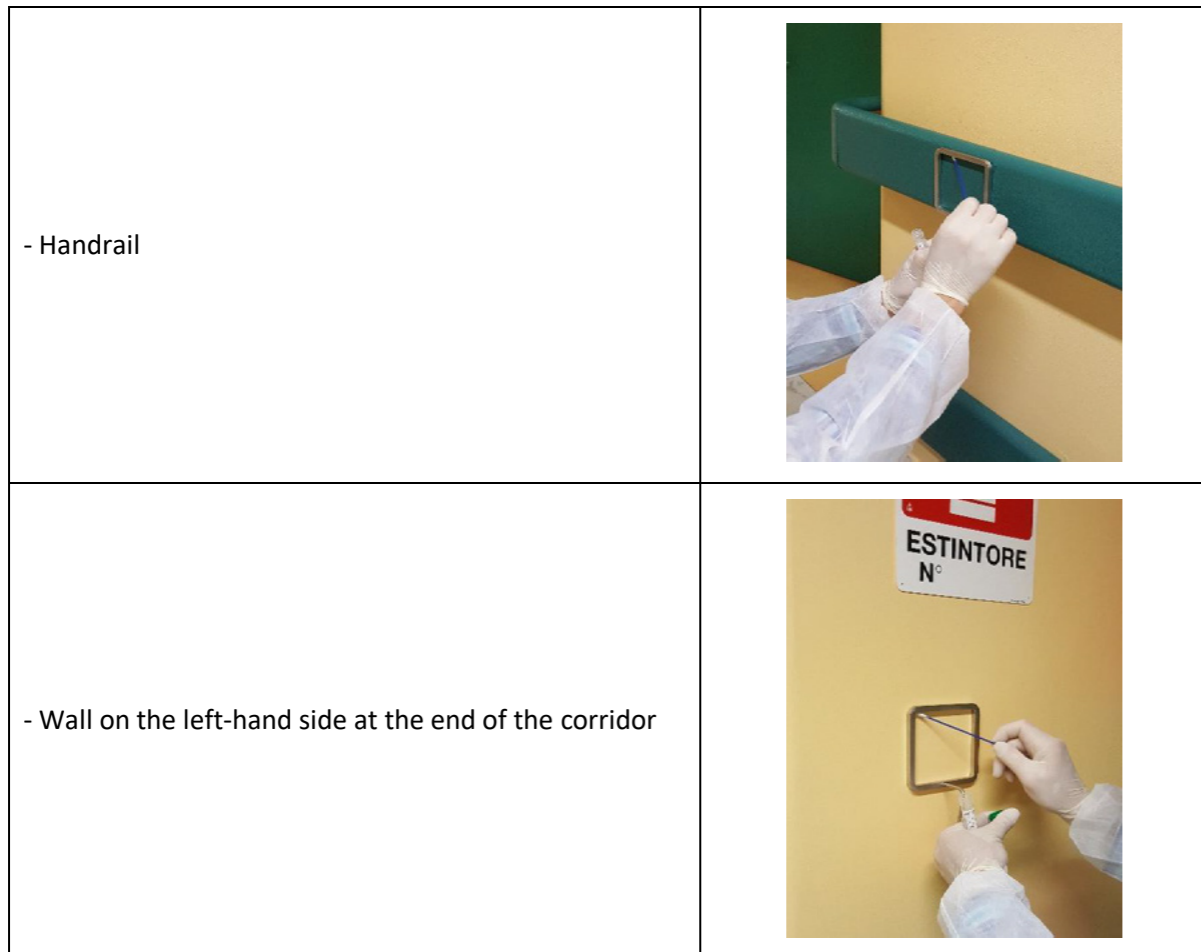
Environmental samples were harvested periodically (twice-weekly) and simultaneously from both the treated ward and the control ward to evaluate efficacy.

The selected sampling points (identical for both wards) were as follows:

#### Surfaces



- Coffee vending machine keypad



The surfaces were chosen as they were deemed to have the highest contamination rate and, thus, of more significance for the objectives of the study.

In the same manner, samples of the ambient air were harvested with an active SAS sampler in the waiting room, neat the lift, and near the coffee machine.

Air



The following were measured in each sample:

- Total bacterial load at 37°C;
- Moulds and yeasts;
- Coagulase-positive staphylococci.

Samples were harvested for four weeks, on Tuesdays and Thursdays, immediately after the end of visiting hours and before any environmental cleaning operation, so as to monitor the worst pollution conditions possible.

**Results obtained**

Ambient air

The results obtained on the values of airborne contamination are set out below, comparing the environmental data of the two wards.

t (days)	Control Ward CFU/m <sup>3</sup>	Ward Treated with CUBE CFU/m <sup>3</sup>	Daily reduction %
0	2100	300	85.71%
2	1100	310	71.82%
7	2000	420	79.00%
9	300	50	83.33%
14	2300	30	98.70%
16	1200	270	77.50%
21	1300	140	89.23%
23	900	100	88.89%
<b>Average</b>	<b>1400</b>	<b>203</b>	
<b>Total reduction %</b>	<b>86%</b>		

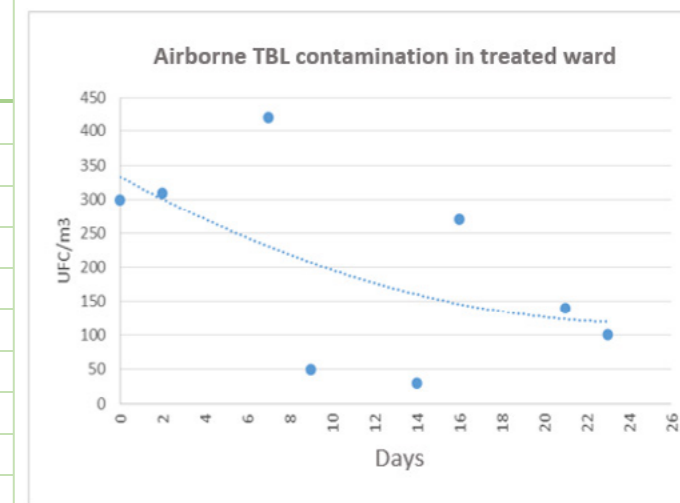


Figure 13 - TABLE: trends of the contamination from Total Bacterial Load measured in the air in the two wards that formed the object of the experiment. The daily reduction % refers to the values per sampling day in the two wards of the study; the total reduction %, instead, refers to the average values that were found in total in the two types of ward. GRAPH: TBL trend during the experiment only in the “treated” ward.

From the results presented, one may clearly appreciate that the microbial contamination tends to decrease over time in the treated ward, being reduced to one-third at the end of the experiment. The subsequent comparison of the data obtained in the control ward with those from the treated ward makes it very clear that the use of the CUBE unit immediately resulted in a significant improvement, with a reduction of the contamination by a total of 86% (average values).

Table 2 - Trends of the contamination from Moulds and Yeasts (table on the left) and Staphylococci (table on the right) found in the air of the two wards of the experiment. The daily reduction % refers to the values per sampling day in the two wards of the study; the total reduction %, instead, refers to the average values that were found in total in the two types of ward.

t (days)	Control Ward CFU/m <sup>3</sup>	Treated Ward (CUBE) CFU/m <sup>3</sup>	Daily reduction %	t (days)	Control Ward CFU/m <sup>3</sup>	Treated Ward (CUBE) CFU/m <sup>3</sup>	Daily reduction %
0	80	0	100.00%	0	60	0	100.00%
2	210	0	100.00%	2	12	0	100.00%
7	150	0	100.00%	7	19	0	100.00%
9	180	0	100.00%	9	22	0	100.00%
14	170	0	100.00%	14	20	0	100.00%
16	210	0	100.00%	16	24	0	100.00%
21	100	0	100.00%	21	0	0	100.00%
23	60	0	100.00%	23	0	0	100.00%
<b>Average</b>	<b>145</b>	<b>0</b>		<b>Average</b>	<b>20</b>	<b>0</b>	
<b>Reduction %</b>	<b>100%</b>			<b>Reduction %</b>	<b>100%</b>		

In this case, one may observe that the presence of the CUBE unit in the treated ward in fact rendered the environment absolutely inhospitable for the germs searched (Moulds and Yeasts, Coagulase-positive staphylococci) which, on the other hand, were practically ever present in the other ward. In this case, therefore, one observed a total reduction of the contamination by 100% (average values).

**Work surfaces**

Similarly to the results relating to ambient air, below please find the contamination values obtained from the analysis of the surfaces from which samples were harvested.

Table 3 - Trends of the contamination from Total Bacterial Load measured on the sample surfaces in the two wards that formed the object of the experiment.

TBL	Control Ward			Treated Ward (CUBE)		
	Keypad	Handrail	Wall	Keypad	Handrail	Wall
t (days)						
0	1400	1200	9100	800	400	620
2	1400	9000	3900	140	40	60
7	2100	700	800	400	180	150
9	350	400	1000	60	70	90
14	500	1200	610	290	180	90
16	1400	2300	730	200	210	130
21	900	1000	1600	70	80	120
23	1000	810	1100	80	85	90
<b>Average</b>	<b>1131</b>	<b>2076</b>	<b>2355</b>	<b>255</b>	<b>156</b>	<b>169</b>

In this case it is possible to point out the following decrease percentages of the average values found for each type of surface in the two wards:

Table 4 - Reduction of microbial contamination by sample surface. Comparison between the surfaces of the treated ward/the surfaces of the control ward

TBL	Keypad	Handrail	Wall
Reduction %	77%	93%	93%

The graphs below show that the microbial contamination tends to progressively decrease over time on all surfaces of the treated ward, from which samples were harvested, in a wholly similar manner to that observed with regard to the air.

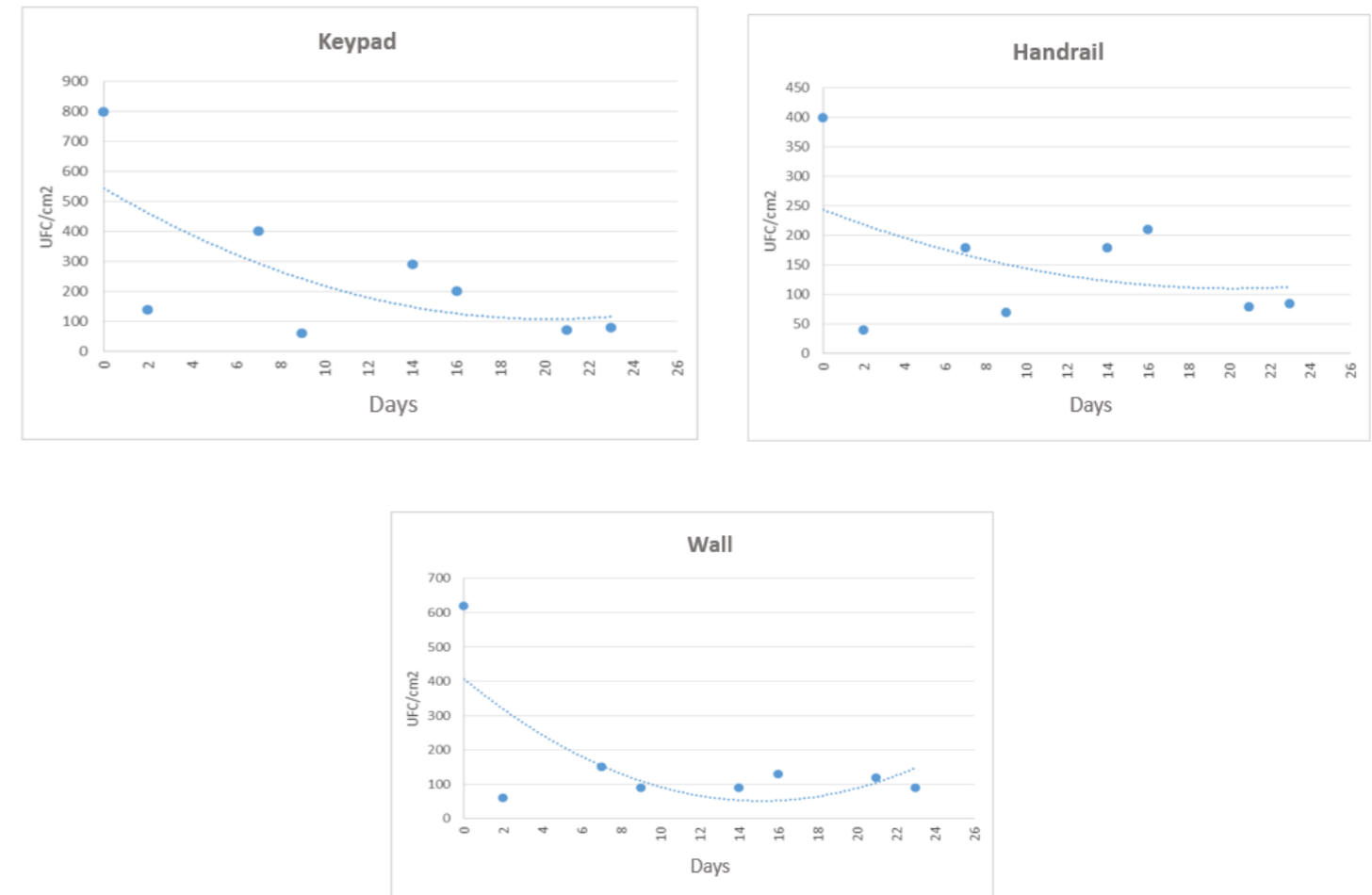


Figure 14 - Trend of the contamination by TBL on the surfaces of the ward treated with CUBE

The results presented clearly show that the treatment of ambient air with the CUBE unit is also beneficial to the surfaces, revealing a clear decreasing tendency of the total microbial load on the surfaces from which samples were taken during the experiment. The reduction is present both when comparing the average values of surface contamination in the two wards (table 18) and when evaluating the trend over time in the treated ward (figure 45).

In this case, the reduction percentages observed were as follows:

Table 5 - Reduction of microbial contamination by sampled surface in the treated ward. Comparison between surfaces at the start/end of treatment

TBL	Keypad	Handrail	Wall
Reduction %	90%	78%	85%

The results for the other two analysed parameters are as follows.

Table 6 Trend of contamination from Moulds and Yeasts (upper table) and Coagulase-positive staphylococci (lower table) found on the sample surfaces in the two wards that formed the object of the experiment.

ML	Control Ward			Treated Ward (CUBE)		
	Keypad	Handrail	Wall	Keypad	Handrail	Wall
t (days)						
0	0	0	120	0	0	0
2	0	0	100	0	0	0
7	0	50	140	0	0	0
9	0	0	200	0	0	0
14	0	0	160	0	0	0
16	0	85	180	0	0	0
21	0	0	40	0	0	0
23	0	0	80	0	0	0
Average	0	17	128	0	0	0

SC+	Control Ward			Treated Ward (CUBE)		
	Keypad	Handrail	Wall	Keypad	Handrail	Wall
t (days)						
0	40	0	30	0	0	0
2	80	0	0	0	0	0
7	70	0	0	0	0	0
9	130	0	0	0	0	0
14	110	70	0	0	0	0
16	19	45	0	0	0	0
21	0	0	0	0	0	0
23	30	0	0	0	0	0
Average	60	14	4	0	0	0

With the following reduction values

MF	Keypad*	Handrail	Wall
Reduction %	0%	100%	100%

\* moulds and yeasts were never found, in neither of the two wards

SC+	Keypad	Handrail	Wall
Reduction %	100%	100%	100%

The following conclusions may be drawn from the data presented:

- The application of the CUBE systems resulted in a constant improvement of the air quality for all research parameters, with differences in contamination between the “treated” ward and the “control” ward of at least two orders of magnitude; said differences were obvious from the very first day of treatment and became increasingly more marked as the treatment went on;

- The “treated” ward showed a significant reduction of the contamination values, this being particularly obvious when evaluating the values of the Total Bacterial Load at 37°C; in the case of the “treated” ward, pollutants from anthropic sources (evidenced by the presence of Coagulase-positive staphylococci) were found to be fully under control, with a constant absence of the pathogen in all samples analysed. Also fungi (some of which potentially pathogenic) were found to be undetectable, further proof of the optimal hygiene levels of the ambient air;

- As happened in the ORs, the use of ionised air resulted in a marked decrease of the contamination levels of the surfaces from which samples were harvested, direct proof of the potential inherent in the use of this technology. In particular, the result obtained on the coffee machine keypad is worthy of being highlighted. This is a surface that very often comes into contact with the hands of visitors, staff and patients, is often overlooked during routine sanitisation operations and is thus able to transfer potential infectious microbial agents from one subject to another.

As shown by the results presented, this surface confirms its “potential” in the control ward, with extremely high contamination values. These data are counterbalanced by the data obtained in the machine located in the “treated” ward, where we observed the disappearance of the staphylococci and a dramatic and significant decrease in the total bacterial loads.

#### Advantages of the possible use of the NTP treatment for Clinical Risk – reduction of the Risk of Infection

The results shown prove that the biocidal activity of the NTP technology is of great interest. In particular, it became clear that it is very effective when it comes to disinfecting surfaces in a really short time. Furthermore, the possibility of combining the ionisation and filtration treatment creates very interesting prospects.

Indeed, one may envisage a mobile device that would be able to perform the air disinfection and filtration treatment wherever the need arises at any given time.

For example, in the OR it could be configured as a unit that can complement the purification of the ambient air performed by the ducted treatment system. In this way, the device would contribute to the “decontamination” of the particulate emitted during surgery in the OR, by recirculating air that has already been treated through a HEPA ultrafilter. If this additional filtration were to be combined with ionisation via NTP, it would guarantee the presence of extremely clean air.

Its ability to sanitise contaminated surfaces would also introduce additional guarantees, contributing to the improvement of environmental hygiene and to a reduction in the possible emergence of infections.

A hypothetical “typical” scenario might be as follows:

- Start of the day in the OR. Standard air treatment system in operation + recirculation system on a HEPA filter;
- Interval between two operations. Start of the operation of the air ionisation and surface disinfection system;
- End of the day. Deep cleaning of the OR. Switching off the standard air treatment system. Switching on the air ionisation system.

This would result in the significant advantage of starting the day with a clean room that has been consistently disinfected by the continuous operation of the treatment system; it would also guarantee an OR that is ready for use within a shorter time in the event of night-time emergency.

Aside from the results in the OR, the study has proven that the use of NTP air, albeit produced with smaller and simplified devices, has resulted in indisputable benefits for the environmental quality in the ward that was subject to treatment, where airborne contamination was decidedly low, the microorganisms present on the surfaces were markedly reduced, while, at the same time, the pathogenic Staphylococci disappeared. In this case one could envisage complementing the current environmental sanitisation system with the installation of three CUBE units per ward, leaving them on without interruption with a minimal program that entails 2 minutes of operation followed by an 8-minute pause, with the possibility of increasing the operation times in particular cases (e.g. presence of specific subjects with a high infection risk).

In conclusion, the use of NTP technology, which has been proven – in the OR and in the wards – to be able to reduce airborne microbial contamination over time and to facilitate the sanitisation of surfaces, may very likely also contribute to the achievement and maintenance of better hygiene/sanitary conditions, helping clinical risk management.

## Indicators for the final check of the service

### PERFORMANCE INDICATORS

#### Physical performance

Decrease % of possible microbial contamination:

#### WARD

**AVERAGE DECREASE\*: 86%**

*\* the values refer to the airborne Total Bacterial Load*

This figure reflects almost exactly the result obtained in the OR experiment, as described in the final Report on Service 2.1

#### OR

First experiment: **100%**; Second experiment: **75%**

**AVERAGE DECREASE\*: 87.5%**

*\* the values refer to the airborne Total Bacterial Load*

Together, therefore, they prove that the effect of the NTP system, regardless of its size and of the premises in which it is placed, if sized correctly for the actual needs, is able to produce perfectly reproducible results, as further guarantee of its potential in terms of reduction of the Clinical Risk with regard to Hospital Infections.

## Bibliography

(1) “Manual for training healthcare providers - Patient safety and management of the clinical risk”

[http://www.salute.gov.it/portale/documentazione/p6\\_2\\_2\\_1.jsp?lingua=italiano&id=640](http://www.salute.gov.it/portale/documentazione/p6_2_2_1.jsp?lingua=italiano&id=640)

## 13. SCIENTIFIC ARTICLES

SCIENTIFIC ARTICLES ON VIRAL AND BACTERIAL SANITIZATION BY MEANS OF NON THERMAL PLASMA

SCIENTIFIC ARTICLES ON INORGANIC POLLUTANT REMOVAL

SCIENTIFIC ARTICLES ON ORGANIC POLLUTANT (VOC) REMOVAL

## ATTACHMENT 13.1

---

### *SCIENTIFIC ARTICLES ON VIRAL AND BACTERIAL SANITIZATION BY MEANS OF NON THERMAL PLASMA*

Leipold, M.L. (2004). Evaluation of the roles of reactive species, heat, and UV radiation in the inactivation of bacterial cells by air plasmas at atmospheric pressure. *International Journal of Mass Spectrometry*, 233 (1-3), 81-86

Ming zhang, Jun Kyun Oh, Luis Cisneros-Zevallos, Mustafa Akbulut – (2013) bactericidal effects of nonthermal low-pressure oxygen plasma on *S. typhimurium* LT2 attached to fresh produce surfaces. *Journal of Food Engineering* 119 (2013) 425-432.

Michael J. Gallagher, A. G. (2004). Non-thermal plasma application in air sterilization. Conference Paper in IEEE International Conference on Plasma Science.

Puligundla Pradeep and Mok Chulkyoon (2016) – Non-thermal plasmas (NTPs) for inactivation of viruses in abiotic environment. *Research Journal of Biotechnology*. Vol 11 (6) June (2016)

Cold plasma, a new hope in the field of virus inactivation (2020) – Arijana Filipić, Ion Gutierrez-Aguirre, Gregor Primc, Miran Mozetič, David Dobnik. PII: S0167-7799(20)30108-6, DOI: <https://doi.org/10.1016/j.tibtech.2020.04.003>, Reference: TIBTEC 1923

Inactivation of airborne porcine reproductive and respiratory syndrome virus (PRRSv) by a packed bed dielectric barrier discharge non-thermal plasma.



## Bactericidal effects of nonthermal low-pressure oxygen plasma on *S. typhimurium* LT2 attached to fresh produce surfaces



Ming Zhang<sup>a,\*</sup>, Jun Kyun Oh<sup>b</sup>, Luis Cisneros-Zevallos<sup>c,\*</sup>, Mustafa Akbulut<sup>a,b,\*</sup>

<sup>a</sup>Artie McFerrin Department of Chemical Engineering, Materials Science and Engineering Program, Texas A&M University, College Station, TX 77843-3122, United States

<sup>b</sup>Materials Science and Engineering Program, Texas A&M University, College Station, TX 77843-3122, United States

<sup>c</sup>Department of Horticultural Sciences, Texas A&M University, College Station, TX 77843-2133, United States

### ARTICLE INFO

#### Article history:

Received 25 March 2013

Received in revised form 17 May 2013

Accepted 31 May 2013

Available online 19 June 2013

#### Keywords:

Oxygen plasma  
Bactericidal effect  
Sanitization  
Fresh produce

### ABSTRACT

This work investigates the feasibility of nonthermal low-pressure oxygen plasma on sanitization of spinach, lettuce, tomato and potato surfaces from *Salmonella enterica* subsp. *enterica* serovar Typhimurium str. LT2 (*Salmonella typhimurium* LT2). It was shown that the time of exposure and plasma power density were two critical parameters influencing the bactericidal efficiency. Surface roughness and hydrophobicity did not influence the sanitization of produce. Oxygen plasma was more effective than washing with 3% H<sub>2</sub>O<sub>2</sub> on eliminating *S. typhimurium* LT2 on spinach. Plasma treatment chemically changed a very thin section of tomato wax cuticle layer by oxidation reaction and decomposition of carbon chains, which could readily and completely be removed by water. Overall, this study confirms that nonthermal oxygen plasma can be a new effective method of sanitization for fresh produce.

© 2013 Elsevier Ltd. All rights reserved.

### 1. Introduction

Fruits and vegetables play an important role in our diet and health by providing essential vitamins, minerals, and fibers. Human pathogens can reach and attach fruit and vegetable surfaces during growth, harvest, transportation and further handling from animal and human sources. Contaminated fruits and vegetables in particular the ones that are consumed raw can lead to foodborne illnesses. In recent years, the number of documented outbreaks of human infections associated with the consumption of contaminated fruits and vegetables has increased (Berger et al., 2010; Van Boxtael et al., 2013).

Typical approaches for the sanitization of pathogenic microorganisms involve the use of heat, pressure, liquid or gas chemical disinfectants, and ionizing or non-ionizing radiation. However, because of their fragile nature, high temperature methods are not suitable for the decontamination of fresh produce. With outbreaks of foodborne illnesses occurring more frequently, the development of novel nonthermal methods to reduce and eliminate bacterial pathogens from fresh produce has received increasing attention (Parish et al., 2003a,b). To this end; X-rays, ultrasound, ultraviolet

light, oscillating magnetic fields, pulsed light, and high voltage arc discharge based methods have recently been considered in the context of fresh produce safety (Zhang et al., 2011; Moosekian et al., 2012; Garcia Loredo et al., 2013; Odriozola-Serrano et al., 2013).

Among novel methods of bacterial sanitization, nonthermal plasma-based sanitization approaches has displayed promising outcomes in decontaminating living tissues and biomaterials from various microorganisms (Ragni et al., 2010; Ermolaeva et al., 2011; Noriega et al., 2011). Effectiveness of nonthermal plasma in decontaminating pathogenic bacteria is attributed to a combination of effects including the formation of electrons, ions, free radicals and excited molecules, as well as UV radiation (Moisan et al., 2001; Laroussi and Leipold, 2004; Kong et al., 2009). The key advantages of nonthermal plasma technologies are their relatively simple and inexpensive design, short processing times, absence of toxicity, and lack of residue formation (Rossi et al., 2009; Roth et al., 2010; Rupf et al., 2010). Its effectiveness against pathogenic bacteria and the above mentioned advantages have prompted an interest in the use of the nonthermal plasma-based approaches in food safety. For instance, Deng et al. (2007) has demonstrated the applicability of nonthermal atmospheric plasma technology for the pasteurization of almonds. The technology was found to effectively reduce *Escherichia coli* on almond by almost a 5 log factor after 30-s treatment at 30 kV and 2000 Hz. Ragni et al. (2010) investigated the efficacy of resistive barrier discharge (RBD) plasma for decontamination of shell egg surfaces and

\* Corresponding authors. Address: Materials Science and Engineering Program, Texas A&M University, College Station, TX 77843-3122, United States. Tel.: +1 609 964 6174; fax: +1 979 845 6446 (M. Akbulut).

E-mail addresses: [lcisnero@tamu.edu](mailto:lcisnero@tamu.edu) (L. Cisneros-Zevallos), [makbulut@mail.che.tamu.edu](mailto:makbulut@mail.che.tamu.edu) (M. Akbulut).



observed reductions up to 2.5 log CFU/eggshell and 4.5 log CFU/eggshell for *Salmonella enteritidis* using air with low and high moisture contents, respectively, after 90 min of RBD plasma treatment. Noriega et al. (2011) investigated the efficiency of nonthermal atmospheric gas plasmas for decontaminating chicken skin and muscle inoculated with *Listeria innocua* and observed a 1 log reduction on skin, and a 3 log reductions on muscle under optimal conditions.

The studies on the efficiency of nonthermal plasma on bacteria responsible for foodborne illnesses when they are attached to fresh produce surfaces is very limited. Niemira and Sites (2008) reported the use of cold air plasma to inactivate human pathogens inoculated on golden delicious apples. The reductions of *Salmonella* Stanley and *E. coli* O157: H7 ranged from 2.9 to 3.7 and 3.4 to 3.6 respectively, after treatment for 3 min at 30 kV and 60 Hz with flow rate of 40 l/min. Fresh produce surfaces may favor bacterial proliferation specially if rich in nutrients (Thunberg et al., 2002; Johnston et al., 2005), through biofilm formation and protection in crevices (i.e. microscale roughnesses and valleys between the asperities of the produce surface) (Burnett and Beuchat 2000; Burnett et al., 2000). Thus, there is a need to correctly assess the feasibility of nonthermal plasma in sanitizing fresh produce surfaces (Niemira, 2012).

In general, non-thermal plasma is generated from either atmospheric pressures or low pressures. Both atmospheric and low pressure plasma generates same species and same electron densities range (Schutze et al., 1998). Therefore, they have similar plasma sanitization mechanics (Moisan et al., 2001; Laroussi, 2005). The main advantage of the atmospheric-pressure plasmas is that they do not require vacuum systems to operate. However, under atmospheric conditions, higher voltages are required to generate plasma. To be specific, the voltage required to initiate the ionization decreases from ~10,000 V to ~100 V if the pressure reduces from atmospheric pressure to  $10^{-3}$  atm for a 1-cm gap between electrode plates (Lieberman and Lichtenberg, 2005). At higher voltages, often arcing occurs between the electrodes. The arcing may damage and burn fragile surfaces such as fresh produce surfaces. Considering that the low pressure vacuum packaging has been used for packaging of many fresh produces (An et al., 2009) and the abovementioned points, the use of low-pressure plasma sanitization instead of atmospheric-pressure one has certain advantages.

Accordingly, this paper investigated the bactericidal effect of nonthermal low-pressure oxygen plasma on *Salmonella enterica* subsp. *enterica* serovar Typhimurium LT2 (*S. typhimurium* LT2) attached on fresh lettuce, spinach, tomato, and potato surfaces. This microorganism was selected because data from the US-CDC foodborne outbreak surveillance system show that the most commonly reported microorganisms associated with fresh produce foodborne illness outbreaks are *Salmonella* spp. (Sivapalasingam et al., 2004). Oxygen was selected as the gas source because oxygen was found to be one of the best sanitization agents (Bol'shakov et al., 2004). Furthermore, four possible combinations of surface roughness and hydrophilicity including hydrophobic smooth, hydrophobic rough, hydrophilic smooth, and hydrophilic rough surfaces were covered through the selected produce. This is possible since spinach and potato are relatively rough, while tomato and lettuce are relatively smooth, and spinach and tomato are relatively hydrophobic, while lettuce and potato are relatively hydrophilic. These properties can influence sanitization efficacy in some sanitization methods, especially liquid based methods (Ukuku and Fett, 2006; Fransisca and Feng, 2012). In the present study, the efficiency of a nonthermal oxygen plasma method was compared with that of washing with aqueous solutions of  $H_2O_2$ . Associated physicochemical changes upon the plasma treatment were also reported.

## 2. Materials and methods

### 2.1. Preparation of produce surface

Spinach, lettuce, tomato and potato were purchased from a local grocery store (Wal-Mart, College Station, TX, USA). After mildly washed for 30 s using 1 L of deionized water, the produce was dried using tissue paper. Then, spinach, lettuce, tomato skin and potato skin were cut into square pieces of 1 cm × 1 cm. The produce pieces were immobilized on a silica wafer using a double sided adhesive carbon tape.

### 2.2. Preparation of inoculum

Rifampicin-resistant *S. enterica* subsp. *enterica* serovar Typhimurium str. LT2 (*S. typhimurium* LT2; ATCC 700720) was obtained from the ATCC (Manassas, VA, USA) and maintained on slants of tryptic soy agar (TSA; Becton, Dickinson and Co., Sparks, MD, USA) at 5 °C. Working cultures were obtained by transferring a loop of culture from TSA slants to 9.0 mL of tryptic soy broth (TSB; Becton, Dickinson and Co.) and incubating aerobically without agitation at 37.5 °C for 24 h. After 24 h, a loop of culture was transferred to a fresh 9 mL of TSB and incubated aerobically without agitation at 37.5 °C for 24 h. After incubation, the culture was transferred to a 15 mL conical centrifuge tube (Thermo-Fisher Scientific, Inc.). Bacterial cells were collected by centrifugation at  $2191 \times g$  in a Jouan B4i centrifuge (Thermo-Fisher Scientific, Inc.) for 15 min at 22 °C. The resulting pellet was suspended in 9.0 mL of Milli Q (MQ) water and washed by centrifugation for 15 min at 22 °C; the entire centrifugation and washing procedure was repeated identically three times. After the final cycle, the pellet was suspended in 9.0 mL MQ water and used immediately in the inoculation experiments. This resulted in an inoculum concentration of  $8 \pm 0.4 \times 10^{10}$  CFU/ml, and determined via selective plating on TSA. Survivors were enumerated following 24 h aerobic incubation at 37.5 °C.

### 2.3. Nonthermal oxygen plasma treatment

Plasma treatment experiments were performed by March CS-1701 Reactive Ion Etching system (March Plasma Systems, Inc., CA, USA). The system consists of four modules: a reaction chamber/process controller, a solid state radio frequency (RF) power generator, a vacuum pump and an oxygen source (Fig. 1A). By applying a strong RF electromagnetic field to the wafer

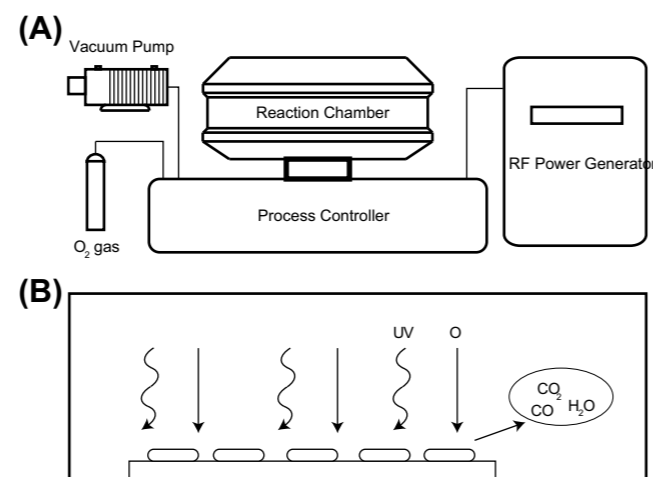


Fig. 1. Schematic illustration of (A) oxygen plasma system, and (B) plasma sanitization in reaction chamber.

platter, plasma is initiated in the system using oxygen gas. The system runs at an RF frequency of 13.56 MHz with a maximum power output of 600 W. The chamber is 15 cm in interior diameter with 2.5 cm spacing between electrodes. When the gas in the chamber is exposed to the oscillating electric field at high frequency and energy, the electrons of the gas start to gain energy, eventually ionizing to atoms. The initial ionization will provide more energy to the system to cause further ionizations in a chain reaction manner, ultimately filling the chamber with plasma, which could react with the treated surface (Fig. 1B). The RF power applied and pressure of the chamber are two main parameters influencing the density and temperature of the plasma (Chen and Chang, 2003). In the present study, we investigated the effect of plasma power and exposure time on the bactericidal properties of the oxygen plasma. To ensure the reproducibility of the results, each experiment was repeated at least three times.

Plasma chemistry of pure oxygen RF plasma has been well identified. Mogul et al. (2003) studied emission spectrum for pure O<sub>2</sub> plasma discharge powered by a 13.56 MHz radio frequency at 100 W and 500 mTorr (67 Pa). They found the presence of excited atomic oxygen, oxygen cation, dioxygen cation, and neutral excited dioxygen in plasma. Bol'shakov et al. (2004) also found the similar results when they studied oxygen plasma generated at 13.56 MHz in the range of 13–67 Pa and pressure and 100–300 W power. These emission spectrum results were also consistent with the previously published oxygen spectra of oxygen plasmas (Carl et al., 1990; Tuszewski et al., 1995). Since the plasma in this paper was generated under similar experiment conditions (13.56 MHz, 34 Pa, 50–350 W), species in plasma in this paper is expected to consist of excited atomic oxygen, oxygen cation, dioxygen cation, and neutral excited dioxygen as well.

### 2.4. Inoculation of produce surfaces

The experimental protocol for the inoculation of produce surfaces used in plasma treatment studies was as follows: Initially, 100  $\mu$ l of bacterial inoculum at  $8 \pm 0.4 \times 10^{10}$  CFU/ml was added dropwise and distributed evenly onto produce surfaces (1 cm × 1 cm pieces) and the produce surfaces were air-dried at room temperature for ~4 h. After the inoculated surface was placed in the chamber, the chamber was first evacuated at 13 Pa, and then the chamber was filled with O<sub>2</sub> to 30 Pa with a gas flow rate of 10 sccm. After the plasma treatment at room temperature, the chamber was ventilated with air to reach atmospheric pressure. To compare the efficacy of plasma sanitization with that of H<sub>2</sub>O<sub>2</sub> washing, some of inoculated surfaces (spinach) were rinsed in 3% H<sub>2</sub>O<sub>2</sub> solution for 600 s instead of the plasma treated. Both of the treated produce surfaces were then used for bacterial counting.

### 2.5. Enumeration of inoculum organisms

The numbers of *S. typhimurium* LT2 cells on the produce surfaces were measured for each exposure time and power density of plasma treatment. Once the treated surfaces were removed from the plasma chamber, these were put in 9 ml test tubes of 0.1% of peptone water. The tubes were shaken on a Mini Shaker (VWR International, LLC) at 900 rpm for 10 min. Serial dilutions of the suspension were made and plated on TSA supplemented with 80  $\mu$ g/ml rifampicin. Survivors were enumerated following 24 h aerobic incubation at 37.5 °C.

### 2.6. Water contact angle measurement

The relative hydrophobicity of produce surface was evaluated using water contact angle measurements. One drop of Milli-Q

water was placed on a produce surface and allowed to equilibrate for 30 s before making any measurements. A digital camera was used to take the images for angle measurement. For each specimen, at least three contact angle measurements were conducted.

### 2.7. Scanning electron microscopy (SEM)

SEM (JSM-7500F, JEOL, Peabody, MA, USA) was used for three purposes in this study: to determine morphology (roughness) of the neat produce surfaces; to characterize the physical changes on the produce surface due to oxygen plasma treatment; and to compare the bacterial attachment behavior of the produce surfaces. To study the effect of surface property on bacteria adhesion, produce surfaces rinsed into *S. typhimurium* LT2 solution for 5 min and then dry in a hood at room temperature for overnight. SEM images were obtained from there with or without the above treatment. Prior to the SEM studies, the samples were coated with

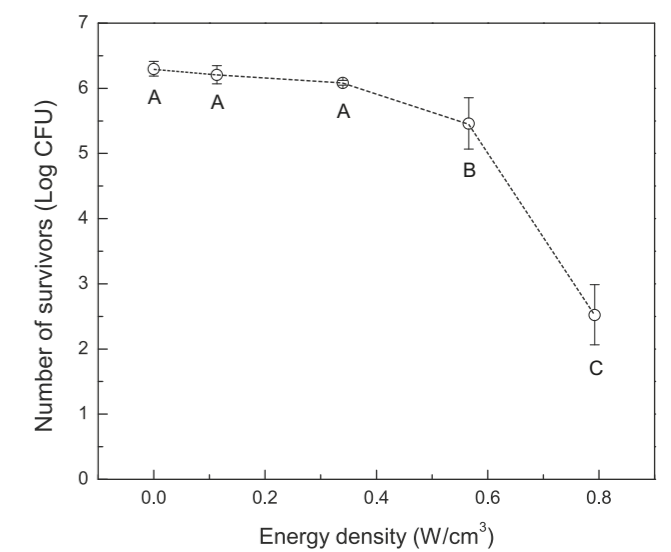


Fig. 2. Survival curve of *S. typhimurium* LT2 on spinach after plasma treatment for 100 s as a function of plasma power density. Treatments with same letters are not significantly different based on Tukey's test ( $p \leq 0.05$ ).

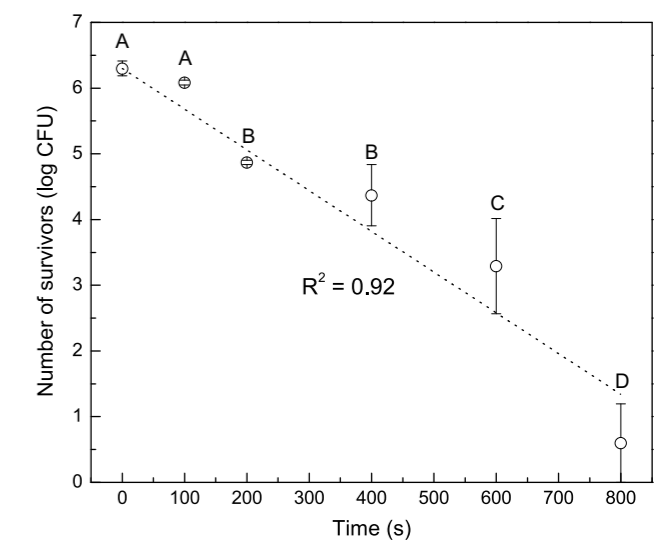


Fig. 3. Survival curve of *S. typhimurium* LT2 on spinach after plasma treatment at 0.34 W/cm<sup>3</sup> for different times of exposures. Treatments with same letters are not significantly different based on Tukey's test ( $p \leq 0.05$ ).

a 50-nm layer of Au by sputter coater (Cressington 105HR, Cressington, England) to ensure electrical conductivity.

2.8. Nuclear magnetic resonance (NMR)

Proton nuclear magnetic resonance (H NMR) was used to investigate chemical changes induced by oxygen plasma treatment. Tomato skin with and without exposure to the oxygen plasma was placed in deuterated chloroform (CDCl<sub>3</sub>) and sonication for 5 min

to dissolve non-polar compounds and in deuterated water (D<sub>2</sub>O) to dissolve polar ones. The extracted compounds were transferred into 5 mm NMR tubes and analyzed using a Bruker 400 MHz NMR spectrometer (Bruker, Billerica, MA, USA) at 298 K.

2.9. Statistical analysis

All experiments were replicated at least three times. Numbers of survival bacteria were converted to log CFU and means and

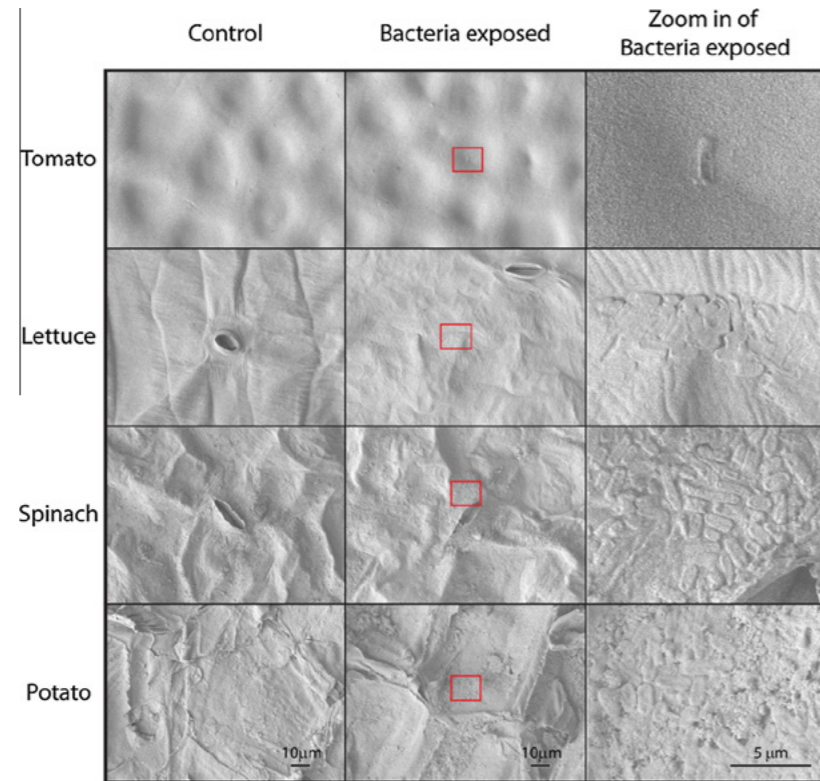


Fig. 4. SEM micrographs of four produce surfaces with or without exposing to bacteria dispersion for 5 min. Red rectangles indicates the areas from which higher magnification images were obtained. (For interpretation of the references to color in this figure legend, the reader is referred to the web version of this article.)

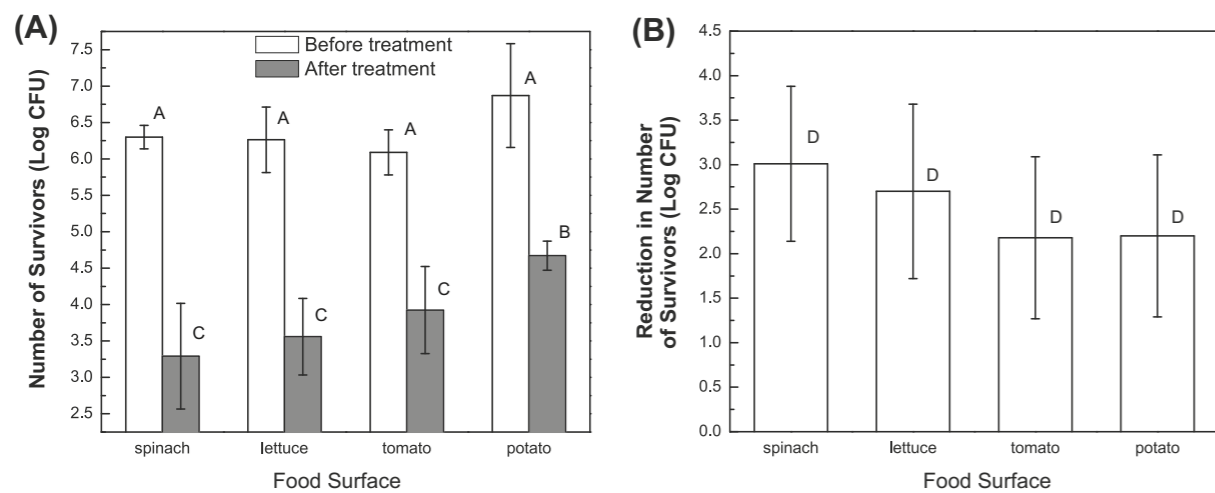


Fig. 5. (A) Number of surviving *S. typhimurium* LT2 on different produce surfaces before and after plasma treatment of 600 s at 0.34 W/cm<sup>3</sup>. (B) Corresponding Log reductions in number of surviving *S. typhimurium* LT2 on different food surfaces. Treatments with same letters are not significantly different based on Tukey's test (p < 0.05).

standard deviations were calculated. Analyses of variance were conducted using JMP (SAS Cary, NC, USA) and mean separation tests performed using a post hoc Tukey's test (p < 0.05).

3. Results and discussion

3.1. Effect of plasma energy density on bactericidal efficiency

Fig. 2 shows the number of surviving *S. typhimurium* LT2 on spinach surface as a function of actual power output of radio frequency (RF) per unit volume of the reaction chamber (power density) of plasma for a given time (t = 100 s). The number of survivors decreased with increasing power density in a nonlinear manner: At low power densities the bactericidal effect increased weakly while at large power densities the bactericidal effect

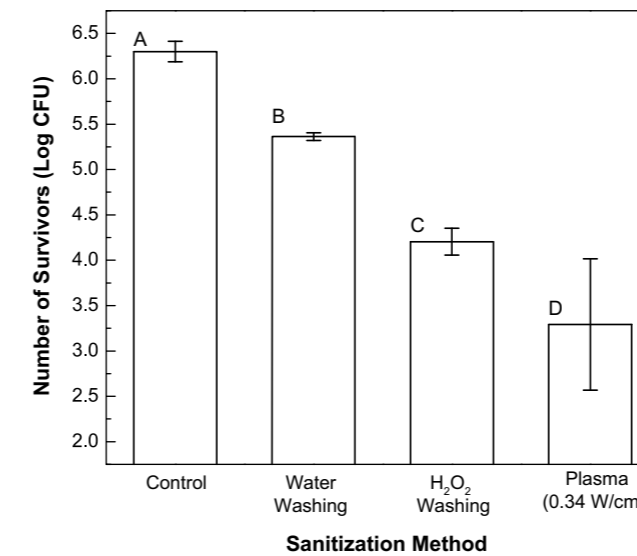


Fig. 6. Number of surviving *S. typhimurium* LT2 for different sanitization methods on spinach surface. Duration of each treatment method was kept constant, i.e. an exposure time of 600 s. Treatments with different letters were significantly different based on Tukey's test (p < 0.05).

increased strongly (p < 0.05). Given higher plasma energy densities give rise to higher intensities of UV irradiation, UV photons, and reactive species such as O, O\*, and O<sub>2</sub>\* (Laroussi and Leipold, 2004; Wu et al., 2012), it is reasonable that bactericidal effect increased with increase power density. No visual damage was observed for power densities up to 0.57 W/cm<sup>3</sup>. However, the spinach surface showed some signs of etching at a power density of 0.79 W/cm<sup>3</sup> and an exposure time of 100 s. Thus, although higher energy densities can allow better sanitization, care must be taken to prevent damage on the produce surface.

3.2. Effect of plasma exposure time on bactericidal efficiency

Fig. 3 shows number of *S. typhimurium* LT2 on spinach surface as a function of time of plasma exposure at a power density of 0.34 W/cm<sup>3</sup> (output power of 150 W). The logarithmic number of surviving bacteria before the exposure (t = 0) was 6.3 ± 0.1. The complete sanitization was achieved at 800 s (≤1 log CFU). No visible side effect was observed on the spinach after a plasma treatment of 800 s at 0.34 W/cm<sup>3</sup>. The logarithmic numbers of viable bacteria decreased linearly with increasing plasma exposure time. This finding implies the number of surviving microorganisms decreased, as an exponential function of time. This trend is consistent with other plasma sanitization studies involving other types of surfaces (Herrmann et al., 1999; Moisan et al., 2002). The half-life of the bacteria killing reaction is about 48 s at a power density of 0.34 W/cm<sup>3</sup>. Accordingly, an exposure time of 317 s decreases the total number of surviving *S. typhimurium* LT2 to 1.0%, and an exposure time of 635 s decreases to 0.01%.

3.3. Effect of food surface on bactericidal efficiency

Tomato, lettuce, spinach, and potato were selected due to their different surface properties. The water contact angles are 107 ± 6 for tomato, 81 ± 7 for spinach, 57 ± 4 for lettuce, and <30 for potato. SEM micrographs showed that tomato and lettuce were relatively smooth while spinach and potato were relatively rough (Fig. 4). Rough and hydrophilic surface (potato) favored for bacteria adhesion, while smooth and hydrophobic surface (tomato) hindered bacterial adhesion (Fig. 4). This behavior is consistent with the previous studies also showing that these surface properties

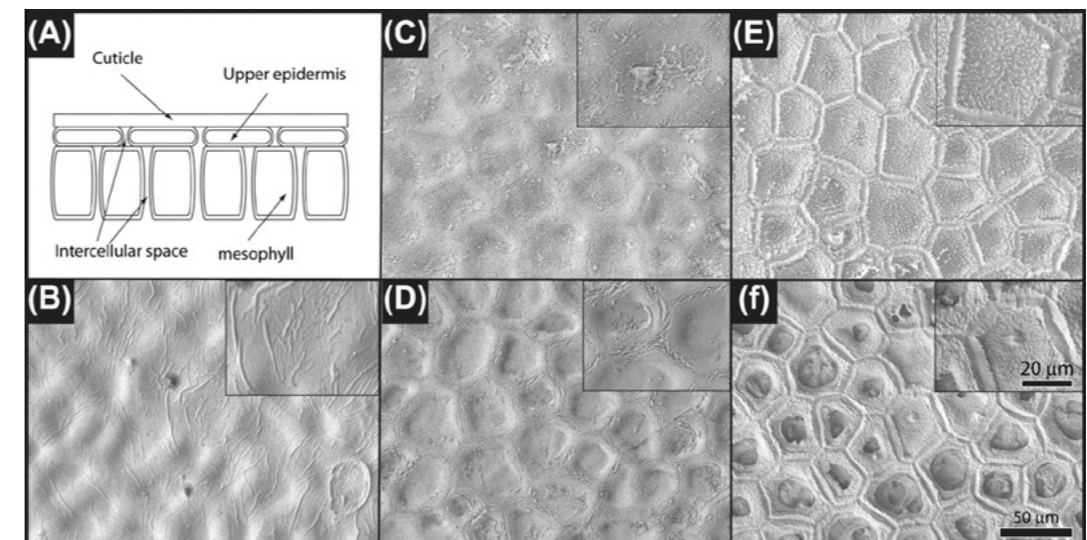


Fig. 7. An illustration of tomato surface (A); SEM images of tomato before plasma treatment (B); after plasma treated for 100 s (C) and then rinsing in MQ water (D); after plasma treated for 600 s (E) and then rinsing in MQ water (F).

(roughness and hydrophobicity) can influence bacterial adhesion (Bruinsma et al., 2001; Wang et al., 2009).

To better understand the effect of produce surface properties on the efficiency of plasma sanitization, we conducted plasma sanitization experiments using four different produce surfaces: tomato (smooth hydrophobic), lettuce (smooth hydrophilic), spinach (rough hydrophobic), and potato (rough hydrophilic). The number of viable bacteria after drying and after plasma treatment for 600 s at 0.34 W/cm<sup>3</sup> is shown in Fig. 5A. Initial viable bacteria were the same for all surfaces ( $p < 0.05$ ); and after treatments, all surfaces showed lower bacteria counts, still the same for all surfaces ( $p < 0.05$ ) with exception of a slight higher value for potatoes. However, when reporting reductions in numbers of the viable bacteria, these were  $3.0 \pm 0.9$ ,  $2.7 \pm 1.0$ ,  $2.2 \pm 0.9$  and  $2.2 \pm 0.9$  for spinach, lettuce, tomato and potato, respectively with no significant difference among them ( $p < 0.05$ ). Accordingly, we confirm that surface properties of roughness and hydrophobicity have no impact on oxygen plasma sanitization. Upon 600 s plasma treatment at 0.34 W/cm<sup>3</sup>, no visible damage was observed for all produce surfaces.

#### 3.4. Comparison to hydrogen peroxide washing

Hydrogen peroxide treatment is one of the most common sanitization methods for vegetable and fruit surfaces (Parish et al. 2003a,b; Ukuku and Fett, 2006). Therefore, we compared the efficiencies of the nonthermal oxygen plasma treatment method with a hydrogen peroxide treatment and water washing using spinach surface (Fig. 6). Duration of each treatment method was kept constant, i.e. an exposure time of 600 s. The logarithmic number of surviving bacteria decreased from  $6.3 \pm 0.1$  to  $5.4 \pm 0.1$  after water washing. The survival number decreased to  $4.2 \pm 0.1$  upon a 600 s exposure to 3% H<sub>2</sub>O<sub>2</sub> while the number further decreased to  $3.4 \pm 0.4$  for the case of 600 s plasma treatment at 0.34 W/cm<sup>3</sup>.

When surface characteristics such as roughness and hydrophobicity promote the formation of a physical barrier for aqueous media penetration, the effectiveness of H<sub>2</sub>O<sub>2</sub> treatment decreases (Ukuku and Fett, 2006; Fransisca and Feng, 2012). We hypothesize that the barrier is due to micro-air pockets which protect the microorganisms from the sanitizer. On the other hand, the length scale (~angstrom) of gas reactive species is much smaller than the length scale of surface roughness of produce surfaces (several micrometers). Therefore, the crevices and micro-air pockets do not hinder the plasma sanitization. The difference in the efficiency of plasma and peroxide treatment is attributed to this phenomenon.

#### 3.5. Physical changes occurring on produce surfaces after plasma treatment

SEM was used to study the physical changes occurring on produce due to the nonthermal oxygen plasma treatment (Fig. 7). Typical produce surfaces like tomato cuticle are covered by a wax layer followed by a layer of cutin or cutin blends of wax and cell wall substances such as carbohydrates. Below the cuticle are the epidermis and mesophyll cells (Fig. 7A). As observed in Fig. 7B, tomato surfaces exhibited regular ridge-and-valley structures. Because the outermost layer is covered with cuticle, it was not possible to directly visualize the upper epidermis. Upon an exposure of 100 s to oxygen plasma at 0.34 W/cm<sup>3</sup> (output power of 150 W), the surface roughness increased slightly and very small amount of debris was observed on the surfaces (Fig. 7C). After rinsing with water, the debris was almost completely removed and intercellular spaces became slightly more apparent (Fig. 7D). There was no sign of damage in epidermis at this point.

Upon an exposure of 600 s to oxygen plasma at 0.34 W/cm<sup>3</sup>, intercellular space could be observed through the translucent cuticle layer, indicating removal of the wax cuticle layer (Fig. 7E). In addition, the surface became roughness. When water rinsing follow the plasma treatment, the epidermal cells seem to be damaged, indicating a possible partial removal of the cuticle layer with an exposure of 600 s to oxygen plasma at 0.34 W/cm<sup>3</sup> (Fig. 7F) The damage was more evident after water washing, since the plasma treatment may convert hydrophobic groups from wax to small molecule weight hydrophilic forms and water can dissolve and etch away the hydrophilic groups easier.

In general, SEM studies suggest that short exposure times have no major effects on the produce surface while long exposure times may partially damage the cuticle layer and epidermis cells. Depending on the produce type, the removal of the cuticle layer may reduce the storage and shelf life of produce (Kissinger et al., 2005; Saladie et al., 2007). However, given that coating of produce surfaces with edible wax or other coatings is becoming widespread (Park, 1999; Dávila-Aviña et al., 2012), if necessary, the removed cuticle layer can be substituted with an edible wax layer. In essence, the time and power density of nonthermal plasma treatment needs to be optimized for each produce surface to ensure an acceptable level of cuticle/upper epidermis removal and bacterial sanitization.

#### 3.6. Chemical changes occurring on produce surfaces after plasma treatment

To characterize such chemical changes taking place on produce surface upon nonthermal oxygen plasma treatment (e.g., tomato surface, 100 s, 0.34 W/cm<sup>3</sup>), we relied on NMR. NMR spectra obtained using CDCl<sub>3</sub> extraction indicated that the signal intensity of proton at ~1–2 ppm, which is presumably due to R-CH<sub>2</sub>CH<sub>3</sub>, R-CH(CH<sub>3</sub>)<sub>2</sub>, or R-C(CH<sub>3</sub>)<sub>3</sub> groups, decreased after the plasma treatment (Fig. 8A). NMR spectra obtained using D<sub>2</sub>O extraction showed that the signal intensity of proton at ~2–3 ppm, which is presumably due to R-CO-CH<sub>3</sub>, R-CO-CH<sub>2</sub>CH<sub>3</sub> or R-CH<sub>2</sub>COOH groups, increased after plasma treatment (Fig. 8B). These findings are consistent with previous studies focusing on the chemical effects of oxygen plasma on mineral oils (Korzec et al., 1994; Jing et al., 2005), polymers (Hillborg et al., 2000; Calvimontes et al., 2011) and other organic materials (Li and Horita, 2000). Accordingly, NMR results suggest that when tomato surfaces are treated by nonthermal oxygen plasma, the wax cuticle layer can be oxidized to form aldehyde and carboxylic acid groups and/or further oxidized (decomposition of carbon chains) to CO<sub>2</sub> and H<sub>2</sub>O, which would be removed from the tomato surface (Fig. 8c).

#### 4. Conclusion

In the present study, we have investigated the efficiency of non-thermal low-pressure oxygen plasma treatment on sanitization of fresh produce surfaces and the associated physicochemical changes taking place on surface cuticle layers. It was shown that the time of exposure and plasma power density were two critical parameters influencing the bactericidal efficiency of nonthermal oxygen plasma treatment. The half-life of the oxygen plasma killing reaction of *S. typhimurium* LT2 was about 48 s at power density of 0.34 W/cm<sup>3</sup>. The sanitization method worked equally well for rough hydrophobic (spinach), rough hydrophilic (lettuce), smooth hydrophobic (tomato) and smooth hydrophilic (potato) produce. For a given time, the bactericidal efficacy of nonthermal oxygen plasma was found to be 1 order of magnitude better than that of 3% H<sub>2</sub>O<sub>2</sub> treatment for *S. typhimurium* LT2 on spinach surface. It was also shown that oxygen plasma treatment (0.34 W/cm<sup>3</sup>) only affects the wax cuticle layer under conditions of short- to intermediate-exposure times. However for long exposure times, wax cuticle layer and upper epidermis cells may be damaged. Oxygen plasma changed the wax surface chemistry through oxidation reactions forming aldehyde and carboxylic acid, and by decomposition of carbon chains. Water rinsing could easily remove these residues from the produce surface. Overall, the nonthermal oxygen plasma treatment shows a potential for the efficient sanitization of fresh produce surfaces.

#### Acknowledgement

This project was supported by Agriculture and Food Research Initiative Competitive Grant No. 2011-67017-30028 from the USDA National Institute of Food and Agriculture.

#### References

An, D.S., Park, E., et al., 2009. Effect of hypobaric packaging on respiration and quality of strawberry and curled lettuce. *Postharvest Biology and Technology* 52 (1), 78–83.  
 Berger, C.N., Sodha, S.V., et al., 2010. Fresh fruit and vegetables as vehicles for the transmission of human pathogens. *Environmental Microbiology* 12 (9), 2385–2397.  
 Bol'shakov, A.A., Cruden, B.A., et al., 2004. Radio-frequency oxygen plasma as a sterilization source. *Aiaa Journal* 42 (4), 823–832.  
 Bruinsma, G.M., van der Mei, H.C., et al., 2001. Bacterial adhesion to surface hydrophilic and hydrophobic contact lenses. *Biomaterials* 22 (24), 3217–3224.  
 Burnett, S.L., Beuchat, L.R., 2000. Human pathogens associated with raw produce and unpasteurized juices, and difficulties in decontamination. *Journal of Industrial Microbiology & Biotechnology* 25 (6), 281–287.  
 Burnett, S.L., Chen, J.R., et al., 2000. Attachment of *Escherichia coli* O157: H7 to the surfaces and internal structures of apples as detected by confocal scanning laser microscopy. *Applied and Environmental Microbiology* 66 (11), 4679–4687.  
 Calvimontes, A., Mauersberger, P., et al., 2011. Effects of oxygen plasma on cellulose surface. *Cellulose* 18 (3), 803–809.  
 Carl, D.A., Hess, D.W., et al., 1990. Oxidation of silicon in an electron cyclotron resonance oxygen plasma: kinetics, physicochemical, and electrical properties. *Journal of Vacuum Science & Technology A: Vacuum, Surfaces, and Films* 8 (3), 2924–2930.  
 Chen, F.F., Chang, J.P., 2003. *Lecture Notes on Principles of Plasma Processing*. Kluwer Academic/Plenum Publishers, New York.  
 Dávila-Aviña, J., Villa-Rodríguez, J., et al., 2012. Effect of edible coatings on bioactive compounds and antioxidant capacity of tomatoes at different maturity stages. *Journal of Food Science and Technology*, 1–7.  
 Deng, S., Ruan, R., et al., 2007. Inactivation of *Escherichia coli* on almonds using nonthermal plasma. *Journal of Food Science* 72 (2), M62–M66.  
 Ermolaeva, S.A., Varfolomeev, A.F., et al., 2011. Bactericidal effects of non-thermal argon plasma *in vitro*, in biofilms and in the animal model of infected wounds. *Journal of Medical Microbiology* 60 (1), 75–83.  
 Fransisca, L., Feng, H., 2012. Effect of surface roughness on inactivation of *Escherichia coli* O157:H7 87-23 by new organic-acid surfactant combinations on alfalfa, broccoli, and radish seeds. *Journal of Food Protection* 75 (2), 261–269.  
 Garcia Loreda, A.B., Guerrero, S.N., et al., 2013. Impact of combined ascorbic acid/CaCl<sub>2</sub>, hydrogen peroxide and ultraviolet light treatments on structure, rheological properties and texture of fresh-cut pear (William var.). *Journal of Food Engineering* 114 (2), 164–173.  
 Herrmann, H.W., Henins, I., et al., 1999. Decontamination of chemical and biological warfare (CBW) agents using an atmospheric pressure plasma jet (APPJ). *Physics of Plasmas* 6 (5), 2284–2289.  
 Hillborg, H., Ankner, J.F., et al., 2000. Crosslinked polydimethylsiloxane exposed to oxygen plasma studied by neutron reflectometry and other surface specific techniques. *Polymer* 41 (18), 6851–6863.  
 Jing, G.S., Eluru, H.B., et al., 2005. Paraffin surfaces for culture-based detection of mycobacteria in environmental samples. *Journal of Micromechanics and Microengineering* 15 (2), 270–276.  
 Johnston, L.M., Jaykus, L.A., et al., 2005. A field study of the microbiological quality of fresh produce. *Journal of Food Protection* 68 (9), 1840–1847.  
 Kissinger, M., Tuvia-Alkalai, S., et al., 2005. Characterization of physiological and biochemical factors associated with postharvest water loss in ripe pepper fruit during storage. *Journal of the American Society for Horticultural Science* 130 (5), 735–741.  
 Kong, M.G., Kroesen, G., et al., 2009. Plasma medicine: an introductory review. *New Journal of Physics* 11.  
 Korzec, D., Rapp, J., et al., 1994. Cleaning of metal parts in oxygen radio-frequency plasma – process study. *Journal of Vacuum Science & Technology A: Vacuum Surfaces and Films* 12 (2), 369–378.  
 Laroussi, M., 2005. Low temperature plasma-based sterilization: overview and state-of-the-art. *Plasma Processes and Polymers* 2 (5), 391–400.  
 Laroussi, M., Leipold, F., 2004. Evaluation of the roles of reactive species, heat, and UV radiation in the inactivation of bacterial cells by air plasmas at atmospheric pressure. *International Journal of Mass Spectrometry* 233 (1–3), 81–86.  
 Li, X., Horita, K., 2000. Electrochemical characterization of carbon black subjected to RF oxygen plasma. *Carbon* 38 (1), 133–138.  
 Lieberman, M.A., Lichtenberg, A.J., 2005. *Principles of plasma discharges and materials processing*. Wiley-Interscience, Hoboken, NJ.  
 Mogul, R., Bolapos, et al., 2003. Impact of low-temperature plasmas on deionococcus radiodurans and biomolecules. *Biotechnology Progress* 19 (3), 776–783.  
 Moisan, M., Barbeau, J., et al., 2001. Low-temperature sterilization using gas plasmas: a review of the experiments and an analysis of the inactivation mechanisms. *International Journal of Pharmaceutics* 226 (1–2), 1–21.  
 Moisan, M., Barbeau, J., et al., 2002. Plasma sterilization. *Methods mechanisms. Pure and Applied Chemistry* 74 (3), 349–358.

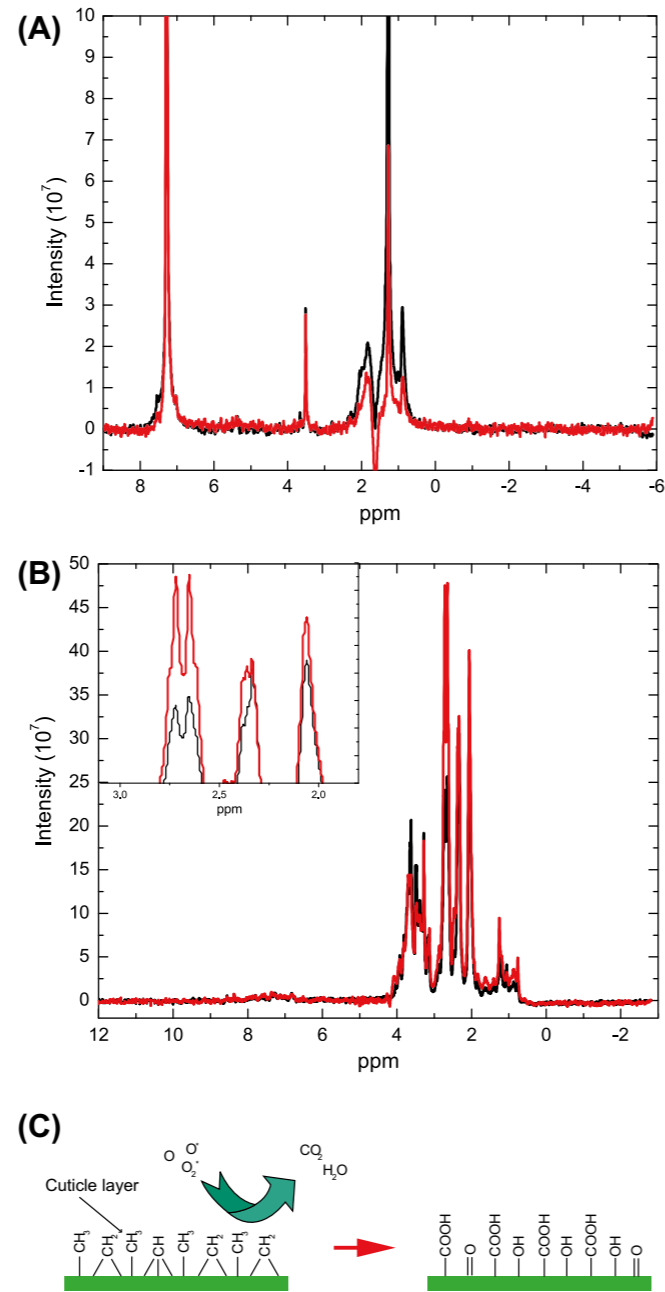


**Fig. 8.** (A) <sup>1</sup>H-NMR spectrum of solution obtained through extraction of tomato skin in CDCl<sub>3</sub>; (B) <sup>1</sup>H-NMR spectrum of solution obtained through extraction of tomato skin in D<sub>2</sub>O. Black lines indicate "before plasma treatment", and red lines indicate "after the plasma treatment"; and (C) An illustration of potential chemical changes taking place on produce surface upon oxygen plasma treatment. (For interpretation of the references to color in this figure legend, the reader is referred to the web version of this article.)

Moosekian, S.R., Jeong, S., et al., 2012. X-ray irradiation as a microbial intervention strategy for food. *Annual Review of Food Science and Technology* 3, 493–510.

Niemira, B.A., 2012. Cold plasma decontamination of foods. *Annual Review of Food Science and Technology* 3 (3), 125–142.

Niemira, B.A., Sites, J., 2008. Cold plasma inactivates salmonella stanley and *Escherichia coli* O157:H7 inoculated on golden delicious apples. *Journal of Food Protection* 71 (7), 1357–1365.

Noriega, E., Shama, G., et al., 2011. Cold atmospheric gas plasma disinfection of chicken meat and chicken skin contaminated with *Listeria innocua*. *Food Microbiology* 28 (7), 1293–1300.

Odriozola-Serrano, I., Aguiló-Aguayo, I., et al., 2013. Pulsed electric fields processing effects on quality and health-related constituents of plant-based foods. *Trends in Food Science & Technology* 29 (2), 98–107.

Parish, M., Beuchat, L., et al., 2003a. Methods to reduce/eliminate pathogens from fresh and fresh-cut produce. *Comprehensive Reviews in Food Science and Food Safety* 2, 161–173.

Parish, M.E., Beuchat, L.R., Suslow, T.V., Harris, L.J., Garrett, E.H., Farber, J.N., Busta, F.F., 2003b. Methods to reduce/eliminate pathogens from produce and fresh-cut produce. *Comprehensive Reviews in Food Science and Food Safety* 2 (Suppl. s1), 161–173.

Park, H.J., 1999. Development of advanced edible coatings for fruits. *Trends in Food Science & Technology* 10 (8), 254–260.

Ragni, L., Berardinelli, A., et al., 2010. Non-thermal atmospheric gas plasma device for surface decontamination of shell eggs. *Journal of Food Engineering* 100 (1), 125–132.

Rossi, F., Kylian, O., et al., 2009. Low pressure plasma discharges for the sterilization and decontamination of surfaces. *New Journal of Physics* 11.

Roth, S., Feichtinger, J., et al., 2010. Characterization of bacillus subtilis spore inactivation in low-pressure, low-temperature gas plasma sterilization processes. *Journal of Applied Microbiology* 108 (2), 521–531.

Rupf, S., Lehmann, A., et al., 2010. Killing of adherent oral microbes by a non-thermal atmospheric plasma jet. *Journal of Medical Microbiology* 59 (2), 206–212.

Saladie, M., Matas, A.J., et al., 2007. A reevaluation of the key factors that influence tomato fruit softening and integrity. *Plant Physiology* 144 (2), 1012–1028.

Schutze, A., Jeong, J.Y., et al., 1998. The atmospheric-pressure plasma jet: a review and comparison to other plasma sources. *IEEE Transactions on Plasma Science* 26 (6), 1685–1694.

Sivapalasingam, S., Friedman, C.R., et al., 2004. Fresh produce: a growing cause of outbreaks of foodborne illness in the United States, 1973–1997. *Journal of Food Protection* 67 (10), 2342–2353.

Thunberg, R.L., Tran, T.T., et al., 2002. Microbial evaluation of selected fresh produce obtained at retail markets. *Journal of Food Protection* 65 (4), 677–682.

Tuszewski, M., Scheuer, J.T., et al., 1995. Composition of the oxygen plasmas from two inductively coupled sources. *Journal of Vacuum Science & Technology A: Vacuum, Surfaces, and Films* 13 (3), 839–842.

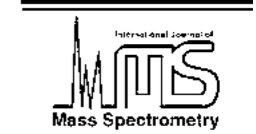
Ukuku, D.O., Fett, W.F., 2006. Effects of cell surface charge and hydrophobicity on attachment of 16 *Salmonella* serovars to cantaloupe rind and decontamination with sanitizers. *Journal of Food Protection* 69 (8), 1835–1843.

Van Boxtael, S., Habib, I., et al., 2013. Food safety issues in fresh produce: bacterial pathogens, viruses and pesticide residues indicated as major concerns by stakeholders in the fresh produce chain. *Food Control* 32 (1), 190–197.

Wang, H., Feng, H., et al., 2009. Effect of surface roughness on retention and removal of *Escherichia coli* O157:H7 on surfaces of selected fruits. *Journal of Food Science* 74 (1), E8–E15.

Wu, H., Sun, P., et al., 2012. Reactive oxygen species in a non-thermal plasma microjet and water system: generation, conversion, and contributions to bacteria inactivation—an analysis by electron spin resonance spectroscopy. *Plasma Processes and Polymers* 9 (4), 417–424.

Zhang, H.Q., Barbosa-Cánovas, G.V., et al., 2011. *Nonthermal Processing Technologies for Food*. Ames, Iowa, Wiley-Blackwell/IFT Press, Chichester, West Sussex, UK.



## Evaluation of the roles of reactive species, heat, and UV radiation in the inactivation of bacterial cells by air plasmas at atmospheric pressure

M. Laroussi\*, F. Leipold

*Department of Electrical and Computer Engineering, Old Dominion University, 231 Kaufman Hall, Norfolk, VA 23529, USA*

Received 2 October 2003; accepted 13 November 2003

### Abstract

Recently, non-equilibrium, atmospheric pressure air plasmas have been shown to possess excellent germicidal properties. A number of studies have shown that air plasmas are capable of inactivating a wide range of microorganisms in the matter of few seconds to few minutes. However, until now little information regarding quantitative measurements of the various plasma agents that can potentially participate in the inactivation process has been published. In this paper, emission spectroscopy and gas detection are used to evaluate important plasma inactivation factors such as UV radiation and reactive species. Our measurements show that for non-equilibrium, atmospheric pressure air plasmas, it is the oxygen-based and nitrogen-based reactive species that play the most important role in the inactivation process.

© 2004 Elsevier B.V. All rights reserved.

*Keywords:* Microorganism; Air plasma; Discharge; Reactive species; Sterilization

### 1. Introduction

The inactivation of harmful microorganisms such as bacteria can be achieved by chemical and/or physical means, such as heat, chemical solutions and gases, and radiation [1]. Most conventional sterilization techniques are associated with some level of damage to the material or medium supporting the microorganisms. This does not present a problem in cases where material preservation is not an issue. However, in cases where it is imperative not to damage the materials to be sterilized, conventional methods are either not suitable at all or offer very impractical and/or tedious and time consuming solutions. This situation led to the development of new techniques that are at least as effective as established ones, but with added superior characteristics such as short processing times, non-toxicity, and medium preservation. Amongst these new methods, non-equilibrium atmospheric pressure plasmas have been shown to present a great promise [2–5].

In this paper, the identification and potential role of each inactivation agent generated by the plasma is assessed. Generally, various gas mixtures can be used to optimize the

production of an agent or another and to optimize the efficiency of the inactivation process. The analysis presented here, however, is for low temperature atmospheric pressure plasmas generated in air. For information on plasma sterilization using other gas mixtures such as O<sub>2</sub>/CF<sub>4</sub>, or at low pressures, the reader is referred to Refs. [6–8].

### 2. Identification of the inactivation factors and assessment of their roles

Under plasma exposure, bacterial cells can be inactivated by one of four known factors or by a synergistic combination of these. These factors are the heat, UV radiation, charged particles, and reactive neutral species. The extent of the influence of each factor depends on the plasma operating parameters such as power and gas mixture and flow rate. Here, we present relative, and when possible, absolute measurements of the presence of these agents in an atmospheric pressure air plasma generated by a Dielectric Barrier Discharge (DBD). Since our experiments are conducted with the biological sample placed at some distance from the plasma (remote exposure), the effects of charged particles (electrons and ions) will not be discussed. A comprehensive study of the effects of charging bacterial cells by a plasma can be found in Ref. [9].

\* Corresponding author. Tel.: +1-757-683-2416; fax: +1-757-683-3220.  
E-mail address: mlarouss@odu.edu (M. Laroussi).

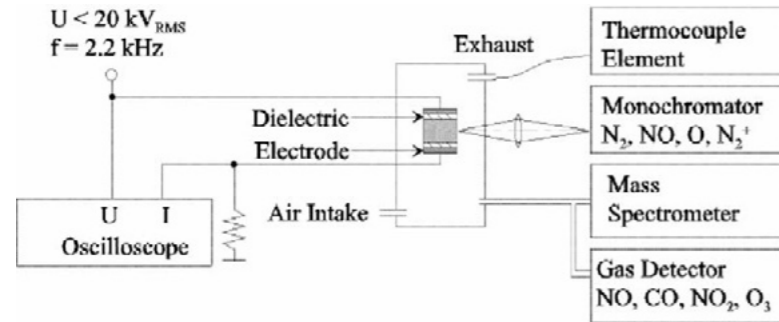


Fig. 1. Experimental setup of DBD air plasma generator and related diagnostics.

A schematic of the experimental setup showing the DBD and the diagnostics used in our evaluations is presented in Fig. 1. The electrodes of our DBD consist of two symmetrical aluminum plates covered by 1 mm thick sheets of alumina (Al<sub>2</sub>O<sub>3</sub>). The distance between the electrodes is adjustable, up to 1.25 cm. Water cooling of the electrodes allows us to keep the temperature close to room temperature. The applied voltage and the discharge current are monitored by means of a high voltage probe and a current viewing resistor, respectively. The discharge was operated at power levels up to 20 W at an electrode separation of about 7 mm. Optical emission spectroscopy, mass spectroscopy, and gas detection (for NO<sub>2</sub>, NO, and O<sub>3</sub>) were used to diagnose the plasma contents.

### 2.1. Heat and its potential effect

It has long been known that heat has detrimental effects on living cells. Therefore, heat-based sterilization techniques were developed and commercially used for applications that do not require medium preservation. In heat-based conventional sterilization methods, both moist heat and dry heat are used. In the case of moist heat, such as in an autoclave, a temperature of 121 °C at a pressure of 15 psi is used [10]. Dry heat sterilization requires temperatures close to 170 °C and treatment times of about 1 h [10].

To assess if heat plays a role in the case of an air plasma, the gas temperature in the discharge was determined by comparing the experimentally measured rotational bands structure of the 0–0 transition of the 2nd positive system of nitrogen with simulated spectra at different temperatures. In addition, the temperature in a sample, placed 2 cm away from the discharge, was measured by a thermocouple probe.

Fig. 2 shows the measured and calculated rotational bands of the 0–0 transition of the 2nd positive system of N<sub>2</sub>, for a power of 10 W. It indicates that the gas temperature remains close to room temperature. A variation in power from 2 to 15 W showed no significant change in the relative spectral distribution. This indicates a power-independent temperature in the range between 2 and 15 W at a gas flow rate of 10 l/min. The gas temperature for various gas flow rates at a power consumption of 10 W was also investigated. The re-

sults are shown in Fig. 3. For a very low flow (0.5 l/min), a gas temperature of 340 K was found. Increasing the airflow causes the gas temperature to approach room temperature (300 K).

Fig. 4 shows the increase in the temperature of the biological sample under treatment for various dissipated power

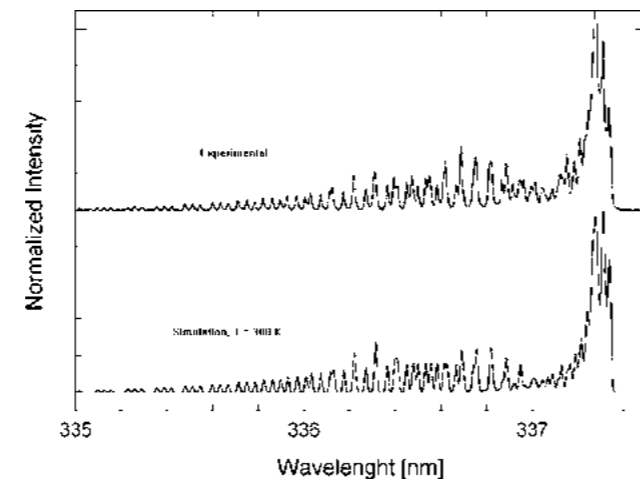


Fig. 2. Measured and calculated rotational bands of the 0–0 transition of the second positive system of nitrogen. The spectra are intentionally shifted vertically for better comparison.

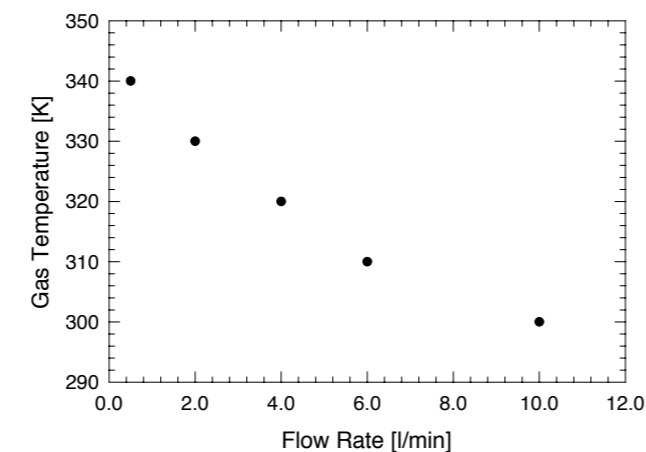


Fig. 3. Gas temperature vs. gas flow rate for a power of 10 W.

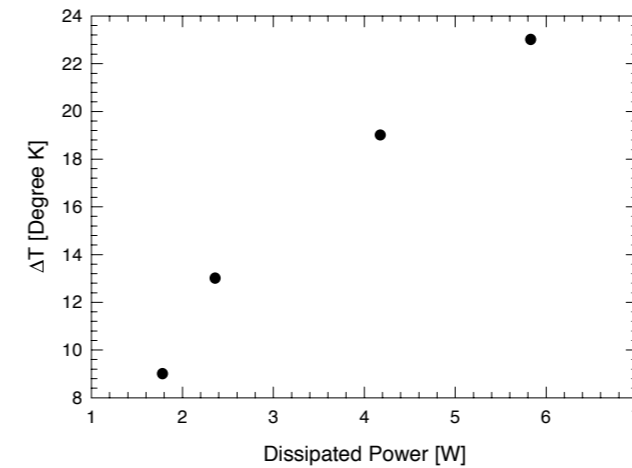


Fig. 4. Increase of sample temperature vs. plasma dissipated power.

levels, as measured by a thermocouple. At our typical running power levels, a maximum increase of 21° was observed. Therefore, based on these measurements no substantial thermal effects on bacterial cells are expected.

### 2.2. Ultraviolet radiation and its potential role

From early times humans have known that sunlight has beneficial hygienic effects. This is of course due the presence of UV radiation in the sunlight spectrum. Amongst UV effects on cells of bacteria is the dimerization of thymine bases in their DNA strands. This inhibits the bacteria's ability to replicate properly. Wavelengths in the 220–280 nm range and doses of several mW s/cm<sup>2</sup> are known to have the optimum effect [11].

Spectroscopic and absolute power measurements were conducted to quantify the UV contribution to the inactiva-

tion process in the case of an air plasma. Our results show that no significant UV emission occurs below 285 nm. This is illustrated in Fig. 5. Power measurements with a calibrated UV detector in the 200–300 nm wavelength region revealed that the power density of the emitted UV radiation is below 50 μW/cm<sup>2</sup> and is essentially independent of the air flow rate. At this power levels we expect the UV not to play a significant direct role in the sterilization process by low temperature air plasmas.

### 2.3. Reactive species and their role

In high-pressure non-equilibrium plasma discharges, reactive species are generated through various collisional pathways, such as electron impact excitation and dissociation. Reactive species play an important role in all plasma–surface interactions. Air plasmas are excellent sources of reactive oxygen species (ROS) and reactive nitrogen species (RNS), such as atomic oxygen (O), ozone (O<sub>3</sub>), hydroxyl (OH), NO, NO<sub>2</sub>, etc. Some reaction pathways that lead to the generation of these species in air plasmas are:

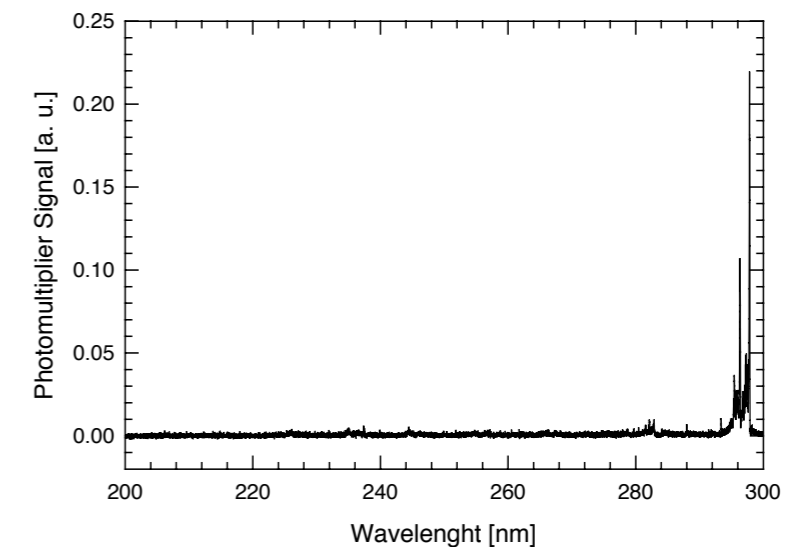
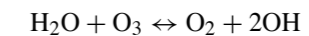
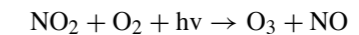
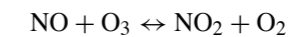
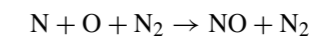
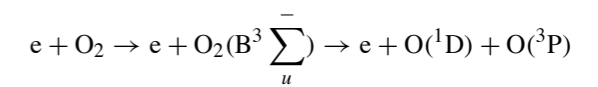
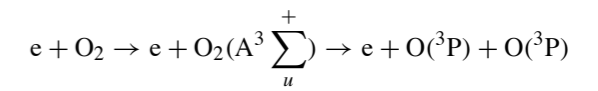


Fig. 5. UV spectrum of a DBD in air in the 200–300 nm wavelength range.

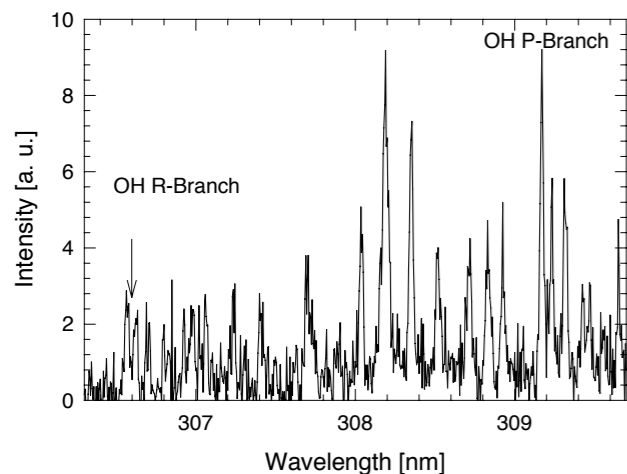
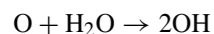
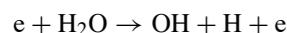


Fig. 6. Emission spectrum from a DBD in air showing OH band heads.



The following are measurements of oxygen, hydroxyl, ozone, and nitrogen dioxide obtained from a DBD operated in atmospheric pressure air. Relative concentration of atomic oxygen in the DBD, as measured by detecting the oxygen lines at 615.597 and 615.678 nm, showed that the concentration of atomic oxygen decreased less than 20% as the flow rate was increased from 1 to 18 l/min. The presence of OH was measured by means of emission spectroscopy, looking for the rotational band of OH A–X (0–0) transition. This molecular band has a branch at about 306.6 nm (R branch) and another one at 309.2 nm (P branch). Fig. 6 shows the

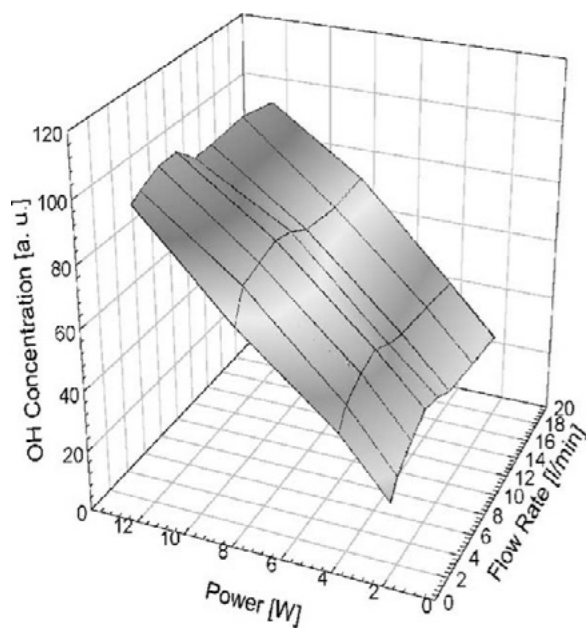


Fig. 7. Relative OH concentration as a function of plasma dissipated power and air flow rate.

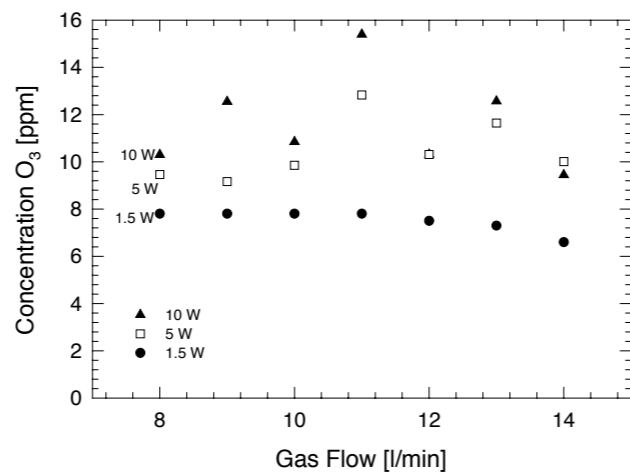


Fig. 8. Ozone concentration generated in a DBD in air as a function of air flow rate and at three power levels (1.5, 5, and 10 W).

emission spectrum in the range between 306 and 310 nm and it indicates the OH band heads. Fig. 7 shows the relative concentration of OH in the discharge as a function of the air flow rate and dissipated power, assuming that the rotational band intensity represents the OH concentration. The ozone concentration was measured for varying flow rates and at various power levels by a calibrated ozone detector. The results are shown in Fig. 8. Ozone germicidal effects are caused by its interference with cellular respiration. Nitrogen dioxide was measured as a function of the air flow rate and for different power levels by a calibrated gas detecting system and the results are shown in Fig. 9.

The reactive species mentioned above have direct impact on the cells of microorganisms, and especially on their outermost membranes. These membranes are made of lipid bilayers, an important component of which is unsaturated fatty acids. The unsaturated fatty acids give the membrane a gel-like nature. This allows the transport of the biochemical

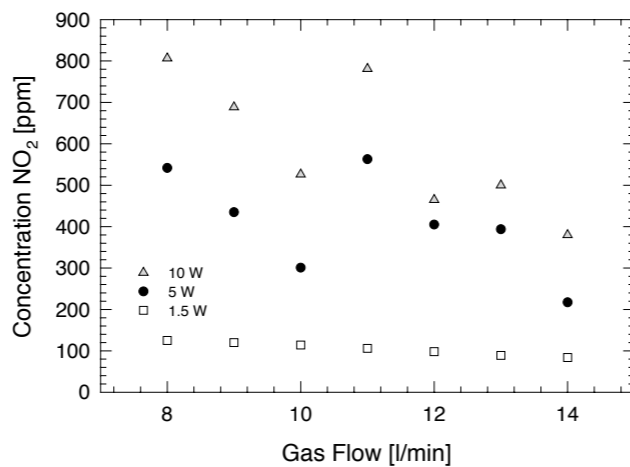


Fig. 9. Concentration of nitrogen dioxide generated in a DBD in air as a function of air flow rate and at three power levels (1.5, 5, and 10 W).

by-products across the membrane. Since unsaturated fatty acids are susceptible to attacks by hydroxyl radical (OH) [12], the presence of this radical can therefore compromise the function of the membrane lipids whose role is to act as a barrier against the transport of ions and polar compounds in and out of the cells [13]. Imbedded in the lipid bilayer are protein molecules which also control the passage of various compounds. Proteins are basically linear chains of aminoacids. Aminoacids are also susceptible to oxidation when placed in the radical-rich environment of the plasma. Therefore, the reactive species generated by air plasmas are expected to greatly compromise the integrity of the cells of microorganisms, leading to their eventual destruction.

### 3. Correlation between the presence of reactive species and inactivation kinetics

One kinetics measurement parameter, which has been used extensively by researchers studying sterilization by plasma, is what is referred to as the “D” value (Decimal value). The D-value is the time required to reduce an original concentration of microorganisms by 90%, or if the “kill” curve is plotted on a semi-logarithmic scale, the D-value is determined as the time for a one log<sub>10</sub> reduction.

To show the effects of reactive species on the destruction of bacteria, kill curves were plotted for three different gaseous conditions: helium only, 97% helium/3% oxygen mixture, and air, all at atmospheric pressure. Spores of the *Bacillus* genus were used since they are hard to kill and are accepted metrics for biological sterilization. When helium is used, only very small concentrations of radicals originating from impurities are expected. When helium is mixed with oxygen, oxygen-based species such as O and O<sub>3</sub> are generated. When air is used, both oxygen-based and nitrogen-based species are generated.

Fig. 10 shows a comparison between the inactivation kinetics in the case of helium and when a 97%–3% helium/oxygen mixture, respectively, was used. After 10 min of treatment time the surviving spore population percentage

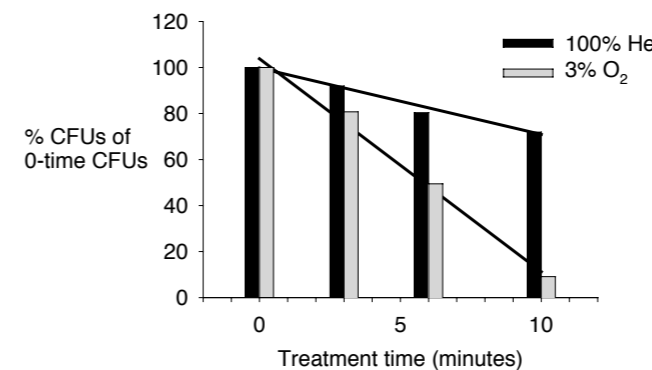


Fig. 10. Percent of surviving *Bacillus* spores vs. plasma treatment time for helium (black) and helium/oxygen mixture (97% He, 3% O<sub>2</sub>) (gray).

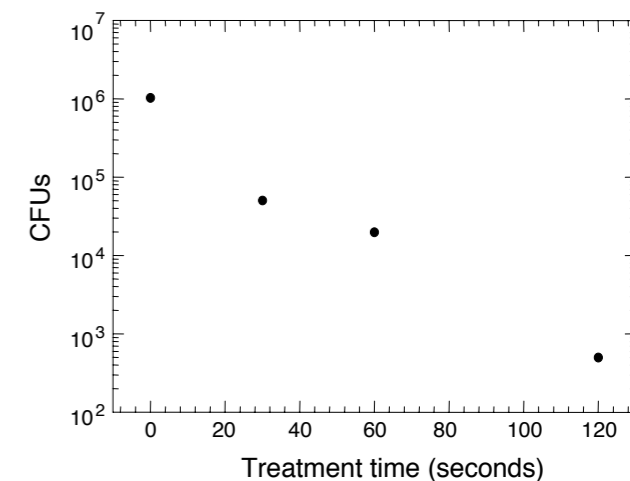


Fig. 11. Colony forming units of *Bacillus* spores vs. treatment time by a low temperature, atmospheric pressure air plasma.

was still much greater than 10%, when only helium was used as the operating gas. In fact the D-value in this case was greater than 20 min. When the helium/oxygen mixture was used, as shown in Fig. 10, a D-value of 10 min was achieved. Fig. 11 shows the inactivation kinetics of an air plasma. A D-value close to 20 s was achieved in this case. This is a 30 times faster inactivation process than the previous case. Since heat and UV radiation were shown not to play an important role for cold air plasmas, the dramatic increase in inactivation efficacy is attributed to the presence of the chemically reactive species such as NO, NO<sub>2</sub>, O, O<sub>3</sub>, etc. . . . .

### 4. Conclusion

Low temperature, atmospheric pressure plasmas have been shown to possess very effective germicidal characteristics. Their relatively simple and inexpensive designs, as well as their non-toxic nature, give them the potential to replace conventional sterilization methods in the near future. This is a most welcome technology in the healthcare arena where re-usable, heat sensitive medical tools are becoming more and more prevalent.

In this paper, based mainly on non-intrusive optical diagnostics and gas detection systems, we conclude that in the case of low temperature air plasmas, it is the highly reactive species such as O, OH, and NO<sub>2</sub> that play the most crucial role in the destruction of microorganisms. Heat and UV radiation may play a secondary role, but we expect their effects to be either minimal or indirect.

### Acknowledgements

Work supported by a grant from the US Air Force Office of Scientific Research.

M. Laroussi, F. Leipold / *International Journal of Mass Spectrometry* 233 (2004) 81–86

References

[1] S.S. Block, *Encyclopedia of Microbiology*, vol. 4, Academic Press, 1992, p. 87.  
 [2] M. Laroussi, *IEEE Trans. Plasma Sci.* 24 (3) (1996) 1188.  
 [3] H.W. Herrmann, I. Henins, J. Park, G.S. Selwyn, *Phys. Plasmas* 6 (5) (1999) 2284.  
 [4] J.G. Birmingham, D.J. Hammerstrom, *IEEE Trans. Plasma Sci.* 28 (1) (2000) 51.  
 [5] M. Laroussi, *IEEE Trans. Plasma Sci.* 30 (4) (2002) 1409.  
 [6] S. Lerouge, M.R. Werthheimer, R. Marchand, M. Tabrizian, L.H. Yahia, *J. Biomed. Mater. Res.* 51 (2000) 128.  
 [7] S. Moreau, M. Moisan, J. Barbeau, J. Pelletier, A. Ricard, *J. Appl. Phys.* 88 (2000) 1166.  
 [8] M. Moisan, J. Barbeau, S. Moreau, J. Pelletier, M. Tabrizian, L.H. Yahia, *Int. J. Pharm.* 226 (2001) 1.  
 [9] M. Laroussi, A. Mendis, M. Rosenberg, *New J. Phys.* 5 (2003) 41.1.  
 [10] S.S. Block, *Disinfection, Sterilization, and Preservation*, Lea & Febiger, Philadelphia, 1983.  
 [11] A. Norman, *J. Cell Comp. Physiol.* 44 (1954) 1.  
 [12] T.C. Montie, K. Kelly-Wintenberg, J.R. Roth, *IEEE Trans. Plasma Sci.* 28 (1) (2000) 41.  
 [13] F.A. Bettleheim, J. March, *Introduction to General, Organic & Biochemistry*, 4th ed., Saunders College Pub., 1995.

See discussions, stats, and author profiles for this publication at: <https://www.researchgate.net/publication/261415267>

# Non-thermal plasma application in air sterilization

Conference Paper in *IEEE International Conference on Plasma Science* · January 2004

DOI: 10.1109/PLASMA.2004.1339779

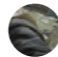
CITATIONS


9


READS

950


5 authors, including:

 **Michael Gallagher**  
 Drexel University  
 20 PUBLICATIONS 313 CITATIONS  
[SEE PROFILE](#)

 **Alexander F. Gutsol**  
 Actively searching for new opportunity  
 179 PUBLICATIONS 7,188 CITATIONS  
[SEE PROFILE](#)

 **Greg Fridman**  
 AAPlasma LLC  
 157 PUBLICATIONS 5,721 CITATIONS  
[SEE PROFILE](#)

Some of the authors of this publication are also working on these related projects:

 **Project** PLASMA FOR AIR AND WATER STERILIZATION [View project](#)

 **Project** Non-thermal Plasma-based Technology in Infection Control [View project](#)

All content following this page was uploaded by [Alexander F. Gutsol](#) on 02 April 2015.

The user has requested enhancement of the downloaded file.

# Non-Thermal Plasma Applications in Air-Sterilization

Michael J. Gallagher<sup>1</sup>, Alexander Gutsol<sup>1</sup>, Gary Friedman<sup>2</sup>, Alexander Fridman<sup>1</sup>

<sup>1</sup>Department of Mechanical Engineering & Mechanics, Drexel University, Philadelphia, PA

<sup>2</sup>Department of Electrical & Computer Engineering, Drexel University, Philadelphia, PA  
Drexel Plasma Institute, Drexel University, Philadelphia, Pennsylvania, USA

## Abstract

In our present study, two non-thermal plasma devices, dielectric barrier discharge and magnetically-rotated gliding arc, are being used to sterilize air containing high concentrations of viral and bacterial bioaerosols. A Pathogen Detection and Remediation Facility was designed for bioaerosol generation, containment, and sampling during plasma sterilization experiments.

**Keywords:** non-thermal plasma, sterilization; decontamination, airborne virus, bacteria, influenza

## 1. Introduction

The improvement of indoor air quality has been a challenge since the dawn of heating, ventilation, and air conditioning (HVAC) systems. Incidents like the infamous outbreak of Legionnaires disease in 1976 in Philadelphia and the recent increasing threat of bioterrorism have raised awareness of the dangers of airborne microorganisms in indoor environments. In recent years, non-thermal atmospheric pressure plasma has been the focus of research as an improved method for the sterilization of air from biological contaminants. Non-thermal plasma has been proven to inactivate many different types of microorganisms, such as viruses and bacteria, on surfaces of materials, but there have been few scientific studies of air sterilization using non-thermal plasma. Also, of the few researchers that have been able to use plasma to decontaminate a moving air stream, many rely on high efficiency particulate air (HEPA) filters to remove a large portion of microorganisms. HEPA filters are effective at trapping particles down to 0.5 microns in size; however, studies have shown that they are not as effective at capturing airborne viruses, which are among the smallest (20-300nm) known microorganisms [1]. HEPA filters also cause significant pressure losses in HVAC systems giving rise to higher energy and maintenance costs. There are several alternative methods for air cleaning, which include electrostatic precipitators, Ultraviolet Germicidal Irradiation (UVGI) devices, and some portable negative air ionizers, that are all capable of reducing particulates and even certain levels of microbial contamination in indoor environments. However, many of these methods are not proven as an efficient and cost effective means of eliminating airborne viruses. In this ongoing scientific study, we will examine the sterilization effect of two types of non-thermal plasma; dielectric barrier discharge (DBD) and magnetically-rotated gliding arc on air contaminated with high concentrations of aerosolized Influenza A virus. A non-pathogenic unicellular bacterium known as *Synechococcus Elongatus*, or Cyanobacteria, was also used in initial trials to demonstrate the decontamination ability of active chemical species generated from dielectric barrier discharge for bacteria in water and to provide benchmark data regarding bioaerosol sampling efficiency.

## 2. Non-thermal plasma for air sterilization

Although Dielectric Barrier Discharge (DBD) and magnetically-rotated Gliding Arc [2] are quite different in terms of current-voltage characteristics and operational power levels, both devices can provide a high concentration of active chemical species, which are a necessary component of the sterilization process. There are two main sterilization effects that bioaerosols are subjected to as they are passed through each plasma device: the direct interaction with the lethal environment of the discharge itself and the downstream interaction with active chemical species, such as ozone (O<sub>3</sub>) and hydroxyl (OH), produced by the discharge. Figure 1 below shows a photo of the DBD device which consists of a thin plane of wires with equally spaced air gaps of 1.5 mm. The high voltage electrodes are coated with a quartz capillary dielectric that has an approximate wall

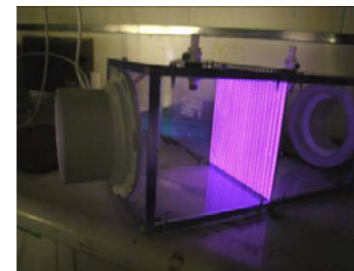


Figure 1. Dielectric Barrier Discharge for air sterilization

thickness of 0.5 mm and the device requires 14 kV for breakdown while consuming less than 200 watts of power. DBD is a low temperature discharge that is very efficient for the production of ozone, which is a strong oxidizer and proven microbial disinfectant [3-6]. The second discharge, magnetically-rotated Gliding Arc, generates a transitional non-thermal plasma and has a relatively low translational gas temperature with a high electron temperature. Gliding Arc uses a strong magnetic field to rotate and elongate an initial thermal arc resulting in rapid convective cooling, keeping the passing air flow near room temperature. This type of discharge has a large power density that can work at atmospheric pressure, but is still very efficient in providing active species. The Gliding Arc device is eight inches in diameter which keeps air velocity low allowing for greater uniformity of treatment. In figure 2, the arc is partially elongated at the center electrode. Additionally, both DBD and gliding arc devices have been designed to prevent an air pressure loss during operation and are capable of retrofit into existing HVAC systems.

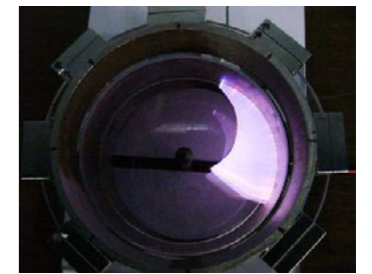


Figure 2. Magnetically Rotated Gliding Arc

## 3. Preliminary experiments with plasma-water decontamination

To understand the decontamination effectiveness of DBD, we designed a simple experiment to test the effect of active chemical species generated from this discharge on cyanobacteria suspended in liquid growth medium. Approximately 35 ml of liquid with cyanobacteria was placed in a Petri dish at a distance of 30 mm from the surface of the plasma discharge. A small fan forced air through the discharge at a direction normal to the surface of the liquid.

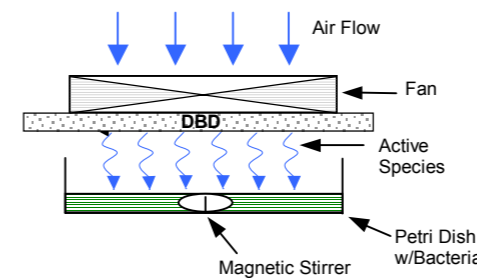


Figure 3. Water decontamination experiment using Dielectric Barrier Discharge (DBD).

Figure 3 shows a diagram of the experimental setup. The DBD discharge produces 0.11 mg of ozone per liter of air, most of which was directed toward the liquid-gas interface as the solution was stirred with a magnetic stir bar. After 3.9 minutes of treatment, we demonstrated more than a 2-log reduction (99.3%) of bacteria in the solution. We attribute ozone as the main active species responsible for the inactivation of bacteria in this case because of its longer lifetime in comparison to hydroxyl. A similar experiment was performed by Moreau, et al. [7] to demonstrate the lethal effect of a gliding arc discharge on strain of a bacterial plant pathogen, *Erwina*, suspended in a liquid medium.

## 4. Air Decontamination / Sterilization

In order to prove that non-thermal plasma is the main factor responsible for sterilization, one must first build a system that is capable of creating, handling, and analyzing dense concentrations of viable bioaerosols. Designing and building an air sterilization system is challenging because there are many factors that contribute to losses of aerosolized microorganisms in moving air streams. These factors include diffusion of aerosol to walls of the air flow system, desiccation stress on the microorganism due to evaporation of bioaerosol droplets in flight, and inertial and gravitational forces which can remove larger droplets from the air stream. The factors causing these losses must be carefully considered in order to avoid misinterpretation of sterilization data and may also be one reason why bioaerosol sterilization studies are limited in comparison to studies involving water or surface sterilization. Careful attention to these potential sources of error will yield greater accuracy and validity in distinguishing non-thermal plasma as the true sterilizing agent. Figure 4 below shows a scheme of the Pathogen Detection and Remediation Facility (PDRF) which is a plug flow reactor that was designed for



bioaerosol generation, containment, and sampling. It was designed to simulate conditions commonly found in an HVAC system: it has an overall volume of 250 liters, and can operate at flow rates up to 25 liters per second. The PDRF houses interchangeable non-thermal plasma devices, DBD and Magnetic Gliding Arc, which are connected to the system with four inch (10 cm) diameter flexible piping. At a flow rate of 25 L/s, the residence time, that is, the time for one droplet to make one revolution through the system, is approximately 10 seconds. An air sampling system is included in the PDRF and was designed to take as large volume air sample as possible (~ 1 liter) in a short period of time (~ 1 second) so that we do not disturb the flow inside the system and can evaluate the viability of the bioaerosol as a function of treatment time.

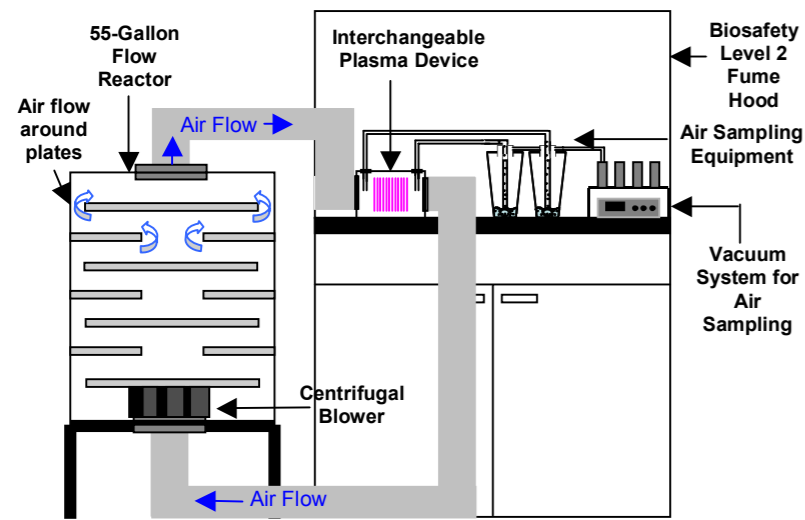


Figure 4. Pathogen Detection and Remediation Facility (PDRF)

Liquid impingement was chosen as the air sampling method for our system, as opposed to filtration or impaction, because it minimizes desiccation stress and allows for the direct deposition of the microorganism into growth media.

The AGI-30 liquid impinger is a commonly used bioaerosol sampler and it operates by drawing a sample of air through an inlet tube submerged in a solution, thereby causing the air stream to strike the liquid bed trapping aerosols in the solution through forces of inertia [8]. The AGI-30 impinger contains a critical orifice that contains one exit port and limits the maximum air sampling rate to 12.5 liters per minute [9]. To accommodate our desired sampling rate of 1 liter per second, we modified the AGI-30 by increasing its overall volume and replacing the standard critical orifice with a hollow spherical tip with several exit ports. Several calibration experiments performed with our modified AGI-30 impinger demonstrated reproducibility in terms of sampling efficiency. In these experiments, a Collison nebulizer was connected directly to the modified liquid impinger and after five minutes of continuous sampling in each trial, we obtained a stable sampling efficiency rating of 3.5%. Some may not consider this as an optimal efficiency rating, however, when sampling bioaerosols, reproducibility is often considered more important than the efficiency rating because the final conclusions are derived from internal comparisons between various data collected using the same samplers [9].

Several additional calibration experiments were performed in which cyanobacteria aerosol (droplet size: 1.5 micron) was injected into the Pathogen Detection and Remediation Facility (PDRF) not for the purpose of sterilization, but to identify all bioaerosol losses from diffusion, inertia, and evaporation, thereby establishing accurate controls before non-thermal plasma is introduced. In these experiments, a Collison nebulizer was used to generate the bioaerosol, the air flow rate was fixed at 25 liters per second, and the lifetime of droplets was measured by periodic air sampling with two modified liquid impingers. For all experiments described here, the system was prehumidified with sterile de-ionized water until the internal surface of the system walls were wet prior to input of the bioaerosol. Initial results showed a very poor recovery of cyanobacteria bioaerosol from the PDRF in comparison to air sampler calibration experiments. When examining the sources of loss: diffusion, inertia, and evaporation, we ruled out inertial forces because air velocity is relatively low and the aerosol droplets are small (1-2 microns). Also, our estimate of droplet diffusion time to the wall is approximately 40 minutes, well beyond the upper time limit of these trials. The effect of small droplet evaporation, however, can be prominent because the saturation pressure around a small droplet is high in comparison to the saturation pressure near the wet walls of the system. To test the effect of evaporation on the survivability of cyanobacteria, we performed two experiments: the first (Experiment A) in which additional humidity was applied continuously with the bioaerosol using an additional nebulizer with sterile de-ionized water, and the

second (Experiment B) without additional humidification. Our results, which are described in figure 5 below, show that additional humidification reduces the rate of inactivation of aerosolized cyanobacteria, by desiccation stress compared to the results of experiments without additional humidification.

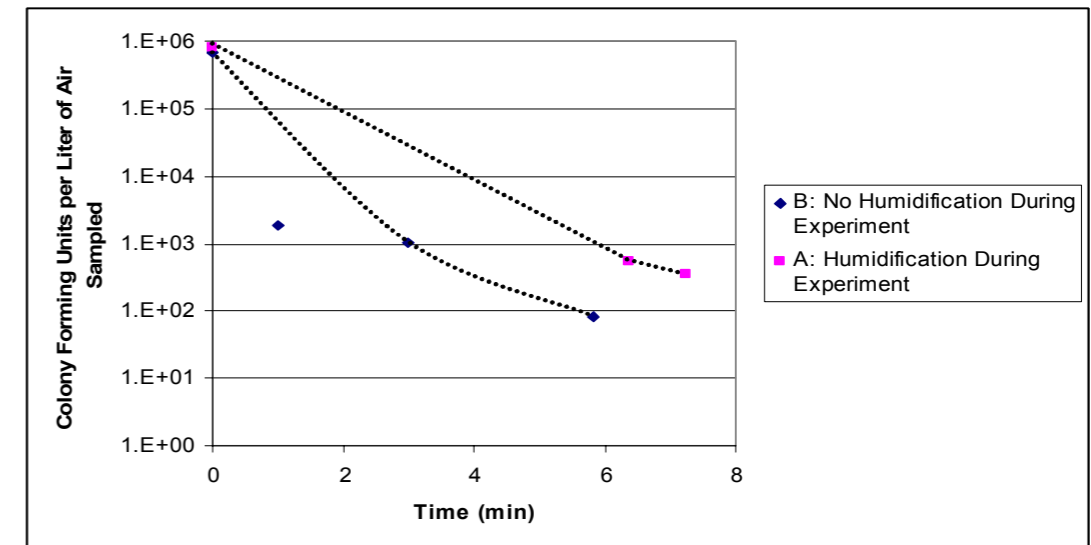


Figure 5. Evaluation of the effect of droplet evaporation on the survivability of aerosolized cyanobacteria. Experiment A minimizes evaporation by providing constant humidity.

The experimentally estimated maximum lifetime of aerosolized Cyanobacteria is 10 minutes, which is far below the estimated diffusion time of droplets to the walls of the system. We desire to have the ability to recover viable cyanobacteria over an extended period of time (tens of minutes) so that when we perform sterilization experiments with non-thermal plasma, we have enough time to take several air samples and thus acquire many data points to accurately describe the rate of inactivation. To determine if the droplets were indeed still present in the air flow after 10 minutes, we added a laser to the system to characterize the optical density of the bacterial aerosol over time. Figure 6 shows an image of the illuminated laser beam at the first minute of the experiment when the concentration of viable Cyanobacteria is high. Illumination from the laser beam slowly decayed over a period of nearly 2 hours indicating that aerosolized bacteria were still present in the flow, however, they were non-viable. Similar results were reported by Ehresmann & Hatch, who described the optical density of aerosolized unicellular bacteria lasting up to four hours at high humidity (92-94%) with viability lasting only minutes [10]. These calibration experiments with Cyanobacteria provided us with a basic understanding of the flow characteristics of the Pathogen Detection and Remediation Facility and efficiency of our air sampling system. This was a necessary step before working with viral bioaerosols because immunoassay detection methods used to quantify viruses are less accurate than the serial dilution methods used to quantify Cyanobacteria in these calibration experiments. Sterilization experiments with Cyanobacteria and Influenza A virus are in progress and we expect to have results in the summer of 2005.

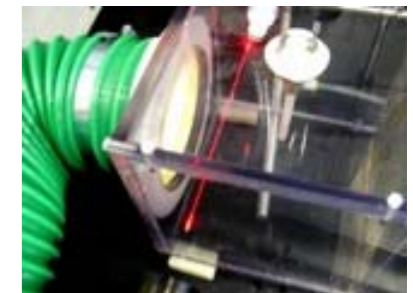


Figure 6. A laser beam illuminates the dense concentration of bioaerosol

### 5. Plasma chemistry sterilization modeling

The results from our experiments with the PDRF will be used to verify a model of plasma chemical sterilization [11]. We have composed a physiochemical model of the oxidizing effects of the active chemical species

generated by non-thermal plasma on many different types of microorganisms. We are investigating the individual sterilizing effects of hydroxyl radicals (OH), ozone (O<sub>3</sub>), ultraviolet radiation (UV) as there is a large amount empirical data regarding the role of each of these components for the sterilization of various bacteria, viruses, and spores in various media. Our model combines this data with the chemical kinetics of non-thermal plasma to predict the rate of destruction of microorganisms under varying conditions.

This research is supported by Telemedicine and Advanced Technology Research Center of the US Department of Defense (TATRC of DoD) through Civilian Medical Response Center (CiMeRC).

## References

- [1] Harstad, J.B. Evaluation of air filters with submicron viral aerosols and bacterial aerosols. American Industrial Hygiene Association Journal. May-June (1969).
- [2] Gangoli, S., Gutsol, A. and Fridman A. Rotating Non-Equilibrium Gliding Arc Plasma Disc for Enhancement in Ignition and Combustion of Hydrocarbon Fuels, ISPC-17, August 7-12, 2005, Toronto, Canada.
- [3] Kowalski, W.J., Bahnfleth, W.P., and Whittam, T.S. Bactericidal effects of high airborne ozone concentrations on escherichia coli and staphylococcus aureus. Ozone Sci. Engin. 20 (1998).
- [4] Kowalski, W.J., W.P. Bahnfleth, B.A. Striebig, and T.S. Whittam. Demonstration of a hermitic airborne ozone disinfection system: studies on E. coli. American Industrial Hygiene Association Journal. March-April (2003).
- [5] Ishizaki, K., Shinriki N., and Matsuyama H. Inactivation of bacillus spores by gaseous ozone. Journal of Applied Bacteriology 60 (1986).
- [6] Burlison G.R., Murray T.M., Pollard M. Inactivation of viruses and bacteria by ozone, with and without sonication. Applied Microbiology 29, 3 (1975).
- [7] Moreau M., Feuilloley M.G.J., Orange N., and Brisset J.-L. Lethal effect of the gliding arc discharges on Erwinia spp. Journal of Applied Microbiology. 98 (2005).
- [8] Perry, J.H. Chemical engineers' handbook, 2nd ed. McGraw-Hill, New York. (1941).
- [9] Cown WB, Kethley TW, Fincher EL. The critical-orifice liquid impinger as a sampler for bacterial aerosols. Applied Microbiology 5 (1957).
- [10] Ehresmann D.W., Hatch M.T. Effect of relative humidity on the survival of airborne unicellular algae. Applied Microbiology 29:3 (1975).
- [11] Gangoli, S., Gallagher, M., Dolgopolsky, A., Gutsol, A. and Fridman A. Sterilization of Microorganisms using Non-Thermal Dielectric Barrier Discharge Plasma – Statistically based Chemical Kinetics Model, ISPC-17, August 7-12, 2005, Toronto, Canada.

See discussions, stats, and author profiles for this publication at: <https://www.researchgate.net/publication/304639945>

## Non-thermal plasmas (NTPs) for inactivation of viruses in abiotic environment

Article · June 2016

CITATIONS  
9



READS  
1,136

2 authors:

 **Pradeep Puligundla**  
Gachon University  
75 PUBLICATIONS 791 CITATIONS  
[SEE PROFILE](#)

 **Chulkyoon Mok**  
Gachon University  
67 PUBLICATIONS 785 CITATIONS  
[SEE PROFILE](#)

Some of the authors of this publication are also working on these related projects:

-  UGC-MRP Research project during the year 2007-2010 [View project](#)
-  Encapsulation of epigallocatechin gallate in zein/chitosan nanoparticles for controlled applications in food system [View project](#)

All content following this page was uploaded by Pradeep Puligundla on 11 July 2016.

The user has requested enhancement of the downloaded file.

## Review Paper:

# Non-thermal plasmas (NTPs) for inactivation of viruses in abiotic environment

Puligundla Pradeep and Mok Chulkyoon\*

Department of Food Science and Biotechnology, Gachon University, Seongnam 13120, KOREA  
mokck@gachon.ac.kr**Abstract**

Despite several successful disinfection strategies, process of controlling the environmental survival and transmission of human pathogenic viruses is becoming increasingly more difficult because of their emerging resistance to disinfectants. Therefore, range of non-chemical methods of inactivation is being explored extensively as an alternative. Especially, non-thermal, chemical-free techniques find wide application in the inactivation of air-borne, water and food-borne and surface-borne viruses. Among such methods, the application of non-thermal plasmas (NTPs) for viral inactivation is a relatively new technique and is quite promising. The present review evaluates comprehensively the studies of virucidal effect of NTPs against human pathogenic viruses in abiotic environment.

**Keywords:** Non-thermal plasma, pathogenic virus, inactivation, disinfection, abiotic environment.

**Introduction**

Medically-important viruses continue to survive and evolve in abiotic environment despite several successful disinfection strategies to control them. This is primarily due to the resistance of several viruses to disinfectants and sterilants, especially to chemical-based ones and continuous appearance of mutations. Also, the highly related viruses can exhibit different disinfection kinetics when treated with the same biocide which makes virus inactivation complicated<sup>8,14</sup>.

The mode of transmission of several groups of viruses to humans is through contaminated food, water and air, person-to-person transmission via contaminated environmental surfaces or objects and direct person-to-person contact<sup>11,34</sup>. It is known that viruses pass into the environment from clinically ill or carrier hosts although they do not replicate outside living animals or people; they are maintained and transported to susceptible hosts<sup>33</sup>. Viruses are less tolerant to heat and therefore lose infectivity rapidly on heat treatment. However, heat-induced inactivation is not always suitable and non-thermal sterilization methods may be required to deactivate viruses on thermolabile surfaces or materials and heat-sensitive foodstuffs. Several non-chemical, non-thermal technologies have been developed to combat surface-borne, food- and water-borne viruses. Such methods uses ionizing radiation,

UV irradiation, pulsed light, pulsed electric field, supercritical fluids, high hydrostatic pressure processing and gas plasma<sup>7,13,16,20,38</sup>.

The use of atmospheric pressure, nonthermal plasmas (NTPs) is a promising approach for sterilization and disinfection of both viable and nonviable surfaces<sup>5</sup>. NTPs have been used for a range of biomedical applications including microbial inactivation, sterilization and disinfection<sup>17,23,27</sup>. The sterilants produced by the nonthermal plasma killed or inactivated a wide range of organisms, spores and viruses<sup>43</sup>. The potential advantages of NTPs over chemical disinfectants include simplicity of design and operation<sup>47</sup>, utilization of nontoxic gases, an absence of toxic residues<sup>36</sup> and production of a large quantity of diverse microbicidal active species. Plasmas are not only capable of inactivating or killing bacteria and viruses; they can also dislodge these dead microorganisms from the surfaces of the objects being sterilized<sup>12</sup>.

**Fundamentals of non-thermal plasmas:** Plasma is defined as a neutral ionized gas with a net neutral charge. It is constituted by different species including ions (both positive and negative), electrons, atoms, free radicals, photons and excited and nonexcited molecules<sup>18</sup>. A neutral gas can be converted to plasma by applying energy in several forms including electric, thermal or magnetic fields and radio or microwave frequencies, thereby resulting in an increase in the kinetic energy of the electrons of constituent gas atoms. This causes interatomic collisions in the gas resulting in the formation of aforementioned plasma constituents. Plasma can be categorized based on the relative energetic levels of electrons and heavy particles of plasma into thermal (equilibrium plasma) and nonthermal or cold (non-equilibrium plasma). Thermal plasmas are generated at high pressure ( $\geq 10^5$  Pa) and consume substantial power (up to 50 MW) to be generated.

On the other hand, NTPs can be generated at lower pressures using less power. They are characterized by an electron temperature much higher than that of the gas temperature and thus do not present a local thermodynamic equilibrium. Such plasma can be generated by electric discharges in lower pressure gases<sup>30</sup>.

NTPs are further divided into two other categories: low-pressure plasmas ( $10^{-4}$  to  $10^{-2}$  kPa) and atmospheric-pressure plasmas. The atmospheric plasma sources can be classified regarding their excitation mode into distinct groups - the DC (direct current) and low frequency

discharges; the plasmas which are ignited by radio frequency waves and the microwave discharges<sup>41</sup>. The DC and low frequency discharges can work, depending on their design either with a continuous or a pulsed mode. The arc plasma torches belong to continuous working mode whereas corona discharge, dielectric barrier discharge (DBD) and microplasma belong to pulsed DC discharges. The NTP technology has potential application for microbial inactivation on surfaces and other thermally-sensitive materials.

**Plasma species responsible for inactivation:** In general, heat is not a major contributor to the sterilization effect using non-thermal plasmas. In atmospheric pressure plasmas, UV photons are not the main microbicidal agents<sup>22,28</sup>. On contrary, however, some authors claim that UV photons, under specific operating conditions, can be the dominant inactivation species<sup>10,31</sup>. Several researchers claimed that the chemically reactive neutral species such as O, O<sub>2</sub>\*, O<sub>3</sub>, OH\*, NO and NO<sub>2</sub> can significantly contribute to the plasma sterilization process, especially at atmospheric pressures<sup>17,26,27</sup>. It has been shown that discharges containing oxygen provide a strong germicidal effect<sup>19,35</sup>. Moreover, discharges containing oxygen also generate ozone (O<sub>3</sub>) which is known to have a strong bactericidal effect<sup>27</sup>. Also, the presence of moisture in discharge gas plays a significant role in bactericidal action by generating hydroxyl (OH) radicals in the plasma which can chemically attack the outer structures of bacterial cells. Therefore, the best bactericidal effects were achieved in moistened oxygen and air<sup>24</sup>.

Reactive species of low-temperature plasma are believed to play a dominant role in hepatitis B virus deactivation process<sup>39</sup>. Virucidal action of reactive oxygen species (ROS) has been demonstrated. Wu et al<sup>46</sup> reported that the ROS species namely OH radicals and atomic oxygen were associated with the inactivation of MS2 viruses by the atmospheric-pressure cold plasma. In addition, ROS have been shown to be implicated in the inactivation of MS2 coliphage by an in-house-built kilohertz-driven atmospheric pressure, nonthermal plasma jet<sup>5</sup>. In the case of feline calicivirus (FCV) inactivation by cold atmospheric gaseous plasma (CGP), the chemical interaction of ROS and reactive nitrogen species (RNS) such as singlet oxygen (O<sub>2</sub>\*), ozone (O<sub>3</sub>) and superoxide (O<sub>2</sub><sup>-</sup>) or peroxyacid, has been shown to play a key role<sup>1</sup>. Sakudo et al<sup>37</sup> found that hydrogen peroxide-like molecules which can create oxidative stress, were predominantly responsible for inactivation of influenza virus by N<sub>2</sub> gas plasma.

**Inactivation mechanisms:** Nonthermal plasma may be employed to inactivate a wide range of microorganisms such as bacteria, spores, fungi, viruses and prions. The mechanism of interaction of plasma with living systems is complex and is not well known. This is mainly due to the complexity of biology and partly due to the complexity of plasma. The charged species of plasma, especially ions, are

believed to play a key role in plasma-living cell interaction<sup>15</sup>. In direct plasma exposure, both positive and negative ions have been reported to possess relatively the same effect. The charged species interact chemically and not through physical phenomena such as shear stress, ion bombardment damage or thermal effects. The charged particles might play a significant role in the rupture of outer cell membranes, especially in gram-negative bacteria which possess thin outer membranes and a thin murein layer<sup>29</sup>.

The specific mechanisms that lead to virus inactivation by NTPs are also unclear. Previous studies demonstrated that exposure to NTPs results in modification and/or degradation of viral proteins and nucleic acids and also lipids in enveloped viruses. Yasuda et al<sup>48</sup> attributed inactivation of  $\lambda$  phage by atmospheric pressure DBD to the damage of coat proteins and found DNA damage hardly contributed to the inactivation. It has been shown that singlet oxygen <sup>1</sup>O<sub>2</sub> can cause inactivation of MS2 phage by rendering the genome nonreplicable and significant genome decay and also through minor effects on host binding and genome injection into the host<sup>45</sup>.

It was hypothesized in the case of FCV inactivation by CGP that both ROS and RNS species can potentially react with the capsid protein, leading to protein peroxidation and destruction of the capsid. In addition, reactive species can damage the viral RNA, leading to reduced gene expression and elimination of viral RNA, or both<sup>1</sup>. The degradation of viral proteins including nucleoprotein, hemagglutinin and neuraminidase was observed when N<sub>2</sub> gas plasma was used for influenza A and B viruses inactivation<sup>37</sup>. In addition, the injury of viral RNA genome and the inactivation of hemagglutination were observed after N<sub>2</sub> gas plasma treatment. It was concluded that these changes were possibly due to changes in the viral envelope because of modification of the lipid content. They also concluded that oxidation may be the most important factor in the inactivation, degradation and modification of influenza virus by N<sub>2</sub> gas plasma.

**Studies on decontamination of viruses using NTPs**

**Noroviruses:** Noroviruses are frequently implicated in human gastroenteritis. Noroviruses spread directly from one person to another and via surfaces, often in crowded facilities. Disinfection of surfaces that come into contact with infected humans is essential for the prevention of cross-contamination and further transmission of the virus. The use of atmospheric pressure, nonthermal plasmas is a promising approach to sterilization and/or disinfection of both viable and nonviable surfaces. The virucidal efficacy of atmospheric pressure, nonthermal plasma jet operated at varying helium/oxygen feed gas concentrations against MS2 bacteriophage, which is widely employed as a convenient surrogate for human norovirus, has been investigated<sup>5</sup>. In this study, the log reductions in MS2 viability after 3 min of the plasma exposure were 3

$\log_{10}$  (99.9%) and the reductions exceeded 7  $\log_{10}$  after 9 min exposure.

The ability of non-thermal plasma to inactivate human enteric virus surrogates on stainless steel surfaces has been investigated<sup>40</sup>. During the experimental procedure, cultivable human norovirus surrogates, feline calicivirus (FCV-F9) and murine norovirus (MNV-1) and bacteriophage MS2 at  $\sim 7 \log$  plaque-forming units (PFU)/ml were inoculated and dried on sterile stainless steel coupons. These coupons were treated with the one atmosphere uniform glow discharge plasma for 0, 1, 2, 5 and 10 min. FCV-F9 exhibited reduction of 2.34 and 3.55  $\log$  PFU after 1 and 2 min respectively and to non-detectable levels after 5 and 10 min. MNV-1 was reduced by 0.56, 1.61, 1.95 and 3.16  $\log$  PFU after 1, 2, 5 and 10 min respectively. And, MS2 was reduced by 2.03 and 5.46  $\log$  PFU after 2 and 5 min respectively and to non-detectable levels after 10 min<sup>40</sup>.

The impact of cold atmospheric pressure plasma (CAPP) on the inactivation of a clinical human outbreak norovirus (NoV), GII.4, has been investigated<sup>2</sup>. In this study, NoV-positive stool sample at three different dilutions was prepared and subsequently treated with CAPP for various lengths of time, up to 15 min. Increased NoV reduction was observed with the increase of CAPP treatment time. CAPP reduced the initial quantity of  $2.36 \times 10^4$  genomic equivalents/ml sample by 1.23  $\log_{10}$  and 1.69  $\log_{10}$  genomic equivalents/ml after 10 and 15 min exposure respectively ( $P < 0.01$ ). CAPP treatment of surfaces carrying a lower viral load reduced NoV by at least 1  $\log_{10}$  after CAPP exposure for 2 min ( $P < 0.05$ ) and 1 min ( $P < 0.05$ ) respectively. The results suggest that NoV can be inactivated by CAPP treatment.

Human norovirus is one of the leading causes of viral foodborne illnesses. NTPs have been used to combat norovirus contamination in food. In a study, inactivation effect of atmospheric pressure plasma (APP) jets against murine norovirus (MNV-1), as a norovirus (NoV) surrogate, associated with three types of fresh meats—beef loin, pork shoulder and chicken breast, was investigated by Bae et al<sup>6</sup>. The reduction in MNV-1 titers [initial inoculums of  $10^7$  plaque-forming units (PFU)] was  $> 2 \log_{10}$  PFU/ml in the three types of meat following the treatment with APP jets for 5–20 min. Under 5 min treatment time, there were no significant differences ( $P > 0.05$ ) in the  $L^*$ ,  $a^*$  and  $b^*$  values and the water content (%) value between untreated and APP jet-treated samples. Although the TBARS values, an indicator of meat rancidity, gradually increased with increase of APP jet treatment times, they were below 1.0 mg MA/kg. The results of the study indicate that 5 min of APP jet treatment was effective in  $> 99\%$  reduction of MNV-1 titer without concomitant changes in meat quality.

In another study, the *in vitro* virucidal activity of radio frequency atmospheric pressure plasma jet against feline

calicivirus (FCV), a surrogate of human norovirus, was demonstrated<sup>1</sup>. Exposure of FCV to 1.0, 1.5, 2.0, 2.5 and 3 W Ar plasma for 15 to 180 s led to gradual reductions in the FCV titer ranging from 0.33 to 2.66, 0.66 to 4.00, 0.88 to 4.66, 0.99 to 5.55 and 1.11 to 5.55  $\log_{10}$  TCID<sub>50</sub>/0.1 ml respectively. More than 99.999% of FCV was inactivated (more than 5  $\log_{10}$  TCID<sub>50</sub>/0.1 ml reduction) after exposure to 2.5 and 3 W plasma for 120 s. Additionally, virucidal effects of four combinations of plasma gas mixtures (Ar, Ar plus 1% O<sub>2</sub>, Ar plus 1% dry air and Ar plus 0.27% water) were studied. Of these, Ar plus 1% O<sub>2</sub> plasma treatment showed the highest virucidal effect: more than 6.0  $\log_{10}$  units of the virus after 15 s of exposure<sup>1</sup>.

**Hepatitis A and B:** Hepatitis A virus (HAV) is a small, foodborne, environmentally stable, single-stranded RNA containing non-enveloped virus that causes enteric infections in humans. Atmospheric pressure plasma (APP) jets were found effective against HAV associated with fresh meats. After 5–20 min treatment with APP jets, the reduction in HAV titers (initial inoculums of  $10^6$  PFU) were  $> 1 \log_{10}$  PFU/ml in the three types of meat (beef loin, pork shoulder and chicken breast)<sup>6</sup>.

Hepatitis B is a viral infection that attacks the liver and can cause both acute and chronic disease. Hepatitis B virus (HBV) is relatively stable in the environment and remains viable for at least 7 days on environmental surfaces at room temperature<sup>9</sup>. Shi et al<sup>39</sup> evaluated the effectiveness of low-temperature plasma (LTP) induced by dielectric barrier discharge (DBD) for HBV deactivation. LTP was used to treat HBV in the blood (serum) of hepatitis B patients with HBsAg, HBeAg and anti-HBc positive at time intervals of 10, 20, 30 and 40 s. A 100  $\mu$ L of diluted HBV serum was spread evenly on cover glass for each experiment which is operated in atmospheric air with the room temperature of  $\sim 20^\circ\text{C}$  and the relative humidity of  $\sim 60\%$ . They found a gradual decrease of the copy numbers of HBV DNA with the increase in plasma exposure time. After the 40-s LTP treatment, a five-order magnitude decrease in the copy number of HBV DNA, from the original  $1.33 \times 10^7$  IU/ml to  $0.74 \times 10^2$  IU/ml was noted.

**Newcastle disease virus (NDV) and avian influenza virus (AIV):** Newcastle disease (ND) in many species of birds is commonly caused by highly pathogenic NDV which can result in 100% mortality<sup>4</sup>. Avian influenza (AI), also called bird flu, is an infectious viral disease of birds caused by avian influenza virus (AIV). Outbreaks of high-pathogenicity AI have been reported as a threat to both humans and animals<sup>21</sup>. These are two of the most important pathogens in poultry. In a study, for the purpose of vaccine preparation, an alternating current (AC) atmospheric pressure non-thermal plasma (NTP) jet with Ar/O<sub>2</sub>/N<sub>2</sub> as the operating gas was used to inactivate a Newcastle disease virus (NDV, LaSota) strain and H9N2 avian influenza virus (AIV, A/Chicken/Hebei/WD/98)<sup>44</sup>. The results showed that complete inactivation could be

achieved with 2 min of NTP treatment for both NDV and AIV.

**Adenoviruses:** Adenoviruses usually, depending on the serotype, cause mild diseases ranging from respiratory tract to gastrointestinal infections. They are double-stranded DNA viruses without envelope and are physically stable due to the protein capsid. They can tolerate deviations from neutral pH, moderate increases in heat and are relatively resistant to UVC. For disinfection, chlorine bleach or autoclaving (20 min at  $121^\circ\text{C}$  at 1 bar) is used<sup>49</sup>. Experiments with cold atmospheric plasma (CAP) to inactivate adenovirus have been performed. A surface micro-discharge in air was used as the plasma source. Within 240 s of CAP treatment, inactivation of up to 6 decimal log levels was achieved<sup>49</sup>. The results indicate that the inactivation of adenovirus was achieved by a synergetic effect of all possible species produced (apart from ozone) in the non-equilibrium plasma chemistry—electrons, charged and uncharged particles, excited atoms and molecules, reactive species and UV light.

**Herpes Simplex Virus:** Herpes keratitis (HK) is a viral infection of the eye caused by the herpes simplex virus (HSV). HSV is the common cause of cornea-derived blindness and infection-associated blindness in developed nations. Although acyclovir and its derivatives have been successful in HK patients, the virus prevalence and emergence of acyclovir-resistant strains of herpes simplex virus (HSV) are becoming a challenge<sup>25, 32</sup>. Therefore, for suppressing HSV infection in the cornea, development of novel nonpharmacologic methods may be of therapeutic interest. In a study, Alekseev et al<sup>3</sup> have investigated the antiviral properties of liquids treated with nonthermal dielectric barrier discharge (DBD) plasma. In this study, herpes simplex virus type 1 (HSV-1) infected human corneal epithelial cells and explanted corneas were exposed to culture medium treated with nonthermal DBD plasma.

As a result, a dose-dependent reduction of viral genome replication, the cytopathic effect and the overall production of infectious viral progeny were observed. Genome replication was inhibited more than 90% at the 40-sec treatment intensity. And, no detrimental effects in explanted human corneas were reported due to the DBD plasma treatments which were confirmed by toxicity studies<sup>3</sup>. The study results confirmed that nonthermal DBD plasma can potentially be used to suppress corneal HSV-1 infection *in vitro* and *ex vivo* without causing pronounced toxicity.

**Influenza and paramyxoviruses:** Virus-induced respiratory infections are major causes of upper and lower respiratory tract infections. Influenza viruses and paramyxoviruses are the major pathogens involved in such infections. The mode of transmission is mainly airborne i.e. by direct transmission through droplets from infected cases. Systems that can control virus transmission will reduce the

burden of these infections. A new process for the generation of a cold oxygen plasma (COP) by subjecting air to high-energy deep-UV light with an effective radiation spectrum between 180 nm and 270 nm has been developed by Biozone Scientific Technology. The efficiency of COP against different airborne respiratory viruses, namely respiratory syncytial virus (RSV), human parainfluenza virus type 3 (hPIV-3) and Influenza A (H5N2), was evaluated. A reduction of 6.5, 3.8 and 4  $\log$  (10) TCID<sub>50</sub>/ml of the titre of the hPIV-3, RSV and influenza virus A (H5N2) suspensions respectively was noted<sup>42</sup>. Therefore, it has been concluded that the COP technology is an efficient and innovative strategy to control airborne virus dissemination.

Another study showed that N<sub>2</sub> gas plasma generated by a high-voltage pulse using a static induction (SI) thyristor power supply effectively inactivated influenza virus<sup>37</sup>. In this study, influenza virus (A/PR/8/34)-infected allantoic fluid dried on a cover glass was subjected to treatment with N<sub>2</sub> gas plasma (1.5 kilo pulses per second; 0, 1, 5 min). Samples were collected with pure water and injected into embryonated eggs. After incubation for 48 h, no nucleoprotein of influenza virus was detected in fluid from embryonated eggs that had been treated with N<sub>2</sub> gas plasma for 5 min. It has been concluded that influenza virus was inactivated within 5 min of N<sub>2</sub> gas plasma treatment.

**Bacteriophages:** Antimicrobial activity of the PlasmaSol nonthermal plasma sterilizer apparatus (PlasmaSol Corporation, Hoboken, NJ, USA) against temperate  $\lambda$  bacteriophage C-17 (ATCC 23724-B1) and lytic bacteriophage (Rambo; Microphage) was examined by Venezia et al<sup>43</sup>. Exposure of the both phages at concentrations of  $10^6$  PFU/ml<sup>-1</sup> had resulted in at least 4–6  $\log_{10}$  reduction in viability following 10 min of exposure. The early stage inactivation of bacteriophage lambda ( $\lambda$  phage) in the presence of atmospheric pressure cold plasma was demonstrated by Yasuda et al<sup>48</sup>. In this study, a DBD device which generates typical atmospheric cold plasma was employed to treat the PET film containing  $\lambda$  phage particles, under neutral pH and near the room temperature. After 20 s discharge treatment, the number of infectious phages decreased quickly and 6-orders of magnitude inactivation was achieved. The time required for one  $\log_{10}$  reduction of phages ( $D$  value) was about 3 s<sup>48</sup>.

In another study, the inactivation effect of atmospheric-pressure cold plasma (APCP) against MS2 bacteriophages was examined. Airborne MS2 bacteriophages were exposed to APCP produced using the power levels of 20, 24 and 28 W and gas carriers [ambient air, Ar-O<sub>2</sub> (2%, vol/vol) and He-O<sub>2</sub> (2%, vol/vol)] for subsecond time intervals. The APCP treatment, wherein ambient air was used as the gas carrier at 28 W for 0.12 s, inactivated more than 95% (1.3-log reduction) of the viruses in the air<sup>46</sup>. However, about the same level of inactivation was achieved for waterborne MS2 viruses with an exposure time of less than 1 min when

they were directly subjected to the APCP treatment for up to 3 min.

### Conclusion

All these studies clearly indicate the virucidal effect of NTPs. Researchers so far have focused on preliminary studies of inactivation of viruses using NTPs by randomly choosing clinically-important viruses. However, more systematic studies are needed to evaluate the relative susceptibility of the different groups of viruses to NTPs. The inactivation studies indicate that the degree of inactivation of a particular virus is completely dependent on the type of plasma being used, length of plasma exposure and other experimental conditions. Also, mechanism of inactivation of the same virus with two different NTPs seems to vary with the composition of plasma reactive species. As the number of studies is limited regarding the inactivation of viruses using NTPs, more studies are warranted. Future studies need to give more emphasis to proof-of-mechanism for NTPs-induced inactivation.

### References

1. Aboubakr H.A., Williams P., Gangal U., Youssef M.M., El-Sohaimy S.A.A., Bruggeman P.J. and Goyal S.M., Virucidal effect of cold atmospheric gaseous plasma on feline calicivirus, a surrogate for human norovirus, *Appl. Environ. Microbiol.*, **81**, 3612–3622 (2015)
2. Ahlfeld B., Li Y., Boulaaba A., Binder A., Schotte U., Zimmermann J.L., Morfill G. and Klein G., Inactivation of a foodborne norovirus outbreak strain with nonthermal atmospheric pressure plasma, *MBio*, **6**, e02300–14 (2015)
3. Alekseev O., Donovan K., Limonnik V. and Azizkhan-Clifford J., Nonthermal dielectric barrier discharge (DBD) plasma suppresses herpes simplex virus type 1 (HSV-1) replication in corneal epithelium, *Trans. Vis. Sci. Tech.*, **3(2)**, 2 (2014)
4. Alexander D., Newcastle disease and other avian paramyxoviruses, *Revue. Sci. Tech.*, **19**, 443–462 (2000)
5. Alshraideh N.H., Alkawarek M.Y., Gorman S.P., Graham W.G. and Gilmore B.F., Atmospheric pressure, nonthermal plasma inactivation of MS2 bacteriophage: effect of oxygen concentration on virucidal activity, *J. Appl. Microbiol.*, **115**, 1420-1426 (2013)
6. Bae S.C., Park S.Y., Choe W. and Ha S.D., Inactivation of murine norovirus-1 and hepatitis A virus on fresh meats by atmospheric pressure plasma jets, *Food Res. Int.*, **76**, 342–347 (2015)
7. Baert L., Debevere J. and Uyttendaele M., The efficacy of preservation methods to inactivate foodborne viruses, *Int. J. Food Microbiol.*, **131**, 83–94 (2009)
8. Baxter C.S., Hofmann R., Templeton M.R., Brown M. and Andrews R.C., Inactivation of adenovirus types 2, 5 and 41 in drinking water by UV light, free chlorine and monochloramine, *J. Environ. Eng.*, **133**, 95–103 (2007)

9. Bond W.W., Favero M.S., Petersen N.J., Gravelle C.R., Ebert J.W. and Maynard J.E., Survival of hepatitis B virus after drying and storage for one week, *Lancet*, **1**, 550-1 (1981)
10. Boudam M.K., Moisan M., Saoudi B., Popovici C., Gherardi N. and Massines F., Bacterial spore inactivation by atmospheric-pressure plasmas in the presence or absence of UV photons as obtained with the same gas mixture, *J. Phys. D: Appl. Phys.*, **39**, 3494-3507 (2006)
11. Cáceres V.M., Kim D.K., Bresee J.S., Horan J., Noel J.S., Ando T., Steed C.J., Weems J.J., Monroe S.S. and Gibson J.J., A viral gastroenteritis outbreak associated with person-to-person spread among hospital staff, *Infect. Cont. Hosp. Ep.*, **19**, 162-167 (1998)
12. Chau T.T., Kao K.C., Blank G. and Madrid F., Microwave plasmas for low temperature dry sterilization, *Biomaterials*, **17**, 1273-1277 (1996)
13. Chun H., Kim J., Chung K., Won M. and Song K.B., *Listeria monocytogenes*, *Salmonella enterica* serovar Typhimurium and *Campylobacter jejuni* in ready-to-eat sliced ham using UV-C irradiation, *Meat Sci.*, **83**, 599–603 (2009)
14. Cromeans T.L., Kahler A.M. and Hill V.R., Inactivation of adenoviruses, enteroviruses and murine norovirus in water by free chlorine and monochloramine, *Appl. Environ. Microbiol.*, **76**, 1028–1033 (2010)
15. Dobrynin D., Fridman G., Friedman G. and Fridman A., Physical and biological mechanisms of direct plasma interaction with living tissue, *New J. Phys.*, **11**, 115020 (2009)
16. Feng K., Divers E., Ma Y. and Li J., Inactivation of a human norovirus surrogate, human norovirus virus-like particles and vesicular stomatitis virus by gamma irradiation, *Appl. Environ. Microbiol.*, **77**, 3507–3517 (2011)
17. Fridman A., Plasma Chemistry, Cambridge University Press, New York (2008)
18. Hati S., Mandal S., Vij S., Minz P.S., Basu S., Khetra Y., Yadav D. and Dahiya M., Nonthermal plasma technology and its potential applications against foodborne microorganisms, *J. Food Process Pres.*, **36**, 518–524 (2012)
19. Herrmann H.W., Henins I., Park J. and Selwyn G.S., Decontamination of chemical and biological warfare, (CBW) agents using an atmospheric pressure plasma jet (APPJ), *Phys. Plasmas*, **6**, 2284-2289 (1999)
20. Hirneisen K.A., Black E.P., Casciarino J.L., Fino V.R., Hoover D.G. and Kniel K.E., Viral inactivation in foods: A review of traditional and novel food-processing technologies, *Compr. Rev. Food. Sci. F.*, **9**, 3–20 (2010)
21. Horimoto T. and Kawaoka Y., Influenza: lessons from past pandemics, warnings from current incidents, *Nat. Rev. Microbiol.*, **3**, 591–600 (2005)
22. Kelly-Wintenberg K., Montie T.C., Brickman C., Roth J.R., Carr A.K., Sorge K., Wadsworth L.C. and Tsai P.P.Y., Room temperature sterilization of surfaces and fabrics with a one

- atmosphere uniform glow discharge plasma, *J. Ind. Microbiol. Biotechnol.*, **20**, 69-74 (1998)
23. Kong M.G., Kroesen G., Morfill G., Nosenko T., Shimizu T., van Dijk J. and Zimmermann J.L., Plasma medicine: an introductory review, *New J. Phys.*, **11**, 115012 (2009)
  24. Kuzmichev A.I., Soloshenko I.A., Tsiolko V.V., Kryzhanovsky V.I., Bazhenov V.Y., Mikhno I.L. and Khomich V.A., Feature of sterilization by different type of atmospheric pressure discharges, 7<sup>th</sup> International Symposium on High Pressure Low Temperature Plasma Chemistry - Hakone VII, Greifswald (Germany), 402-406 (2001)
  25. Laibson P.R., Resistant herpes simplex keratitis, *Clin. Exp. Ophthalmol.*, **38**, 227–228 (2010)
  26. Laroussi M., Low temperature plasma-based sterilization: Overview and state-of-the-art, *Plasma Process Polym.*, **2**, 391-400 (2005)
  27. Laroussi M., Nonthermal decontamination of biological media by atmospheric pressure plasmas: Review, analysis, and prospects. *IEEE T. Plasma Sci.*, **30**, 1409-1415 (2002)
  28. Laroussi M., Sterilization of contaminated matter with an atmospheric pressure plasma, *IEEE T. Plasma Sci.*, **24**, 1188-1191 (1996)
  29. Mendis D.A., Rosenberg M. and Azam F., A note on the possible electrostatic disruption of bacteria, *IEEE T. Plasma Sci.*, **28**, 1304-1306 (2000)
  30. Moreau M., Orange N. and Feuilloley M.G.J., Non-thermal plasma technologies: New tools for bio-decontamination, *Biotechnol. Adv.*, **26**, 610–617 (2008)
  31. Morent R. and De Geyter N., Inactivation of Bacteria by Non-Thermal Plasmas, Biomedical Engineering - Frontiers and Challenges, Prof. Reza Fazel, ed., In Tech, 25-54 (2011)
  32. Piret J. and Boivin G., Resistance of herpes simplex viruses to nucleoside analogues: mechanisms, prevalence and management, *Antimicrob. Agents Ch.*, **55**, 459–472 (2011)
  33. Pirtle E.C. and Beran G.W., Virus survival in the environment, *Rev. Sci. Tech. Off. Int. Epiz.*, **10**, 733-748 (1991)
  34. Richards G.P., Enteric virus contamination of foods through industrial practices: a primer on intervention strategies, *J. Ind. Microbiol. Biotechnol.*, **27**, 117–125 (2001)
  35. Richardson J.P., Dyer F.F., Dobbs F.C., Alexeff I. and Laroussi M., On the use of the resistive barrier discharge to kill bacteria: Recent results, 27<sup>th</sup> IEEE International Conference on Plasma Science - ICOPS2000, New Orleans (USA), 109-109 (2000)
  36. Rossi F., Kylian O., Rauscher H., Hasiwa M. and Gilliland D., Low pressure plasma discharges for the sterilization and decontamination of surfaces, *New J. Phys.*, **11**, 115017 (2009)

37. Sakudo A., Misawa T., Shimizu N. and Imanishi Y., N<sub>2</sub> gas plasma inactivates influenza virus mediated by oxidative stress, *Front. Biosci.*, **6**, 69-79 (2014)
38. Sakudo A., Onodera T. and Tanaka Y., Inactivation of viruses, In Sakudo A. and Shintani H., ed., Sterilization and Disinfection by Plasma, Chapter 2.4, Nova Scientific, 49-60 (2010)
39. Shi X.M., Zhang G.J., Wu X.L., Peng Z.Y., Zhang Z.H., Shao X.J. and Chang Z.S., Effect of low-temperature plasma on deactivation of hepatitis B virus, *IEEE T. Plasma Sci.*, **40**, 2711-2716 (2012)
40. Su X., Golden D.A. and D'Souza D.H., Inactivation of Human Enteric Virus Surrogates on Stainless Steel Surfaces by Non-thermal Plasma, International Association for Food Protection, Annual Meeting, Charlotte, NC (2013)
41. Tendero C., Tixier C., Tristant P., Desmaison J. and Leprince P., Atmospheric pressure plasmas: A review, *Spectrochim. Acta B*, **61**, 2-30 (2006)
42. Terrier O., Essere B., Yver M., Barthélémy M., Bouscambert-Duchamp M., Kurtz P., VanMechelen D., Morfin F., Billaud G., Ferraris O., Lina B., Rosa-Calatrava M. and Moules V., Cold oxygen plasma technology efficiency against different airborne respiratory viruses, *J. Clin. Virol.*, **45**, 119-124 (2009)
43. Venezia R.A., Orrico M., Houston E., Yin S.M. and Naumova Y.Y., Lethal activity of nonthermal plasma sterilization against microorganisms, *Infect. Cont. Hosp. Ep.*, **29**, 430–436 (2008)
44. Wang G. et al, Non-thermal plasma for inactivated-vaccine preparation, *Vaccine*, <http://dx.doi.org/10.1016/j.vaccine.2015.10.099> (2016)
45. Wigginton K.R., Pescon B.M., Sigstam T., Bosshard F. and Kohn T., Virus inactivation mechanisms: impact of disinfectants on virus function and structural integrity, *Environ. Sci. Technol.*, **46**, 12069–12078 (2012)
46. Wu Y., Liang Y., Wei K., Li W., Yao M., Zhang J. and Grinshpun S.A., MS2 virus inactivation by atmospheric-pressure cold plasma using different gas carriers and power levels, *Appl. Environ. Microbiol.*, **81**, 996-1002 (2015)
47. Yardimci O. and Setlow P., Plasma sterilization: opportunities and microbial assessment strategies in medical device manufacturing, *IEEE T. Plasma Sci.*, **38**, 973–981 (2010)
48. Yasuda H., Miura T., Kurita H., Takashima K. and Mizuno A., Biological evaluation of DNA damage in bacteriophages inactivated by atmospheric pressure cold plasma, *Plasma Process Polym.*, **7**, 301–308 (2010)
49. Zimmermann J.L., Dumler K., Shimizu T., Morfill G.E., Wolf A., Boxhammer V., Schlegel J., Gansbacher B. and Anton M., Effects of cold atmospheric plasmas on adenoviruses in solution, *J. Phys. D: Appl. Phys.*, **44**, 505201 (2011).

(Received 29<sup>th</sup> January 2016, accepted 15<sup>th</sup> February 2016)

\*\*\*\*\*

## Journal Pre-proof

Cold plasma, a new hope in the field of virus inactivation

Arijana Filipić, Ion Gutierrez-Aguirre, Gregor Primc, Miran Mozetič, David Dobnik



PII: S0167-7799(20)30108-6

DOI: <https://doi.org/10.1016/j.tibtech.2020.04.003>

Reference: TIBTEC 1923

To appear in: *Trends in Biotechnology*

Please cite this article as: A. Filipić, I. Gutierrez-Aguirre, G. Primc, et al., Cold plasma, a new hope in the field of virus inactivation, *Trends in Biotechnology* (2020), <https://doi.org/10.1016/j.tibtech.2020.04.003>

This is a PDF file of an article that has undergone enhancements after acceptance, such as the addition of a cover page and metadata, and formatting for readability, but it is not yet the definitive version of record. This version will undergo additional copyediting, typesetting and review before it is published in its final form, but we are providing this version to give early visibility of the article. Please note that, during the production process, errors may be discovered which could affect the content, and all legal disclaimers that apply to the journal pertain.

© 2020 Published by Elsevier.

## Cold plasma, a new hope in the field of virus inactivation

Arijana Filipić<sup>1,2,\*@</sup>, Ion Gutierrez-Aguirre<sup>1</sup>, Gregor Primc<sup>3</sup>, Miran Mozetič<sup>3</sup>, David Dobnik<sup>1</sup>

<sup>1</sup>Department of Biotechnology and Systems Biology, National Institute of Biology, Večna pot 111, 1000 Ljubljana, Slovenia<sup>@</sup>

<sup>2</sup>Jožef Stefan International Postgraduate School, Jamova cesta 39, 1000 Ljubljana, Slovenia

<sup>3</sup>Department of Surface Engineering and Optoelectronics, Jožef Stefan Institute, Jamova cesta 39, 1000 Ljubljana, Slovenia<sup>@</sup>

\*Correspondence: [arijana.filipic@nib.si](mailto:arijana.filipic@nib.si) (A. Filipić)

<sup>@</sup>Twitter accounts: @ArijanaFilipic, @NIB\_FITO\_SI, @DepartmentF4

**Keywords:** Virus, virus inactivation, cold plasma, reactive oxygen and nitrogen species

**Abstract**

Viruses can infect all cell-based organisms, from bacteria to humans, animals, and plants. They are responsible for numerous cases of hospitalization, many deaths, and widespread crop destruction, which all result in an enormous medical, economical, and biological burden. Each of the currently used decontamination methods have important drawbacks. Cold plasma has entered this field as a novel, efficient, and clean solution for virus inactivation. Here, we present the recent developments in this promising field of cold-plasma-mediated virus inactivation, and describe the applications and mechanisms of the inactivation. This is a particularly relevant subject as viral pandemics, such as the COVID-19 pandemic, expose the need for alternative viral inactivation methods to replace, complement or upgrade existing ones.

**When viruses meet plasma**

Viruses are the most abundant and diverse microbes on our planet. They have inhabited the Earth for billions of years [1], so they have adapted to various environments and are now found across all ecosystems. Viruses have contributed to the evolution of life on Earth, and can be beneficial for preserving ecosystems and important natural Earth cycles, such as the carbon cycle in the sea [2]. On the other hand, pathogenic viruses cause tens to hundreds of millions of plant, animal and human infections annually, which result in high crop losses and numerous deaths (Box 1). Therefore, inactivating harmful viruses is crucial for better quality of life.

Viruses can be transmitted directly from one infected individual to another, or indirectly via contaminated intermediates, such as surfaces, objects, air, food, and water. Transmission via contaminated surfaces and aerosols has shown to be of great importance in the COVID-19 pandemic, caused by severe acute respiratory syndrome coronavirus 2 (SARS-CoV-2) [3]. Water is also becoming an increasingly important transmission route for pathogenic viruses. This has arisen from global climate change and the continued increasing water demand, combined with inefficient virus removal by traditional water treatments, and with re-use of wastewater for irrigation purposes [4,5]. Pathogenic waterborne viruses are important contributors to one of the most important global risks we are facing today, the scarcity of potable water [6]. Various inactivation methods are used to prevent viral spread in different matrices but unfortunately, the ideal method has yet to be discovered (Box 1). Thus, there is an urgent need for an environmentally friendly treatment that produces neither waste nor toxic by-products, does not use toxic chemicals, is easy and safe to work with, and is also efficient in terms of viral

inactivation. The emergence of cold plasma (CP) treatments for virus inactivation aims to provide a solution to all of these features.

Plasma is the fourth state of matter. It is a partially or fully ionized gas where the atoms and/or molecules are stripped of their outer-shell electrons (Box 2) [7]. Among its complex constituents, ultraviolet (UV) radiation and **reactive oxygen and/or nitrogen species (RONS)** (see Glossary) provide the most important antimicrobial properties [8]. UV can damage nucleic acids [9], while RONS can oxidize nucleic acids, proteins, and lipids, with different affinities that depend on the species [10]. These inherent properties of plasma, and more specifically of CP, have motivated extensive studies on the use of CP for inactivation of various pathogenic microorganisms. Here, the main target has been bacteria, with investigations across different fields, such as food production [11], medicine, and dentistry [12]. These have even extended to oncotherapy applications, where cancer cells are targeted instead of pathogenic microorganisms [13].

The scientific niche of plasma-mediated virus inactivation is a relatively young field of research (for reviews, see [14,15]), which started only about 20 years ago [16]. This is despite the decades-old knowledge that ozone that is usually synthesized from O<sub>2</sub> subjected to plasma conditions can inactivate viruses [17]. However, over the last few years, the number of publications in the CP-virus field has doubled, and the research has expanded from only defining the virucidal properties of plasma to describing its modes of inactivation.

This review offers a comprehensive overview of the latest progress and achievements in the CP-virus field. It also describes and discusses the modes of CP-mediated virus inactivation, and the reactive species responsible for it.

## **Cold plasma inactivation of viruses**

Almost every study on CP inactivation of viruses is unique, as they either use a specific plasma source (e.g. **dielectric barrier discharge [DBD]**, **plasma (micro)jet**) (Figure 1) with different characteristics (e.g. power, gas, treatment time), or they deal with the treatment of different liquid volumes (from microliters to several milliliters), matrices (e.g. water, other solutions, surfaces, cells), and viruses (surrogates of human viruses, human, animal and plant viruses). Such wide diversity makes it difficult to directly compare these studies and to define the mechanistic conclusions or any universal inactivation parameters. To simplify these complexities, we will consider here the individual types of viruses that have been subjected to CP treatments. For a complete list of the treatments published to date, please see Tables S1 and S2.

### **Human viruses**

#### *Enteric viruses*

CP treatments have been often focused on **enteric viruses**, such as norovirus, adenovirus, and hepatitis A virus. These are the leading causes of **acute gastroenteritis**, the second most common infectious disease worldwide, which is responsible for high levels of hospitalization and deaths [18]. Working with human viruses can pose serious health hazards, thus such studies require specialized laboratories and equipment. Moreover, infectivity assessments of important enteric viruses, such as norovirus, have been limited due to a lack of cultivation methods [19]. For these reasons, these viruses are often replaced by surrogate viruses.

Animal viruses such as feline calicivirus (FCV), murine norovirus (MNV), and Tulane virus (TV) have been used as surrogates for norovirus due to their similar sizes,



morphologies and genetic material. Furthermore, these surrogate viruses are easy to culture/reproduce, and are safe to work with [19]. Opinions are divided over which of these surrogate viruses best resembles the stability of norovirus, and the final choice strongly depends on the inactivation method used and the environmental properties [13–15]. In addition to animal viruses, bacteriophages (viruses that infect bacteria), can be used as surrogates for enteric viruses, and for other human pathogens (Box 3).

Enteric viruses and their surrogates have been successfully treated in aqueous solutions [20–22] and other liquid media [23], and also on the surfaces of food [24–26], stainless-steel [25,27], and glass [28,29]. Three of these studies have reported on the comparative use of both surrogates and enteric viruses [23,25,27]. It was shown that the inactivation of a chosen surrogate virus is more efficient than that of the target enteric virus [23,27], suggesting that the effects of CP on such surrogates might not always mirror their effects on the enteric virus counterparts, and should thus be interpreted with caution.

Norovirus is one of the most, if not the most, problematic enteric virus. Its inactivation in comparison to FCV as its surrogate has been investigated using CP for diluted stool samples on a stainless-steel surface and lettuce leaves. As no infectivity assays are available to date for norovirus, the inactivation was determined using **ethidium-monoazide-coupled reverse-transcriptase quantitative real-time PCR (EMA-RT-qPCR)** [25]. A decrease of ~2.6 log units of gene copies was observed after 5 min treatment with DBD on both of these surfaces. Here, the inactivation of the surrogate FCV measured by EMA-RT-qPCR in the same medium on the stainless-steel surface was similar to that of norovirus, although the cell-culture-based infectivity assays showed complete FCV inactivation after 3 min (also

confirmed in [20]). The underestimation of FCV inactivation based on EMA-RT-qPCR in comparison with the infectivity assay might also indicate underestimation of norovirus inactivation. Since FCV and norovirus were similarly affected by the CP treatment, FCV can be considered as an appropriate surrogate. However, it still needs to be determined if this would also apply when using different treatment conditions.

FCV was inactivated by DBD plasma torch also on a glass surface [28], indicating that both this device, and the previously mentioned DBD, have a good potential to inactivate enteric viruses on the objects of various surfaces. On the other hand, the inactivation of adenovirus on a glass surface with a pulsed high-voltage source that sustains plasma at 0.5 bar was not as successful and would thus not be as suitable as DBDs for this purpose [29].

One of the most successful inactivation in liquid medium, including the work on bacteriophages (Box 3), was achieved by 15 s treatment of FCV using plasma jet [21,22]. This extremely short treatment time indicates that such plasma jet could be an important tool for enteric virus inactivation in liquids, however based on its present configuration, it would be limited to treatment of smaller objects contaminated with potentially infected droplets.

Different CP sources were also applied on the surfaces of various foods, such as blueberries [24], lettuce [25,26], and meat [30], where viruses were successfully inactivated without altering the appearance of the treated food. It was also shown that DBD could be used to treat packaged food [26], however, inactivation was not as good as in case of non-packaged food and therefore this process would require further improvements before its implementation. Application of CP in food industry

for decontamination has multiple advantages over the most widely used thermal processing of food, as it can sustain freshness and quality of food with minimal impact on the environment due to shorter treatment times and energy requirements [11]. One must be careful when using CP for treating sensitive material such as food, as despite CP is in general at room temperature at the point of application, the temperatures can rise in some cases due to the specific CP generation conditions. To prevent thermal damage during treatments of sensitive materials, the CP discharge needs to be placed far enough from the treated material [24] and/or have additional cooling provided. Another option is to use indirect treatments with plasma-activated liquids.

#### *Respiratory viruses*

Treatments of the respiratory viruses influenza A and B (for review, see [14]) and respiratory syncytial virus (RSV) [31] have only been performed with the already mentioned pulsed high-voltage CP source. RSV is the most frequent causative agent of lower respiratory tract infections in infants, and it is one of the most important viruses in pediatric medicine, particularly as it spreads easily through contact with contaminated surfaces [32]. Even though CP treatment completely inactivated RSV on a glass surface after 5 min [31], a simpler and more portable plasma configuration would be needed for efficient decontamination of hospital surfaces, while the previously described one would be practical only for decontamination of tools and smaller objects. Some respiratory viruses can also remain stable as aerosols for longer periods of time, such as SARS-CoV-2, and in order to stop their spread, it is crucial to treat the air, not just surfaces (see section Animal viruses and Box 3).

#### *Sexually transmitted viruses*

Human immunodeficiency virus (HIV) is one of the most important sexually transmitted pathogens, and one of the greatest challenges to public health in general (<https://www.who.int/news-room/facts-in-pictures/detail/hiv-aids>). Three shots for a total of 45 s with a plasma jet were applied to macrophages prior to their infection with HIV [33]. Upon infection, this treatment reduced the viral reverse-transcriptase activity by over two-thirds, and it impaired the other steps required for successful virus infection, without any cytotoxic effects on the macrophages. In contrast, another study reported the increasing cytotoxicity of the treated cells with the decrease of virus concentration [34].

Despite these promising results, there are some limitations for deploying such strategy in real-life scenarios, including the extraction of macrophages from the sick individual in order to treat them by CP, and their delivery back into the body. Such issues will need to be solved before CP is to be considered as an alternative HIV treatment option in the future.

#### *Animal viruses*

Three important animal pathogens have been treated by CP: avian influenza virus (AIV), Newcastle disease virus (NDV), and porcine reproductive and respiratory syndrome virus (PRRSv). All three viruses pose a significant threat to global food security and economic stability. Some strains of AIV viruses can cause up to 100% mortality in chickens (<https://www.cdc.gov/flu/avianflu/influenza-a-virus-subtypes.htm>), and some strains of NDV can cause up to 100% mortality in different avian species [35]. This is why prevention of their spread by vaccination is essential. Vaccines for both viruses would benefit from the improvements that would allow them to be more cost-effective, provide higher immune protection and decrease the

risks of disease development, by ensuring complete viral inactivation without affecting the antigens responsible for inducing the immune response [36,37]. For this purpose, CP was used as a possible inactivation step in vaccine preparation [35]. Complete inactivation was achieved after a 2-min treatment with a plasma jet. This was shown to be a perfect time for vaccine preparation, as longer treatment times can alter the antigen determinants responsible for immunogenicity. Both vaccines have been used to successfully induce the production of specific antibodies, and the NDV vaccine induced even higher antibody titers compared to the traditionally inactivated vaccines. Additional prevention method to stop the spread of these viruses would be decontamination of surfaces and tools that are in contact with potentially infected poultry by using CP-activated disinfection solutions. It has been shown that at specific ratios, CP-activated distilled water, 0.9% NaCl and 0.3% H<sub>2</sub>O<sub>2</sub> completely inactivated viruses, and the chicken embryos attained 100% survival [38].

PRRSv is economically one of the most important pathogens in the pork industry that can be transmitted as aerosols and stay infective after travelling long distances, making it a potential threat even to distant barns [39,40]. Most commonly used methods for air treatment in general rely on either physically limiting virus transmission (such as various filters) or on lowering virus infectivity (such as UV-radiation). CP could potentially achieve both goals, stopping the viral spread and abolishing virus infectivity, by charge-driven filtration and RONS, respectively [39–41]. Aerosolized PRRSv has been treated in two studies by different DBDs [39,40]. Promising results with complete virus inactivation (~3.5 log reduction), were achieved by one DBD system [39], while the other system was only partially successful [40] and authors have suggested potential improvements that would increase inactivation efficiency. Based on these and the results on bacteriophages

(Box 3), we can conclude that CP has great potential to be used for direct air disinfection, which could also be utilized in the fight against COVID-19-like outbreaks. Nevertheless, issues such as the high ozone production (Box 3) will have to be addressed and solved before such treatment becomes a part of a regular practice.

#### *Plant viruses*

Plant viruses were the first viruses to be discovered [42]. Although most virus-to-plant transmission occurs via insects [42], the increasing re-use of untreated wastewater and the use of closed irrigation systems as an answer to water scarcity are promoting viral spread. Plant viruses can result in tremendous economic losses that have been estimated at approximately 30 billion US dollars annually [43]. Despite this, there are only two reports on their deactivation by CP treatments. Inactivation of the most important potato viral pathogen, potato virus Y (PVY), in water samples was achieved using plasma jet [7]. This water-transmissible virus [44] was successfully inactivated in polluted and clean water with treatments of only 5-min and 1-min, respectively. Other economically relevant plant viruses that are highly stable, resistant to classic inactivation methods, and water-transmissible are the members of the genus *Tobamovirus*, such as tobacco mosaic virus (TMV). Despite the inherent stability of TMV, a 10-min treatment by DBD was shown to be enough to inactivate it [45].

Since enormous quantities of water are being used for irrigation (up to 70% of global water usage), closed irrigation systems or reuse of wastewater are being increasingly utilized, enabling the spread of plant pathogens and high crop losses. Based on the results on efficient inactivation of important resilient plant viral

pathogens by CP, we believe that the use of plasma as a decontamination tool in agriculture has a high potential and deserves additional attention, especially in the upcoming global warming scenario.

### **Proposed mechanisms of inactivation**

An understanding of the underlying mechanisms of virus inactivation by CP is crucial to be able to fine-tune CP treatments before their deployment in industrial, medical, and agricultural environments, and to more easily predict all possible outcomes, which include potential formation of undesired by-products that do not contribute to the inactivation.

#### *Reactive species responsible for inactivation*

The main consensus between the diverse studies to date is that the formation of ROS and/or RNS is the main feature of CP that contributes to viral inactivation, while UV radiation and temperature changes remain as minor contributors or have no effect at all. Different methods have been used to measure and identify the RONS (Table 1), which is a challenging task due to their short life span.

Singlet O<sub>2</sub> (<sup>1</sup>O<sub>2</sub>) was shown to be the most important ROS for inactivation of FCV [21,22,28] and phage T4 [46]. <sup>1</sup>O<sub>2</sub> causes oxidative modification of histidine residues and a shift in molecular mass of methionine residues [21]. It also reacts with cysteine, tyrosine, and tryptophan, and oxidizes guanine [46]. Ozone (O<sub>3</sub>) has been used as the main [20] or an additional inactivation factor [21,22] in FCV treatment, and it was proposed to also have roles in the inactivation of MS2 [41] and adenovirus [47]. Hydrogen peroxide (H<sub>2</sub>O<sub>2</sub>) has been suggested to be crucial for inactivation of RSV [31] and influenza A virus [48], but to have a secondary role in inactivation of FCV [22], PVY [7], and adenovirus [29]. RNS have been proposed as the principal

inactivation factors only in studies with FCV, where the main RNS species were ONOOH (in an acidic environment) [22,28], ONOO<sup>-</sup> [28], or NO<sub>x</sub> [20]. Other groups have measured increases in different RONS during CP treatments [7,33,35,45,49] (Table 1), but these studies did not expand their research to determine the precise involvement of each of the RONS in virus inactivation.

In summary, RONS are the main contributors to CP-mediated virus inactivation; however, the particular reactive species that have the essential roles vary and are highly dependent on the experimental conditions, such as the gas used for the CP generation, the matrix, the virus treated and the method used for RONS determination. Increased availability and development of more accurate methods for measurement of RONS and UV intensity will enable determination of the exact CP properties that are crucial for viral inactivation. In addition to determination of the CP properties that contribute the most to viral inactivation, for a better mechanistic understanding of the inactivation process, it is also important to explore which virus component is disrupted.

#### *Modes of virus inactivation*

The viral capsid, or envelope, is the first contact point with the host, and for efficient recognition of a virus by the cell receptors, it is important that their outer structure is more or less intact. Once in the cells, the viral genome takes over the process of replication. Therefore, these two components are the most important ones for the evaluation of virus inactivation (Table 1).

Capsid protein damage and nucleic acid degradation were reported for bacteriophages T4 [46], MS2 [49] and λ [50], as well as NDV [38] and FCV [21]. In the case of the enveloped virus influenza A, in addition to capsid and nucleic acid

damage, changes in lipid components from the envelope have been reported [48]. Only in the case of bacteriophage  $\lambda$  [50] and FCV [21] has it been shown that the main mode of inactivation was degradation of the capsid proteins, which preceded the degradation of nucleic acids. In other studies, it was not possible to determine which degradation path contributed more to the decay in viral infectivity. The beforementioned detailed study of FCV [21] identified primary targets of the CP oxidation, which included specific amino acids in different regions of the capsid protein, and specific functional peptide residues in the capsid protein region that were responsible for virus attachment and entry into the host cell. CP treatments resulted in nucleic acid degradation for FCV [28] and PVY [7], for which protein degradation was not measured, and for adenovirus [29], RSV [31], and TMV [45], where nucleic-acid degradation was indicated as the only mode of inactivation (the viral proteins or their subunits stayed intact).

It is evident that the high oxidative power of CP derivatives can disrupt virus integrity at both the structural and genomic levels by affecting both proteins and nucleic acids. Minor disruption or conformational changes of the capsid proteins (or the lipid envelope when present) caused by RONS can result in loss of viral infectivity, due to disruption of the virus binding to the receptors on the host-cell surface. In cases where the genomic nucleic acids are damaged, viruses will no longer be infective, as an intact genetic material is needed for virus genome translation and replication.

Even in cases where the damage was shown to be inflicted only to nucleic acids, it is likely that the RONS had also damaged or disrupted the outer protein layer to a certain extent, as otherwise it would not be possible for the RONS to penetrate the virus and reach the genetic material.

One of the challenges for the study of the modes of viral inactivation is the selection of the appropriate method. Methods used for determination of protein degradation are either not as sensitive as the molecular methods used to determine nucleic acid degradation, or they target only specific protein subunits, and hence can sometimes overlook other changes to the proteins. Future studies using combinations of the state-of-the-art methods to assess both types of damage will help with more accurate interpretation of how the damage occurs. These include cryo-electron microscopy, mass spectrometry, and long-read sequencing, along with methods based on nucleic acid amplification, like quantitative PCR and digital PCR.

### Concluding Remarks

Diverse CP sources can completely inactivate or significantly reduce the infectivity of numerous human, animal and plant pathogenic viruses on or in various matrices (Figure 2, Key Figure). However, as indicated from various studies (Table S1), virus inactivation is highly dependent on the treatment properties, so the optimal parameters need to be chosen on a case-by-case basis.

Based on the recent developments in the CP-virus field described here, we anticipate that CP will be one of the most effective and environmentally friendly tools for inactivation of different viruses in the near future. Ultimately, its use should lead to reduced human, animal and plant infections, and along with this, lower economic and biological burdens. We believe that one of the fields of virus inactivation where plasma can represent a more significant breakthrough is water decontamination. It could inactivate problematic enteric viruses and resilient plant viruses for either human consumption and/or for agricultural purposes. In any case, it will first be necessary to evaluate the potential adverse genotoxic and cytotoxic effects of

plasma-activated water on humans and plants. Additionally, a field of CP application that may gain relevance as a response to viral outbreaks (like SARS-CoV-2), would in our opinion be CP-mediated air purification and incorporation of CP in protective masks and respirators (Box 3), which could help to palliate the sanitary burden caused by any future outbreaks. There is also potential in decontaminating small-surface objects, such as tools and food. Even with the promising initial results, using CP in medicinal treatments or vaccine preparation would still require significant research before their actual implementation.

Despite the high efficiency of virus inactivation, the exact modes of action and the plasma functionality in scaled-up systems remain largely unexplored (see Outstanding Questions), and further research needs to be focused in this direction. This insufficient knowledge of plasma/virus interaction presents the biggest obstacle in the expansion of this field. To understand this interaction, it is important to know the flux of reactive species (RONS or radiation) on the surface of the virus, the probability for the reaction of a particular type of reactive species with the virus, and any synergetic effects between different reactive species for viral deactivation. None of these parameters are currently understood completely. Another issue to be dealt with is how to scale up CP reactors without altering the composition and amount of reactive species achieved at small scale. This could be overcome by a scale-out approach, where several small-scale reactors could be used in parallel, increasing the amount of treated material but maintaining the desired plasma composition. Such an approach would also abolish the need for specialized equipment for characterizing plasma chemistry in scaled-up systems, as they would be the same as the ones already characterized at laboratory scale.

In view of environment protection, novel environmentally friendly decontamination methods are needed. We think that CP should replace current chemical decontamination practices, as it does not produce excessive waste and can efficiently inactivate viruses in or on different media and surfaces. CP usage will likely spread in different directions to help coping with upcoming global challenges, such as the scarcity of clean water and the detrimental effects of future viral epidemics or pandemics like COVID-19. CP in combination with other existing technologies could help to improve virus inactivation through synergistic effects, thus providing an ultimate decontamination tool.

## Acknowledgements

This work was financially supported by the Slovenian Research Agency (research core funding No P4 – 0407, project No. L4-9325 and program for young researchers in the accordance with »agreement on (co) financing research activity in 2019« No. 1000-18-0105), Ministry of Agriculture, Forestry and Food and wastewater treatment plant JP Centralna Čistilna Naprava Domžale-Kamnik d.o.o. We want to thank Assoc. Prof. Dr. Jana Žel for her valuable input on the manuscript.

## References

- 1 Nasir, A. and Caetano-Anollés, G. (2015) A phylogenomic data-driven exploration of viral origins and evolution. *Sci. Adv.* 1, e1500527
- 2 Wilhelm, S.W. and Suttle, C.A. (1999) Viruses and nutrient cycles in the sea aquatic food webs. *Bioscience* 49, 781–788
- 3 van Doremalen, N. *et al.* (2020) Aerosol and Surface Stability of SARS-CoV-2 as Compared with SARS-CoV-1. *N. Engl. J. Med.* DOI:10.1056/NEJMc2004973
- 4 Shrestha, S. *et al.* (2018) Virological quality of irrigation water sources and pepper mild mottle virus and tobacco mosaic virus as index of pathogenic virus contamination level. *Food Environ. Virol.* 10, 107–120
- 5 Mehle, N. and Ravnkar, M. (2012) Plant viruses in aqueous environment - Survival, water mediated transmission and detection. *Water Res.* 46, 4902–4917
- 6 World Economic Forum. (2020). *The Global Risks Report 2020 15th Edition. Insight Report.* Geneva.
- 7 Filipić, A. *et al.* (2019) Cold atmospheric plasma as a novel method for inactivation of potato virus Y in water samples. *Food Environ. Virol.* 11, 220–228
- 8 Guo, J. *et al.* (2015) Bactericidal effect of various non-thermal plasma agents and the influence of experimental conditions in microbial inactivation: A review. *Food Control* 50, 482–490
- 9 USEPA. (2006). *Ultraviolet disinfection guidance manual for the final long term 2 enhanced surface water treatment rule.* Washington, DC.
- 10 Mittler, R. (2017) ROS Are Good. *Trends Plant Sci.* 22, 11–19
- 11 Bourke, P. *et al.* (2018) The potential of cold plasma for safe and sustainable food production. *Trends Biotechnol.* 36, 615–626
- 12 Sakudo, A. *et al.* (2019) Disinfection and sterilization using plasma technology: fundamentals and future perspectives for biological applications. *Int. J. Mol. Sci.* 20, 5216
- 13 Dai, X. *et al.* (2018) The emerging role of gas plasma in oncotherapy. *Trends Biotechnol.* 36, 1183–1198

- 14 Puligundla, P. and Mok, C. (2016) Non-thermal plasmas (NTPs) for inactivation of viruses in abiotic environment. *Res. J. Biotechnol.* 11, 91–96
- 15 Weiss, M. *et al.* (2017) Virucide properties of cold atmospheric plasma for future clinical applications. *J. Med. Virol.* 89, 952–959
- 16 Kelly-Wintenberg, K. *et al.* (1999) Use of a one atmosphere uniform glow discharge plasma to kill a broad spectrum of microorganisms. *J. Vac. Sci. Technol. A* 17, 1539–1544
- 17 Burleson, G.R. *et al.* (1975) Inactivation of viruses and bacteria by ozone, with and without sonication. *Appl. Microbiol.* 29, 340–4
- 18 McMinn, B.R. *et al.* (2017) Bacteriophages as indicators of faecal pollution and enteric virus removal. *Lett. Appl. Microbiol.* 65, 11–26
- 19 Cromeans, T. *et al.* (2014) Comprehensive comparison of cultivable norovirus surrogates in response to different inactivation and disinfection treatments. *Appl. Environ. Microbiol.* 80, 5743–5751
- 20 Nayak, G. *et al.* (2018) Reactive species responsible for the inactivation of feline calicivirus by a two-dimensional array of integrated coaxial microhollow dielectric barrier discharges in air. *Plasma Process. Polym.* 15, 1–12
- 21 Aboubakr, H.A. *et al.* (2018) Cold argon-oxygen plasma species oxidize and disintegrate capsid protein of feline calicivirus. *PLoS One* 13, e0194618
- 22 Aboubakr, H.A. *et al.* (2016) Inactivation of virus in solution by cold atmospheric pressure plasma: identification of chemical inactivation pathways. *J. Phys. D: Appl. Phys.* 49, 1–17
- 23 Takamatsu, T. *et al.* (2015) Microbial inactivation in the liquid phase induced by multigas plasma jet. *PLoS One* 10, e0132381
- 24 Lacombe, A. *et al.* (2017) Nonthermal inactivation of norovirus surrogates on blueberries using atmospheric cold plasma. *Food Microbiol.* 63, 1–5
- 25 Aboubakr, H.A. *et al.* (2020) In situ inactivation of human norovirus GII.4 by cold plasma: Ethidium monoazide (EMA)-coupled RT-qPCR underestimates virus reduction and fecal material suppresses inactivation. *Food Microbiol.* 85, 103307
- 26 Min, S.C. *et al.* (2016) Dielectric barrier discharge atmospheric cold plasma inhibits *Escherichia coli* O157:H7, *Salmonella*, *Listeria monocytogenes*, and *Tulane virus* in Romaine lettuce. *Int. J. Food Microbiol.* 237, 114–120

- 27 Park, S.Y. and Ha, S. Do (2018) Assessment of cold oxygen plasma technology for the inactivation of major foodborne viruses on stainless steel. *J. Food Eng.* 223, 42–45
- 28 Yamashiro, R. *et al.* (2018) Key role of singlet oxygen and peroxyxynitrite in viral RNA damage during virucidal effect of plasma torch on feline calicivirus. *Sci. Rep.* 8, 17947
- 29 Sakudo, A. *et al.* (2016) Nitrogen gas plasma generated by a static induction thyristor as a pulsed power supply inactivates adenovirus. *PLoS One* 11, e0157922
- 30 Bae, S.C. *et al.* (2015) Inactivation of murine norovirus-1 and hepatitis A virus on fresh meats by atmospheric pressure plasma jets. *Food Res. Int.* 76, 342–347
- 31 Sakudo, A. *et al.* (2017) Crucial roles of reactive chemical species in modification of respiratory syncytial virus by nitrogen gas plasma. *Mater. Sci. Eng. C* 74, 131–136
- 32 Toivonen, L. *et al.* (2019) Respiratory syncytial virus infections in children 0–24 months of age in the community. *J. Infect* 80, 69–75
- 33 Volotskova, O. *et al.* (2016) Cold atmospheric plasma inhibits HIV-1 replication in macrophages by targeting both the virus and the cells. *PLoS One* 11, e0165322
- 34 Amiran, M.R. *et al.* (2016) In vitro assessment of antiviral activity of cold atmospheric pressure plasma jet against the human immunodeficiency virus (HIV). *J Med Microbiol Infec Dis* 4, 62–67
- 35 Wang, G. *et al.* (2016) Non-thermal plasma for inactivated-vaccine preparation. *Vaccine* 34, 1126–1132
- 36 Dimitrov, K.M. *et al.* (2017) Newcastle disease vaccines—A solved problem or a continuous challenge? *Vet. Microbiol.* 206, 126–136
- 37 Jang, H. *et al.* (2018) Efficacy and synergy of live-attenuated and inactivated influenza vaccines in young chickens. *PLoS One* 13, e0195285
- 38 Su, X. *et al.* (2018) Inactivation efficacy of nonthermal plasma-activated solutions against Newcastle disease virus. *Appl. Environ. Microbiol.* 84, e02836-17



- 39 Nayak, G. *et al.* (2020) Rapid inactivation of airborne porcine reproductive and respiratory syndrome virus using an atmospheric pressure air plasma. *Plasma Process. Polym.* DOI: 10.1002/ppap.201900269
- 40 Xia, T. *et al.* (2020) Inactivation of airborne porcine reproductive and respiratory syndrome virus (PRRSv) by a packed bed dielectric barrier discharge non-thermal plasma. *J. Hazard. Mater.* 393, 122266
- 41 Xia, T. *et al.* (2019) Inactivation of airborne viruses using a packed bed non-thermal plasma reactor. *J. Phys. D. Appl. Phys.* 52, 255201
- 42 Lefeuvre, P. *et al.* (2019) Evolution and ecology of plant viruses. *Nat. Rev. Microbiol.* 17, 632-644
- 43 Nicaise, V. (2014) Crop immunity against viruses: Outcomes and future challenges. *Front. Plant Sci.* 5, 1–18
- 44 Mehle, N. *et al.* (2014) Survival and transmission of potato virus Y, pepino mosaic virus, and potato spindle tuber viroid in water. *Appl. Environ. Microbiol.* 80, 1455–1462
- 45 Hanbal, S.E. *et al.* (2018) Atmospheric - pressure plasma irradiation can disrupt tobacco mosaic virus particles and RNAs to inactivate their infectivity. *Arch. Virol.* 163, 2835–2840
- 46 Guo, L. *et al.* (2018) Mechanism of virus inactivation by cold atmospheric-pressure plasma and plasma-activated water. *Appl. Environ. Microbiol.* 84, 1–10
- 47 Zimmermann, J.L. *et al.* (2011) Effects of cold atmospheric plasmas on adenoviruses in solution. *J. Phys. D. Appl. Phys.* 44, 505201
- 48 Sakudo, A. *et al.* (2014) N<sub>2</sub> gas plasma inactivates influenza virus mediated by oxidative stress. *Front. Biosci.* 6, 69–79
- 49 Wu, Y. *et al.* (2015) MS2 virus inactivation by atmospheric-pressure cold plasma using different gas carriers and power levels. *Appl. Environ. Microbiol.* 81, 996–1002
- 50 Yasuda, H. *et al.* (2010) Biological evaluation of DNA damage in bacteriophages inactivated by atmospheric pressure cold plasma. *Plasma Process. Polym.* 7, 301–308
- 51 Koonin, E. V. and Starokadomskyy, P. (2016) Are viruses alive? The replicator paradigm sheds decisive light on an old but misguided question.

- Stud. Hist. Philos. Sci. Part C Stud. Hist. Philos. Biol. Biomed. Sci.* 59, 125–134
- 52 Roossinck, M.J. and Baz, E.R. (2017) Symbiosis: Viruses as Intimate Partners. *Annu. Rev. Virol.* 4, 123-139
- 53 Milone, M.C. and O'Doherty, U. (2018) Clinical use of lentiviral vectors. *Leukemia* 32, 1529–1541
- 54 Wang, D. *et al.* (2019) Adeno-associated virus vector as a platform for gene therapy delivery. *Nat. Rev. Drug Discov.* 18, 358–378
- 55 Mehle, N. *et al.* (2018) Water-Mediated Transmission of Plant, Animal, and Human Viruses. In *Advances in virus research* (Malmstrom, C. M., ed), pp. 85–128, Academic Press
- 56 Staggemeier, R. *et al.* (2015) Animal and human enteric viruses in water and sediment samples from dairy farms. *Agric. Water Manag.* 152, 135–141
- 57 Zhang, T. *et al.* (2006) RNA viral community in human feces: Prevalence of plant pathogenic viruses. *PLoS Biol.* 4, 0108–0118
- 58 Lyon, B.A. *et al.* (2014) Integrated chemical and toxicological investigation of UV-chlorine/ chloramine drinking water treatment. *Environ. Sci. Technol.* 48, 6743–6753
- 59 Machala, Z. and Pavlovich, M.J. (2018) A New Phase in Applied Biology. *Trends Biotechnol.* 36, 577–578
- 60 Mozetič, M. *et al.* (2019) Introduction to Plasma and Plasma Diagnostics. In *Non-thermal plasma technology for polymeric materials: applications in composites, nanostructured materials and biomedical fields* (Thomas, S., Mozetic M., Cvelbar U., Spatenka P., Praveen K.M., eds), pp. 23-65, Elsevier
- 61 Ehlbeck, J. *et al.* (2011) Low temperature atmospheric pressure plasma sources for microbial decontamination. *J. Phys. D. Appl. Phys.* 44, 013002
- 62 Bruggeman, P.J. *et al.* (2016) Plasma–liquid interactions: a review and roadmap. *Plasma Sources Sci. Technol.* 25, 053002
- 63 Labay, C. *et al.* (2019) Production of reactive species in alginate hydrogels for cold atmospheric plasma-based therapies. *Sci. Rep.* 9, 1–12
- 64 McMinn, B.R. *et al.* (2017) Bacteriophages as indicators of faecal pollution and enteric virus removal. *Lett. Appl. Microbiol.* 65, 11–26
- 65 Machala, Z. *et al.* (2019) Chemical and antibacterial effects of plasma activated water: correlation with gaseous and aqueous reactive oxygen and

nitrogen species, plasma sources and air flow conditions. *J. Phys. D. Appl. Phys.* 52, 034002

- 66 Alekseev, O. *et al.* (2014) Nonthermal dielectric barrier discharge (DBD) plasma suppresses herpes simplex virus type 1 (HSV-1) replication in corneal epithelium. *Transl. Vis. Sci. Technol.* 3, 2
- 67 Jakober, C. and Phillips, T (California Environmental Protection Agency, Air Resources Board). (2008) *Evaluation of ozone emissions from portable indoor air cleaners: electrostatic precipitators and ionizers*. Sacramento, CA

## Figure legends

**Figure 1: Examples of the most used plasma sources for virus inactivation in different matrices.** These include some different types of (micro)jets **(a)** and dielectric barrier discharges **(b)**, and various matrices that have been inoculated with viruses and treated using cold plasma **(c)**: left to right: meat, blueberries, lettuce, glass, stainless steel, water, buffer or other liquid medium, air, cells).

## Figure 2, Key Figure: Inactivation of viruses using cold plasma. (a)

Morphologically different viruses under treatment with cold plasma. **(b)** Close-up of the cold-plasma properties that are responsible for viral inactivation. The most essential particles in virus inactivation are reactive oxygen and/or nitrogen species (RONS), although UV radiation and charged particles (e.g. ions, electrons) can also have some role. Molecules in the ground state are neutral and do not have any effects on virus inactivation. Cold plasma can target both the viral proteins and their nucleic acids (or even the virus envelope, when present). **(c)** After the cold-plasma treatment, the virus particles and nucleic acids are partially or completely degraded to non-infective particles that cannot cause any harm to their hosts.

**Table 1.** Mechanisms of viral inactivation by plasma.

Virus	Reactive oxygen and/or nitrogen species involved in	Mode of virus inactivation		Methods for identification of virus inactivation		Methods used for cold-plasma characterization <sup>b</sup>	References
		Protein	DNA/RN A	Protein	DNA/RN A		

	inactivation <sup>a</sup>	degr	A	ion	degradat		
		adat	degr		ion		
		ion	adat				
			ion				
<b>Bacteriophage</b>							
λ	NA	Yes	Yes	SDS- PAGE alone, or in combinati on with <i>in-vitro</i> packagin g	Agarose gel electroph oresis alone, or in combinat ion with <i>in-vitro</i> packagin g	Optical emission spectroscopy	[ 5 0 ] ]
MS2 <sup>c</sup>	↑O	Yes	Yes	SDS- PAGE gel electroph oresis	RT-PCR, agarose gel electroph oresis	Optical emission spectroscopy	[ 4 9 ] ]
MS2	O <sub>3</sub> <sup>f</sup>	NA	No	Not measure d	RT- qPCR	Ozone sensor	[ 4 1 ] ]
T4	<sup>1</sup> O <sub>2</sub> <sup>g</sup>	Yes	Yes	SDS- PAGE	Agarose gel	H <sub>2</sub> O <sub>2</sub> /peroxidase assay kit,	[ 4 ]

						electroph oresis	nitrite/nitrate colorimetric assay kit, electron spin resonance	6 ] ]
<b>Animal surrogate of enteric virus</b>								
FCV <sup>d</sup>	<sup>1</sup> O <sub>2</sub> or ONOOH (in acidic conditions) <sup>g</sup> , O <sub>3</sub> <sup>h</sup> , H <sub>2</sub> O <sub>2</sub> , NO <sub>2</sub> <sup>-f</sup> .	Yes	NA	SDS- PAGE, LC- MS/MS	Not measure d	Colorimetric assay with titanium sulfate, Griess assay, LC/MS equipped with electrospray ionization ion source, fluorescence probe, spectrophotometry	[ 2 2 ] ]	
FCV	<sup>1</sup> O <sub>2</sub> and ONOO <sup>-</sup> or ONOOH (acidic conditions) <sup>g</sup>	NA	Yes	Not measure d	RT- qPCR	Optical emission spectroscopy, UV test strips, Griess assay, H <sub>2</sub> O <sub>2</sub> test strips	[ 2 8 ] ]	
FCV	<sup>1</sup> O <sub>2</sub> <sup>g</sup> , O <sub>3</sub> <sup>h</sup>	Yes	Yes	EMA-RT- qPCR, EMA-RT- PCR, SDS- PAGE	RT-PCR, RT- qPCR, sequenci ng	Indirect measurements with LC-MS/MS	[ 2 1 ] ]	
FCV	NO <sub>x</sub> , O <sub>3</sub> <sup>g</sup>	NA	NA	Not measure d	Not measure d	UV light meter, UV absorption spectroscopy, Griess	[ 2 0 ]	

						assay	]
<b>Human virus</b>							
Adenovirus	H <sub>2</sub> O <sub>2</sub> <sup>f</sup>	No	Yes	Immuno- chromatography and Western blotting	PCR, qPCR	H <sub>2</sub> O <sub>2</sub> , nitrite and nitrate test strips	[ 2 9 ]
Adenovirus	O <sub>3</sub> <sup>f</sup>	NA	NA	Not measured	Not measured	Optical spectrometer, UV-Power meter, photometric ozone analyzer	[ 4 7 ]
Influenza A and B virus <sup>e</sup>	H <sub>2</sub> O <sub>2</sub> <sup>g</sup>	Yes	Yes	Hemagglutination assays, ELISA, Western blotting	RT- qPCR	Chemical indicator strips, multichannel spectrophotometer, gas detector	[ 4 8 ]
RSV	H <sub>2</sub> O <sub>2</sub> <sup>g</sup>	No	Yes	Immuno- chromatography kits	RT-PCR, RT- qPCR	Active O <sub>2</sub> test strips	[ 3 1 ]
HIV	↑O <sub>2</sub> <sup>+</sup> , O, NO, N <sub>2</sub> (second positive), N <sub>2</sub> <sup>+</sup>	NA	Yes	Not measured	qPCR	Optical emission spectroscopy	[ 3 3 ]
<b>Animal virus</b>							

NDV	↑Oxidation/ reduction potential, H <sub>2</sub> O <sub>2</sub> , OH <sup>·</sup> , NO <sup>·</sup>	Yes	Yes	Bradford protein assay kits	Agilent 2100 bioanalyz er	Oxidation/reduction potential probe, H <sub>2</sub> O <sub>2</sub> assay kit, electrical conductivity meter, electron spin resonance	[ 3 8 ]
NDV, AIV	↑Oxidation/ reduction potential, O, NO, OH	NA	NA	Not measure d	Not measure d	Oxidation/reduction potential probe, optical emission spectroscopy	[ 3 5 ]
<b>Plant virus</b>							
TMV	↑H <sub>2</sub> O <sub>2</sub> , NO <sub>3</sub> <sup>-</sup> , HNO <sub>2</sub> , N <sub>2</sub> O <sub>2</sub> , NO <sub>2</sub> <sup>-</sup>	No	Yes	Western blotting	RT-PCR	Optical absorption spectroscopy, chemical probe	[ 4 5 ]
PVY	H <sub>2</sub> O <sub>2</sub> <sup>f</sup> . ↑OH, O	NA	Yes	Not measure d	RT-PCR	Optical emission spectroscopy, H <sub>2</sub> O <sub>2</sub> test strips	[ 7 ]

<sup>a</sup> ↑: In case where the increase of reactive oxygen and/or nitrogen species was only measured but their importance in inactivation was not determined

<sup>b</sup> Measurements of pH and temperature are excluded as are scavenger experiments and other methods used for indirect identification of RONS

<sup>c</sup> Methods to determine modes of viral inactivation were applied only for treated solutions

<sup>d</sup> Methods to determine modes of viral inactivation were applied only for plasma ignited in 99% Ar and 1% O<sub>2</sub>

<sup>e</sup> The only group that noticed degradation of viral envelope using Fourier-Transform InfraRed (FT-IR) spectrophotometer. ELISA was done only for Influenza B, Western blotting, RT-qPCR, hemagglutination and FT-IR only for Influenza A

<sup>f</sup> Some role in the inactivation, it is not defined how important it is

<sup>g</sup> The main role in the inactivation

<sup>h</sup> Very important but does not have the main role in the inactivation  
Abbreviations: ELISA, enzyme-linked immunosorbent assay; EMA, ethidium monoazide; LC-MS, liquid chromatography-mass spectrometry; MS/MS, tandem mass spectrometry; NA, not applicable; PCR, polymerase chain reaction; RT-PCR, Reverse transcription PCR; RT-qPCR, Reverse transcription real-time PCR; SDS-PAGE, sodium dodecyl sulfate-polyacrylamide gel electrophoresis

#### **Box 1.** Viruses and methods for their disinfection.

Viruses are microscopic agents that can infect all existing forms of cellular life. Their classification as living organisms has historically been a question of interesting, almost philosophical debate, but what it is definitely unquestionable is that they are one of the most powerful engines of evolution on the planet [51]. Most viruses are not harmful, and some of them are even beneficial for their hosts [52]. In recent years, viruses have been increasingly used towards human wellbeing. For example, lentiviruses [53] and adeno-associated viruses [54] are being genetically engineered to formulate state-of-the-art gene therapies. Nevertheless, viruses have a bad reputation as causative agents of various human, animal and plant diseases. This is no surprise, as they were the main players in numerous epidemics and pandemics throughout history (<https://www.who.int/emergencies/diseases/managing-epidemics/en/>). Several viral agents have contributed to the well-deserved 'biohazard' fame of viruses, including influenza, Ebola, HIV and coronavirus SARS-

CoV-2 that causes COVID-19 disease. Despite not being such 'viral celebrities', waterborne viruses pose increasingly serious health and economic burdens in the present era that is threatened by climate change and scarcity of potable water.

Different physical and chemical treatments have been traditionally applied for inactivation of viruses. Chlorine, alcohols, acids, alkalis, and bleach are examples of chemical disinfectants, while UV radiation, filtration, pressure and temperature are among the physical ones [55]. The method of choice depends greatly on the matrix to be disinfected and on the virus targeted for inactivation. Waterborne viruses, including enteric viruses [56] and plant tobamoviruses [57], are among the most stable of the viruses. To inactivate such stable viruses in such a delicate matrix, the disinfection method needs to be strong enough to inactivate the virus, and at the same time it needs to be non-toxic to maintain the quality and properties of the water. It is now known that chlorination, a traditionally used method for water disinfection, is not efficient enough for inactivation of certain viruses, and in the long term, it can pose a risk to human health due to release of toxic by-products [58]. In more recent years, novel waterborne viral inactivation technologies have been developed, such as membrane filtration, reverse osmosis, UV and ozone treatments, and hydrodynamic cavitation, each of which has their own pros and cons. The frequent disadvantages of these technologies are cost inefficiency, scalability problems, and unsustainable power usage. Laboratory scale studies suggest that cold plasma has the potential to overcome these problems, but actual confirmation will only arrive with studies focused on pilot or industrial scale deployment of plasma-based disinfection devices.

**Box 2.** Let's talk about plasma

Plasma is the most abundant state of matter in the visible universe, as it comprises 99% of it. The sun and other stars, nebulae, solar winds, lightning, and aurora borealis are all in plasma state. Plasma TVs, neon and fluorescent lights are the best-known man-made uses of plasma. Generally, plasma contains free electrons, atoms, and molecules in neutral, ionized and/or excited states (including reactive oxygen and nitrogen species). Plasma of many gases represents an extensive source of ultraviolet and vacuum ultraviolet radiation [59]. The possibility to use a particular or a combination of constituents makes plasma a unique material-treatment technique.

On a rough scale, plasma can be divided into thermal or equilibrium plasma, where all particles have roughly the same temperature (average kinetic energy of random motion), and non-thermal, non-equilibrium, or cold plasma, where light electrons have much higher temperatures compared to heavy atoms and molecules, which often remain close to room temperature. In other words, cold plasma is at the point of application at room temperature, and as such, it is suitable for treating any biological material, be it solid, liquid, or an aerosol. Cold plasma can be further classified into low pressure and atmospheric pressure. The latter is limited to the volume where there are large electric fields, while low-pressure plasma spreads in a large volume [60]. Cold plasma is usually sustained with an electrical discharge. The gas temperature usually remains almost unaffected, but the chemical reactivity is huge comparing to the source gas due to the presence of reactive species. In most cases of virus inactivation, the atmospheric-pressure plasma has been used, for practical considerations (for more information on various plasma sources used in microbial decontamination, see [61]).

Plasmas are used in various industries, mainly for tailoring surfaces of solids (e.g. oxidation, cleaning, nanostructuring, binding different atom/ molecule groups), including destruction of microorganisms such as viruses. Plasma can also be used for treatment of liquids, however, inactivation of viruses in liquid media is much more challenging, compared to surfaces, as plasma cannot be sustained in liquids, but only in gaseous bubbles inside the liquid or above the liquid surface. Depending on the place of their generation, RONS interact with either the surface of bubbles or the surface of liquid, where many dissolve. They can then diffuse within the liquid, and might eventually interact with the virus. Furthermore, UV radiation penetrates liquids with a penetration depth that depends enormously on the wavelength, and the concentration and type of impurities [62]. There are various techniques for measuring both long- and short-lived RONS in liquids [63], but they are not used frequently by authors working on the destruction of viruses. Many authors state the discharge parameters (voltage, current, power) rather than plasma parameters (concentration of reactive species), which are necessary to compare various plasma sources. The plasma-virus scientific niche is therefore in its infancy at present.

**Box 3.** Bacteriophages as surrogates and an alternative cold plasma treatment

Bacteriophages are the first choice in many studies to establish proof of concept for virus inactivation methods, due to their many advantages. They are relatively inexpensive to culture/produce, easy and safe to work with, they can be produced in large quantities, and plaque-based infectivity assays are time efficient [64]. However, care must be taken when interpreting the results, as they might not always correlate with the response of the actual virus to the inactivation method.

The very first study that triggered the expansion of the plasma-virus field was conducted on bacteriophages [16]. In recent years, bacteriophages have been used to test the use of CP for air purification [41,49], and to study CP effects on waterborne viral pathogens [46,49].

Bacteriophages have been successfully inactivated in water, where almost complete inactivation of MS2 was obtained after 3 min using a plasma microjet [49].

Waterborne MS2, T4 and  $\phi$ 174 were treated directly with surface DBD or indirectly with CP-activated water [46]. All three of these phages were successfully inactivated with both of these treatments, but with shorter treatment times needed for inactivation of  $\phi$ 174 and MS2, compared to T4 (Table S1). In general, CP-activated liquids are gaining a lot of attention [65], as they can be produced in more controlled ways compared to direct CP treatments. Such a strategy is likely to be a better choice when working with irregular and very sensitive samples, as CP-activated liquids can be applied evenly and can reduce potentially unwanted mechanical changes in a treated material [66].

Airborne human viral pathogens pose a serious threat to human health. In two studies, aerosolized MS2 bacteriophages were successfully inactivated by CP after

only 0.12 s [49] or 0.25 s [41] of contact time of the aerosol with the plasma.

Although these are very promising results, one of the biggest concerns when using plasma for air purification is the production of ozone, as it can be hazardous at high concentrations. Every future application of plasma should consider this, and thus aim to lower ozone concentrations below the recommended limit [67]. Another plasma-based alternative to protect against aerosolized pathogenic viruses would be using a protective mask equipped with a miniature plasma source. Such a mask would have the potential to stop the spread of various viruses, like SARS-CoV-2, that are transmitted by droplets, as droplets are ideal for dissolution of radicals due to the large surface-to-volume ratio. Here, the problem again arises from the fact that the radicals like ozone and nitric oxides would be inhaled so a mask would have to include a radical catalyzer, or even better, a two-membrane mask, where the first plasma membrane would inactivate the virus, while the second membrane would serve as a catalyzer for unhealthy plasma created species. We believe that such innovative mask configuration could be highly beneficial in future outbreaks.

## Glossary

**Acute gastroenteritis:** Inflammation of the gastrointestinal tract that is mainly caused by viruses, especially rotavirus and norovirus. The most common symptoms are vomiting, diarrhea, and abdominal pain.

**Dielectric barrier discharge (DBD):** Plasma is created when the processing gas is guided between an insulator with electrodes on the opposite side.

**Ethidium-monoazide-coupled reverse-transcriptase qPCR (EMA-RT-qPCR):** This method combines the nucleic acid intercalating dye that polymerizes nucleic acid upon exposure to light (ethidium monoazide), which prevents the targeted part of the genome from PCR amplification. As a result, the EMA-RT-qPCR method should only detect infectious viruses with an intact capsid after treatment. This has been proposed to be used instead of infectivity assays.

**Enteric viruses:** A very diverse group of human viruses that are most commonly transmitted via the fecal-oral route (including contaminated food and water), including norovirus, rotavirus, hepatitis A, sapovirus, astrovirus and adenovirus. They infect the gastrointestinal tract, where they replicate and are then excreted in high concentrations. They can cause illness at low doses, and they can survive in the environment for long periods of time, as they are resistant to physiological changes like pH and temperature.

**Polymerase chain reaction (PCR):** A method frequently used in molecular biology for amplification of targeted parts of nucleic acids. Different versions of PCR can be used qualitatively and/or quantitatively. The most often quantitative methods used are real-time PCR (qPCR) and the more advanced version, digital PCR (dPCR).

**Plasma (micro)jet:** Plasma is created by blowing a gas next to or through an electrode.

**Plaque-forming units (PFUs):** A measure of the number of viral particles that form plaques in a certain volume of a sample under examination.

**Reactive oxygen and nitrogen species (RONS):** ROS (e.g.  $O_3$ ,  $O$ ,  $O_2^*$ ,  $H_2O_2$ ,  $OH^\cdot$ ,  $^1O_2$ ) are partially reduced or excited forms of oxygen, and RNS (e.g.  $N$ ,  $N_2^*$ ,  $NO$ ,  $NO_2$ ,  $NO_2^-$ ,  $NO_3^-$ ,  $ONOO^-$ ,  $ONOOH$ ) are the most common nitrogen- and nitric-

oxide-derived compounds. RONS have crucial and versatile roles in the maintenance of normal functions of different cells in most organisms.

**Virus inactivation:** To decrease the infection of a host by a virus. The most reliable method to determine the inactivation efficiency is an infectivity assay, in which appropriate hosts (e.g. bacterial or eukaryotic cells, plants, chicken embryos) are inoculated with a virus. The inoculation is followed by the observation/ measurement of different factors, such as the formation of plaques, cytopathic effects and symptoms in plants, survival of the embryos or the integrity of viral nucleic acids.



## Outstanding questions

1. What cold plasma source conditions will enable optimal efficiency of targeted virus inactivation in terms of the required treatment times and energy consumption?
2. Which reactive oxygen and/or nitrogen species are the most relevant for inactivation of a given virus in a given matrix, how to optimize production of such relevant RONS, and which methods should be used for their accurate determination?
3. Does ultraviolet radiation have a synergetic effect with reactive oxygen and/or nitrogen species in virus inactivation?
4. What are the main viral components that are affected by different cold plasma-mediated virus inactivation strategies, and which viral characterization methods should be used in each experiment to get a precise answer? Should a standardized protocol be developed for this purpose?
5. What is the scale-up potential of cold-plasma treatments?
6. Can cold plasma cause cytotoxic or genotoxic damage when used for virus inactivation in specific matrices that will come in contact with human, plant, and animal tissues?
7. Would the combination of cold plasma with already established methods, such as chlorine treatment, or some new environmentally friendly methods such as cavitation, have a synergistic effect on the virus inactivation? Would such synergy contribute to shorter treatment times, lower energy consumption and decreased environmental burden?

## Highlights

- Pathogenic viruses are becoming an increasing burden for health, agriculture and the global economy. Classic disinfection methods have some downsides, so innovative solutions for virus inactivation are urgently needed.
- Cold plasma can be used as an environmentally friendly tool for virus inactivation. It can inactivate different human, animal, and plant viruses in various matrices.
- When using cold plasma for virus inactivation it is important to set up the right parameters and to choose treatment durations that allow particles to interact with the contaminated material.
- Reactive oxygen and/or nitrogen species have been shown to be responsible for virus inactivation through effects on capsid proteins and/or nucleic acids. Development of more accurate methods will provide information on which plasma particles are crucial in each experiment, and how exactly do they affect viruses.



## Inactivation of airborne porcine reproductive and respiratory syndrome virus (PRRSv) by a packed bed dielectric barrier discharge non-thermal plasma

T. Xia<sup>a,\*</sup>, M. Yang<sup>b</sup>, I. Marabella<sup>c</sup>, E.M. Lee<sup>d</sup>, B. Olson<sup>c</sup>, D. Zarling<sup>c</sup>, M. Torremorell<sup>b</sup>, H.L. Clack<sup>a</sup>

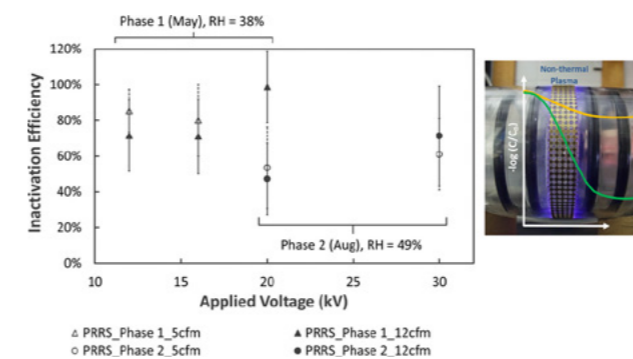
<sup>a</sup> Civil and Environmental Engineering, University of Michigan, Ann Arbor, MI, United States

<sup>b</sup> Veterinary Population Medicine, University of Minnesota, St. Paul, MN, United States

<sup>c</sup> Mechanical Engineering, University of Minnesota, Minneapolis, MN, United States

<sup>d</sup> Mechanical, Materials and Aerospace Engineering, Illinois Institute of Technology, Chicago, IL, United States

### GRAPHICAL ABSTRACT



### ARTICLE INFO

**Keywords:**  
Non-thermal plasma  
Airstream inactivation  
PRRSv  
TCID<sub>50</sub>  
qPCR

### ABSTRACT

Porcine reproductive and respiratory syndrome virus (PRRSv) is one of the most significant airborne viruses impacting the pork industry in the US. Non-thermal plasmas (NTPs) are electrical discharges comprised of reactive radicals and excited species that inactivate viruses and bacteria. Our previous experiments using a packed bed NTP reactor demonstrated effective inactivation of bacteriophage MS2 as a function of applied voltage and power. The present study examined the effectiveness of the same reactor in inactivating aerosolized PRRSv. A PRRSv solution containing  $\sim 10^5$  TCID<sub>50</sub>/ml of PRRSv VR2332 strain was aerosolized at 3 ml/min by an air-jet nebulizer and introduced into 5 or 12 cfm air flow followed by NTP exposure in the reactor. Twin impingers upstream and downstream of the reactor collected samples of the virus-laden air flow for subsequent TCID<sub>50</sub> assay and qPCR analyses. An optical particle sizer measured upstream and downstream aerosol size distributions, giving estimates of aerosol filtration by the reactor. The results showed that PRRSv was inactivated to a similar degree as MS2 at the same conditions, with the maximum 1.3-log inactivation of PRRSv achieved at 20 kV and 12 cfm air flow rate. The results demonstrate the potential of properly optimized NTPs in controlling PRRSv transmission.

\* Corresponding author at: M6075 SPH II, 1415 Washington Heights, Ann Arbor, MI, 48109, United States.  
E-mail address: [xiatian@umich.edu](mailto:xiatian@umich.edu) (T. Xia).

<https://doi.org/10.1016/j.jhazmat.2020.122266>

Received 13 October 2019; Received in revised form 4 February 2020; Accepted 8 February 2020

Available online 10 February 2020

0304-3894/ © 2020 Elsevier B.V. All rights reserved.

## 1. Introduction

Airborne transmission of livestock or zoonotic diseases such as Newcastle disease, avian influenza, foot-and-mouth disease, and porcine reproductive and respiratory syndrome (PRRS), just to name a few, greatly threaten global food security, agricultural industry and public health by causing significant losses in production, high mortality, decrease in productivity, stoppage of exports, etc.. This is particularly significant in the face of ongoing climate change, especially for pathogens whose efficiency of airborne transmission through the atmosphere may change in counterintuitive ways. In addition, animals can experience a greater degree of exposure to ambient atmospheric conditions or unconditioned outdoor air compared to humans. Foot and mouth disease is considered as the top foreign animal disease threat to US agriculture (Colby, 2013), and the 2014–2015 outbreak of highly pathogenic avian influenza in the US caused an average of 50,000 bird losses per operation for turkeys and over 1 million bird losses per operation for table-egg laying chickens where the disease was confirmed (Ramos et al., 2017).

In the case of the pork industry, porcine reproductive and respiratory syndrome virus (PRRSv), an enveloped virus that appeared in the US in the 1980s (Keffaber, 1989), has drawn increasing research attention due to its significant impact on pork production and ability to be transmitted in air over kilometers. It was estimated that in 2011 the outbreaks of PRRSv in the US national breeding- and growing-pig herd overall cost \$664 million annually due to productivity losses, 45 % of which occurred in the breeding herd (Holtkamp et al., 2013). Outbreaks of PRRSv in China caused great economic losses and gained public concern due to the emergence of highly pathogenic strains. In 2006, a highly pathogenic PRRSv disease outbreak emerged in China, with its clinical signs being prolonged high fever, red discoloration of the body, and blue ears associated with high mortality of infected pigs. It quickly spread to 12 provinces and significantly impacted the country's pork industry (Tian et al., 2007). In 2014, another novel NADC30-like strain of PRRSv emerged in China (Zhou et al., 2015), which was virulent to pigs but is less pathogenic than the highly virulent PRRSv discovered in 2006 (Sun et al., 2016). Since late 1990s, research has shown that PRRSv can survive in aerosols and be transmitted through airborne pathways. PRRSv can be released in aerosols from infected pig barns and has been found in aerosols generated when swine manure collection tanks are pumped out (Millerick-May et al., 2016). Once released, the virus can be transmitted in ambient air over several kilometers (up to 9.1 km as reported) from the source (Otake et al., 2010) and can potentially cause outbreaks in distant barns. The airborne transmission of PRRSv can be affected by many environmental factors, such as aerosol concentration, aerosol size distribution, ambient temperature, relative humidity (RH), and solar radiation. It is reported that PRRSv can survive longer in aerosols at lower ambient temperature and lower relative humidity (Hermann et al., 2007). Open-air factors with unidentified chemical nature (Hood, 2009) may also have adverse effects to the survival of viruses in aerosols. In 2019, Arruda et al. gave a detailed and comprehensive literature review on the previous research projects, findings and current knowledge gaps of PRRSv aerosols and airborne PRRSv transmission (Arruda et al., 2019).

The most commonly applied technologies to control airborne pathogens in both human-occupied buildings and animal confinements are the collection of bioaerosols on filters, such as HEPA, MERV 14 and MERV 16 filters, and UV germicidal irradiation (UVGI). HEPA filtration has been proven to be very effective in removal of bioaerosols from airstreams. (Farnsworth et al. (2006)) reported  $96.5 \pm 1.5$  % bacterial collection efficiency of *B. subtilis* by HEPA filtration. The study also examined HEPA filtration of three virus species, and reported no viable virus recovered from the downstream sampler. A study by (Dee (2011)) found that new PRRSv outbreaks were recorded at 20 % of farms with ventilation air filters installed as compared to 92 % of farms without such filters in the control group. The use of HEPA filters comes with

several limitations, including high filter replacement costs; high pressure drops, and the associated increase in energy consumption of the HVAC system to maintain desired ventilation rate. In the case of agricultural buildings, there are also high reconstruction costs to achieve an air-tight building envelope and eliminate potential air infiltration (Pitkin et al., 2009a). Lastly, collection of bioaerosols on HEPA filters does not actually inactivate the pathogens, with the possibility of re-emitting more environmentally resilient pathogens into the ambient air during filter replacement and disposal processes (Miaskiewicz-Peska and Lebkowska, 2012). Effective UVGI disinfection requires a sufficiently high light intensity, achieved through a combination of a number of bulbs and exposure time in a carefully designed ventilation system. UV inactivation efficiency is also to some degree influenced by the susceptibility of the pathogen (Bolashikov and Melikov, 2009). UVGI has been shown to diminish the transmission of Mycobacterium tuberculosis from patients occupying hospital wards to guinea pigs raised in an exposure chamber (Riley, 1961), and prevent the spread of rubella within army barracks (Wheeler et al., 1945). The application of UVGI in indoor air disinfection is limited by the need to avoid the adverse health effects of UV on humans and livestock. In the indoor environment, UV lights can be installed in the upper regions of the room near the ceiling to avoid exposing the occupants to UV light. The process, however, is passive in nature and can only inactivate pathogens transported by upward air currents into the UVGI treatment zone. In many cases, UV radiation alone is not effective enough in instantaneous air disinfection, and is often applied in conjunction with HEPA filters: airborne pathogens are collected on filter surfaces and inactivated by UV radiation (Memarzadeh et al., 2010). However, UV light is unable to penetrate deeply into HEPA filters, where collected pathogens may survive and re-enter the air flow. The energy consumption of the UV system is also significant, and broken bulbs should be detected and replaced periodically. In all, of the two defining characteristics of infectious aerosols - transport and infectivity (Pitkin et al., 2009b) - particulate filters only address transport and UVGI mainly addresses infectivity. Non-thermal plasmas (NTPs) address both characteristics by 1) electrostatic removal of larger particles (> 1  $\mu\text{m}$  approx.) and 2) sterilization of the remaining smaller particles by direct plasma exposure. NTPs are stable electrical discharges containing excited and ionized species and radicals that are orders of magnitude more reactive than ozone ( $\text{O}_3$ ) (Xiao et al., 2014), the more familiar, less effective, and more persistent oxidant used by indoor air cleaners. Radicals and excited species are thought to vigorously attack the bacterial cell membrane or virus capsid, leading to damage that causes a loss in structural integrity and eventual pathogen inactivation. NTPs have already been proven for surface disinfection, inactivating biological pathogens on the surfaces of food products (Perni et al., 2008; Noriega et al., 2011) and treatment of skin diseases (Heinlin et al., 2010). NTPs have also been thoroughly studied for destruction of gaseous pollutants, the radicals and excited species having been shown to destroy a wide variety of gaseous volatile hydrocarbons such as those emitted from industrial processes (Xiao et al., 2014) as well as gaseous pollutants such as nitrous and sulfur oxides ( $\text{NO}_x$  and  $\text{SO}_x$ ) emitted from combustion (McAdams, 2001). However, the intersection of these two established applications of NTPs - disinfection of an air stream - is substantially complicated by the fact that viruses and bacteria act as charged aerosols suspended in the gas stream, both the aerosols and the gas responding separately to the electric fields and flow of charged ions that form the foundation of NTPs. Another concern of applying NTP inactivation in animal confinements is that the elevated concentrations of chemically reducing species such as  $\text{NH}_3$  and  $\text{H}_2\text{S}$ , common emissions from urine and manure in animal confinements, have the potential to react with the plasma-generated oxidative species, possibly reducing the inactivation efficiency of NTP.

Our previous research (Xia et al., 2019) has developed a packed bed NTP reactor and demonstrated inactivation of airborne bacteriophage MS2 by the reactor as a function of applied voltage and power with a

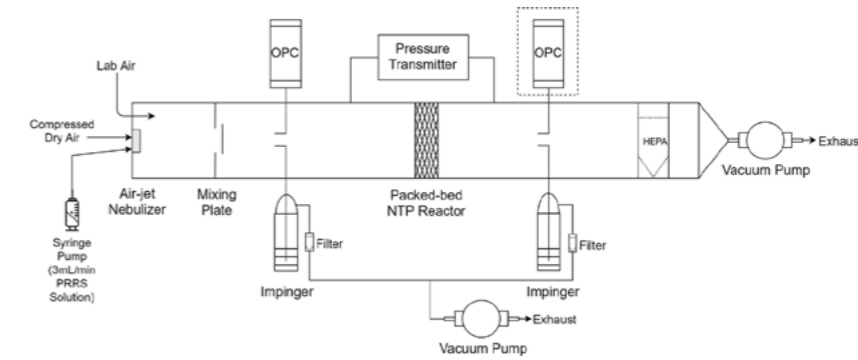


Fig. 1. Schematic of the small-scale wind tunnel setup at University of Minnesota with the NTP reactor mounted in the middle test section. One OPC is indicated with a dashed box since only one OPC instrument was available, its location alternated between upstream and downstream sampling probes during each test.

maximum inactivation of 2-log at 30 kV peak-to-peak voltage and 2.08 W ( $734 \text{ J/m}^3$  at 170 LPM). The objective of the present study is to measure the inactivation of aerosolized PRRSv by the same packed bed NTP reactor and compare the results with our previous bacteriophage MS2 inactivation results to investigate if the packed bed NTP reactor has different performance inactivating an enveloped airborne virus (PRRSv) versus a non-enveloped virus (bacteriophage MS2). Using virus stocks and wind tunnel facilities provided by the University of Minnesota, the packed bed NTP reactor was tested for effectiveness in inactivating aerosolized PRRSv.

## 2. Materials and methods

### 2.1. Experimental apparatus

The tests of PRRSv inactivation by NTP were conducted using a small-scale non-recirculating wind tunnel located at the University of Minnesota. A schematic of the experimental setup is shown in Fig. 1. The wind tunnel has an inside duct diameter of 3.5", an overall length of 96" and can operate in a volumetric flow rate range from approximately 3–30 cfm. An induced draft (ID) fan is connected at the outlet of the wind tunnel and the volumetric flow rate is maintained by measuring the pressure drop (OMEGA Differential Pressure Transmitter P X 653-10D5V) across a calibrated orifice meter installed near the tunnel exit and applying the necessary voltage to the vacuum pump downstream of the tunnel. Temperature and relative humidity in the tunnel and absolute pressure are measured and taken into account in the volumetric flow rate measurements. The flow rate is calculated and maintained using Proportional-Integral-Derivative (PID) feedback control in LabView. Data acquisition by the LabView software is facilitated by a National Instruments USB-6001 DAQ. A HEPA filter is installed at the exit of the tunnel to prevent contamination or release of the PRRSv into the laboratory.

The packed bed NTP reactor was mounted in the test section of the wind tunnel (shown in Fig. 1) and was tested at volumetric flow rates of 5 and 12 cfm. The design and schematic of the dielectric barrier discharge (DBD) packed bed NTP reactor are described in detail in our previous paper (Xia et al., 2019a). The Plexiglas tube wall serves as the dielectric barrier which would promote microdischarge generation. Two grounded electrodes, compressing 500 inert borosilicate glass beads (0.25-inch diameter) in between, formed the packed bed setup which can further enhance the microdischarge by partial discharges at the contact points between the glass beads for more effective plasma species-viral aerosol interactions.

An air-jet large particle generator (LPG) atomizer was installed at the entrance of the tunnel and used to generate PRRSv challenge aerosols. A PRRSv solution from a 65 ml syringe was feed into the LPG atomizer using a syringe pump set (New Era Pump Systems Inc. NE-300) at a constant liquid feed rate of 3 mL/min. Dry and filtered

dispersion air at a volumetric flow rate of 1.5 L per minute (LPM) was directed into the dispersion air inlet of the atomizer to help aerosolize the virus solution reaching the atomizer nozzle. After aerosolization, the PRRSv aerosols were diluted and dried with lab air drawn into the wind tunnel, and the air was mixed thoroughly using a downstream orifice mixing plate, which generates turbulence to achieve uniform aerosol distribution in the air flow. Isokinetic probes were installed upstream and downstream of the packed bed NTP reactor to extractively sample from the wind tunnel flow at 2.8 LPM, and the droplet number concentrations in the sampled air were measured by a portable optical particle counter (OPC, TSI AeroTrak model 9306-V2). An aerosol diluter was used to prevent coincidence errors in the OPC. Two additional isokinetic probes were installed as well upstream and downstream of the packed bed NTP reactor at the same locations as the OPC probes, which extractively sampled the wind tunnel air flow at a nominal volumetric flow rate of 9 LPM. The sampled air was drawn by a vacuum pump through two identical liquid impingers (Ace Glass, Inc. 125 mL 24/25 Impinger), leading to collection of infectious and inactivated PRRSv aerosols in the 20 mL impinger collection fluid (Dulbecco's Modified Eagle Medium (DMEM)). The pressure drop across the NTP reactor was measured by another differential pressure transmitter (Omega P X 653-03D5V).

### 2.2. Experimental procedure

#### 2.2.1. NTP inactivation testing procedure

The tests of airborne PRRSv inactivation by the packed bed NTP reactor took place in two phases, in May and August 2017, over the course of four months to allow time for samples collected in the first phase to be analyzed by the Veterinary Diagnostic Lab at Univ. of Minnesota. The two-phase tests were designed because there was initial concern that the sensitivity of PRRSv titration, which is limited by the initial titer of infective PRRSv that is aerosolized, might lead to a situation where no infective virus was detected downstream of the reactor, resulting in uncertainty as to whether such a result represented a 100 % inactivation or evidence of reaching the lower detection limit. As a result, Phase 1 employed the lowest voltages to make sure to the extent possible that as little of the virus was inactivated. Test conditions in the second phase employed higher voltages after analyses showed the results of Phase 1 yielded partial inactivation.

In the first phase (May data), the NTP reactor was operated at voltages of 12, 16, and 20 kV, and the highest NTP discharge power was 0.56 W achieved at 20 kV. In the second phase (August data), voltages of 30 kV were applied in the reactor using a second power supply, resulting in about 2.08 W discharge power in the NTP reactor (Xia et al., 2019a). For each voltage setting, the PRRSv inactivation by the packed bed NTP reactor was examined under two air flow rates (5 cfm and 12 cfm), and all tests were conducted in triplicate. In both Phase 1 and Phase 2 (May and August), two control tests, either with the reactor

deactivated (no voltage supplied) or with the reactor removed from the wind tunnel, were also conducted in duplicate. At the beginning of each test, the vacuum pump downstream of the sampling train was turned on to reach a constant desired flow rate through the wind tunnel, after which the syringe pump and compressed air supplied to the air-jet nebulizer were turned on to initiate PRRSV aerosolization. When consistent mist was observed emitting from the nebulizer, the packed bed NTP reactor was activated (for reactor-on tests only), and the sampling pumps downstream of the impingers were turned on to start the 20-minute impinger sampling. Only one OPC was available for this study, which was switched between upstream and downstream sampling probes, consecutively making a 5-minute upstream particle size distribution (PSD) measurement, a 5-minute downstream PSD measurement, and then another 5-minute upstream PSD measurement during the 20-minute testing period. The two 5-minute upstream PSD data were averaged as an estimation of the synchronous upstream PSD when the downstream PSD was actually measured. The OPC had six particle size bins (set to 0.3  $\mu\text{m}$ , 0.5  $\mu\text{m}$ , 1  $\mu\text{m}$ , 3  $\mu\text{m}$ , 5  $\mu\text{m}$  and 10  $\mu\text{m}$ ) and was set to report the differential particle number concentrations between adjacent bin sizes. It was assumed that the log-average of the two adjacent bin sizes was the average droplet size for the corresponding measured differential number concentrations.

### 2.2.2. PRRSV virus preparation, aerosolization and collection

PRRSV VR2332 reference strain was propagated in MARC-145 cells and titrated to  $10^5$  TCID<sub>50</sub>/mL (50 % Tissue Culture Infectious Dose per milliliter). The virus was aliquoted and frozen at  $-80^\circ\text{C}$  until used. For each test, a syringe was filled with 65 mL of PRRSV at  $10^5$  TCID<sub>50</sub>/mL, placed into a New Era pump system, model NE-1000 multi-phaser, and aerosolized into the testing chamber at 3 mL/min via an air-jet nebulizer for 20 min. Room temperature and relative humidity (RH) level were measured during each test by a portable humidity/temperature pen (Traceable 4093). During each test, air samples were collected with twin impingers, placed upstream and downstream of NTP reactor, for 20 min. Each impinger was filled with 20 mL of DMEM supplemented with 1.5 mg/mL of bovine serum albumin fraction V 7.5 %, 1X antibiotic-antimycotic, 0.0015 mg/mL of Trypsin-TPCK, and 0.05 mg/mL of gentamicin. After 20 min sampling time, the volume of supplemented DMEM in each impinger was measured, recorded, aliquoted into 3 tubes and frozen at  $-80^\circ\text{C}$  until tested. The collected impinger samples were submitted to the Veterinary Diagnostic Lab at the University of Minnesota for quantitative RT-PCR analysis and TCID<sub>50</sub> assay analysis.

### 2.2.3. Quantitative RT-PCR (RT-qPCR)

Samples were quantified for PRRSV using quantitative RT-PCR as previously described (Cho et al., 2006). A standard curve based on transcript RNA with a quantitative linear range from  $1 \times 10^3$  copies/ $\mu\text{L}$

to  $1 \times 10^6$  copies/ $\mu\text{L}$  was used to determine the RNA copy number/mL. The copy number/mL results were consecutively converted to copies/ $\text{m}^3$  of air. The detection limit of PRRSV quantitative RT-qPCR is approximately 1000 copies/mL, which is equivalent to approximately  $8 \times 10^4$  copies/ $\text{m}^3$  of air in this study.

### 2.2.4. Sample titration

Samples were serially diluted 5-fold. 100  $\mu\text{L}$  of the serial dilution was plated onto 96-wells plates containing MARC-145 cells in 4 replicates. Plated samples were incubated for 7 days at  $37^\circ\text{C}$  with 5 % CO<sub>2</sub>. At day 7, plates were removed and cytopathic effect (CPE) was read and recorded. TCID<sub>50</sub>/mL was calculated using the Spearman-Kärber method and consecutively converted to TCID<sub>50</sub>/ $\text{m}^3$  of air. The detection limit of PRRSV TCID<sub>50</sub> is 1.43 TCID<sub>50</sub>/100  $\mu\text{L}$ , which is equivalent to approximately 1200 TCID<sub>50</sub>/ $\text{m}^3$  of air in this study.

### 2.2.5. Testing the effects of liquid accumulation on NTP performance

During the experiment, it was observed that compared with the previous bacteriophage MS2 inactivation tests (Xia et al., 2019a), more virus solution droplets (mainly DMEM in this study) reached and impacted on the packed bed and accumulated in the reactor between the glass beads, likely due to higher RH conditions of the supplied air, shorter distance between the atomizer and the packed bed NTP reactor, and potentially larger droplets produced by the air-jet large particle generator. The accumulated virus solution may have promoted virus aerosol filtration by the packed bed, but could also have led to re-emission of viral aerosols from the reactor into the region downstream. In addition, increase of RH and accumulation of liquid inside the packed bed may change the NTP discharge scenario, serve as a protective reservoir for suspended viruses, and affect reactive species formation by the reactor. To examine the effects of accumulated DMEM solutions, another set of tests was conducted at the University of Michigan using bacteriophage MS2 as the target virus. 5 mL and 10 mL DMEM solution were sprayed directly into the packed bed before each test and the reduction of airborne infectious MS2 from upstream to downstream of the DMEM-soaked packed bed NTP reactor were examined with the reactor powered by the 20 kV power supply at 170 LPM air flow rate. The setup of the sampling line, the methodology of MS2 ultrasonic atomization, and the virus sample analysis methods were described in detail in our previous paper (Xia et al., 2019a).

## 3. Results and discussion

### 3.1. Droplet size distribution

For all powered-reactor tests, particle size distributions (PSD) were measured both upstream and downstream of the packed bed NTP

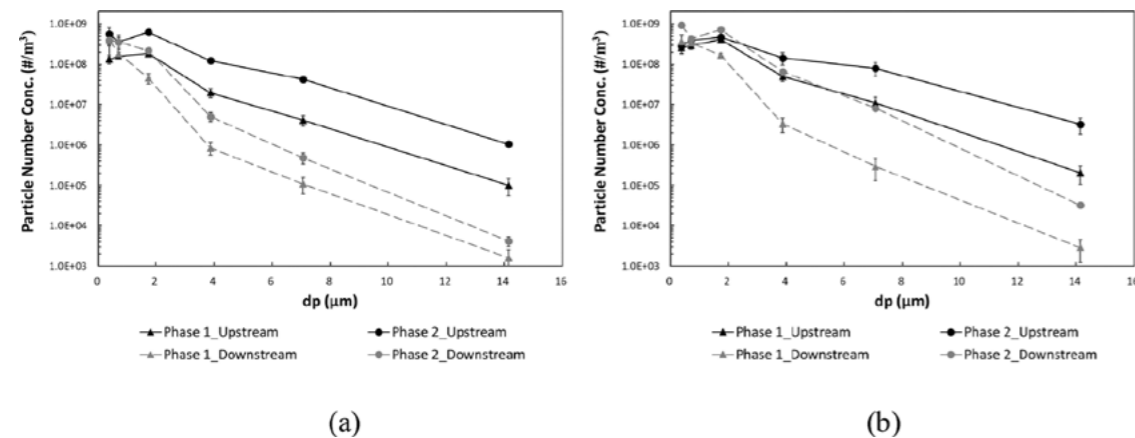


Fig. 2. Average droplet size distributions both upstream and downstream of the reactor in each test program phase (Phase 1 and Phase 2) for wind tunnel flow rates of (a) 12 cfm and (b) 5 cfm.

reactor under two flow rates, and the results were averaged for each phase of the test program and each flow rate (Fig. 2). From Fig. 2 it is evident that the OPC measurements were quite consistent with small confidence intervals, indicating that the virus solution aerosolization process was repeatable and the packed bed had relatively consistent filtration efficiencies regardless of the applied voltage level (which is proved by PSD data comparison between different applied voltages in the same test program phase with the same flow rate). The PSD plots confirm that aerosols generated by air-jet nebulizers are polydisperse in size with large proportions of droplets over 5  $\mu\text{m}$  in diameter, which agrees with other reports on aerosol PSDs generated by air-blast atomization (Lorenzetto and Lefebvre, 1977; Steckel and Eskandar, 2003). The upstream sampling probe was installed about 40" (101.6 cm) downstream of the air-jet nebulizer, which was only about a quarter of the distance between the ultrasonic atomizer and upstream sampling port (144", 365.8 cm) in our previous bacteriophage MS2 inactivation setup (Xia et al., 2019a). The shorter distance led to more incomplete aerosol evaporation, and as a result more coarse droplets (with droplet diameter  $d_p$  ranging from 2.5–10  $\mu\text{m}$ ) would reach the reactor where they would be filtered by the packed bed and accumulate as a bulk liquid in the reactor. This inference was proved by experimental observations: during all PRRSV inactivation tests in both test program phases, bulk virus solution was found accumulating between the glass beads in the packed bed NTP reactor, while for all MS2 tests conducted in University of Michigan, no liquid accumulation was found with an ultrasonic atomizer expected to generate aerosols with smaller and more uniform size distribution (Steckel and Eskandar, 2003) and using a dry (RH typically < 10 %) compressed air supply. It should be noted in interpreting the results that the accumulated virus solution is undesirable since it may cause re-emission of aerosols from the packed bed, change the NTP discharge phenomena, serve as a protective reservoir for suspended viruses, and impact reactive species formation by the reactor.

The two plots in Fig. 2 illustrate how virus solution aerosolization and packed bed filtration would change with changing flow rate and flow relative humidity. In the same test program phase, the upstream droplet number concentration is generally higher at 5 cfm (Fig. 2b) than that at 12 cfm flow rate (Fig. 2a), due to reduced dilution and slower droplet evaporation at lower air flow rate. The average RH of the ambient room air (which was the major air source of the wind tunnel flow) in Phase 2 was 49 %, higher than the ambient condition in Phase 1 (38 %), while the air temperature remained relatively constant ( $22.2^\circ\text{C}$  in Phase 1 and  $23.2^\circ\text{C}$  in Phase 2). Higher inlet RH in Phase 2 caused slower droplet evaporation, and as a result more droplets in all sizes were found upstream of the reactor in Phase 2 in both Fig. 2a and 2b. Comparison between upstream and downstream PSD in both plots provides a measure of the packed bed filtration effects on various size droplets. Fig. 2a showed that the number concentrations of droplets larger than 1  $\mu\text{m}$  reduced significantly from upstream to downstream of the reactor, which should be mainly due to filtration by the packed bed and size reduction through evaporation, and larger droplets had more significant decreases in number concentration due to their low mobility and large surface area and thus rapid evaporation. Concentrations of submicron droplets (droplets smaller than 1  $\mu\text{m}$ ), however, increased from upstream to downstream of the reactor, potentially due to re-aerosolization of virus solutions accumulated in the packed bed, and evaporation of super micron droplets to submicron sizes. Fig. 2b showed similar droplet number concentration changing trends, while concentrations of droplets between 1  $\mu\text{m}$  and 7  $\mu\text{m}$ , especially in Phase 2, showed less reduction compared with the 12 cfm data. This should be due to slower evaporation of droplets larger than 7  $\mu\text{m}$  to this size range at 5 cfm. At 12 cfm, these droplets may evaporate faster and fall into the submicron region before reaching the downstream sampling probe. These observations and hypotheses are confirmed by comparing droplet penetration (downstream concentration divided by upstream concentration) in the two phases at two flow rates (Fig. 3). From Fig. 3, it is

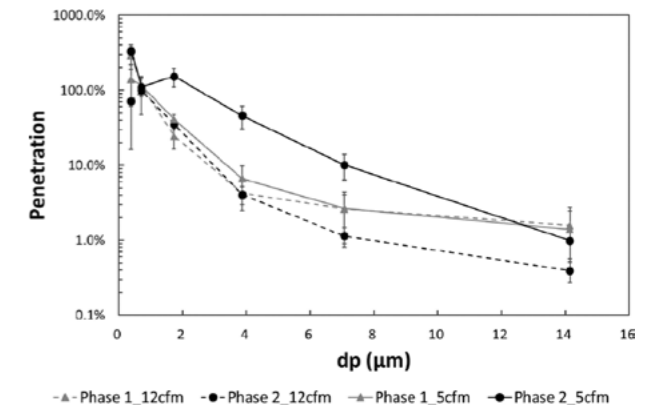


Fig. 3. Penetration of particles (downstream number concentration / upstream number concentration) in each OPC size bin measured at two flow rates in the two test program phases.

evident that in Phase 1 droplets had similar penetration through the reactor at both flow rates, and 1  $\mu\text{m}$ –5  $\mu\text{m}$  droplets had slightly higher penetration at 5 cfm. In Phase 2 at 12 cfm, the penetration of droplets smaller than 4  $\mu\text{m}$  had similar values as the Phase 1 data, while droplets larger than 4  $\mu\text{m}$  had less penetration, likely due to the increased amount of virus solution accumulated in the packed bed at higher RH. At 5 cfm in Phase 2, the penetration curve was quite different from the other three, with significantly higher droplet penetration in the range 2  $\mu\text{m}$ –7  $\mu\text{m}$ . It is likely that at this air-to-water mass flow ratio, the RH in the wind tunnel exceeded the critical RH predicted by our previous droplet evaporation numerical model (Xia et al., 2020), which prevented rapid liquid evaporation and led to more 2  $\mu\text{m}$ –7  $\mu\text{m}$  droplets reaching the downstream sampling probe. Based on the OPC data and assuming spherical droplets, the average volumetric droplet penetration through the packed bed was 10.6 % in Phase 1 at 12 cfm, 13.7 % in Phase 1 at 5 cfm, 6.2 % in Phase 2 at 12 cfm, and 22.2 % in Phase 2 at 5 cfm.

### 3.2. PRRSV filtration and inactivation by the packed-bed NTP

In this study, TCID<sub>50</sub> analysis of the twin upstream and downstream impinger samples collected in each test provided a measure of the reduction in viable PRRSV for all mechanisms. qPCR analysis of the upstream and downstream samples was performed with TCID<sub>50</sub> analysis and provided a measure of the reduction in the PRRSV genome irrespective of changes in viability caused by NTP exposure; in the context of the present study, reductions in the abundance of the PRRSV genome were interpreted as packed bed filtration. Such filtration effects could also be inferred from TCID<sub>50</sub> analyses showing reductions in viable PRRSV between the upstream and downstream impinger samples collected when the reactor was not powered. The latter method, however, were not applied in this study since it can yield greater uncertainties with two groups of tests (reactor-on and reactor-off) conducted separately, which might have experienced different RH conditions, varied virus solution aerosolization and evaporation phenomena, or have different viable PRRSV concentration in the initial solution filled into the syringe pump. In addition, the previous bacteriophage MS2 inactivation study used qPCR data as the indication of packed bed filtration, so it is preferable to apply the same analytical method in order to compare results between the two studies. Reductions in viable PRRSV from TCID<sub>50</sub> analyses, after correcting for packed bed filtration according to the qPCR data, yielded the inactivation of PRRSV by the reactor solely due to NTP exposure.

Table 1 summarizes the measured abundance of PRRSV genome copies (in RNA copies/ $\text{m}^3$ ) and abundance of infective PRRSV (in TCID<sub>50</sub>/ $\text{m}^3$ ) in the tunnel air flow before- (upstream, U) and after- (downstream, D) NTP treatment. Averages of  $8.1$ – $73.5 \times 10^{10}$  RNA

**Table 1**  
Summary of the measured abundance of PRRSv genome copies (in RNA copies/m<sup>3</sup>) and abundance of infective PRRSv (in TCID<sub>50</sub>/m<sup>3</sup>) in the tunnel air flow before- (upstream, U) and after- (downstream, D) NTP treatment.

Phase	Voltage (kV)	Tunnel air flow Rate (cfm)	Replicates	Acceptable Replicates		10 <sup>10</sup> RNA copies/m <sup>3</sup>	SD	10 <sup>5</sup> TCID <sub>50</sub> /m <sup>3</sup>	SD
1	20	12	3	1	U	8.10	—	167.62	—
					D	1.87	—	0.53	—
1	16	12	3	3	U	12.32	5.65	5.42	2.92
					D	1.88	1.78	0.20	0.15
1	12	12	3	1	U	16.73	—	8.73	—
					D	5.96	—	0.88	—
1	20	5	3	2	U	73.47	69.43	108.10	146.73
					D	6.19	2.70	1.27	0.59
1	16	5	3	1	U	36.90	—	11.48	—
					D	9.11	—	0.57	—
1	12	5	3	2	U	28.87	1.45	44.47	2.96
					D	8.71	3.33	2.02	1.51
2	30	12	3	2	U	14.57	2.31	26.20	26.46
					D	0.70	0.05	0.19	0.03
2	20	12	6	3	U	8.67	2.91	20.53	19.45
					D	0.62	0.11	0.35	0.20
2	30	5	3	1	U	18.57	—	16.62	—
					D	1.95	—	0.68	—
2	20	5	6	3	U	18.38	4.02	22.05	21.24
					D	3.37	0.83	1.54	1.41

(SD: standard deviation; U: upstream; D: downstream).

copies/m<sup>3</sup> were detected in the air flow upstream of NTP treatment, and 0.6–9.1 × 10<sup>10</sup> RNA copies/m<sup>3</sup> were detected downstream. In terms of infective PRRSv concentration, 5.4–167.6 × 10<sup>5</sup> TCID<sub>50</sub>/m<sup>3</sup> were detected upstream of NTP and 0.2–2.0 × 10<sup>5</sup> TCID<sub>50</sub>/m<sup>3</sup> were detected in the downstream flow. Comparing the TCID<sub>50</sub> results with qPCR at the upstream location, there was ~5-log inactivation of PRRSv in the aerosols before reaching the reactor, which is comparable with our previous research (Xia et al., 2019a) and should be due to the evaporation of droplets and intensive air-jet nebulization (Niven et al., 1995). Three to six replicates were conducted for each applied voltage and tunnel flow rate combination, however, only one to three replicates yielded physical results. The rejected replicates yielded unphysical results with either the abundance of infective PRRSv or the number of genome copies higher at the downstream location than at the upstream location. Degradation of the airborne PRRSv by attack from reactive species within the non-thermal plasma would not be expected to result in either an increase in TCID<sub>50</sub> or an increase in the number of PRRSv genome copies at the downstream sampling location. The increase in TCID<sub>50</sub> or PRRSv genome copies data could be due to sampling or analysis errors or accumulation of virus solution in the packed bed and the resulting potential re-aerosolization of PRRSv into the downstream flow. Repeating tests may not reduce these errors with the present experimental design, since each replicated test may experience different RH conditions, varied virus solution aerosolization and evaporation phenomena, or have different viable PRRSv concentration in the initial solution filled into the syringe pump. As shown in Table 1, tests with two to three replicates may result in average values with relatively large standard deviations and thus fail to reduce the uncertainty level. The inherent errors and uncertainties of this study is acknowledged in the following discussions and figures.

The PRRSv inactivation efficiency by NTP was calculated based on the ratio of downstream to upstream abundance of viable PRRSv, normalized by the ratio of downstream to upstream abundance of PRRSv genome copies determined by qPCR. The results are plotted in Fig. 4. For data acquired in Phase 1 (May), the figure illustrates the increasing trend in inactivation efficiency with increasing applied voltage, as expected, and the generally lower inactivation efficiency at the higher air flow rate (12 cfm) as compared to the lower air flow rate (5 cfm). These trends are as expected and agree with those observed in previous results involving inactivation of bacteriophage MS2 conducted at University of Michigan (Xia et al., 2019a). The measured PRRSv inactivation levels

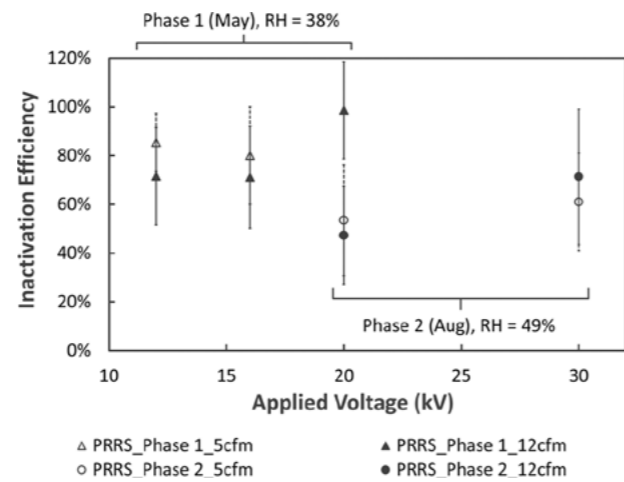


**Fig. 4.** Comparison of Phase 1 (May) and Phase 2 (August) PRRSv inactivation by NTP treatment at two air flow rates (5cfm and 12 cfm) and four voltages (12, 16, 20, and 30 kV).

by NTP are close to the relevant NTP inactivation levels reported by other research groups using different NTP reactor designs inactivating different bioaerosol species (Vaze et al., 2010; Wu et al., 2015). Vaze et al. constructed a 28 kV 600 μs pulse dielectric barrier grating discharge NTP reactor, which achieved 29%–97% inactivation (0.15–1.5 log) of aerosolized *E. coli* during the 10 s treatment time (Vaze et al., 2010). Wu et al. applied 14 kV 10 kHz AC power to a miniature wire-cylinder DBD reactor, and the reactor achieved ~80% inactivation (0.9 log) of aerosolized bacteriophage MS2 during a 0.12 s treatment time (with 20 W power) (Wu et al., 2015). Evident from the Phase 1 data presented in Fig. 4 is the fact that under similar experimental conditions, the effectiveness of the NTP in inactivating PRRSv aerosols was somewhat higher than the demonstrated effectiveness for inactivating MS2 with the same device at the same conditions; however, the large uncertainty in the results as indicated by the large confidence intervals allows only for a conclusion that the two viruses were likely inactivated comparably. Data acquired in Phase 2 (August), however, showed reduced inactivation efficiency. With 20 kV supplied voltage, the measured inactivation efficiency at both flow rates in Phase 2 was 30%–50% lower than the values acquired in Phase 1 or in the MS2 inactivation

study (Xia et al., 2019a). When the supplied voltage was increased from 20 kV to 30 kV, and the estimated discharge power was increased from 0.56 W at 20 kV (237 J/m<sup>3</sup> at 5 cfm) to 2.08 W at 30 kV (881 J/m<sup>3</sup> at 5 cfm), the packed bed NTP reactor showed increased PRRSv inactivation efficiencies at both flow rates, which were still lower than the values acquired with 20 kV power supply in Phase 1 or during the MS2 inactivation study (Xia et al., 2019a). It was found in our previous study that the bacteriophage MS2 inactivation by the packed bed NTP reactor with 30 kV power supply can lead to at least 2-log (99%) viable MS2 reduction (Xia et al., 2019a), which was significantly higher than the 30 kV results presented in Fig. 4. It is likely that the reduced NTP inactivation efficiency observed in Phase 2, as well as the large confidence intervals for all PRRSv inactivation results in both phases of the PRRSv test program, were due to increased accumulation of bulk virus solution (in this study DMEM) in the packed bed.

As discussed in previous paragraphs, incomplete evaporation of the PRRSv-laden droplets of DMEM was consistent throughout both Phase 1 and Phase 2 tests, while prior tests involving MS2 inactivation achieved complete or near complete droplet evaporation after several modifications to the experimental apparatus: lengthening the distance between the introduction of the droplets into the airstream and the NTP reactor; supplementing ambient air with dry compressed air (RH < 10%), and thereby lowering relative humidity and speeding evaporation; and producing smaller droplets via an ultrasonic atomizer. These remedies were not available or not possible for the current project. As a result, the significant unanswered question regarding the present results is the impacts, if any, of the persistent presence of liquid DMEM in fine droplets exposed to the non-thermal plasma and accumulating in the NTP reactor itself. DMEM is a solution of glucose in water. One hypothesis is that residual DMEM on aerosols or as aerosols passing through the NTP reactor may have the effect of protecting PRRSv from oxidation by the reactive species generated by the plasma. Whereas H<sub>2</sub>O alone, when dissociated, produces additional reactive species in the form of H<sup>+</sup> and OH<sup>-</sup>, hydrocarbons would act more as a sink for the plasma-generated species, consuming them in the course of their complete oxidation. There exists a separate branch of plasma environmental remediation that involves using plasmas to oxidize chemical contaminants in water supplies or wastewater. Support for this hypothesis came from preliminary tests prior to Phase 1. Prior testing at University of Michigan using MS2 phage determined that ozone (O<sub>3</sub>) produced by the NTP reactor had the potential to accumulate in the downstream impinger fluid, a phosphate buffered saline (PBS) consisting of small amounts of sodium and phosphorous salts dissolved in water. The dissolved ozone was found to continuously inactivate MS2 phage in the impinger during and after testing, potentially leading to a high bias in inactivation efficiency results. To compensate for this, sodium sulfite was routinely added to the PBS during MS2 testing, serving to consume O<sub>3</sub> and prevent inactivation of MS2 phage while in the impinger. However, when similar tests were conducted exposing PRRSv in DMEM to dissolved O<sub>3</sub>, the results showed no inactivation of PRRSv in DMEM by O<sub>3</sub>, suggesting that O<sub>3</sub> was consumed by oxidation reactions with the hydrocarbons in DMEM and therefore unavailable to chemically attack the PRRSv in solution. A second potential effect of residual DMEM could be in influencing the electrical properties of the packed bed and the strength or distribution of the plasma therein. In the packed bed, the plasma exists in the voids between the beads where the electric field increases above the threshold where electrical breakdown occurs in air. Accumulation of DMEM (approximate conductivity σ = 1.4 S/m (Chen et al., 2009)) in these spaces could provide a conductive electrical pathway that prevents such electric fields from forming. This, too, would be expected to reduce the apparent inactivation efficiency of tests involving DMEM as compared to tests in which evaporation of the liquid phase was more complete.

In order to test these hypotheses and the potential effects of accumulated DMEM, experiments were conducted after Phase 2 in which the packed bed NTP reactor was pre-soaked with known amounts of

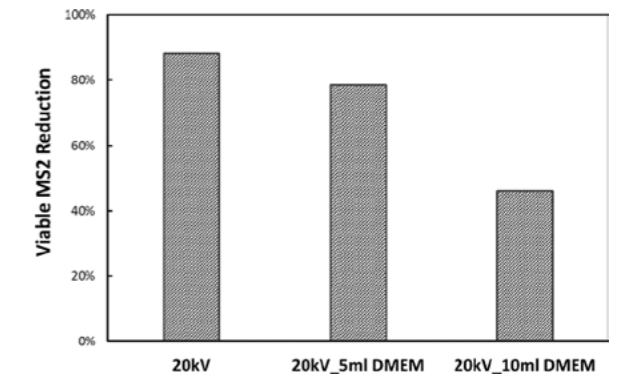


**Fig. 5.** Reduction (filtration + inactivation) of viable bacteriophage MS2 in response to 5 ml and 20 ml of DMEM added to and held within the NTP packed bed.

DMEM (5 mL or 10 mL), and the inactivation of MS2 aerosols by the “wet” reactor was measured. Fig. 5 shows the results of these tests in the form of viable MS2 reduction, comprising both physical filtration and NTP inactivation (with 20 kV), comparing samples collected at the upstream pre-treatment location against those collected at the downstream post-treatment location. The degree of viable MS2 reduction induced by the 20 kV reactor when dry was acquired from the previous bacteriophage MS2 inactivation study. With 5 mL DMEM sprayed into the packed bed, the viable MS2 reduction decreased from 88% (dry reactor) to 79%, and with 10 mL DMEM added, the viable MS2 reduction was further reduced to 46%. The figure proves that increasingly accumulated DMEM in the packed bed would reduce viable MS2 reduction from upstream to downstream locations of the packed bed NTP reactor, potentially by quenching reactive plasma species or preventing electric field build up for NTP discharge. With regard to the electrical effects, it seemed that the residual DMEM in the packed bed NTP reactor can increase the amplitude of transmitted current without changing the amplitude and waveform of the applied voltage. With 20 kV applied to the dry packed bed NTP reactor, the current had an amplitude of 0.40 mA. The addition of 5 ml of MEM to the packed bed increased the current amplitude to 0.48 mA, and the addition of 10 ml of MEM to the packed bed further increased the current amplitude to 0.56 mA. This was reasonable since the accumulation of liquid in the packed bed could reduce the overall resistance of the reactor and thus increasing the transmitted current. This discharge environment, however, may not be favorable for plasma generation, since more current would pass through the conductive liquid without ionizing air in the packed bed.

#### 4. Conclusion

In summary, this study provides the first demonstration of NTP inactivation of an airborne pathogen relevant to livestock. Both the non-enveloped bacteriophage MS2, and the enveloped PRRS virus were likely inactivated to comparable degrees. The highest PRRSv inactivation efficiency was 98.6% achieved in Phase 1 (May) with 20 kV voltage supplied to the packed bed NTP reactor at the wind tunnel flow rate of 12 cfm. However, size, composition of DMEM droplets and relative humidity were all likely contributors to variability in measured inactivation. Accumulated DMEM bulk liquid in the packed bed can reduce the reactor’s efficiency on viable PRRSv reduction, potentially through quenching reactive plasma species or preventing electric field build up for NTP discharge. Future studies with improved virus aerosolization methods and more consistent and dryer inlet air supply should be conducted to further examine how non-enveloped and enveloped viruses react to NTP inactivating environment. Overall, the results show promising results to inactivate airborne PRRSv by NTP and offer potential alternatives to pork producers to enhance their

biosecurity practices.

#### Supporting information

None.

#### Funding sources

This project is funded by the National Pork Board, under award # 16-098. The MS2-related work is supported by the National Institute of Food and Agriculture, U.S. Department of Agriculture, under award # 2016-67030-24892.

#### CRedit authorship contribution statement

**T. Xia:** Methodology, Investigation, Formal analysis, Writing - original draft, Writing - review & editing, Visualization. **M. Yang:** Methodology, Investigation, Formal analysis. **I. Marabella:** Methodology, Investigation. **E.M. Lee:** Methodology, Investigation. **B. Olson:** Methodology. **D. Zarling:** Methodology. **M. Torremorell:** Conceptualization, Funding acquisition, Writing - review & editing. **H.L. Clack:** Conceptualization, Funding acquisition, Writing - review & editing.

#### Declaration of Competing Interest

EML and HLC are affiliated with Taza Aya LLC; HLC is co-founder and CTO. TX, MY, IM, BO, DZ, and MT all declare no competing financial interest.

#### Acknowledgements

This project is funded by the National Pork Board, under award # 16-098. The MS2-related work is supported by the National Institute of Food and Agriculture, U.S. Department of Agriculture, under award # 2016-67030-24892. Any opinions, findings, conclusions, or recommendations expressed in this publication are those of the author(s) and do not necessarily reflect the view of the U.S. Department of Agriculture. The authors thank Minmeng Tang for helping in the experimental setup and Prof. Krista R. Wigginton and Yinyin Ye (Univ. of Michigan) for helping us with the MS2 inactivation test. The authors also thank Prof. John Foster and Selman Mujovic (Univ. of Michigan) for helping in the design and power consumption measurements of the packed bed NTP reactor used in this research.

#### References

- Arruda, A.G., Tousignant, S., Sanhueza, J., Vilalta, C., Poljak, Z., Torremorell, M., Alonso, C., Corzo, C.A., 2019. Aerosol detection and transmission of porcine reproductive and respiratory syndrome virus (PRRSV): what is the evidence, and what are the knowledge gaps? *Viruses* 11 (8), 712.
- Bolashikov, Z.D., Melikov, A.K., 2009. Methods for air cleaning and protection of building occupants from airborne pathogens. *Build. Environ.* 44 (7), 1378–1385.
- Chen, M.-T., Jiang, C., Vernier, P.T., Wu, Y.-H., Gundersen, M.A., 2009. Two-dimensional nanosecond electric field mapping based on cell electroporability. *PMC Biophys.* 2 (1), 9.
- Cho, J.G., Dee, S.A., Deen, J., Guedes, A., Trincado, C., Fano, E., Jiang, Y., Faaberg, K., Collins, J.E., Murtaugh, M.P., 2006. Evaluation of the effects of animal age, concurrent bacterial infection, and pathogenicity of porcine reproductive and respiratory syndrome virus on virus concentration in pigs. *Am. J. Vet. Res.* 67 (3), 489–493.
- Colby, M.M., 2013. DHS S&T's Agricultural Defense Program Overview. National Center for Foreign Animal and Zoonotic Disease Defense (FAZD).
- Dee, S., 2011. An Assessment of Air Filtration for Reducing the Risk of PRRSV Infection in Large Breeding Herds in Swine Dense Regions. NPB #09-209. .

- Farnsworth, J.E., Goyal, S.M., Kim, S.W., Kuehn, T.H., Raynor, P.C., Ramakrishnan, M., Anantharaman, S., Tang, W., 2006. Development of a method for bacteria and virus recovery from heating, ventilation, and air conditioning (HVAC) filters. *J. Environ. Monit.* 8 (10), 1006–1013.
- Heinlin, J., Morfill, G., Landthaler, M., Stolz, W., Isbary, G., Zimmermann, J.L., Shimizu, T., Karrer, S., 2010. Plasma medicine: possible applications in dermatology. *JDDG* 8 (12), 968–976.
- Hermann, J., Hoff, S., Muñoz-Zanzi, C., Yoon, K.-J., Roof, M., Burkhardt, A., Zimmerman, J., 2007. Effect of temperature and relative humidity on the stability of infectious porcine reproductive and respiratory syndrome virus in aerosols. *Vet. Res.* 38 (1), 81–93.
- Holtkamp, D.J., Kliebenstein, J.B., Neumann, E.J., Zimmerman, J.J., Rotto, H.F., Yoder, T.K., Wang, C., Yeske, P.E., Mowrer, C.L., Haley, C.A., 2013. Assessment of the economic impact of porcine reproductive and respiratory syndrome virus on United States pork producers. *J. Swine Health Prod.* 21 (2), 72–84.
- Hood, A., 2009. The effect of open-air factors on the virulence and viability of airborne *Francisella tularensis*. *Epidemiol. Infect.* 137 (6), 753–761.
- Keffaber, K., 1989. Reproductive failure of unknown etiol-ogy. *Am. Assoc. Swine Pract. Newsl* 1, 1–9.
- Lorenzetto, G., Lefebvre, A.H., 1977. Measurements of drop size on a plain-jet airblast atomizer. *Aiaa J.* 15 (7), 1006–1010.
- McAdams, R., 2001. Prospects for non-thermal atmospheric plasmas for pollution abatement. *J. Phys. D Appl. Phys.* 34 (18), 2810.
- Memarzadeh, F., Olmsted, R.N., Bartley, J.M., 2010. Applications of ultraviolet germicidal irradiation disinfection in health care facilities: effective adjunct, but not stand-alone technology. *Am. J. Infect. Control* 38 (5), S13–S24.
- Miaskiewicz-Peska, E., Lebkowska, M., 2012. Comparison of aerosol and bioaerosol collection on air filters. *Aerobiologia* 28 (2), 185–193.
- Millerick-May, M.L., Ferry, E., Benjamin, M., May, G.A., 2016. Routine Manure Removal From Swine Operations: a Potential Mechanism for Pathogen Dispersion. *Michigan Pork Symposium*, Lansing, Michigan.
- Niven, R.W., Ip, A.Y., Mittelman, S., Prestrelski, S., Arakawa, T., 1995. Some factors associated with the ultrasonic nebulization of proteins. *Pharm. Res.* 12 (1), 53–59.
- Noriega, E., Shama, G., Laca, A., Díaz, M., Kong, M.G., 2011. Cold atmospheric gas plasma disinfection of chicken meat and chicken skin contaminated with *Listeria innocua*. *Food Microbiol.* 28 (7), 1293–1300.
- Otake, S., Dee, S., Corzo, C., Oliveira, S., Deen, J., 2010. Long-distance airborne transport of infectious PRRSV and *Mycoplasma hyopneumoniae* from a swine population infected with multiple viral variants. *Vet. Microbiol.* 145 (3-4), 198–208.
- Perni, S., Liu, D.W., Shama, G., Kong, M.G., 2008. Cold atmospheric plasma decontamination of the pericarps of fruit. *J. Food Prot.* 71 (2), 302–308.
- Pitkin, A., Otake, S., Dee, S., Acvm, D.M.P.D., 2009a. Biosecurity Protocols for the Prevention of Spread of Porcine Reproductive and Respiratory Syndrome Virus. Swine Disease Eradication Center. University of Minnesota College of Veterinary Medicine, pp. 1–17.
- Pitkin, A., Deen, J., Dee, S., 2009b. Use of a production region model to assess the airborne spread of porcine reproductive and respiratory syndrome virus. *Vet. Microbiol.* 136 (1-2), 1–7.
- Ramos, S., MacLachlan, M., Melton, A., 2017. Impacts of the 2014-2015 Highly Pathogenic Avian Influenza Outbreak on the US Poultry Sector.
- Riley, R.L., 1961. Airborne pulmonary tuberculosis. *Bacteriol. Rev.* 25 (3), 243.
- Steckel, H., Eskandar, F., 2003. Factors affecting aerosol performance during nebulization with jet and ultrasonic nebulizers. *Eur. J. Pharm. Sci.* 19 (5), 443–455.
- Sun, Z., Wang, J., Bai, X., Ji, G., Yan, H., Li, Y., Wang, Y., Tan, F., Xiao, Y., Li, X., 2016. Pathogenicity comparison between highly pathogenic and NADC30-like porcine reproductive and respiratory syndrome virus. *Arch. Virol.* 161 (8), 2257–2261.
- Tian, K., Yu, X., Zhao, T., Feng, Y., Cao, Z., Wang, C., Hu, Y., Chen, X., Hu, D., Tian, X., 2007. Emergence of fatal PRRSV variants: unparallelled outbreaks of atypical PRRS in China and molecular dissection of the unique hallmark. *PLoS One* 2 (6), e526.
- Vaze, N.D., Gallagher, M.J., Park, S., Fridman, G., Vasilets, V.N., Gutsol, A.F., Anandan, S., Friedman, G., Fridman, A.A., 2010. Inactivation of bacteria in flight by direct exposure to nonthermal plasma. *IEEE Trans. Plasma Sci.* 38 (11), 3234–3240.
- Wheeler, S., Ingraham, H., Hollaender, A., Lill, N., Gershon-Cohen, J., Brown, E., 1945. Ultra-violet light control of air-borne infections in a naval training center: preliminary report. *Am. J. Public Health Nations Health* 35 (5), 457–468.
- Wu, Y., Liang, Y., Wei, K., Li, W., Yao, M., Zhang, J., Grinshpun, S.A., 2015. MS2 virus inactivation by atmospheric-pressure cold plasma using different gas carriers and power levels. *Appl. Environ. Microbiol.* 81 (3), 996–1002.
- Xia, T., Kleinheksel, A., Lee, E., Qiao, Z., Wigginton, K., Clack, H., 2019. Inactivation of airborne viruses using a packed bed non-thermal plasma reactor. *J. Phys. D Appl. Phys.* 52 (25), 255201.
- Xia, T., Kleinheksel, A., Wigginton, K.R., Clack, H.L., 2020. Suspending Viruses in an Airstream Using a Consumer-grade Ultrasonic Humidifier. In preparation. .
- Xiao, G., Xu, W., Wu, R., Ni, M., Du, C., Gao, X., Luo, Z., Cen, K., 2014. Non-thermal plasmas for VOCs abatement. *Plasma Chem. Plasma Process.* 34 (5), 1033–1065.
- Zhou, L., Wang, Z., Ding, Y., Ge, X., Guo, X., Yang, H., 2015. NADC30-like strain of porcine reproductive and respiratory syndrome virus, China. *Emerging Infect. Dis.* 21 (12), 2256.



# ATTACHMENT 13.2

## SCIENTIFIC ARTICLES ON INORGANIC POLLUTANT REMOVAL

Wen-Jun Liang, H.-P. F.-X.-Q. (2011). Performance of non-thermal DBD plasma reactor during the removal of hydrogen sulfide. *Journal of Electrostatics* Volume 69, Issue 3, 206-213.



## Performance of non-thermal DBD plasma reactor during the removal of hydrogen sulfide

Wen-Jun Liang\*, Hong-Ping Fang, Jian Li, Feng Zheng, Jing-Xin Li, Yu-Quan Jin

College of Environmental & Energy Engineering, Beijing University of Technology, No.100 Ping Le Yuan, Chaoyang District, Beijing 100124, PR China

### ARTICLE INFO

#### Article history:

Received 4 January 2010  
Received in revised form  
11 September 2010  
Accepted 25 March 2011  
Available online 9 April 2011

#### Keywords:

Non-thermal plasma  
Dielectric barrier discharge  
Lissajous diagram  
Specific energy density  
Hydrogen sulfide

### ABSTRACT

Destruction of hydrogen sulfide using dielectric barrier discharge plasma in a coaxial cylindrical reactor was carried out at atmospheric pressure and room temperature. Three types of DBD reactor were compared in terms of specific energy density (SED), equivalent capacitances of the gap (Cg) and the dielectric barrier (Cd), energy yield (EY), and H<sub>2</sub>S decomposition. In addition, byproducts during the decomposition of H<sub>2</sub>S and destruction mechanism were also investigated. SED for all the reactors depended almost linearly on the voltage. In general, Cg decreased with increasing voltage and with the existence of pellet material, while Cd displayed the opposite trend. The removal efficiency of H<sub>2</sub>S increased substantially with increasing AC frequency and applied voltage. Longer gas residence times also contributed to higher H<sub>2</sub>S removal efficiency. The choice of pellet material was an important factor influencing the H<sub>2</sub>S removal. The reactor filled with ceramic Raschig rings had the best H<sub>2</sub>S removal performance, with an EY of 7.30 g/kWh. The likely main products in the outlet effluent were H<sub>2</sub>O, SO<sub>2</sub>, and SO<sub>3</sub>.

© 2011 Elsevier B.V. All rights reserved.

### 1. Introduction

There is a growing concern that malodorous pollution at sewage and industrial wastewater treatment plants is not only a nuisance in the ambient environment but may also produce adverse health effects in humans. The odors are mainly caused by sulfurous compounds such as hydrogen sulfide (H<sub>2</sub>S), which has an extremely low odor threshold, is highly toxic and has a characteristic rotten-egg smell [1]. Prolonged exposure to a concentration of 300 ppm of H<sub>2</sub>S in the air has caused death, and concentrations exceeding 2000 ppm can be fatal to humans are exposed for only a few minutes [2]. Therefore, the effective removal of these sulfur compounds from air is highly desired.

Traditional methods to control the emissions of gaseous odor-causing materials into the atmosphere include absorption (wet scrubbing), adsorption, incineration (either thermal or catalytic), masking and biofiltration [3–10]. Unfortunately, all these technologies may have limitations when removing odor-causing substances from gas streams. Absorption and adsorption transfer odor-causing materials from the gas phase to scrubbing liquids or solid adsorbents, potentially causing other forms of pollution while resolving

the odor problems. Incineration can be effective in controlling odor-causing substances. However, the possibility of generating other air pollutants such as NO<sub>x</sub>, potential poisoning of the catalyst, and relatively high cost associated with this technology should be taken into account. The technical and economic limitations of traditional odor control methods are particularly important for low concentration odor abatement. Nowadays, some new oxidation technologies such as microwave discharge [11] and photocatalytic oxidation [12–14] are also used to remove odor gases.

Due to some unique advantages (rapid reaction at ambient temperature under atmospheric pressure and achievement of high electron energies within a short residence time) as well as ease of operation, non-thermal plasma (NTP) processing has received considerable attention. Recent progress in applying NTP technology to the control of polluting gases such as acidifying components (SO<sub>2</sub> [15,16], NO<sub>x</sub> [17,18]) and volatile organic compounds [19–22] is very encouraging. While plasma technology has been used to remove H<sub>2</sub>S [18,23–26], in our opinion, the combination of plasma and pellets in the reactor is likely to be more effective. There are also opportunities for further work – very few studies have been carried out using AC of 100–400 Hz, and reports on the byproducts formed during H<sub>2</sub>S decomposition in dielectric barrier discharge (DBD) systems are few. Many literatures reported the pollutants removal with plasma reactor, in which the spherical ceramic pellets were filled.

\* Corresponding author. Tel.: +86 10 67392080.  
E-mail address: [liangwenj1978@hotmail.com](mailto:liangwenj1978@hotmail.com) (W.-J. Liang).

In the present paper, we present a new DBD plasma reactor, filled with glass beads or ceramic Raschig rings as “pellets”. The main objective of this study is to compare the decomposition of H<sub>2</sub>S with and without the pellets. The electrical parameters during the discharge process and the energy efficiency for H<sub>2</sub>S removal were investigated at the same time. The byproducts during the decomposition of H<sub>2</sub>S were also evaluated, enabling destruction mechanisms to be discussed.

## 2. Experimental setup

### 2.1. Experimental apparatus

The schematic diagram of the experimental setup for the present study is shown in Fig. 1. The setup consisted of a DBD plasma reactor, an AC power supply (0–100 kV, 50–500 Hz, sine wave), a continuous flow gas supply system and electric and gaseous analytical systems. H<sub>2</sub>S (99.9%, Beijing Zhaoge Special Gas Co.) was mixed with compressed air through a mixing chamber and then introduced into the DBD reactor. The flow rate and H<sub>2</sub>S concentration were adjusted by mass flow controllers (MFC). The coaxial cylindrical DBD reactor was made of PMMA with an inner diameter of 28 mm and wall thickness of 2 mm wrapped with an iron mesh, 20 cm long, which acted as a ground electrode. The inner discharge electrode was a tungsten wire, 1.25 mm diameter, placed on the axis of the reactor. The relative humidity in the reactor was controlled at 30% with a thermohygrometer. Ceramic Raschig rings or glass pellets were chosen as pellets and were packed randomly packed into the DBD reactor. When a sufficiently high voltage was applied to the reactor, micro-discharges began, initiating a series of chemical reactions.

### 2.2. Analyses and procedures

The concentrations of H<sub>2</sub>S before and after plasma treatment were determined by a spectrophotometric method. H<sub>2</sub>S in the gas stream was absorbed by a solution of N,N-dimethyl-p-phenylenediamine in acid, to which FeCl<sub>3</sub> was added afterward to form methylene blue. H<sub>2</sub>S was then determined by measuring absorbance at 665 nm with a spectrophotometer (UV/vis 2000, Shanghai Precision & Scientific Instrument CO., LTD, China). A typical standard curve relating absorbance to the mass of H<sub>2</sub>S in solution is shown in Fig. 2. A linear relationship between absorbance and mass of H<sub>2</sub>S in solution was observed with a correlation coefficient of 0.999. The initial concentration of H<sub>2</sub>S was 30 ppm and the gas flow rate in the reactor was 8–18 L/min.

The H<sub>2</sub>S removal efficiency is calculated as:

$$\eta_{H_2S}(\%) = \frac{C_{in} - C_{out}}{C_{in}} \times 100 \quad (1)$$

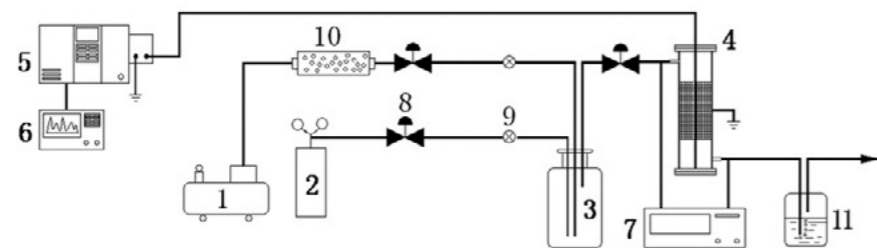


Fig. 1. Schematic diagram of the experimental setup 1. Air compressor 2. H<sub>2</sub>S gas cylinder 3. Mixing chamber 4. DBD reactor 5. AC power supply 6. Oscillograph 7. Spectrophotometer 8. MFC 9. Needle valve 10. Gas filtration system 11. Absorbent.

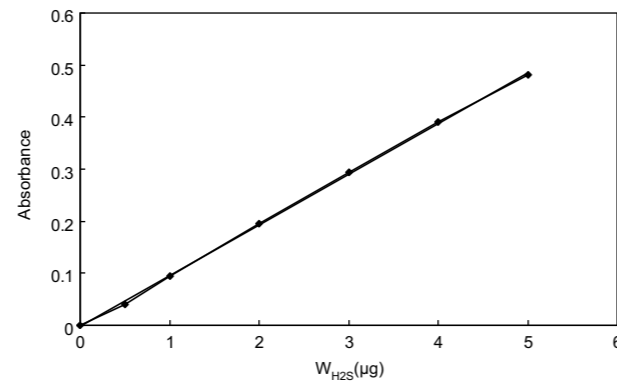


Fig. 2. Typical standard curve for light absorbance with the mass of H<sub>2</sub>S.

where  $C_{in}$  and  $C_{out}$  denote the inlet and outlet concentrations ( $mg/m^3$ ) of H<sub>2</sub>S respectively.

The products of the reaction were detected by GC–MS (Trace DSQ, USA). Intermediate product analysis was done using EI mode, 70 eV and full scan. The byproducts were also analyzed by an ion chromatography (IC) (Metrohm 861, Switzerland).

The surface areas of the pellets used in the experiment were measured using gas adsorption principles (Detected by Micromeritics, NOVA 1000, USA).

### 2.3. Electrical measurements

The plasma was generated at atmospheric pressure and room temperature. The voltage and current waves were measured by an oscilloscope (Tektronix 2014). To investigate the electric characteristics of the discharge, the voltage applied to the reactor was sampled by a 12500:1 voltage divider. The current was determined from the voltage drop across a shunt resistor ( $R_3 = 10\text{ k}\Omega$ ) connected in series with the ground electrode. In order to obtain the total charge and discharge power simultaneously, a capacitor ( $C_m = 2\text{ }\mu\text{F}$ ) was inserted between the reactor and the ground. The electrical power provided to the discharge was measured using the V–Q Lissajous diagram [27]. The discharge power is directly proportional to the area of the parallelogram in the diagram and can be calculated according to the relation:

$$P = f \cdot C_m \cdot S \quad (2)$$

where  $C_m$  is the  $2\text{ }\mu\text{F}$  measuring capacitance,  $f$  is the frequency and  $S$  is the area of the parallelogram.

In addition to energy consumption, the equivalent capacitance during the discharge process is an important parameter. The two gradients of the parallelogram of the V–Q Lissajous diagram

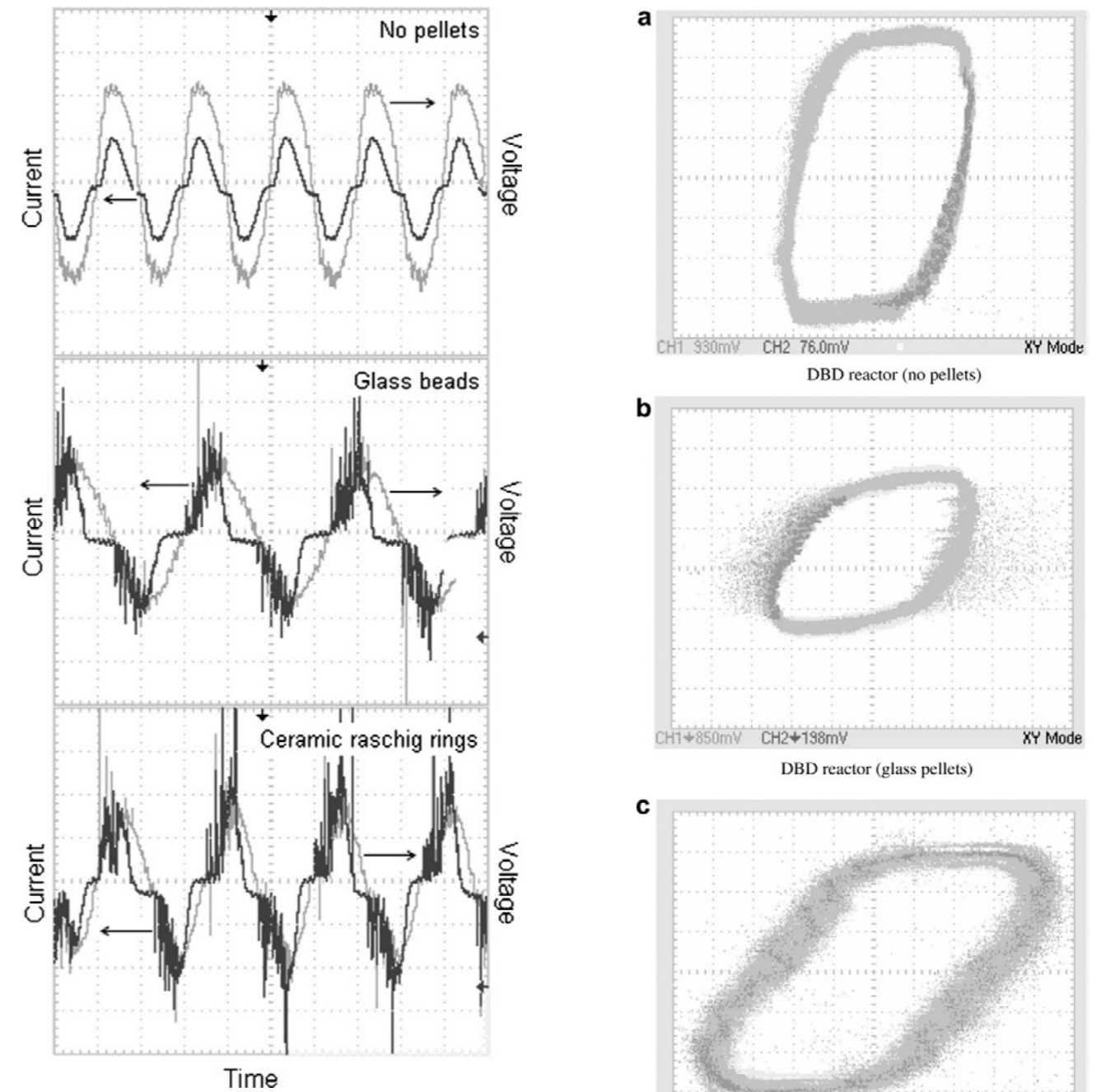


Fig. 3. Waveforms of applied voltage and discharge current (13 kV applied voltage, 300 Hz frequency).

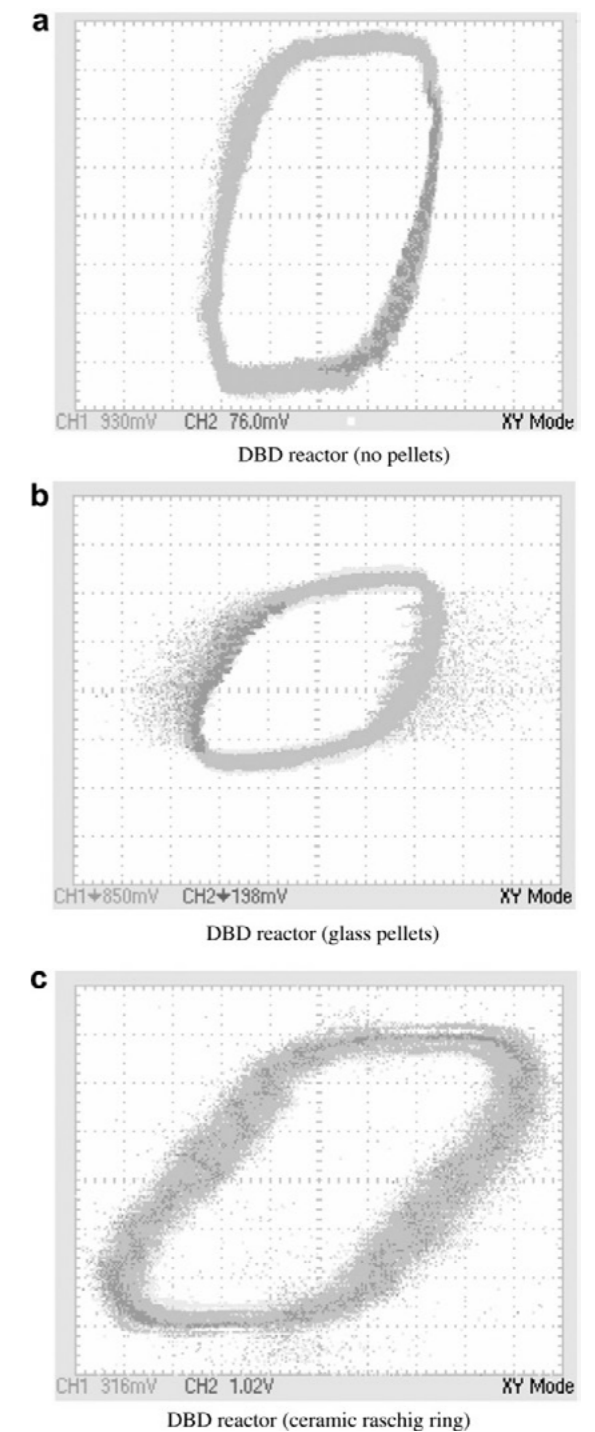


Fig. 4. Typical Lissajous figures for three kinds of dielectric barrier discharge (13 kV applied voltage, 300 Hz frequency).

represent the capacitances in the equivalent circuit of the reactor. In this paper,  $C$ ,  $C_d$ , and  $C_g$  denote the total equivalent capacitance, the equivalent capacitance of the dielectric barrier and the equivalent capacitance of the gap, respectively. The relationship between them can be expressed as:

$$C = \frac{C_d \times C_g}{C_d + C_g} \quad (3)$$

The specific energy density (SED) was defined as the average power dissipated in the discharge, divided by the total gas flow rate:

$$SED \left( \frac{J}{l} \right) = \frac{P(W)}{Q(l/min)} \times 60 \quad (4)$$

where  $P$  and  $Q$  denote the discharge power ( $W$ ) and gas flow rate ( $l/min$ ).

As a measure of the energy efficiency, the energy yield (EY) was defined:



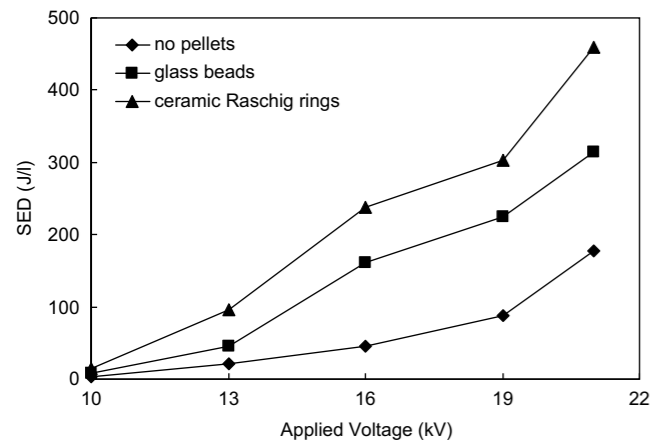


Fig. 5. Variation of SED as a function of applied voltage.

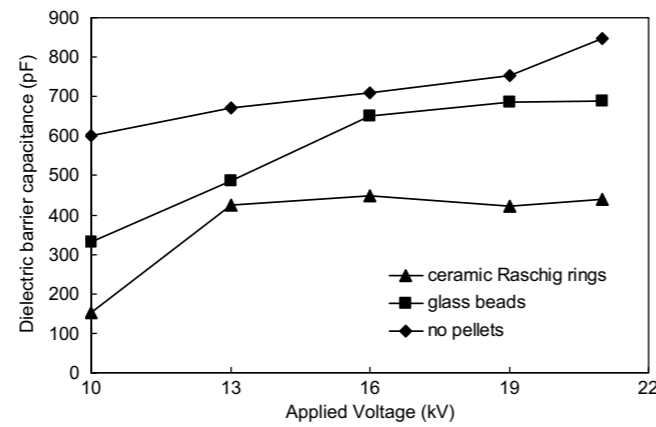


Fig. 7. Variation of dielectric barrier capacitance as a function of applied voltage.

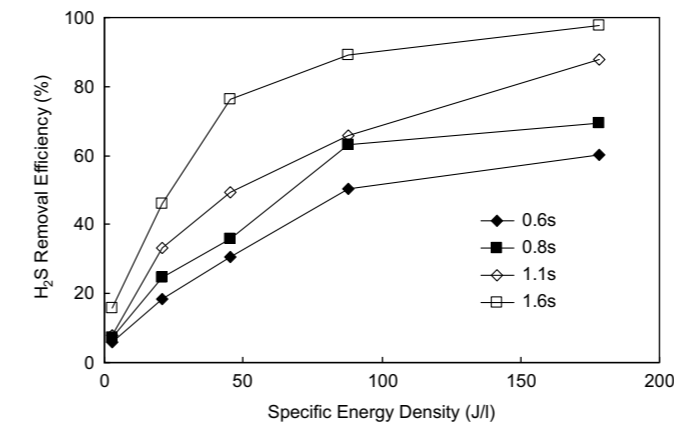


Fig. 9. H<sub>2</sub>S removal as a function of SED under different gas residence time inlet concentration was 30 ppm; and frequency was 300 Hz.

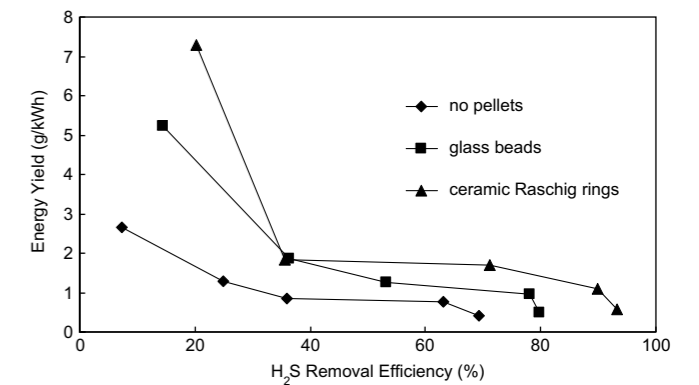


Fig. 11. Relationship between energy yield and H<sub>2</sub>S removal Inlet concentration was 30 ppm; gas residence time was 0.8 s; and frequency was 300 Hz.

$$EY(g/kWh) = \frac{C_{in} - C_{out}}{SED} \times 3.6 \quad (5)$$

where  $C_{in}$  and  $C_{out}$  denote the inlet and outlet concentrations ( $mg/m^3$ ) of H<sub>2</sub>S respectively.

### 3. Results and discussion

#### 3.1. Electrical discharge characteristics

Typical applied voltage and discharge current waveforms for various reactors are shown in Fig. 3. The applied voltage was 13 kV (300 Hz, sinusoidal waveform), and was slightly distorted by the microdischarge current, especially when the reactor contained pellets. These micro-discharges, which were uniformly distributed over the surface of the dielectric, were of nanosecond duration and generated radicals, excited atomic or molecular species that initiate plasma chemical reactions. Obviously, the number of micro-discharge pulses in the presence of pellets was much larger than without pellets. The number of microdischarge is directly related to the pollutant decomposition via non-thermal plasma. The discharge voltage and current showed typical barrier discharge waveforms; that is, the microdischarge current appeared when the applied voltage passed through certain values (discharge onset voltages) to the positive or negative maximum, which is in agreement with the literature [27]. Typically, the voltage charge Lissajous figure of the

three kinds of reactors was shaped like a parallelogram, as shown in Fig. 4. The area of this parallelogram was equal to the energy dissipated during one period of the voltage [28]. Fig. 5 shows the variation in SED as a function of applied voltage in the presence and absence of pellets. The SED values for reactors with different pellets were generally in the order: ceramic Raschig rings reactor > glass beads reactor > no pellets reactor under the same experimental conditions. When the applied voltage was below 13 kV, the SED of the ceramic Raschig rings reactor was slightly higher than that of the glass beads reactor and the no pellets reactor. At an applied voltage of 13 kV, the SEDs for the three reactors were 21 J/l (no pellets), 45 J/l (glass beads) and 96 J/l (ceramic Raschig rings). This order was maintained with further increase in voltage, as the SED increased substantially for all reactors, particularly those containing pellets. As the applied voltage increased from 13 to 21 kV, the SED of the reactors increased from 21 J/l to 178 J/l (no pellets), 45 J/l to 315 J/l (glass beads), and 96 J/l to 459 J/l (ceramic Raschig rings). In an electric field, materials such as ceramics and glass are able to store energy. The relative dielectric constants of the ceramic and glass at normal temperature and pressure were 9.16 and 4.10, which meant that the energy storage ability of the ceramic was higher than that of glass. At low applied voltage, there was little effect of the materials in the electric field, and the plasma was mainly of the type referred to as corona discharge, which occurs in regions of high electric field near electrically stressed wire edges. When the voltage was high enough, dielectric barrier discharge began to occur, and the pellets

stored more energy as the electric field strength increased. More micro-discharges appeared under these electric fields, which resulted in initiation of chemical reactions between H<sub>2</sub>S molecules, radicals and electrons.

For DBD plasma, the plasma reactor can be regarded as equivalent to a capacitive load, so the equivalent capacitance of the gap ( $C_g$ ) and the equivalent capacitance of the dielectric barrier ( $C_d$ ) are important parameters. In accordance with methods in literature [29,30],  $C_g$  and  $C_d$  for our experiments were calculated using V-Q Lissajous diagrams. Fig. 6 shows the equivalent gap capacitance ( $C_g$ ) as a function of applied voltage for the different kinds of DBD reactor. In general,  $C_g$  decreased gradually with increasing applied voltage. At the same time,  $C_g$  of the DBD reactor with ceramic Raschig rings decreased sharply when the applied voltage was 10–16 kV. For the reactor with ceramic Raschig rings, when the applied voltage increased from 10 to 21 kV,  $C_g$  decreased from 19 pF to 6 pF. This is consistent with the observations reported by Takaki et al. [30].

The equivalent capacitance of the dielectric barrier ( $C_d$ , obtained by V-Q Lissajous diagrams) as a function of applied voltage is shown in Fig. 7. All the reactors displayed the same general trend, with  $C_d$  increasing with higher applied voltage.  $C_d$  values for the various reactors were in the order: no pellets reactor > glass beads reactor > ceramic Raschig rings reactor. When the applied voltage increased from 10 kV to 21 kV, the  $C_d$  values changes as follows: no pellets reactor increased from 600 pF to 847 pF; ceramic Raschig rings reactor increased from 151 pF to 441 pF; glass beads reactor increased

#### 3.2. H<sub>2</sub>S decomposition in the plasma

##### 3.2.1. Effect of applied frequency on H<sub>2</sub>S decomposition

Experiments were conducted to determine the dependence of H<sub>2</sub>S removal efficiency on AC frequency and applied voltage, as shown in Fig. 8. Both the number and average energy of electrons and active radicals apparently increased with increasing applied voltage and AC frequency, leading to higher H<sub>2</sub>S removal efficiency. When the frequency was lower than 300 Hz, H<sub>2</sub>S removal efficiency increased slowly with frequency, while it increased sharply when frequency was higher than 300 Hz. The dependence of  $\eta_{H_2S}$  on applied voltage was similar to the dependence on frequency. An increase in AC frequency from 100 Hz to 400 Hz, resulted in an increase in H<sub>2</sub>S removal efficiency from 6.8% to 7.8% with for an applied voltage of 10 kV, and a very significant increase from 40.4% to 82.8% was observed when the applied voltage was 21 kV. When the amplitude of the applied voltage is low, the voltage across the discharge gap is not high enough to ignite the plasma. Once the voltage was high enough to cause breakdown of the gas, the charge was phase shifted with respect to the voltage due to resistive losses in the charge [29].

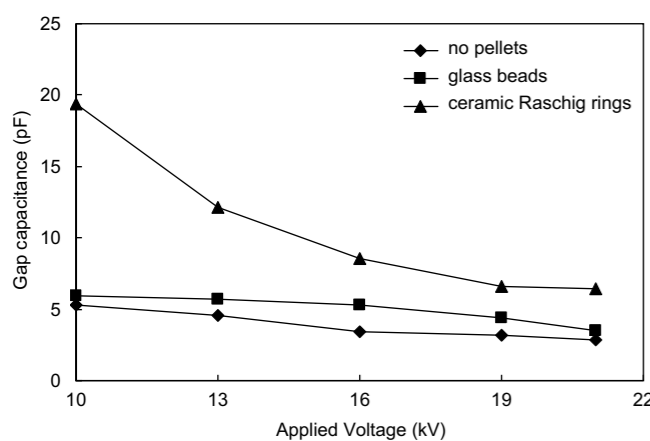


Fig. 6. Variation of gap capacitance as a function of applied voltage.

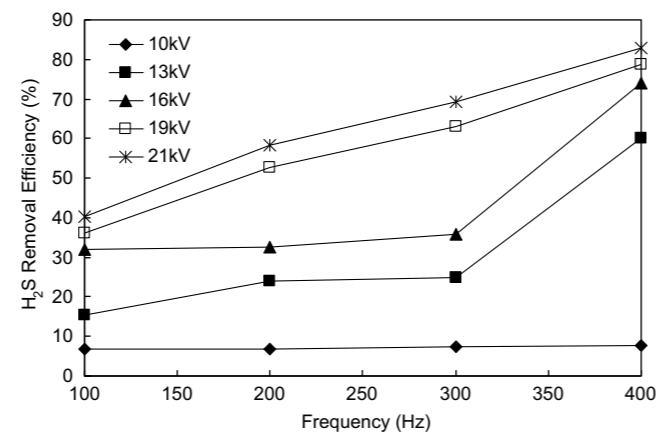


Fig. 8. H<sub>2</sub>S removal as a function of frequency under different applied voltage inlet concentration was 30 ppm; gas flow rate was 0.25l/s, and residence time was 0.8 s.

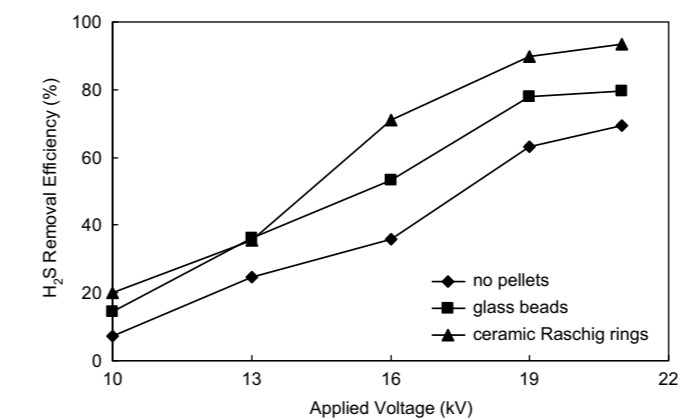


Fig. 10. H<sub>2</sub>S removal as a function of applied voltage for different reactors inlet concentration was 30 ppm; gas residence time was 0.8 s; and frequency was 300 Hz.

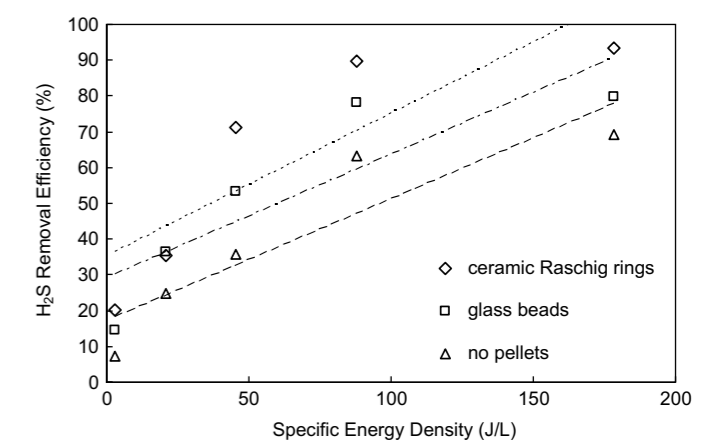


Fig. 12. Relationship between  $\eta$  and SED and linear fits for different reactors.

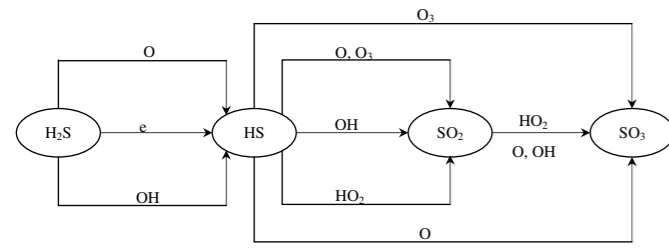


Fig. 13. Dominant pathways leading to the destruction of H<sub>2</sub>S molecules.

These resistive losses arise as free electrons or radicals transfer all or part of their kinetic energy to the target molecules through inelastic collisions, leading to destruction of the target molecule.

According to the investigation by Xia et al. [17], when their plasma system was operated for a long enough time, the temperature of the whole plasma zone was observed to increase from 150 °C to 250 °C with peak voltage rising from 3 kV to 9 kV and fixed frequency of 20 kHz. In our experiment, during the course of plasma discharge, the temperature of the plasma zone was only 5–8 °C higher than room temperature.

### 3.2.2. Effect of gas residence time on H<sub>2</sub>S decomposition

Fig. 9 presents the influence of gas residence time and SED on H<sub>2</sub>S decomposition. Similar trends were observed for different gas residence times. It is found that the effect of increasing the gas residence time depends on the SED – a sharp increase in removal efficiency was observed when the SED was lower than 87.9 J/l while only a slight increase resulted when the SED was higher than 87.9 J/l. Longer gas residence times result in a larger probability of collisions between H<sub>2</sub>S molecules and electrons and radicals, and hence enhance the removal of H<sub>2</sub>S. Furthermore, with increasing SED, the energy throughout the entire discharge volume was increasing, leading to micro-discharges throughout the reactor and stimulating the chemical reactions between H<sub>2</sub>S molecules and electrons and radicals. Similar experiment results were obtained by Xia et al. [11,17].

### 3.2.3. Effect of pellets on H<sub>2</sub>S removal

Fig. 10 represents the H<sub>2</sub>S removal process for DBD reactors containing different pellets as a function of applied voltage. The H<sub>2</sub>S

removal efficiencies followed the same trend, that is,  $\eta_{\text{H}_2\text{S}}$  was enhanced with increasing applied voltage. The H<sub>2</sub>S removal efficiency of three reactors was in the order ceramic Raschig rings reactor > glass beads reactor > no pellets reactor for the same experimental conditions. For example, at 10 kV applied voltage, the efficiency values were: 20.2% (ceramic Raschig rings reactor), 14.5% (glass beads reactor) and 7.4% (no pellets reactor), while at 21 kV applied voltage, the values were 93.3%, 79.7% and 69.3% respectively. Durme et al. [31] indicated that packing pellets are helpful for expanding the discharge region because the streamers (or micro-discharges) are apt to propagate along the solid surfaces. Our experiment results demonstrate that the packing material is an important factor influencing H<sub>2</sub>S removal. In our experiment, the BET surface areas of the ceramic Raschig rings and glass beads were 0.2461 m<sup>2</sup>/g and 0.0353 m<sup>2</sup>/g. This implies that more H<sub>2</sub>S molecules, electrons and radicals could react with one another on the ceramic pellet surface than on the glass pellet surface. And both reactors with pellets had higher H<sub>2</sub>S decomposition ability than the no pellets reactor. As mentioned above in Fig. 5, we observed that the SED values of the different pellet reactors were in the order ceramic Raschig rings reactor > glass beads reactor > no pellets reactor under the same experimental conditions, which means more energetic electrons and radicals were generated in the ceramic Raschig rings reactor than the other reactors, which is consistent with the observed higher H<sub>2</sub>S removal efficiency.

### 3.3. Energy efficiency for H<sub>2</sub>S removal

We have used the energy yield (EY) to characterize the H<sub>2</sub>S removal ability of each plasma reactor. From Equation (5), it can be seen that EY is inversely proportional to SED. Fig. 11 illustrates the relationship between EY and H<sub>2</sub>S removal efficiency for the three reactors. Obviously, as the H<sub>2</sub>S removal efficiency increased, the energy yield decreased for all reactors. The highest EY was 7.30 g/kWh for the ceramic Raschig rings reactor. Once the removal efficiency ratio for the glass beads reactor and ceramic Raschig rings reactor exceeded 35%, the EY stabilized at about 1.8 g/kWh, double the energy efficiency of the no pellets reactor.

The decomposition rate of H<sub>2</sub>S molecules depends on both the concentration of H<sub>2</sub>S itself and the concentrations of the active species generated in the reactor. The concentrations of active

species generated are proportional to the discharge power. This leads to the important relationship between H<sub>2</sub>S removal and discharge power, as shown in Equation (6).

$$\eta = \text{SED} \times K_d + b \quad (6)$$

where  $K_d$  is the reaction rate constant, and  $b$  is the intercept.

Variation in  $\eta$  as a function of SED is given in Fig. 12. The reaction rate constants for ceramic, glass and no pellet reactors were 0.3982, 0.3453 and 0.3397, respectively. The ceramic Raschig rings reactor had the best H<sub>2</sub>S decomposition capability of all the reactors.

### 3.4. Destruction mechanism for H<sub>2</sub>S and analysis for by-products

A DBD plasma generates electrons with sufficient energy to cause the formation of gas-phase radicals, thereby driving the reactions of decomposition and oxidation of H<sub>2</sub>S to form end products including H<sub>2</sub>O, SO<sub>2</sub>, and SO<sub>3</sub>. The removal of H<sub>2</sub>S probably depends on two mechanisms: (a) direct removal caused by the collision of electrons and (b) reaction between H<sub>2</sub>S molecules and gas-phase radicals (indirect gas-phase radical reaction). Gas-phase radicals may consist of O<sup>•</sup>, OH<sup>•</sup>, HO<sub>2</sub><sup>•</sup> and O<sub>3</sub>. Suggested reactions at normal temperature and pressure are shown in Equations (7)–(18) [11,14–16,25,26].

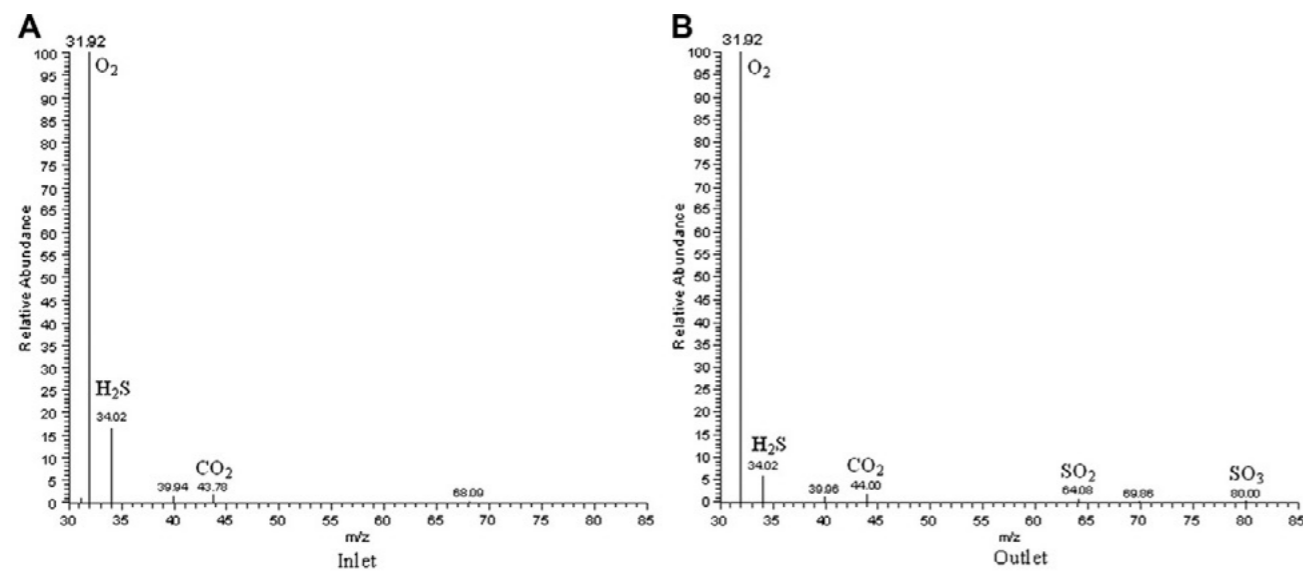
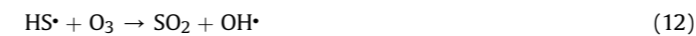


Fig. 14. Mass spectrogram of inlet and outlet products.

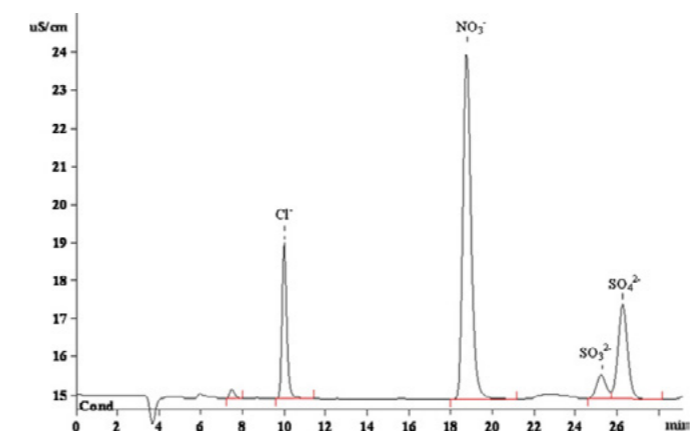


Fig. 15. Products in inlet and outlet gas.



It can be seen from these reactions that generation of HS radicals is a very important step resulting in further oxidation and removal of H<sub>2</sub>S molecules. The dominant pathways for the removal of H<sub>2</sub>S are described in Fig. 13.

In our experiments, the contents of both the inlet gas and outlet effluent were confirmed through GC-MS. From the mass spectrograms of inlet and outlet gases in Fig. 14A and B, we could determine that the main components of the inlet gas were O<sub>2</sub>, H<sub>2</sub>S and CO<sub>2</sub>, while in the outlet gas, the main products were O<sub>2</sub>, less H<sub>2</sub>S, CO<sub>2</sub>, SO<sub>2</sub> and SO<sub>3</sub>. The assignment of the peaks at  $m/z = 39.94$ ,  $68.09$  and  $69.86$  requires further investigation.

To confirm the products of H<sub>2</sub>S decomposition, the gas products were sampled into distilled water and the ion chromatography (IC) technique was employed to analyze products qualitatively. As shown in Fig. 15, the main anions were Cl<sup>-</sup>, NO<sub>3</sub><sup>-</sup>, SO<sub>4</sub><sup>2-</sup>, and no other anions were detected in the sample using IC. The SO<sub>2</sub> and SO<sub>3</sub> in outlet gas are the products of H<sub>2</sub>S decomposition, while the NO<sub>3</sub><sup>-</sup> is assumed to result from nitrogen oxides in the effluent. The origin of Cl<sup>-</sup> is unclear at this stage.

## 4. Conclusions

The abatement of H<sub>2</sub>S with non-thermal DBD plasma was experimentally investigated in a coaxial cylindrical reactor. The main results are that the efficiencies (as measured by the SED) for reactors containing different pellets were in the order: ceramic Raschig rings reactor > glass beads reactor > no pellets reactor under the same experimental conditions.  $\eta$  generally decreased gradually with increasing applied voltage, but  $K_d$  increased with higher applied voltage. Both the number and average energy of the electrons and active radicals increased with increased applied voltage or AC frequency, which led to higher H<sub>2</sub>S removal efficiency. Longer gas residence times (which result in greater collision probability between H<sub>2</sub>S molecules and electrons and radicals) enhanced the removal of H<sub>2</sub>S, as did the choice of pellet material. The highest EY was 7.30 g/kWh for the ceramic Raschig rings reactor. The likely major products in the outlet effluent were H<sub>2</sub>O, SO<sub>2</sub>, and SO<sub>3</sub>.

## Acknowledgment

This work was supported by the Youth Scientific Research Fund of BJUT(X1005013200802).

## References

- [1] B. Mills, Review of methods of odor control, *Filtr. Sep.* 32 (1995) 146–152.
- [2] M. Tomar, T.H.A. Abdullah, Evaluation of chemicals to control the generation of malodorous hydrogen sulfide in waste water, *Water Res.* 28 (1994) 2545–2552.
- [3] D. Gabriel, M.A. Deshusses, Retrofitting existing chemical scrubbers to bio-trickling filters for H<sub>2</sub>S emission control, *Proc. Natl. Acad. Sci. U S A* 100 (2003) 6308–6312.
- [4] M.A. Daley, C.L. Mangun, J.A.D. Barr, S. Riha, A. Lizzio, G. Donnals, J. Economy, Adsorption of SO<sub>2</sub> onto oxidized and heat-treated activated carbon fibers (ACFs), *Carbon* 35 (1997) 411–417.
- [5] A. Bagreev, S. Katikaneni, S. Parab, T.J. Bandoz, Desulfurization of digester gas: prediction of activated carbon bed performance at low concentrations of hydrogen sulfide, *Catal. Today* 99 (2005) 329–337.
- [6] D.N. Thanh, K. Block, T.J. Bandoz, Adsorption of hydrogen sulfide on montmorillonites modified with iron, *Chemosphere* 59 (2005) 343–353.
- [7] M.N. Bae, M.K. Song, Y. Kim, K. Seff, The catalytic activity of vanadium pentoxide film modified electrode on the electrochemical oxidation of hydrogen sulfide in alkaline solutions, *Micropor. Mesopor. Mater.* 63 (2003) 21–31.
- [8] X.H. Wang, T.H. Sun, J. Yang, L. Zhao, J.P. Jia, Low-temperature H<sub>2</sub>S removal from gas streams with SBA-15 supported ZnO nanoparticles, *Chem. Eng. J.* 142 (2008) 48–55.
- [9] L.A. Fenouil, S. Lynn, Study of calcium-based sorbents for high-temperature H<sub>2</sub>S removal. 1. Kinetics of H<sub>2</sub>S sorption by uncalcined limestone, *Ind. Eng. Chem. Res.* 34 (1995) 2324–2333.

- [10] L.A. Fenouil, S. Lynn, Study of calcium-based sorbents for high-temperature H<sub>2</sub>S removal. 2. Kinetics of H<sub>2</sub>S sorption by calcined limestone, *Ind. Eng. Chem. Res.* 34 (1995) 2334–2342.
- [11] L.Y. Xia, D.H. Gu, J. Tan, W.B. Dong, H.Q. Hou, Photolysis of low concentration H<sub>2</sub>S under UV/VUV irradiation emitted from microwave discharge electrodeless lamps, *Chemosphere* 71 (2008) 1774–1780.
- [12] R. Portela, B. Sánchez, J.M. Coronado, R. Candal, S. Suárez, Selection of TiO<sub>2</sub>-support: UV-transparent alternatives and long-term use limitations for H<sub>2</sub>S removal, *Catal. Today* 129 (2007) 223–230.
- [13] R. Portela, M.C. Canela, B. Sánchez, F.C. Marques, A.M. Stumbo, R.F. Tessinari, J.M. Coronado, S. Suárez, H<sub>2</sub>S photodegradation by TiO<sub>2</sub>/M-MCM-41 (M = Cr or Ce): deactivation and by-product generation under UV-A and visible light, *Appl. Catal. B* 84 (2008) 643–650.
- [14] E. Subramanian, J.O. Baeg, S.M. Lee, S.J. Moon, K.J. Kong, Dissociation of H<sub>2</sub>S under visible light irradiation ( $\lambda \geq 420$  nm) with FeGaO<sub>3</sub> photocatalysts for the production of hydrogen, *Int. J. Hydrogen Energy* 33 (2008) 6586–6594.
- [15] M.D. Bai, Z.T. Zhang, M.D. Bai, C.W. Yi, X.Y. Bai, Removal of SO<sub>2</sub> from gas streams by oxidation using plasma-generated hydroxyl radicals, *Plasma Chem. Plasma Process* 26 (2006) 177–186.
- [16] M.B. Chang, J.H. Balbach, M.J. Rood, M.J. Kushner, Removal of SO<sub>2</sub> from gas streams using a dielectric barrier discharge and combined plasma photolysis, *J. Appl. Phys.* 69 (1991) 4409–4417.
- [17] L.Y. Xia, L. Huang, X.H. Shu, R.X. Zhang, W.B. Dong, H.Q. Hou, Removal of ammonia from gas streams with dielectric barrier discharge plasmas, *J. Hazard. Mater.* (2007). doi:10.1016/j.jhazmat.2007.06.070.
- [18] M.B. Chang, T.D. Tseng, Gas-phase removal of H<sub>2</sub>S and NH<sub>3</sub> with dielectric barrier discharges, *J. Environ. Eng.* 122 (1996) 41–46.
- [19] C.L. Chang, T.S. Lin, Decomposition of toluene and acetone in packed dielectric barrier discharge reactors, *Plasma Chem. Plasma Process* 25 (2005) 227–243.
- [20] H.H. Kim, H. Kobara, A. Ogata, S. Futamura, Comparative assessment of different non-thermal plasma reactors on energy efficiency and aerosol formation from the decomposition of gas-phase benzene, *IEEE Trans. Ind. Appl.* 41 (2005) 206–214.
- [21] Z.L. Ye, Y.N. Zhang, P. Li, L.Y. Yang, R.X. Zhang, H.Q. Hou, Feasibility of destruction of gaseous benzene with dielectric barrier discharge, *J. Hazard. Mater.* 156 (2008) 356–364.
- [22] M.B. Chang, J.S. Chang, Abatement of PFCs from semiconductor manufacturing processes by nonthermal plasma technologies: a critical review, *Ind. Eng. Chem. Res.* 45 (2006) 4101–4109.
- [23] V. Dalaine, J.M. Cormier, S. Pellerin, P. Lefauchaux, H<sub>2</sub>S destruction in 50 Hz and 25 kHz gliding arc reactors, *J. Appl. Phys.* 84 (1998) 1215–1221.
- [24] J.J. Ruan, W. Li, Y. Shi, Y. Nie, X. Wang, T.E. Tan, Decomposition of simulated odors in municipal wastewater treatment plants by a wire-plate pulse corona reactor, *Chemosphere* 59 (2005) 327–333.
- [25] D.J. Helfritsch, Pulsed corona discharge for hydrogen sulfide decomposition, *IEEE Trans. Ind. Appl.* 29 (1993) 882–886.
- [26] H.B. Ma, P. Chen, R. Ruan, H<sub>2</sub>S and NH<sub>3</sub> removal by silent discharge plasma and ozone combo-system, *Plasma Chem. Plasma Process* 21 (2001) 611–624.
- [27] K. Takaki, K. Urashima, J.S. Chang, Ferro-electric pellet shape effect on C<sub>2</sub>F<sub>6</sub> removal by a packed-bed-type nonthermal plasma reactor, *IEEE Trans. Plasma Sci.* 32 (2004) 2175–2183.
- [28] M. Kraus, B. Eliasson, U. Kogelschatz, A. Wokaun, CO<sub>2</sub> reforming of methane by the combination of dielectric-barrier discharges and catalysis, *Phys. Chem. Chem. Phys.* 3 (2001) 294–300.
- [29] M. Magureanu, N.B. Mandache, V.I. Parvulescu, Ch. Subrahmanyam, A. Renken, L. Kiwi-Minsker, Improved performance of non-thermal plasma reactor during decomposition of trichloroethylene: optimization of the reactor geometry and introduction of catalytic electrode, *Appl. Catal. B* 74 (2007) 270–277.
- [30] K. Takaki, M. Shimizu, S. Mukaigawa, T. Fujiwara, Effect of electrode shape in dielectric barrier discharge plasma reactor for NO<sub>x</sub> removal, *IEEE Trans. Plasma Sci.* 32 (2004) 32–38.
- [31] J.V. Durme, J. Dewulf, C. Leys, H. Langenhove, Combining non-thermal plasma with heterogeneous catalysis in waste gas treatment: a review, *Appl. Catal. B* 78 (2008) 324–333.



## ATTACHMENT 13.3

### SCIENTIFIC ARTICLES ON ORGANIC POLLUTANT (VOC) REMOVAL

Osman Karatum, M. A. (2106). A comparative study of dilute VOCs treatment in a non-thermal plasma reactor. *Chemical Engineering Journal* 294, 308-315.

J. Karuppiaha, E. Linga Reddya, P. Manoj Kumar Reddya, B. Ramarajua, R. Karvembub, Ch. Subrahmanyama (2012) – Abatement of mixture of volatile organic compounds (VOCs) in a catalytic non-thermal plasma reactor. *Journal of Hazardous Material* 237-238 (2012) 283-289.

Carlos M. Nunez, G. H. (2012). Corona Destruction: An Innovative Control Technology for VOCs and Air Toxics. *Waste*, 242-247.

Shijie Lia, Xiaoqing Danga, Xin Yua, Ghulam Abbasb, Qian Zhanga, Li Cao (2020) – The application of dielectric barrier discharge non-thermal plasma in VOCs abatement: A review – *Chemical Engineering Journal* 388 (2020) 124275.



## A comparative study of dilute VOCs treatment in a non-thermal plasma reactor



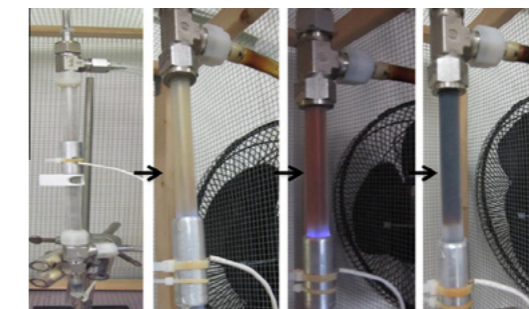
Osman Karatum<sup>1</sup>, Marc A. Deshusses\*

Department of Civil and Environmental Engineering, Duke University, United States

### HIGHLIGHTS

- The treatment of 7 dilute VOCs vapors in air using non-thermal plasma was investigated.
- Very fast degradation rates were obtained.
- Benzene and MEK were most difficult to degrade while hexane was the easiest.
- Large residual ozone concentrations were observed.
- Tar-like deposits was observed when treating ethylbenzene and toluene.

### GRAPHICAL ABSTRACT



### ARTICLE INFO

#### Article history:

Received 13 January 2016  
Received in revised form 29 February 2016  
Accepted 1 March 2016  
Available online 5 March 2016

#### Keywords:

Non-thermal plasma  
Dielectric barrier discharge  
Deposits  
VOCs removal  
Air pollution control

### ABSTRACT

Non-thermal plasma (NTP) is an emerging technology for the treatment of volatile organic compounds (VOCs) in polluted point source air streams. Here, a dielectric barrier discharge NTP was used to evaluate the treatment efficiency of several common VOCs at constant experimental conditions (gas residence time of 0.016 s in the plasma zone, 95–100 ppm<sub>v</sub> average inlet VOC concentration in air). When treated as single pollutant with a specific input energy (SIE) of 350 J L<sup>-1</sup>, the removal efficiency of the VOC followed the following sequence: methyl ethyl ketone (50%), benzene (58%), toluene (74%), 3-pentanone (76%), methyl tert-butyl ether (80%), ethylbenzene (81%), and n-hexane (90%). The effects of pollutant structure on VOC removal efficiency were investigated. The highest removal efficiencies were observed for compounds with the highest percentage of hydrogen in their molecular structures. During treatment of toluene and ethylbenzene vapors, a dark brown, tar-like deposit formed inside the plasma reactor. The deposit formation rate depended on both treated VOCs as well as on experimental conditions such as VOC concentration, and SIE.

© 2016 Elsevier B.V. All rights reserved.

### 1. Introduction

The emission of volatile organic compounds (VOCs) from anthropogenic sources is an important factor associated with

human and environmental health, and has both local and global impacts. For example, benzene emissions have been linked to childhood leukemia in Houston, TX [1], a high correlation between VOC emissions and some types of cancer (i.e., brain, endocrine system, and skin) has been reported [2] and many VOCs are precursors to ozone formed by photochemical reactions leading to increased asthma [3].

Different technologies have been used for controlling VOCs, including adsorption, incineration, condensation and biological treatment [4–6]. Adsorption is generally cost-effective only for low concentrations of VOCs, whereas incineration and condensation are best used for high VOC concentrations [7]. For air streams

\* Corresponding author at: Dept. of Civil and Environmental Engineering, 127C Hudson Hall, Box 90287, Duke University, Durham, NC 27708-0287, United States. Tel.: +1 919 660 5480; fax: +1 919 660 5219.

E-mail addresses: [osman.karatum@duke.edu](mailto:osman.karatum@duke.edu) (O. Karatum), [marc.deshusses@duke.edu](mailto:marc.deshusses@duke.edu) (M.A. Deshusses).

<sup>1</sup> Dept. of Civil and Environmental Engineering, 121 Hudson Hall, Box 90287, Duke University, Durham, NC 27708-0287, United States. Tel.: +1 919 265 8248; fax: +1 919 660 5219.

<http://dx.doi.org/10.1016/j.cej.2016.03.002>

1385-8947/© 2016 Elsevier B.V. All rights reserved.

with medium to low concentrations of VOCs, biological treatment methods (e.g., biofiltration) have proven to be effective, however biofiltration is only applicable to the treatment of biodegradable pollutants [4].

An emerging air pollution control technology is non-thermal plasma (NTP) which has the potential to treat high flows for both low (<100 ppm<sub>v</sub>) to high (>1000 ppm<sub>v</sub>) concentrations of pollutants [8–11]. In particular, NTP or cold plasma has been used to treat air contaminated with elemental mercury, H<sub>2</sub>S, SO<sub>2</sub>, NO<sub>x</sub>, odors, and VOCs such as toluene, benzene, acetone, and trichloroethylene [12–19].

In NTP, electrons and their surroundings are not in thermal equilibrium. Electric discharges in the gas heat the electrons instead of the gas itself, and the resulting high energy electrons, active radicals and ions promote numerous chemical reactions in the ionized zones thus produced. While NTP is a very promising development for a variety of applications [20,21], it also has some drawbacks, notably low energy efficiency, incomplete oxidation of the pollutants undergoing treatment, and the formation of undesired by-products [22–24]. For example, the low selectivity of the oxidation reactions can lead to toxic by-product formation such as CO, NO<sub>x</sub>, and O<sub>3</sub> [25,26] and typical values for VOC conversion to CO<sub>2</sub> are only 30–70% [27,28]. In light of this, the original motivation for the present study was to explore and demonstrate the feasibility of combining NTP treatment with a biotrickling filter, as a possible means for effective treatment of low concentrations of selected VOCs (including recalcitrant ones such as hexane) in air. The vision was that NTP would only provide partial breakdown of the VOC and that incompletely oxidized by-products would subsequently be removed biologically in a biotrickling filter. This would capitalize on the high efficiency of NTP for initial breakdown of hard to biodegrade VOCs and rely on effective biotreatment for completing treatment similar to other studies combining advanced oxidation with biological treatment [29,30]. Thus, experiments were conducted with a NTP operated at a very short gas residence time and treating selected VOC vapors. However, these experiments revealed that the treated VOCs were preferably converted to all the way to CO<sub>2</sub> without the formation of partially oxidized volatile intermediates suggesting that the NTP as used was unsuitable as a pretreatment to a biotrickling filter. On the other hand, a significant amount of solid was found to deposit inside our NTP reactor, and thus the focus of the study was shifted toward characterizing the fate of common VOCs while undergoing treatment and understanding NTP's critical limitations.

## 2. Materials and methods

### 2.1. NTP reactor, conditions, and analytical

NTP was generated using a dielectric discharge barrier (DBD) consisting of a cylindrical quartz tube (9 mm inner diameter, 266 mm length, 3.5 mm thick) fitted with an aluminum cylindrical sleeve (5 cm long, 3.2 mm thick) serving as the external electrode. The internal high voltage electrode was a stainless steel rod (6.32 mm outer diameter, 40 cm long) positioned in the center of the quartz tube running along the axial direction of the reactor. Thus, the discharge gap was 1.34 mm, and the total volume of the plasma zone in the reactor was 1.6 mL. Note that the plasma reactor did not include any catalyst or packing materials. A schematic of the experimental setup is shown in Fig. 1. The excitation frequency for the DBD was kept constant at 22 kHz and the voltage was varied ranging from 7 to 10 kV using a PVM500 dielectric barrier corona driver (Information Unlimited, Amherst, NH).

The synthetic VOC-laden air stream (6.6 L min<sup>-1</sup>) was produced using compressed air from our central laboratory air system which produces dry and oil-free compressed air from ambient air. A metered stream of compressed air was passed through the headspace of a 500 mL flask containing small vials filled with the selected VOC. This VOC-laden stream was then diluted with another metered stream of compressed air at room temperature to the prescribed VOC concentration (95 ppm<sub>v</sub> or 100 ppm<sub>v</sub>). For experiments with humid air, the main air stream was split prior to being mixed with the VOC vapor and part of it was sparged in a container filled with deionized water. The dry and moist air streams were combined such that the resulting air reached the target relative humidity of 30% at 20–22 °C.

The VOC concentrations at the inlet and outlet of the plasma reactor were determined using a GC (Shimadzu 2014, Kyoto, Japan) equipped with flame ionization detector (FID). The concentrations of CO<sub>2</sub> in the reactor influent and effluent were determined using a non-dispersive infrared portable CO<sub>2</sub> meter (Vaisala Carbon Dioxide Meter-GMP70, Louisville, CO). Carbon monoxide effluent concentrations were determined using Dräger tubes (Sugarland, TX), and the ozone concentration was measured by the iodometric method (Iodometric Method, Standardized Procedure 001/96, International Ozone Association) after absorption of a metered air stream into solutions of KI. Elemental analysis of the deposits was conducted by the Duke Environmental Stable Isotope Laboratory using a Carlo Erba Elemental Analyzer. The temperature of the

discharge zone was measured with a surface mounted K-type thermocouple attached to the outer electrode. Another thermocouple was placed in the effluent air downstream of the plasma reactor. The thermocouples were connected to a data logger to record temperature at 5-s intervals. Average temperatures were reported.

### 2.2. Electrical measurements

One of the most important parameters for assessing plasma reactors for air or gas treatment is the specific input energy (SIE), which is the power dissipated in the plasma divided by the gas flow rate and thus has units of J L<sup>-1</sup>. The SIE was determined using Eq. (1) [31].

$$\text{SIE (J L}^{-1}\text{)} = \frac{\text{Power (W)}}{\text{Flow Rate (L s}^{-1}\text{)}} \quad (1)$$

The discharge power was determined using the charge (*Q*) accumulated on a non-inductive capacitor (*C* = 0.22 μF) calculated (using *V* = *Q*/*C*) from the voltage measured using a high frequency data acquisition (Nationals Instruments, NI, USB-5132) (see Fig. SM-1 in supplementary information). Plotting *Q* vs. the voltage measured across the capacitor allows calculation of the power (i.e., the so-called *Q*-*V* Lissajous method). The multiplication of frequency with the area of the parallelogram formed by *Q* vs. *V* is equal to the discharge power in the DBD reactor (Fig. SM-2). Real-time calculation of the discharge power was carried out by a custom LabView (National Instruments, Austin, TX) code using Matlab sub-routines.

### 2.3. Experimental protocol

All experiments were carried out at room temperature (20–22 °C) and atmospheric pressure. The selected VOCs were toluene, benzene, ethylbenzene, methyl ethyl ketone (MEK), methyl tert-butyl ether (MTBE), 3-pentanone, and n-hexane. These VOCs were selected to determine the effect of the molecular structure (e.g., aromatics, ketones, or alkanes) on the removal of these VOCs in the NTP reactor and because of their frequent occurrence as air pollutants. Experiments were conducted at a constant air flow rate (6.6 L min<sup>-1</sup> corresponding to a contact time of 0.016 s in the plasma zone) and a constant inlet concentration of VOCs (95 ppm<sub>v</sub>). Determination of the VOC removal, effluent CO<sub>2</sub>, O<sub>3</sub> concentrations, and

mass of deposit was performed at selected SIEs ranging from 50 to 300 J L<sup>-1</sup>. Subsequently, VOCs that caused the formation of deposits inside the plasma reactor were tested at a constant inlet concentration (100 ppm<sub>v</sub>), flow rate (6.6 L min<sup>-1</sup>), and SIE (360 J L<sup>-1</sup>) in order to determine the relationship between VOC removal, the rate of deposit formation, and the time until reactor clogging.

## 3. Results and discussion

### 3.1. Influence of SIE on VOC removal efficiency

The effect of SIE on the removal efficiency (RE) of VOCs was investigated first. Many studies have reported that when keeping the SIE constant, increasing the VOC concentration and/or the air flow rate decreased the RE, and that increasing the SIE at a constant air flow rate and inlet pollutant concentration increased pollutant removal [7,32]. As will be discussed in more details in Section 3.4, the VOCs were primarily converted to CO<sub>2</sub> and some unaccounted fraction (possibly CO), and no partially degraded volatile organics were detected by GC. The absence of partially oxidized by-products had been explained by Nunez et al. [14] by the fact that once the reaction is initiated, the heat of the reaction is generally sufficient to sustain the completion of the oxidation to CO<sub>2</sub>. Fig. 2 shows the removal efficiency of the seven VOCs tested as a function of SIE. Clearly, the RE increased proportionally with SIE, however, both the removal of the VOCs and the effect of the SIE depended on the specific compound being treated. Selected results of this study are summarized and compared to others in Table 1. Holzer et al. [28] investigated the treatment of MTBE and toluene vapors; the addition of a catalyst in their NTP system resulted in much higher removal efficiencies (>90%) even at very high inlet concentrations (240 and 450 ppm<sub>v</sub>). Delagrangé et al. [24] reported that the oxidation of high concentrations of toluene required higher SIEs in the absence of a catalyst. In non-catalyst applications, Mista and Kacprzyk [33] focused on the removal of toluene using a direct current (DC) back corona discharge reactor at room temperature and found very low RE (15%), despite using relatively high SIE (400 J L<sup>-1</sup>). One likely reason for the lower removal may be the additional electrode (described as a passive electrode used for the back-ionization process), which could have resulted in non-homogenous distribution of energetic electrons. Differences in experimental conditions can also cause differences in reactor performance, hence the interest in systematic studies like

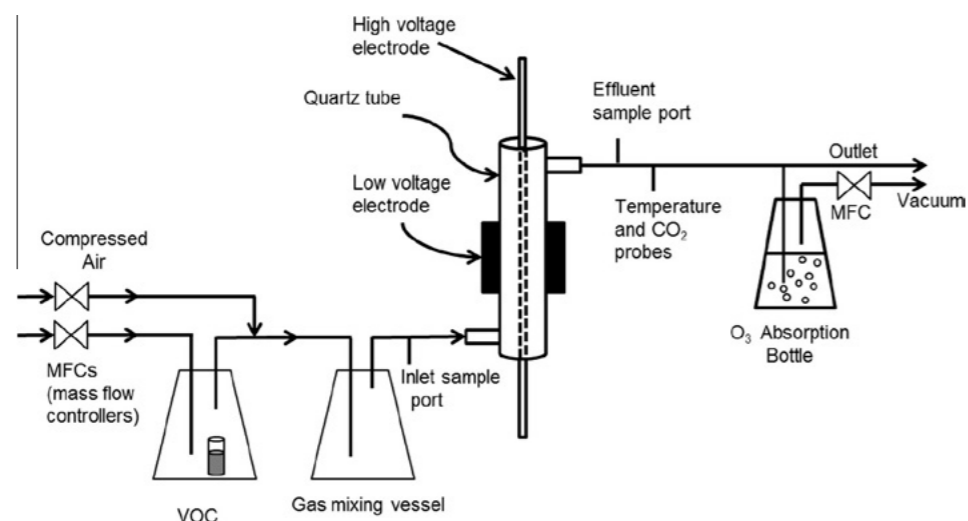


Fig. 1. General schematic of the experimental set up (see Figs. SM-1 and SM-2 for power monitoring setup).

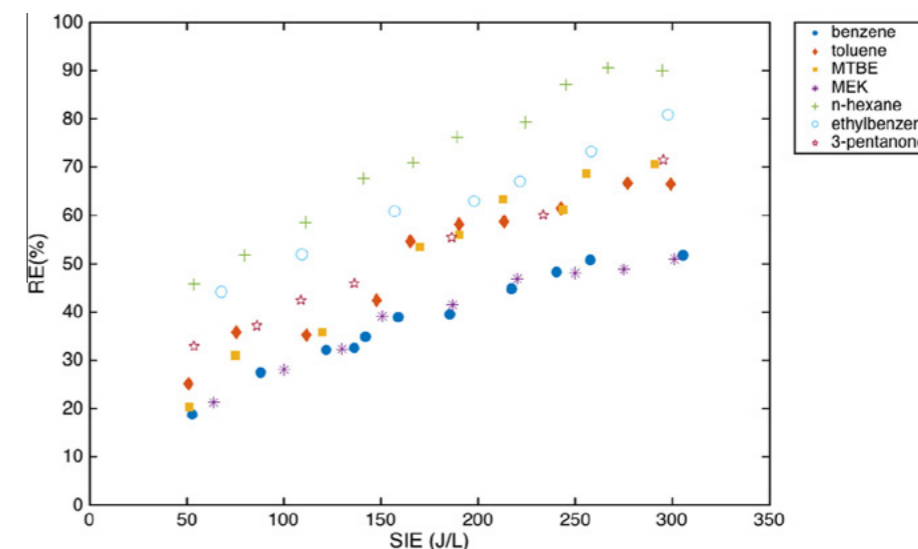
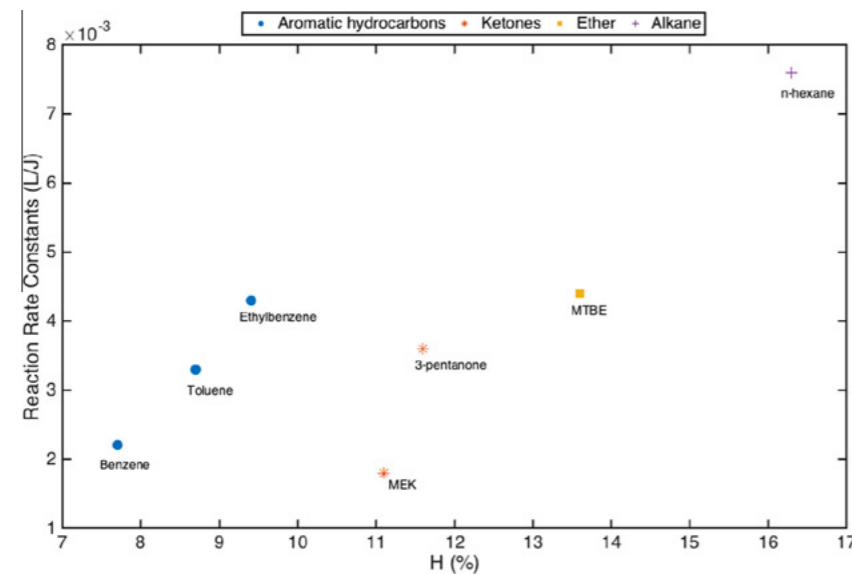


Fig. 2. Removal efficiencies (REs) of selected VOCs as a function of applied specific input energy (SIE) for a flow rate of 6.6 L min<sup>-1</sup> and an inlet VOCs concentration of 95 ppm<sub>v</sub>.

**Table 1**

Comparison of selected removal efficiencies (RE) for this and other studies (some using a catalyst).  $C_{in}$  = inlet concentration, RE = removal efficiency, SIE = specific input energy, V = voltage, ND = no data.

VOCs	$C_{in}$ (ppm <sub>v</sub> )	RE (%)	SIE (J L <sup>-1</sup> )	Gap (mm)	V (kV)	Catalyst	g VOC removed/kW h	References
Toluene	95	74	360	1.3	7–10	None	2.6	This study
Toluene	200	15	400	ND	12 (DC)	None	1.0	[33]
Toluene	50	95.9	756	8.0	30	MnO <sub>2</sub>	0.86	[34]
Toluene	450	90	2400	1.5–10	0–35	BaTiO <sub>3</sub> and LaCoO <sub>3</sub>	2.3	[28]
Toluene	240	55	172	6.0	0–40	MnO <sub>2</sub> /AC	10.4	[24]
MTBE	95	80	360	1.3	7–10	None	2.7	This study
MTBE	200	~100	1300	1.5–10	0–35	BaTiO <sub>3</sub> and LaCoO <sub>3</sub>	2.0	[28]



**Fig. 3.** Calculated reaction rate constants of the VOCs as a function of the hydrogen weight fraction H% (w/w) for the tested VOCs for a constant inlet concentration (95 ppm<sub>v</sub> in dry air) and SIE (360 J L<sup>-1</sup>).

ours for comparison purposes. Guo et al. [34] reported that higher oxygen content in the gas stream resulted in slightly lower removal of toluene. Overall, our removal data seem to indicate yields better than most (but not all) of the selected NTP studies (see the column (g VOC removed per kWh) in Table 1), although in absolute terms, the energy demand for VOC treatment in NTP remains quite high. One possible explanation for the lower yield is that significant amounts of ozone were formed in our experiments as discussed below, and that parasitic discharges occurred on the outer electrode (in some instances, ozone could be detected in the laboratory). Both account for some of the energy input not converted into beneficial reactions.

### 3.2. Determination of the overall reaction rate constants

Knowing the overall reaction rate constant is important to compare systems and to predict the removal of VOCs in NTP reactors. A previously published first-order kinetic model was used [35,36]. This model (Eqs. (2) and (3)) is semi-empirical and does not attempt to describe the detailed chemistry occurring in the plasma reactor. Instead, it lumps all processes into a simple equation that often provides an adequate overall kinetic relationship. The model has been shown to be generally applicable when the VOC removal does not exceed 95% [37].



$$\frac{[\text{VOC}]}{[\text{VOC}]_0} = e^{-\text{SIE}/\beta} \quad (3)$$

where  $\dot{O}$  represents the oxygen radicals produced in the discharge zone of the plasma, and  $[\text{VOC}]_0$  is the inlet concentration of the VOC. The  $\beta$  (J L<sup>-1</sup>) parameter is thus determined by regression of the natural logarithm of  $[\text{VOC}]/[\text{VOC}]_0$  vs. SIE. The slope of the straight line ( $-1/\beta$ ) is (minus) the reaction rate constant  $k$  (L J<sup>-1</sup>). The  $k$  and  $\beta$  values obtained for the seven VOCs that were tested (for the dry air condition) are reported in Table SM-1. Similar reaction rate constants values were reported for some of the VOCs by others ([23,38]). The reaction rate values reported in Table SM-1 allow direct comparison of the reactivity of the tested VOCs since all conditions were kept the same. The results highlight that important differences exist in the reactivity of the VOCs that were selected in our study, allowing some examination of structure-activity relationships.

It has been suggested that the hydrogen weight fraction of the pollutant undergoing treatment is an important factor affecting the reactivity of VOCs in NTP reactors [39]. This is believed to be because molecules with a greater number of methyl groups tend to be more reactive, with a proton lost or gained at the methyl group [14]. In Fig. 3, the reaction rate constant for each VOC was plotted vs. the hydrogen weight fraction. Indeed, the trend shows that a greater hydrogen fraction generally resulted in a greater reaction rate (in particular  $k$  for hexane far exceeded all others). This trend and proposed mechanism might explain why simple hydrocarbons are better removed compared to aromatics or ketones. In addition, removal of aromatic compounds (e.g., ethylbenzene, toluene and benzene) seem to follow their own trend with respect to their hydrogen fractions. Overall, this was not unexpected. For example, Cho et al. found that molecules

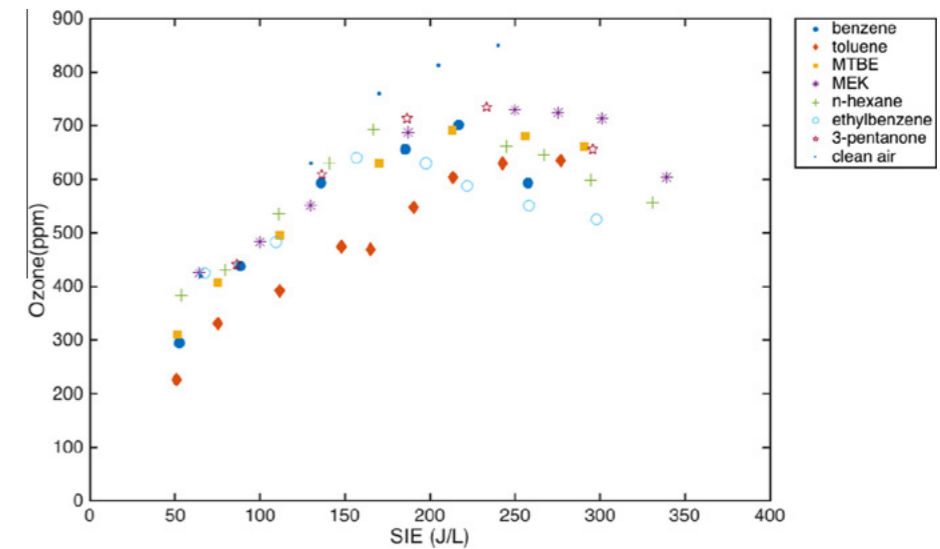


**Fig. 4.** SIE impact on effluent ozone concentration at a flow rate of 6.6 L min<sup>-1</sup>. Typical standard deviations for the ozone measurements were 40–60 ppm<sub>v</sub>.

with oxygen or chlorine lead to formation of volatile products in the plasma, which in turn enhanced the decomposition of VOCs [39]. Another correlation was attempted between  $k$  and the ionization potentials as a measure of how easily the electrons in a molecule respond to a perturbation. The results are shown in Fig. SM-3 did not lead to any obvious trend adding further evidence that reaction mechanisms are complex. Clearly, in order to develop better predictive models based on chemical structures, many more VOCs should be tested in a systematic and quantitative manner.

### 3.3. Influence of SIE on ozone production

Ozone production was quite important, with outlet concentrations ranging from 300 to 900 ppm<sub>v</sub> depending on the specific conditions (Fig. 4). Production of O<sub>3</sub> was greater in the absence of VOCs at higher SIE (>200 J L<sup>-1</sup>) because ozone is consumed by the oxidation of VOCs. Using this logic, one would expect ozone concentrations to be lower when treating pollutants that are well removed, but this was not the case, highlighting the fact that degradation of the VOC vapor follows complex mechanisms. A similar decrease in ozone concentration during VOC treatment was reported by Holzer et al. [28], while Oda [23] observed that presence of VOC (i.e., TCE) first decreased the ozone concentration (4000 ppm<sub>v</sub>–1000 ppm<sub>v</sub>), and then remained constant. Two likely reasons for the difference between studies are (1) the different types of high voltage rods (bolt type or coil type) and/or (2) that a lower SIE could cause different trends in ozone production and consumption. These different types of electrodes (e.g., wire, rod or a bolt) in barrier discharge reactors might change the stability of the discharge from the electrode to the dielectric wall (barrier). Here, as expected, ozone production increased with increasing SIE up to 200 J L<sup>-1</sup> (Fig. 4), but at higher SIE (>200 J L<sup>-1</sup>), ozone production decreased. This decrease may be caused by different mechanisms. One possible explanation is that the temperature in the NTP increased (by about 10 °C; temperature in discharge zone was 40 ± 6 °C) with greater SIEs, and ozone is known to decompose faster at higher temperatures [23]. Another possible explanation proposed by Liang et al. [40] is that at higher SIE, a greater density of high energy electron reacts with ozone thereby lowering its concentrations. Finally, it is possible that NO<sub>x</sub> (in particular NO<sub>2</sub>) were formed at high SIE as was described by several authors (see e.g., Shin and Yoon, 2013) [41]. Unfortunately, NO<sub>x</sub> were not measured in the reactor effluent. In any case, detailed studies would be

needed to confirm and quantify the contribution of each of these mechanisms. Obviously, both NO<sub>x</sub> and ozone are unwanted in the effluent of an air pollution control device and their formations also reduce the energy efficiency of the process. One approach to lower ozone generation is to use a catalyst in situ or post plasma applications. For example, using a MnO<sub>2</sub>/SMF catalyst in-situ decreased ozone formation from 800 ppm<sub>v</sub> to 500 ppm<sub>v</sub> [32]. Another study also concluded that MnO<sub>2</sub> catalyst (this time post-plasma) decreased ozone production while increasing the removal of benzene vapors [15].

### 3.4. Formation of deposit

The treatment of toluene and ethylbenzene vapors resulted in a deposit forming inside the plasma zone, whereas no deposit was observed during the treatment of the other five VOCs tested. Deposits were observed first as color changes (yellow–brown) to solid surfaces (electrodes, outlet tubing) as well as a significant amount of small dark brown particles accumulating at the exit port of the plasma reactor (see Graphical Abstract, Figs. SM-4 and SM-5). These deposits were dark brown in color and gave off a petroleum- or tar-like odor. This came as a surprise, since the NTP published literature is relatively silent on the formation of such deposits. Only a few papers [34,42,43] briefly mention similar observations, but thorough and quantitative determinations are lacking. Guo et al. [34] reported that a yellow product was observed after the treatment of toluene vapors in a DBD, and described it as an aromatic polymer. A few reports exist on deposit formation after the treatment of VOCs with non-thermal plasma and catalyst hybrid systems [44–46]. They generally described the deposits as polymeric substances, or carbonaceous deposits, some were identified as benzoic acid crystals. Deposit formation increased with decreasing flow rate or reducing the SIE. Another study by Demidiouk et al. [42] found that solid particles formed during the treatment of toluene vapors, but not during butyl acetate. These papers only focused on the qualitative aspects of the deposits.

Thus, an important question was to determine what percentage of the treated pollutant was transformed into these deposits. The carbon content in the deposit was determined to be 54 ± 1% by mass and nitrogen was 2.9 ± 0.1%. As shown in Fig. 5, between 1% and 3% (as carbon) of the toluene or ethylbenzene fed to the reactor was recovered as deposit. This number still leaves a fairly

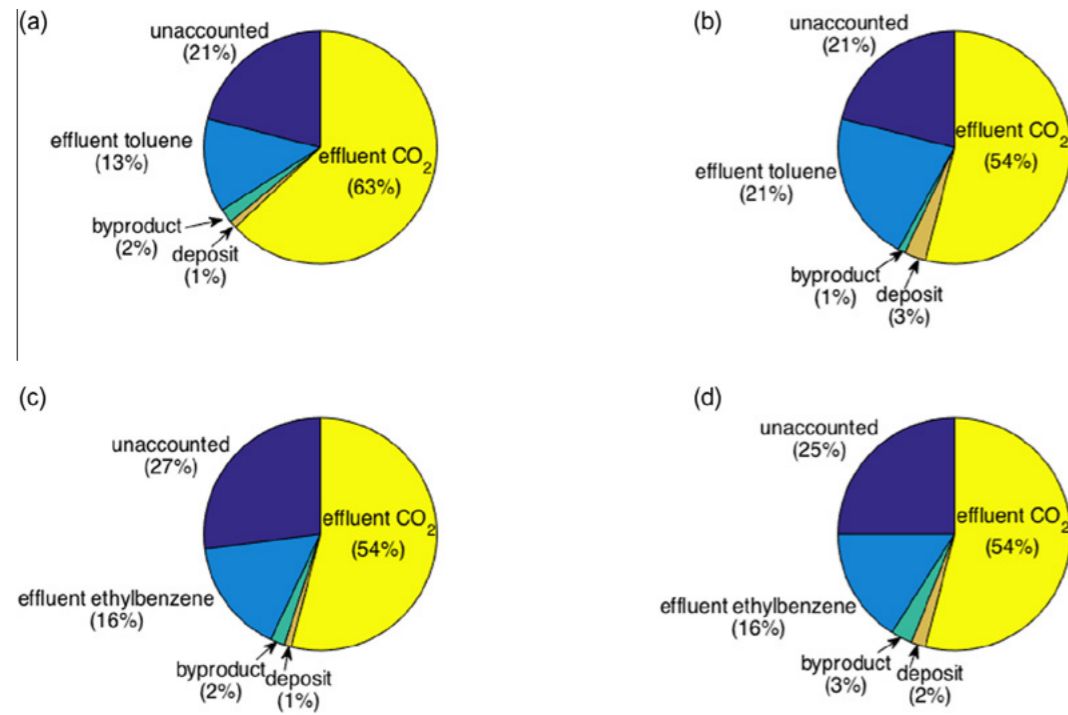


Fig. 5. Fate of influent pollutant (as carbon mass fraction) during VOC treatment under dry and humid air conditions. (a) Toluene, dry air; (b) toluene, 30% RH; (c) ethylbenzene, dry air; (d) ethylbenzene, 30% RH. Experimental conditions: constant inlet concentration (100 ppm<sub>v</sub>), flow rate (6.6 L min<sup>-1</sup>), and SIE (360 J L<sup>-1</sup>).

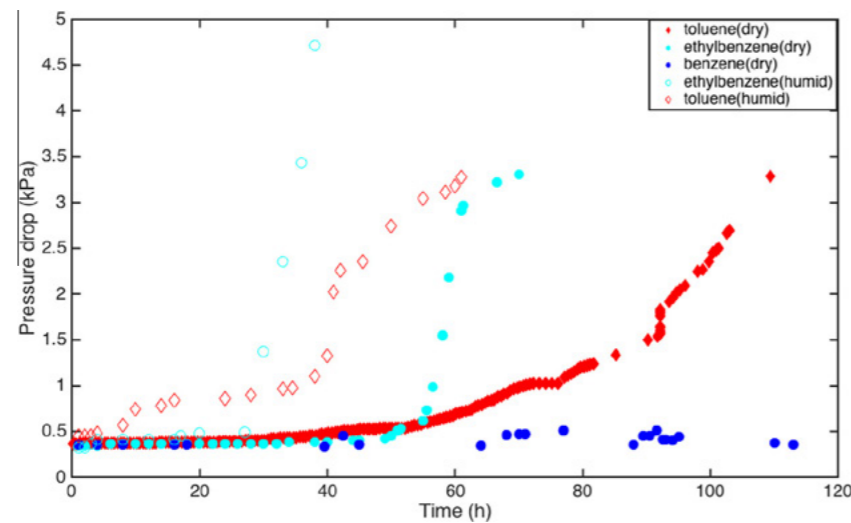


Fig. 6. Pressure drop determined as a function of time. Experimental conditions were 360 J L<sup>-1</sup> SIE, a gas flow rate of 6.6 L min<sup>-1</sup>, and 100 ppm<sub>v</sub> inlet concentration.

large fraction of the carbon unaccounted; it is quite possible that some semi- or non-volatiles left via the exhaust instead of being deposited, and thus could be part of the carbon labeled as “unaccounted”. It was reported that higher concentrations of treated VOCs (i.e., 1000 ppm<sub>v</sub> styrene) produced more (60–70%) deposits inside a plasma reactor [35]. In our experiments, the CO concentration in the exhaust was measured, but was always below our detection limit of 20 ppm<sub>v</sub>. It is only in selected experiments (not shown) conducted at SIE >700 J L<sup>-1</sup> that CO in the exhaust rose to about 50 ppm<sub>v</sub>. Because of the relatively high detection limit of CO, CO could well be a major fraction of the carbon unaccounted for in Fig. 5. If this was indeed the case, it would be consistent with the large amount of CO observed by Yu-fang et al. [47].

The time required for the deposit to cause significant clogging was determined by measuring the pressure drop over the reactor (Fig. 6). An increase in the pressure drop across the reactor could cause serious malfunctions, leakages, or fractures in the dielectric tubes. As shown in Fig. 6, a greater deposit formation was observed in humid conditions while no deposit was observed with benzene. This contrasts with Cal et al. [48] who reported deposit formation during benzene vapor treatment and could easily dissolve it with a small amount of water. Here, the deposit was different in nature from that of Cal et al.; it was not water soluble, and required an organic solvent (ethanol or methanol) to remove it. In addition to the greater amount of deposit yield in humid conditions, the structure and visual aspects of the deposit in humid conditions

was different than in dry conditions. Under humid air condition, the deposit formed a more compact than under dry air conditions and some (unidentified) crystals could be seen (see Fig. SM5). The results of Fig. 6 show that when deposits occur, they can cause reactor malfunction if not managed properly. Solutions can include special reactor designs and/or specific operating procedures. For example, Zhang et al. [49] demonstrated that increasing the volume of the discharge zone and placing additional dielectric tube (i.e., double tube dielectric barrier discharge reactor) could overcome the solid deposit accumulation inside the plasma zone.

#### 4. Conclusions

In this study, the treatment of selected volatile organic vapors in a DBD-type non-thermal plasma reactor was evaluated. Experiments conducted at the same operating conditions for all VOCs allowed to determine how the treatment performance was affected by the nature of the pollutant and by the SIE.

The main findings can be summarized as follows:

- Removal of 95 ppm<sub>v</sub> of the tested VOCs at 350 J L<sup>-1</sup> followed the following sequence: methyl ethyl ketone (50%), benzene (58%), toluene (74%), 3-pentanone (76%), methyl tert-butyl ether (80%), ethylbenzene (81%), and *n*-hexane (90%). The treated VOCs were primarily oxidized to CO<sub>2</sub>.
- The solid deposits that formed when treating toluene and ethylbenzene vapors can be problematic. About 1–3% of the total inlet carbon was recovered as a deposit for the treatment of 100 ppm<sub>v</sub> ethylbenzene and toluene at 360 J L<sup>-1</sup>. When humid air was treated, a greater fraction of the treated pollutant was recovered as deposit and reactor clogging happened sooner. However, deposits from treating benzene were minor and did not clog the reactor within the duration of the experiments.
- Deposits also accumulated downstream the dielectric tube. They did not change the reactor's removal efficiency, but caused clogging problems over time.
- The hydrogen content of the molecules undergoing treatment was a reasonable predictor for the trends in VOC reaction rate constants (*k*). Molecules with a greater hydrogen content were more reactive and better removed.
- As a by-product, effluent ozone concentrations increased with the SIE, but leveled off or decreased at high SIEs (>200 J L<sup>-1</sup>). The high outlet ozone concentrations (200–900 ppm<sub>v</sub>) decrease the process's energy efficiency and need further consideration.

#### Appendix A. Supplementary data

Supplementary data associated with this article can be found, in the online version, at <http://dx.doi.org/10.1016/j.cej.2016.03.002>.

#### References

- S.R. Hanna, R. Paine, D. Heinold, E. Kintigh, D. Baker, Uncertainties in air toxics calculated by the dispersion models AERMOD and ISC3T3 in the Houston ship channel area, *J. Appl. Meteorol. Climatol.* 46 (2007) 1372–1382.
- M.L. Boeglin, D. Wessels, D. Henshel, An investigation of the relationship between air emissions of volatile organic compounds and the incidence of cancer in Indiana counties, *Environ. Res.* 100 (2006) 242–254.
- S.I.V. Sousa, M.C.M. Alvim-Ferraz, F.G. Martins, Health effects of ozone focusing on childhood asthma: what is now known—a review from an epidemiological point of view, *Chemosphere* 90 (2013) 2051–2058.
- J.S. Devinny, M.A. Deshusses, T.S. Webster, *Biofiltration for Air Pollution Control*, Lewis Publishers, New York, 1998.
- D. Gabriel, H.H.J. Cox, M.A. Deshusses, Conversion of full-scale wet scrubbers to biotrickling filters for H<sub>2</sub>S control at publicly owned treatment works, *J. Environ. Eng.* 130 (2004) 1110–1117.

- Q. Hu, C. Wang, K. Huang, Biofiltration performance and characteristics of high temperature gaseous benzene, hexane and toluene, *Chem. Eng. J.* 279 (2015) 689–695.
- G. An, Y. Sun, T. Zhu, X. Yan, Degradation of phenol in mists by a non-thermal plasma reactor, *Chemosphere* 84 (2011) 1296–1300.
- B.M. Penetrante, S.E. Schultheis, Non-thermal plasma techniques for pollution control: part A—overview, fundamentals and supporting technologies and part B—electron beam and electrical discharge processing, *NATO ASI Ser Ser G* 84 (2011) 1296–1300.
- B.M. Penetrante, M.C. Hsiao, J.N. Bardsley, B.T. Merritt, G.E. Vogtlin, A. Kuthi, C. P. Burkhardt, J.R. Bayless, Identification of mechanisms for decomposition of air pollutants by non-thermal plasma processing, *Plasma Sources Sci. Technol.* 6 (1997) 251–259.
- S. Schmid, M.C. Jecklin, R. Zenobi, Degradation of volatile organic compounds in a non-thermal plasma air purifier, *Chemosphere* 79 (2010) 124–130.
- S. Lu, L. Chen, Q. Huang, L. Yang, C. Du, X. Li, J. Yan, Decomposition of ammonia and hydrogen sulfide in simulated sludge drying waste gas by a novel non-thermal plasma, *Chemosphere* 117 (2014) 781–785.
- A. Mizuno, J.S. Clements, R.H. Davis, A method for the removal of sulfur dioxide from exhaust gas utilizing pulsed streamer corona for electron energization, *IEEE Trans. Ind. Appl.* 3 (1986) 516–522.
- T. Yamamoto, K. Ramanathan, P. Lawless, D.S. Ensor, J.R. Newsome, N. Plaks, G. H. Ramsey, Control of volatile organic compounds by an ac energized ferroelectric pellet reactor and a pulsed corona reactor, *IEEE Trans. Ind. Appl.* 28 (1992) 528–534.
- C.M. Nunez, G.H. Ramsey, W.H. Ponder, J.H. Abbott, L.E. Hamel, P.H. Kariher, Corona destruction: an innovative control technology for VOCs and air toxics, *J. Air Waste Manage. Assoc.* 43 (1993) 242–247.
- S. Futamura, A. Zhang, H. Einaga, H. Kabashima, Involvement of catalyst materials in nonthermal plasma chemical processing of hazardous air pollutants, *Catal. Today* 72 (2002) 259–265.
- Y. Byun, D.J. Koh, D.N. Shin, Removal mechanism of elemental mercury by using non-thermal plasma, *Chemosphere* 83 (2011) 69–75.
- L. Huang, L. Xia, X. Ge, H. Jing, W. Dong, H. Hou, Removal of H<sub>2</sub>S from gas stream using combined plasma photolysis technique at atmospheric pressure, *Chemosphere* 88 (2012) 229–234.
- T. Zhu, R. Chen, N. Xia, X. Li, X. He, W. Zhao, T. Carr, Volatile organic compounds emission control in industrial pollution source using plasma technology coupled with F-TiO<sub>2</sub>/γ-Al<sub>2</sub>O<sub>3</sub>, *Environ. Technol.* 36 (2015) 1405–1413.
- J. Liu, J. Wang, X. Cao, R. Zhang, H. Hou, Decomposition of gaseous toluene using a continuous flow discharge plasma reactor with new configurations, *Environ. Technol.* 36 (2015) 3084–3093.
- C.A. Aggelopoulos, P. Svarnas, M.I. Klapa, C.D. Tsakiroglou, Dielectric barrier discharge plasma used as a means for the remediation of soils contaminated by non-aqueous phase liquids, *Chem. Eng. J.* 270 (2015) 428–436.
- K.B. Andersen, J.A. Beukes, A. Feilberg, Non-thermal plasma for odour reduction from pig houses – a pilot scale investigation, *Chem. Eng. J.* 223 (2013) 638–646.
- K. Urashima, J.S. Chang, Removal of volatile organic compounds from air streams and industrial flue gases by non-thermal plasma technology, *IEE Trans. Dielectr. Electr. Insul.* 7 (2000) 602–614.
- T. Oda, Non-thermal plasma processing for environmental protection: decomposition of dilute VOCs in air, *J. Electrostat.* 57 (2003) 293–311.
- S. Delagrèze, L. Pinard, J.M. Tatibouet, Combination of a non-thermal plasma and a catalyst for toluene removal from air: manganese based oxide catalysts, *Appl. Catal. B* 68 (2006) 92–98.
- U. Roland, F. Holzer, F.D. Kopinke, Improved oxidation of air pollutants in a non-thermal plasma, *Catal. Today* 73 (2002) 315–323.
- R. Zhu, Y. Mao, L. Jiang, J. Chen, Performance of chlorobenzene removal in a nonthermal plasma catalysis reactor and evaluation of its byproducts, *Chem. Eng. J.* 279 (2015) 463–471.
- D.E. Tevault, Carbon monoxide production in silent discharge plasmas of air and air-methane mixtures, *Plasma Chem. Plasma Process.* 7 (1987) 231–242.
- F. Holzer, F.D. Kopinke, U. Roland, Influence of ferroelectric materials and catalysts on the performance of non-thermal plasma (NTP) for the removal of air pollutants, *Plasma Chem. Plasma Process.* 25 (2005) 595–611.
- Z. Runye, K. Christian, C. Zhuowei, L. Lichao, Y. Jianming, C. Jianmeng, Styrene removal in a biotrickling filter and a combined UV-biotrickling filter: steady- and transient-state performance and microbial analysis, *Chem. Eng. J.* 275 (2015) 168–178.
- Y. Jianming, L. Wei, C. Zhuowei, J. Yifeng, C. Wenji, C. Jianmeng, Dichloromethane removal and microbial variations in a combination of UV pretreatment and biotrickling filtration, *J. Hazard. Mater.* 268 (2014) 14–22.
- T.C. Manley, The electric characteristics of the ozonator discharge, *Trans. Electrochem. Soc.* 84 (1943) 83–96.
- C. Subrahmanyam, M. Magureanu, A. Renken, L. Kiwi-Minsker, Catalytic abatement of volatile organic compounds assisted by non-thermal plasma: Part 1. A novel dielectric barrier discharge reactor containing catalytic electrode, *Appl. Catal. B* 65 (2006) 150–156.
- W. Mista, R. Kacprzyk, Decomposition of toluene using non-thermal plasma reactor at room temperature, *Catal. Today* 137 (2008) 345–349.
- Y.F. Guo, D.Q. Ye, K.F. Chen, J.C. He, W.L. Chen, Toluene decomposition using a wire-plate dielectric barrier discharge reactor with manganese oxide catalyst in situ, *J. Mol. Catal. A Chem.* 245 (2006) 93–100.
- G.K. Anderson, H. Snyder, J. Coogan, Oxidation of styrene in a silent discharge plasma, *Plasma Chem. Plasma Process.* 19 (1999) 131–151.

- [36] T. Zhang, Q. Li, Y. Liu, Y. Duan, W. Zhang, Equilibrium and kinetics studies of fluoride ions adsorption  $CeO_2/Al_2O_3$  composites pretreated with non-thermal plasma, *Chem. Eng. J.* 168 (2011) 665–671.
- [37] L.A. Rosocha, R.A. Korzekwa, Advanced oxidation and reduction processes in the gas phase using non-thermal plasmas, *J. Adv. Oxid. Technol.* 4 (1999) 247–264.
- [38] L.A. Rosocha, G.K. Anderson, L.A. Bechtold, J.J. Coogan, H.G. Heck, M. Kang, W.H. McCulla, R.A. Tennant, P.J. Wantuck, Treatment of hazardous organic wastes using silent discharge plasmas, *Non-Thermal Plasma Techniques for Pollution Control*, NATO ASI Series, Springer, Berlin 34 (1993) 281–308.
- [39] D.L. Cho, D.C. Chung, G.S. Kim, Decomposition and solidification of hazardous volatile organic compounds through plasma chemical reactions, *J. Ind. Eng. Chem.* 13 (2007) 287–291.
- [40] W.J. Liang, L. Ma, H. Liu, J. Li, Toluene degradation by non-thermal plasma combined with a ferroelectric catalyst, *Chemosphere* 92 (2013) 1390–1395.
- [41] H.H. Shin, W.S. Yoon, Hydrocarbon effects on the promotion of non-thermal plasma  $NO-NO_2$  conversion, *Plasma Chem. Plasma Process.* 23 (2003) 681–704.
- [42] V. Demidiouk, S.I. Moon, J.O. Chae, Toluene and butyl acetate removal from air by plasma-catalytic system, *Catal. Commun.* 4 (2003) 51–56.
- [43] M.S. Gandhi, A. Ananth, Y.S. Mok, J.I. Song, K.H. Park, Time dependence of ethylene decomposition and byproducts formation in a continuous flow dielectric-packed plasma reactor, *Chemosphere* 91 (2013) 685–691.
- [44] M. Magureanu, D. Piroi, N.B. Mandache, V.I. Parvulescu, V. Parvulescu, B. Cojocaru, C. Cadigan, R. Richards, In situ study of ozone and hybrid plasma Ag–Al catalysts for the oxidation of toluene: evidence of the nature of the active sites, *Appl. Catal. B.* 104 (2011) 84–90.
- [45] H.L. Chen, H.M. Lee, S.H. Chen, M.B. Chang, S.J. Yu, S.N. Li, Removal of volatile organic compounds by single-stage and two-stage plasma catalysis systems: a review of the performance enhancement mechanisms, current status, and suitable applications, *Environ. Sci. Technol.* 43 (2009) 2216–2227.
- [46] M. Magureanu, N.B. Mandache, Toluene oxidation in a plasma-catalytic system, *J. Appl. Phys.* 99 (2006) 123301–123304.
- [47] G. Yu-fang, Y. Dai-qi, T. Ya-feng, C. Ke-fu, Humidity effect on toluene decomposition in a wire-plate dielectric barrier discharge reactor, *Plasma Chem. Plasma Process.* 26 (2006) 237–249.
- [48] M.P. Cal, M. Schluep, Destruction of benzene with non-thermal plasma in dielectric barrier discharge reactors, *Environ. Prog.* 20 (2001) 151–156.
- [49] H. Zhang, K. Li, C. Shu, Z. Lou, T. Sun, J. Jia, Enhancement of styrene removal using a novel double-tube dielectric barrier discharge (DDBD) reactor, *Chem. Eng. J.* 265 (2014) 107–118.



Contents lists available at SciVerse ScienceDirect

Journal of Hazardous Materials

journal homepage: [www.elsevier.com/locate/jhazmat](http://www.elsevier.com/locate/jhazmat)

## Abatement of mixture of volatile organic compounds (VOCs) in a catalytic non-thermal plasma reactor

J. Karuppiah<sup>a</sup>, E. Linga Reddy<sup>a</sup>, P. Manoj Kumar Reddy<sup>a</sup>, B. Ramaraju<sup>a</sup>, R. Karvembu<sup>b</sup>, Ch. Subrahmanyam<sup>a,\*</sup>

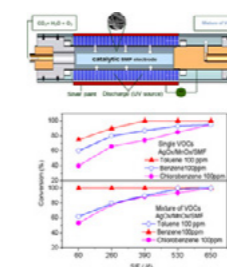
<sup>a</sup> Energy and Environmental Research Laboratory, Department of Chemistry, Indian Institute of Technology, Hyderabad 502205, India

<sup>b</sup> Department of Chemistry, National Institute of Technology, Tiruchirappalli 620015, India

### HIGHLIGHTS

- Oxidation of mixture of VOCs in a catalytic dielectric barrier discharge reactor.
- Synergy effect on integration of catalyst to plasma.
- Positive effect of water vapor during removal of mixture of VOCs.
- Best activity of  $AgO_x/MnO_x$  under humid conditions.

### GRAPHICAL ABSTRACT



### ARTICLE INFO

#### Article history:

Received 29 May 2012  
Received in revised form 17 August 2012  
Accepted 18 August 2012  
Available online 24 August 2012

#### Keywords:

VOC abatement  
SMF  
Ozone  
Non-thermal plasma  
Synergy

### ABSTRACT

Total oxidation of mixture of dilute volatile organic compounds was carried out in a dielectric barrier discharge reactor with various transition metal oxide catalysts integrated in-plasma. The experimental results indicated the best removal efficiencies in the presence of metal oxide catalysts, especially  $MnO_x$ , whose activity was further improved with  $AgO_x$  deposition. It was confirmed water vapor improves the efficiency of the plasma reactor, probably due to the formation of hydroxyl species, whereas, in situ decomposition of ozone on the catalyst surface may lead to nascent oxygen. It may be concluded that non-thermal plasma approach is beneficial for the removal of mixture of volatile organic compounds than individual VOCs, probably due to the formation of reactive intermediates like aldehydes, peroxides, etc.

© 2012 Elsevier B.V. All rights reserved.

### 1. Introduction

Volatile organic compounds (VOCs) are one of the major contributors to the atmospheric pollution and may have adverse effects on human health [1]. Technical VOC mixtures of different chemical character such as aromatic hydrocarbons, alkanes, alcohols, acetates and ketones are utilized for commercial and industrial applications such as paints, chemical plants, and printing

industries. Exposure to VOCs has implications in a number of human diseases, including cancer, cardiovascular and several insusceptible diseases [2]. As some of the VOCs are carcinogenic more rigorous environmental regulations have to be followed in order to reduce the VOCs emission [1–3]. There are many conventional methods for VOCs reduction including adsorption, absorption, catalytic oxidation and thermal incineration. These techniques are not effective, especially for dilute concentrations (<1000 ppmv), where non-thermal plasma (NTP) generated at atmospheric pressure may be energy saving due to fast ignition response and generation of highly energetic electrons that may contribute to plasma chemistry reactions [2–6]. Further, a synergy

\* Corresponding author. Tel.: +91 40 23016050; fax: +91 40 23016032.  
E-mail address: [csubbu@iith.ac.in](mailto:csubbu@iith.ac.in) (Ch. Subrahmanyam).



between NTP and catalytic action is expected with suitable catalyst integration with plasma in order to overcome the low selectivity problems of NTP [4–6]. As the typical industrial emissions comprise a blend of VOCs, an effective technology for the oxidative decomposition of VOCs is desirable [7,8]. Catalytic NTP technique has often been tested for the removal of various single component VOCs, but reports on VOCs mixture are limited [9,10]. During the present study, a mixture of VOCs of different nature was tested with NTP combined with MnO<sub>x</sub> and AgO<sub>x</sub>/MnO<sub>x</sub> catalysts and results were compared with NTP alone. Influence of various parameters like design of the reactor, catalyst, presence of water vapor, concentration of VOCs, nature of the by-products formed and ozone formation inside the NTP reactor has been studied.

## 2. Experimental set-up

### 2.1. Materials

Toluene (TOL), benzene (BZ) chlorobenzene (CB), manganese acetate tetrahydrate and silver nitrate were also purchased from

$$\text{Conversion of CB (\%)} = \frac{[\text{CB}]_{\text{in}} - [\text{CB}]_{\text{out}}}{[\text{CB}]_{\text{in}}} \times 100\%$$

$$\text{Conversion of TOL (\%)} = \frac{[\text{TOL}]_{\text{in}} - [\text{TOL}]_{\text{out}}}{[\text{TOL}]_{\text{in}}} \times 100\%$$

$$\text{Conversion of BZ (\%)} = \frac{[\text{BZ}]_{\text{in}} - [\text{BZ}]_{\text{out}}}{[\text{BZ}]_{\text{in}}} \times 100\%$$

$$\text{Global selectivity of CO}_{\text{SCO}} = \frac{[\text{CO}]_{\text{out}}}{6 \times ([\text{BZ}]_{\text{in}} - [\text{BZ}]_{\text{out}}) + 7 \times ([\text{TOL}]_{\text{in}} - [\text{TOL}]_{\text{out}}) + 6 \times ([\text{CB}]_{\text{in}} - [\text{CB}]_{\text{out}})} \times 100\%$$

$$\text{Global selectivity of CO}_2 S_{\text{CO}_2} = \frac{[\text{CO}_2]_{\text{out}}}{6 \times ([\text{BZ}]_{\text{in}} - [\text{BZ}]_{\text{out}}) + 7 \times ([\text{TOL}]_{\text{in}} - [\text{TOL}]_{\text{out}}) + 6 \times ([\text{CB}]_{\text{in}} - [\text{CB}]_{\text{out}})} \times 100\%$$

$$S_{\text{CO}_x} = S_{\text{CO}} + S_{\text{CO}_2}$$

Merck (Germany). All the solutions were prepared with deionized water. Sintered metal fiber (SMF) filters made of stainless steel consisting of thin uniform metal fibers of diameter 30 μm, wetness capacity of ~30 wt% and porosity of ~80% were acquired, Southwest Screens and Filters SA, Belgium.

### 2.2. Catalyst supported SMF preparation

Manganese oxide and silver supported manganese oxide on SMF were prepared by wet chemical route. The SMF was first oxidized at 873 K for 3 h, followed by impregnation with manganese acetate aqueous solutions of desired concentration. Then it was dried at room temperature followed by calcination in air at 773 K for 5 h to obtain MnO<sub>x</sub>/SMF, whereas, AgO<sub>x</sub>/MnO<sub>x</sub>/SMF were prepared by deposition of AgNO<sub>3</sub> and drying at room temperature followed by calcination at 773 K for 5 h. Finally, SMF filters were subjected to an electrical hot press to shape them into cylindrical form giving the desired discharge gap of 2.5 mm.

### 2.3. Experimental procedure

A detailed description of the reactor has been given elsewhere [11]. Briefly, the dielectric discharge was generated in a cylindrical quartz tube with an inner diameter of 18.5 mm. One end of the SMF electrode was connected through a stainless steel rod to AC high voltage, whereas the other end was connected to the inlet gas stream through a Teflon tube. The gas after passing the discharge zone diffuses through the SMF and was analyzed with a gas chromatograph at the outlet. The discharge length was 10 cm and

discharge gap was fixed at 2.5 mm during the destruction of VOCs. V-Q Lissajous method was used to determine the discharge power (W) from which specific input energy (SIE) was calculated by dividing power (W) with flow rate (l/s). SIE in the present study was varied in between 60 and 650 J/l by changing the amplitude of AC high voltage (14–22 kV/50 Hz). The VOCs BZ, CB and TOL were introduced with a motor driven syringe pump and were mixed with air at a flow rate of 250 ml/min at standard temperature and pressure and were fed into the plasma reactor with a Teflon tube. Conversion at each voltage was measured after 30 min. The concentration of VOCs at the outlet of reactor was measured with a gas chromatograph (Varian 450) equipped with a flame ionization detector and a VF1 capillary column (50 m length, 0.25 mm thickness), whereas an on-line GC-MS (Thermo Fisher Scientific) was used to identify the by-products formed. The formation of CO<sub>2</sub> and CO was simultaneously monitored with an online infrared gas analyser (Analyser Instruments Company, India), whereas ozone formed in the plasma reactor was measured with UV absorption ozone monitor (API-450 NEMA). As the volume change due to chemical reactions is negligible, global selectivity of CO<sub>2</sub> and CO<sub>x</sub> was defined as follows:

where all concentrations are in ppmv.

## 3. Results and discussion

The present study has been aimed at the removal of mixture of VOCs of different nature. However, in order to understand the oxidation behavior of VOCs in a mixture, initial experiments were carried out with single component VOCs over MnO<sub>x</sub>/SMF, AgO<sub>x</sub>/MnO<sub>x</sub>/SMF and SMF and the results are presented in Fig. 1. As seen in Fig. 1a, SMF showed least conversion compared to modified catalysts. At 60 J/l, MnO<sub>x</sub>/SMF showed conversion of 30, 50 and 60%, respectively for CB, BZ and TOL and with increasing SIE to 650 J/l, conversion increased up to 90, 90 and 100%, respectively. Interestingly, AgO<sub>x</sub>/MnO<sub>x</sub>/SMF catalyst showed higher conversion compared to MnO<sub>x</sub>/SMF in the entire SIE range. Even at 60 J/l, AgO<sub>x</sub>/MnO<sub>x</sub>/SMF showed 45, 60 and 75% for CB, BZ and TOL. Even though, during the decomposition of VOCs total oxidation is desired, in general, NTP leads to the formation of undesired products and the selectivity to CO<sub>2</sub> may not be 100%. As seen in Fig. 1b, selectivity to CO<sub>x</sub> (CO + CO<sub>2</sub>) was never 100%, indicating the formation of by products along with carbonaceous deposits on the walls of the reactor. For the VOCs tested in the present study, the selectivity to CO<sub>2</sub> followed the order SMF < MnO<sub>x</sub> < AgO<sub>x</sub>/MnO<sub>x</sub>/SMF.

### 3.1. Plasma-catalytic oxidation of mixture of VOCs

The performance of various catalytic electrodes during the destruction of 200 ppm of mixture of VOCs (50 ppm CB, 100 ppm BZ and 50 ppm TOL) in the SIE range of 60–650 J/l was tested. As seen in Fig. 2a, SMF without any modification showed ~100% conversion

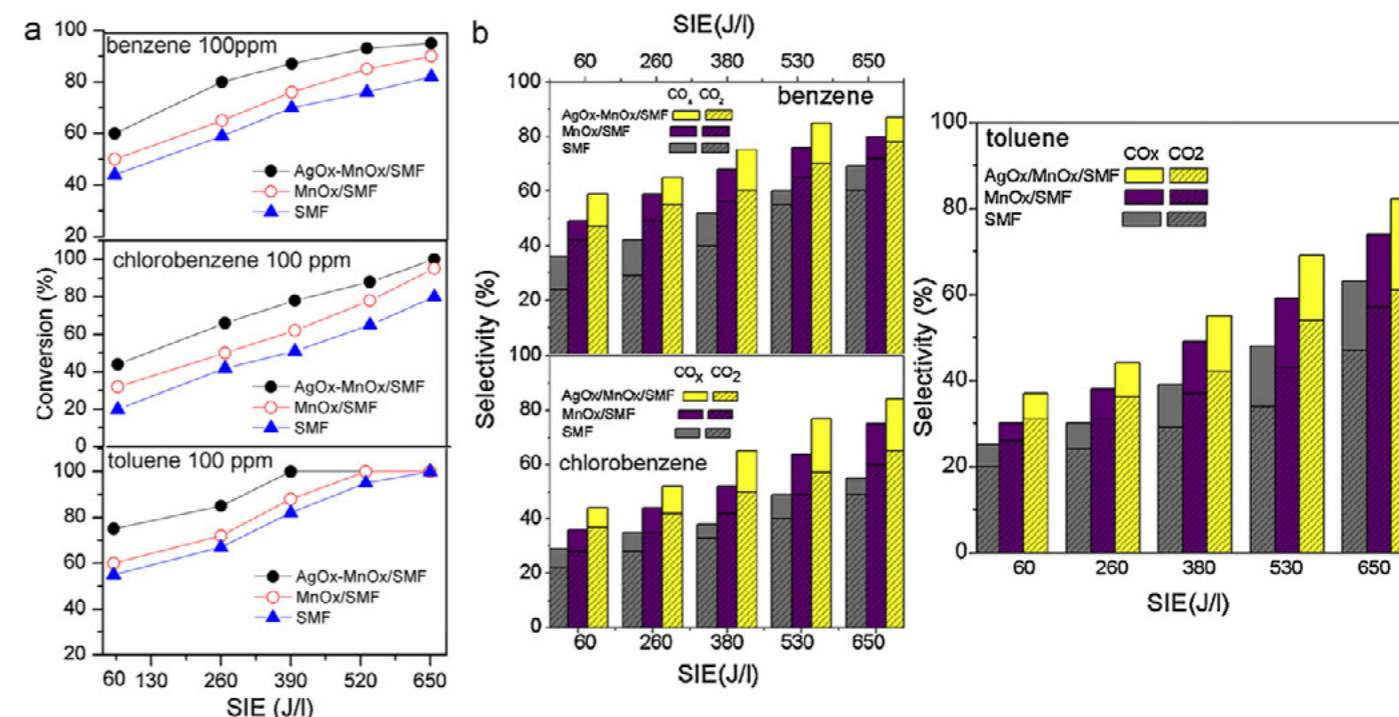


Fig. 1. Influence of SIE and SMF modification during the destruction of VOCs. (a) Conversion and (b) selectivity (SIE 60–650 J/l and 100 ppm of VOCs).

of TOL even at 60 J/l, whereas, under the same input energy conversion of BZ and CB was only around 65%. Nearly the same results were observed for MnO<sub>x</sub>/SMF, whereas, AgO<sub>x</sub>/MnO<sub>x</sub>/SMF showed better performance than SMF and MnO<sub>x</sub>/SMF, where the conversion of BZ and CB increased to 70 and 80%, respectively. SMF showed complete conversion of BZ and CB only at 530 J/l, whereas, with AgO<sub>x</sub>/MnO<sub>x</sub>/SMF the same result was obtained even at 400 J/l. AgO<sub>x</sub>/MnO<sub>x</sub>/SMF showed better activity over SMF and MnO<sub>x</sub>/SMF throughout the range of the present study. Among all electrodes, AgO<sub>x</sub>/MnO<sub>x</sub>/SMF under dry condition showed the high activity for all the VOCs. Interesting observation is that AgO<sub>x</sub>/MnO<sub>x</sub>/SMF under humid conditions showed 100% conversion of the mixture of VOCs at 300 J/l, whereas, relatively high energy (420 J/l) was needed with unmodified SMF.

Fig. 2b presents the global selectivity of CO<sub>x</sub> (CO + CO<sub>2</sub>) for various catalysts during the destruction of 200 ppm of VOCs mixture. As seen in Fig. 2b, increasing SIE leads to higher CO<sub>x</sub> selectivity and among the catalysts studied, AgO<sub>x</sub>/MnO<sub>x</sub> electrodes showed best selectivity (up to ~85–95%), whereas, SMF showed only 65% even at 650 J/l. Fig. 2b also presents the CO<sub>2</sub> selectivity that also followed a similar trend to that of conversion, where AgO<sub>x</sub>/MnO<sub>x</sub>/SMF showed the highest selectivity of close to 80% under dry condition. Hence, for the mixture of VOCs, SMF showed poor carbon balance for VOCs mixture. During the present study trace amounts of by products (aldehyde, aromatic acids, alcohol etc.) were detected at the reactor outlet.

Most of the industrial oxidation processes produce flue gases containing water vapor, thus the effect of water vapor on VOC oxidation process always needs careful investigation [12,13]. The effect of water vapor on oxidation of VOCs mixture has been examined by employing a feed gas containing 50–100 ppm of each VOC in 2% of water vapor (20,000 ppmv). Fig. 2a and b shows the conversion and selectivity to CO<sub>x</sub> as a function of SIE. As seen from Fig. 2, AgO<sub>x</sub>/MnO<sub>x</sub>/SMF under humid conditions showed ~85–90% conversion even at 60 J/l, especially for CB and BZ, against 70 and 80% conversion under dry conditions. The complete conversion was achieved with AgO<sub>x</sub>/MnO<sub>x</sub>/SMF/humid air at SIE of 280 J/l. CO<sub>x</sub>

and CO<sub>2</sub> selectivity was always high under humid conditions over AgO<sub>x</sub>/MnO<sub>x</sub>/SMF. For example at 650 J/l, AgO<sub>x</sub>/MnO<sub>x</sub>/SMF showed ~95% selectivity to CO<sub>2</sub> under humid conditions, whereas for dry mixture, it was around 80%. A similar trend was earlier reported by Gerasimov and Kim during the destruction of VOCs, where on addition of water vapor conversion increased due to in situ formation of OH radicals [5,12].

### 3.2. Decomposition of ozone on metal oxide catalysts

During the present study, SMF electrode modified by transition metal oxides shifted the product distribution toward total oxidation. It was generally believed that ozone decomposition on the metal oxide surface may lead to the formation of a strong oxidant atomic oxygen that may improve the selectivity to total oxidation [11,14–19]. In order to understand the role of ozone during the oxidation of mixture of VOCs, its concentration at the outlet was measured. It has been observed that 850, 450 and 350 ppm of ozone formed at 260 J/l (Fig. 3) with SMF, MnO<sub>x</sub>/SMF and AgO<sub>x</sub>/MnO<sub>x</sub>/SMF, respectively, whereas under humid conditions ozone concentration with AgO<sub>x</sub>/MnO<sub>x</sub>/SMF catalyst was zero. This decrease in the ozone concentration under humid air suggests the formation of atomic oxygen [Eqs. (3) and (4)] on the catalyst surface that may improve the CO<sub>2</sub> selectivity [12,20].



Also, even in dry conditions, MnO<sub>x</sub> and AgO<sub>x</sub>/MnO<sub>x</sub>/SMF decreased ozone conversion, which is in agreement with the better performance over SMF, which changed the product distribution toward the total oxidation of mixture (Fig. 3). Even though MnO<sub>x</sub> facilitates the ozone decomposition leading to formation of atomic

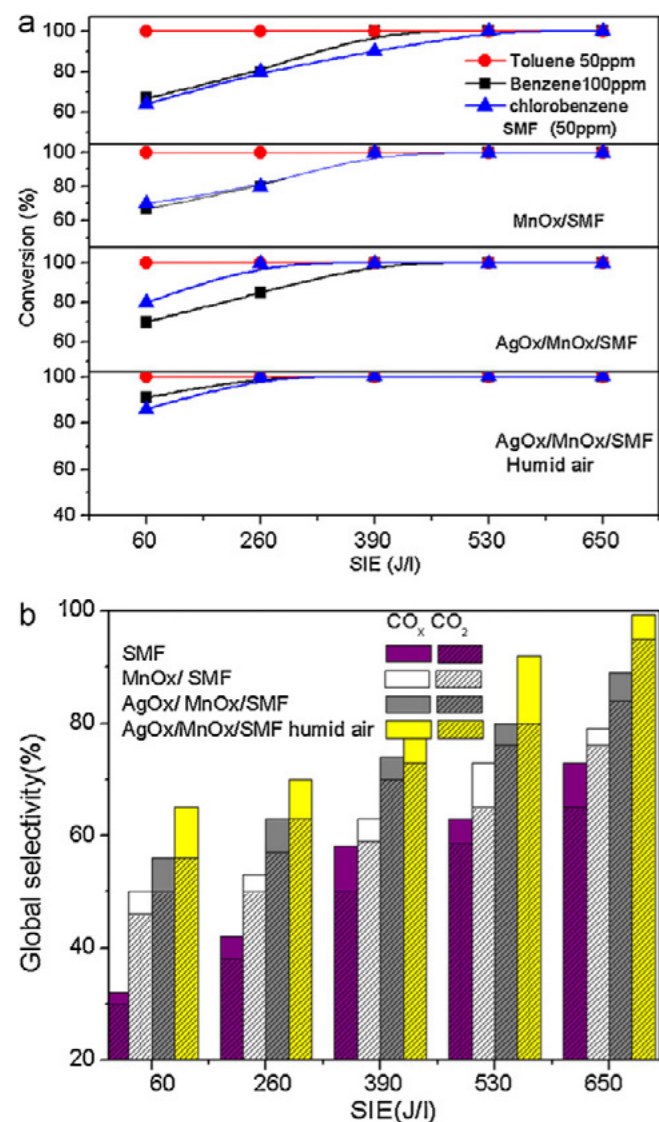


Fig. 2. Influence of SIE and SMF modification during the destruction dry and humid air of mixture VOCs. (a) Conversion and (b) selectivity (SIE 60–650 J/l and 200 ppm of VOCs).

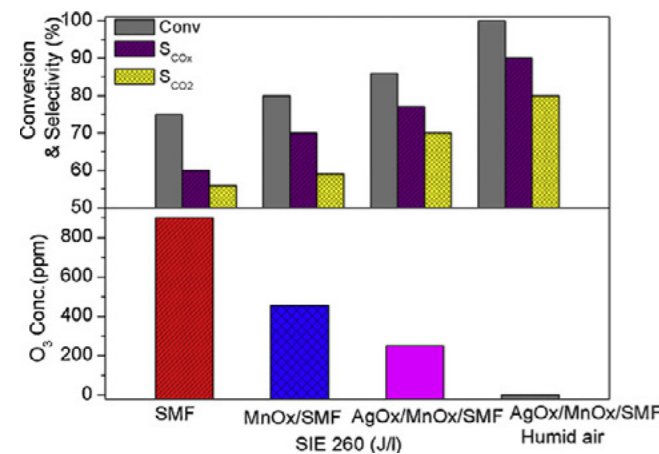


Fig. 3. Activity of SMF electrodes in plasma reactor during ozone decomposition with dry and humid air and influence of ozone concentration in the reactor on decomposition of mixture of VOCs at 260 J/l.

oxygen, AgO<sub>x</sub>/MnO<sub>x</sub> on humid conditions destroyed ozone completely and showed the best performance.

Some transition-metal oxides may deactivate in NTP due to the poisoning effect of carbonaceous deposit, whereas, during the present study, the reactivity of AgO was stable. The oxygen species produced on Ag may be remarkably active in the oxidative process compared with other transition-metal oxides. Reactions (5) and (6) are envisaged to proceed via the dissociative adsorption of O<sub>3</sub> on AgO, which decomposes to atomic oxygen [21,22]:



The distribution of oxygen atom on Ag surface followed by the formation of chemisorbed oxygen is thermodynamically favored over bulk oxide [22]. The heat of adsorption of oxygen on Ag ( $\Delta H = -177.2 \text{ kJ mol}^{-1} \text{ O}_2$ ) is larger than the enthalpy of formation of silver oxides ( $\Delta H = -60.6 \text{ kJ mol}^{-1} \text{ O}_2$ ) [21]. Once the surface is completely covered, the formation of silver oxides from ozone decomposition becomes thermodynamically favored as shown in Eq. (6). Exposure of oxide catalysts to water vapor results in adsorption of H<sub>2</sub>O molecules that may then dissociates into OH<sup>-</sup> and H<sup>+</sup>, forming surface hydroxyl group.

### 3.3. Performance of the reactor on individual and mixture of VOCs decomposition

In order to understand the nature of individual VOCs (100 ppm) and its presence in the mixture (100 ppm each) was tested in the SIE range 60 and 650 J/l with SMF electrode modified with AgO<sub>x</sub>/MnO<sub>x</sub> and the results are presented in Fig. 4a and b. The experiment was performed under dry conditions. Interesting observation is that conversion of any individual VOC is less than that in the mixture. For example conversion of TOL was 75% at 60 J/l, whereas it was close to 100% in the mixture at the same input energy. A similar trend was observed for BZ and CB where higher conversion was observed in the mixture. At 60 J/l, the removal efficiencies for the mixture was 100, 60 and 50%, whereas, for individual VOCs it was only 75, 60 and 40%, respectively for TOL, BZ and CB. Selectivity to CO<sub>x</sub> was shown in Fig. 4b. As seen from Fig. 4b, selectivity to CO<sub>x</sub> for individual VOC was around 80% at 650 J/l, against ~95% for the mixture. Hence, during the destruction of individual and mixture of VOCs, individual VOC demands high energy than mixture. A single component VOC may generate reactive intermediates/radicals. As seen from the data presented in the manuscript; conversion of any VOC was higher in a mixture when compared to individual one. Hence, it may be concluded that treatment of VOCs mixture may enhance the utilization efficiency of active species generated in NTP like high energy electrons and or radicals. This may be due to the possible reactions taking place with excited and/or partially decomposed molecules in the mixture.

In order to understand the observed phenomena, two fundamental types of chemisorption processes on the catalyst surface can be proposed namely, molecular or associative chemisorption, in which all bonds of the adsorbate molecules are retained. Whereas, dissociative chemisorption proceeds via cleavage of adsorbate molecules and fragmented species will be adsorbed on the catalyst surface. As the dissociative chemisorption is always exothermic, the reaction enthalpy is large and positive. Similar observation was made by some authors that the VOCs can be easily activated in a mixture [23–25]. Piotrowska and Syczewska found that the oxidation of n-butyl acetate was high in a mixture of aromatics and alcohols [25]. These activations are probably due to the exothermic

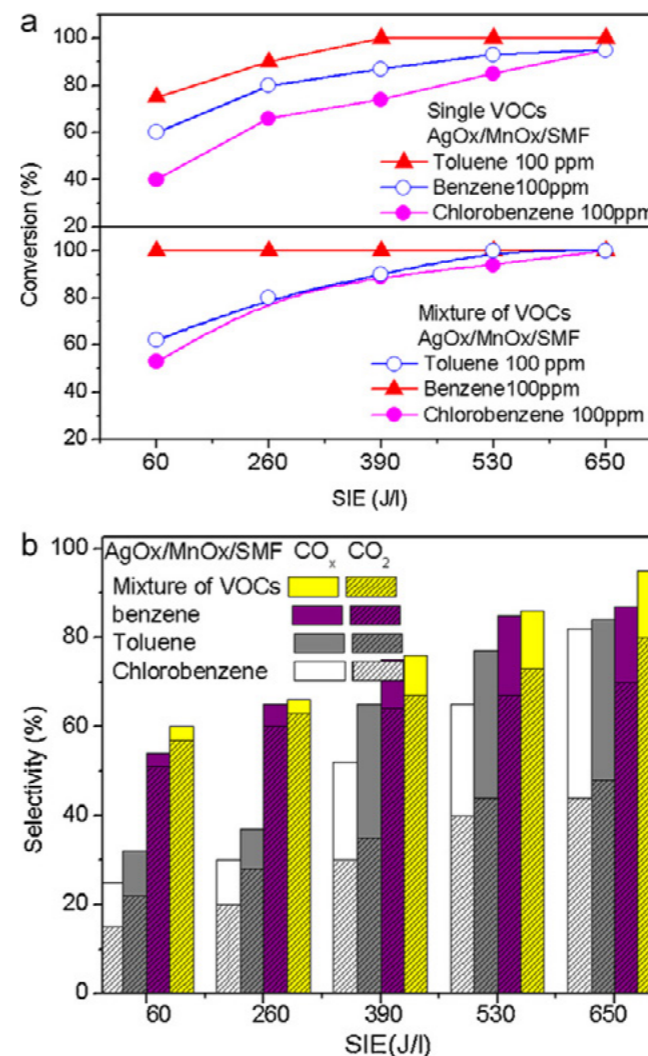


Fig. 4. Influence of single VOCs and mixture of VOCs on AgO<sub>x</sub>–MnO<sub>x</sub>/SMF electrode. (a) Conversion and (b) selectivity to CO<sub>x</sub> and CO<sub>2</sub>.

character of the complete oxidation reaction, which would raise locally the surface temperature of the catalyst [24]. Conversion at each voltage was recorded only after 30 min and the surface area of 5 wt% of catalyst on SMF was less than 10 m<sup>2</sup>/g, hence the activation of VOCs in NTP is due to exothermic nature of the oxidation reactions.

### 3.4. Performance of the reactor for conversion of VOCs at higher initial concentrations

During the present study, concentration of VOCs mixture was changed from 200 to 400 ppm in order to understand the performance of the reactor at higher concentration of VOCs. The experiment was performed under dry conditions. Fig. 5a presents the activity of various catalytic electrodes during the conversion of 400 ppm of VOCs mixture in the SIE range 60–650 J/l. As seen in Figs. 2a and 5a, with increasing the mixture of VOCs concentration from 200 to 400 ppm, the conversion of CB decreased from 80 to 60% at SIE of 60 J/l with AgO<sub>x</sub>/MnO<sub>x</sub>/SMF. However, as seen from Fig. 5a SMF modification with MnO<sub>x</sub> and AgO<sub>x</sub>/MnO<sub>x</sub> showed slightly better conversion than unmodified SMF. For 400 ppm of VOCs mixture the activity of the studied catalysts followed the trend AgO<sub>x</sub>/MnO<sub>x</sub>/SMF > MnO<sub>x</sub>/SMF > SMF. Selectivity to the CO<sub>x</sub> was

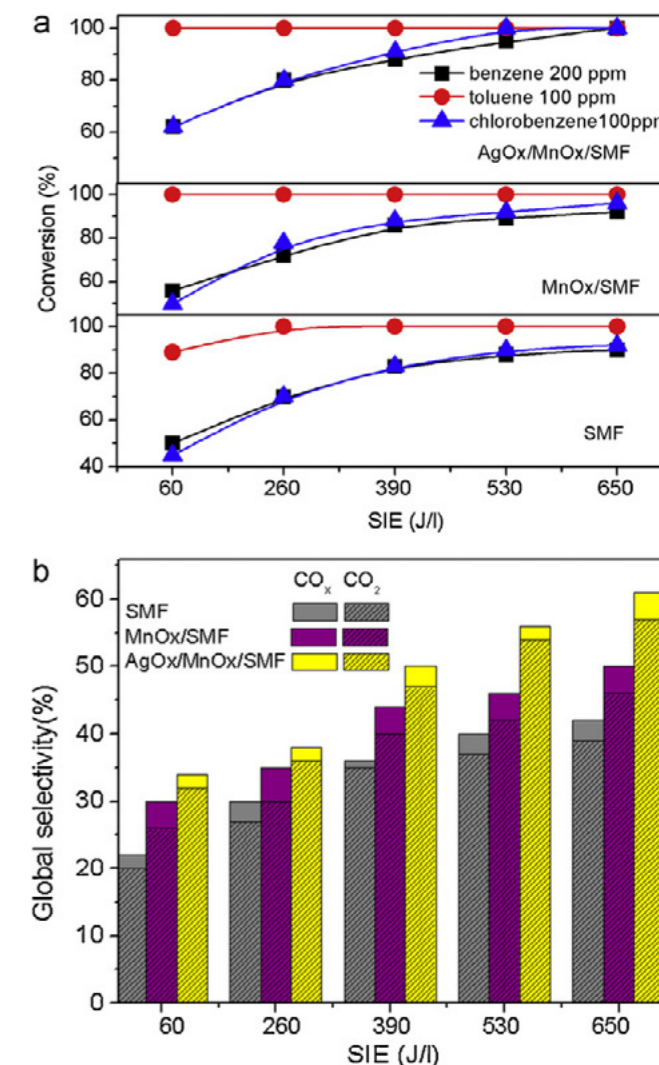


Fig. 5. Activity of SMF electrodes for higher VOC concentrations. (a) Conversion and (b) selectivity to CO<sub>x</sub> and CO<sub>2</sub>.

shown in Fig. 5b. As seen from Figs. 2b and 5b, for 400 ppm of VOC mixture ~40% selectivity to CO<sub>x</sub> was observed at 260 J/l, whereas under the same conditions, for 200 ppm of VOCs mixture, selectivity to CO<sub>x</sub> was around 70% for AgO<sub>x</sub>/MnO<sub>x</sub>/SMF. Hence, during the destruction of 200 ppm of VOC mixture, at any SIE, selectivity to CO<sub>x</sub> and CO<sub>2</sub> was high. For 400 ppm of VOCs mixture, SMF showed ~35% selectivity to CO<sub>2</sub> at 260 J/l, whereas AgO<sub>x</sub>/MnO<sub>x</sub>/SMF showed around 40% CO<sub>2</sub> selectivity even at 260 J/l and reached 65% at 650 J/l. A similar trend was observed on MnO<sub>x</sub>/SMF. Hence, selectivity toward total oxidation of VOCs mixture increases with metal oxide integrated NTP reactor and among the catalysts, AgO<sub>x</sub>/MnO<sub>x</sub>/SMF under humid conditions showed improved performance toward total oxidation.

### 3.5. Reaction products and mechanism of mixture of VOCs decomposition

The chromatogram and GC–MS spectra for the identification of intermediate products during the degradation of mixture of VOCs are given in the supporting information. All detected compounds were identified using the NIST98 library database with fit values higher than 35–95% probability (Table S1 in the supporting information).

Catalytic oxidation of mixture of VOCs was studied over modified SMF catalysts and it was observed that carbon balance was not 100%. High removal efficiencies not always accompanied by high CO<sub>x</sub> or CO<sub>2</sub> selectivity and formation of by-products like NO<sub>x</sub>, ozone, partially fragmented products (benzaldehyde, ethyl benzene, aromatic or higher aliphatic hydrocarbons, aliphatic acids, aromatic acids and alcohols) were observed by GC–MS. Little amounts of polymeric deposits are formed on the walls of the plasma reactor and on the inner electrode, however, they were not analyzed. MnO<sub>x</sub> and AgO<sub>x</sub>/MnO<sub>x</sub> catalysts integration to plasma not only increased the selectivity to CO<sub>2</sub>, but also decreased the by-products like aromatic and aliphatic acids and alcohols. Besides these by-products, the formation of HCl and Cl<sub>2</sub> is also expected from chlorobenzene [26,27]. Close to 60 ppm of NO was detected under dry conditions at SIE of 260J/l, whereas, under humid conditions it increased to ~150 ppm. With increasing SIE to >400J/l, NO concentration approached zero, probably due to chemical reactions of NO with active species like O, OH radicals and O<sub>3</sub> that may lead to the formation of HNO<sub>3</sub>. Nitric acid formation was confirmed by acid–base titration of the water after bubbling gas stream for 4 h. It has been reported that in NTP process, NO molecules may be oxidized to NO<sub>2</sub> and finally to HNO<sub>3</sub> [14,28].

Concerning the reaction mechanism responsible for the removal of VOCs mixture in plasma, decomposition by direct electron impact is unlikely, due to the low concentration of mixture of VOCs in air. Urashima and Chang, and Vandenbroucke et al. suggested that VOCs oxidation takes place by either radicals, negative or positive ions [2,29]. It is proposed that the initial steps of VOCs decomposition differ depending on the plasma regime applied, however, it is generally accepted that ionic reaction may be favored in both dry and humid conditions. The presence of mixture has a beneficial effect on the amount and type of undesired side products, notably ozone and NO<sub>x</sub>. Thus, VOC mixture reduces the formation of ozone and promotes the conversion of NO<sub>x</sub> to HNO<sub>3</sub>. The formation of nitric acid, a desirable side product which is more readily disposed than the NO<sub>x</sub> is favored. NO<sub>2</sub> is formed from oxidation of NO coupled to the conversion of organic peroxyradicals (ROO\*) to the corresponding oxy radicals (RO\*) and may promote the VOC oxidation to CO<sub>2</sub> [2,29,30].

In the same context, MnO<sub>x</sub> and AgO<sub>x</sub> facilitate the formation of atomic oxygen by ozone decomposition. As observed from the data presented, AgO<sub>x</sub>/MnO<sub>x</sub> on humid conditions destroyed ozone completely and showed the best performance. Hence, a possible decomposition mechanism expected to be VOC derived radicals such organic radicals (R\*) generated during plasma reactions are trapped by molecular oxygen (via ozone decomposition on catalytic oxide surface) to form a peroxy radical (ROO\*) and oxyradical (RO\*) [31–36]. The reactions of such radicals either via hydrogen abstraction by molecular oxygen and/or fragmentation lead to carbonyl derivatives, notably aldehydes and ketones. These carbonyl intermediates may form the ultimate oxidation products, CO<sub>2</sub> and water [37,38]. Earlier studies found that the catalytic oxidation and degree of destruction for a compound may also depend on VOCs mixture [38–41].

#### 4. Conclusions

In this work, the enhanced removal of mixture of VOCs in air using a DBD reactor operating at ambient conditions was reported. The present study reveals that NTP is an energy-efficient technology for complete diminution of dilute VOCs of different nature. It also reveals that plasma catalytic approach not only enhances the conversion of mixture of VOCs, but also improves the product selectivity to total oxidation. The experimental results during the oxidation of dilute VOCs mixture indicated that the removal

efficiencies of mixture of VOCs enhanced significantly in the presence of metal oxide catalysts, especially MnO<sub>x</sub>, whose activity was further improved with AgO<sub>x</sub> deposition. Water vapor may facilitate the formation of strong oxidant hydroxyl radical on the catalyst surface. It may be concluded that NTP assisted removal of VOCs from a mixture appeared to be beneficial than the individual VOCs, probably due to the formation of reactive intermediates like aldehydes, peroxides, etc. However, the selectivity to total oxidation needs further improvement. These findings implied that NTP is a promising technique for the removal of mixture of VOCs with MnO<sub>x</sub> and AgO<sub>x</sub>/MnO<sub>x</sub> catalysts integration.

#### Acknowledgements

This work was supported by the Department of Science and Technology (DST) – New Delhi, India under SERC scheme. The authors gratefully acknowledge the generous support by Profs. Albert Renken and Kiwi-Minsker, EPFL, Switzerland.

#### Appendix A. Supplementary data

Supplementary data associated with this article can be found, in the online version, at <http://dx.doi.org/10.1016/j.jhazmat.2012.08.040>.

#### References

- [1] A.P. Jones, Indoor air quality and health, *Atmos. Environ.* 33 (1999) 4535–4564.
- [2] A.M. Vandenbroucke, R. Morent, N.D. Geyter, C. Leys, Non-thermal plasmas for non-catalytic and catalytic VOC abatement, *J. Hazard. Mater.* 195 (2011) 30–54.
- [3] S. Schmid, M.C. Jecklin, R. Zenobi, Degradation of volatile organic compounds in a non-thermal plasma air purifier, *Chemosphere* 79 (2010) 124–130.
- [4] A.M. Harling, D. Glover, J.C. Whitehead, K. Zhang, Novel method for enhancing the destruction of environmental pollutants by the combination of multiple plasma discharges, *Environ. Sci. Technol.* 42 (2008) 4546–4550.
- [5] G. Gerasimov, Modelling study of electron-beam polycyclic and nitro-polycyclic aromatic hydrocarbons treatment, *Radiat. Phys. Chem.* 76 (2007) 27–36.
- [6] H.L. Chen, H.M. Lee, S.H. Chen, M.B. Chang, S.J. Yu, S.N. Li, Removal of volatile organic compounds by single-stage and two-stage plasma catalysis systems: a review of the performance enhancement mechanisms, current status, and suitable applications, *Environ. Sci. Technol.* 43 (2009) 2216–2227.
- [7] C. Fitzsimmons, F. Ismail, J.C. Whitehead, J.J. Wilman, The chemistry of dechloromethane destruction in atmospheric-pressure gas streams by a dielectric packed-bed plasma reactor, *J. Phys. Chem. A* 104 (2000) 6032–6038.
- [8] L.Y. Jin, R.H. Ma, J.J. Lin, L. Meng, Y.J. Wang, M.F. Luo, Bifunctional Pd/Cr<sub>2</sub>O<sub>3</sub>–ZrO<sub>2</sub> catalyst for the oxidation of volatile organic compounds, *Ind. Eng. Chem. Res.* 50 (2011) 10878–10882.
- [9] H. Wang, D. Li, Y. Wu, L. Jie, G. Li, Removal of four kinds of volatile organic compounds mixture in air using silent discharge reactor driven by bipolar pulsed power, *J. Electrostat.* 67 (2009) 547–553.
- [10] Z. Yue, L.I. Duan, W. Hongchang, Removal of volatile organic compounds (VOCs) mixture by multi-pin-mesh corona discharge combined with pulsed high-voltage, *Plasma Sci. Technol.* 12 (2010) 702–707.
- [11] Ch. Subrahmanyam, A. Renken, L. Kiwi-Minsker, Catalytic abatement of volatile organic compounds assisted by non-thermal plasma: Part 1. A novel dielectric barrier discharge reactor containing catalytic electrode, *Appl. Catal. B: Environ.* 65 (2006) 150–156.
- [12] J.C. Kim, Factors affecting aromatic VOC removal by electron beam treatment, *Radiat. Phys. Chem.* 65 (2002) 429–435.
- [13] L.F. Liotta, Catalytic oxidation of volatile organic compounds on supported noble metals, *Appl. Catal. B: Environ.* 100 (2010) 403–412.
- [14] J. Karuppiyah, R. Karvembu, Ch. Subrahmanyam, The catalytic effect of MnO<sub>x</sub> and CoO<sub>x</sub> on the decomposition of nitrobenzene in a non-thermal plasma reactor, *Chem. Eng. J.* 180 (2012) 39–45.
- [15] Ch. Subrahmanyam, M. Magureau, D. Laub, A. Renken, L. Kiwi-Minsker, Non-thermal plasma abatement of trichloroethylene enhanced by photocatalysis, *J. Phys. Chem. C* 111 (2007) 4315–4318.
- [16] H. Einaga, A. Ogata, Benzene oxidation with ozone over supported manganese oxide catalysts: effect of catalyst support and reaction conditions, *J. Hazard. Mater.* 164 (2009) 1236–1241.
- [17] H. Einaga, A. Ogata, Catalytic oxidation of benzene in the gas phase over alumina-supported silver catalysts, *Environ. Sci. Technol.* 44 (2010) 2612–2617.
- [18] U. Roland, F. Holzer, F.D. Kopinke, Improved oxidation of air pollutants in a non-thermal plasma, *Catal. Today* 73 (2002) 315–323.

- [19] A.M. Harling, D.J. Glover, J.C. Whitehead, K. Zhang, The role of ozone in the plasma-catalytic destruction of environmental pollutants, *Appl. Catal. B: Environ.* 90 (2009) 157–161.
- [20] S. Imamura, M. Ikebata, Decomposition of ozone on a silver catalyst, *Ind. Eng. Chem. Res.* 30 (1991) 217–221.
- [21] F. Besenbacher, J.K. Nørskov, Oxygen chemisorption on metal surfaces: general trends for Cu, Ni and Ag, *Prog. Surf. Sci.* 44 (1993) 5–66.
- [22] C.I. Carlisle, T. Fujimoto, W.S. Sim, D.A. King, Atomic imaging of the transition between oxygen chemisorption and oxide film growth on Ag{1 1 1}, *Surf. Sci.* 470 (2000) 15–31.
- [23] D.M. Papenmeier, J.A. Rossin, Catalytic-oxidation of dichloromethane, chloroform, and their binary-mixtures over a platinum alumina catalyst, *Ind. Eng. Chem. Res.* 33 (1994) 3094–3103.
- [24] N. Burgos, M. Paulis, M.M. Antxustegi, M. Montes, Deep oxidation of VOC mixtures with platinum supported on Al<sub>2</sub>O<sub>3</sub>/Al monoliths, *Appl. Catal. B: Environ.* 38 (2002) 251–258.
- [25] A.M. Piotrowska, K. Syczevska, Destruction of volatile organic mixtures by catalytic combustion, *Environ. Prot. Eng.* 15 (1989) 115–125.
- [26] H.R. Snyder, G.K. Anderson, Effect of air and oxygen content on the dielectric barrier discharge decomposition of chlorobenzene, *IEEE Trans. Plasma Sci.* 26 (1998) 1695–1699.
- [27] M. Dilmeghani, K.O. Zahir, Kinetics and mechanism of chlorobenzene degradation in aqueous samples using advanced oxidation processes, *J. Environ. Qual.* 30 (2001) 2062–2070.
- [28] L. Xia, L. Huang, Shu, R. Zhang, W. Dong, H. Hou, Removal of ammonia from gas stream with dielectric barrier discharge plasmas, *J. Hazard. Mater.* 152 (2008) 113–119.
- [29] K. Urashima, J.S. Chang, Removal of volatile organic compounds from air streams and industrial flue gases by non-thermal plasma technology, *IEEE Trans. Dielect. Elect. Insul.* 7 (2000) 602–614.

- [30] M.J. Kirkpatrick, W.C. Finney, B.R. Locke, Plasma-catalyst inter-actions in the treatment of volatile organic compounds and NO<sub>x</sub> with pulsed corona discharge and reticulated vitreous carbon Pt/Rh-coated electrodes, *Catal. Today* 89 (2004) 117–126.
- [31] M. Schiorlin, E. Marotta, M. Rea, C. Paradisi, Comparison of toluene removal in air at atmospheric conditions by different corona discharges, *Environ. Sci. Technol.* 43 (2009) 9386–9392.
- [32] Y. Xi, C. Reed, Y.K. Lee, S.T. Oyama, Acetone oxidation using ozone on manganese oxide catalysts, *J. Phys. Chem. B* 109 (2005) 17587–17596.
- [33] B. Dhandapani, S.T. Oyama, Gas phase ozone decomposition catalysts, *Appl. Catal. B: Environ.* 11 (1997) 129–166.
- [34] K. Genov, V. Georgiev, T. Bataklijev, D.K. Sarker, Ozone decomposition over silver-loaded perlite, *Int. J. Civil Environ. Eng.* 3 (2011) 202–205.
- [35] H. Einaga, S. Futamura, T. Ibusuki, Complete oxidation of benzene in gas phase by platinumized titania photocatalysts, *Environ. Sci. Technol.* 35 (2001) 1880–1884.
- [36] J. Ma, N.J.D. Graham, Degradation of atrazine by manganese-catalyzed ozonation: influence of humic substances, *Water Res.* 33 (1999) 785–793.
- [37] L. Yang, C. Hu, Y. Nie, J. Qu, Catalytic ozonation of selected pharmaceuticals over mesoporous alumina-supported manganese oxide, *Environ. Sci. Technol.* 43 (2009) 2525–2529.
- [38] R.K. Sharma, B. Zhou, S. Tong, K.T. Chuane, Catalytic destruction of volatile organic compounds using supported platinum and palladium hydrophobic catalysts, *Ind. Eng. Chem. Res.* 34 (1995) 4310–4317.
- [39] S.K. Gangwal, M.E. Mullins, J.J. Spivey, P.R. Caffrey, B.A. Tichenor, Kinetics and selectivity of deep catalytic oxidation of n-hexane and benzene, *Appl. Catal.* 36 (1988) 231–247.
- [40] B.A. Tichenor, M.A. Palazzolo, Destruction of volatile organic compounds via catalytic incineration, *Environ. Prog.* 6 (1987) 172–176.
- [41] J.J. Spivey, Complete catalytic oxidation of volatile organics, *Ind. Eng. Chem. Res.* 26 (1987) 2165–2180.



## Corona Destruction: An Innovative Control Technology for VOCs and Air Toxics

Carlos M. Nunez , Geddes H. Ramsey , Wade H. Ponder , James H. Abbott , Larry E. Hamel & Peter H. Kariher

To cite this article: Carlos M. Nunez , Geddes H. Ramsey , Wade H. Ponder , James H. Abbott , Larry E. Hamel & Peter H. Kariher (1993) Corona Destruction: An Innovative Control Technology for VOCs and Air Toxics, *Air & Waste*, 43:2, 242-247, DOI: 10.1080/1073161X.1993.10467131

To link to this article: <https://doi.org/10.1080/1073161X.1993.10467131>

Published online: 06 Mar 2012.

Submit your article to this journal [↗](#)

Article views: 615

View related articles [↗](#)

Citing articles: 105 View citing articles [↗](#)

Full Terms & Conditions of access and use can be found at <https://www.tandfonline.com/action/journalInformation?journalCode=uawm20>

### CONTROL TECHNOLOGY

# Corona Destruction: An Innovative Control Technology for VOCs and Air Toxics

**Carlos M. Nunez, Geddes H. Ramsey, Wade H. Ponder and James H. Abbott**  
Air and Energy Engineering Research Laboratory  
Environmental Protection Agency  
Research Triangle Park, North Carolina

**Larry E. Hamel and Peter H. Kariher**  
Acurex Corporation  
Research Triangle Park, North Carolina

This paper discusses the work and results to date leading to the demonstration of the corona destruction process at pilot scale. The research effort in corona destruction of volatile organic compounds (VOCs) and air toxics has shown significant promise for providing a valuable contribution to critical U.S. Environmental Protection Agency and national goals of reducing the health effects associated with exposures to hazardous air pollutants. The corona destruction technology could be especially useful in future years in helping industry meet the residual risk requirements of the Clean Air Act Amendments of 1990.

Since 1988, EPA has conducted research in the area of corona destruction of VOCs and air toxics. EPA's interest in corona destruction of molecular species started with modeling of a point-plane reactor for destroying toxic organic compounds. EPA's goal is to develop a technology capable of controlling low concentration streams at low capital and operating costs. The purpose of this work is to develop an industrial scale corona reactor capable of efficiently and cost-effectively destroying VOCs and air toxics at ambient temperature and pressure. Results show that corona destruction is a promising control technology for many VOC-contaminated air streams, especially at low concentrations. Cost comparisons are presented for corona destruction and conventional control devices, carbon adsorption, catalytic incineration and thermal incineration.

The research effort in corona destruction of volatile organic compounds (VOCs) and air toxics has shown significant promise for providing a valuable contribution to critical EPA and national goals of reducing the health effects associated with exposures to hazardous air pollutants. The corona destruction technology could be especially useful in future years in helping industry meet the residual risk requirements of the Clean Air Act Amendments of 1990.

Since 1988, EPA's Air and Energy Engineering Research Laboratory has conducted research in the area of corona destruction of VOCs and air toxics. EPA's interest in corona destruction of molecular species started with modeling of a point-plane reactor for destroying toxic organic compounds.<sup>1</sup> The emerging concern for excessive concentrations of ambient ozone, for which many VOCs are precursors,

the need to develop technology to control low concentration streams, and the economic advantages of ambient temperature operation provided impetus for the work on high intensity corona reactor devices.

The purpose of this work is to develop an industrial scale corona reactor capable of efficiently and cost-effectively destroying VOCs and air toxics at ambient temperature and pressure.

The work and results to date leading to the demonstration of the corona destruction process at pilot scale are presented in this paper.

#### Background

The initial work at EPA involved investigating the viability of corona destruction as an effective device for VOCs. The initial tests were run with toluene and were very successful. The next phase of the research program involved developing the destruction mechanism and prediction theory for destruction of other hydrocarbons. Even though corona destruction was able to destroy toluene, an understanding of the reaction mechanisms, both chemically and electrically, is necessary before larger systems can be successfully designed. Thus, a series of experiments was conducted using 10 compounds, and the destruction efficiency and ionization potential of each compound was examined to determine the possible existence of a statistical correlation. The compounds tested were benzene, cyclohexane, ethanol, hexane, hexene, methane, methylene chloride, methyl ethyl ketone, styrene and toluene. Preliminary results indicate that a relationship exists between ionization potential and ease of destruction for VOCs, the lower the ionization potential, the easier the compounds are destroyed.

Corona destruction has several advantages over conventional control devices as shown in Table I. The compounds that we have tested have been oxidized to carbon dioxide, carbon monoxide, and water, plus, in the case of chlorinated compounds, chlorine and hydrochloric acid. The exhaust streams have been analyzed thoroughly with a gas chromatograph/flame ionization detector (GC/FID) and gas chromatograph/mass spectroscopy (GC/MS), and no intermediate compounds have been found. Since the contami-

Copyright 1993 - Air & Waste Management Association

**Table I.** Benefits of corona destruction over conventional technologies.

- Performs effectively and economically at very low concentrations
- Operates at ambient temperature
- Eliminates disposal or treatment problems associated with carbon adsorption
- Eliminates sensitivity to poisoning by sulfur or halogen containing compounds
- Requires no auxiliary fuel
- Requires low maintenance

nants are destroyed, the problem of disposing of collected toxins is avoided.

Two corona destruction processes have been evaluated for their potential in destroying VOCs and air toxics. One of the corona destruction processes uses high dielectric barium titanate pellets in a packed-bed reactor across which a high voltage alternating current (AC) is applied. The micro-electric fields developed in the interstitial spaces between the pellets form a multiplicity of corona sites which generate electrons. These electrons initiate the reactions that lead to destruction of the challenge gas species. The second process consists of a wire-in-tube reactor which is energized by high voltage nanosecond pulses. These techniques have the potential of generating very energetic electrons without wasting power by accelerating ions.

The corona processes operate at ambient temperature. The corona is generated in the packed-bed of barium titanate pellets or along the wire in the pulsed reactor. The necessity of heating the contaminated air streams to the temperature required for a catalyst or for thermal incineration to work is avoided.

The corona destruction processes were also evaluated as a means to control very low concentrations of contaminants in air streams. Experiments with contaminant streams using 10 ppmv single component VOCs in air demonstrated the ability to destroy the contaminant beyond the detection limit of our analytical equipment (< 10 ppbv). Corona destruction may be an alternative control technology for low concentration streams where conventional control devices such as catalytic incineration and carbon adsorption have disadvantages, either economical or technical. Preliminary power estimates for the corona process indicate that the power requirement for VOC destruction is approximately 3 W/ft<sup>3</sup> (106 J/sec/m<sup>3</sup>). As shown in Figure 1, the annual operating costs of corona destruction fall below the costs of catalytic incineration and thermal incineration.<sup>2</sup> The annual operat-

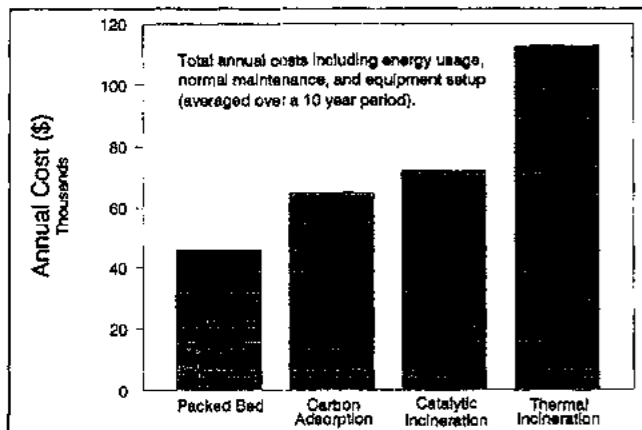


Figure 1. Estimated costs of corona process and conventional VOC control technologies.

**Table II.** Potential source categories for the application of corona destruction.**Industrial**

- Painting and coating operations
- Semiconductor and electric component manufacture
- Food and pharmaceutical processing
- Site remediation

**Commercial**

- Commercial paint operations (body shops)
- Furniture manufacturers
- Dry cleaning establishments
- Restaurants

ing costs for these technologies are based on a contaminated air stream at ambient conditions with a flowrate of 3000 acfm and an organic concentration of less than 100 ppmv. For these reasons, corona destruction may be well suited to destroy VOCs and air toxics in the outlet stream from operations such as the ones shown in Table II.

One of our current program objectives is to test the corona reactor on a larger scale. Experiments are currently underway to prove the feasibility of the packed-bed reactor on a 20 to 50 cfm (0.57 to 1.42 m<sup>3</sup>/min) stream. At this stage, the reactor design can be optimized as to dimensions and power requirements. Other program objectives include demonstration of this technology on an industrial scale and commercialization of corona destruction as a VOC control alternative.

The purpose of this work is to determine if VOCs can be destroyed in these high intensity corona reactors. In setting up the original feasibility-of-concept experiments, an attempt was made to relate the work to the greatest extent possible to current problems threatening the environment. For these experiments both non-halogenated and halogenated compounds were evaluated.

**Theory of Corona Destruction**

Although several theoretical concepts are still being evaluated to describe the destruction pathways for several families of hydrocarbons, the following discussion provides some of the most likely mechanisms for VOC destruction in a corona process.

Electrons undergo both elastic and inelastic collisions as they travel through energy fields. In an elastic collision, the electron retains the majority of its kinetic energy. Under the influence of the strong electric field, free electrons are accelerated. They undergo an elastic collision at the end of each free path length. The electrons continue to increase in energy until the energy becomes high enough to allow the electrons to undergo an inelastic collision. During an inelastic collision the electron transfers all or part of its kinetic energy to the particle with which it has collided. Inelastic collisions result in a change to the target particle or molecule such as ionization, dissociation or excitation.<sup>3</sup> In an inelastic collision, significant amounts of energy are transferred from an electron to the target species. Examples of these inelastic collisions are:

- Electron attachment by electronegative gases to form negative ions.
- Dissociation of molecular species into smaller fragments including formation of free radicals.
- Excitation of molecular and elemental species.
- Ionization to form positive ions and additional free electrons (a Townsend avalanche develops under favorable circumstances, generating many additional free electrons).

- Breaking down of molecular species into their elemental components.

The amount of energy required for the above events varies by type of event and molecular/elemental species. Energy requirements for different types of events are less than 5 eV for electron attachment and 5 to 25 eV to form positive ions by electron removal.<sup>4</sup> An electron volt (eV) is defined as the energy that an electron acquires (or loses) in passing through a 1 V change in potential. The electron volt is a particularly useful unit of measurement for this work because it allows an easy comparison of electrical energy input required for destruction of the target molecules. The probability of one of the above events occurring is expressed by the collision cross section which is mainly a function of concentration. The probability that the event will occur is dependent on the electron's having achieved the energy level needed for the event.

At atmospheric pressure and ambient temperatures, an electron's energy level can increase by a fraction of 1 eV in one mean free path length, if the mean free path length is parallel to an electric field of 20 to 30 kV/cm. At atmospheric pressure and ambient temperature a mean free path length is about 1 x 10<sup>-7</sup> m.

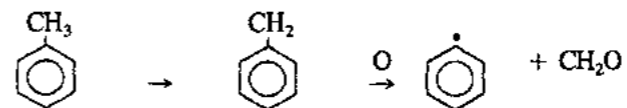
In addition to the above effects of inelastic electron collisions, there are also photoelectric effects (ionization, dissociation, excitation, etc.) which are either activated by or result in the emission of a photon. The events that can occur are very much interrelated.

In summary, the picture that is presented is one of high complexity when the possibility of electron collisions and the effects of photons are considered. The energy distribution in a swarm of energetic electrons ranges from very low to very high, with the majority centered around some median value. Therefore, electrons having a wide range of energies will undergo various types of inelastic collisions such as attachment, excitation and ionization. For a mixture of gases the picture becomes even more complex.

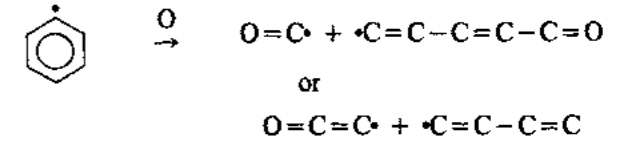
The power input to the bench-scale packed-bed reactor was measured, allowing the calculation of the energy introduced for a unit of time. For a typical toluene concentration of about 200 ppmv the energy introduced per toluene molecule was about 400 eV (9300 kcal/g-mole). The carbon byproducts were CO<sub>2</sub> and CO. The ratio of CO<sub>2</sub> to CO was about 2:1.

A number of reaction mechanisms are possible in the corona destruction of aromatic hydrocarbons. Three of the reactions are presented and discussed. The first reaction mechanism involves initial attack of the hydrocarbon molecule with an energized oxygen molecule. The other two reaction mechanisms, which involve breaking a C-C bond in the ring or removing a hydrogen from one of the carbons in the ring, have a lower probability.<sup>5</sup>

A mechanism likely to occur in the destruction of toluene is the oxidation of the methyl group of the molecule. Toluene has a resonance structure where a proton is lost or gained at the methyl group which should result in a more reactive site. The methyl group serves as an electron donor to the phenyl group. An excited oxygen molecule would attack the methyl group and the following reaction would proceed:



The CH<sub>2</sub>O radical rapidly reacts to form a CHO radical which goes to CO. The benzene radical reacts as follows:



The O=C or O=C=C radical reacts with oxygen to form CO<sub>2</sub>. The other radical oxidizes rapidly to CHO and then to CO.<sup>2</sup> Although the reaction to form CO rather than CO<sub>2</sub> is favored at low temperatures, high temperatures may be generated at the pellets, which would explain the favored formation of CO<sub>2</sub>. A CO<sub>2</sub> molecule is formed when the ring breaks, but the CO reaction is favored in the remainder of bond destruction reactions. This accounts for the approximately 1.7:1 ratio of CO<sub>2</sub> to CO observed experimentally.

The energies of bond formation/destruction are:<sup>3</sup>

C-C	3.6 eV
C=C	6.3 eV
C=C (in ring)	5.5 eV
C-H	4.3 eV
C-O	3.7 eV
C=O	7.7 eV
C=O (in CO <sub>2</sub> )	8.3 eV
C-Cl	3.5 eV

During the destruction of a toluene molecule, energy is required to break a C-H bond by an electron or by reaction with oxygen. The radical formed will react with an excited oxygen molecule, e.g., singlet oxygen (<sup>1</sup>Σ<sub>g</sub><sup>+</sup> and <sup>1</sup>Δ<sub>g</sub>) to form a C-O bond.<sup>6</sup> The energy released when the C-O bond forms is more than enough to break the adjacent C-C bonds. Therefore, the energy for the reaction once past the initiation energy must come from the oxidation of the toluene itself.<sup>7</sup> Because 20 percent of the gas is oxygen and since the oxygen molecule is one of the easiest to excite, the excitation of the oxygen molecule is consequently the most likely mechanism occurring in the process. The potential energies for the ground state and the first four electronically excited states of oxygen are shown in Table III.

The addition of energy greater than 7 eV causes dissociation of the oxygen molecule to one atom in the ground state and one in the 1st excitation state.<sup>8</sup> Many other excited states of oxygen are possible inside the corona destruction reactor.

The benzene molecule should react similarly to the toluene molecule, but slightly more energy would be required to initiate the benzene reaction. Instead of the excited oxygen attacking the methyl group of the toluene molecule, the point of attack in the benzene molecule would have to be the ring structure or a C-H bond. The bond energies would favor an attack of the C-H bond (4.3 eV for the C-H bond compared to 5.5 eV for the C=C bond). This is slightly

**Table III.** The potential energies for the excited state of oxygen.

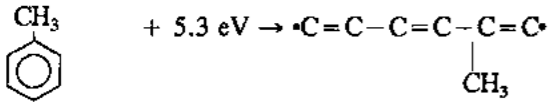
State of Oxygen Molecule	Energy Required eV	Comments
Ground state	0	
1st excitation	0.98	Forbidden transition
2nd excitation	1.63	Allowed; half-life of about 10 seconds; collisionally relaxing to 1st excitation state
3rd excitation	4.25	Theoretically forbidden
4th excitation	6.00	Allowed; creates two oxygen atoms in the ground state via a non-radiative transition

higher than the C-C bond energy which would be the point of attack in the toluene molecule (3.6 eV for the C-C bond). Therefore, since a higher energy is required to initiate the reaction of the benzene molecule, destruction of benzene should be lower than toluene under similar conditions. This was confirmed by our laboratory results.

The second possible reaction is the breaking of a C-C bond in the chain by a sufficiently energetic electron. This reaction is of the type:



in which [AB] is a radical. For the toluene molecule, the ring structure has a greater affinity for an electron than does the methyl group. The energy required to break a C-C bond in the toluene ring is 5.3 eV (123 kcal/g-mole). For toluene, cleavage of an arbitrary C-C bond would be:



The fragment on the right-hand side of the above reaction equation is a radical. The energy required for the ionization of toluene is 8.5 eV (195 kcal/g-mole). Consequently, the collision cross section for the C-C bond cleavage is considerably less than that for the ionization.

Once a C-C bond is broken and the free radical is formed, the free radical is able to react with oxygen. The heat of oxidation of toluene is 39 eV (901 kcal/g-mole) when going to CO<sub>2</sub> and 22 eV (497 kcal/mole) when going to CO.<sup>3</sup> Either pathway will supply sufficient energy to sustain the oxidation of all carbon molecules once the reaction starts.

For this second reaction to occur, electrons would have to achieve 5.3 eV to sever a C-C bond. Many electrons do achieve the higher energy levels, but not all.

A final reaction possibility is removing a hydrogen from the ring structure by electron collision. The energy required to break a C-H bond is about 4.3 eV. Once the C-H bond is broken the reaction will proceed by the same mechanism as the primary reaction suggested above. This mechanism would also account for the CO/CO<sub>2</sub> formation.

The intermediate steps in the oxidation require the attachment of an oxygen to a severed carbon bond or to a site where a hydrogen was removed. The energy released by attachment of the oxygen is sufficient to break an adjacent C-C bond, which provides the site for the next oxygen attachment. The most likely intermediate byproduct is the radical CHO which is favored at low temperatures. The CHO radical leads to the formation of CO; higher temperature reactions favor the formation of CO<sub>2</sub>. Note that once a C-C bond in the ring is severed, the radical that is formed has two active ends for attachment of an oxygen.

In all the suggested mechanisms, once the reaction of the individual molecule is initiated, the destruction of the molecule proceeds to completion since no other lower molecular weight species are found during analysis. If the molecule were not completely oxidized, other hydrocarbon byproducts would appear in the exhaust stream. The absence of other hydrocarbons has been confirmed by GC/MS. For operating conditions in which less than 100 percent destruction is deliberately achieved, the unreacted toluene molecules remain intact, which is evident in GC/MS.

### Results and Discussion

The packed-bed corona reactor makes use of a bed of ferroelectric pellets across which an AC electric field is impressed. A total of 10 hydrocarbons (benzene, cyclo-

hexane, ethanol, hexane, hexene, methane, methylene chloride, methyl ethyl ketone, styrene and toluene) were tested in the bench-scale packed-bed reactor. The bench-scale packed-bed reactor is depicted in Figure 2.

The pellets must be made of a material with a high dielectric constant. In this case the material is barium titanate with a dielectric constant ranging from 15 to 12,000.<sup>9</sup> The dielectric constant for barium titanate varies due to temperature, bead size and impurities. The barium titanate pellets are energized by an AC voltage applied through porous stainless steel plates. Corona appears at the contact points of the pellets when an AC electric field is generated as low as about 1 kV/cm. Sparking across the bed occurs for fields of 5 to 8 kV/cm, depending upon the size of the pellets. The reactor obviously uses more energy during sparking; however, the reactor performance is not improved proportionally to the increased amount of power applied during sparking. The most efficient operating point will be below sparking conditions.

The work required to remove a given electron from its atomic orbit and place it at rest at an infinite distance, is called the ionization potential.<sup>8</sup> Since all the compounds evaluated in the laboratory were not destroyed equally in the packed-bed corona reactor, the first method attempted to predict the destruction efficiency was based on ionization potential (see Table IV). Other parameters evaluated were heat of combustion, size of molecule, molecule bonding energy, Gibbs free energy and enthalpy. From the parameters evaluated to estimate the destruction of compounds in the packed-bed corona reactor, the ionization potential was the value that best correlated with destruction efficiency, i.e., the higher the ionization potential, the lower the destruction at constant operating conditions. As shown in Figure 3, factors other than ionization potential may explain the deviations from the predicted destruction efficiencies. In addition to the great ionization power of electrons, they also have the property of attaching to many molecular and atomic species to form negative gas ions. Electron attachment is greatest for atoms in the upper right-hand region of the periodic table. For example, methylene chloride has

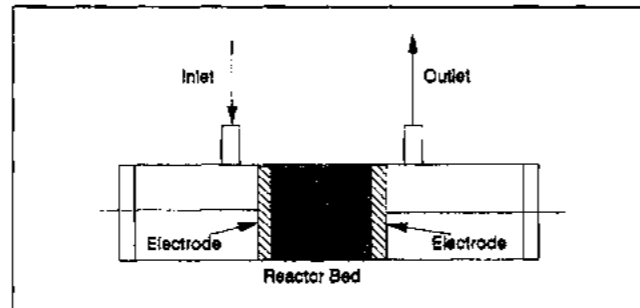


Figure 2. Bench-scale packed-bed corona destruction reactor.

Table IV. Ionization energies of selected molecules, eV.

Nitrogen	15.6	Formaldehyde	10.9
Hydrogen	15.4	Methanol	10.9
Carbon Monoxide	14.0	Hexane	10.2
Carbon Dioxide	13.8	Nitrogen Dioxide	9.8
Methane	13.0	Methyl Ethyl Ketone	9.5
Nitrous Oxide	12.9	Hexene	9.4
Ozone	12.8	Cyclohexane	9.4
Water	12.6	Benzene	9.3
Oxygen	12.1	Nitric Oxide	9.3
Methylene Chloride	11.3	Toluene	8.8
		Naphthalene	8.1

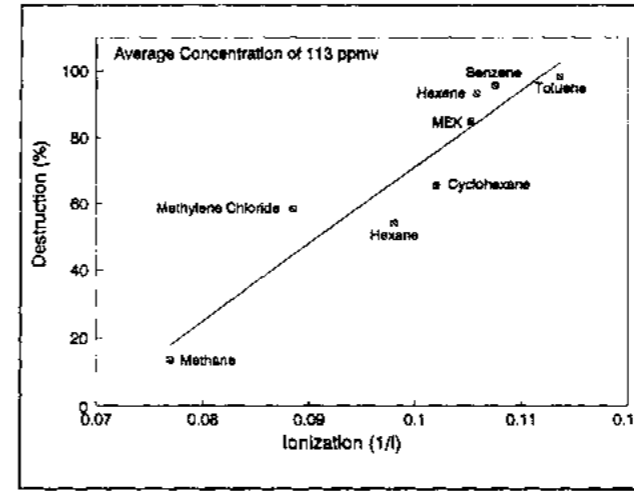


Figure 3. Destruction of VOCs as a function of ionization potential.

a higher ionization potential than hexane; however, the destruction efficiency is higher. This is probably due to the high electronegativity of the chlorine atom which will increase the chance of electron attachment to the chlorine atom.

A test matrix consisting of three sets of eight runs for a total of 24 runs was performed using toluene in the bench scale corona reactor. This test matrix was designed to support the calculation of material and energy balances, characterize wall effects, and determine the magnitude of systematic and random errors. Two reactor sizes (diameters of 2.23 and 3.18 cm), two face velocities (1.8 and 5.3 cm/sec), two residence times (0.48 and 1.43 seconds), and two toluene concentrations (50 and 250 ppmv) were used for the test matrix. The reactor length was 2.5 cm. The reactors were placed in an oven at 50 °C to maintain a constant temperature. Before each block of eight runs was initiated, the reactors were disassembled, the pellets were replaced by an equal weight of unused pellets, and the reactors were reassembled. Figures 4 and 5 show the outlet concentration of toluene, CO<sub>2</sub> and CO obtained during these experiments for toluene inlet concentrations of 50 and 250 ppmv, respectively. Each reactor performance was controlled by the gas flowrate (face velocity and residence time). The product of face velocity and residence time was maintained at about 2.5 cm for both reactors (R<sub>1</sub> and R<sub>2</sub>). The carbon balance for the test matrix varied from 102 to 105 percent.

In Figure 6, the effect of voltage on reactor performance for the large reactor (R<sub>2</sub>) and for a toluene concentration of 50 ppmv is shown. For voltages over 15 kV complete destruction of toluene was obtained.

The electric power for these experiments was measured using a digital oscilloscope connected to the corona reactor. The circuitry used to measure both voltage and amperage is depicted in Figure 7. Since the current signal is not of a sinusoidal form,  $e_i \cos \theta$  was not used to estimate power consumption. Power was calculated by integrating the area under the power curve using Simpson's rule. The power curve is the result of multiplying each data point of the current curve with the corresponding data point of the voltage curve. The voltage and amperage for one cycle (16.7 ms) was analyzed using a customized spreadsheet program. Figure 8 is an example of the graphical output from the power curve analysis.

### Conclusions

The packed-bed corona destruction process shows significant promise as an alternative control method for re-

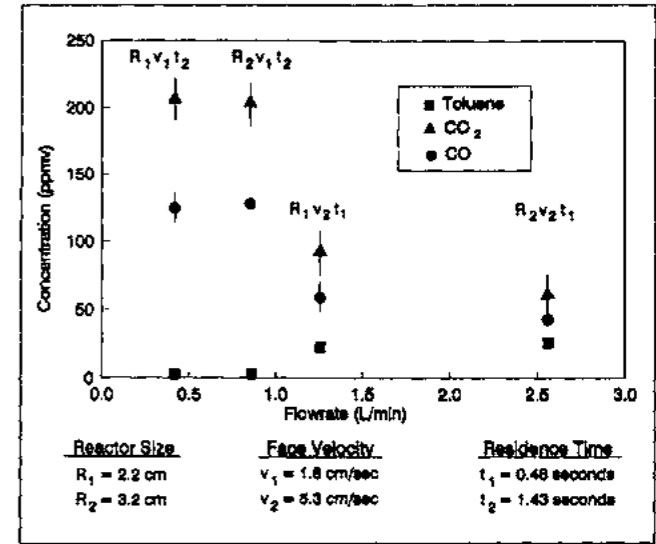


Figure 4. Outlet concentration of toluene, CO<sub>2</sub>, and CO at various flowrates (toluene inlet concentration of 50 ppmv).

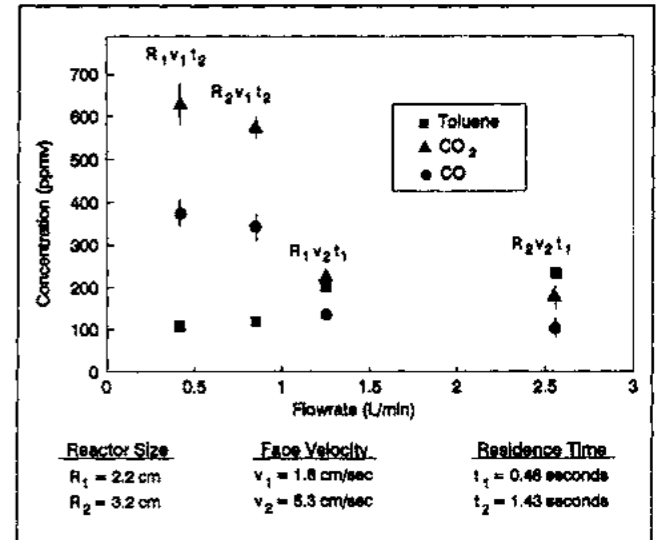


Figure 5. Outlet concentration of toluene, CO<sub>2</sub>, and CO at various flowrates (toluene inlet concentration of 250 ppmv).

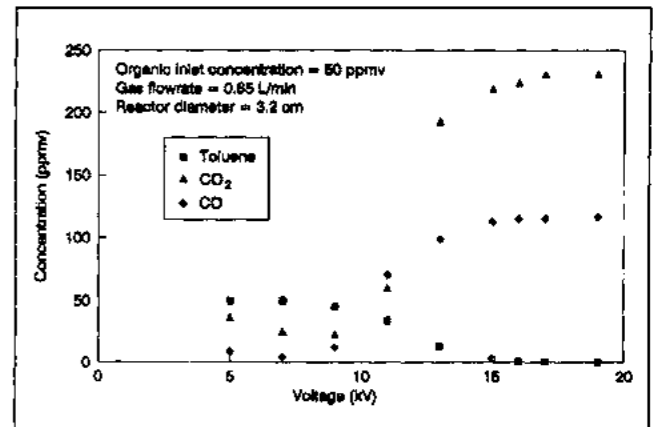


Figure 6. Toluene, CO<sub>2</sub>, and CO outlet concentration as a function of voltage.

ducing VOC and air toxics emissions from industrial and commercial operations. Preliminary data show that this technology is technically and economically feasible. When the corona destruction process is compared to conventional control technologies such as carbon adsorption, catalytic



## Review

## The application of dielectric barrier discharge non-thermal plasma in VOCs abatement: A review

Shijie Li<sup>a</sup>, Xiaoqing Dang<sup>a,\*</sup>, Xin Yu<sup>a</sup>, Ghulam Abbas<sup>b</sup>, Qian Zhang<sup>a,\*</sup>, Li Cao<sup>a</sup><sup>a</sup> School of Environment & Municipal Engineering, Xi'an University of Architecture & Technology, Xi'an 710055, China<sup>b</sup> Department of Chemical Engineering and Technology, University of Gujrat, Gujrat 50700 Pakistan

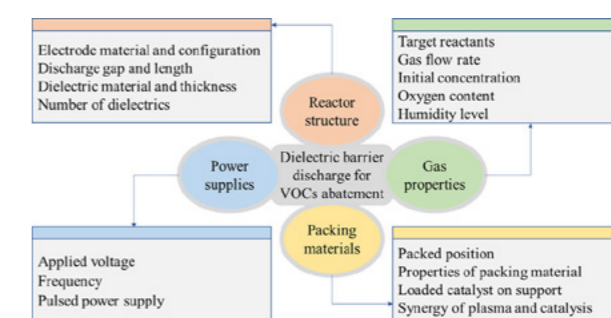
## HIGHLIGHTS

- The history, microdischarge formation and application of DBD were presented.
- The effect of reactor structure, power supplies, packing materials and gas properties on VOCs removal were described.
- The discussion of the above factors was based on discharge behaviors, VOCs removal and mineralization rate, and by-products.
- The practical implementation of DBD in VOCs abatement were examined.
- Future trends on DBD for VOCs treatment were given.

## ARTICLE INFO

**Keywords:**  
Dielectric barrier discharge  
Volatile organic compounds  
Reactor structure  
Power supplies  
Packing material  
Gas properties  
Practical application

## GRAPHICAL ABSTRACT



## ABSTRACT

This review describes the history and current status of dielectric barrier discharge (DBD) non-thermal plasma (NTP) for volatile organic compounds (VOCs) abatement. Firstly, the history of DBD, the formation of micro-discharge and its environmental applications were presented. Next, the status quo of DBD for VOCs removal was discussed in detail from four aspects: reactor structure (include electrode material and configuration, discharge gap and length, dielectric material and thickness, and number of dielectrics), power supplies (include applied voltage, frequency and pulsed power supply), packing materials (include packed position, properties of packing material, loaded catalyst on support and synergy of plasma and catalysis) and gas properties (include target reactants, gas flow rate, initial concentration, oxygen content and humidity level). The description of these factors is mainly based on their effects on discharge characteristics and VOCs decomposition in DBD. Subsequently, a number of aspects related to the practical implementation of DBD for VOCs treatment were described. Finally, future trends were suggested based on the existing research works.

## 1. Introduction

As the pollution of particulate matter, SO<sub>x</sub> and NO<sub>x</sub> gradually decreases, the abatement of volatile organic compounds (VOCs) emitted from various industries is becoming a matter of wider concern for

researchers and environmentalist. Most VOCs have high photochemical reactivity and react easily with NO<sub>x</sub> to form ozone [1,2]. Meanwhile VOCs are key precursor of secondary organic aerosols, which are significant components of fine particulate matter [3–5]. In addition to the adverse effects on the environment, VOCs also have hazards for human

\* Corresponding authors.

E-mail addresses: [xiaoqingdang@hotmail.com](mailto:xiaoqingdang@hotmail.com) (X. Dang), [zhangqian2018@xauat.edu.cn](mailto:zhangqian2018@xauat.edu.cn) (Q. Zhang).<https://doi.org/10.1016/j.cej.2020.124275>

Received 14 October 2019; Received in revised form 8 January 2020; Accepted 28 January 2020

Available online 30 January 2020

1385-8947/© 2020 Elsevier B.V. All rights reserved.

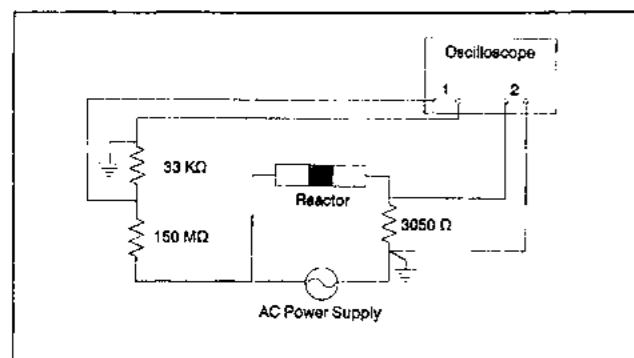


Figure 7. Voltage and current measurement system.

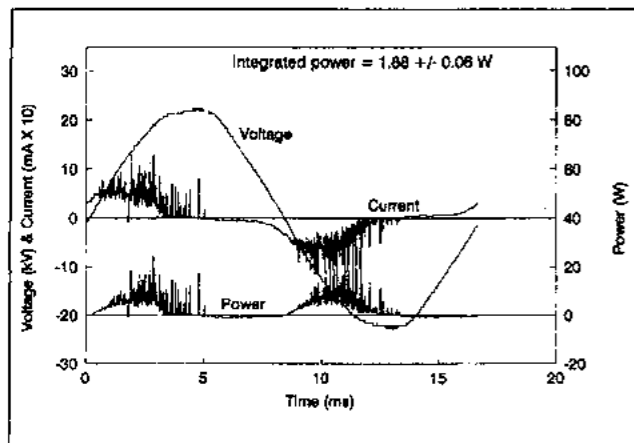


Figure 8. Power curve for the bench-scale packed-bed corona reactor.

incineration, and thermal incineration, the corona process demonstrates several significant advantages over the conventional control methods. These advantages are listed in Table I.

Conventional control technologies usually fail either technically or economically in effectively controlling VOC and air toxics at very low concentrations. In the corona destruction process, the lower the concentration the lower the power required to achieve excellent performance. Based on the durability of the bed packing material, ease of assembly, and simplicity of the hardware required, packed-bed corona destruction requires very little maintenance.

In catalytic and thermal incineration systems, relatively high temperatures are required to obtain the desired performance. This usually translates to a high cost of operation. In addition, when the inlet organic concentration is low, auxiliary fuel is needed to maintain proper incineration of the pollutants. However, the corona destruction process operates at ambient temperature, thus substantially reducing operating costs. Unlike catalytic systems, the corona process is not sensitive to poisoning by sulfur or halogen containing compounds.

Corona destruction also eliminates the problem associated with the treatment and disposal of the adsorbent used in carbon adsorption. Although the use of carbon adsorption in recovering VOCs may be cost-effective at high adsorbate concentrations, its performance dramatically declines when the adsorbate concentration is low. The application of carbon adsorption at low concentrations then becomes prohibitive.

Corona destruction is an effective alternative control method for a variety of VOCs and air toxics. Its destruction efficiency for VOCs such as benzene, cyclohexane, ethanol, hexane, hexene, methane, methylene chloride, methyl ethyl ketone, styrene and toluene may be predicted from the ionization potential and types of bonds in the molecules.

During the tests of destruction of VOCs and air toxics by the corona process, no products of incomplete reaction are formed. When the compounds were treated with the corona, molecules either were completely destroyed or passed through the reactor unaffected. More complex compounds and mixtures will have to be tested to determine if these promising results hold true in practical applications. The percentage of molecules destroyed can be predicted and controlled by appropriate reactor design and specification of operational parameters.

The performance of the corona destruction system can be enhanced by either increasing the power input or adjusting the residence time in the reactor to achieve a high degree of destruction for VOCs.

## References

1. G.H. Ramsey, N. Plaks, C.A. Vogel, et al., "The destruction of volatile organic compounds by an innovative corona technology," Presented at *The Eighth Symposium on the Transfer and Utilization of Particulate Control Technology*, San Diego, CA, March 20-23, 1990.
2. S. Moore, *HAP-PRO User's Manual*, Version 1.0, EPA-600/8-91-211a (NTIS PB92-135904) (manual), EPA-600/8-91-211b (diskettes), October 1991.
3. H.J. White, *Industrial Electrical Precipitation*, Addison-Wesley Publishing Co., Reading, MA, 1963.
4. G.C. Pimentel, R.D. Spratley, *Chemical Bonding Clarified Through Quantum Mechanics*, Holden-Day, Inc., San Francisco, CA, January 1970.
5. J.A. Miller, G.A. Fisk, "Combustion chemistry," *Chem. Engineer. News* 65:22 (1987).
6. *Advances in Environmental Sciences*, Volume 1, J.N. Pitts, R.L. Metcalf, Eds., Wiley and Sons, New York, 1969, p. 310.
7. R.J. Heinsohn, P.M. Becker, "Effects of Electric Fields on Flames," in *Combustion Technology: Some Modern Developments*, Academic Press, New York, 1974.
8. B.J. Finlayson-Pitts, J.N. Pitts, Jr., *Atmospheric Chemistry: Fundamentals and Experimental Techniques*, John Wiley & Sons, New York, 1986, p. 220-225.
9. *CRC Handbook of Chemistry and Physics*, R.C. Weast, Ed., CRC Press, Inc., Cleveland, OH, 1975, p. E-60.

## About the Authors

C.M. Nunez, G.H. Ramsey, W.H. Ponder and J.H. Abbott are with the Air and Energy Engineering Research Laboratory, U.S. Environmental Protection Agency, Research Triangle Park, NC 27711. L.E. Hamel and P.H. Kariker are with Acurex Corporation, P.O. Box 13109, Research Triangle Park, NC 27709. This manuscript was submitted for peer review on April 17, 1992. The revised manuscript was received on November 19, 1992.

health. Many VOCs are carcinogenic, affecting the central nervous system, causing respiratory diseases [6–8], etc.

In order to reduce the emission of VOCs, three techniques have been developed, namely source, process and terminal control. Although the first two techniques can decrease the production or emission of VOCs, end-of-pipe solution is still essential. End-of-pipe techniques include the recovery and destruction of VOCs. The former refers to the transfer or concentration of VOCs from exhaust gas, including adsorption [9,10], condensation [11], absorption [12] and membrane separation [13]. The latter means decomposing VOCs into harmless substances such as CO<sub>2</sub> and H<sub>2</sub>O, including thermal oxidation [14], biological treatment [15,16], catalytic oxidation [17–19], photocatalysis [20–22], thermal plasma [23] and non-thermal plasma [24,25]. Recent reviews have highlighted the benefits and drawbacks of different techniques available for VOCs removal [26–29]. Among these techniques, adsorption and thermal oxidation are the most widely applied ones in the industrial sector. However, for the adsorption, the saturated adsorbents need to be desorbed and the desorbed gas requires further treatment, and thermal oxidation is high in energy consumption by heating a large amount of gas [30]. Alternatively, non-thermal plasma (NTP) is widely deemed to have the following merits: (1) Its energy efficiency is higher than that of thermal oxidation. (2) It operates at atmospheric pressure and room temperature. (3) It can be easily integrated with various packing materials. (4) It can be quickly switched on/off [31–33].

Although Francis Hauksbee created the first gas discharge in 1705 and Siemens invented the first silent discharge (also referred to as dielectric barrier discharge) device for producing ozone in 1857 [34], until 1928, the term ‘plasma’ was proposed by Irving Langmuir to describe a ‘region containing balanced charges of ions and electrons [35]. In other words, plasma is a partially or fully ionized gas consisting of electrons, atoms, ions and ground state, metastable and excited molecules. It is worth noting that not all balanced charges of ionized gas are plasma. In plasma, the spatial scale of the ‘region’ should be much larger than Debye length ( $\lambda_D$ ) and the density of charged species should be sufficiently large. The term of temperature is commonly used to quantitatively describe plasma. In thermal plasma, the temperature of heavy particles (ions, atoms, molecules and radicals) and electrons is similar, indicating that almost all its species are at thermal equilibrium. In non-thermal plasma, the temperature is beyond thermal equilibrium, and the temperature of electrons ( $10^4$ – $10^5$  K) is much higher than heavy particles (300–1000 K) due to the differences in their mass [36]. For environmental pollution control, thermal plasma processes are used for the decontamination of solids like sludge, filter ash, municipal waste and hospital waste [37], while non-thermal plasma is mainly applied to the control of gaseous pollutants like SO<sub>x</sub>, NO<sub>x</sub> and VOCs [38].

Accelerated in an electric field, electrons in NTP reach a temperature of 10000 K to 250000 K (1–20 eV) due to their light mass [39]. Bombarded by these high-energy electrons, the ground state molecules (e.g. N<sub>2</sub>, O<sub>2</sub>) become metastable (N<sub>2</sub><sup>m</sup>, O<sub>2</sub><sup>m</sup>) or excited (N<sub>2</sub><sup>\*</sup>, O<sub>2</sub><sup>\*</sup>). These metastable and excited state particles collide with each other and with ground state molecules or are again bombarded by electrons, and processes such as ionization, dissociation and Penning dissociation occur in the electric field. Through these multi-step physical and chemical reactions, free radicals and ions are formed. These free radicals (e.g. ·O, ·OH) are ideal oxidants that react with gaseous contaminants and intermediates generated from the collision of electrons and precursors to form harmless products like CO<sub>2</sub> and H<sub>2</sub>O. These chemical

changes can be realized in NTP at low temperature, while they are only possible in combustion systems and thermal discharge at much higher temperature (> 1000 K) [36]. NTP can be produced through various ways, including dielectric barrier discharge [40–42], pulsed/AC/DC corona discharge [43,44], electron-beam [45,46], gliding arc discharge [47,48], microwave plasma [49,50], etc. Among them, DBD (include silent, surface and dielectric packed bed discharge) reactor is considered to have the following advantages: (1) Its geometrical configuration is very simple; (2) It can be scaled up for industrial application without additional difficulties; (3) It is available to get reliable, efficient and affordable power supplies; (4) It requires no vacuum chambers with delicate windows like electron beam; (5) The plasma conditions in DBD are stable and reproducible [51,52]. Theoretically, DBD plasma has lower energy efficiency compared to other types of plasma such as gliding arc. However, this demerit can be compensated by optimizing reactor configuration and packing the reactor with suitable catalysts. In addition, most of the current researchers on VOCs removal by NTP use DBD reactors, especially in the presence of catalysts. However, there are few reviews focusing on the application of DBD in VOCs abatement. Therefore, it is necessary to pay special attention to DBD rather than various discharge types to gain insight into VOCs removal by NTP.

This review presents an overview of the applications of dielectric barrier discharge NTP in VOCs abatement. In the first part, an introduction of DBD is given, including the history, microdischarge formation and environmental applications of DBD. In the next four parts, the influence of reactor structure (including electrode material and configuration, discharge gap and length, dielectric material and thickness, and number of dielectrics), power supplies (including applied voltage, frequency and pulsed power supply), packing materials (including packed position, properties of packing material, loaded catalyst on support and synergy of plasma and catalysis) and gas properties (including target reactants, gas flow rate, initial concentration, oxygen content and humidity level) on discharge characteristics and VOCs removal in DBD reactor are discussed. Subsequently, a number of aspects associated to the practical application of DBD for VOCs abatement are discussed. In the last part, conclusions and future trends for this promising technique are described.

## 2. What is dielectric barrier discharge?

### 2.1. History

It has been over 150 years since the invention of dielectric barrier discharge by W. Siemens in 1857 [53]. The first DBD device focused on the ozone generation and it was the earliest environmental application of an NTP. As presented in Fig. 1, the device consists of two coaxial cylindrical glass tubes and high voltage and ground electrodes, which were attached on the inner surface of the inner tube and the outer surface of the outer tube, respectively. Air or oxygen passed through a narrow annular gap between two glass tubes, where discharge happened. Since then, DBD was primarily applied to generate ozone for water disinfection. In addition to industrial application, the processes of ozone and nitrogen oxide formation in DBD became a significant research area for many decades [54]. An important work was made by K. Buss (1932), who photographed the traces of current filaments on dielectric plates (as depicted in Fig. 2) and pointed out that air breakdown occurs in these filaments [55]. Then, a lot of works on these

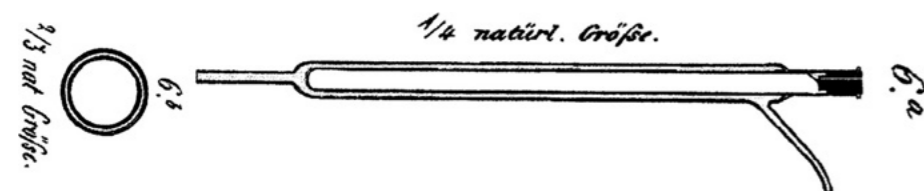


Fig. 1. Historic ozone generator of W. Siemens, 1857 [53].

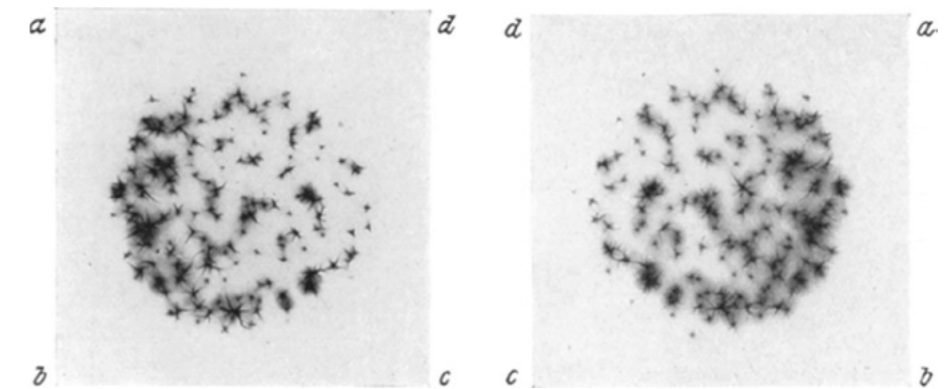


Fig. 2. Photographic footprints of current filaments [55].

current filaments was documented. Another considerable step was taken in 1943 by T. C. Manley, who proposed a method for determining the dissipated power in DBD by measuring closed Lissajous figures [56]. Around 1970, extensive studies were conducted to better understand the physical and chemical processes in DBD. These research efforts not only improved the performance of ozone generator, but also promoted the application of DBD in other fields, including surface modification, excimer UV lamps, CO<sub>2</sub> lasers, plasma display panels, contamination control and greenhouse gas recycling and utilization [57]. The abatement of VOCs with DBD began around 1990. More details about the history of DBD can be found in Kogelschatz's reviews [51,57–60].

### 2.2. Micro-discharge formation

Dielectric barrier discharge is characterized by inserting one or more dielectrics between the high voltage and the ground electrode. As illustrated in Fig. 3, there are two common DBD reactor configurations, namely panel and cylinder. Since DC cannot pass through insulating dielectric, the power applied to a DBD should be AC or pulsed high voltage power. The gas discharge characteristics between the two electrodes will change due to the presence of the dielectric. An intact dielectric can limit the amount of accumulated charge and avoid spark or arc in the discharge gap. The material commonly used as a dielectric barrier is glass or silica glass, and in some special cases ceramics or polymer layers are also used.

When the electric field strength of the discharge gap is large enough to cause breakdown, the electron density at certain regions reaches a critical value, and a large number of independent short-lived current filaments (i.e. micro-discharge) are produced. The common appearance of micro-discharges in a DBD at atmospheric pressure is shown in Fig. 4.

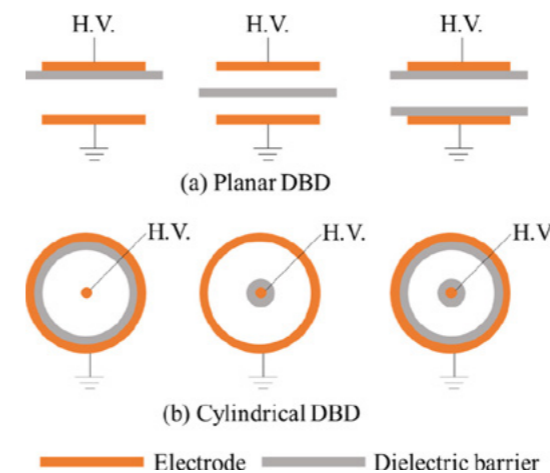


Fig. 3. Illustrations of various DBD reactors.

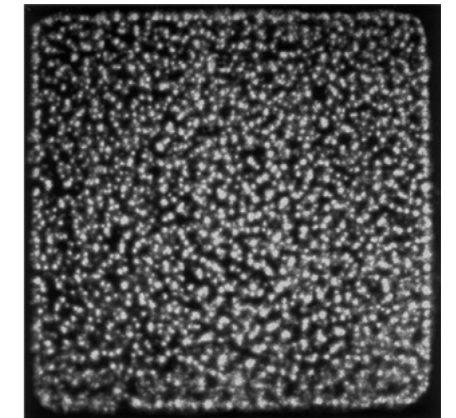


Fig. 4. End-on view of microdischarges in atmospheric-pressure air [51].

Each micro-discharge has an approximately cylindrical plasma channel with a radius about 100 μm. A single micro-discharge develops rapidly in few nanoseconds to tens of nanoseconds and propagates at the dielectric surface to form a surface discharge, which has a larger radius than the original current filaments channel. As a result, the transferred charge accumulates and decreases the electric field strength. As the electric field is further weakened, the micro-discharge extinguished when the attachment of electrons exceeded ionization. Every time the polarity of the AC voltage changes, a new micro-discharge is created at the original position. Fig. 5 depicts the model of an individual micro-discharge. The charges transported by a single micro-

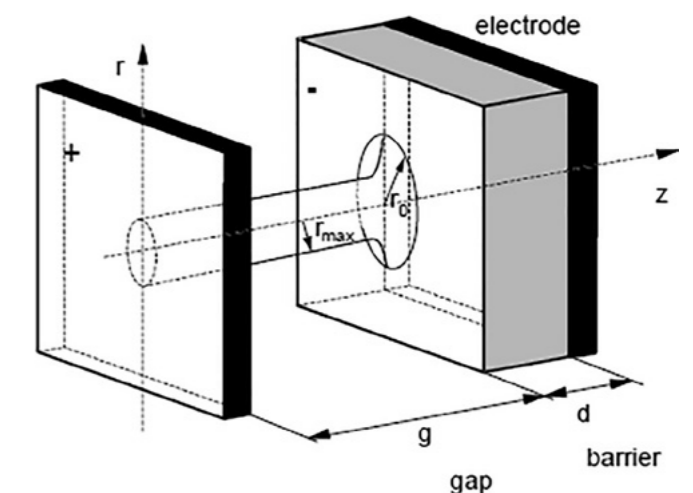


Fig. 5. The shape of a single microdischarge [64].



discharge are in the order of 100 pC and the energies are in order of  $\mu\text{J}$  [61].

It is noteworthy that filamentary discharge is not the only form of discharge in DBD. There are various discharge types such as filamentary, regularly patterned or diffuse, laterally homogeneous discharges that can exist in DBD [62]. In the study by Starostin et al. [63], different types of DBD were observed, including stationary filaments, Townsend discharge, non-stationary microdischarges and glow. They investigated the pathways of formation and temporal evolution of the diffuse glow-like DBD at atmosphere pressure by means of optical (fast imaging camera) and electrical diagnostics.

### 2.3. Environmental application

**Ozone production:** Since 1857, ozonizer has been the most widely used application of DBD. The formation of ozone involves two steps. First, the oxygen was bombarded by electrons and dissociated into oxygen atoms, and then oxygen reacts with these atoms to form ozone. Usually, a third collision partner like  $\text{O}_2$ ,  $\text{N}_2$  will participate in the latter reaction. The time scale for ozone formation during atmospheric discharge is about 10  $\mu\text{s}$  in oxygen and 100  $\mu\text{s}$  in air. The yield of ozone is affected by the feed gas composition, supply voltage, gas temperature, dielectric thickness and electrode configuration [65,66]. Since the low stability of ozone requires operation at low temperatures, an effective cooling system is necessary in an ozonizer. The development of power supply units and process control has greatly contributed to the improvement of ozonizer performance. For example, at a fixed input power, the use of high frequency power makes it possible to operate at a lower voltage. Recently, a substantial progress in an effective ozone generation was achieved by a pulse discharge usage [67,68]. As the fundamental physical and chemical processes of DBD are similar, some research results on ozonizer can inspire other environmental applications.

**Air pollution control:** The application of DBD on air pollution control primarily involves the abatement of gaseous contaminants like  $\text{NO}_x$ ,  $\text{SO}_2$ ,  $\text{H}_2\text{S}$  and VOCs. Depending on the chemical process, there are two strategies for removing  $\text{NO}_x$ : oxidation and reduction. Whether it is a stationary source (e.g. coal-fired fuel gas) or a mobile source (e.g. diesel and gasoline exhaust), the most widely used technique of removing  $\text{NO}_x$  at present is selective catalyst reduction (SCR). However, activation of the SCR catalyst requires high temperature conditions (about 300°C). Instead, DBD can be operated at room temperature without heating bulk gas. In addition, the possibility of ammonia leakage, catalyst poisoning or blockage and the construction of solution stations will affect the use of SCR [69–71]. For a stationary source like coal-fired power plants, the SCR and wet flue gas desulfurization (WFGD) could effectively eliminate  $\text{NO}_x$  and  $\text{SO}_x$ . However, the separate treatment system has the demerit of complicated treatment process, large construction space and high investment cost [72]. Non-thermal plasma is a promising technique for simultaneous removal of  $\text{SO}_2$  and  $\text{NO}_x$ . Recent studies have shown that DBD can effectively remove  $\text{SO}_2$  and  $\text{NO}_x$  simultaneously at low energy consumption [73–75]. DBD can also be applied to remove  $\text{H}_2\text{S}$ , which emit from sewage industrial wastewater treatment plants [76,77].

Unlike  $\text{SO}_2$ ,  $\text{NO}_x$  and  $\text{H}_2\text{S}$ , VOCs involve many kinds of organic substances and their molecular structure are usually more complex. Using DBD for VOCs abatement starts from around 1990, because the concern for the pollution of VOCs was realized later than  $\text{SO}_2$  and  $\text{NO}_x$ . Table 1 gives an overview of researches on the degradation of VOCs by DBD in past 30 years. In the early years, packed bed reactor meant packing a dielectric material in an AC corona discharge reactor and it can be considered as a special dielectric barrier discharge. Before 2000, most of the experiments on DBD degradation of VOCs were without packing materials or catalyst, and the removal efficiency was used as the main evaluation index of reactor performance. Subsequently, combining the catalyst with DBD opened a new window for the

research of VOCs abatement. In the past two decades, extensive research on catalysts in DBD has been carried out, such as different packing materials and metal supported catalysts, the location of the catalyst, and the like. In addition to its combination with catalysts, some researchers have focused their attention on configuration improvements in DBD reactor and the destruction of mixture of various VOCs. Since organic by-products are unavoidable in the degradation process of VOCs, it is necessary to use mineralization rate (also refers to as  $\text{CO}_x$  selectivity) and  $\text{CO}_2$  selectivity rather than just removal efficiency as evaluation index. The type of organic by-products generated during VOCs degradation has not been discussed detailly in this review, as it is mainly used to speculate about the VOCs decomposition pathways. It is also worth noting that some pilot scale experiments have been carried with gas flow rates of several hundred  $\text{m}^3/\text{h}$ , which is of great significance for the practical application of DBD.

### 2.4. Summary

Dielectric barrier discharge was invented some 150 years ago, i.e., over a century earlier than its application in VOCs abatement. In the past 100 years, the physical characteristics and chemical processes of DBD have been extensively investigated, and tremendous achievements were obtained. The chemical reaction channels in DBD are provided by a large number of current filaments (micro-discharges) and their formation process and physical characteristics have been clarified. However, filamentary discharge is not the only discharge mode in DBD. In fact, DBD can be operated in the form of filamentary, regularly patterned or diffuse, laterally homogeneous discharges. Studying how VOCs are degraded in discharge forms other than filamentary discharge may provide a new window for VOCs removal in DBD. Although VOCs abatement is an emerging field in DBD application, there are a large number of experimental and theoretical studies on DBD itself or on ozone generation, which are available in history for reference. Therefore, while focusing on the status quo and looking into the future, we should also review history, and there may be some serendipity can be found. On the other hand, there is also a lot of research on  $\text{SO}_x$  and  $\text{NO}_x$  removal as well as energy applications (e.g.  $\text{CO}_2$  conversion [78], dry reforming of methane [79,80] and ammonia synthesis [81,82]) in DBD, which may provide inspiration for VOCs abatement.

## 3. Effect of reactor structure

### 3.1. Electrode material and configuration

The material and structure of the high voltage and ground electrodes directly affect the discharge characteristics of DBD reactor, thereby affecting the degradation performance of VOCs. The high voltage electrode can be made of stainless steel [115], tungsten [116], molybdenum [94], copper [117], nickel [118], brass [119], iron, metallic oxide [120], sintered metal fiber [121] or MWNTs (Multi-walled carbon nanotubes)/sponge [122] with a structure of wire [123], rod [124], bolt [125] and coil [126]. The discharge current and electrical field distribution of plasma reactor is directly affected by work function and secondary electron emission of the cathode [127]. Jin et al. [128] used a plasma reactor with different high voltage electrodes (tungsten, copper and steel) to degrade toluene and xylene, indicating that the removal efficiency of VOCs is positively correlated with the secondary electron emission coefficient of electrodes. Jahanmiri et al. [119] investigated the influence of electrode material on naphtha cracking through a pulsed DBD plasma reactor and found that process energy efficiency was in the order of: steel > Al  $\gg$  brass > Fe > Cu. Yao et al. [120] observed a remarkable discharge currents increase in the reactor with  $\text{MgO}/\text{NiO}/\text{Ni}$  cathode and  $\text{NiO}/\text{Ni}$  cathode than the one with Ni cathode and discharges with oxide cathodes displayed better toluene decomposition performance than the one with Ni cathode. The geometry of inner electrode affects the formation of micro-discharge

**Table 1**  
An overview of researches on the degradation of VOCs by DBD.

Reactor type	Power supply	Flow rate / residence time	Packing materials	Target pollutant (ppm)	RE	MR/ $\text{S}_{\text{CO}_2}$	Ref.	Year
Packed bed	60 Hz	0.2,0.8 L/min 7.9 s	BaTiO <sub>3</sub>	Toluene (23–235) CH <sub>2</sub> Cl <sub>2</sub> (500,1000)	100 95		[83]	1992
Silent discharge	4.5 kHz	10 L/min		CFC-113 (500,1000)	67		[84]	1993
Surface discharge	5,10 kHz, 6.8 kV	1.5, 3.6, 8.0 s		TEC (500)	~90		[85]	1993
DBD	60 Hz, 16–19 kV	1.0–2.0 L/min		CFC-22(1000)	90		[86]	1995
Dielectric & surface discharge	50 Hz, 5–50 kHz, 4.5–30 kV	0.35 L/min, 2.7 s		Formaldehyde (40–120)	97		[87]	1996
Packed bed	60 Hz, 18 kHz, 3–16.4 kV	0.2 L/min	BaTiO <sub>3</sub>	Trichloroethylene (1000)	99		[88]	1996
Packed bed	15–19 kV	0.3–1 L/min 0.3–1 L/min 3 L/min, 3–12 s		Toluene (57–234) o-xylene (200)	100 100		[89]	1997
Packed bed	50 Hz, 5–8 kV	0.5–1.5 L/min, 3.0–8.9 s	BaTiO <sub>3</sub>	TCE (200)	98.1		[90]	1998
Packed bed, sequential	50 Hz, 3–11 W	0.2 L/min	BaTiO <sub>3</sub> , Al <sub>2</sub> O <sub>3</sub> , Ag, Co, Cu, Ni/Al <sub>2</sub> O <sub>3</sub>	Toluene (50–400)	80		[91]	1999
Double DBD & packed bed	10–27 kV	1 L/min	BaTiO <sub>3</sub>	MEK (125)	80		[92]	1999
Packed bed	50 Hz	0.2 L/min	BaTiO <sub>3</sub> , Al <sub>2</sub> O <sub>3</sub>	Butane (1000)	94		[93]	2000
Packed bed DBD	60 Hz, 12–21 kV	1.0–2.0 L/min	$\gamma$ -Al <sub>2</sub> O <sub>3</sub>	Benzene (200)	99		[94]	2001
Packed bed DBD, PPC & IPC	50 Hz, 12.5 kV	0.1 L/min	$\gamma$ -Al <sub>2</sub> O <sub>3</sub> , $\alpha$ -Al <sub>2</sub> O <sub>3</sub> , silica gel, quartz powder	Benzene (500), Toluene (480), Xylene (480), Cumene (450), Diethylether (500, 800), Dichloromethane (460)	95		[95]	2002
DBD	14–16 kV	0.5–1.5 L/min		Benzene (200)	69		[96]	2003
Packed bed DBD	100–600 Hz	4 L/min	Ag/TiO <sub>2</sub>	p-terphenyl	100	63	[97]	2003
Packed bed DBD	50 Hz	0.5 L/min	NaY, HY, Ferrierite, HMordenite	p-xylene (0–500)	~85	95	[98]	2004
DBD, catalytic electrode	12.5–22.5 kV, 200–450 Hz	0.5 L/min	MnOx, CoOx/Sintered metal fiber	Benzene (203–210)	87	76 ( $\text{S}_{\text{CO}_2}$ )	[99]	2005
Packed bed DBD, PPC & IPC	16.5–17.5 kV, 10.25–13.25 kHz	1 L/min	BaTiO <sub>3</sub> , $\gamma$ -Al <sub>2</sub> O <sub>3</sub> , Ag <sub>2</sub> O, MnO <sub>2</sub> /Al <sub>2</sub> O <sub>3</sub>	Toluene (100–1000)	100	~80	[100]	2007
Packed bed DBD, sequential	9–12 kV, 2 kHz	0.6 L/min (ad), 0.06 L/min (de)	Ag/HZSM-5	Toluene (500)	~100	~100	[101]	2009
Packed bed DBD, PPC & IPC	1 kHz	0.5 L/min	Ba-CuO-Cr <sub>2</sub> O <sub>3</sub> /Al <sub>2</sub> O <sub>3</sub>	Acetaldehyde (1000) n-eicosane	~97		[102]	2010
DBD, catalytic electrode	50 Hz, 14–22 kV	0.25 L/min	MnOx, AgOx/Sintered metal fiber	Toluene (100)	~70		[103]	2012
Packed bed DBD	15–20 kV, 50–500 Hz	8.7 L/min	BaTiO <sub>3</sub> , TiO <sub>2</sub> /Al <sub>2</sub> O <sub>3</sub>	Dichloromethane (200)	100	~82	[104]	2013
Packed bed DBD	50 Hz, 0–15 kV	0.3 L/min	MnOx/SBA-15	Toluene (100)	90	~85	[105]	2014
Packed bed DBD	5–9 kV, 10 kHz	3–15 s	CeO <sub>2</sub> /HZSM-5, CuO/MnO <sub>2</sub> , Ag/TiO <sub>2</sub>	Chlorobenzene (50–250)	~75	~82	[106]	2015
DBD	7–10 kV, 22 kHz	6.6 L/min		Toluene, benzene, ethylbenzene, methyl ethyl ketone, methyl tert-butyl ether, 3-pentanone, and n-hexane (95)	50–90	54–63 ( $\text{S}_{\text{CO}_2}$ )	[107]	2016
DBD	0–30 kV, 50 Hz	250–500 m <sup>3</sup> /h	CeO <sub>2</sub> -MnOx	Isovaleraldehyde (2–10)	5–35		[108]	2016
Packed bed DBD	15–24 W	0.13–0.4 L/min		Toluene (500–2500)	95.94	90.73 ( $\text{S}_{\text{CO}_2}$ )	[109]	2017
Sliding DBD	0–60 kV	0.3 L/min	TiO <sub>2</sub>	Toluene (100)	~62	~80 ( $\text{S}_{\text{CO}_2}$ )	[110]	2018
TiO <sub>2</sub> /UV-DBD	30 kV, 50 Hz	1, 2 m <sup>2</sup> /h		Butyraldehyde (11–90)	40	72	[111]	2018
Packed bed DBD	11 kV, 350–750 Hz	1000 m <sup>3</sup> /h	Halloysite	Ammonia (11–90)	83		[112]	2018
Packed bed DBD	10.1 kHz	1 L/min	LaMO <sub>3</sub> (M: Mn, Fe, Co)	VOCs from compost plant (13.1–21.5)	62.9		[113]	2019
				Ethyl acetate (100)	98.8	78.6	[113]	2019

(continued on next page)

Table 1 (continued)

Reactor type	Power supply	Flow rate / residence time	Packing materials	Target pollutant (ppm)	RE	MR/ $S_{CO_2}$	Ref.	Year
Packed bed DBD, sequential	10 kHz	0.5 L/min (ad), 0.5–1.2 L/min (de)	Ag/ZSM-5	Toluene (61.35 $\mu$ mol)	100	96.83	[114]	2019

RE: removal efficiency, MR: mineralization rate,  $S_{CO_2}$ : selectivity of  $CO_2$

and the discharge gap. For example, the sharp edge of bolt electrode can distort the surrounding electric field, resulting in more high-energy electrons than the rod and wire one [129]. The coil electrode exhibits lower gap capacitance than rod and bolt electrodes, indicating that the dielectric loss in the barrier can be decreased by coil electrode [130]. As the diameter of inner electrode increases, the discharge gap reduces, thereby increasing the average electric field strength, resulting in more active species. Also, a large diameter means a large surface area, resulting in more secondary electron emission [131].

The materials that make up the ground electrodes are similar to the high voltage electrodes, but the structure is different, especially for cylindrical reactors. Typically, the ground electrode is a wire, tape, sheet or mesh that wrapped around the surface of dielectric. Some researchers also used silver paste as a ground electrode [132,133]. Bahri et al. [134] investigated the effect of ground electrode configuration on ozone production. The results showed that  $Ag_{paste}$  has higher energy yield than  $Al_{foil}$  and  $stainless-steel_{mesh}$ . There is no secondary electron emission at ground electrode, so the difference between various electrodes is mainly due to its structure rather than material. When a foil or mesh used as ground electrode, streamers or corona discharges are formed in the void between electrode and dielectric [97]. The energy used to ionize air in the outer of dielectric can be considered as “wasted energy”, meaning that it does not contribute to the degradation of VOCs or the production of ozone. Using silver paste as ground electrode, the gap between electrode and dielectric barrier can be eliminated [133,135]. Thereby more energy is used to ionize the gas inside reactor, resulting in higher energy yield and better degradation of VOCs.

### 3.2. Discharge gap and length

A suitable discharge gap is significant for VOCs abatement in DBD. On the one hand, increasing the discharge gap increases the gas residence time, which facilitates the removal of VOCs. On the other hand, increasing the discharge gap reduces the average electric field strength, which is detrimental to the abatement of VOCs. In addition, if the discharge gap is changed by changing the diameter of cathode, the secondary electron emission of the cathode also affects the degradation of VOCs. The discharge gap of DBD reactor in laboratory usually ranges from 1 to about 15 mm. Magureanu et al. [136] compared the removal efficiency of trichloroethylene (TCE) for various discharge gap in the range of 1–5 mm. The results showed that shorter gap (1–3 mm) is more favorable for the conversion of TCE. However, in the dry reforming of methane experiments conducted by Khoja et al [137], the conversion of methane and  $CO_2$  increased first and then decreased with the increase of discharge gap (1–5 mm). A higher power density can be achieved at a constant discharge power, and current filaments are more likely to cover the entire discharge volume with a small gap [138]. But if the gap is too short, arc or spark discharge may occur, and the interaction between target contamination molecule and active species might be limited due to a short residence time. Therefore, to obtain a good performance of DBD for VOCs abatement, both discharge gap and the residence time should be considered.

The discharge length also plays a significant role in DBD degradation of VOCs. By increasing the effective discharge length, lower voltage is required to achieve the plasma ignition. An increase of the discharge length leads to a higher effective electrode surface, resulting in more micro-discharge inside the reactor, which increases the probability of gas breakdown [134]. In addition, increasing the discharge length will increase the residence time of VOCs in the plasma zone, which is advantageous for the decomposition of VOCs due to the increased chance of collision between VOCs molecule and energetic electrons and other reactive species. Chang et al. [139] investigated the degradation of styrene with various discharge length (10, 20, 30, 40, 50, 60 cm) and found that the input power increased linearly with discharge lengths. The selectivity of  $CO_2$  also improved with the increase of discharge length. The same experimental results were

obtained by Zhang et al. [140]. However, at a fixed input power, a long discharge length means a smaller power density due to the enlarged plasma region. Moreover, increasing the discharge length results in higher energy loss due to heat dissipation of dielectric barrier [141]. As a result, increasing the discharge length may reduce energy efficiency.

### 3.3. Dielectric material and thickness

The insulating dielectric material in DBD reactor can be glass [142], quartz [143], plexiglas [144], pyrex [145], alumina [146], mullite [147], ceramics [148], polytet [149], polyethylene terephthalate [150], teflon and epoxy resin [151]. Among these materials, quartz is the most widely used due to its moderate price and commercial availability. The dielectric permittivity affects the discharge characteristics of DBD, which affects the degradation of VOCs. Since the dielectric capacitance and the gas gap capacitance are connected in series in the circuit, increasing the dielectric capacitance increases the electric field strength of the discharge gap which results in more micro-discharge. Zhu et al. [152] investigated the influence of dielectric material on toluene removal and found that the discharge current and toluene removal rate of the 99-ceramic reactor were higher than that of quartz reactor. They attributed this difference to the higher relative permittivity of 99-ceramic (5–10) than quartz (3.5–4.5). In the study of Khoja et al. [137], it was observed that the conversion of methane and  $CO_2$  of aluminum dielectric reactor were slightly higher than that of quartz. They believe this is because the surface of aluminum reactor is porous and rough, which increases the gas residence time. Therefore, the longer residence time in aluminum reactor allowed more collision between gas molecules and energetic electrons due to its porous peculiarity. Moreover, Meiners et al. [153] found that the reactor with MgO dielectric has higher electron densities than that of aluminum reactor at the same input energy. They attributed this to the higher secondary electron emission of MgO (0.11) than that of alumina (0.099).

The performance of the DBD reactor is also affected by the thickness of dielectric barrier, which typically ranges from 1 to 3 mm. As the thickness of the dielectric barrier increases, the required plasma ignition voltage increases and the current pulses reduces [153]. Mei et al. [138] investigated the influence of dielectric material thickness on  $CO_2$  conversion and they pointed out that increasing the thickness of the quartz dielectric reduced the conversion of  $CO_2$  at a fixed specific energy input due to a decreased transferred charge. Interestingly, Ozkan et al. [147] observed the opposite results. In their study, a thick dielectric is more conducive to  $CO_2$  conversion due to the formation of more micro-discharge. Therefore, the influence of dielectric thickness on the performance of DBD reactor is not certain, but it is related to other conditions of the system. In addition, the thickness of the dielectric barrier cannot be chosen at will. Because most dielectric material are fragile, electrical breakdown may occur if it is too thin.

### 3.4. Number of dielectrics

Although most of the current DBD reactors contain only one dielectric, the first DBD reactor created by Siemens consisted of two dielectrics. An important reason why double dielectric barrier discharge (DDBD) is less of concern is that its structure is more complicated than single dielectric barrier discharge (SDBD). The electric field strength of discharge gap is uniform in planar DBD, whereas in cylindrical DBD it is related with the distance to high voltage electrode. As a result, the difference between DDBD and SDBD is more remarkable for cylindrical reactor than for planar reactor. Therefore, the DDBD discussed later is mainly used for cylindrical reactors. As depicted in Fig. 6, there are two different configurations of DDBD reactors, one of which is that the high voltage electrode is separated from inner dielectric barrier and the other is closely attached. For latter, both electrodes are not in contact with plasma, so the electrodes can be protected from plasma corrosion and etching. However, the former contains two different discharge

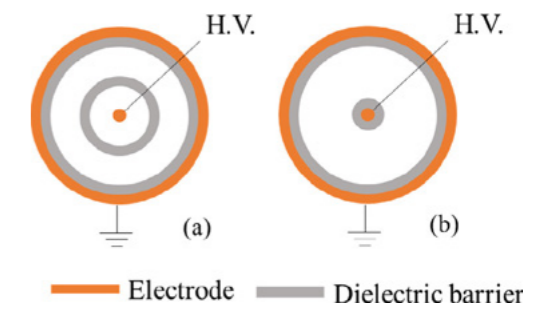


Fig. 6. Configuration of DDBD reactors.

regions, which may be more advantageous for the decomposition of VOCs. In the study by Jiang et al. [130], it was demonstrated that benzene could be degraded in both discharge regions and the highest benzene removal efficiency could be obtained while utilizing two regions simultaneously.

Some studies have shown that VOCs can be efficiently removed in DDBD [154,155], but there are not many studies comparing DDBD with traditional SDBD. Fig. 7 presented the current and voltage waveforms of DDBD and SDBD. Obviously, the current pulses in SDBD are more than DDBD, which means more micro-discharges are formed in SDBD. Since micro-discharge is developed from the cathode, the inner dielectric barrier of DDBD will prevent the advancement of micro-discharge to the inner surface of the outer dielectric. As a result, SDBD consumes much more power than DDBD (Fig. 8). However, a large input power does not mean that the removal efficiency of VOCs is destined to be higher. Because there is a lot of energy that is dissipated in the form of heat, which heats the gas and dielectric barrier. Zhang et al. [156] used DBD to degrade styrene and found that DDBD has higher mineralization rate and energy utilization efficiency than SDBD. In fact, since DDBD has a strong and a weak discharge zone with one power supply, it can be considered as a special two-stage reactor that achieves high mineralization of VOCs and inhibits the generation of by-product like ozone and  $NO_x$ . Much of the information about VOCs removal in DDBD is still not clear enough and further research is needed.

### 3.5. Summary

Although the geometry of DBD reactor is simple, its specific structure is diverse. Various structural features, such as electrode material and configuration, discharge gap and length, dielectric material and thickness, and number of dielectrics will affect the discharge characteristic of DBD, and thus influence VOCs removal performance. In most case, optimization of these structures will result in enhanced electric field or increased discharge current, which will increase the removal and mineralization rate of VOCs. However, by-products such as residual  $O_3$  and  $NO_x$  will also increase without a suitable catalyst. Exceptionally, in double dielectric barrier discharge (DDBD) reactor, the discharge current will be significantly reduced compared with a single barrier reactor, but the VOCs removal efficiency may be increased. This could be due to a change in discharge type in DDBD reactor. Actually, in the area of VOCs abatement by DBD, there is not much research on the optimization of reactor structure compared with plasma-catalysis. Moreover, most of these existing studies do not explain explicitly how the discharge characteristics are altered by these factors. This is largely due to the lack of electrical diagnostics for discharge behaviors and the complexity of gas discharges. In the near future, the application of advanced plasma diagnostics (such as intensified charge coupled device (ICCD) imaging) and fluid modeling will provide new opportunities for investigating how these reactor structures affect VOCs removal.

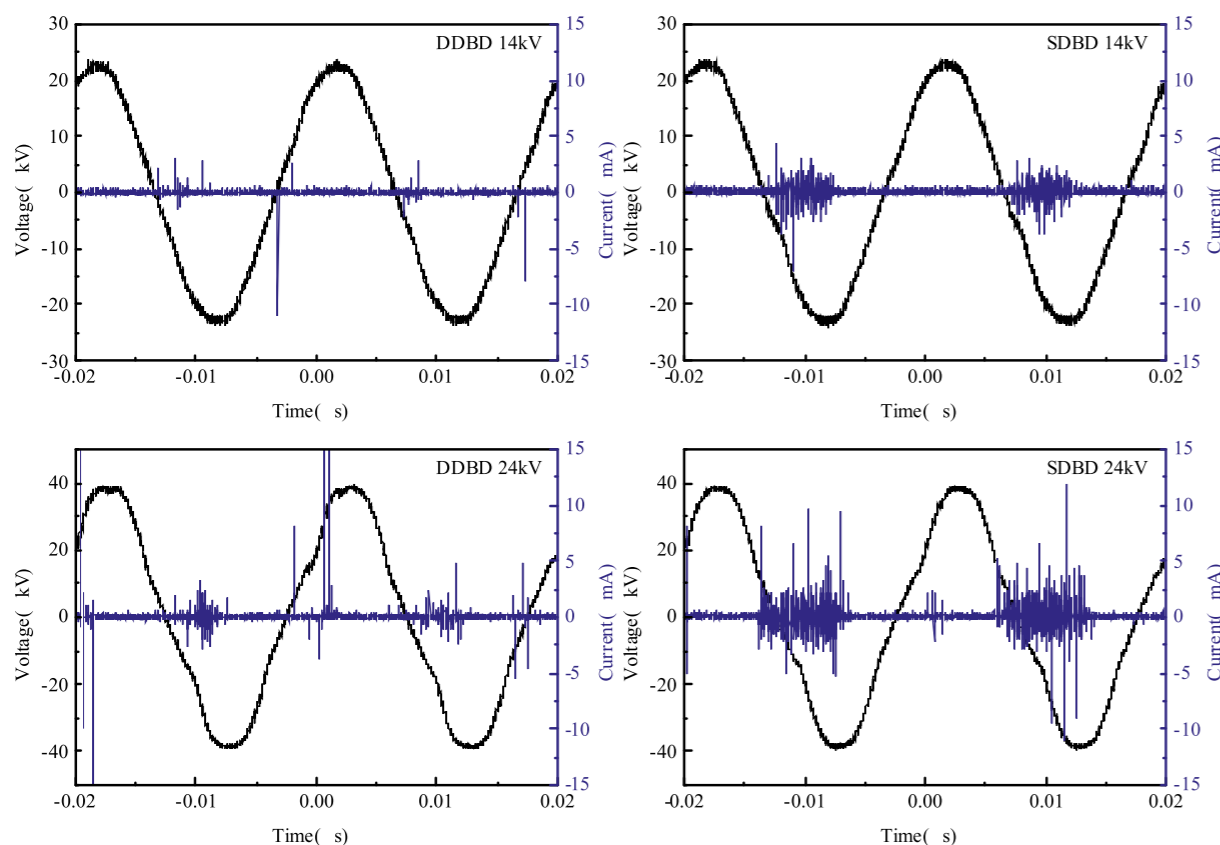


Fig. 7. Voltage and current waveform of DDBD and SDBD.

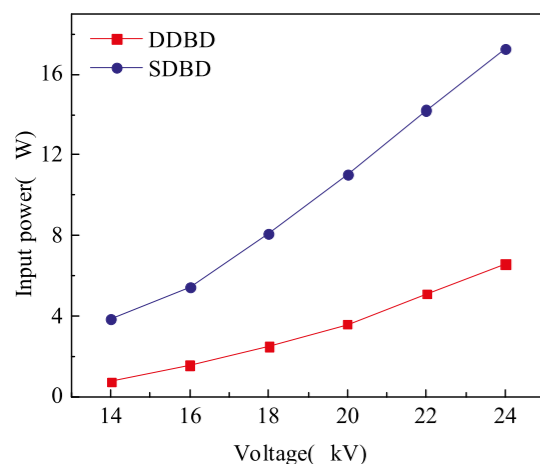


Fig. 8. The input power of DDBD and SDBD.

#### 4. Effect of power supplies

##### 4.1. Applied voltage

The applied voltage is one of the most significant parameters for DBD removal of VOCs. The voltage applied to DBD reactor is in the range of few kV to around 30 kV. At a fixed discharge gap, a high applied voltage means a strong electric field strength. Therefore, an increase in voltage causes an increase in the kinetic energy of free electrons, causing an increase in the collision cross section of electrons with other particles, meaning that the gaseous molecule or atom is more susceptible to ionization and dissociation. As depicted in Fig. 7, both the number and intensity of current pluses increase with rising voltage, which means more micro-discharges are formed at a high voltage.

Therefore, VOCs are more easily removed at high voltages. Because the chemical bonds of VOCs molecules are more easily destroyed by higher energy electrons, and a large number of active species means that VOCs can be more fully decomposed. Although enhancing the applied voltage can increase the removal efficiency and mineralization rate of VOCs, however, it is not the case that the higher the voltage the better. Firstly, a high voltage means more ozone and nitrogen oxides [157,158], which are considered as undesirable by-products in the exhaust. Secondly, if the voltage is too high, arc or spark discharge may occur [159], and the dielectric barrier may be broken down. Finally, a high voltage causes more energy to be dissipated as thermal energy by heating a large amount of gas and dielectric barrier, which may result in reduced energy efficiency of VOCs removal [160–162]. Hence, choosing a suitable voltage is significant for the abatement of VOCs in DBD.

##### 4.2. Frequency

The frequency of AC applied to DBD for removing VOCs ranges from several tens of Hz to several tens of kHz. The same number of identical micro-discharges is produced in each period. Therefore, a higher frequency means that more micro-discharges are generated in a fixed time [51]. Therefore, a higher frequency means that more micro-discharges are generated in a fixed time, which is beneficial to the decomposition of VOCs. At a frequency of 200 to 450 Hz, Subrahmanyam et al. [163] found that the COx selectivity of toluene destruction increased with elevating frequency. In the study by Liang et al. [131], the removal efficiency of toluene raised with increasing frequency from 10 to 35 kHz, but the energy yield decreased. However, Ozkan et al. [164] used DBD to split carbon dioxide and observed that the conversion of CO<sub>2</sub> decreased slightly with increasing frequency (16.2–28.6 kHz). They thought this may be due to a drop in the electron density involved in CO<sub>2</sub> splitting. In each half-cycle, the number of current pulses at low

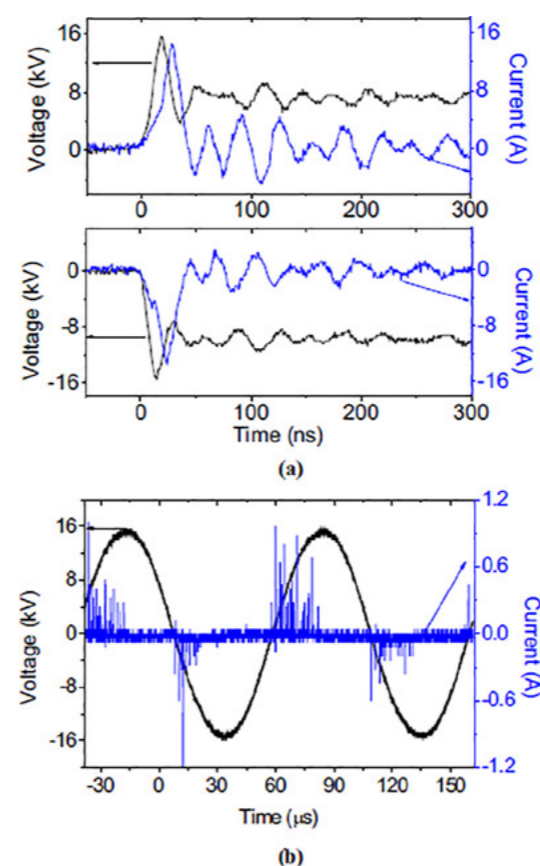


Fig. 9. Typical voltage and current waveforms of (a) nanosecond pulsed discharge and (b) AC discharge [173].

frequency is more than higher frequency [164–166]. At high frequencies, multiple breakdowns do not occur during discharge due to insufficient time in between the voltage cycles [166]. Moreover, the formation of micro-discharge may be choked if the electron transit time is longer than voltage cycle. Therefore, the input power is positively correlated with frequency but not proportional. In addition, the energy efficiency of VOCs abatement reduces with elevating frequency [131]. Another notable feature of high frequencies is that it can reduce the breakdown voltage at a fixed input power. Because by operating at high frequencies, the DBD discharge exhibits a high memory voltage due to the accumulation of charge on the surface of dielectric [167]. In summary, the choice of a suitable frequency is important and it may also refer to the applied voltage.

##### 4.3. Pulsed power supply

In addition to sinusoidal alternating current, pulsed high voltage power can also be applied in DBD reactors to generate non-thermal plasma at atmospheric pressure. The typical voltage and current waveform of AC and pulse discharges is significantly different (Fig. 9). For AC discharge, many comb-like filaments (also known as localized micro-discharge) appear on the edge of the voltage polarity reversal, indicating that AC discharge is filamentary mode. The discharges mainly occur at the first peaks of both positive and negative pulse voltage, this means that only the first peaks are effective for discharge. However, the peak current of pulsed discharge is much higher than that of AC discharge at the same applied voltage. As a result, the deposition power of pulse discharge is much higher than that of AC discharge at the same repetition rates and applied voltage [168]. Although the threshold voltage of discharge is relatively low for AC DBD, but its discharges are inhomogeneous and consist of some bright spots [169].

In contrast, for pulsed DBD, the discharge is homogeneous and without any bright spot or irregular distribution mode. In [170], Yuan et al. reported that both ·OH formation and energy efficiency of bipolar pulse power were superior than those driven by AC power. Wang et al. [171] investigated the effect of power supply mode on removal of benzene and found that at the same input power, the removal efficiency and CO<sub>2</sub> selectivity of benzene of bipolar pulsed power were higher than those of AC power. For pulsed discharge DBD, in addition to applied voltage and frequency, pulse rise time, pulse-forming capacitance and pulsed modes also affect its discharge characteristics. Chirumamilla et al. [172] investigated the influence of microsecond (μs) and nanosecond (ns) pulse on NO abatement and observed that the nanosecond is more efficient for NO conversion. The energy transfer efficiency is closely related with the pulse-forming capacitor (Cp). In [149], Jiang et al. reported that the toluene decomposition efficiency increases and the energy yield reduces with the increase of Cp. Jiang et al. [110] also researched the effect of pulsed modes on toluene destruction, indicating that the removal efficiency and energy yield decrease in the order of: ± pulse > + pulse > - pulse. Although pulsed DBD seems to be superior to AC DBD in VOCs abatement, AC power supply is widely applied due to economic reasons.

#### 4.4. Summary

The power supply has a significant effect on VOCs removal in a given DBD reactor. Generally, increasing the applied voltage amplitude will increase the removal and mineralization rate of VOCs, but more by-products (O<sub>3</sub> and N<sub>2</sub>O) will be generated. In addition, a high voltage amplitude can also lead to low energy efficiency. Increasing the frequency will result in more micro-discharges in a fixed time, leading to an increase in removal and mineralization rate of VOCs, but also a raise in residual O<sub>3</sub> and NOx formation and a decrease in energy efficiency. Therefore, it is imperative to choose a proper applied voltage amplitude and frequency to trade off removal efficiency, mineralization rate, by-products formation, and energy yield. Compared with AC power, a much higher pulsed current can be obtained in a short time for pulsed power at the same applied voltage. In addition, the discharge is more homogeneous in pulsed DBD than AC DBD. Although pulsed DBD exhibits good VOCs abatement performance, it is not widely used for economic reasons. In the future, using DBD to remove VOCs may benefit from the development of new power supplies.

#### 5. Effect of packing materials

In order to improve the removal efficiency of VOCs by DBD, several approaches have been developed, such as optimizing the reactor configuration, electrode or power supplies. However, most of these approaches increase VOCs removal efficiency at the expense of producing more undesired by-products (O<sub>3</sub> and NOx), which hinder the industrial application of DBD. In addition to the above approaches, packed bed DBD has also been extensively investigated and it is considered to be the most promising method because it can simultaneously increase removal efficiency of VOCs and suppress by-products at low energy consumption. In packed bed DBD reactors, a packing material is positioned in plasma zone or downstream of plasma zone. In the former case, there are synergistic effects between plasma and packing material, which promotes the degradation of VOCs. The electrical and morphological properties and the loaded catalyst of packing material all influence the characteristics of plasma and thus affect VOCs removal efficiency as well as by-product production.

##### 5.1. Packed position

As illustrated in Fig. 10, the common types of packed bed DBD reactor include one- and two-stage configurations. In one-stage system (a) (also referred to as in plasma catalysis-IPC), the packing material is

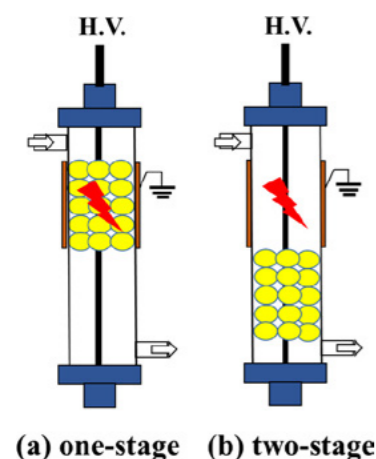


Fig. 10. Types of packed bed DBD reactors according to packing material position.

positioned in the plasma region of DBD reactor. In contrast, packing material is located in the downstream of plasma zone in two-stage system (b) (also referred to as post plasma catalysis-PPC). In PPC configuration, only long-lived species like  $O_3$  and metastable particles can reach the packing region, while short-lived species such as electrons and radicals are quenched before interacting with packing material. Conversely, for an IPC system, both short-lived and long-lived species will interact with the packing material and, more importantly, the packing material will influence the discharge characteristic of DBD reactor. As a result, there is the chance of contributions from electron- and photon-induced processes, surface discharge, radicals and excited species [174], which are significant for VOCs degradation. There is no doubt that the PPC system has an advantage in ozone suppression for VOCs abatement. However, as concerned for the removal efficiency of VOCs, it is difficult to assert which configuration is better. Although in most cases, IPC configuration is superior to PPC in VOCs removal [100,157,175–180], some studies have shown that PPC system is better than IPC [102,181]. Moreover, in the research by Durme et al. [182], IPC or PPC system is better related to the type of catalyst.

Besides the location of packing material, operational process is another important basis for packed bed DBD reactor classification. According to whether the plasma is turned on when VOCs-containing gas enters the reactor, there are continuous and sequential processes. In a sequential operating system, VOCs are first adsorbed onto the packing material and then plasma is switched on to degrade adsorbed VOCs. A significant advantage of sequential process is that its energy efficiency is higher than for continuous operation [183]. A fact that cannot be ignored is that both IPC and PPC configuration can be operated continuously or sequentially. Therefore, the packed bed DBD reactor includes four systems, namely continuous IPC (CIPC), continuous PPC (CPPC), sequential IPC (SIPC) and sequential PPC (SPPC). In a CPPC system, VOCs are partially decomposed and then reach the downstream packing region if the VOCs-containing gas stream passes through discharge zone. For the SPPC system, VOCs are only degraded in the packed area since VOCs have been adsorbed before plasma is turned on. In some studies of CPPC system [102,181], the VOCs-containing gas stream is in parallel with the gas stream through DBD reactor, and the two gas streams were mixed and then passed through packed zone. Hence, in CPPC system and SPPC system with parallel gas flow, the DBD reactor acts as an ozone generator.

Anyhow, the combination of plasma and catalyst exhibits multiple advantages in terms of removal efficiency, mineralization rate and energy efficiency of VOCs abatement. In an IPC configuration, a better understanding of the interaction between plasma and catalyst is significantly important for further optimization of a given system. Therefore, the discussion of the next few sections is based on the IPC

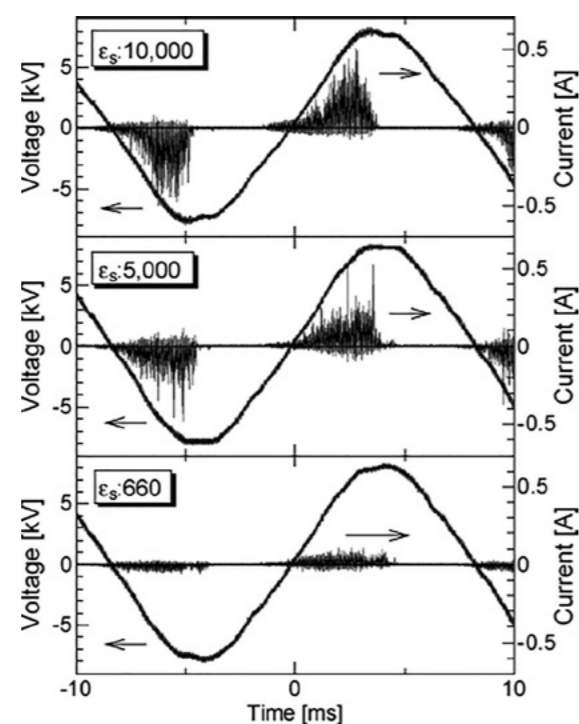


Fig. 11. Waveforms of voltage and current for various dielectric constant of sphere pellet at 14 kVpp applied voltage [190].

system.

## 5.2. Properties of packing material

Usually the materials packed in DBD reactor include ferroelectrics ( $BaTiO_3$ ,  $CaTiO_3$ ,  $SrTiO_3$ ), metal oxides ( $CeO_2$ ,  $\gamma-Al_2O_3$ ,  $MnO_x$ ), semiconductors ( $TiO_2$ ,  $WO_3$ ) and zeolites (ZSM, HY, 13X, SBA, MCM). These materials can be filled alone in the reactor or after loading with metal catalyst. The electrical, surface and morphological properties of these materials significantly affect the discharge characteristics of DBD and the performance of VOCs decomposition.

**Dielectric constant:** DBD reactor is actually a capacitor in which the capacitance of the dielectric and the gas are connected in series in an equivalent circuit. The introduction of a packing material means that a new capacitor is added to the series circuit. Since the packing material generally has a dielectric constant greater than that of air, a packed bed reactor can store more energy than DBD alone during a single discharge. At the same applied voltage, there is a greater discharge current when DBD is packed with a material with a high permittivity, as illustrated in Fig. 11. In addition, material with high permittivity reduce breakdown voltage and enhance local electric field strength, thereby increasing VOCs removal efficiency [184]. In [185], benzene conversion increased with increasing dielectric constant (20 to 1100), but the conversion is not obviously affected when the permittivity is in the range of 1600–15000. Gallon et al. [186] pointed out that the effect of permittivity in the range of less than 100 plays a very minor role in the reduction of breakdown voltage in DBD. Therefore, dielectric constant of packing material will only have a significant effect on the performance of DBD under a certain range. Recently, some fluid model studies have provided more information for understanding the discharge characteristics of packed bed DBD. In a fluid model investigation by Laer et al. [187], the results indicated that the enhancement of permittivity on electric is limited to a certain value of permittivity, being 9 for a micro-gap and 100 for a mm-gap. Also, the enhanced electric field results in a higher electron temperature, but a lower electron density. In [188], Zhang et al. reported that smaller pore sizes only yield enhanced

ionization for smaller dielectric constants (i.e., up to  $\epsilon_r = 200, 150$ , and 50 for pore sizes of 50, 30, and 10  $\mu m$ ). This means that plasma is more easily formed inside pores of low permittivity materials. Hence, the porosity of packing material cannot be neglected when investigating the influence of permittivity on VOCs removal. Moreover, the dielectric constant of packing material is affected by temperature and humidity, both of which are variable in DBD. As the temperature increases, the packing material becomes more resistive rather than capacitive [189], which is confirmed by the fact that the shape of V-Q Lissajous figure changes from a parallelogram to an ellipse [51]. Therefore, an increase in temperature lowers dielectric constant, which may result in a decrease of VOCs removal efficiency.

**Surface properties:** DBD reactor packed with porous material is more favorable for the decomposition of VOCs than with non-porous materials because porous material has a strong adsorption capacity, and micro-discharge may be formed in its inner pores. Gandhi et al. [191] examined the performance of porous and nonporous  $\alpha$ -alumina ( $\alpha-Al_2O_3$ ) for the degradation of ethylene in a DBD reactor and the results indicated that the decomposition efficiency obtained with the porous  $\alpha$ -alumina was higher than that with the nonporous one. For porous packing materials, their surface properties such as specific surface area and pore size play a significant role in VOCs decomposition by DBD. The surface area of material is directly related to its adsorption capacity for VOCs, which affects the residence time of VOCs in reactor and the probability of collision between VOCs and active species. As the  $S_{BET}$  of flake-like HZSM-5 decreased from 366 to 341  $m^2/g$ , the carbon balance of toluene removal reduced significantly from 81.9% to 65.8% [118]. In study by Wang et al. [109], the highest removal efficiency of toluene and  $CO_2$  selectivity were obtained in a catalyst (Ce1Mn1) with the largest surface area (84.1  $m^2/g$ ). However, a high surface area does not necessarily mean a high VOCs removal performance. For example, ZSM-5 (306.6  $m^2/g$ ) has a larger surface area than  $\gamma-Al_2O_3$  (175.1  $m^2/g$ ), but  $\gamma-Al_2O_3$  has a higher toluene mineralization rate than ZSM-5 [192]. This is because  $\gamma-Al_2O_3$  has a higher dielectric constant than ZSM-5 and thus has a better discharge performance. Moreover, the surface area is reduced after metal is loaded on the support, but VOCs removal efficiency is improved [193,194]. Wang et al. [195] investigated toluene degradation over different  $MnO_2$  polymorphs and found that  $\alpha$ - $MnO_2$  showed the best toluene conversion, but its surface area is lower than  $\gamma$ - $MnO_2$  and  $\delta$ - $MnO_2$ . Therefore, in addition to surface area, the dielectric constant and crystal structure of packing material and the presence of metal catalyst all significantly affect the degradation of VOCs.

Porous material is more susceptible to adsorbing molecules that are smaller in size than its pore size. Compared to ferrierite, benzene is more easily assimilated into the micropore in HY [132]. Because the molecular size of benzene is 5.9  $\text{\AA}$ , which is smaller than the pore size of HY (7.4  $\text{\AA}$ ) but greater than ferrierite (4.3–5.3  $\text{\AA}$ ). As the pore size of HZSM-5 decreased from 0.533 to 0.522 nm, the equilibrium adsorption capacity of toluene decreased from 39.70 to 30.32 mg/g, and removal efficiency decreased from 84.9% to 79.8% [118]. In contrast, the pore size of  $\gamma-Al_2O_3$  is larger than that of 13X zeolite, but the adsorption capacity of  $\gamma-Al_2O_3$  is poor [143]. Therefore, the pore size of packing material should not be too large nor too small, and pore size slightly larger than the target molecular size is preferable. Considering that both discharge enhancement and adsorption capacity are important for VOCs removal, combining materials with different properties may give a better performance. After mechanically mixing ZSM-5 and  $\gamma-Al_2O_3$ ,  $TiO_2$  or  $BaTiO_3$ , the mineralization of toluene is significantly improved compared to ZSM-5 alone [115]. In addition, the shape of pores will also influence the electric field enhancement and thus the plasma properties. In the study by Zhang et al. [196], the strongest electric field enhancement occurs at the opening and bottom corners of the conical pore with small opening, at the bottom of the conical pore with large opening and at the bottom corners of cylindrical pore.

**Size and shape:** Since the micro-discharge mainly occurs near the contact point of packing material, increasing the size of packing

material decreases the number of contact points and causes a decrease in the number of micro-discharges. However, the amount of charge transferred by a single micro-discharge will be intensified [197]. Ogata et al. [185] studied the influence of  $BaTiO_3$  pellets size on benzene degradation and the result indicated that the benzene decomposition efficiency was: 1 mm  $\approx$  2 mm  $>$  3 mm. For a given pellet size, the total contact points between packing material will be affected by the reactor size. Therefore, the optimum packing material size may vary for different reactors. In addition, it should be noted that these low particle sizes may be optimal at lab scale conditions but not adequate to pilot or industrial scaled system due to the higher gas velocities.

Although spherical particles are the most widely used packing materials, they are not morphologically advantageous for enhancing discharge. Because a strong local electric field is more likely to appear near sharp edges. In the study by Chang et al. [198], three different shapes were tested for  $BaTiO_3$ . The discharge current has a relationship of the order: small hollow  $>$  large hollow  $>$  cylinder  $>$  sphere, which indicates that reactor filled with hollow  $BaTiO_3$  may be more efficient for VOCs removal. Takaki et al. [190] researched the influence of  $BaTiO_3$  shapes on  $C_2F_6$  degradation. The sequence of discharge current was as follows: hollow cylinder  $>$  cylinder  $>$  sphere. As a result, the energy efficiency for  $C_2F_6$  abatement in the reactor with hollow cylinder and sphere were 3.7 and 2.5 g/kWh, respectively. Furthermore, the pressure drops of the reactor with hollow cylindrical is lower than that with sphere [198], which is advantageous for industrial applications.

## 5.3. Loaded catalyst on support

Although most packing material can improve the removal of VOCs by discharge enhancement and/or adsorption, metal catalysts are still necessary to obtain desired performance, such as suppressing residual ozone. An important part of plasma catalyzed removal of VOCs is to find a suitable combination of metal (e.g.: Ag, Co, Ni, Fe, Mn, Ce and Cu) and support. Fig. 12 illustrated a plausible pathway of VOCs degradation in a plasma-driven catalysts system. According to Kim [126], the VOCs decomposition process occurs primarily on the surface of packing material rather than on the loaded metal catalyst. However, the supported metal catalyst facilitates further oxidation of CO and carbon balance.

The type, loading amount, shape and size of supported metal catalyst will affect VOCs abatement. Although there has been a lot of research on plasma catalytic abatement of VOCs, it has not been concluded so far which catalyst is the best for a given target pollutant. Table 2 gives an overview of VOCs removal by different catalysts in plasma. It is clear that the sequence of catalyst for VOCs degradation is not consistent in different studies. For example, for the decomposition of benzene, Ag is superior to Cu in [144] but the opposite result was obtained in [178]. This means that the performance of catalyst in plasma is not only related to the target pollutant, but also to the reactor configuration, packing position, type of support and the like. The difference between various metal catalysts at a given condition depends primarily on their ability to decompose ozone into oxygen radicals ( $O^{2-}$ ,  $O_2^{2-}$ ,  $O^-$ ), which are indispensable in the degradation of VOCs. Ozone molecules are adsorbed and decomposed in oxygen vacancies, which are electron-deficient as Lewis acid sites [199].

The loading amount of metal catalyst has an optimum value. Below this value, the increase in the amount is beneficial to VOCs degradation, and greater than this value is unfavorable. This is because a large loading amount can provide more active sites, however, an amount above a certain value will reduce the surface area of the catalyst. In [144], the benzene removal efficiency increased with the increase of Ag loading in the range of 4–15 wt%, and then decreased at higher loading amount. Wu et al. [201] investigated the effect of Ni loading of  $NiO/\gamma-Al_2O_3$  on toluene abatement and the result indicated that 5 wt% is the optimum value. When the loading of Ni exceeded a certain value,

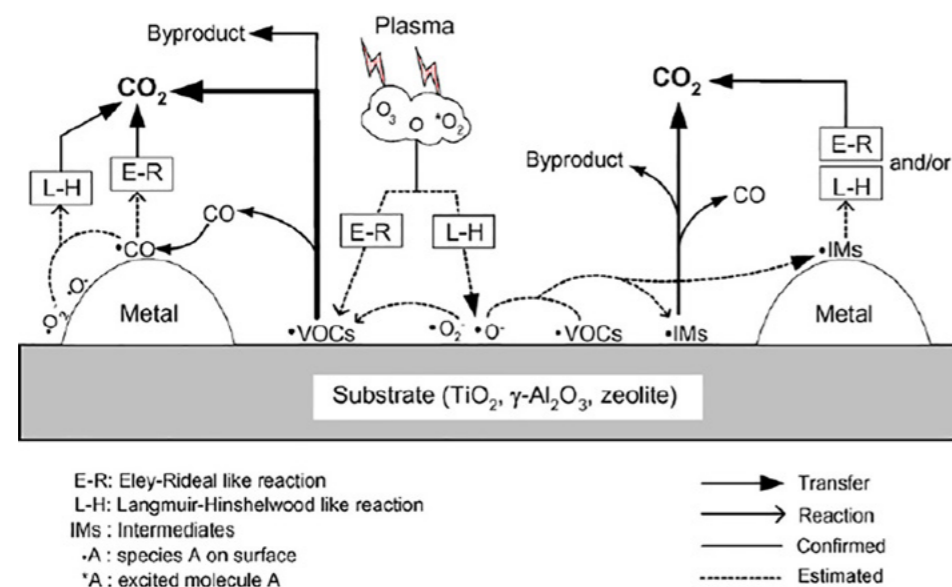


Fig. 12. Plausible mechanism for the plasma-driven catalysis of VOCs [126].

multilayer or bulk NiO may occur, resulting in a decrease of active component area exposed to air.

In the study by Peng et al. [203], the shape effect of Pt/CeO<sub>2</sub> catalysts on catalytic oxidation of toluene was elucidated. The immobilized Pt particles on nanorods, nanoparticles, and nanocubes CeO<sub>2</sub>. Pt/CeO<sub>2</sub>-rods achieved the best catalytic performance due to its best reducibility and highest concentration of surface oxygen vacancies. Further, they found the size effect of Pt nanoparticles in the range of 1.3 to 2.5 nm [204]. Due to the optimum balance of Pt dispersion and concentration of oxygen vacancy in CeO<sub>2</sub>, Pt/CeO<sub>2</sub>-1.8 exhibited the best catalytic activity. Although the two studies applied catalytic oxidation, the results are useful for plasma-catalytic process.

Recently, some studies have shown that more effective degradation of VOCs can be obtained by combining two different metal catalysts such as Mn-Co [160,205], Ag-Mn [117,123,193], Mn-Ce [109,193,202,205,206], Mn-Cu [202], Ag-Ce [207], Cu-Ce [208]. The molar ratio of two metals will significantly affect the activity of catalyst. The optimum molar ratio of Ag-Mn was 1:2 for xylene abatement in [117], which is due to the higher proportion of surface-adsorbed O and better reducibility through the synergy between Ag and Mn. In [109], the best ratio of Ce-Mn was 1:1 for toluene destruction. This is because Ce1Mn1 catalyst has higher surface area, more oxygen vacancies and higher mobility of oxygen species. In addition to mixing ratio, the impregnation sequence of different metals will also affect the degradation of VOCs if catalyst is prepared by impregnation method. For example, when Mn is first impregnated [Ag-Mn(F)/ $\gamma$ -Al<sub>2</sub>O<sub>3</sub>], a longer breakthrough time and better mineralization rate of toluene was observed compared to first Ag impregnation and co-impregnation [209]. This is attributed to the larger amount of Ag<sup>+</sup> on catalyst surface and the

better promotion of surface-active oxygen migration in Ag-Mn(F)/ $\gamma$ -Al<sub>2</sub>O<sub>3</sub>.

#### 5.4. Synergy of plasma and catalysis

**Effect of catalyst on plasma.** The discharge characteristics of DBD reactor are obviously changed after the introduction of catalytic/non-catalytic packing materials in plasma region. In a fully packed bed DBD, the discharge mode partially changes from bulk streamers to more intense surface streams that is distributed along the surface of packing material. This phenomenon has been confirmed by Kim et al. [210–212] through ICCD imaging and several numerical investigations [213,214]. The formation of micro-discharge will also be affected. The propagation of micro-discharge will be limited between the voids of packing material particles rather than the entire discharge gap. As a result, the number and intensity of micro-discharges increase, which leads to an elevation in the average energy of electrons and thus promoting the degradation of VOCs. Since most packing materials are porous, it is possible for micro-discharges to form in these pores. Holzer et al. [95] demonstrated the formation of short-lived active species in intra-particle volume by comparing the degradation of VOCs in porous and non-porous alumina. Moreover, Zhang et al. [215] investigated micro-discharge formation inside catalyst pore by a fluid model and believed that plasma species can be formed in micron-sized pores. Packing material also reduces the breakdown voltage, thereby increasing energy efficiency. In was observed that the breakdown voltage decreased from 3.3 to 0.75 kV with the addition of Ni/Al<sub>2</sub>O<sub>3</sub> catalyst in a DBD reactor [216]. In addition to physical properties, the chemical characteristics of plasma are also altered by the presence of catalyst. For

instance, ozone is easily decomposed by catalysts to produce oxygenated radicals, which have higher oxidation activity, thus enhancing the decomposition of VOCs [109,217].

**Effect of plasma on catalyst:** Since NTP can be applied as a material surface modification technique, it can also be used for catalyst preparation. When the catalyst is exposed to plasma, active sites will be more uniform and particle size will be decreased, thereby increasing the activity and stability of catalyst [39,218]. Smaller Pt particle size and higher dispersion of nanoparticles were observed on Pt/CeO<sub>2</sub> after plasma treatment [219]. In addition, a change in the concentration of oxygen vacancies and Ce<sup>3+</sup> in Pt/CeO<sub>2</sub> indicates that the oxidation state of catalyst can be changed by plasma. After 8 h of plasma process, parent Ti–O bonds in TiO<sub>2</sub> was reduced [174]. The energy of the Pd–support bond increases during plasma treatment, causing a rise in the degree of dispersion and sintering resistance of Pd, thereby a higher stability [220]. The adsorption behavior of catalyst in plasma is different from conventional thermal catalytic process. Compared to molecules, atoms and radicals are more susceptible to adsorption by catalysts due to their lower energy barriers. For thermal catalysis, atoms and radicals can only be produced by dissociative chemisorption of stable precursors. However, in plasma catalyst, a large amount of radicals and atoms around the boundary layer can be directly adsorbed with a low energy [36]. Therefore, plasma catalysis will provide new reaction pathways, which leads to reduced activation energy and higher reaction rate [189]. In addition to affecting the process of adsorption and surface reactions, plasma also promotes the desorption of products by electron and ion bombardment. The gas temperature in NTP is typically less than 400 K, which generally does not result in thermo-catalytic activation. However, hotspots can be created between corners of adjacent pellets and sharp edges due to local intense electric fields [39]. Furthermore, the metal particles dispersed on the support have a high electrical conductivity, and Joule heating is generated as discharge spreads along the surface [221]. Hence, VOCs may be degraded partially through thermal catalysis.

#### 5.5. VOCs decomposition mechanisms

In order to verify the degradation pathway of VOCs in packed-bed DBD, various surface analysis techniques such as gas chromatography-mass spectrometry (GC–MS), X-ray photoelectron spectroscopy (XPS), Raman and infrared were used to identify the species that are present on catalytic surface during plasma processing. However, these analyses were performed when the catalyst was removed from the DBD reactor. Therefore, some weakly adsorbed intermediates may have been lost before detection, so that only limited information on the catalyst surface can be obtained. The application of in-situ detection technique will provide more real and detailed information about the intermediates. Xu et al. [222] used an in-situ FT-IR spectroscopy to evaluate toluene abatement process in continuous and sequential systems with NiO/Al<sub>2</sub>O<sub>3</sub> packed. The results indicated that toluene was gradually removed and organic intermediates were mostly destructed after 90 min reaction in sequential system, while the types of organic by-products accumulated on catalyst surface in continuous system, and eventually impeded the further steps of toluene decomposition. In order to investigate the difference in degradation of adsorbed toluene in IPC and PPC systems, Jia et al. [175] used two complementary in situ diagnostics (diffuse reflectance infrared fourier transform spectroscopy (DRIFTS) and transmission fourier transform infrared spectroscopy using Sorbent track (ST) device) to dynamically probing toluene surface coverage and adsorbed intermediates on CeO<sub>2</sub>. As depicted in Fig. 13 (a), for PPC system, the toluene surface coverage decreased as soon as the plasma was turned on and the surface concentrations of benzyl alcohol and benzaldehyde gradually increased until plateau was reached. Different from benzyl alcohol and benzaldehyde, the production of surface benzoic acid started beyond 500 s. Compared to PPC system, some similar trends were observed in IPC configuration (Fig. 13 (b)). However, the

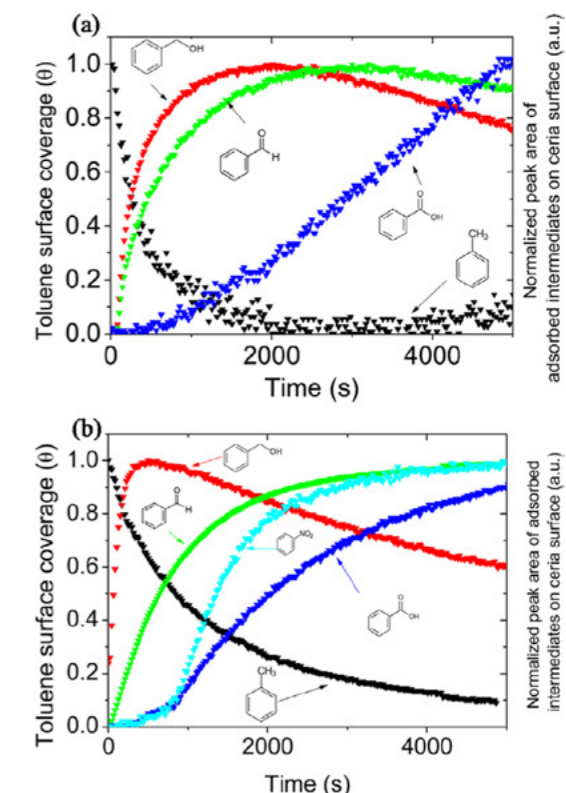


Fig. 13. Evolution of toluene and adsorbed intermediates surface coverage on CeO<sub>2</sub> as a function of post situ (a) and in situ (b) NTP exposure time [175].

concentration of benzyl alcohol in IPC increased faster than that in PPC and the formation of nitrobenzene in IPC was observed. In addition, IPC showed a higher reaction rate of toluene decomposition than PPC system. This was attributed to the fact that the toluene on catalytic surface is simultaneously exposed to long- and short-lived species in IPC, while only long-lived species contributed to toluene degradation.

Although in situ detection can provide more reliable and detailed information about the intermediates on catalyst surface, it is still hard to sketch the real map of VOCs degradation. Based on these experimental results, using computational chemistry to obtain the reaction pathways can lead to a better understanding of reaction dynamics in plasma-catalysis systems. To our best knowledge, there is currently no research on the application of computational chemistry to plasma-catalyzed oxidation of VOCs. However, in other fields of plasma catalysis, some studies can be referenced. Shirazi et al. [223] conducted a density functional theory (DFT) study of Ni-catalyzed plasma dry for methane reforming. They inspected many activation barriers, from the early stage of adsorption of major chemical fragments derived from CH<sub>4</sub> and CO<sub>2</sub> molecules up to the formation of value-added chemicals at the surface. The results indicated that the hydrogenation of a chemical fragment on the hydrogenated crystalline surface is energetically favored compared to the simple hydrogenation of the chemical fragment at the bare Ni (1 1 1) surface. The surface-bound H atoms and the remaining chemical fragments at the crystalline surface will facilitate the catalytic conversion of the fragments generated from CH<sub>4</sub> and CO<sub>2</sub>. They believed that the retention of methane fragments, especially CH<sub>3</sub>, in the presence of surface bound H atoms can be regarded as an identifier for the choice of a suitable catalyst.

#### 5.6. Summary

Plasma catalysis is considered as the most promising way to improve the performance of DBD in VOCs abatement due to its excellent capability in the enhancement of mineralization rate and energy

Table 2  
VOCs removal by different type of catalyst.

Reactor	Target pollutant	Support	Catalyst performance	Reference
CIPC	Ethyl acetate		LaCoO <sub>3</sub> > LaMnO <sub>3</sub> > LaFeO <sub>3</sub> (MR)	[113]
CPPC	Benzene	$\gamma$ -Al <sub>2</sub> O <sub>3</sub>	AgOx > MnOx > CuOx > FeOx (RE)	[144]
CIPC	Acetone	$\gamma$ -Al <sub>2</sub> O <sub>3</sub>	CuOx > MnOx ≈ CoOx > NiOx > CeOx (RE)	[200]
SPPC	Toluene	HZSM-5	Ag–Mn > Ce–Mn > Mn > Ag > Ce (MR)	[193]
CIPC	Toluene	$\gamma$ -Al <sub>2</sub> O <sub>3</sub>	NiO > MnO <sub>2</sub> > CeO <sub>2</sub> > Fe <sub>2</sub> O <sub>3</sub> > CuO (RE)	[201]
CIPC/PPC	Toluene	Al <sub>2</sub> O <sub>3</sub>	Au > Ag > Cu > Co (RE)	[177]
SIPC/SPPC	Benzene	HZ	Ce > Cu > Zn > Ag > Fe > Mn > Ni > Co (MR)	[178]
CPPC	Methanol	$\gamma$ -Al <sub>2</sub> O <sub>3</sub>	Mn–Cu > Mn–Ce > Mn > Cu ≥ Ce (RE)	[202]

Here MR and RE refer to mineralization rate and removal efficiency, respectively.

efficiency as well as the suppression of by-products. There are four types of packed-bed DBD system according to the catalyst packing position and operation process, namely CIPC, CPPC, SIPC and SPPC. For an IPC system, the properties of packing material (such as dielectric constant, surface properties, size and shape) will directly affect the discharge characteristics of DBD and VOCs decomposition performance. These effects can be partially confirmed by measuring the discharge characteristics, represented by the current–voltage waveforms and Lissajous figures obtained by an oscilloscope. Recently, the application of ICCD imaging and fluid modeling has made it possible to gain a deeper insight of discharge characteristics. It is foreseeable that effects such as packing material shape on discharge characteristics will be explored by these advanced methods. Since temperature plays a significant role in plasma catalyst system, investigating the change and distribution of temperature in packed-bed DBD through fluid modeling may yield some vital findings. The loading of metal catalyst on packing material will further improve VOCs removal performance, which is affected by the type, loading amount, shape and size of supported metal catalyst. In a plasma catalysis system, there are synergistic effects between the catalyst and plasma. However, the fundamental physical and chemical processes of the interactions between plasma and catalyst are still not well understood. As a result, the selection of catalyst and operating conditions in plasma process is still based on trial and error approach. The dynamically monitoring of intermediates on catalyst surface through in situ detection technique can provide a deeper understanding about VOCs decomposition mechanism in plasma catalysis system. Combined with the results from in situ analysis, computational chemistry makes it possible to tailor the catalyst for a specific chemical reaction process. More details about the synergy of plasma and catalyst can be accessed in recent reviews [34,36,39,61,79,189,218,224–230].

## 6. Effect of gas properties

### 6.1. Target pollutants

There are > 100 kinds of VOCs emitted from various industrial processes, which is a major difficulty in VOCs abatement. Table 3 summarizes the abatement of different common VOCs as well as odors (such as dimethylamine, dimethyl sulfide, acetaldehyde) by DBD reactor. According to the difference in chemical structure, these VOCs include aromatics, ketones, aldehydes, alcohols, esters, alkanes, alkenes and halocarbons. The degree of difficulty for various VOCs decomposition in DBD may be related to its chemical structure, ionization

potential and hydrogen content (mass percentage). Karatum et al. [107] chose methyl ethyl ketone, benzene, toluene, 3-pentanone, methyl *tert*-butyl ether, ethylbenzene, and n-hexane as target reactants to degrade in a DBD reactor. The results showed that the molecule (n-hexane) with the highest hydrogen content has the highest removal efficiency (90%). The reaction rate constants of different VOCs are significantly positively correlated with their hydrogen weight fraction. Moreover, aromatic compounds follow their own trend with respect to their hydrogen content. In [231], a higher hydrogen content results in higher removal efficiency for aromatic hydrocarbons (benzene, toluene and xylene), ketones (propanone, 2-butanone and 2-pentanone) and esters (ethyl acetate, ethyl propionate and ethyl butyrate) but the results were in the reverses order for alkanes (n-pentane, n-hexane and cyclohexane). However, there is no obvious relationship between removal efficiency and hydrogen content when considering all four types of VOCs. Hence, the relationship between hydrogen content and removal efficiency may only be applicable to different VOCs with similar chemical structures. Further, the lower the ionization potential, the higher the reactivity of VOCs and radicals, which gives rise to the higher degradation efficiency of VOCs. In addition, the three alkanes deviate from the main trend due to their inclusion of more single bonds, which are more easily destroyed in NTP. In the study by Kim et al. [232], no correlation between the ionization potential and VOCs degradation was observed in plasma driven catalyst reactor, which indicates that the decomposition mechanism of VOCs in packed bed reactor is different from NTP alone. Moreover, the effect of chemical structure on removal rate is not negligible, e.g., the presence of double or triple bonds of CC are beneficial for initial activation during VOCs destruction [233]. In terms of total energy demand, single bonds are cracked more easily than double bonds. However, the second bond of a double bond needs low energy levels to be activated and, afterwards, transformation of the activated single bonded compounds is preferred in comparison to the non-activated single bond compound. Hill et al. found that at an input energy of 100 J/ L, the removal rates were 16% and 68% for propane and propene, respectively [234]. This is due to the limited number of available pathways to initiate propane removal. The influence of functional groups is also noteworthy. For example, the reason why the toluene removal rate is greater than that of benzene is more likely due to the presence of methyl group in toluene than its higher hydrogen content.

### 6.2. Gas flow rate

The gas flow rate significantly affects the performance of VOCs

degradation in DBD reactor. A higher gas flow rate means that more VOCs molecules pass through the reaction zone per unit time, resulting in a reduction in the number of active species available for each molecule. In addition, a higher gas flow rate results in a shorter residence time, which reduces the probability of collision between VOCs molecules and active particles. As a result, increasing the gas flow rate leads to a decrease in VOCs removal efficiency and CO<sub>2</sub> selectivity. For example, in [109], when the gas flow rate varies from 0.13 to 0.4 L/ min, the residence time is reduced from 4.3 s to 1.4 s, the toluene decomposition efficiency is reduced from 93.39% to 80.84%, and the CO<sub>2</sub> selectivity is lowered from 92.53% to 72.18%. However, increasing the gas flow rate significantly enhances the energy efficiency for a given system [206], as the active species can be more fully utilized at a high gas flow rate. If VOCs are decomposed by a sequential processing, the effect of gas flow rate will be different from continuous processing. In sequential treatment, VOCs are first adsorbed on packing material and then degraded by plasma. On the one hand, if the discharge gas flow rate is too low, there may be insufficient oxygen active species to react with the adsorbed VOCs, resulting in a decrease in mineralization rate and CO<sub>2</sub> selectivity. On the other hand, as the discharge gas flow rate increases, the specific input energy and residence time are reduced, which is detrimental to the degradation of VOCs. In [114], the toluene mineralization rate and CO<sub>2</sub> selectivity with discharge gas flow rate of 1.0 L/min are higher than that of 0.5 and 1.2 L/min. Interestingly, in [291], as the discharge gas flow rate (0.025, 0.05, 0.1 and 0.2 L/min) increases, the CO<sub>2</sub> selectivity increases while the CO selectivity decreases, and the mineralization rate (or COx selectivity) remains constant. Therefore, the effect of gas flow rate on VOCs degradation in sequential treatment is dependent on the specific experimental conditions.

### 6.3. Initial concentration

DBD is primarily applied to treat low concentration VOCs, typically less than 1000 ppm. Under a given operating condition, the amount of active species such as high-energy electrons and radicals generated in the DBD reactor is constant. Therefore, increasing the initial concentration of VOCs leads to a decrease in the number of active species that react with each molecule, resulting in a decrease in removal efficiency and mineralization rate of VOCs. In [161], the initial toluene concentration increased from 25 to 125 ppm, the removal efficiency and mineralization rate decreased from 70.58% to 39.32% and from 19.60% to 6.68%, respectively. However, increasing the initial concentration will increase the amount of VOCs removed [106], thereby increasing energy efficiency. This is because the probability of collision between VOCs active species is higher when a higher number of VOCs are introduced into the reactor per unit time. In [248], the energy efficiency increased from 0.56 to 1.18 g/kWh when the initial concentration of acetone increased from 100 to 300 ppm. For sequential processing, the performance of VOCs removal is related to the amount of stored VOCs rather than the initial concentration. In [114], as the toluene storage increased from 53.17 to 65.44 μmol, the carbon balance decreased from 98.26% to 92.36%, and the energy efficiency increased from 1.925 to 2.369 g/kWh. The reason for this result is similar to the influence of initial concentration on VOCs decomposition in continuous treatment. In addition, increasing the concentration or adsorbed amount of VOCs will cause more active species to contribute to VOCs decomposition. As a result, the formation of O<sub>3</sub> and NOx is suppressed.

### 6.4. Oxygen content

Since oxygen plays a significant role in the degradation of VOCs in DBD, the oxygen content in the discharge gas significantly affects the performance of VOCs abatement. For DBD process alone, the degradation efficiency of VOCs generally increases first and then decreases with the increase of oxygen content. In pure nitrogen, VOCs are removed by

collision with electrons and active metastable nitrogen atoms and molecules. After adding oxygen, the active oxygen atoms and molecules as well as OH radicals participate in the decomposition of VOCs, thereby enhancing the removal efficiency of VOCs [268]. However, when the oxygen content exceeds a certain value, the formation of NOx and O<sub>3</sub> begins to prevail, which consumes a large amount of active species derived from oxygen and nitrogen, resulting in less degradation of VOCs. In addition, the reaction rate of O<sub>3</sub> towards VOCs is too small to contribute to VOCs degradation.

Several studies have reported the dependence of VOCs decomposition on oxygen content in DBD and the maximum efficiency was obtained at 5% O<sub>2</sub> for toluene [292], 4% for dichloromethane [268], 2% for trifluoromethane [148], 3–5% for benzene [126], 5% for p-xylene [96]. The influence of oxygen content on COx selectivity is different from VOCs removal efficiency. In [293], the selectivity of CO<sub>2</sub> and COx increased with the increase of oxygen concentration, but according to Kim [126], the selectivities of CO and CO<sub>2</sub> were much less affected by the partial pressure of O<sub>2</sub> compared with decomposition efficiency. Unlike DBD alone, a high oxygen content enhances VOCs decomposition in packed bed reactor. After introducing catalyst, reactive oxygen species (such as ·O, O<sup>2-</sup> and O<sup>·</sup>) can be produced from lattice oxygen and interaction with ozone. As the oxygen concentration increases, a large amount of ozone is formed, most of which is decomposed into active oxygen species on the surface of catalyst, thereby increasing the decomposition efficiency and COx selectivity of VOCs. In [126], the increase of O<sub>2</sub> concentration elevated both the degradation efficiency of benzene and CO<sub>2</sub> selectivity regardless of the type of catalysts (TiO<sub>2</sub>, γ-Al<sub>2</sub>O<sub>3</sub>, zeolites). If the target reactant contains oxygen atoms, the effect of oxygen content on VOCs decomposition may differ from the above results. In [249], the removal efficiency of acetone is decreased with increasing oxygen concentration with or without packing materials (γ-Al<sub>2</sub>O<sub>3</sub>, α-Al<sub>2</sub>O<sub>3</sub> and glass beads). This is because acetone is less reactive with oxygen species than other VOCs such as toluene and benzene.

### 6.5. Humidity level

Since industrial VOCs containing exhaust gases usually contain water vapors, the effect of humidity on the degradation of VOCs in DBD is not negligible. The presence of water vapor cannot be neglected in VOCs removal by NTP since it can be decomposed into ·OH, which has a stronger oxidation power than other active species such as oxygen atoms and metastable nitrogen molecules and atoms. In a DBD reactor with photo-catalytic electrode (SMF/TiO<sub>2</sub>), the concentration of ·OH at a relative humidity (RH) of 80% is approximately three times than that at 10% RH [294]. The discharge characteristics of DBD are affected by the presence of water. Water vapor may cover the surface of the dielectric, resulting in reduced surface resistance and increased dielectric capacitance, which leads to decline of total transferred discharge [295].

Similar to oxygen, the addition of suitable water may facilitate the decomposition of VOCs due to the high oxidizing power of ·OH. However, if too much water is introduced, the high-energy electrons will be quenched by the electronegative water molecules, so that the density and average energy of electrons are lowered, resulting in a decrease in the number of active species. Many studies have reported that the highest VOCs removal efficiency can be obtained at a suitable humidity level. For example, at 20% RH for toluene [296], at 30% for benzene [207], at 70% for ethanethiol [297]. In other studies [93,181,201,298,299], the decomposition of VOCs is decreased with the increase of humidity level. The difference in these findings may be due to the variety of VOCs and experimental conditions. Fan et al. [300], found that different VOCs have different sensitivity to water vapor. Humidity suppressed benzene removal, while toluene decomposition was slightly enhanced by increasing RH from 30% to 50–80% and p-xylene conversion was insensitive to water vapor. In packed bed DBD reactor, the presence of water vapor may poison the catalyst by covering a portion of active sites, which are available for VOCs and O<sub>3</sub>

**Table 3**  
Overview of various VOCs degraded by DBD.

Classification	VOCs	Reference
Aromatics	Toluene	[33,109,114,118,143,149,157,161,235–239]
	Benzene	[101,129,178,207,240–243]
	Styrene	[116,139,140,156,232,244]
	Xylene	[96,117,232,245–247]
Ketones	Acetone	[41,200,248–250]
Aldehydes	Formaldehyde	[86,179,208,251,252]
	Acetaldehyde	[94,145,253]
Alcohols	Methanol	[42,202,206,254]
	Ethanol	[255,256]
Esters	Ethyl acetate	[113,154,231]
Alkanes	Methane	[155,180,257,258]
	Propane	[234,259–264]
Alkenes	Ethylene	[176,191,265]
	Propene	[234,258,259,266]
Halocarbons	Dichloromethane	[267–271]
	Tetrachloromethane	[272–274]
	Chlorobenzene	[103,106,133,205,275,276]
	Trifluoromethane	[148,277–279]
Odors	Trichloroethylene (TCE)	[136,272,280–285]
	Dimethylamine, dimethyl sulfide, acetaldehyde, ammonia, dimethyl sulphide, thiols, hydrothion	[112,233,286–290]

adsorption [299]. Therefore, the resistance to water should be considered when choosing a catalyst.

As for the influence of water vapor on COx selectivity, the results reported by various studies are also different. In [161] and [207], the highest COx yield and CO<sub>2</sub> selectivity were obtained at 30% RH, which is consistent with the effect of humidity on decomposition efficiency. In other studies [93,240,296], increasing humidity enhances CO<sub>2</sub> selectivity due to the further oxidation of intermediates by ·OH. The presence of catalyst affects the influence of humidity on CO<sub>2</sub> selectivity. In [300], the CO<sub>2</sub> selectivity by DBD alone increased while that by packed bed DBD decreased with the increase of RH. The humidity level also affects the formation of O<sub>3</sub> and NOx. Generally, an increase in humidity results in a decrease in O<sub>3</sub> concentration due to the quench of high energy electrons by water molecular, which led to the decrease of atomic oxygen, and then decreased the amount of ozone in the plasma [201]. Intriguingly, Jiang et al. observed a reverse trend in a PPC system and they attributed it to the competitive adsorption between H<sub>2</sub>O and O<sub>3</sub> molecules on the catalyst [207]. For NO<sub>2</sub>, its concentration decreases with increasing humidity level in both NTP alone and PPC systems [207]. This was because high water vapor in discharge plasma tends to induce electron attachment reaction and thereby reduce the energetic electron density and mean electron energy, resulting in a decreased total production of active species.

### 6.6. Summary

In a given DBD reactor, VOCs removal performance is affected by various gas properties, such as the type of target pollutants, gas flow rate, initial concentration, oxygen content and humidity level. The degree of difficulty for different VOCs decomposition in DBD may be related to its chemical structure, functional groups, ionization potential and hydrogen content. In continuous systems, an increase in gas flow rate will reduce the gas retention time, which lead to a reduction in VOCs removal and mineralization rates, but will increase energy efficiency. In sequential systems, the influence of gas flow rate on VOCs removal is dependent on specific experimental conditions. Similarly, increasing the initial concentration leads to a decrease in removal and mineralization rate of VOCs, but an increase in energy efficiency. For sequential processing, what matters is the amount of stored VOCs rather than the initial concentration. A appropriate level of oxygen content and water vapor will facilitate the decomposition of VOCs due to the formation of highly oxidizing species (such as ·O and ·OH). An increase in oxygen content will lead to an increase in ozone, which is hard to oxidize VOCs but is easily decomposed into strong oxidizing species by catalyst. In contrast, too much water vapor will cover the active sites of the catalyst, thereby poisoning the catalyst. These results about the effect of gas properties on VOCs abatement are of great significance for the practical application of DBD. However, most of these results were obtained from laboratory-scale experiments. In the future, more efforts should focus on using DBD to remove VOCs-containing gases which are close to industrial conditions.

### 7. Practical application

Although DBD exhibits various merits for VOCs abatement, its commercial implementation is still scarce. There are barriers that need to be addressed, such as the formation of stable organic by-products, residual O<sub>3</sub> and NOx, and the sensibility to humidity. Theoretically, the presence of suitable catalysts can alleviate these problems, which has been confirmed in many laboratory experiments. However, the performance of plasma catalysis for the treatment of industrial VOCs-containing exhaust gas is still uncertain. Therefore, before the industrial application of DBD (with or without catalyst) for VOCs removal, a large number of pilot experiments should be performed. Table 4 presents some scale-up experiments on DBD removal of VOCs. In these experiments, VOCs-containing exhaust gas come from industrial processes or

**Table 4**  
Scaled-up experiments of DBD system for VOCs abatement.

Equipment	Power supply	Flow rate m <sup>3</sup> /h	RH	Pollutant	RE	Reference
DBD (10 tubes)	3–10.5 kV, 1.12–3.4 kW	509	50	Benzene (2050.8–3243 mg/m <sup>3</sup> )	40.5–59.2	[301]
DBD + post catalyst	7–8 kV, 350–400 Hz, 0.3–0.6 kW	196	-	Emissions of water treatment plants(odor 96300–265100 OU/m <sup>3</sup> )	57–90	[290]
DBD (40 tubes)	25–100 kV, 1 kHz	100	-	Toluene 100 mg/m <sup>3</sup>	~25–90	[303]
DBD	10 kV, 1 kHz, 150 W	2.5–5	40	Oil shale processing plant:butyl acetate (30–110 ppm)	~26–71	[305]
DBD + photocatalyst	0–30 kV, 50 Hz	350	53	Animal quartering centers: isobutyraldehyde, isovaleraldehyde, 2-methylbutyraldehyde, and dimethyl disulfide, 30 mg/m <sup>3</sup> (total)	65,55,75,25	[302]
DBD + zeolite + Biotrickling filter	11 kV, 520 Hz, 1.5–1.6 kW	1000	25–80	Emissions of sludge centrifugation(odor 200–1400 OU/m <sup>3</sup> )	~95	[233]

laboratories, and in most cases the gas flow rate is about several hundred cubic meters. These industrial waste gases are emitted from water treatment plants, oil shale processing plant, animal quartering centers and sludge centrifugation. Most of these experiments were conducted in the bypass of the emission duct during the industrial process. Unlike laboratory, the conditions of the process gases to be treated were varying (fluctuation of pollutants concentration, humidity and flow rate). As a result, the performance of DBD may be poorer than the results obtained from laboratory, in which the gas conditions are carefully controlled and are generally single-component. Nevertheless, it is not difficult to meet the local legislative limitations since the inlet gas concentration is usually relatively low. In addition, multiple DBD systems can be arranged in series to improve VOCs removal efficiency. In the study by Ye et al. [301], the removal rates of benzene increased from 58.2% with one DBD system to 92.7% with three DBD system in series at 10.5 kV. Surely, this was achieved at the expense of increasing constructional and operational costs.

Upon inspection of these scale-up experiments, DBD system appeared to exhibit high potential for odor elimination. Over 90% of odor abatement were achieved in several studies [233,290], in which DBD system was combined with other techniques such as catalyst, adsorber and biotrickling filter. At the same time, the destruction of methane [233] and dimethyl disulfide (DMS) [302] was unsatisfactory, which is consistent with the results obtained from laboratory experiments. For the degradation of different VOCs in laboratory and in the case of real gases, the degree of difficulty should be the same. In other words, the results gained in laboratory are significant for the treatment of industrial VOCs despite the different gas conditions.

During the scale-up experiment, some unpredictable situations may occur due to the changes in operating conditions. Therefore, the comparison of lab-scale and pilot-scale test is imperative. Liang et al. [303] evaluated the performance of toluene decomposition in two DBD reactors with different scale. They found that the toluene removal rate in lab-scale reactor was higher than that in pilot-scale reactor at the same applied voltage. This was due to the fact that the discharge gap of pilot-scale reactor (6 mm) is larger than that of lab-scale reactor (2.5 mm). However, the pilot-scale reactor exhibited a higher energy efficiency than lab-scale reactor at the same amount of exhaust gas. They attributed this to the much weaker wall effect in pilot-scale reactor compared to lab-scale reactor. Assadi et al. [108] investigated the capacities of isovaleraldehyde (3-methylbutanal) removal in laboratory scale (planar and cylindrical reactor) and pilot scale reactors and they believed that the plasma reactor scale-up for pollutant removal can be feasible.

The feasibility of industrial application for DBD to remove VOCs is not only relates to pollutants degradation performance, but also depends on its construction and operational costs. Ye et al. [301] calculated the treatment cost of benzene destruction in DBD (509 m<sup>3</sup>/h, RH = 50%) and concluded that the cost ranged from 0.24 to 0.52 \$/10<sup>3</sup> m<sup>3</sup> at the voltage of 6–10.5 kV. Dobslaw et al. [233] estimated the construction and operational costs of using the combined NTP-mineral adsorber – biotrickling filter process to treat waste gas from sludge centrifugation in a waste water treatment plan. For treatment of 20,000 m<sup>3</sup>/h of waste gas at an annual operation time of 8000 h, the construction and operational costs were 11.17 \$/(m<sup>3</sup>/h) and 0.53 \$/10<sup>3</sup> m<sup>3</sup>, respectively. Martini et al. [304] have made hypotheses on fixed and variable costs for a Q = 50,000 m<sup>3</sup>/h BDB system and concluded that the DBD fixed cost and the annual variable cost were 33.99 \$/(m<sup>3</sup>/h) and 0.0112 \$/10<sup>3</sup> m<sup>3</sup>, respectively. The costs in the above two studies were calculated based on original data and the exchange rate of € and \$ (1€ = 1.1175\$). It should be pointed out that Dobslaw's research included the construction and operational costs of adsorber and biotrickling filter, which was not considered in Martini's economic analysis. Even if the two costs are added in Martini's study, the results of the two economic analyses are still very different, which may be correlated to the balance between fixed and variable costs. Currently, economic data on the application of DBD for VOCs abatement is scarce.

Therefore, more research is needed to illustrate the economic viability of DBD.

Based on the above-mentioned pilot scale studies, the prospects for the application of DBD in VOCs abatement are clearer. There are a number of aspects which are correlated to the practical use and targets for DBD systems can be discussed.

**Adaptability to gas conditions** The real gas conditions are more complicated than those in laboratories. Since many industrial waste gases contain fine particles or aerosols, so a filter for dust retention is necessary before the gas enters DBD reactors. In the industrial process, the pollutant concentration, moisture and flow rate of the exhaust gas fluctuate randomly. Hence, the DBD equipment's capability for pollutants treatment should be able to adjust as the gas conditions change. This can be achieved by adjusting the applied voltage. Specifically, when the pollutant load is at a low level, the DBD can work at a lower voltage to save energy and prevent over oxidation, which results in a large amount of O<sub>3</sub> and NOx formation. Similarly, the voltage should be raised with the increase of pollutant load to ensure removal rate. Various industrial processes such as printing and painting are operated intermittently, which means that the waste gas is not continuously generated. Therefore, VOCs treating equipment should be able to be turned on and off at any time. For DBD, this requirement is easily met because there is no warm-up stage.

**Acceptable construction and operational cost** Construction costs mainly include pipes, DBD casing, DBD stacks, DBD power supply and ventilator. Among these fixed costs, DBD stacks and power supply account for the majority. The operational cost will be dictated predominantly by electricity cost, which consists of power supply and ventilator consumption. For plasma catalysis systems, the cost of catalyst purchase and disposal needs to be considered. The price of commercially viable catalysts ranges from several \$ to hundreds \$ per kg. Therefore, in practical applications, there should be a compromise between the cost and efficiency of the catalyst. In addition, the disposal of deactivated catalyst after a long period of use cannot be ignored. For commercial applications, with or without a catalyst, the total cost of DBD for VOCs abatement should be comparable to thermal oxidation technique.

**By-products formation** The formation of undesired by-products is inevitable during the degradation of VOCs in DBD. The mineralization rate of VOCs in DBD is generally less than 50% in the absence of catalysts. This means that more than half of initial pollutants are converted into organic by-products. Some of these by-products are emitted in a gaseous form, and the rest are deposited in the form of aerosols on dielectric barrier surface or electrodes. The long-term accumulation of these aerosols will inevitably affect the normal operation of DBD and may even cause accidents. Hence, these deposited by-products should be cleaned in due course of time. The presence of catalysts can reduce but cannot eliminate the formation of organic by-products. As a result, the catalyst may be deactivated by the gradual deposition of by-products. Currently, there are few studies related to the deactivation of catalysts during VOCs removal in DBD. Although ozone is an oxidant, it hardly reacts with VOCs in the absence of catalysts. This is why a large amount of ozone can be detected in the exhaust gas while the mineralization rate is low. Depending on the reactor configuration and applied voltage, the residual ozone concentration ranges from tens to thousands of ppm. Nevertheless, the residual ozone can be easily decomposed if a suitable catalyst is located downstream of the discharge zone in both IPC and PPC systems. As for nitrogen oxides, they can also be reduced by appropriate catalysts.

**Safety** The security risks in the operation of DBD equipment cannot be ignored. Firstly, the concentration of VOCs to be treated should be below the explosion limit. Secondly, fine particles such as oil or paint mist should be effectively filtered before the exhaust gas enters DBD. These particles can be deposited on the electrode or the dielectric surface and may cause accidents during discharge. Thirdly, insulators on the high-voltage input should be protected from contamination and

condensation to avoid creepage and creeping discharge. Lastly, the organic by-products deposited in the equipment should be cleaned in due course of time. These deposits may be ignited by local high temperature during discharge and cause accidents. Most of these deposits can be cleaned by alcohol. Therefore, maintenance and cleaning of the DBD equipment during VOCs treatment are significant for its safe operation.

**Modularity** DBD reactor can be easily scaled up based on actual demands. In order to treat high gas flows, several modules can be used in series or in parallel, which provides a high degree of flexibility. The number of modules required depends on the gas volume and the treatment capacity of single modules. The connection mode of each module can be determined according to the space of the site. Other benefits of modularity include the flexibility of transportation and high utilization of space.

These benefits, requirements and associated issues are helpful in identifying the applicability of DBD for VOCs abatement and smooth operation of DBD equipment in industrial setting.

## 8. Conclusions and perspectives

The application of dielectric barrier discharge non-thermal plasma in VOCs abatement was discussed along with the history, micro-discharge formation and environmental application of DBD. Subsequently, the effect of reactor configuration, power supplies, packing materials and gas properties on discharge characteristics and VOCs degradation in DBD were presented. A desirable DBD reactor should have high VOCs removal efficiency and mineralization rate, as well as low by-products. In order to achieve this goal, various aspects, such as optimization of reactor structure, application of advanced power supply and the introduction of catalysts need to be considered. In addition, investigating the influence of gas properties such as initial concentration, flow rate and humidity level on VOCs abatement can provide an important reference for the industrial applications of DBD. Based on several pilot scale experiments, a number of aspects associated to the practical implementation and targets for DBD systems were discussed.

In the past three decades, a huge number of researches have been implemented and great achievements have been made, which paved for the practical application of DBD in VOCs abatement. However, the mechanisms behind these experimental results are still veiled, and commercial applications of DBD on VOCs removal are still scarce. Therefore, future work should be carried out from both theoretical and practical aspects.

In terms of theory, it mainly lies in the understanding of the discharge process and the degradation pathways of VOCs in the presence or absence of a catalyst. In the early days, the discharge process information such as consumed power was mainly obtained through oscilloscopes. Recently, the application of fast imaging technique has made it possible to directly observe the discharge behavior such as the propagation of streamers on catalyst surface. Further, the information about variation and distribution of the temperature and density of electrons during discharge can be gained through fluid modeling. Through these advanced means, a better insight into the discharge behavior could be obtained, such as electric field enhancement in packed bed DBD reactors, plasma streamer propagation in packed bed DBD reactors and plasma streamer penetration in catalyst pores. In the near future, the discharge mechanism of packed bed DBD will be more fully understood. Unexpectedly, few researchers have focused on the impact of reactor structure on discharge behavior through these advanced means and methods.

About VOCs decomposition mechanisms, most of them were speculated from the information obtained by ex situ detection techniques. To date, the underlying physical and chemical processes of VOCs degradation with or without catalyst are still not clear enough. This is mainly because the survival time of reactive species such as radicals and electrons in plasma and the intermediates generated from VOCs are too

short to be detected. Recently, the application of direct in situ detection has provided more information for understanding the mechanism for VOCs decomposition. Further, the results obtained by in situ measurements can be used in conjunction with computational chemistry such as DFT (Density Functional Theory) to gain a better insight into the reaction pathways of packed-bed DBD systems.

Although a deep insight into the mechanisms of discharge and VOCs degradation can provide theoretical guidance for reactor optimization and catalyst tailoring, it is a difficult task to unveil these mechanisms due to the complexity of plasma behavior, especially in the presence of catalysts. Therefore, in addition to theoretical research, we can also focus on practical aspects to promote the industrial application of DBD in VOCs abatement through process improvement and scale-up experiments. The possible research areas that needs to be explored are as follows:

1) Since real exhaust gas contains many types of VOCs, it is useful to investigate the performance of DBD on mixed VOCs removal.

2) Many studies have shown that sequential DBD process (adsorption with plasma off and oxidation with plasma on) exhibits high energy efficiency. Therefore, it is necessary to undertake research work in this field to testify the practical performance of this operation process.

3) It is promising to combine DBD with other waste air treatment techniques to develop more energy efficient systems. For instance, DBD can be operated as a pre-treatment stage to decompose VOCs into hydrophilic substances, which can be effectively removed by a subsequent biological treatment. More research efforts are needed to identify the potential of these combined systems.

4) In most case, high mineralization rates can be obtained in IPC systems, while PPC system is effective for the suppression of residual ozone. The addition of a downstream catalyst to an IPC system may provide a pragmatic solution to treat VOCs efficiently while ensuring a low residual ozone level. On the other hand, it may be difficult for a single catalyst to effectively remove various types of VOCs simultaneously. A multistage arrangement with different catalysts may be a valid option to address this issue. Therefore, the investigation of multistage catalytic systems is crucial in terms of both residual ozone elimination and complex VOCs mixtures treatment.

5) At present, pilot-scale experiments on industrial VOCs removal by DBD are scarce, which has led to insufficient information and guidance for its practical implementation. In order to promote the commercial application of DBD in VOCs abatement, more scale-up experiments and economic analysis need to be performed in the future.

## Declaration of Competing Interest

The authors declare that they have no known competing financial interests or personal relationships that could have appeared to influence the work reported in this paper.

## Acknowledgments

This work was financially supported by National Key R&D Program of China (No. 2017YFC0212204), Shaanxi Key R&D Program (No. 2018ZDCXL-SF-02-04), Youth Talents Lifting Project of Science and Technology Association in Shaanxi Provinces Universities and Colleges (No. 20190703), Special Research Project of Education Department of Shaanxi Province (No. 19JK0453), Key Research and Development Program of Shaanxi Province (No. 2018-ZDXM3-01).

## References

- Z. Tan, K. Lu, M. Jiang, R. Su, H. Dong, L. Zeng, S. Xie, Q. Tan, Y. Zhang, Exploring ozone pollution in Chengdu, southwestern China: A case study from radical chemistry to O<sub>3</sub>-VOC-NO<sub>x</sub> sensitivity, *Sci. Total. Environ.* 636 (2018) 775–786.
- Y. Yan, L. Peng, R. Li, Y. Li, L. Li, H. Bai, Concentration, ozone formation potential and source analysis of volatile organic compounds (VOCs) in a thermal power station centralized area: A study in Shouzhou, China, *Environ. Pollut.* 223 (2017)

- 295–304.
- L. Hui, X. Liu, Q. Tan, M. Feng, J. An, Y. Qu, Y. Zhang, N. Cheng, VOC characteristics, sources and contributions to SOA formation during haze events in Wuhan, Central China, *Sci. Total. Environ.* 650 (2019) 2624–2639.
- W. Wei, Y. Li, Y. Wang, S. Cheng, L. Wang, Characteristics of VOCs during haze and non-haze days in Beijing, China: Concentration, chemical degradation and regional transport impact, *Atmos. Environ.* 194 (2018) 134–145.
- R.J. Huang, Y. Zhang, C. Bozzetti, K.F. Ho, J.J. Cao, Y. Han, K.R. Daellenbach, J.G. Slowik, S.M. Platt, F. Canonaco, P. Zotter, R. Wolf, S.M. Pieber, E.A. Bruns, M. Crippa, G. Ciarelli, A. Piazzalunga, M. Schwikowski, G. Abbaszade, J. Schnelle-Kreis, R. Zimmermann, Z. An, S. Szidat, U. Baltensperger, I. El Haddad, A.S. Prevot, High secondary aerosol contribution to particulate pollution during haze events in China, *Nature* 514 (2014) 218–222.
- R. Hu, G. Liu, H. Zhang, H. Xue, X. Wang, Levels, characteristics and health risk assessment of VOCs in different functional zones of Hefei, *Ecotox. Environ. Safe.* 160 (2018) 301–307.
- M.A. Bari, W.B. Kindziarski, Ambient volatile organic compounds (VOCs) in Calgary, Alberta: Sources and screening health risk assessment, *Sci. Total. Environ.* 631–632 (2018) 627–640.
- D. Wang, L. Nie, X. Shao, H. Yu, Exposure profile of volatile organic compounds receptor associated with paints consumption, *Sci. Total. Environ.* 603–604 (2017) 57–65.
- X. Zhang, B. Gao, A.E. Creamer, C. Cao, Y. Li, Adsorption of VOCs onto engineered carbon materials: A review, *J. Hazard. Mater.* 338 (2017) 102–123.
- H. Wang, B. Wang, J. Li, T. Zhu, Adsorption equilibrium and thermodynamics of acetaldehyde/acetone on activated carbon, *Sep. Purif. Technol.* 209 (2019) 535–541.
- B. Belaisaoui, Y.L. Moullec, E. Favre, Energy efficiency of a hybrid membrane/condensation process for VOC (Volatile Organic Compounds) recovery from air: A generic approach, *Energy* 95 (2016) 291–302.
- A.S.R. Castillo, P.F. Biard, S. Guihéneuf, L. Paquin, A. Amrane, A. Couvert, Assessment of VOC absorption in hydrophobic ionic liquids: Measurement of partition and diffusion coefficients and simulation of a packed column, *Chem. Eng. J.* 360 (2019) 1416–1426.
- W. Yang, H. Zhou, C. Zong, Y. Li, W. Jin, Study on membrane performance in vapor permeation of VOC/N<sub>2</sub> mixtures via modified constant volume/variable pressure method, *Sep. Purif. Technol.* 200 (2018) 273–283.
- X. Hao, R. Li, J. Wang, X. Yang, Numerical simulation of a regenerative thermal oxidizer for volatile organic compounds treatment, *Environ. Eng. Res.* 23 (2018) 397–405.
- H. Wu, H. Yan, Y. Quan, H. Zhao, N. Jiang, C. Yin, Recent progress and perspectives in biotrickling filters for VOCs and odorous gases treatment, *J. Environ. Manage.* 222 (2018) 409–419.
- D. Dobslaw, J. Schöller, D. Krivak, S. Helbich, K.H. Engesser, Performance of different biological waste air purification processes in treatment of a waste gas mix containing tert-butyl alcohol and acetone: A comparative study, *Chem. Eng. J.* 355 (2019) 572–585.
- Z. Zhang, Z. Jiang, W. Shangguan, Low-temperature catalysis for VOCs removal in technology and application: A state-of-the-art review, *Catal. Today* 264 (2016) 270–278.
- C. Yang, G. Miao, Y. Pi, Q. Xia, J. Wu, Z. Li, J. Xiao, Abatement of various types of VOCs by adsorption/catalytic oxidation: A review, *Chem. Eng. J.* 370 (2019) 1128–1153.
- J. Guo, C. Lin, C. Jiang, P. Zhang, Review on noble metal-based catalysts for formaldehyde oxidation at room temperature, *Appl. Surf. Sci.* 475 (2019) 237–255.
- W. Zou, B. Gao, Y.S. Ok, L. Dong, Integrated adsorption and photocatalytic degradation of volatile organic compounds (VOCs) using carbon-based nanocomposites: A critical review, *Chemosphere* 218 (2019) 845–859.
- Z. Shayegan, C.S. Lee, F. Haghghat, TiO<sub>2</sub> photocatalyst for removal of volatile organic compounds in gas phase – A review, *Chem. Eng. J.* 334 (2018) 2408–2439.
- A.H. Mamaghani, F. Haghghat, C.S. Lee, Photocatalytic oxidation technology for indoor environment air purification: The state-of-the-art, *Appl. Catal. B: Environ.* 203 (2017) 247–269.
- S.H. Chen, O. Živný, A. Mašláni, S.W. Chau, Abatement of fluorinated compounds in thermal plasma flow, *J. Fluorine Chem.* 217 (2019) 41–49.
- J.C. Whitehead, Plasma catalysis: A solution for environmental problems, *Pure Appl. Chem.* 82 (2010) 1329–1336.
- S.K.P. Veerapandian, N.D. Geyter, J.M. Giraudon, J.F. Lamonier, R. Morent, The Use of Zeolites for VOCs Abatement by Combining Non-Thermal Plasma, Adsorption, and/or Catalysis: A Review, *Catalysts* 9 (2019).
- A.K.G.F.I. Khan, Removal of Volatile Organic Compounds from polluted air, *J. Loss Prevent. Proc.* 13 (2000) 527–545.
- G.R. Parmar, N.N. Rao, Emerging Control Technologies for Volatile Organic Compounds, *Crit. Rev. Env. Sci. Tec.* 39 (2008) 41–78.
- A. Luengas, A. Barona, C. Hort, G. Gallastegui, V. Platel, A. Elias, A review of indoor air treatment technologies, *Rev. Environ. Sci. Bio.* 14 (2015) 499–522.
- C. Dai, Y. Zhou, H. Peng, S. Huang, P. Qin, J. Zhang, Y. Yang, L. Luo, X. Zhang, Current progress in remediation of chlorinated volatile organic compounds: A review, *J. Ind. Eng. Chem.* 62 (2018) 106–119.
- K.H. Kim, J.E. Szulejko, P. Kumar, E.E. Kwon, A.A. Adelodun, P.A.K. Reddy, Air ionization as a control technology for off-gas emissions of volatile organic compounds, *Environ. Pollut.* 225 (2017) 729–743.
- F. Thevenet, L. Sivachandiran, O. Guaitella, C. Barakat, A. Rousseau, Plasma-catalyst coupling for volatile organic compound removal and indoor air treatment: a review, *J. Phys. D: Appl. Phys.* 47 (2014).
- A. Bogaerts, E.C. Neyts, Plasma Technology: An Emerging Technology for Energy Storage, *ACS Energy Lett.* 3 (2018) 1013–1027.
- B. Lee, D.W. Kim, D.W. Park, Dielectric barrier discharge reactor with the segmented electrodes for decomposition of toluene adsorbed on bare-zeolite, *Chem. Eng. J.* 357 (2019) 188–197.
- E.C. Neyts, K.K. Ostrikov, M.K. Sunkara, A. Bogaerts, Plasma Catalysis: Synergistic Effects at the Nanoscale, *Chem. Rev.* 115 (2015) 13408–13446.
- R.N. Franklin, N.S.J. Braithwaite, 80 Years of Plasma, *Plasma Sources Sci. T.* 18 (2009).
- J.C. Whitehead, Plasma-catalysis: the known knowns, the known unknowns and the unknown unknowns, *J. Phys. D: Appl. Phys.* 49 (2016).
- T. Hammer, Application of Plasma Technology in Environmental Techniques, *Contrib. Plasma Phys.* 39 (1999) 441–462.
- R. McAdams, Prospects for non-thermal atmospheric plasmas for pollution abatement, *J. Phys. D: Appl. Phys.* 34 (2001) 2810–2821.
- A.M. Vandembroucke, R. Morent, N.D. Geyter, C. Leys, Non-thermal plasmas for non-catalytic and catalytic VOC abatement, *J. Hazard. Mater.* 195 (2011) 30–54.
- W.A. Saoud, A.A. Assadi, M. Guiza, S. Loganathan, A. Bouzaza, W. Aboussaoud, A. Ouederni, S. Rtimi, D. Wolbert, Synergism between non-thermal plasma and photocatalysis: Implications in the post discharge of ozone at a pilot scale in a catalytic fixed-bed reactor, *Appl. Catal. B: Environ.* 241 (2019) 227–235.
- X. Li, T. Guo, Z. Peng, L. Xu, J. Dong, P. Cheng, Z. Zhou, Real-time monitoring and quantification of organic by-products and mechanism study of acetone decomposition in a dielectric barrier discharge reactor, *Environ. Sci. Pollut. Res. Int.* 26 (2019) 6773–6781.
- C. Norsic, J.M. Tatibouët, C.B. Dupeyrat, E. Fourré, Methanol oxidation in dry and humid air by dielectric barrier discharge plasma combined with MnO<sub>2</sub>-CuO based catalysts, *Chem. Eng. J.* 347 (2018) 944–952.
- X. Zhang, F. Feng, S. Li, X. Tang, Y. Huang, Z. Liu, K. Yan, Aerosol formation from styrene removal with an AC/DC streamer corona plasma system in air, *Chem. Eng. J.* 232 (2013) 527–533.
- J.V. Durme, J. Dewulf, W. Sysmans, C. Leys, H.V. Langenhove, Abatement and degradation pathways of toluene in indoor air by positive corona discharge, *Chemosphere* 68 (2007) 1821–1829.
- J.H. Park, J.W. Ahn, K.H. Kim, Y.S. Son, Historic and futuristic review of electron beam technology for the treatment of SO<sub>2</sub> and NO<sub>x</sub> in flue gas, *Chem. Eng. J.* 355 (2019) 351–366.
- Y.S. Son, T.H. Kim, C.Y. Choi, J.H. Park, J.W. Ahn, T.V. Dinh, Treatment of toluene and its by-products using an electron beam/ultra-fine bubble hybrid system, *Radiat. Phys. Chem.* 144 (2018) 367–372.
- F. Zhu, X. Li, H. Zhang, A. Wu, J. Yan, M. Ni, H. Zhang, A. Buekens, Destruction of toluene by rotating gliding arc discharge, *Fuel* 176 (2016) 78–85.
- H. Zhang, F. Zhu, X. Li, R. Xu, L. Li, J. Yan, X. Tu, Steam reforming of toluene and naphthalene as tar surrogate in a gliding arc discharge reactor, *J. Hazard. Mater.* 369 (2019) 244–253.
- Y. Qin, G. Niu, X. Wang, D. Luo, Y. Duan, Status of CO<sub>2</sub> conversion using microwave plasma, *J. CO<sub>2</sub> Util.* 28 (2018) 283–291.
- A.G. Zherlitsyn, V.P. Shiyann, P.V. Demchenko, Microwave plasma torch for processing hydrocarbon gases, *Resource Efficient Technol.* 2 (2016) 11–14.
- U. Kogelschatz, Dielectric-barrier Discharges Their History, Discharge Physics, and Industrial Applications, *Plasma Chem. Plasma P.* 23 (2003) 1–46.
- Plasma Chem Plasma Process 34 (5) (2014) 1033–1065, <https://doi.org/10.1007/s11090-014-9562-0>.
- W. Siemens, Ueber die elektrostatistische Induction und die Verzögerung des Stroms in Flaschendrahten, *Ann. Phys. Chem.* 178 (1857) 66–122.
- B. Eliasson, M. Hirth, U. Kogelschatz, Ozone synthesis from oxygen in dielectric barrier discharges, *J. Phys. D: Appl. Phys.* 20 (1987) 1421–1437.
- K. Buss, Die elektrodenlose Entladung nach Messung mit dem Kathodenszilligraphen, *Archiv für Elektrotechnik* 26 (1932) 261–265.
- T.C. Manley, The Electric Characteristics of the Ozonator Discharge, *J. Electrochem. Soc.* 84 (1943) 83–96.
- U. Kogelschatz, B. Eliasson, W. Egli, Dielectric-Barrier Discharges. Principle and Applications, *J. PHYS IV FRANCE* 4 (1997) 46–66.
- B. Eliasson, U. Kogelschatz, Modeling and Applications of Silent Discharge Plasmas, *IEEE T. Plasma Sci.* 19 (1991) 309–323.
- U. Kogelschatz, B. Eliasson, W. Egli, From ozone generators to flat television screens: history and future potential of dielectric-barrier discharges, *Pure Appl. Chem.* 71 (1999) 1819–1828.
- U. Kogelschatz, Fundamentals and applications of dielectric-barrier, discharges (2000).
- Plasma Chem Plasma Process 36 (1) (2016) 185–212, <https://doi.org/10.1007/s11090-015-9662-5>.
- U. Kogelschatz, Collective phenomena in volume and surface barrier discharges, *J. Phys. Conf. Series* 257 (2010).
- S.A. Starostin, P.A. Premkumar, M. Creator, E.M. van Veldhuizen, H. de Vries, R.M.J. Paffen, M.C.M. van de Sanden, On the formation mechanisms of the diffuse atmospheric pressure dielectric barrier discharge in CVD processes of thin silica-like films, *Plasma Sources Sci. Technol.* 18 (2009).
- H.E. Wagner, R. Brandenburg, K.V. Kozlov, A. Sonnenfeld, P. Michel, J.F. Behnke, The barrier discharge: basic properties and applications to surface treatment, *Vacuum* 71 (2003) 417–436.
- Y. Sun, F. Zhang, Investigation of influencing factors in ozone generation using dielectric barrier discharge, *Proceedings of the 9th International Conference on Properties and Applications of Dielectric Materials*, 2009, pp. 614–617.
- K. Takaki, Y. Hatanaka, K. Arima, S. Mukaiyama, T. Fujiwara, Influence of electrode configuration on ozone synthesis and micro-discharge property in dielectric



- barrier discharge reactor, *Vacuum* 83 (2008) 128–132.
- [67] S. Jodzis, M. Zięba, Energy efficiency of an ozone generation process in oxygen, Analysis of a pulsed DBD system, *Vacuum* 155 (2018) 29–37.
- [68] L.S. Wei, D.K. Yuan, Y.F. Zhang, Z.J. Hu, G.P. Dong, Experimental and theoretical study of ozone generation in pulsed positive dielectric barrier discharge, *Vacuum* 104 (2014) 61–64.
- [69] P. Talebizadeh, M. Bahaie, R. Brown, H. Rahimzadeh, Z. Ristovski, M. Arai, The role of non-thermal plasma technique in NO<sub>x</sub> treatment: A review, *Renew. Sust. Energ. Rev.* 40 (2014) 886–901.
- [70] Z. Adnan, S. Mir, M. Habib, Exhaust gases depletion using non-thermal plasma (NTP), *Atmos. Pollut. Res.* 8 (2017) 338–343.
- [71] M. Bahaie, P. Davari, P. Talebizadeh, F. Zare, H. Rahimzadeh, Z. Ristovski, R. Brown, Performance evaluation of non-thermal plasma on particulate matter, ozone and CO<sub>2</sub> correlation for diesel exhaust emission reduction, *Chem. Eng. J.* 276 (2015) 240–248.
- [72] S. Ma, Y. Zhao, J. Yang, S. Zhang, J. Zhang, C. Zheng, Research progress of pollutants removal from coal-fired flue gas using non-thermal plasma, *Renew. Sust. Energ. Rev.* 67 (2017) 791–810.
- [73] S. Cui, R. Hao, Dong Fu, Integrated method of non-thermal plasma combined with catalytic oxidation for simultaneous removal of SO<sub>2</sub> and NO, *Fuel* 246 (2019) 365–374.
- [74] S. Cui, R. Hao, D. Fu, An integrated system of dielectric barrier discharge combined with wet electrostatic precipitator for simultaneous removal of NO and SO<sub>2</sub>: Key factors assessments, products analysis and mechanism, *Fuel* 221 (2018) 12–20.
- [75] B.M. Obradovic, G.B. Sretenovic, M.M. Kuraica, A dual-use of DBD plasma for simultaneous NO(x) and SO<sub>2</sub> removal from coal-combustion flue gas, *J. Hazard. Mater.* 185 (2011) 1280–1286.
- [76] W.J. Liang, H.P. Fang, J. Li, F. Zheng, J.X. Li, Y.Q. Jin, Performance of non-thermal DBD plasma reactor during the removal of hydrogen sulfide, *J. Electrostat.* 69 (2011) 206–213.
- [77] X. Dang, J. Huang, L. Kang, T. Wu, Q. Zhang, Research on Decomposition of Hydrogen Sulfide Using Nonthermal Plasma with Metal Oxide Catalysis, *Energy Procedia* 16 (2012) 856–862.
- [78] R. Snoeckx, A. Bogaerts, Plasma technology - a novel solution for CO<sub>2</sub> conversion? *Chem. Soc. Rev.* 46 (2017) 5805–5863.
- [79] A.H. Khoja, M. Tahir, N.A.S. Amin, Recent developments in non-thermal catalytic DBD plasma reactor for dry reforming of methane, *Energ. Convers. Manage.* 183 (2019) 529–560.
- [80] W.C. Chung, M.B. Chang, Review of catalysis and plasma performance on dry reforming of CH<sub>4</sub> and possible synergistic effects, *Renew. Sust. Energ. Rev.* 62 (2016) 13–31.
- [81] P. Peng, P. Chen, C. Schiappacasse, N. Zhou, E. Anderson, D. Chen, J. Liu, Y. Cheng, R. Hatzenbeller, M. Addy, Y. Zhang, Y. Liu, R. Ruan, A review on the non-thermal plasma-assisted ammonia synthesis technologies, *J. Clean. Prod.* 177 (2018) 597–609.
- [82] J. Hong, S. Praver, A.B. Murphy, Plasma Catalysis as an Alternative Route for Ammonia Production: Status, Mechanisms, and Prospects for Progress, *ACS Sustain. Chem. Eng.* 6 (2017) 15–31.
- [83] T. Yamamoto, K. Ramanathan, P.A. Lawless, D.S. Ensor, J.R. Newsome, N. Plaks, G.H. Ramsey, C.A. Vogel, L. Hammel, Control of Volatile Organic Compounds by an ac Energized Ferroelectric Pellet Reactor and a Pulsed Corona Reactor, *IEEE Trans. Ind. Appl.* 28 (1992) 528–534.
- [84] D. Evans, L.A. Rosocha, G.K. Anderson, J.J. Coogan, M.J. Kushner, Plasma remediation of trichloroethylene in silent discharge plasmas, *J. Appl. Phys.* 74 (1993) 5378–5386.
- [85] T. Oda, T. Takahashi, H. Nakano, S. Masuda, Decomposition of Fluorocarbon Gaseous Contaminants by Surface Discharge-Induced Plasma Chemical Processing, *IEEE Trans. Ind. Appl.* 29 (1993) 787–792.
- [86] M.B. Chang, C.C. Lee, Destruction of Formaldehyde with Dielectric Barrier Discharge Plasmas, *Environ. Sci. Technol.* 29 (1995) 181–186.
- [87] T. Oda, R. Yamashita, T. Takahashi, S. Masuda, Atmospheric Pressure Discharge Plasma Processing for Gaseous Air Contaminants, *IEEE Trans. Ind. Appl.* 32 (1996) 227–232.
- [88] T. Yamamoto, J.S. Chang, A.A. Berezin, H. Kohno, S. Honda, A. Shibuya, Decomposition of Toluene, o-Xylene, Trichloroethylene, and Their Mixture Using a BaTiO<sub>3</sub> Packed-Bed Plasma Reactor, *J. Adv. Oxid. Technol.* 1 (1996) 67–78.
- [89] M.B. Chang, C.C. Chang, Destruction and Removal of Toluene and MEK from Gas Streams with Silent Discharge Plasmas, *Aiche J.* 43 (1997) 1325–1330.
- [90] S. Futamura, A. Zhang, G. Prieto, T. Yamamoto, Factors and Intermediates Governing Byproduct Distribution for Decomposition of Butane in Nonthermal Plasma, *IEEE Trans. Ind. Appl.* 34 (1998) 967–974.
- [91] A. Ogata, K. Yamanouchi, K. Mizuno, S. Kushiyama, T. Yamamoto, Decomposition of Benzene Using Alumina-Hybrid and Catalyst-Hybrid Plasma Reactors, *IEEE T. Ind. Appl.* 35 (1999) 1289–1295.
- [92] J. Chae, S. Moon, H. Sun, K. Kim, V.A. Vassiliev, E.M. Mikhopol, A Study of Volatile Organic Compounds Decomposition with the Use of Non-Thermal Plasma, *KSME Int. J.* 13 (1999) 647–655.
- [93] A. Ogata, N. Shintani, K. Yamanouchi, S. Kushiyama, K. Mizuno, T. Yamamoto, Effect of Water Vapor on Benzene Decomposition Using a Nonthermal-Discharge Plasma Reactor, *Plasma Chem. Plasma P.* 20 (2000) 453–467.
- [94] M.B. Chang, H.M. Lee, Gas-Phase Removal of Acetaldehyde via Packed-Bed Dielectric Barrier Discharge Reactor, *Plasma Chem. Plasma P.* 21 (2001) 329–343.
- [95] F. Holzer, U. Roland, F.D. Kopinke, Combination of non-thermal plasma and heterogeneous catalysis for oxidation of volatile organic compounds Part 1. Accessibility of the intra-particle volume, *Appl. Catal. B: Environ.* 38 (2002) 163–181.
- [96] H.M. Lee, M.B. Chang, Abatement of Gas-phase p-Xylene via Dielectric Barrier Discharges, *Plasma Chem. Plasma P.* 23 (2003) 541–558.
- [97] H.H. Kim, S.M. Oh, A. Ogata, S. Futamura, Decomposition of benzene using AgTiO<sub>2</sub> packed plasma-driven catalyst reactor influence of electrode configuration and Ag-loading amount, *Catal. Lett.* 96 (2004) 189–194.
- [98] S.M. Oh, H.H. Kim, A. Ogata, S. Futamura, D.W. Park, Effect of zeolite in surface discharge plasma on the decomposition of toluene, *Catal. Lett.* 99 (2005) 101–104.
- [99] C. Subrahmanyam, M. Magureauu, A. Renken, L. Kiwi-Minsker, Catalytic abatement of volatile organic compounds assisted by non-thermal plasma, *Appl. Catal. B: Environ.* 65 (2006) 150–156.
- [100] Vladimir Demidyuk, J. Christopher Whitehead, Influence of temperature on gas-phase toluene decomposition in plasma-catalytic system, *Plasma Chem. Plasma Process* 27 (1) (2007) 85–94, <https://doi.org/10.1007/s11090-006-9045-z>.
- [101] H.Y. Fan, C. Shi, X.S. Li, D.Z. Zhao, Y. Xu, A.M. Zhu, High-efficiency plasma catalytic removal of dilute benzene from air, *J. Phys. D Appl. Phys.* 42 (2009) 1–5.
- [102] Atsushi Ogata, Keiichi Saito, Hyun-Ha Kim, Masami Sugawara, Hirofumi Aritani, Hisahiro Einaga, Performance of an Ozone Decomposition Catalyst in Hybrid Plasma Reactors for Volatile Organic Compound Removal, *Plasma Chem Plasma Process* 30 (1) (2010) 33–42, <https://doi.org/10.1007/s11090-009-9206-y>.
- [103] J. Karuppiah, E.L. Reddy, P.M. Reddy, B. Ramaraju, R. Karvembu, C. Subrahmanyam, Abatement of mixture of volatile organic compounds (VOCs) in a catalytic non-thermal plasma reactor, *J. Hazard. Mater.* 237–238 (2012) 283–289.
- [104] W.J. Liang, L. Ma, H. Liu, J. Li, Toluene degradation by non-thermal plasma combined with a ferroelectric catalyst, *Chemosphere* 92 (2013) 1390–1395.
- [105] *Plasma Chem Plasma Process* 34 (5) (2014) 1141–1156, <https://doi.org/10.1007/s11090-014-9556-y>.
- [106] R. Zhu, Y. Mao, L. Jiang, J. Chen, Performance of chlorobenzene removal in a non-thermal plasma catalysis reactor and evaluation of its byproducts, *Chem. Eng. J.* 279 (2015) 463–471.
- [107] O. Karatum, M.A. Deshusses, A comparative study of dilute VOCs treatment in a non-thermal plasma reactor, *Chem. Eng. J.* 294 (2016) 308–315.
- [108] A.A. Assadi, A. Bouzaza, D. Wolbert, Comparative study between laboratory and large pilot scales for VOCs removal from gas streams in continuous flow surface discharge plasma, *Chem. Eng. Res. Des.* 106 (2016) 308–314.
- [109] B. Wang, C. Chi, M. Xu, C. Wang, D. Meng, Plasma-catalytic removal of toluene over CeO<sub>2</sub>-MnOx catalysts in an atmosphere dielectric barrier discharge, *Chem. Eng. J.* 322 (2017) 679–692.
- [110] N. Jiang, L. Guo, C. Qiu, Y. Zhang, K. Shang, N. Lu, J. Li, Y. Wu, Reactive species distribution characteristics and toluene destruction in the three-electrode DBD reactor energized by different pulsed modes, *Chem. Eng. J.* 350 (2018) 12–19.
- [111] W.A. Saoud, A.A. Assadi, M. Guiza, A. Bouzaza, W. Aboussaoud, I. Soutrel, A. Ouederni, D. Wolbert, S. Rtimi, Abatement of ammonia and butyraldehyde under non-thermal plasma and photocatalysis: Oxidation processes for the removal of mixture pollutants at pilot scale, *Chem. Eng. J.* 344 (2018) 165–172.
- [112] D. Dobslaw, O. Ortinghaus, C. Dobslaw, A combined process of non-thermal plasma and a low-cost mineral adsorber for VOC removal and odor abatement in emissions of organic waste treatment plants, *J. Environ. Chem. Eng.* 6 (2018) 2281–2289.
- [113] Y. Cai, X. Zhu, W. Hu, C. Zheng, Y. Yang, M. Chen, X. Gao, Plasma-catalytic decomposition of ethyl acetate over LaMO<sub>3</sub> (M = Mn, Fe, and Co) perovskite catalysts, *J. Ind. Eng. Chem.* 70 (2019) 447–452.
- [114] Mohammad Sharif Hosseini, Hassan Asilian Mahabadi, Rasoul Yarahmadi, Removal of Toluene from Air Using a Cycled Storage-Discharge (CSD) Plasma Catalytic Process, *Plasma Chem Plasma Process* 39 (1) (2019) 125–142, <https://doi.org/10.1007/s11090-018-9938-7>.
- [115] C. Qin, H. Guo, P. Liu, W. Bai, J. Huang, X. Huang, X. Dang, D. Yan, Toluene abatement through adsorption and plasma oxidation using ZSM-5 mixed with  $\gamma$ -Al<sub>2</sub>O<sub>3</sub>, TiO<sub>2</sub> or BaTiO<sub>3</sub>, *J. Ind. Eng. Chem.* 63 (2018) 449–455.
- [116] H. Zhang, K. Li, L. Li, L. Liu, X. Meng, T. Sun, J. Jia, M. Fan, High efficient styrene mineralization through novel NiO-TiO<sub>2</sub>-Al<sub>2</sub>O<sub>3</sub> packed pre-treatment/post-treatment dielectric barrier discharge plasma, *Chem. Eng. J.* 343 (2018) 759–769.
- [117] N. Jiang, C. Qiu, L. Guo, K. Shang, N. Lu, J. Li, Y. Zhang, Y. Wu, Plasma-catalytic destruction of xylene over Ag-Mn mixed oxides in a pulsed sliding discharge reactor, *J. Hazard. Mater.* 369 (2019) 611–620.
- [118] W. Xu, K. Lin, D. Ye, X. Jiang, J. Liu, Y. Chen, Performance of Toluene Removal in a Nonthermal Plasma Catalysis System over Flake-Like HZSM-5 Zeolite with Tunable Pore Size and Evaluation of Its Byproducts, *Nanomaterials (Basel)* 9 (2019).
- [119] A. Jahanmiri, M.R. Rahimpour, M.M. Shirazi, N. Hooshmand, H. Taghvaei, Naphtha cracking through a pulsed DBD plasma reactor: Effect of applied voltage, pulse repetition frequency and electrode material, *Chem. Eng. J.* 191 (2012) 416–425.
- [120] X. Yao, N. Jiang, J. Li, N. Lu, K. Shang, Y. Wu, An improved corona discharge ignited by oxide cathodes with high secondary electron emission for toluene degradation, *Chem. Eng. J.* 362 (2019) 339–348.
- [121] J. Karuppiah, R. Karvembu, C. Subrahmanyam, The catalytic effect of MnOx and CoOx on the decomposition of nitrobenzene in a non-thermal plasma reactor, *Chem. Eng. J.* 180 (2012) 39–45.
- [122] Y. Zhang, J. Nie, C. Yuan, Y. Long, M. Chen, J. Tao, Q. Wang, Y. Cong, CuO/Cu/Ag/MWNTs/sponge electrode-enhanced pollutant removal in dielectric barrier discharge (DBD) reactor, *Chemosphere* 229 (2019) 273–283.
- [123] C. Qin, X. Dang, J. Huang, J. Teng, X. Huang, Plasma-catalytic oxidation of adsorbed toluene on Ag-Mn/ $\gamma$ -Al<sub>2</sub>O<sub>3</sub>: Comparison of gas flow-through and gas circulation treatment, *Chem. Eng. J.* 299 (2016) 85–92.
- [124] M. Bahri, F. Haghighat, S. Rohani, H. Kazemian, Metal organic frameworks for gas-phase VOCs removal in a NTP-catalytic reactor, *Chem. Eng. J.* 320 (2017) 308–318.
- [125] M.S. Gandhi, Y.S. Mok, S.B. Lee, H. Park, Effect of various parameters for butane decomposition under ambient temperature in a dielectric barrier discharge non-thermal plasma reactor, *J. Taiwan Inst. Chem. E.* 44 (2013) 786–794.
- [126] H.H. Kim, A. Ogata, S. Futamura, Oxygen partial pressure-dependent behavior of various catalysts for the total oxidation of VOCs using cycled system of adsorption and oxygen plasma, *Appl. Catal. B: Environ.* 79 (2008) 356–367.
- [127] H. Baránková, L. Bárdos, Effect of the electrode material on the atmospheric plasma conversion of NO in air mixtures, *Vacuum* 84 (2010) 1385–1388.
- [128] X. Jin, Y. Zhang, X. Jiang, R. Wang, Analysis of electrode material effect on organic exhaust gas decomposition by pulse plasma, *China Environ. Sci.* 18 (1998) 213–217.
- [129] N. Jiang, N. Lu, J. Li, Y. Wu, Degradation of Benzene by Using a Silent-Packed Bed Hybrid Discharge Plasma Reactor, *Plasma Sci. Technol.* 14 (2012) 140–146.
- [130] N. Jiang, N. Lu, K. Shang, J. Li, Y. Wu, Effects of electrode geometry on the performance of dielectric barrier/packed-bed discharge plasmas in benzene degradation, *J. Hazard. Mater.* 262 (2013) 387–393.
- [131] W. Liang, J. Li, J. Li, Y. Jin, Abatement of toluene from gas streams via ferroelectric packed bed dielectric barrier discharge plasma, *J. Hazard. Mater.* 170 (2009) 633–638.
- [132] H.H. Kim, A. Ogata, S. Futamura, Effect of different catalysts on the decomposition of VOCs using flow-type plasma-driven catalysis, *IEEE T. Plasma Sci.* 34 (2006) 984–995.
- [133] L. Sivachandiran, J. Karuppiah, C. Subrahmanyam, DBD plasma reactor for oxidative decomposition of Chlorobenzene, *Int. J. Chem. React. Eng.* 10 (2012).
- [134] M. Bahri, F. Haghighat, S. Rohani, H. Kazemian, Impact of design parameters on the performance of non-thermal plasma air purification system, *Chem. Eng. J.* 302 (2016) 204–212.
- [135] H.H. Kim, S.M. Oh, A. Ogata, S. Futamura, Decomposition of gas-phase benzene using plasma-driven catalyst (PDC) reactor packed with Ag/TiO<sub>2</sub> catalyst, *Appl. Catal. B: Environ.* 56 (2005) 213–220.
- [136] M. Magureauu, N.B. Mandache, V.I. Parvulescu, C. Subrahmanyam, A. Renken, L. Kiwi-Minsker, Improved performance of non-thermal plasma reactor during decomposition of trichloroethylene Optimization of the reactor geometry and introduction of catalytic electrode, *Appl. Catal. B: Environ.* 74 (2007) 270–277.
- [137] A.H. Khoja, M. Tahir, N.A.S. Amin, Dry reforming of methane using different dielectric materials and DBD plasma reactor configurations, *Energ. Convers. Manage.* 144 (2017) 262–274.
- [138] D. Mei, X. Tu, Conversion of CO<sub>2</sub> in a cylindrical dielectric barrier discharge reactor: Effects of plasma processing parameters and reactor design, *J. CO<sub>2</sub> Util.* 19 (2017) 68–78.
- [139] Chung-Liang Chang, Hsunling Bai, Shu-Jen Lu, Destruction of Styrene in an Air Stream by Packed Dielectric Barrier Discharge Reactors, *Plasma Chem Plasma Process* 25 (6) (2005) 641–657, <https://doi.org/10.1007/s11090-005-6818-8>.
- [140] H. Zhang, K. Li, T. Sun, J. Jia, Z. Lou, L. Feng, Removal of styrene using dielectric barrier discharge plasmas combined with sol-gel prepared TiO<sub>2</sub> coated  $\gamma$ -Al<sub>2</sub>O<sub>3</sub>, *Chem. Eng. J.* 241 (2014) 92–102.
- [141] B. Wang, W. Yan, W. Ge, X. Duan, Methane conversion into higher hydrocarbons with dielectric barrier discharge micro-plasma reactor, *J. Energ. Chem.* 22 (2013) 876–882.
- [142] U. Roland, F. Holzer, F.D. Kopinke, Combination of non-thermal plasma and heterogeneous catalysis for oxidation of volatile organic compounds, *Appl. Catal. B: Environ.* 58 (2005) 217–226.
- [143] C. Qin, H. Guo, W. Bai, J. Huang, X. Huang, X. Dang, D. Yan, Kinetics study on non-thermal plasma mineralization of adsorbed toluene over  $\gamma$ -Al<sub>2</sub>O<sub>3</sub> hybrid with zeolite, *J. Hazard. Mater.* 369 (2019) 430–438.
- [144] N. Jiang, C. Qiu, L. Guo, K. Shang, N. Lu, J. Li, Y. Wu, Post Plasma-Catalysis of Low Concentration VOC Over Alumina-Supported Silver Catalysts in a Surface/Packed-Bed Hybrid Discharge Reactor, *Water Air Soil Poll.* 228 (2017) 113.
- [145] A.S. Chipper, N.B. Simiand, F. Jorand, S. Pasquiers, G. Popa, C. Postel, Influence of water vapour on acetaldehyde removal efficiency by DBD, *J. Optoelectron. Adv.* M. 8 (2006) 208–212.
- [146] J.H. Byeon, J.H. Park, Y.S. Jo, K.Y. Yoon, J. Hwang, Removal of gaseous toluene and submicron aerosol particles using a dielectric barrier discharge reactor, *J. Hazard. Mater.* 175 (2010) 417–422.
- [147] A. Ozkan, T. Dufour, A. Bogaerts, F. Reniers, How do the barrier thickness and dielectric material influence the filamentary mode and CO<sub>2</sub> conversion in a flowing DBD? *Plasma Sources Sci. T.* 25 (2016).
- [148] M.S. Gandhi, Y.S. Mok, Decomposition of trifluoromethane in a dielectric barrier discharge non-thermal plasma reactor, *J. Environ. Sci.* 24 (2012) 1234–1239.
- [149] Nan Jiang, Cheng Qiu, Lianjie Guo, Kefeng Shang, Na Lu, Jie Li, Yan Wu, Improved Performance for Toluene Abatement in a Continuous-Flow Pulsed Sliding Discharge Reactor Based on Three-Electrode Configuration, *Plasma Chem Plasma Process* 39 (1) (2019) 227–240, <https://doi.org/10.1007/s11090-018-9939-6>.
- [150] A.S. Chipper, A. Nastuta, G. Rusu, G. Popa, Electrical characterisation of a double DBD in He at atmospheric pressure used for surface treatments, *J. Optoelectron. Adv. M.* 9 (2007) 2926–2931.
- [151] H. Ma, P. Chen, M. Zhang, X. Lin, R. Ruan, Study of SO<sub>2</sub> Removal Using Non-thermal Plasma Induced by Dielectric Barrier Discharge (DBD), *Plasma Chem. Plasma P.* 22 (2002) 239–254.
- [152] T. Zhu, J. Li, W.J. Liang, Y.Q. Jin, Experimental Research on Toluene Decomposition with High Frequency DBD, *High Voltage Eng.* 35 (2009) 359–363.
- [153] A. Meiners, M. Leck, B. Abel, Efficiency enhancement of a dielectric barrier plasma discharge by dielectric barrier optimization, *Rev. Sci. Instrum.* 81 (2010) 113507.
- [154] M.F. Mustafa, X. Fu, Y. Liu, Y. Abbas, H. Wang, W. Lu, Volatile organic compounds (VOCs) removal in non-thermal plasma double dielectric barrier discharge reactor, *J. Hazard. Mater.* 347 (2018) 317–324.
- [155] M.F. Mustafa, X. Fu, W. Lu, Y. Liu, Y. Abbas, H. Wang, M.T. Arslan, Application of non-thermal plasma technology on fugitive methane destruction: Configuration and optimization of double dielectric barrier discharge reactor, *J. Clean. Prod.* 174 (2018) 670–677.
- [156] H. Zhang, K. Li, C. Shu, Z. Lou, T. Sun, J. Jia, Enhancement of styrene removal using a novel double-tube dielectric barrier discharge (DDBD) reactor, *Chem. Eng. J.* 256 (2014) 107–118.
- [157] K.L. Pan, M.B. Chang, Plasma catalytic oxidation of toluene over double perovskite-type oxide via packed-bed DBD, *Environ. Sci. Pollut. Res. Int.* 2019.
- [158] Z. Bo, H. Hao, S. Yang, J. Zhu, J. Yan, K. Cen, Vertically-oriented graphenes supported Mn<sub>3</sub>O<sub>4</sub> as advanced catalysts in post plasma-catalysis for toluene decomposition, *Appl. Surf. Sci.* 436 (2018) 570–578.
- [159] H. Zhang, K. Li, T. Sun, J. Jia, X. Yang, Y. Shen, J. Wang, Z. Lou, The removal of styrene using a dielectric barrier discharge (DBD) reactor and the analysis of the by-products and intermediates, *Res. Chem. Intermediat.* 39 (2012) 1021–1035.
- [160] T. Chang, Z. Shen, Y. Huang, J. Lu, D. Ren, J. Sun, J. Cao, H. Liu, Post-plasma-catalytic removal of toluene using MnO<sub>2</sub>-Co<sub>3</sub>O<sub>4</sub> catalysts and their synergistic mechanism, *Chem. Eng. J.* 348 (2018) 15–25.
- [161] T. Chang, J. Lu, Z. Shen, Y. Huang, D. Lu, X. Wang, J. Cao, R. Morent, Simulation and optimization of the post plasma-catalytic system for toluene degradation by a hybrid ANN and NSGA-II method, *Appl. Catal. B: Environ.* 244 (2019) 107–119.
- [162] T. Zhu, Y.D. Wan, J. Li, X.W. He, D.Y. Xu, X.Q. Shu, W.J. Liang, Y.Q. Jin, Volatile organic compounds decomposition using nonthermal plasma coupled with a combination of catalysts, *Int. J. Environ. Sci. Tech.* 8 (2011) 621–630.
- [163] C. Subrahmanyam, A. Renken, L. Kiwi-Minsker, Catalytic abatement of volatile organic compounds assisted by non-thermal plasma, *Appl. Catal. B: Environ.* 65 (2006) 157–162.
- [164] A. Ozkan, T. Dufour, T. Silva, N. Britun, R. Snyders, A. Bogaerts, F. Reniers, The influence of power and frequency on the filamentary behavior of a flowing DBD—application to the splitting of CO<sub>2</sub>, *Plasma Sources Sci. T.* 25 (2016) 025013.
- [165] I. Radu, R. Bartnikas, M.R. Wertheimer, Frequency and voltage dependence of glow and pseudoglow discharges in helium under atmospheric pressure, *IEEE T. Plasma Sci.* 31 (2003) 1363–1378.
- [166] S. Gadkari, S. Gu, Numerical investigation of co-axial DBD: Influence of relative permittivity of the dielectric barrier, applied voltage amplitude, and frequency, *Phys. Plasmas* 24 (2017) 053517.
- [167] R.V. Barrientos, J.P. Sotelo, M.P. Pacheco, J.S.B. Read, R.L. Callejas, Analysis and electrical modelling of a cylindrical DBD configuration at different operating frequencies, *Plasma Sources Sci. T.* 15 (2006) 237–245.
- [168] J.M. Williamson, D.D. Trump, P. Bletzinger, B.N. Ganguly, Comparison of high-voltage ac and pulsed operation of a surface dielectric barrier discharge, *J. Phys. D: Appl. Phys.* 39 (2006) 4400–4406.
- [169] H. Jiang, T. Shao, C. Zhang, Z. Niu, Y. Yu, P. Yan, Y. Zhou, Comparison of AC and Nanosecond-Pulsed DBDs in Atmospheric Air, *IEEE T. Plasma Sci.* 39 (2011) 2076–2077.
- [170] D. Yuan, S. Tang, J. Qi, N. Li, J. Gu, H. Huang, Comparison of hydroxyl radicals generation during granular activated carbon regeneration in DBD reactor driven by bipolar pulse power and alternating current power, *Vacuum* 143 (2017) 87–94.
- [171] H. Wang, D. Li, Y. Wu, J. Li, G. Li, Effect of Power Supply Mode on Removal of Benzene by DBD-Catalysis, *High Voltage Eng.* 35 (2009) 2759–2763.
- [172] V.R. Chirumamilla, W.F.L.M. Hoeben, F.J.C.M. Beckers, T. Huiskamp, E.J.M. Van Heesch, A.J.M. Pemen, Experimental Investigation on the Effect of a Microsecond Pulse and a Nanosecond Pulse on NO Removal Using a Pulsed DBD with Catalytic Materials, *Plasma Chem Plasma Process* 36 (2) (2016) 487–510, <https://doi.org/10.1007/s11090-015-9670-5>.
- [173] S. Zhang, W. Wang, P. Jiang, D. Yang, L. Jia, S. Wang, Comparison of atmospheric air plasmas excited by high-voltage nanosecond pulsed discharge and sinusoidal alternating current discharge, *J. Appl. Phys.* 114 (2013) 163301.
- [174] A.E. Wallis, J.C. Whitehead, K. Zhang, Plasma-assisted catalysis for the destruction of CFC-12 in atmospheric pressure gas streams using TiO<sub>2</sub>, *Catal. Lett.* 113 (2007) 29–33.
- [175] Z. Jia, X. Wang, F. Thevenet, A. Rousseau, Dynamic probing of plasma-catalytic surface processes: Oxidation of toluene on CeO<sub>2</sub>, *Plasma Process. Polym.* 14 (2017) 1600114.
- [176] Q.H. Trinh, Y.S. Mok, Effect of the adsorbent/catalyst preparation method and plasma reactor configuration on the removal of dilute ethylene from air stream, *Cataly. Today* 256 (2015) 170–177.
- [177] H.T. Quoc An, T. Pham Huu, T. Le Van, J.M. Cormier, A. Khacef, Application of atmospheric non thermal plasma-catalysis hybrid system for air pollution control: Toluene removal, *Cataly. Today* 176 (2011) 474–477.
- [178] Hong-Yu Fan, Xiao-Song Li, Chuan Shi, De-Zhi Zhao, Jing-Lin Liu, Yan-Xia Liu, Ai-Min Zhu, Plasma Catalytic Oxidation of Stored Benzene in a Cycled Storage-Discharge (CSD) Process: Catalysts, Reactors and Operation Conditions, *Plasma Chem Plasma Process* 31 (6) (2011) 799–810, <https://doi.org/10.1007/s11090-011-9320-5>.
- [179] X. Fan, T. Zhu, Y. Sun, X. Yan, The roles of various plasma species in the plasma and plasma-catalytic removal of low-concentration formaldehyde in air, *J. Hazard. Mater.* 196 (2011) 380–385.
- [180] T.P. Huu, S. Gil, P.D. Costa, A.G. Fendler, A. Khacef, Plasma catalytic hybrid

- reactor Application to methane removal, *Cataly. Today* 257 (2015) 86–92.
- [181] H. Huang, D. Ye, X. Guan, The simultaneous catalytic removal of VOCs and O<sub>3</sub> in a post-plasma, *Cataly. Today* 139 (2008) 43–48.
- [182] J. Van Durme, J. Dewulf, W. Sysmans, C. Leys, H. Van Langenhove, Efficient toluene abatement in indoor air by a plasma catalytic hybrid system, *Appl. Catal. B: Environ.* 74 (2007) 161–169.
- [183] L. Sivachandiran, F. Thevenet, A. Rousseau, Isopropanol removal using Mn<sub>x</sub>O<sub>y</sub> packed bed non-thermal plasma reactor: Comparison between continuous treatment and sequential sorption/regeneration, *Chem. Eng. J.* 270 (2015) 327–335.
- [184] S. Veerapandian, C. Leys, N. De Geyter, R. Morent, Abatement of VOCs Using Packed Bed Non-Thermal Plasma Reactors: A Review, *Catalysts* 7 (2017).
- [185] A. Ogata, N. Shintani, K. Mizuno, S. Kushiyama, T. Yamamoto, Decomposition of Benzene Using a Nonthermal Plasma Reactor Packed with Ferroelectric Pellets, *IEEE T. Ind. Appl.* 35 (1999) 753–759.
- [186] H.J. Gallon, X. Tu, J.C. Whitehead, Effects of Reactor Packing Materials on H<sub>2</sub> Production by CO<sub>2</sub> Reforming of CH<sub>4</sub> in a Dielectric Barrier Discharge, *Plasma Process. Polym.* 9 (2012) 90–97.
- [187] K.V. Laer, A. Bogaerts, Influence of Gap Size and Dielectric Constant of the Packing Material on the Plasma Behaviour in a Packed Bed DBD Reactor A Fluid Modelling Study, *Plasma Process. Polym.* 14 (2017) 1600129.
- [188] Y.R. Zhang, E.C. Neyts, A. Bogaerts, Influence of the Material Dielectric Constant on Plasma Generation inside Catalyst Pores, *J. Phys. Chem. C* 120 (2016) 25923–25934.
- [189] **Hyun-Ha Kim, Yoshiyuki Teramoto, Atsushi Ogata, Hideyuki Takagi, Tetsuya Nanba, Plasma Catalysis for Environmental Treatment and Energy Applications, *Plasma Chem Plasma Process* 36 (1) (2016) 45–72, <https://doi.org/10.1007/s11090-015-9652-7>.**
- [190] K. Takaki, K. Urashima, J.S. Chang, Ferro-Electric Pellet Shape Effect on C<sub>2</sub>F<sub>6</sub> Removal by a Packed-Bed-Type Nonthermal Plasma, Reactor, *IEEE T. Plasma Sci.* 32 (2004) 2175–2183.
- [191] M.S. Gandhi, A. Ananth, Y.S. Mok, J. Song, K.H. Park, Effect of porosity of  $\gamma$ -alumina on non-thermal plasma decomposition of ethylene in a dielectric-packed bed reactor, *Res. Chem. Intermed.* 40 (2014) 1483–1493.
- [192] S. Li, X. Yu, X. Dang, H. Guo, P. Liu, C. Qin, Using non-thermal plasma for decomposition of toluene adsorbed on  $\gamma$ -Al<sub>2</sub>O<sub>3</sub> and ZSM-5: Configuration and optimization of a double dielectric barrier discharge reactor, *Chem. Eng. J.* 375 (2019) 122027.
- [193] W. Wang, H. Wang, T. Zhu, X. Fan, Removal of gas phase low-concentration toluene over Mn, Ag and Ce modified HZSM-5 catalysts by periodical operation of adsorption and non-thermal plasma regeneration, *J. Hazard. Mater.* 292 (2015) 70–78.
- [194] W. Xu, X. Xu, J. Wu, M. Fu, L. Chen, N. Wang, H. Xiao, X. Chen, D. Ye, Removal of toluene in adsorption–discharge plasma systems over a nickel modified SBA-15 catalyst, *RSC Advances* 6 (2016) 104104–104111.
- [195] T. Wang, S. Chen, H. Wang, Z. Liu, Z. Wu, In-plasma catalytic degradation of toluene over different MnO<sub>2</sub> polymorphs and study of reaction mechanism, *Chinese J. Catal.* 38 (2017) 793–803.
- [196] Y.R. Zhang, E.C. Neyts, A. Bogaerts, Enhancement of plasma generation in catalyst pores with different shapes, *Plasma Sources Sci. T.* 27 (2018).
- [197] H.L. Chen, H.M. Lee, S.H. Chen, M.B. Chang, Review of Packed-Bed Plasma Reactor for Ozone Generation and Air Pollution Control, *Ind. Eng. Chem. Res.* 47 (2008) 2122–2130.
- [198] J.S. Chang, A. Chakrabart, K. Urashima, M. Arai, The Effects of Barium Titanate Pellet Shapes on the Gas Discharge Characteristics of Ferroelectric Packed Bed Reactors, *Proc. Conf. Electr. Insul. Dielectr. Phenom.* (1998).
- [199] J. Li, H. Na, X. Zeng, T. Zhu, Z. Liu, In situ DRIFTS investigation for the oxidation of toluene by ozone over Mn/HZSM-5, Ag/HZSM-5 and Mn-Ag/HZSM-5 catalysts, *Appl. Surf. Sci.* 311 (2014) 690–696.
- [200] X. Zhu, X. Gao, X. Yu, C. Zheng, X. Tu, Catalytic screening for acetone removal in a single-stage plasma-catalysis system, *Cataly. Today* 256 (2015) 108–114.
- [201] J. Wu, Y. Huang, Q. Xia, Z. Li, Decomposition of Toluene in a Plasma Catalysis System with NiO, MnO<sub>2</sub>, CeO<sub>2</sub>, Fe<sub>2</sub>O<sub>3</sub>, and CuO Catalysts, *Plasma Chem. Plasma P.* 33 (2013) 1073–1082.
- [202] C. Norsic, J.M. Tatibouët, C.B. Dupeyrat, E. Fourné, Non thermal plasma assisted catalysis of methanol oxidation on Mn, Ce and Cu oxides supported on  $\gamma$ -Al<sub>2</sub>O<sub>3</sub>, *Chem. Eng. J.* 304 (2016) 563–572.
- [203] R. Peng, X. Sun, S. Li, L. Chen, M. Fu, J. Wu, D. Ye, Shape effect of Pt/CeO<sub>2</sub> catalysts on the catalytic oxidation of toluene, *Chem. Eng. J.* 306 (2016) 1234–1246.
- [204] R. Peng, S. Li, X. Sun, Q. Ren, L. Chen, M. Fu, J. Wu, D. Ye, Size effect of Pt nanoparticles on the catalytic oxidation of toluene over Pt/CeO<sub>2</sub> catalysts, *Appl. Catal. B: Environ.* 220 (2018) 462–470.
- [205] H. Song, F. Hu, Y. Peng, K. Li, S. Bai, J. Li, Non-thermal plasma catalysis for chlorobenzene removal over CoMn/TiO<sub>2</sub> and CeMn/TiO<sub>2</sub>: Synergistic effect of chemical catalysis and dielectric constant, *Chem. Eng. J.* 347 (2018) 447–454.
- [206] X. Zhu, S. Liu, Y. Cai, X. Gao, J. Zhou, C. Zheng, X. Tu, Post-plasma catalytic removal of methanol over Mn–Ce catalysts in an atmospheric dielectric barrier discharge, *Appl. Catal. B: Environ.* 183 (2016) 124–132.
- [207] N. Jiang, J. Hu, J. Li, K. Shang, N. Lu, Y. Wu, Plasma-catalytic degradation of benzene over Ag–Ce bimetallic oxide catalysts using hybrid surface/packed-bed discharge plasmas, *Appl. Catal. B: Environ.* 184 (2016) 355–363.
- [208] X. Zhu, X. Gao, R. Qin, Y. Zeng, R. Qu, C. Zheng, X. Tu, Plasma-catalytic removal of formaldehyde over Cu–Ce catalysts in a dielectric barrier discharge reactor, *Appl. Catal. B: Environ.* 170–171 (2015) 293–300.
- [209] C. Qin, X. Huang, X. Dang, J. Huang, J. Teng, Z. Kang, Toluene removal by sequential adsorption-plasma catalytic process: Effects of Ag and Mn impregnation sequence on Ag-Mn/ $\gamma$ -Al<sub>2</sub>O<sub>3</sub>, *Chemosphere* 162 (2016) 125–130.
- [210] H.J. Gallon, H.H. Kim, X. Tu, J.C. Whitehead, Microscope–ICCD Imaging of an Atmospheric Pressure CH<sub>4</sub> and CO<sub>2</sub> Dielectric Barrier Discharge, *IEEE T. Plasma Sci.* 39 (2011) 2176–2177.
- [211] H.H. Kim, Y. Teramoto, T. Sano, N. Negishi, A. Ogata, Effects of Si/Al ratio on the interaction of nonthermal plasma and Ag/HY catalysts, *Appl. Catal. B: Environ.* 166–167 (2015) 9–17.
- [212] H.H. Kim, A. Ogata, Nonthermal plasma activates catalyst: from current understanding and future prospects, *Eur. Phys. J. Appl. Phys.* 55 (2011) 13806.
- [213] W. Wang, H.H. Kim, K.V. Laer, A. Bogaerts, Streamer propagation in a packed bed plasma reactor for plasma catalysis applications, *Chem. Eng. J.* 334 (2018) 2467–2479.
- [214] S. Gadhkari, S. Gu, Influence of catalyst packing configuration on the discharge characteristics of dielectric barrier discharge reactors: A numerical investigation, *Phys. Plasmas* 25 (2018) 063513.
- [215] Y.R. Zhang, K. Van Laer, E.C. Neyts, A. Bogaerts, Can plasma be formed in catalyst pores? A modeling investigation, *Appl. Catal. B: Environ.* 185 (2016) 56–67.
- [216] X. Tu, H.J. Gallon, M.V. Twigg, P.A. Gorry, J.C. Whitehead, Dry reforming of methane over a Ni/Al<sub>2</sub>O<sub>3</sub> catalyst in a coaxial dielectric barrier discharge reactor, *J. Phy. D: Appl. Phys.* 44 (2011) 274007.
- [217] Z. Wu, Z. Zhu, X. Hao, W. Zhou, J. Han, X. Tang, S. Yao, X. Zhang, Enhanced oxidation of naphthalene using plasma activation of TiO<sub>2</sub>/diatomite catalyst, *J. Hazard. Mater.* 347 (2018) 48–57.
- [218] B. Wang, X. Xu, W. Xu, N. Wang, H. Xiao, Y. Sun, H. Huang, L. Yu, M. Fu, J. Wu, L. Chen, D. Ye, The Mechanism of Non-thermal Plasma Catalysis on Volatile Organic Compounds Removal, *Catal. Surv. Asia* 22 (2018) 73–94.
- [219] B. Wang, B. Chen, Y. Sun, H. Xiao, X. Xu, M. Fu, J. Wu, L. Chen, D. Ye, Effects of dielectric barrier discharge plasma on the catalytic activity of Pt/CeO<sub>2</sub> catalysts, *Appl. Catal. B: Environ.* 238 (2018) 328–338.
- [220] A.S. Pribytkov, G.N. Baeva, N.S. Telegina, A.L. Tarasov, A.Y. Stakheev, A.V. Tel'nov, V.N. Golubeva, Effect of electron irradiation on the catalytic properties of supported Pd catalysts, *Kinet. Catal.* 47 (2006) 765–769.
- [221] S. Kameshima, K. Tamura, Y. Ishibashi, T. Nozaki, Pulsed dry methane reforming in plasma-enhanced catalytic reaction, *Cataly. Today* 256 (2015) 67–75.
- [222] W. Xu, N. Wang, Y. Chen, J. Chen, X. Xu, L. Yu, L. Chen, J. Wu, M. Fu, A. Zhu, D. Ye, In situ FT-IR study and evaluation of toluene abatement in different plasma catalytic systems over metal oxides loaded  $\gamma$ -Al<sub>2</sub>O<sub>3</sub>, *Catal. Commun.* 84 (2016) 61–66.
- [223] M. Shirazi, E.C. Neyts, A. Bogaerts, DFT study of Ni-catalyzed plasma dry reforming of methane, *Appl. Catal. B: Environ.* 205 (2017) 605–614.
- [224] E.C. Neyts, A. Bogaerts, Understanding plasma catalysis through modelling and simulation—a review, *J. Phy. D: Appl. Phys.* 47 (2014).
- [225] H.H. Kim, Y. Teramoto, N. Negishi, A. Ogata, A multidisciplinary approach to understand the interactions of nonthermal plasma and catalyst: A review, *Cataly. Today* 256 (2015) 13–22.
- [226] E.C. Neyts, K. Ostrikov, Nanoscale thermodynamic aspects of plasma catalysis, *Cataly. Today* 256 (2015) 23–28.
- [227] X. Feng, H. Liu, C. He, Z. Shen, T. Wang, Synergistic effects and mechanism of a non-thermal plasma catalysis system in volatile organic compound removal: a review, *Catal. Sci. Technol.* 8 (2018) 936–954.
- [228] H.L. Chen, H.M. Lee, S.H. Chen, M.B. Chang, S.J. Yu, S.N. Li, Removal of Volatile Organic Compounds by Single-Stage and Two-Stage Plasma Catalysis Systems: A Review of the Performance Enhancement Mechanisms, Current Status, and Suitable Applications, *Environ. Sci. Technol.* 43 (2009) 2216–2227.
- [229] H. Puliyalil, D. Lašič Jurković, V.D.B.C. Dasireddy, B. Likozar, A review of plasma-assisted catalytic conversion of gaseous carbon dioxide and methane into value-added platform chemicals and fuels, *RSC Adv.* 8 (2018) 27481–27508.
- [230] W.C. Chung, D.H. Mei, X. Tu, M.B. Chang, Removal of VOCs from gas streams via plasma and catalysis, *Catal. Rev.* 61 (2018) 270–331.
- [231] X. Zhao, X. Liu, J. Liu, J. Chen, S. Fu, F. Zhong, The effect of ionization energy and hydrogen weight fraction on the non-thermal plasma volatile organic compounds removal efficiency, *J. Phy. D: Appl. Phys.* 52 (2019).
- [232] H.H. Kim, A. Ogata, S. Futamura, Atmospheric plasma-driven catalysis for the low temperature decomposition of dilute aromatic compounds, *J. Phy. D: Appl. Phys.* 38 (2005) 1292–1300.
- [233] D. Dobslaw, A. Schulz, S. Helbich, C. Dobslaw, K.-H. Engesser, VOC removal and odor abatement by a low-cost plasma enhanced biotrickling filter process, *J. Environ. Chem. Eng.* 5 (2017) 5501–5511.
- [234] S.L. Hill, H.H. Kim, S. Futamura, J.C. Whitehead, The Destruction of Atmospheric Pressure Propane and Propene Using a Surface Discharge Plasma Reactor, *J. Phys. Chem. A* 112 (2008) 3953–3958.
- [235] J. Li, H. Zhang, D. Ying, Y. Wang, T. Sun, J. Jia, In Plasma Catalytic Oxidation of Toluene Using Monolith CuO Foam as a Catalyst in a Wedged High Voltage Electrode Dielectric Barrier Discharge Reactor: Influence of Reaction Parameters and Byproduct Control, *Int. J. Environ. Res. Public Health* 16 (2019).
- [236] X. Yao, J. Zhang, X. Liang, C. Long, Plasma-catalytic removal of toluene over the supported manganese oxides in DBD reactor: Effect of the structure of zeolites support, *Chemosphere* 208 (2018) 922–930.
- [237] B. Wang, S. Yao, Y. Peng, Y. Xu, Toluene removal over TiO<sub>2</sub>-BaTiO<sub>3</sub> catalysts in an atmospheric dielectric barrier discharge, *J. Environ. Chem. Eng.* 6 (2018) 3819–3826.
- [238] B. Dou, D. Liu, Q. Zhang, R. Zhao, Q. Hao, F. Bin, J. Cao, Enhanced removal of toluene by dielectric barrier discharge coupling with Cu-Ce-Zr supported ZSM-5/TiO<sub>2</sub>/Al<sub>2</sub>O<sub>3</sub>, *Catal. Commun.* 92 (2017) 15–18.
- [239] X. Xu, P. Wang, W. Xu, J. Wu, L. Chen, M. Fu, D. Ye, Plasma-catalysis of metal loaded SBA-15 for toluene removal: Comparison of continuously introduced and adsorption-discharge plasma system, *Chem. Eng. J.* 283 (2016) 276–284.
- [240] L. Mao, Z. Chen, X. Wu, X. Tang, S. Yao, X. Zhang, B. Jiang, J. Han, Z. Wu, H. Lu, T. Nozaki, Plasma-catalyst hybrid reactor with CeO<sub>2</sub>/ $\gamma$ -Al<sub>2</sub>O<sub>3</sub> for benzene decomposition with synergistic effect and nano particle by-product reduction, *J. Hazard. Mater.* 347 (2018) 150–159.
- [241] S. Hamada, H. Hojo, H. Einaga, Effect of catalyst composition and reactor configuration on benzene oxidation with a nonthermal plasma-catalyst combined reactor, *Cataly. Today*, 2018.
- [242] J. Hu, N. Jiang, J. Li, K. Shang, N. Lu, Y. Wu, Degradation of benzene by bipolar pulsed series surface/packed-bed discharge reactor over MnO<sub>2</sub>-TiO<sub>2</sub>/zeolite catalyst, *Chem. Eng. J.* 293 (2016) 216–224.
- [243] X. Dang, C. Qin, J. Huang, J. Teng, X. Huang, Adsorbed benzene/toluene oxidation using plasma driven catalysis with gas circulation: Elimination of the byproducts, *J. Ind. Eng. Chem.* 37 (2016) 366–371.
- [244] X. Zhang, Y. Huang, Z. Liu, K. Yan, Aerosol emission and collection in styrene-contaminated air remediation with a multi-stage plasma system, *J. Electrostat.* 76 (2015) 31–38.
- [245] T. Shou, N. Xu, Y. Li, G. Sun, M.T. Bernards, Y. Shi, Y. He, Mechanisms of Xylene Isomer Oxidation by Non-thermal Plasma via Paired Experiments and Simulations, *Plasma Chem. Plasma P.*, 2019.
- [246] **Plasma Chem Plasma Process 36 (6) (2016) 1501–1515, <https://doi.org/10.1007/s11090-016-9741-2>.**
- [247] T. Kuroki, K. Hirai, R. Kawabata, M. Okubo, T. Yamamoto, Decomposition of Adsorbed Xylene on Adsorbents Using Nonthermal Plasma With Gas Circulation, *IEEE T. Ind. Appl.* 46 (2010) 672–679.
- [248] X. Zhu, X. Tu, D. Mei, C. Zheng, J. Zhou, X. Gao, Z. Luo, M. Ni, K. Cen, Investigation of hybrid plasma-catalytic removal of acetone over CuO/ $\gamma$ -Al<sub>2</sub>O<sub>3</sub> catalysts using response surface method, *Chemosphere* 155 (2016) 9–17.
- [249] C. Zheng, X. Zhu, X. Gao, L. Liu, Q. Chang, Z. Luo, K. Cen, Experimental study of acetone removal by packed-bed dielectric barrier discharge reactor, *J. Ind. Eng. Chem.* 20 (2014) 2761–2768.
- [250] H.Q. Trinh, Y.S. Mok, Plasma-catalytic oxidation of acetone in annular porous monolithic ceramic-supported catalysts, *Chem. Eng. J.* 251 (2014) 199–206.
- [251] K. Saulich, S. Müller, Removal of formaldehyde by adsorption and plasma treatment of mineral adsorbent, *J. Phy. D: Appl. Phys.* 46 (2013).
- [252] D.Z. Zhao, X.S. Li, C. Shi, H.Y. Fan, A.M. Zhu, Low-concentration formaldehyde removal from air using a cycled storage–discharge (CSD) plasma catalytic process, *Chem. Eng. Sci.* 66 (2011) 3922–3929.
- [253] C. Klett, X. Duten, S. Tieng, S. Touchard, P. Jestin, K. Hassouni, A. Vega-Gonzalez, Acetaldehyde removal using an atmospheric non-thermal plasma combined with a packed bed: role of the adsorption process, *J. Hazard. Mater.* 279 (2014) 356–364.
- [254] D.H. Lee, T. Kim, Effect of Catalyst Deactivation on Kinetics of Plasma-Catalysis for Methanol Decomposition, *Plasma Process. Polym.* 11 (2014) 455–463.
- [255] S. Lovasico, N. Blin-Simiand, L. Magne, F. Jorand, S. Pasquiers, Experimental Study and Kinetic Modeling for Ethanol Treatment by Air Dielectric Barrier Discharges, *Plasma Chem Plasma Process* 35 (2) (2015) 279–301, <https://doi.org/10.1007/s11090-014-9601-x>.
- [256] I. Aouadi, J.-M. Tatibouët, L. Bergaoui, MnOx/TiO<sub>2</sub> Catalysts for VOCs Abatement by Coupling Non-thermal Plasma and Photocatalysis, *Plasma Chem Plasma Process* 36 (6) (2016) 1485–1499, <https://doi.org/10.1007/s11090-016-9740-3>.
- [257] H. Lee, D.H. Lee, Y.H. Song, W.C. Choi, Y.K. Park, D.H. Kim, Synergistic effect of non-thermal plasma–catalysis hybrid system on methane complete oxidation over Pd-based catalysts, *Chem. Eng. J.* 259 (2015) 761–770.
- [258] T.P. Huu, L. Sivachandiran, P. Da Costa, A. Khacef, Methane, Propene and Toluene Oxidation by Plasma-Pd/ $\gamma$ -Al<sub>2</sub>O<sub>3</sub> Hybrid Reactor: Investigation of a Synergetic Effect, *Top. Catal.* 60 (2016) 326–332.
- [259] **Tarryn Blackburn, Vladimir Demidyyuk, Sarah L. Hill, J. Christopher Whitehead, The Effect of Temperature on the Plasma-Catalytic Destruction of Propane and Propene: A Comparison with Thermal Catalysis, *Plasma Chem Plasma Process* 29 (6) (2009) 411–419, <https://doi.org/10.1007/s11090-009-9189-8>.**
- [260] J. Tang, W. Zhao, Y. Duan, In-Depth Study on Propane-Air Combustion Enhancement With Dielectric Barrier Discharge, *IEEE T. Plasma Sci.* 38 (2010) 3272–3281.
- [261] P.V. Julien Jarrige, Plasma-enhanced catalysis of propane and isopropyl alcohol at ambient temperature on a MnO<sub>2</sub>-based catalyst, *Appl. Catal. B: Environ.* 90 (2009) 74–82.
- [262] C. Trionfetti, A. Ağiral, J.G.E. Gardeniens, L. Lefteris, K. Seshan, Oxidative Conversion of Propane in a Microreactor in the Presence of Plasma over MgO-Based Catalysts An Experimental Study, *J. Phys. Chem. C* 112 (2008) 4267–4274.
- [263] **Olivier Aubry, Jean-Marie Cormier, Improvement of the Diluted Propane Efficiency Treatment Using a Non-thermal Plasma, *Plasma Chem Plasma Process* 29 (1) (2009) 13–25, <https://doi.org/10.1007/s11090-008-9161-z>.**
- [264] A. Ağiral, C. Trionfetti, L. Lefteris, K. Seshan, J.G.E. Gardeniens, Propane Conversion at Ambient Temperatures C-C and C-H Bond Activation Using Cold Plasma in a Microreactor, *Chem. Eng. Technol.* 31 (2008) 1116–1123.
- [265] Q.H. Trinh, S.B. Lee, Y.S. Mok, Removal of ethylene from air stream by adsorption and plasma-catalytic oxidation using silver-based bimetallic catalysts supported on zeolite, *J. Hazard. Mater.* 285 (2015) 525–534.
- [266] T. Pham, H. Bui, A. Khacef, Oxidation of propene from air by atmospheric plasma-catalytic hybrid system, *J. Serbian Chem. Soc.* 83 (2018) 641–649.
- [267] V. Gaikwad, E. Kennedy, J. Mackie, C. Holdsworth, S. Molloy, S. Kundu, M. Stockenhuber, B. Długogorski, Reaction of dichloromethane under non-oxidative conditions in a dielectric barrier discharge reactor and characterisation of the resultant polymer, *Chem. Eng. J.* 290 (2016) 499–506.
- [268] Z.A. Allah, J.C. Whitehead, P. Martin, Remediation of dichloromethane (CH<sub>2</sub>Cl<sub>2</sub>) using non-thermal, atmospheric pressure plasma generated in a packed-bed reactor, *Environ. Sci. Technol.* 48 (2014) 558–565.
- [269] A.E. Wallis, J.C. Whitehead, K. Zhang, The removal of dichloromethane from atmospheric pressure nitrogen gas streams using plasma-assisted catalysis, *Appl. Catal. B: Environ.* 74 (2007) 111–116.
- [270] A.E. Wallis, J.C. Whitehead, K. Zhang, The removal of dichloromethane from atmospheric pressure air streams using plasma-assisted catalysis, *Appl. Catal. B: Environ.* 72 (2007) 282–288.
- [271] C. Fitzsimmons, F. Ismail, J.C. Whitehead, J.J. Wilman, The Chemistry of Dichloromethane Destruction in Atmospheric-Pressure Gas Streams by a Dielectric Packed-Bed Plasma Reactor, *J. Phys. Chem. A* 104 (2000) 6032–6038.
- [272] B. Ulejczyk, Decomposition of Halocarbons in the Pulsed Dielectric Barrier Discharge, International Conference on Optimization of Electrical & Electronic Equipment (2014) 1053–1059.
- [273] **K. Krawczyk, B. Ulejczyk, H.K. Song, A. Lamenta, B. Paluch, K. Schmidt-Szałowski, Plasma-catalytic Reactor for Decomposition of Chlorinated Hydrocarbons, *Plasma Chem Plasma Process* 29 (1) (2009) 27–41, <https://doi.org/10.1007/s11090-008-9159-6>.**
- [274] A.A. Gushchin, V.I. Grinevich, T.V. Izvekova, E.Yu. Kvitkova, K.A. Tyukanova, V.V. Rybki, The Destruction of Carbon Tetrachloride Dissolved in Water in a Dielectric Barrier Discharge in Oxygen, *Plasma Chem, Plasma P.*, 2019.
- [275] L. Jiang, G. Nie, R. Zhu, J. Wang, J. Chen, Y. Mao, Z. Cheng, W.A. Anderson, Efficient degradation of chlorobenzene in a non-thermal plasma catalytic reactor supported on CeO<sub>2</sub>/HZSM-5 catalysts, *J. Environ. Sci. (China)* 55 (2017) 266–273.
- [276] F.G. Shahrna, A. Bahrami, I. Alimohammadi, R. Yarahmadi, B. Jaleh, M. Gandomi, H. Ebrahim, K.A. Abedi, Chlorobenzene degradation by non-thermal plasma combined with EG-TiO<sub>2</sub>/ZnO as a photocatalyst: Effect of photocatalyst on CO<sub>2</sub> selectivity and byproducts reduction, *J. Hazard. Mater.* 324 (2017) 544–553.
- [277] D.H. Kim, Y.S. Mok, S.B. Lee, Effect of temperature on the decomposition of trifluoromethane in a dielectric barrier discharge reactor, *Thin Solid Films* 519 (2011) 6960–6963.
- [278] D.B. Nguyen, W.G. Lee, Effects of ambient gas on cold atmospheric plasma discharge in the decomposition of trifluoromethane, *RSC Adv.* 6 (2016) 26505–26513.
- [279] D.H. Kim, Y.S. Mok, S.B. Lee, S.M. Shin, Nonthermal Plasma Destruction of Trifluoromethane Using a Dielectric- Packed Bed Reactor, *J. Adv. Oxid. Technol.* 13 (2010) 36–42.
- [280] S. Sultana, A.M. Vandenbroucke, M. Mora, C. Jiménez-Sanchidrián, F.J. Romero-Salguero, C. Leys, N. De Geyter, R. Morent, Post plasma-catalysis for trichloroethylene decomposition over CeO<sub>2</sub> catalyst: synergistic effect and stability test, *Appl. Catal. B: Environ.* 253 (2019) 49–59.
- [281] A.M. Vandenbroucke, M.T. Nguyen Dinh, N. Nuns, J.M. Giraudon, N. De Geyter, C. Leys, J.F. Lamonier, R. Morent, Combination of non-thermal plasma and Pd/LaMnO<sub>3</sub> for dilute trichloroethylene abatement, *Chem. Eng. J.* 283 (2016) 668–675.
- [282] M.T. Nguyen Dinh, J.M. Giraudon, A.M. Vandenbroucke, R. Morent, N. De Geyter, J.F. Lamonier, Manganese oxide octahedral molecular sieve K-OMS-2 as catalyst in post plasma-catalysis for trichloroethylene degradation in humid air, *J. Hazard. Mater.* 314 (2016) 88–94.
- [283] M.T.N. Dinh, J.M. Giraudon, A.M. Vandenbroucke, R. Morent, N. De Geyter, J.F. Lamonier, Post plasma-catalysis for total oxidation of trichloroethylene over Ce–Mn based oxides synthesized by a modified “redox-precipitation route”, *Appl. Catal. B: Environ.* 172–173 (2015) 65–72.
- [284] S. Sultana, Z. Ye, S.K.P. Veerapandian, A. Löfberg, N. De Geyter, R. Morent, J.-M. Giraudon, J.-F. Lamonier, Synthesis and catalytic performances of K-OMS-2, Fe/K-OMS-2 and Fe-K-OMS-2 in post plasma-catalysis for dilute TCE abatement, *Cataly. Today* 307 (2018) 20–28.
- [285] A.M. Vandenbroucke, M. Mora, C. Jiménez-Sanchidrián, F.J. Romero-Salguero, N. De Geyter, C. Leys, R. Morent, TCE abatement with a plasma-catalytic combined system using MnO<sub>2</sub> as catalyst, *Appl. Catal. B: Environ.* 156–157 (2014) 94–100.
- [286] F. Holzer, F.D. Kopinke, U. Roland, Non-thermal plasma treatment for the elimination of odorous compounds from exhaust air from cooking processes, *Chem. Eng. J.* 334 (2018) 1988–1995.
- [287] J. Chen, J. Yang, H. Pan, Q. Su, Y. Liu, Y. Shi, Abatement of malodorants from pesticide factory in dielectric barrier discharges, *J. Hazard. Mater.* 177 (2010) 908–913.
- [288] T. Kuwahara, M. Okubo, T. Kuroki, H. Kametaka, T. Yamamoto, Odor removal characteristics of a laminated film-electrode packed-bed nonthermal plasma reactor, *Sensors (Basel)* 11 (2011) 5529–5542.
- [289] C.W. Park, J.H. Byeon, K.Y. Yoon, J.H. Park, J. Hwang, Simultaneous removal of odors, airborne particles, and bioaerosols in a municipal composting facility by dielectric barrier discharge, *Sep. Purif. Technol.* 77 (2011) 87–93.
- [290] M. Hohr, B. Brandenburg, H. Grosch, S. Weinmann, B. Hansel, Plasma Supported Odour Removal from Waste Air in Water Treatment Plants: An Industrial Case Study, *Aerosol Air Qual. Res.* 14 (2014) 697–707.
- [291] J.S. Youn, J. Bae, S. Park, Y.K. Park, Plasma-assisted oxidation of toluene over Fe/zeolite catalyst in DBD reactor using adsorption/desorption system, *Catal. Commun.* 113 (2018) 36–40.
- [292] Y.F. Guo, D.Q. Ye, K.F. Chen, J.C. He, W.L. Chen, Toluene decomposition using a wire-plate dielectric barrier discharge reactor with manganese oxide catalyst in situ, *J. Mol. Catal. A: Chem.* 245 (2006) 93–100.
- [293] M. Lu, R. Huang, J. Wu, M. Fu, L. Chen, D. Ye, On the performance and mechanisms of toluene removal by FeOx/SBA-15-assisted non-thermal plasma at atmospheric pressure and room temperature, *Cataly. Today* 242 (2015) 274–286.
- [294] J. Chen, Z. Xie, J. Tang, J. Zhou, X. Lu, H. Zhao, Oxidation of toluene by dielectric barrier discharge with photo-catalytic electrode, *Chem. Eng. J.* 284 (2016)

- 166–173.
- [295] Z. Falkenstein, J.J. Coogan, Microdischarge behaviour in the silent discharge of nitrogen - oxygen and water - air mixtures, *J. Phys. D: Appl. Phys.* 30 (1997) 817–825.
- [296] H.P. Nguyen, M.J. Park, S.B. Kim, H.J. Kim, L.J. Baik, Y.M. Jo, Effective dielectric barrier discharge reactor operation for decomposition of volatile organic compounds, *J. Clean. Prod.* 198 (2018) 1232–1238.
- [297] Chengzhu Zhu, Ying Liu, Jun Lu, Zhe Yang, Yunxia Li, Tianhu Chen, Decomposition of Ethanethiol Using Dielectric Barrier Discharge Combined with 185 nm UV-Light Technique, *Plasma Chem Plasma Process* 35 (2) (2015) 355–364, <https://doi.org/10.1007/s11090-014-9609-2>.
- [298] H. Huang, D. Ye, D.Y.C. Leung, Abatement of Toluene in the Plasma-Driven Catalysis: Mechanism and Reaction Kinetics, *IEEE T. Plasma Sci.* 39 (2011) 877–882.
- [299] J. Wu, Q. Xia, H. Wang, Z. Li, Catalytic performance of plasma catalysis system with nickel oxide catalysts on different supports for toluene removal: Effect of water vapor, *Appl. Catal. B: Environ.* 156–157 (2014) 265–272.
- [300] X. Fan, T. Zhu, Y. Wan, X. Yan, Effects of humidity on the plasma-catalytic removal of low-concentration BTX in air, *J. Hazard. Mater.* 180 (2010) 616–621.
- [301] Z. Ye, Y. Zhang, P. Li, L. Yang, R. Zhang, H. Hou, Feasibility of destruction of gaseous benzene with dielectric barrier discharge, *J. Hazard. Mater.* 156 (2008) 356–364.
- [302] A.A. Assadi, A. Bouzaza, I. Soutrel, P. Petit, K. Medimagh, D. Wolbert, A study of pollution removal in exhaust gases from animal quartering centers by combining photocatalysis with surface discharge plasma: From pilot to industrial scale, *Chem. Eng. Process.* 111 (2017) 1–6.
- [303] P. Liang, W. Jiang, L. Zhang, J. Wu, J. Zhang, D. Yang, Experimental studies of removing typical VOCs by dielectric barrier discharge reactor of different sizes, *Process Saf. Environ.* 94 (2015) 380–384.
- [304] L.M. Martini, G. Collier, M. Schiavon, A. Cernuto, M. Ragazzi, G. Dilecce, P. Tosi, Non-thermal plasma in waste composting facilities: From a laboratory-scale experiment to a scaled-up economic model, *J. Clean. Prod.* 230 (2019) 230–240.
- [305] M. Schmidt, I. Jögi, M. Holub, R. Brandenburg, Non-thermal plasma based decomposition of volatile organic compounds in industrial exhaust gases, *Int. J. Environ. Sci. Te.* 12 (2015) 3745–3754.



# NON THERMAL PLASMA AND VIRUS

PAPER

## Inactivation of airborne viruses using a packed bed non-thermal plasma reactor

To cite this article: T Xia *et al* 2019 *J. Phys. D: Appl. Phys.* **52** 255201

View the [article online](#) for updates and enhancements.

### Recent citations

- [A short review of bioaerosol emissions from gas bioreactors: Health threats, influencing factors and control technologies](#)  
Xu-Rui Hu *et al*
- [Factors influencing the antimicrobial efficacy of Dielectric Barrier Discharge \(DBD\) Atmospheric Cold Plasma \(ACP\) in food processing applications](#)  
Ehsan Feizollahi *et al*
- [Rapid inactivation of airborne porcine reproductive and respiratory syndrome virus using an atmospheric pressure air plasma](#)  
Gaurav Nayak *et al*



**IOP | ebooks™**

Bringing together innovative digital publishing with leading authors from the global scientific community.

Start exploring the collection—download the first chapter of every title for free.

# Inactivation of airborne viruses using a packed bed non-thermal plasma reactor

T Xia<sup>1,3</sup>, A Kleinheksel<sup>1</sup>, E M Lee<sup>2</sup>, Z Qiao<sup>1</sup>, K R Wigginton<sup>1</sup> and H L Clack<sup>1</sup>

<sup>1</sup> Department of Civil and Environmental Engineering, University of Michigan, Ann Arbor, MI, United States of America

<sup>2</sup> Department of Mechanical, Materials, and Aerospace Engineering, Illinois Institute of Technology, Chicago, IL, United States of America

E-mail: [xiatian@umich.edu](mailto:xiatian@umich.edu)

Received 28 November 2018, revised 25 March 2019

Accepted for publication 28 March 2019

Published 23 April 2019



CrossMark

## Abstract

Outbreaks of airborne infectious diseases such as measles or severe acute respiratory syndrome can cause significant public alarm. Where ventilation systems facilitate disease transmission to humans or animals, there exists a need for control measures that provide effective protection while imposing minimal pressure differential. In the present study, viral aerosols in an airstream were subjected to non-thermal plasma (NTP) exposure within a packed-bed dielectric barrier discharge reactor. Comparisons of plaque assays before and after NTP treatment found exponentially increasing inactivation of aerosolized MS2 phage with increasing applied voltage. At 30 kV and an air flow rate of 170 standard liters per minute, a greater than 2.3 log reduction of infective virus was achieved across the reactor. This reduction represented ~2 log of the MS2 inactivated and ~0.35 log physically removed in the packed bed. Increasing the air flow rate from 170 to 330 liters per minute did not significantly impact virus inactivation effectiveness. Activated carbon-based ozone filters greatly reduced residual ozone, in some cases down to background levels, while adding less than 20 Pa pressure differential to the 45 Pa differential pressure across the packed bed at the flow rate of 170 standard liters per minute.

Keywords: non-thermal plasma, bioaerosol inactivation, bacteriophage MS2, ozone, plaque assay, qPCR

Supplementary material for this article is available [online](#)

(Some figures may appear in colour only in the online journal)

## Introduction

Airborne infectious disease outbreaks such as measles, tuberculosis, and severe acute respiratory syndrome (SARS) can cause risk of infection by the essential and involuntary action of respiration. Airborne disease transmission, the processes governing it, and the development of protective measures against it, are less understood than transmission via water, food, arthropod vectors, and direct contact with infected individuals. Disease transmission among humans and animals often involves either direct contact with an infected individual or transport across

very short distances; however, pathogen transmission over longer distances can also occur. The SARS outbreak within the Amoy Gardens housing complex in Hong Kong [1] was spread between apartments by sewer main gases drawn in by improperly sized ventilation fans and poorly maintained drains.

Livestock diseases such as Newcastle disease, avian influenza, hoof-and-mouth disease, porcine reproductive and respiratory syndrome (PRRS), and African swine flu are potential threats to global food security. In pork and poultry production, biosecurity measures for preventing the introduction of pathogens into animal confinement buildings primarily protect against disease spread through direct contact between animals and from pathogen-contaminated surfaces. PRRS and avian

and porcine influenza are two examples of high impact diseases for which biosecurity measures have been implemented to prevent airborne transmission. The virus that causes PRRS is understood to survive transmission through the atmosphere in greater numbers when atmospheric conditions are cool, damp, or cloudy [2]. Long-term changes in climate and their influences on infectious disease outbreaks vary by route of transmission and are highly uncertain [3]. While increasing vector populations with increasing annual average temperature and precipitation could increase vector-borne transmission, the influences of changing meteorological conditions on airborne transmission of pathogens are unclear.

In contexts where humans or animals move freely, the potential for disease transmission through direct contact is greater, reducing the importance of airborne transmission and greatly limiting the utility of airborne pathogen inactivation. However, where airborne transmission is or is suspected of being an important transmission route, few mitigation technologies exist. Disinfection by UV irradiation requires UV doses involving a combination of radiative fluxes and exposure times that have been established [4], which are difficult to implement in air. Upper-room UV irradiation relies on natural air circulation patterns within a room to transport airborne pathogens into the illumination zone of a wall-mounted, upward facing UV fixture near the ceiling. Upper room UV was proven effective in reducing TB transmission in hospital wards [5] and rubella transmission within army barracks [6]. UV germicidal irradiation (UVGI) directs UV radiation onto conventional particulate filters within ventilation systems to inactivate bacteria and viruses captured on the filter surfaces [7]; however, viruses and bacteria that migrate into the filter media or that are shielded from the UV source as subsequent particles are collected, are inactivated with lower efficiencies [7]. The US EPA concludes that there is insufficient evidence, and no standard test procedures, for assessing UVGI performance and that UVGI provides virtually no additional protection over the use of conventional HEPA filtration alone [8]. Conventional filtration presents several drawbacks, including the low fluid permeability needed for high particle collection efficiency, which inherently increases the differential pressure across the filter and promotes infiltration of untreated air into indoor spaces at partial vacuum. In buildings not constructed to an air-tight standard, this can lead to high costs of building reconstruction and retrofit.

Two factors govern the potential for disease transmission of airborne pathogens such as viruses and bacteria: aerosol transport and aerosol infectivity [9]. UV radiation alone only addresses aerosol infectivity and particle filtration only addresses aerosol transport. Unlike filtration and UV irradiation, non-thermal plasmas (NTPs) can address *both* transport (by charge-driven filtration) and infectivity (by reaction with reactive plasma species) of airborne pathogens. NTP is a result of electrical discharges within a neutral gas under atmospheric conditions and mainly consists of electrons, ions, and radicals. Unlike thermal plasma, where all constituents are in thermal equilibrium, a NTP in comparison is always in a state of non-equilibrium because the electrons with very light masses can reach higher temperatures ( $10^4$ – $2.5 \times 10^5$  K) and attain higher kinetic energy (1–20 eV) than the rest of

the NTP constituents, which are heavier and at lower temperatures [10]. On these bases, an NTP is also known as non-equilibrium plasma or cold plasma. A commonly applied NTP reactor type is the dielectric barrier discharge (DBD) reactor. DBD or silent discharge refers to the electrical discharge through a dielectric barrier, such as glass, quartz, or alumina. A high voltage AC source is commonly used in a DBD reactor, because the changing polarity of AC is essential to sustain the electrical discharge in a DBD reactor. The dominant electrical discharge mode in a DBD reactor is microdischarge, which is in a form of filaments with nanosecond lifespan. When the microdischarge reaches a dielectric barrier, the dielectric surface allows for the spreading and accumulation of the charges and thus reduces the electric field until the field is completely quenched. The use of an AC source repeats the cycle by generating microdischarge with a different electrical polarity. In studying the effectiveness of removing air pollutants such as methyl tert-butyl ether (MTBE) by NTP, Holzer *et al* [11] utilized a gaseous plasma generated by a DBD reactor using different dielectric barriers including glass,  $\text{Al}_2\text{O}_3$ , and  $\text{TiO}_2$ . Kuwahara *et al* [12] developed a DBD reactor using polyester-laminated electrodes to evaluate the removal characteristics of odorous compounds, including  $\text{NH}_3$  and  $\text{NH}_3$  mixed with  $\text{CH}_3\text{CHO}$ , by NTP. In studying oil mist-to-gas conversion, Park *et al* [13] developed a DBD reactor using thin copper electrodes (0.05 mm thickness) where each electrode was sandwiched in between by two dielectric plates made of alumina (1 mm thickness).

A packed-bed reactor provides a more efficient way of treating trace air pollutants by adding pellets between the electrodes in a corona reactor or a DBD reactor. A typical air pollutant has a concentration in the range of parts per million by volume (ppmv), so direct interactions between the electrons and air pollutants are usually negligible under ambient conditions [10]. In a packed-bed reactor, the electron-impact reactions serve as the main plasma chemistry for air pollutant decomposition [14]. By packing the pellets, electron generation takes place through partial discharges at the pellet contact points within a packed-bed reactor. More specifically, an external electric field applied between the pellets and the electrodes enables polarization, which in turn induces partial discharges and subsequently the electron-impact reactions. While a packed-bed arrangement can provide evenly distributed flows, it can also lead to a higher pressure drop across the packed-bed. Perovskite pellets, such as  $\text{BaTiO}_3$  and  $\text{Al}_2\text{O}_3$  are commonly used dielectric materials for packed-bed reactors. The addition of catalytically active materials can further improve the selectivity of a packed-bed reactor. Mizuno *et al* [15, 16] discovered that a ferroelectric pellet packed-bed reactor was not only capable of collecting particles, but also destroying yeast cells. In studying organic solvents (e.g. MTBE, toluene, and acetone), Holzer *et al* [11] evaluated three packed-bed materials (i.e. glass beads,  $\text{BaTiO}_3$ , and  $\text{PbZrO}_3$ – $\text{PbTiO}_3$ ) and one catalyst (i.e.  $\text{LaCoO}_3$ ) using various cylindrical DBD reactors designs, which showed that the ferroelectric packed-bed reactor using  $\text{BaTiO}_3$  pellets significantly increased the conversion of MTBE and toluene to  $\text{CO}_x$ . Kuwahara *et al* [12] used a ferroelectric packed-bed reactor

to study the decomposition of odorous compounds (i.e. NH<sub>3</sub>) by adding BaTiO<sub>3</sub> pellets to the previously developed DBD reactor, which used polyester-laminated electrodes. The results showed that the DBD reactor with ferroelectric packed-bed pellets could decompose NH<sub>3</sub> at a much faster rate than the DBD reactor alone.

Researchers [17, 18] have reported reductions in infective airborne pathogen concentrations as a result of NTP treatment, results that included confounding effects of extended exposure of viral aerosols to ozone [17] or loss of viral aerosols by charge-driven filtration [18]. In one study, a DBD NTP reactor with 10 s plasma exposure and a very high air flow rate (25 l s<sup>-1</sup>) resulted in 97% *Escherichia coli* inactivation [17]. The research group found that the synergetic action of short-living plasma agents, such as hydroxyl radicals, and plasma-generated ozone, achieved the previously measured 97% in-flight inactivation of aerosolized *E. coli* [19]. Another research group constructed a 12 mm diameter DBD NTP device and reported >95% inactivation of bacteria and 85%–98% inactivation of fungal species with a 24 W reactor energy output and a flow rate of 28.3 LPM (liters per minute) [20]. That same team examined NTP inactivation of MS2 and reported over 95% MS2 airstream inactivation with a 28 W reactor energy output at 12.5 LPM flow rate [18]. None of these research, however, examined the airstream inactivation performance of a reactor with a pack-bed feature.

In this study, we describe the development and performance of a packed-bed NTP in-flight airstream disinfection process. A DBD NTP reactor was constructed to treat an air stream seeded with viral aerosols. Aerosols of bacteriophage MS2 were generated by the evaporation of fine mists produced by ultrasonic atomization. Plaque assay and quantitative polymerase chain reaction (qPCR) analyses were conducted to determine the abundance of infective and total MS2 aerosols, respectively, in the pre- and post-treatment samples. Ultimately, the ability to remove residual ozone with carbon filters was assessed. A maximum of 2.3 log reduction of infective MS2 virus was achieved by the reactor, demonstrating NTP is a viable technology for in-flight disinfection and the prevention of airborne virus transmission.

## Materials and methods

### Experimental setup

The experimental apparatus (figure 1) for NTP inactivation of viral aerosols includes: (1) an induced draft (ID) fan, (2) a DBD reactor, (3) an aerosol generator, (4) a digital oscilloscope, (5) a high voltage amplifier, and (6) a digital function generator. The aerosol generator is a modified consumer-grade cool-mist humidifier (Vicks V5100-N) that piezoelectrically atomizes virus buffer solution containing MS2, a single-stranded RNA bacteriophage. A 10.2 cm (4-inch) ID fan at the end of the apparatus draws ambient air (25%–36% RH) into a flexible duct (8.9 cm (3.5-inch) ID and 4 m (13-ft) length), where mixing occurs between the air and the droplets, allowing for droplet evaporation and thus bioaerosol generation. The droplet evaporation process is further enhanced by

the addition of a facility-supplied stream of dry compressed air (<10% RH; figure 1). The DBD reactor is powered by one of the two AC voltage amplifiers, namely a variable 0 to 20 kV (peak-to-peak) high voltage amplifier (Trek Model-610E) and a 30 kV neon transformer (France 15030 P5G-2UE ServiceMaster). The variable 0 to 20 kV high voltage amplifier is coupled with a digital function generator (BK Precision Model-4052), which outputs 60 Hz sinusoidal AC voltage. The amplifier can output applied voltage (*U*) signals at 1 V/1000 V and two current (*I*) signals, total current and return current, at 1 V/200 μA, which can be monitored directly by a digital oscilloscope (BK Precision Model-2190D). For the 30 kV neon transformer, a high voltage probe (Cal Test Electronics CT2700, 1 V/1000 V) and a Pearson current coil (Model 6585, 1 V/1A) are connected to one of the power supply's high voltage electrodes (the schematic is illustrated in figure S1 in the supplementary information, available online ([stacks.iop.org/JPhysD/52/255201/mmedia](http://stacks.iop.org/JPhysD/52/255201/mmedia))), whose output signals are monitored by the digital oscilloscope. The power (*P*) of the reactor was therefore calculated according to the equation:

$$P = \frac{1}{T} \int_T U \times Idt \quad (1)$$

where *T* is the period of the AC voltage. A honeycomb-structured ozone filter (figure 1; Burnett Process Inc. BP-4810) is located downstream of the reactor to remove ozone from the exhaust. Two impingers installed upstream and downstream (figure 1) of the reactor enabled the quantification of virus inactivation by the NTP reactor.

### NTP and reactor design

The NTP reactor developed in the present study utilizes the characteristics of DBD and packed-bed discharge for the application of viral aerosol inactivation. Figure 2 is a close-up schematic of the DBD packed-bed reactor. The reactor is composed of one larger Plexiglas tube (10.2 cm (4-inch) OD, 9.5 cm (3.75-inch) ID, 20.3 cm (8-inch) length) and two smaller tubes (8.9 cm (3.5-inch) OD, 7.6 cm (3-inch) ID, 30.5 cm (12-inch) length). The smaller tubes slide freely relative to the larger tube due to a clearance of 0.3 cm (0.125-inch). Two rubber O-rings, which sit in the grooves on the OD of the smaller tube permit an air-tight sliding mechanism. As indicated in figure 2, a circular perforated brass plate is installed at the end of each sliding tube to serve as the ground electrode and to evenly distribute the inlet and outlet flow of the reactor. The design of the sliding electrode allows for packed bed depth adjustment ranging between 0.6 and 12.7 cm (0.25 and 6 inches). A brass ring (0.9 mm (0.035-inch) thickness, 2.5 cm (1-inch) width) adhered to the OD of the larger Plexiglas tube serves as the high voltage electrode for the AC high voltage supply. Two flow plugs made of styrofoam (6.35 cm (2.5-inch) OD) are positioned at the center of the reactor to direct the airflow with viral aerosols through an annular region in which the plasma is concentrated (figure 2). The DBD reactor utilizes the microdischarge generated through a dielectric barrier made of Plexiglas. The packed-bed, consisting of 500 inert borosilicate glass beads (0.6 cm (0.25-inch) diameter), further

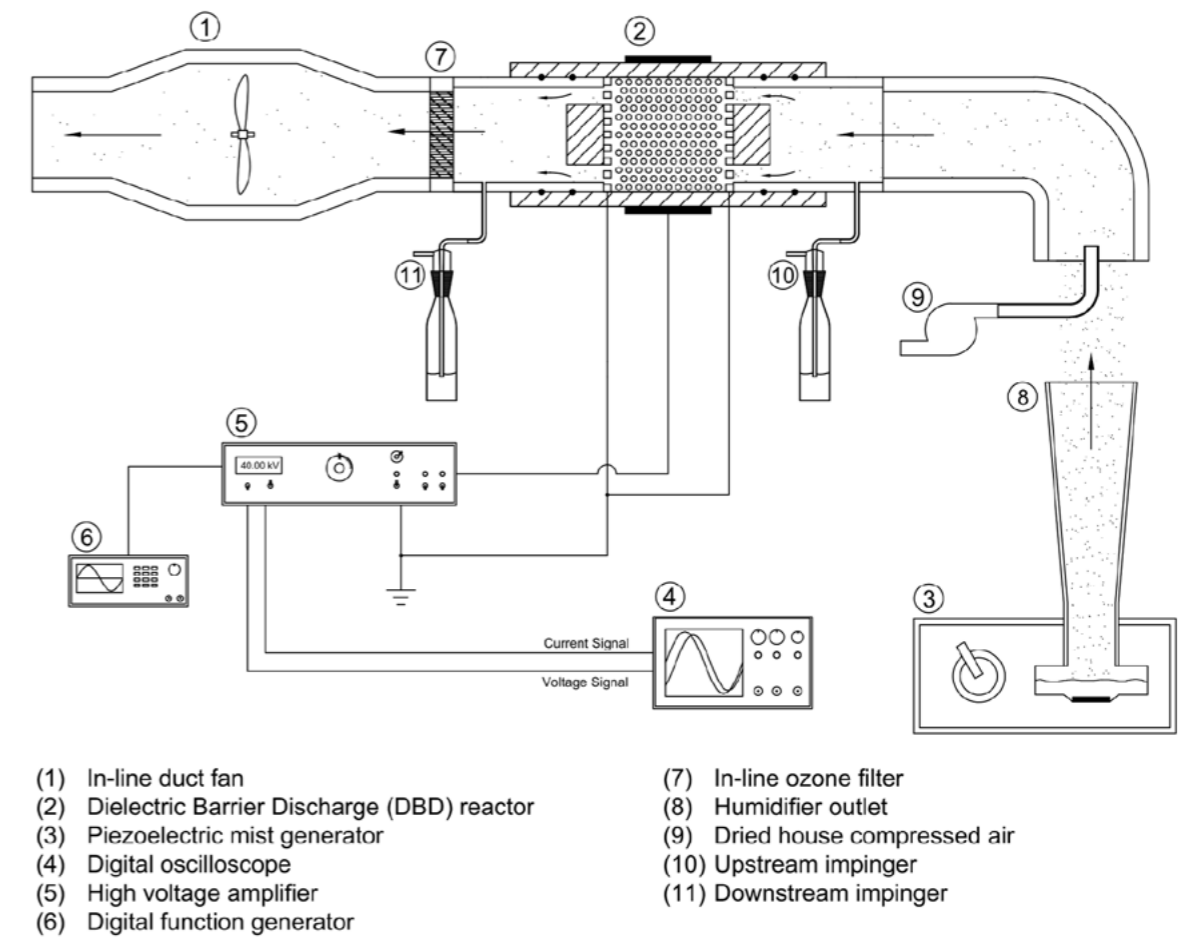


Figure 1. Experimental setup for the inactivation of viral aerosols with the 0–20kV variable amplifier.

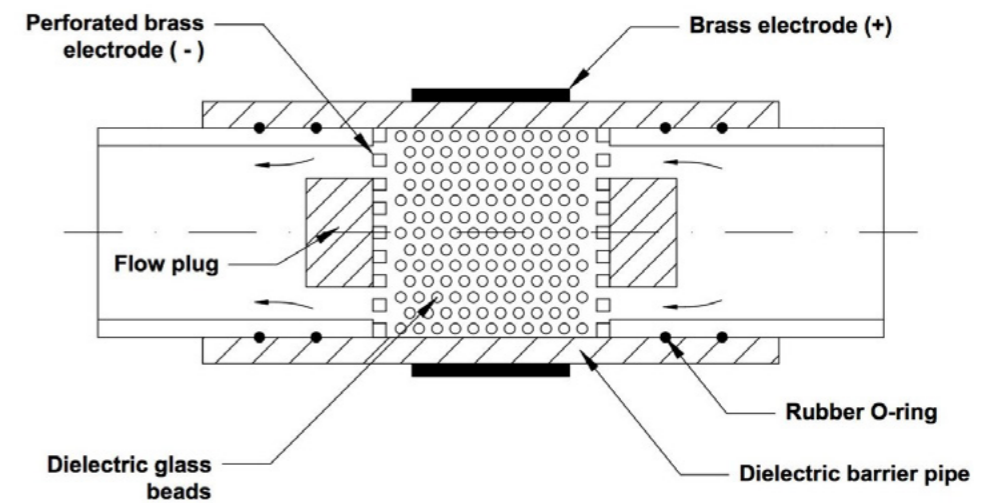


Figure 2. Schematic of the DBD packed-bed reactor.

enhances the microdischarge by partial discharges at the contact points between the glass beads for effective electron-viral aerosol collisions and inactivation process.

### Experimental procedure

During the virus inactivation tests, a consumer-grade ultrasonic humidifier was used to generate MS2 viral aerosols from

the original virus solution. Each inactivation test involved adding 300 ml (for a 60 min test) or 200 ml (for a 30 min test) of MS2 solution consisting of  $\sim 1 \times 10^8$  pfu ml<sup>-1</sup> in phosphate-buffered saline (PBS; 0.78 g NaH<sub>2</sub>PO<sub>4</sub>/L, 0.58 g NaCl/L, pH of 7.5) into the ultrasonic humidifier reservoir. The humidifier was set to built-in power level 2 (labeled as H2) and the atomization rate was approximately 117 ml h<sup>-1</sup> over a 30 min experimental period [21]. The air flow rate through

the sampling train was maintained by the ID fan with a viable transformer (Staco Energy 3PN221B). In each test, the ID fan and humidifier were turned on for five minutes until reaching steady state. Then the packed-bed NTP reactor was activated by the selected high voltage supply. An electric vacuum pump (McMaster-Carr model #4176K11) was turned on to draw samples from the air stream near the inner wall of the pipe through the impingers (ACE Glass 7533-13) upstream and downstream of the reactor at 1 LPM, leading to collection of MS2 aerosols in the 20 ml impinger collection fluid (PBS).

For inactivation tests with the reactor powered by the 0–20 kV variable amplifier, the sampling time was 30 min. For tests with the 30 kV transformer, the sampling time was 60 min in order to collect a higher number of viable viruses within the impinger installed downstream of the reactor (figure 1). Virus samples were also collected directly from the ultrasonic humidifier reservoir before each trial. Plaque assays and reverse transcriptase quantitative polymerase chain reaction (RT-qPCR) assays, both described in detail below, were performed on each sample to determine the concentration of infectious MS2 plaque forming units (pfu/ml) and the concentration of MS2 genome copies (gc/ml) in the PBS collecting solution. To compare the humidifier reservoir samples with impinger samples, all of the acquired infectious MS2 concentrations in aqueous PBS solutions were converted to concentrations in the air stream using the following two mass balance equations:

$$C_{8,air} = \dot{V} \times \frac{C_3}{\dot{Q}_{air}} \quad (2)$$

$$C_{10,air} = \frac{V_{impinger} C_{10}}{\dot{Q}_{sample} t_{sample}}; C_{11,air} = \frac{V_{impinger} C_{11}}{\dot{Q}_{sample} t_{sample}} \quad (3)$$

where  $\dot{V}$  is the average ultrasonic atomization rate ( $117 \text{ ml h}^{-1}$ ),  $C_3$  is the measured infective MS2 concentrations in samples acquired from the humidifier reservoir (position 3 in figure 1) immediately before each test.  $C_{10}$  and  $C_{11}$  are the infective MS2 concentrations in the impingers (positions 10 and 11 in figure 1 respectively).  $C_{8,air}$ ,  $C_{10,air}$  and  $C_{11,air}$  are converted infectious MS2 concentrations in the airstream at the humidifier outlet and at the upstream and downstream sampling points, respectively.  $\dot{Q}_{air}$  is the air flow rate through the apparatus,  $V_{impinger}$  is the volume of PBS in each of the impingers (20 ml), and  $\dot{Q}_{sample}$  and  $t_{sample}$  are, respectively, air flow rates through the impingers (1 LPM) and the standard elapsed time allowed for sampling (30 or 60 min). It should be noted that the MS2 inactivation in the reservoir during atomization is not considered in the calculation of  $C_{8,air}$ , so the calculated results should be good approximations rather than true values. According to our previous study, there may be a 0.3 log reduction of viable MS2 concentration in the humidifier reservoir during the 30 min test, but this inactivation would not affect the estimation of the NTP reactor inactivation efficiency as long as viable MS2 are measured in the upstream impinger [21]. Similarly, total virus genome concentrations (both infective and inactivated) were assessed with qPCR and measured as genome copies per milliliter of solution (gc/ml), corrected with equations (2) and (3), and reported as genome copies per liter of air.

**MS2 propagation and enumeration.** Bacteriophage MS2 (ATCC 15597-B1) and its corresponding *E. coli* host ATCC 15597 was purchased from American Type Culture Collection (ATCC). MS2 was propagated and assayed in its *E. coli* host using previously published methods [22, 23]. The virus stocks were purified using an Econo Fast Protein Liquid Chromatography system (Bio-Rad, USA) with a HiPrep Sephacryl S-400 HR column (GE, USA). The purified virus fractions were concentrated with 100 kDa Amicon ultracentrifugal filters (Millipore, USA), and finally filter-sterilized with 0.22  $\mu\text{m}$  PES membrane filters. The final MS2 stocks ( $\sim 10^{11}$  pfu  $\text{ml}^{-1}$ ) were stored in phosphate buffer (5 mM  $\text{NaH}_2\text{PO}_4$  and 10 mM NaCl, pH 7.5) at 4 °C. In the experiments, the detection limit was 10 pfu  $\text{ml}^{-1}$  since only 100  $\mu\text{l}$  of a sample was used for each plate.

**RT-qPCR.** Viral RNA was extracted from 200  $\mu\text{l}$  MS2 virus samples using Maxwell 16 Viral Total Nucleic Acid Purification Kits (Promega, Madison, WI) according to the manufacturer's instructions. Extracted RNA was eluted using 50  $\mu\text{l}$  of nuclease-free water. The forward primer (5'-CCGCTACCTT-GCCCTAAAC-3') and reverse primer (5'-GACGACAAC-CATGCCAAAC-3') were designed with the Primer3free software (<http://primer3.sourceforge.net/>) and purchased from ThermoFisher Scientific (Grand Island, NY). Extracted MS2 RNA samples and RNA standards were reverse transcribed and amplified in parallel in an Eppendorf Mastercycler ep realplex Real-time PCR System (Eppendorf, Hauppauge, NY). Each reverse transcription-qPCR reaction was run in 20  $\mu\text{l}$  of total volume comprising 10  $\mu\text{l}$  of GoTaq 1-Step Master Mix, 0.4  $\mu\text{l}$  of RT mix, 0.6  $\mu\text{l}$  each of 10  $\mu\text{M}$  forward and reverse primers, 6.4  $\mu\text{l}$  of nuclease-free water and 2  $\mu\text{l}$  of RNA sample (Promega, Madison, WI). The following thermocycling conditions were used: 15 min at 40 °C; 10 min at 95 °C; and 45 cycles of 95 °C for 15 s, 60 °C for 30 s and 72 °C for 40 s, followed by a melting ramp from 68 to 95 °C, with the temperature held for 45 s at 60 °C and for 5 s at all subsequent temperatures.

**Measurements of system performance.** During the experiment, a portable humidity/temperature pen (Traceable 4093) measured the temperature and relative humidity (RH) inside the sampling train upstream of the reactor. An insertable anemometer (Extech 407123) measured the air stream radial velocity profile  $\sim 30.5$  cm (12-inch) downstream of the reactor. The pressure drops across the packed-bed NTP reactor and the ozone filter were measured by a low-pressure differential gauge (Magnehelic 2300-0). When the reactor was powered by the 0–20 kV variable amplifier, an oscilloscope (BK Precision Model-2190D) monitored the applied voltage and current to the packed-bed NTP reactor, from which the input and discharge power can be calculated. When the reactor was powered by the fixed 30 kV transformer, the total input power consumption of the transformer was measured by an electricity power meter (P3 International P4460), and the discharge power was measured by a high voltage probe and a Pearson coil, as discussed in the experimental setup section. To ensure that collected MS2 would not be inactivated in the impinger

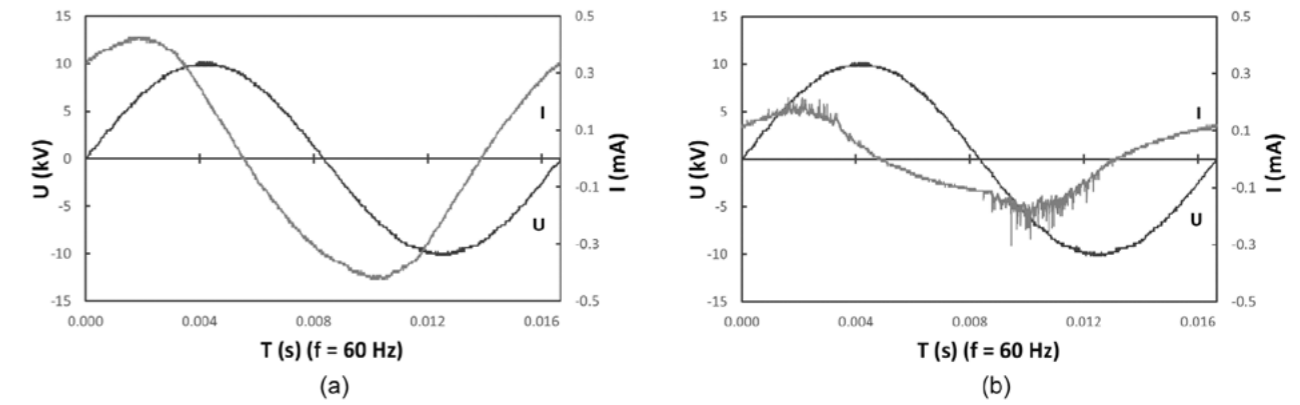


**Figure 3.** Applied voltage and (a) total current or (b) return current waveform acquired by the oscilloscope with 20 kV peak-to-peak voltage.

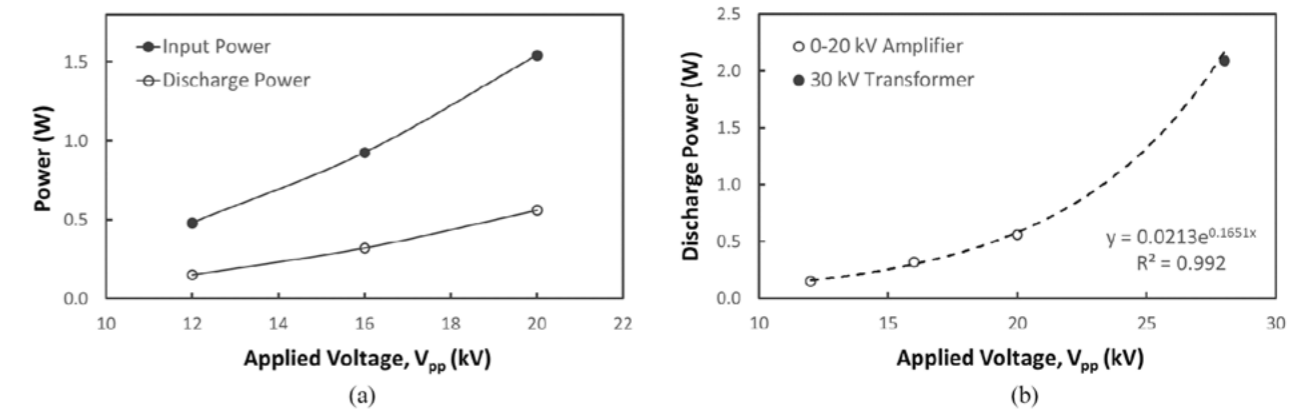


**Figure 4.** (a) Input and discharge power of the reactor at 12 kV, 16 kV and 20 kV applied voltage with the 0–20 kV variable amplifier; (b) estimated discharge power showed a strong exponential correlation with the applied voltage with both high voltage power supplies.

liquid during sampling, 20 ml of  $1 \times 10^6$  pfu  $\text{ml}^{-1}$  MS2-PBS solution was added into the downstream impinger, which was then connected to the downstream sampling port. The packed-bed NTP reactor was either inactivated or activated by the 20 kV voltage supply, and the effluent gas from the reactor was bubbled through the impinger liquid for 15, 30 and 45 min, after which the infectious MS2 concentrations in the impinger were assayed. Ozone generated by the packed-bed NTP reactor when energized had the potential to dissolve into sampling liquid in the downstream impinger and inactivate MS2 during and after sample collection. To quench the ozone in solution, 50 mM of anhydrous sodium sulfite ( $\text{Na}_2\text{SO}_3$ , Fisher Scientific BP355-500) was added into the downstream 20 ml impinger collection liquid. An ozone sensor (EcoSensors A-21ZX) measured the ozone concentration either upstream of the ozone filter (downstream of the reactor) or downstream of the filter to determine the amount of ozone generated by the packed-bed NTP reactor at various power and flow rate levels and to examine the removal efficiency of ozone by the ozone filter.

## Results and discussion

### Operating conditions

In this study, the overall air flow rate through the sampling train was estimated to be 170 LPM at 30% voltage setting

of the ID fan and 330 LPM at 60% voltage setting, by integrating the measured air velocity profile along the pipe radius. The pressure difference upstream and downstream of the NTP DBD packed bed measured at the 170 LPM flow rate was 45 Pa, a reasonably low difference due to the high porosity of the packed bed. The ozone filter was also quite porous, with a honeycomb structure that produced a pressure drop of 20 Pa at the flow rate of 170 LPM. The total pressure drop across the system was about 65 Pa at the flow rate of 170 LPM, or 0.38 Pa/LPM. It was estimated that at 170 LPM, the virus exposure time to NTP species was about 0.25 s.

Typical applied voltage and current waveforms measured by the oscilloscope are presented in figure 3, and all voltage and current waveforms at all voltage setups (12 kV, 16 kV, 20 kV and 30 kV) can be found in the supporting information. Two current waveforms were measured: the total current represented the current supplied into the system and was used to calculate input power; the return current represented the current returned to the supply from the ground electrode, and was used to calculate NTP discharge power. When applied voltage increased from 12 kV to 20 kV, the input power increased from 0.5 W to 1.5 W and the discharge power increased from 0.2 W to 0.6 W, 31%–36% of the input power (figure 4(a)). Kuwahara *et al* [12] reported similar differences (76%) between input and discharge power, and two other research reported that 20%–27% of the input power was converted to

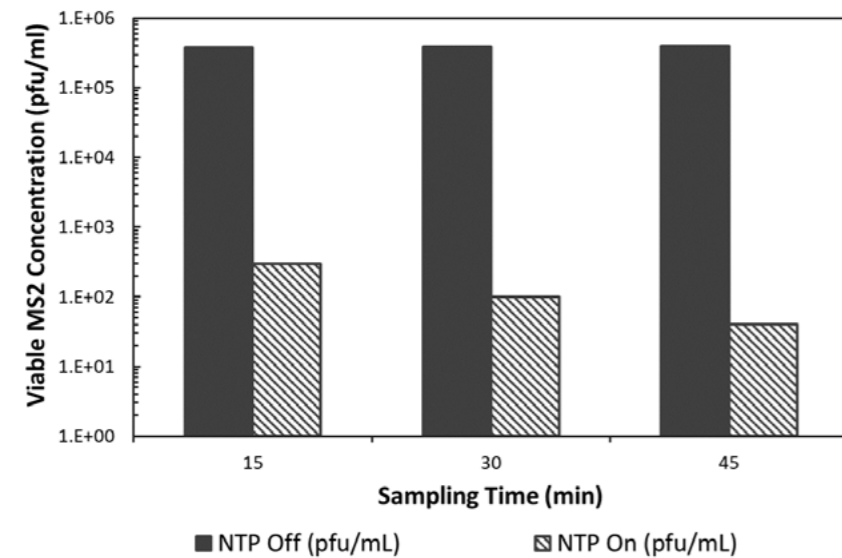


**Figure 5.** Change of infectious MS2 concentration in the downstream impinger with either ozone-free air (reactor off) or ozone-loaded air (reactor activated by 20kV) bubbling through the impinger liquid.

plasma discharge power in their NTP reactor [24, 25]. With the 0–20kV variable amplifier, the maximum discharge power in the reactor was 0.56 W (198 J m<sup>-3</sup> at 170 LPM) at 20kV. With the fixed 30kV neon transformer, the actual peak-to-peak voltage applied to the reactor was 28kV and the total input power consumption was ~21 W measured by the commercial power meter. The estimated discharge power was 2.08 W (734 J m<sup>-3</sup> at 170 LPM), 10% of the input power, according to the high voltage probe and Pearson coil measurements. The estimated discharge power showed a strong exponential correlation with the applied peak-to-peak voltage, no matter which power supply is used (figure 4(b)). In future, the V–Q Lissajous method can be applied to more accurately estimate the discharge power with both the 0–20kV variable amplifier and the 30kV neon transformer.

When ambient air was supplemented with dry compressed air, the initial temperature and RH of the air stream inside the sampling train were 20 °C and 30%, respectively. The addition of water mist from the humidifier into the air stream can induce evaporative cooling, in which the air temperature would be reduced, and the RH would be increased. According to the measurement data, at 170 LPM air flow rate and the humidifier power level 2 (H2; atomization rate of 117 ml h<sup>-1</sup>), both the temperature and RH reached steady state values of 16.5 °C and 60%, respectively, after 30 min.

Control tests were conducted during which 20ml of an MS2 solution (1 × 10<sup>6</sup> pfu ml<sup>-1</sup> in PBS) was added into the downstream impinger and the effluent gas from the reactor was bubbled through the impinger liquid. The concentration of infective viruses when the NTP reactor was off proved that bubbling ozone-free air through the impinger for 45 min did not inactivate the MS2 (figure 5). When the reactor was on, a 3 log reduction in the infective MS2 concentration was observed in the impinger solution over the first 15 min. This indicated that when the reactor was activated by 20kV, the generated ozone dissolved in the impinger liquid and inactivated the sampled MS2. As the goal of these experiments was to inactivate viruses within the reactor and not in the sampling

liquid downstream of the reactor, the ozone that dissolved in the downstream impinger liquid was quenched with 50mM of anhydrous sodium sulfite. According to the measured ozone concentration and the calculated equilibrium dissolved ozone concentration in the impinger liquid (based on Henry’s Law), the added sodium sulfite should be sufficient to quench all of the dissolved ozone during the packed-bed NTP inactivation tests. Control experiments proved that the sodium sulfite did not inactivate MS2 within the experimental timeframe.

#### MS2 Inactivation

The decrease in infective MS2 particles and total MS2 particles across the reactor were assayed by taking samples from the atomizer reservoir and samples from impingers both upstream and downstream of the NTP treatment. Although plaque assay results are normally reported in pfu per ml of solution and qPCR results are reported as gene copies (gc) per ml of solution, our reported concentrations are in pfu or gc per liter of air, which correspond to the overall air flow rate for the case of gross concentrations entering the sampling train, and to the 1 LPM air sampling rate through the impingers.

When the volumetric air flow rate was maintained at 170 LPM and the reactor was off, a ~2.6 log decrease in infective MS2 concentrations from the humidifier outlet to the upstream impinger was observed, as was a ~0.35 log decrease between the upstream and downstream impingers (figure 6). The qPCR results, which reflect the total number of viruses, suggested a decrease of ~1 log between the humidifier outlet and the upstream impinger and a decrease of ~0.35 log between the upstream and downstream impingers (figure 6). The ~1 log decrease in gene copy concentrations from the humidifier outlet (position 8) to the upstream impinger (position 10), which indicates the loss of total (infectious and inactivated) viruses during atomization, may have several causes, including wall losses along the four-meter-long duct. These impacts are discussed in greater detail in Xia et al [21]. The additional 1.6 log reduction in infectious MS2 concentrations

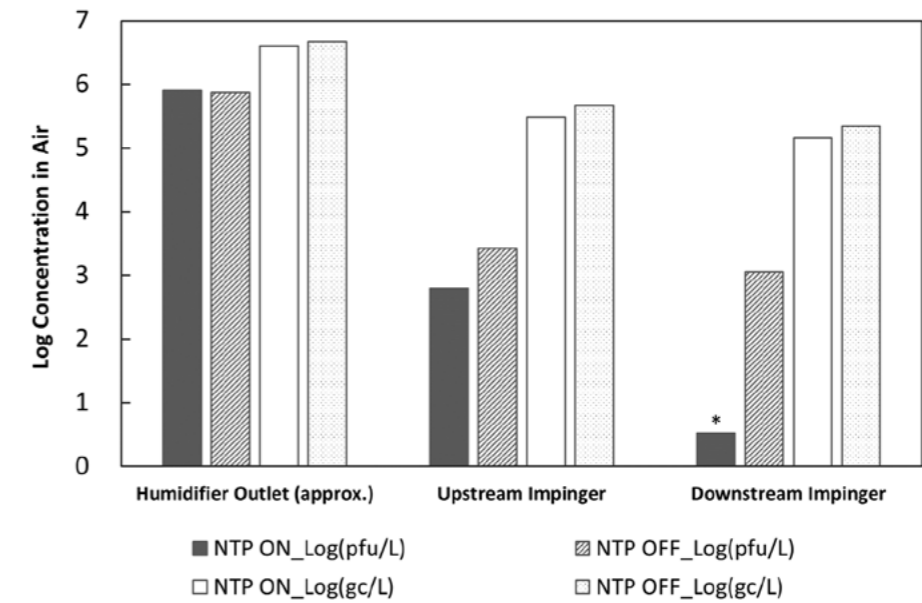


**Figure 6.** Concentrations of viruses in air measured with plaque assays and RT-qPCR in the NTP reactor powered by 30kV AC supply at a 170 LPM air flow rate (\*: detection limit).

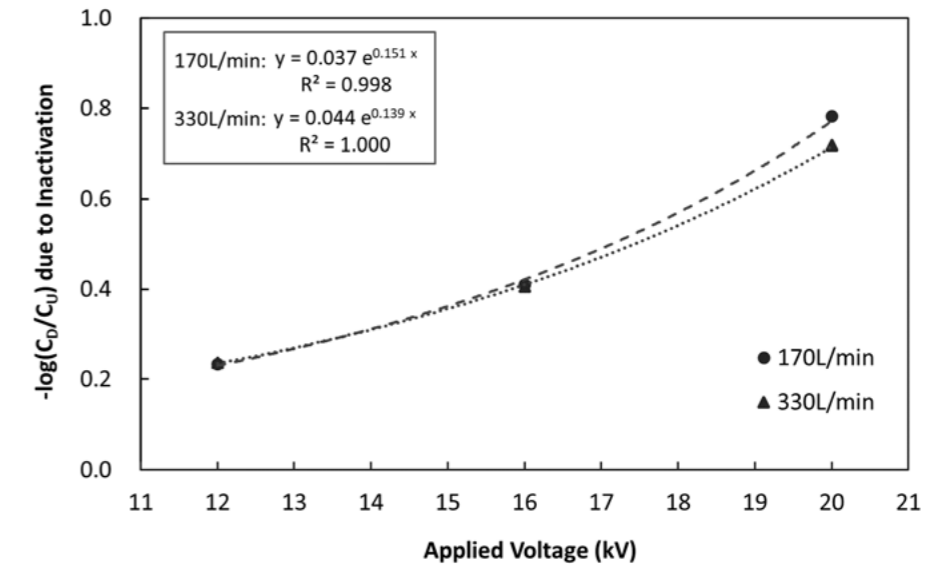


**Figure 7.** Log-reduction of infectious MS2 in airstream due to inactivation of the packed-bed NTP reactor activated by the variable voltage amplifier at 12kV, 16kV and 20kV (C<sub>D</sub> and C<sub>U</sub> represent the downstream and upstream concentrations in air, respectively).

was most likely caused by inactivation during the evaporation process of the atomized MS2-PBS droplets. Based on the qPCR results, the 0.35 log decrease of infectious viruses through the packed bed when the reactor was off was not due to inactivation of viruses in the aerosols and was likely due to physical filtration of the virus by the packed bed.

When the reactor was powered with the 30kV neon transformer, samples collected post-NTP treatment contained infective virus concentrations below our plaque assay limit of quantification (10 pfu ml<sup>-1</sup>). Consequently, the reactor caused a decrease of more than 2.3 log infective MS2 (2 log inactivation if excluding the 0.35 log filtration discussed above) (figure 6). In contrast, the nearly constant reduction in gene copy concentrations with and without power to the reactor

suggests that the virus was inactivated, and not removed physically (figure 6). In Xia et al [21], we discuss the likely mechanisms responsible for the nearly three log reduction in infective MS2 concentration between the introduction of the aerosol at position 8 to the upstream impinger at position 10 (figure 1).

MS2 inactivation was measured over a range of lower voltages (12, 16, and 20kV) and two air flow rates (170 LPM and 330 LPM). Increasing the voltage resulted in an exponential increase in MS2 inactivation by the reactor (figure 7), when the packed-bed filtration effect (an average of 0.14 log) was subtracted. At an air flow rate of 170 LPM and 12kV, an infective virus inactivation reduction across the reactor of 0.23 log was observed. This increased to a 0.78 log reduction at



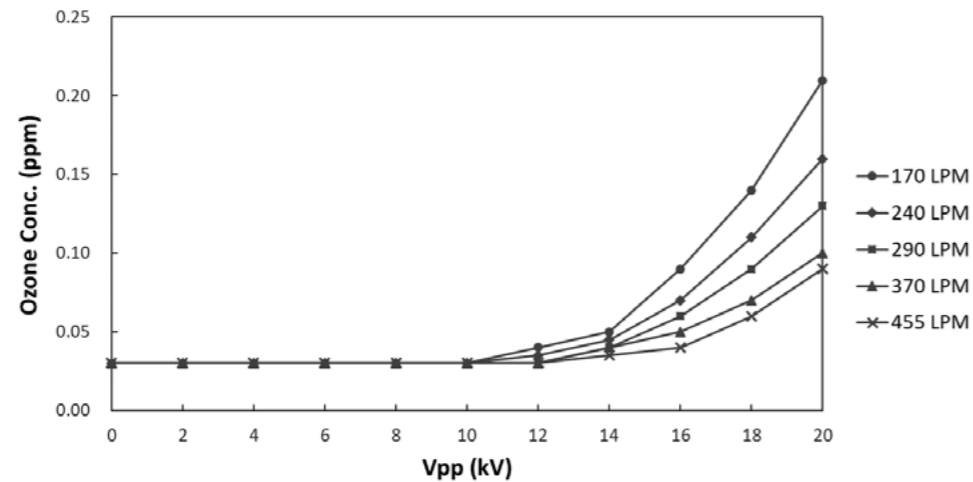


**Figure 8.** Measured ozone concentrations upstream of the ozone filter as a function of  $V_{pp}$  and air flow rate.

20kV. Inactivation of infectious agents by chemical oxidants generally follows a Chick–Watson model, as illustrated by the equation below [26, 27]:

$$\ln\left(\frac{C_D}{C_U}\right) = -kC_{inact}^n t \quad (4)$$

where  $C_D$  and  $C_U$  are downstream and upstream infectious virus concentrations respectively,  $C_{inact}$  is the concentration of the inactivating agent generated by NTP,  $n$  is the coefficient of dilution (usually assumed to be 1),  $t$  is duration of treatment, and  $k$  is a kinetic constant. When the NTP reactor is operating at steady state under steady applied AC voltage,  $C_{inact}$  and treatment time  $t$  should remain constant. Increasing applied voltage to the NTP reactor increases the concentration of reactive ions and electrons ( $C_{inact}$ ) in the plasma, and according to figure 7 and equation (4),  $C_{inact}$  should increase exponentially with increasing applied voltage. This assertion, however, needs to be justified in future plasma species measurements and analysis. Increasing the flow rate to 330 LPM, and consequently reducing the treatment time by approximately 50%, had a small impact on inactivation (figure 7), which indicates that the amount of treated air by the reactor can be increased without having a major impact on inactivation efficiency. This may be because that the predominant species inactivating aerosolized MS2 in this study were short-lived radicals rather than long-lived ozone, whose lifetime is at the scale of nanoseconds [28] and would not be affected by the change of second-scale exposure time. Wu *et al* [18] reported similar limited impact of treatment time on NTP inactivation efficiency. Specifically, the study showed that doubling the treatment time would only cause a 2%–4% further inactivation of waterborne MS2 by plasma gas. Extrapolating the results obtained at 12–20kV and 170 LPM to 30kV according to the trendline would yield an estimated 3.5 log reduction, in agreement with the greater than 2 log reduction obtained with the fixed 30kV neon transformer.

In this study, at the flow rate of 170 LPM, the virus exposure time to NTP species was about 0.25s, and the steady state ozone concentration downstream of the reactor was measured as 0.21ppm at 20kV and 2.08ppm at 30kV. The ozone

dose received by aerosolized MS2 was thereby estimated as  $0.0017 \text{ min mg m}^{-3}$  at 20kV and  $0.017 \text{ min mg m}^{-3}$  at 30kV (assuming room temperature and pressure). According to Tseng and Li [29], 90% (1 log) inactivation of airborne MS2 required an ozone dose of  $1.28 \text{ min mg m}^{-3}$ , which is 75–750 times of the ozone dose provided in this study. It was therefore concluded that ozone acted as a secondary inactivating reagent in this study and that aerosolized MS2 was predominantly inactivated by radicals and other reactive oxygen species (ROS) generated by the packed-bed NTP reactor over the short exposure time.

Our MS2 inactivation results (figures 6 and 7) are comparable with the previous studies. For example, Vaze *et al* applied 28 kV 600  $\mu\text{s}$  pulse discharges to generate NTP, and the reactor achieved 97% inactivation of *E. coli* (1.5 log reduction) during the 10s treatment time [17]. When the plasma generation area was reduced by 25%, the reactor's *E. coli* inactivation efficiency reduced significantly to 29% (0.16 log reduction) [19]. Wu *et al* applied a 14kV 10kHz AC power supply, and at 20 W power level, the reactor achieved ~80% MS2 inactivation (0.9 log reduction) in room air during a 0.12s treatment time [18]. Both of these studies, however, only reported the reductions of viable bioaerosol concentration after the NTP treatment, and did not separate the inactivation effect of the active plasma species from the physical electrostatic precipitation or filtering effect of the reactor.

#### Ozone generation by the NTP reactor

One major concern for NTP-based airstream disinfection is the production of ozone in ventilation air, which can have detrimental impacts on human and animal health [30]. In California, state environmental regulations [31] require that indoor air cleaning devices intended for use in occupied spaces should not produce ozone concentrations greater than 0.05ppm in treated air streams. We therefore adapted consumer-grade activated carbon honeycomb filters, normally installed over exhaust vents of photocopiers and laser printers, for use as a post-NTP treatment ozone filter.

The ozone concentrations were measured in the airstream upstream of the ozone filter (downstream of the packed bed

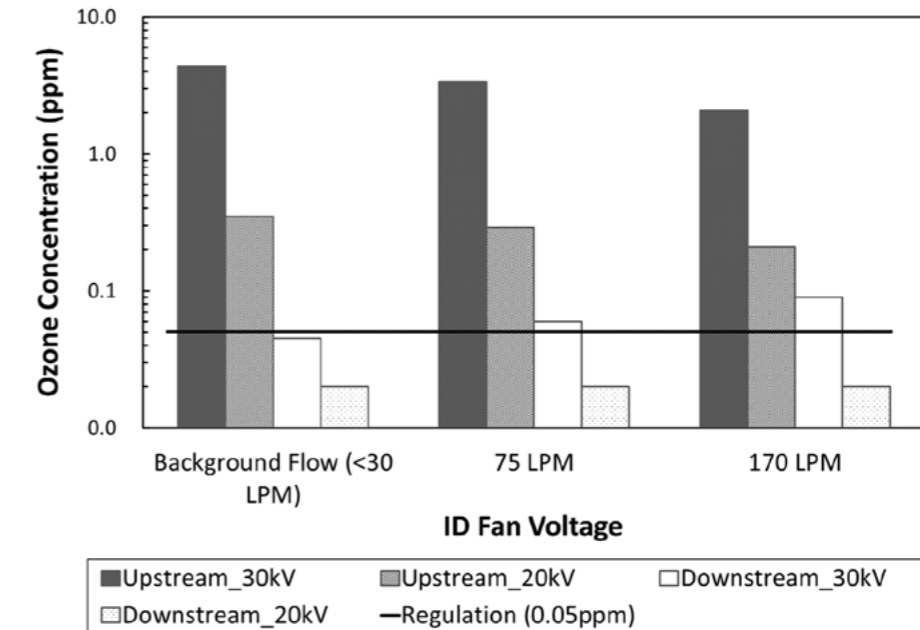


**Figure 9.** Measured ozone concentration upstream and downstream of the single layer ozone filter with either 20kV or 30kV power supply at varied air flow rates. The dashed line represents the ozone standard for indoor air cleaners set by the state of California [31].

section of the reactor), as a function of peak-to-peak voltage ( $V_{pp}$ ) applied by the Trek high voltage power supply (figure 8). The baseline ozone concentration in the room air was 0.03ppm. Results suggest that plasma was not established in the reactor and no ozone was produced until the applied  $V_{pp}$  exceeded 10kV (figure 8). Above 10kV, the ozone concentration downstream of the packed bed and upstream of the ozone filter increased with increasing  $V_{pp}$  and decreased due to reduction of NTP discharge energy density (discharge energy per unit volume of the air flow) with increasing air flow rate, as set by the ID fan. When 20kV AC voltage was applied to the packed-bed NTP reactor and at the 170 LPM flow rate, the highest ozone concentration downstream of the reactor was 0.21ppm.

Ozone concentrations were measured upstream and downstream of a single, centimeter-thick ozone filter under reactor-on conditions at 20kV (discharge power of 0.56 W) and 30kV (discharge power of 2.08 W) over a range of air flow rates (figure 9). Increasing air flow rates corresponded with decreasing upstream ozone concentrations due to reduction of NTP discharge energy density, and increasing downstream ozone concentrations, likely due to increasing space velocity (defined as volumetric flow rate normalized by filter volume) and thus decreasing filter performance. The much higher supplied power of the 30kV power supply, as compared to the 20kV power supply, also produced more ozone, approximately ten times higher at all three flow rate conditions (figure 9). This was likely a result of greater oxygen atom radical (O) production at the higher power, which reacted with the available  $\text{O}_2$  to form more  $\text{O}_3$  [32, 33]. At 170 LPM and 30kV, the single layer of the activated carbon filter reduced upstream ozone concentrations by 96%; however, the downstream  $\text{O}_3$  concentration (0.09ppm) still exceeded the 0.05ppm California standard. The addition of

a second filter would very likely reduce concentrations below the California standard, with little increase in the pressure drop across the filter (20 Pa at the flow rate of 170 LPM).

## Conclusion

In this study, we successfully designed and constructed a packed-bed DBD NTP reactor that was effective at inactivating bacteriophage MS2 in aerosols with minimal pressure drop across the reactor. Ozone generated by the active plasma was effectively reduced to meet regulation standards by the insertion of commercial ozone filters without significant pressure drop. In future applications, the packed-bed depth, the dielectric material, and the air flow rate through the sampling train can be modified to achieve improved performance at various flow conditions.

## Associated content

## Acknowledgment

This article is based upon work that is supported by the National Institute of Food and Agriculture, US Department of Agriculture, under Award No. 2016-67030-24892. Any opinions, findings, conclusions, or recommendations expressed in this publication are those of the author(s) and do not necessarily reflect the view of the US Department of Agriculture. The authors thank Minmeng Tang and Yinyin Ye (University of Michigan) for helping in the experimental setup and plaque assay analysis respectively. The authors also thank Professor John Foster and Selman Mujovic (University of Michigan) for helping in the design and power consumption measurements of the packed-bed NTP reactor used in this research.

## Supporting information

Please see the supplementary material document, available online.

## Author contributions

The manuscript was written through contributions from all authors. All authors have given approval to the final version of the manuscript.

## Funding sources

This article is based upon work that is supported by the National Institute of Food and Agriculture, US Department of Agriculture, under Award No. 2016-67030-24892.

## Notes

E M L and H L C are affiliated with Taza Aya LLC; H L C is co-founder and CEO. T X, A K, Z Q, and K R W all declare no competing financial interest.

## ORCID iDs

T Xia  <https://orcid.org/0000-0002-0601-0467>

## References

- [1] McKinney K R, Gong Y Y and Lewis T G 2006 Environmental transmission of SARS at Amoy Gardens *J. Environ. Health* **68** 26
- [2] Hermann J, Hoff S, Muñoz-Zanzi C, Yoon K-J, Roof M, Burkhardt A and Zimmerman J 2007 Effect of temperature and relative humidity on the stability of infectious porcine reproductive and respiratory syndrome virus in aerosols *Vet. Res.* **38** 81–93
- [3] Ostfeld R S 2009 Climate change and the distribution and intensity of infectious diseases *Ecology* **90** 903–5
- [4] Kowalski W J, Bahnfleth W P, Witham D L, Severin B F and Whittam T S 2000 Mathematical modeling of ultraviolet germicidal irradiation for air disinfection *Quant. Microbiol.* **2** 249–70
- [5] Riley R L 1961 Airborne pulmonary tuberculosis *Bacteriol. Rev.* **25** 243
- [6] Wheeler S M, Ingraham H S, Hollaneder A, Lill N D, Gershon-Cohen J and Brown E W 1945 Ultra-violet light control of air-borne infections in a naval training center: preliminary report *Am. J. Public Health Nation's Health* **35** 457–68
- [7] Memarzadeh F, Olmsted R N and Bartley J M 2010 Applications of ultraviolet germicidal irradiation disinfection in health care facilities: effective adjunct, but not stand-alone technology *Am. J. Infect. Control* **38** S13–24
- [8] USEPA 2018 *Air Cleaners and Air Filters in the Home* (Washington, DC: EPA Office of Radiation and Indoor Air, Indoor Environments Division)
- [9] Pitkin A, Deen J and Dee S 2009 Use of a production region model to assess the airborne spread of porcine reproductive and respiratory syndrome virus *Vet. Microbiol.* **136** 1–7
- [10] Kim H H 2004 Nonthermal plasma processing for air-pollution control: a historical review, current issues, and future prospects *Plasma Process. Polym.* **1** 91–110
- [11] Holzer F, Kopinke F and Roland U 2005 Influence of ferroelectric materials and catalysts on the performance of non-thermal plasma (NTP) for the removal of air pollutants *Plasma Chem. Plasma Process.* **25** 595–611
- [12] Kuwahara T, Okubo M, Kuroki T, Kametaka H and Yamamoto T 2011 Odor removal characteristics of a laminated film-electrode packed-bed nonthermal plasma reactor *Sensors* **11** 5529–42
- [13] Park S S, Kang M S and Hwang J 2015 Oil mist collection and oil mist-to-gas conversion via dielectric barrier discharge at atmospheric pressure *Sep. Purif. Technol.* **151** 324–31
- [14] Vandenbroucke A M, Morent R, De Geyter N and Leys C 2011 Non-thermal plasmas for non-catalytic and catalytic VOC abatement *J. Hazard. Mater.* **195** 30–54
- [15] Mizuno A, Yamazaki Y, Ito H and Yoshida H 1989 AC energized ferroelectric pellet bed precipitator for sterilization and gas clean up *IEEE Industry Applications Society Annual Meeting* pp 2148–53
- [16] Mizuno A, Yamazaki Y, Ito H and Yoshida H 1992 AC energized ferroelectric pellet bed gas cleaner *IEEE Trans. Ind. Appl.* **28** 535–40
- [17] Vaze N D, Arjunan K P, Gallagher M J, Vasilets V N, Gutsol A, Fridman A and Anandan S 2007 Air and water sterilization using non-thermal plasma *16th IEEE Int. Pulsed Power Conf. (IEEE)* pp 1231–5
- [18] Wu Y, Liang Y, Wei K, Li W, Yao M, Zhang J and Grinshpun S A 2015 MS2 virus inactivation by atmospheric-pressure cold plasma using different gas carriers and power levels *Appl. Environ. Microbiol.* **81** 996–1002
- [19] Vaze N D, Gallagher M J, Park S, Fridman G, Vasilets V N, Gutsol A F, Anandan S, Friedman G and Fridman A A 2010 Inactivation of bacteria in flight by direct exposure to nonthermal plasma *IEEE Trans. Plasma Sci.* **38** 3234–40
- [20] Liang Y, Wu Y, Sun K, Chen Q, Shen F, Zhang J, Yao M, Zhu T and Fang J 2012 Rapid inactivation of biological species in the air using atmospheric pressure nonthermal plasma *Environ. Sci. Technol.* **46** 3360–8
- [21] Xia T, Kleinheksel A, Wigginton K R and Clack H L 2019 Suspending viruses in an airstream using a consumer-grade ultrasonic humidifier *Aerosol Sci. Technol.* in preparation
- [22] Pecson B M, Martin L V and Kohn T 2009 Quantitative PCR for determining the infectivity of bacteriophage MS2 upon inactivation by heat, UV-B radiation, and singlet oxygen: Advantages and limitations of an enzymatic treatment to reduce false-positive results *Appl. Environ. Microbiol.* **75** 5544–54
- [23] United States Environmental Protection Agency 2001 *Environmental Protection Agency Method 1601: Male-Specific (f+) and Somatic Coliphage in Water by Two-Step* (Washington, DC: US EPA Office of Water)
- [24] Harling A M, Glover D J, Whitehead J C and Zhang K 2009 The role of ozone in the plasma-catalytic destruction of environmental pollutants *Appl. Catal. B* **90** 157–61
- [25] Ogata A, Mizuno K, Kushiya S and Yamamoto T 1998 Methane decomposition in a barium titanate packed-bed nonthermal plasma reactor *Plasma Chem. Plasma Process.* **18** 363–73
- [26] Chick H 1908 An investigation of the laws of disinfection *J. Hygiene* **8** 92–158
- [27] Watson H 1908 A note on the variation of the rate of disinfection with change in the concentration of the disinfectant *J. Hygiene* **8** 536–42

- [28] Eliasson B and Kogelschatz U 1991 Nonequilibrium volume plasma chemical processing *IEEE Trans. Plasma Sci.* **19** 1063–77
- [29] Tseng C-C and Li C-S 2006 Ozone for inactivation of aerosolized bacteriophages *Aerosol Sci. Technol.* **40** 683–9
- [30] Lippmann M 1989 Health effects of ozone. A critical review *JAPCA* **39** 672–95
- [31] Jakober C and Phillips T 2008 *Evaluation of Ozone Emissions From Portable Indoor Air Cleaners: Electrostatic*

- Precipitators and Ionizers* (Sacramento, CA: California Environmental Protection Agency, Air Resources Board)
- [32] Yehia A and Mizuno A 2013 Ozone generation by negative direct current corona discharges in dry air fed coaxial wire-cylinder reactors *J. Appl. Phys.* **113** 183301
- [33] Penetrante B, Hsiao M, Bardsley J, Merritt B, Vogtlin G, Kuthi A, Burkhardt C and Bayless J 1997 Identification of mechanisms for decomposition of air pollutants by non-thermal plasma processing *Plasma Sources Sci. Technol.* **6** 251–9







































JONIX  
pure living

